IMPERIAL INSTITUTE

OF

AGRICULTURAL RESEARCH, PUSA

PROCEEDINGS

OF THE

ROYAL SOCIETY OF LONDON

SERIES A

CONTAINING PAPERS OF A MATHEMATICAL AND
PHYSICAL CHARACTER

VOL. CXLIV

CONTENTS.

SERIES A   VOL CXLIV

PROCEEDINGS OF

THE ROYAL SOCIETY.

SECTION A — MATHEMATICAL AND PHYSICAL SCIENCES.

Discussion on Heavy Hydrogen

Opening Address

By LORD RUTHERFORD, O M, F R S

In the history of Physical Science, it is a commonplace that a new discovery which at first appears to be of purely scientific interest, ultimately, within a period of twenty years or more, is found to have useful practical applications This is well illustrated by the discovery of the rare gases in the atmosphere, neon, and argon, which are now used in quantity for industrial purposes The fundamental discovery in 1919 of the isotopic constitution of the majority of our elements, so largely due to Aston, at first sight appeared to be of purely scientific significance, but we shall see from the discussion to-day that it may ultimately have wide practical consequences in many directions

It is hardly necessary to discuss in detail the history of the discovery and separation of heavy hydrogen, in which scientific men in the U S A have taken such a leading part   The proof that oxygen was not a simple element but contained two isotopes in small quantity of masses 17 and 18, indicated that there was a small discrepancy of about 2 parts in 10,000 between the measurements of the relative masses of hydrogen and oxygen found by Aston and those found by direct physical and chemical methods.   Birge and Mendel suggested that this discrepancy might be due to the presence of an isotope of mass 2 present in ordinary hydrogen   This gave the necessary impetus to Urey, Brickwedder and Murphy to test whether the presence of H^2 could be detected by direct optical methods.   The experiments were successful in showing a small trace of H^2, estimated initially at about 1 in 4000 of the H^1 isotope.   The wave-length of the α line of H^2 was found to be 1 79 A units greater than for H^1—a result agreeing closely with the theoretical value to be expected for an isotope of hydrogen of mass 2.   The mass of the new isotope was directly

measured by Bainbridge, using a modified type of mass spectrograph, and found to be 2·0136, slightly less than the weight of the ordinary hydrogen molecule 2 0156 in terms of O = 16

We have no definite evidence of the exact constitution of H^2, whether it is to be regarded as a simple entity or built up of two or more constituents. It was at first natural to suppose that the H^2 nucleus might be made up of two protons and a negative electron, but the subsequent discovery of the neutron indicated that it might rather be a close combination of a neutron and a proton Taking Chadwick's value of the mass of the neutron as 1 0067, the sum of the masses of the proton and neutron is 2 0145, while the mass of the H^2 nucleus is slightly less, 2·0136, indicating that the binding energy of the neutron-proton combination is less than 1 million volts. If this be so, it is expected that the H^2 nucleus should be broken up by collision with a swift α-particle In conjunction with Mr Kempton I have made experiments to test this, but have been unable to detect with certainty the presence of any neutrons when heavy water was bombarded by α-particles from polonium. The number of neutrons, if any, was certainly less than 1% of the number of neutrons released from a sheet of beryllium under the same conditions. If the disruption of H^2 with an emission of a neutron occurs, it must happen very rarely compared with the number of violent collisions between the α-particles and the H^2 nucleus

It is interesting to note here a suggestion made by Lawrence He found in his experiments on the bombardment of matter by high speed H^2 ions that a group of protons of nearly the same speed was released from a number of elements In explanation, he suggested that the H^2 nucleus broke up into a neutron and proton either in the bombarded nucleus or in the strong field in its neighbourhood For the conservation of energy to hold, it is necessary to suppose that the mass of the neutron is much lower than that found by Chadwick, viz , 1 0006 instead of 1 0067 On this view, the H^2 nucleus contains a store of energy corresponding to about 5 million volts, and this is occasionally released in nuclear collisions Further experiments are required to test the validity of this idea.

It was of interest to me also to examine whether the fields of force near the H^1 and H^2 nuclei are the same This was tested by comparing the distribution with the velocity of the recoil H^1 and H^2 atoms when α-particles pass through ordinary and heavy hydrogen respectively While the recoil H^2 particles travel, as is to be expected, slightly further than the H^1 particles, to a first approximation the number and distribution of the recoil atoms were about the same in the two cases. Since in a close collision the α-particles and the H^2

nucleus approach within 10^{-12} cm. of each other, these results indicate that the scattering fields are sensibly the same for H^1 and H^2 nuclei, even up to these very small distances

Some success in concentrating H^2 was initially obtained by fractionating liquid hydrogen Washbourn and Urey noted that there was a greater concentration of H^2 in old electrolytic cells and found the H^2 was rapidly enriched in the residues after electrolysis This general method was first used on a large scale by Lewis and Macdonald, of the University of California, in order to obtain concentrated preparation of heavy water By this method they have obtained quantities of heavy water of the order of several hundred cubic centimetres practically in a pure state It has been concluded that one atom of H^2 is normally present with 6500 atoms of ordinary hydrogen. Lewis and his collaborators find that the density of this new water is about 11% higher than that of ordinary water, while its freezing point is 3 8° C and its boiling point 101 42° C The maximum density is found to occur at 11 6° C instead of 4° C as in normal water It is of interest also to refer to another method of concentration by pure diffusion methods Professor Hertz informs me that he has been able to obtain the new isotope in small quantity in a pure state by applying his elaborate diffusion method to ordinary hydrogen He states that he has obtained heavy hydrogen so pure that he has been unable to detect in its spectrum the α line of ordinary hydrogen I shall not discuss further the practical methods of separation, for I hope the methods of obtaining heavy water will be explained to you by Dr Hartock who has been responsible for a preparation of about 25 c c of the new water in the Cavendish Laboratory, for use in experiments on the transformation of matter

It is obvious that this new discovery opens up a wide and important field of work, but I shall leave my chemical colleagues to deal adequately with this question On account of its greater mass, it is to be expected that the rate of diffusion and the rate of chemical reaction will differ when H^2 is substituted for H^1, while the compounds formed with the new isotope are to be expected in some cases to exhibit rather different properties from the normal hydrogen compounds Similarly, this new discovery opens up interesting questions on the effect of heavy water in altering the normal physical and chemical processes in animal and plant life. A certain amount of information is already available in this interesting field of enquiry.

There is one question of much interest to me to which I should like to refer, namely, the use of H^2 nuclei as swift projectiles for studying the transformation of the elements. It was a happy coincidence that when Professor Lewis had

prepared concentrated samples of H^2, Professor Lawrence of the same University had in working order his ingenious apparatus for obtaining high-speed ions corresponding to more than a million volts in energy   Lawrence found that the high speed H^2 ions were often much more effective than protons of equal energy in causing transformations of new kinds in a number of elements. For example, when lithium is bombarded with H^2 ions, α-particles are ejected with speed considerably greater than the swiftest α-particle from radioactive substances.   It is now clear that an H^2 particle occasionally enters the nucleus of lithium mass 6, and the resulting nucleus then breaks up into 2 α-particles, escaping in nearly opposite directions.   The correctness of this view is well shown by the Wilson chamber photographs of the tracks of the α-particles obtained by Dee and Walton   The action of H^2 on the isotope of mass 7 is even more complicated, for Oliphant and I have observed that α-particles are liberated over a wide range of velocities   In this case, it seems that the capture of H^2 by the lithium nucleus of mass 7 results in the break up of the system into two α-particles and a neutron   We estimate that the maximum energy of the ejected neutron may be as great as 15 million volts   We have confirmed this conclusion by finding that neutrons can be detected in numbers corresponding to this mode of transformation using H^2 particles of energy about 200,000 volts   Lauritsen found that a copious supply of neutrons could be obtained by bombarding beryllium with H^2 particles, while Lawrence obtained large numbers from lithium with very fast H^2 particles, but he inclines to believe that most of the neutrons observed in his experiments arise from the break up of the H^2 nucleus into a neutron and a proton

As already mentioned, Lawrence has observed that H^2 bombardment gives rise to one or more groups of fast protons from a number of elements.   These observations have been confirmed by Cockcroft and Walton for several light elements such as Li, C and Fe, using H^2 particles of energy about 500,000 volts, but they have failed to observe proton groups from Cu and Au   In general it appears that the H^2 particle is remarkably effective in causing the transformation of many elements, resulting in a number of substances in the liberation of α-particles as well as protons and neutrons   There can be no doubt that this new projectile, as well as the proton, will prove of great service in studying the processes which take place in the transformation of the elements, and this will give further important information on the structure of nuclei

It is obvious that this new isotope, which can so easily be obtained in reasonable quantity in a pure state, will prove of such great importance to science that it is desirable to give it a definite name.   Urey has proposed the

name " deuterium " for the new isotope It is important also that an appropriate title should be given to the H² nucleus not only as a projectile for atomic transmutations but as a possible constituent of atomic nuclei Lewis has suggested the name " deuton " or " deuteron " for this nucleus While we all realize that the first discoverer has a strong claim in suggesting an appropriate name for a new substance the question of a suitable nomenclature is in this case of such general importance to scientific men that it deserves careful consideration While the name " deuton " is in some ways suitable it has for me the objection that it is liable in the spoken voice to be confused with neutron, and this difficulty is accentuated by the recent discovery that neutrons are often liberated from elements bombarded by deutons In consultation with some of my physical and chemical colleagues some time before these names were announced the name " diplogen " (διπλοῦς—double) for heavy hydrogen and " diplon " for the nucleus seemed to meet with some favour Whatever view may be taken on this question it is important that the new isotope should have a definite symbol allotted to it and the symbol " D " seems appropriate

In this brief statement I have not attempted to deal with a number of interesting points which I hope will receive the attention of subsequent speakers

The PRESIDENT I think it might be well if each speaker would express his opinion on this question of the names ; it would be useful to have the collective opinions of all those who speak.

Dr N V SIDGWICK , F R S   I should like, in compliance with the President's wishes, to express very strong support for the terminology suggested by Lord Rutherford. I do not think that the objection he raised to the term " deuton " because of its similarity to " neutron " is at all an unimportant matter , I have heard from people who were at the meeting of the American Chemical Society at Chicago last summer that they actually had very great difficulty in determining whether a speaker said " neutron " or " deuton " You must remember that this is not like the discovery of a rare earth. It does not much matter to any of us what we call No 61 because we rarely have occasion to refer to a substance like that , but the isotope of hydrogen is going to be one of the most important substances in the coming development of chemistry

The names which Lord Rutherford suggested give us exactly what we want They give us, first of all, the relation between the nucleus of the new isotope and the nucleus of the old isotope, and it is really more sensible to call it " the

double one " than " the second one " because the interesting thing about it is not that it is the second lightest particle , that is a matter of argument and it may be said that the first particle is the proton and the second the thing with atomic number 2 The interesting thing about it is that it is double the first one, and that is the reason for the name Lord Rutherford suggests. Then you have the relation between the particle and the atom as a whole which is given by " diplogen," which means that which makes diplon , and the only way in which you can make the particle is from the atom of the isotope   " Diplogen," too, conveys the obvious analogy to hydrogen, which is the most striking thing about it   " Deutium," " deuterium " or " deuteronium " do not indicate a relation to hydrogen Moreover, when we come to compounds like CH_3D and $C_6H_4D_2$ it is quite easy to call them diplomethane or di-diplobenzene, whereas if you call them deuteromethane or di-deuterobenzene it must be remembered that the prefix " deutero " is a living prefix in scientific terminology, and means not " containing deuterium," but simply " second "

I have been asked to say something on the chemical side of the question, and I will do so as briefly as I can, since I have no new knowledge to produce I want to deal with what we may expect to be the properties of substances made of this new material, as compared with those made of hydrogen, and along what lines we may expect the investigation of the new substance to lead to the discovery of new knowledge

It is to be expected that the atomic volume of the new isotope will be very nearly the same as that of hydrogen, just as the two isotopes of lead have, as far as we know, the same atomic volume Moreover, since the atomic volume is practically the same and the atomic number is the same, the ordinary physical properties of a substance made of this element will only differ slightly from those of a substance made of ordinary hydrogen That is the first point

The second point is that it has been shown by Urey and Rittenberg, on the basis of theoretical physics, that the equilibrium constant for reactions in which the new isotope takes part will not be quite the same as for those in which the old hydrogen takes part The difference is not likely to be more than 50% , thus for the reaction $H_2 + I_2 = 2HI$ they find a difference of 20%

This refers to reactions at the ordinary temperature , if you do them at the absolute zero that difference ought to increase up to infinity, but at the ordinary temperature you may expect rather small differences With regard to this, we have already the experimental evidence of Lewis that the maximum density of D_2O is at 11 6° C , whereas that of ordinary water is at 4° C We all realise,

of course, that water, at any rate at temperatures near freezing point, is made up of a variety of polymers in some sense or another, and that the abnormal change in density near freezing point is due to that fact. Now, it is obvious from the fact that the maximum density for the D_2O is at a different temperature from that of water, that the equilibrium between these polymers or between the various states of water is different for the two substances, and therefore—and this, I think, has not always been noticed—it follows that the differences which have been observed in the physical properties of the heavy water and the light water—the difference of 3.8° in freezing point and 1.4° in boiling point, about $\frac{1}{3}$% in molecular volume and about 1% in molecular refraction—are not the normal differences to be expected, but are bigger, because the equilibrium is different for that substance. They are larger differences than you would expect to find, for instance, in non-associated substances such as benzene and hexadiplobenzene.

The next point is that we should expect to find that the rates of reaction of the new hydrogen will be slower than the rates of reaction of the old, and to an extent which may easily lead to a variation in the ratio of 5 to 1 in the velocity constants of the reaction, and in exceptional types of reaction the differences may be very much greater. This is obviously of great importance, because there are many reactions, particularly in organic chemistry, where it is a matter of dispute whether a hydrogen atom takes part. If you can put one of the diplogen atoms in place of the hydrogen atom and measure the rate, that ought to tell you whether the hydrogen atom does take part in the reaction, or whether the reaction in which that hydrogen atom takes part is slow enough to affect the whole of the rate of the reaction.

Another point is that the discovery of this new isotope enables us to earmark the hydrogen atoms in a compound in very much the same way that Hevesy and Paneth have earmarked the atoms by the use of radioactive isotopes mingled with the other isotopes of the same elements which were not radioactive, but with this tremendous advantage, that whereas they were necessarily confined to the isotopes of the heaviest elements, which form part of only a very limited number of molecules, we are now able to do the same with hydrogen, which is a constituent of more chemical compounds than any other element.

All sorts of obvious applications arise out of this. One is in determining the readiness of reaction of hydrogen in ordinary groupings. Bonhoeffer has already shown that if you dissolve sugar in heavy water and let it crystallise out you get a redistribution, an almost equal partition of the heavy isotope

atoms between the water and the hydroxyl groups in the sugar, but that in those conditions you get no such partition with the hydrogen of the C—H groups of sugar   Sugar consists mainly of H O C H groups , one part redistributes with the water and the other does not redistribute at all   Again, Polanyi has found that DH gas reacts with water in the presence of a catalyst such as platinum black. It is clearly desirable to pursue this line of inquiry further, and it may be expected to throw much light on the nature of the processes involved   In particular, it will be important to find out how far the readiness of the hydrogen to undergo this change is affected in the first place by the nature of the atoms with which it is linked, and secondly—which is also a matter of great importance—by the nature of the other groups in the same molecule   That ought to throw a great deal of light on the nature of the chemical reaction

To give another example of an important development, I may mention the question regarding electrolytic concentration   It is obvious to anyone who has seen the literature on the subject that when we know what the real difference of effective conditions is, the knowledge of that will throw great light on the intimate nature of these electrolytic processes themselves

I have only tried to show a few of the directions in which we may expect the new reagent to be of value, but the most important services it will be found to render to science will be in directions which we do not yet suspect

Dr F. W Aston, F R S   There are only two points which I wish to make In the first place, I should like to emphasize how very small a discrepancy enabled the discovery of this element to be made   The measurement of the atomic weight of hydrogen by chemical and physical methods, as you know, compared with O = 16, is 1 00777, and when I measured the relative masses of hydrogen 1 and oxygen 16 I got 1 00778, and that measurement was made through helium, and therefore might have an accumulated error   The method I used was one in which one had to change the electric field   In the comparison of O⁸ with He⁴ I was able to use a small change of the field, as I could use the atom carbon as a marking point between the two, and I had only to change the field by 33%, but with He⁴ and H₂ I had to change the field 100%, and, if there had been any systematic error, that on the two together might have been quite serious   I did estimate the possible error of the whole bracket as 1·5 parts in 10,000, and I thought it was considerably less

There are three completely different measurements, the chemical atomic weight, the isotopic weight, and the abundance of the rare isotopes of oxygen

made by optical spectrographic observations The accumulated error of those three experiments, of which in one the error might be admittedly 1 5 in 10,000, had to be less than 2 in 10,000 to prove that heavy hydrogen existed I think Urey is to be congratulated as a brave experimenter to attack such a problem with such extraordinarily small differences in which to trust

The only other point to which I desire to refer is that of nomenclature, which I think is extremely important I was at the meeting in Chicago last June at which Urey and Lawrence were present I was interested to note that the discussion threatened to become acrimonious, and I fear that our friends across the Atlantic may not like the suggestion coming from this side I had a talk with Professor Bohr at the time, and he certainly at first insisted that the new isotope should be called hydrogen , he said it was not a new element , it had the atomic number 1, and therefore it was hydrogen I admit that is true, but it is quite impossible to go on with the chemistry of this substance without having a new word for it, and at that meeting I suggested to Professor Urey that, although tradition allows the discoverer to name his discovery, it certainly does not guarantee that the public will use that name We all know the story, for instance, of the "corpuscle," and in quite recent years there is the word "isotope," which is now so altered in meaning that its author would hardly know it My own word, "mass-spectrograph," has also changed I think we ought to have a word which will be as useful as possible, and therefore I strongly support Lord Rutherford's suggestion of "diplogen " and " diplon "

Dr P Harteck   First of all I should like to show you two experiments, illustrating the differences of vapour pressure from normal and heavy water and the different melting points of normal and heavy ice According to Lewis and Macdonald, the vapour pressure of heavy water is smaller than that of normal water , at $25°$ C it is 12% less, and at $60°$ C about 8% less. Normal water has, at room temperature, a vapour pressure of about 24 mm., heavy water a vapour pressure of about 21 mm , a difference of 3 mm At $60°$, heavy water has a vapour pressure of 138 mm against 150 mm for normal water I can show you this difference of vapour pressures with the help of a differential manometer. I have here a U-shaped tube containing mercury , on one side is a little heavy water and on the other side a little normal water , on the one side is the vapour of heavy water and on the other the vapour of normal water, and, at this room temperature, you will see a difference of 3 mm. in the levels. When the temperature increases, the difference will be greater I have another apparatus of the same type which I plunge into hot water, and you can see as a result what a big difference there is !

The second experiment illustrates the difference in melting points. Normal water has a freezing point of 0° C, and heavy water, according to Lewis and Macdonald, 3 8° C   I have here two tubes, in one of which is a white pearl and in the other a blue pearl   They have been placed in a vessel where the temperature was about 1° C, and you will see that the heavy water is still in the form of ice, whereas the normal water has melted

I should now like to make some remarks on the preparation of the heavy water.

Lewis and Macdonald* have described the preparation of heavy hydrogen by means of the electrolysis of an alkaline solution with nickel electrodes. They do not give details of the experimental methods.   There are, however, some precautions which must be observed if the enrichment of the heavy hydrogen (H^2) is to proceed satisfactorily   This paper gives a description of a convenient method of working   For the working out of the method it was a big advantage that slightly enriched samples of water could be examined in the apparatus of Oliphant and Rutherford† in which lithium is bombarded with hydrogen ions   The long range α-particles which are observed are due to collisions involving H^2 according to the equation,

$$H^2 + Li^6 = 2\alpha \ (13 \text{ cm range})$$
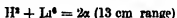
The amount of heavy hydrogen in ordinary water gives a measurable number of disintegration particles, and is a rapid method of estimating the amount of H^2 at weak concentrations

About 60 samples of enriched hydrogen, which had been prepared by electrolysis of normal water under varying experimental conditions, were tested in this way   When the method had been developed the H^2 concentration was determined by density measurements.

The electrolytic cells were made of nickel supplied by the Mond Nickel Co   The cells were soldered carefully on the outside so that practically no solder came in contact with the electrolyte

The electrolysis is begun with $\frac{1}{2}\%$ NaOH   With a current of 150 to 200 amps and cooling water approximately 10° C the temperature of the electrolyte does not rise about 25° C   Grease and organic compounds in general must be carefully avoided   The wet surface is scrubbed with glass paper and steel wool and the electrolysis immediately begun

* 'J Chem Phys,' vol 1, p 341 (1933)

† Oliphant and Rutherford, 'Proc Roy Soc', A, vol 141, p 259 (1933)   Oliphant, Kinsey and Rutherford, 'Proc Roy Soc', A, vol 141, p 722 (1933)

More than 25 electrolyses have been carried out in this manner with four different cells without any case of failure Since the initial concentration of alkali is so small it is possible to electrolyse to a $\frac{1}{40}$ or $\frac{1}{10}$ of the initial volume The solution is then neutralised with CO_2 and the water distilled off, as described by Lewis and Macdonald

The efficiency of the electrolysis seems to be independent of the concentration of alkali over a wide range   No definite increase in efficiency was observed with increasing current density provided this was greater than 0 6 amp /cm.^{2} The temperature dependence of the electrolysis was not investigated since it was always necessary to work at a low temperature to keep down evaporation

If the electrodes are really clean the efficiency has its full value from the beginning

No	V_a cm ^{3}	V_b cm ^{3}	V_a/V_b	% H^2_a	% H^2_b
1	3000	300	10	0 33	2 3
6	3000	100	30	0 33	5 3
15	40	1	40	12 2	100
23	2500	22 5	110	0 48	27
26	120	6	20	12	91 5

As soon as the concentration of H^2 had the value of about 12% the mixture of oxygen and hydrogen coming off from the cell was burnt to water to avoid loss

In the course of these experiments we have obtained enriched samples of heavy water containing from 30% to 98% of heavy hydrogen, corresponding in all to about 25 c c of pure heavy water

Professor F SODDY The questionable extension of the now well-understood term "isotope" to heavy hydrogen and other supposed examples revealed only by band-spectra is, I think, probably responsible for the confusion, since 1927, between the chemical and physical (positive-ray) unit of atomic mass The conception of chemically non-separable varieties of the same element, which dates from 1907–10, had its origin in the absolute chemical identity of radio-elements of different atomic mass, genesis, and modes of disintegration It was followed by the displacement law of radioactive change, arrived at in its final form early in 1913, the critical evidence for which was based mainly on the work of Alexander Fleck in my laboratory at Glasgow The double and single shift of place in opposite directions in the periodic table, which is produced by the expulsion of the α- and the β-ray respectively from the disintegrating

atom, caused the word " isotope " to be coined   To me it was and still is a short term for the individuals of a group of two or more chemically identical elements existing together in constant natural proportion and separable only by the few physical methods that depend directly on the masses and therefore the velocities of the molecules

In the country of its origin at least this independent experimental conception of chemistry has always been overshadowed by the contemporaneous conception of the nuclear atom of Rutherford and Bohr, and the conception of atomic number of van der Broek, as later determined experimentally from X-ray spectra by Moseley, ultimately for all the elements except those of the first short period   The positive ray method of Thomson, Aston's extension of the conception of isotopes to the non-radioactive elements, and his discovery of the whole number rule, furnish now the best proof of the correctness of the conception itself, as it arrived at in the narrower field of radio-chemistry, and particularly the constancy of the natural ratio   The only slight exception with regard to the second criterion, the constancy of natural ratio of isotopes, is boron, examined by Professor Briscoe and others, which is, as Aston has pointed out, most favourable for separability by physical processes such as diffusion

Up to 1929, the chemical and physical methods of determining atomic weights led to the most gratifying agreement for the four elements up to and including oxygen, found by Aston by the mass-spectrograph to be " pure," and for which some of the finest atomic weight data are available   Thus, in terms of oxygen 16, the chemical and physical (mass-spectra) values were as follows —

Nitrogen	14 008 and 14 008
Carbon	12 0025 and 12 0036
Hydrogen	1 00777 and 1 00778

Then, in 1929, from evidence of band spectra, the existence of small proportions of the two isotopes O^{18} and O^{17} was inferred. If these are really isotopes in the original sense, their existence demands the existence also of very nicely equivalent proportions of corresponding isotopes in the other three elements, and sure enough, when looked for, band spectra indicated also the existence of N^{15}, C^{13}, and H^2.

The first point is, and it has not been mentioned to-day, that the heavy hydrogen does not appear to be in nearly sufficient proportion to bring back the concordance between the chemical and physical numbers.   I think Aston

refers to 35,000 to one, and Lord Rutherford to-day gave it about half that.

Lord RUTHERFORD   I said 6500

Professor SODDY   6000, at any rate, is required to bring it back to the right value, and how these proportions can possibly be determined seems to me very difficult to believe , I mean, for these isotopes at any rate it is mere guesswork, and I think the knowledge of what is required to bring the value right must have a certain weight—unconsciously, no doubt—with the investigator   Further, it has been forgotten that this marked difference of chemical character that has been discovered for heavy hydrogen entirely destroys the basis of the prediction   To any chemist who is acquainted with the most extraordinarily careful atomic weight work on which the ratio of hydrogen to oxygen was founded, it is incredible that a substance so easily separable can have had any more effect on the chemical than it does on the physical ratio   One need not go into the question of whether heavy hydrogen is or is not absorbed by palladium or the usual methods by which the chemists purified their gases   Either hydrogen and heavy hydrogen were separated completely or not at all   Otherwise the differences in purification must inevitably lead to differences in the atomic weight determinations   The fact that this value of the chemists was a concordant value, although the two substances are readily separable, seems to me conclusive evidence against the validity of the original prediction   To me it is a comedy of errors , it is not a question of prediction at all

With regard to separability, the instance would appear to be much more analogous to the separation of a pair of homologues, such as zirconium and hafnium, rather than isotopes   As to the criterion of constant ratio, I do not know what the evidence is, but I have yet seen none which would exclude the possibility that we are dealing with substances analogous to oxygen and ozone , that is, that heavy hydrogen is not in natural constant proportion in hydrogen at all, but is formed by the electric discharge or by electrolysis of alkaline solutions under high pressure and current density   Aston quotes in his recent book, " Mass Spectra and Isotopes," the evidence of Sandford, that the band due to $C^{12}C^{12}$ is abnormally intense in the spectra of certain types of stars, and for what stellar evidence is worth to the chemist that shows that these are not isotopes in the original sense of the word

The relative ease with which the light elements are transmuted apparently ought also to make for caution in applying properties inferred from the behaviour

of the heavier elements to those of the first short period, and particularly to hydrogen I have never given a place in the periodic table to this element at all, and therefore regard the expression " hydrogen isotope " as doubly a misnomer It may prove that it is even easier to synthesize heavy hydrogen artificially than to disrupt the light elements

I do not wish to detract in the very least from the intense interest and importance of this discovery I think it is of fundamental importance, and the Americans are to be congratulated on it. I recall that two Americans, McCoy and Ross, in 1907, when confronted with a pair of isotopes, had the courage to call a spade a spade and to declare that radiothorium and thorium are chemically inseparable by any process Heavy hydrogen bids fair, I think, to be one of the great discoveries of the century I hope it may prove valuable not only in smashing up a few atoms, but even more so in smashing some of the physical theories of the present day about the whole of them !

Dr M Polanyi I should like to say a few words about the experiments of Dr Horiuti with hydrogen containing a small percentage of diplogen which have been made with a view to measuring the rate of ionization of diplogen, in connexion with the problem of over-voltage and catalysis If hydrogen containing 1% of diplogen is put into a 100-c c container and 10 c c of water is added, and we add half a gramme of platinum black and shake up the whole at ordinary temperature for 10 minutes, the 1% of diplogen is reduced to $\frac{1}{2}$% This proves the existence of a catalysed interchange between the diplogen and the water

It is well known that platinum is a good hydrogen electrode, and that the function of the hydrogen electrode consists in bringing about equilibrium between hydrogen and the hydrogen ions of the solution in which it is immersed In doing so, the current is caused to pass through the electrode carrying hydrogen atoms in the form of hydrogen ions into the solution, and hydrogen ions at the same time and in the same quantity pass from the solution and form hydrogen If part of the hydrogen on the electrode is substituted by diplogen then these two currents tend to interchange the hydrogen and the diplogen On half a gramme of platinum black there is about 0 2 ampere of current going to and fro in both directions

We have carried out a few experiments to make sure that what we are measuring here is really the actual rate of ionization and not some accidental factor such as diffusion We changed the solution, taking an acid solution, then an alkaline solution, and then a different acid as well as alcoholic solutions,

and we found that as we did so the rate of ionization changed quite considerably, in particular the rate of ionization was very much slower in the alkaline solution than in pure water If we take the rate of ionization in water as 1, $n/1$ hydrochloric acid is 0 7, $n/1$ sulphuric acid 0 2, and $n/4$ NaOH 0 4, in alcohol with 2% water the rate is 0 4 and if we add some alkali to this solution, the ionization disappears, so that we could not measure it in the time used for these experiments.

This shows that we actually measure not the diffusion, which, of course, could not be affected in this way, but the ionization process itself In addition, I think it throws some light on the question of what is the inertia attached to the ionization of hydrogen It is well known that, when hydrogen is formed on an electrode, it is necessary to have a certain over-voltage to force the hydrogen out of the solution, and from this over-voltage one can conclude that there is some chemical or physical resistance which has to be overcome Evidently, this resistance is identical with the inertia attached to the ionization of hydrogen, which we have measured in our experiments We recognize that it depends on the nature of the solution in which the electrode is immersed This indicates very strongly that of the two theories which have been current about the nature of this resistance, at least for platinum, only one can hold good One of these theories assumes that it is the dissociation of the hydrogen into atoms, which is accompanied by inertia, and that this caused over-voltage The other theory assumes that the hydrogen instantaneously decomposes into hydrogen atoms, and that it is the second step, the ionization of the hydrogen from the atomic state to the ionic state, to which over-voltage is due It is evident that the first step, which is really a reaction between hydrogen and platinum, could scarcely be influenced by the nature of the solution, whereas the second step would naturally be strongly influenced by it Therefore, at least, for platinum, the cause of over-voltage must be in an inertia attached to the transition of the hydrogen ion from the solution to the atomic state in its adsorbed form on the platinum.

It seems to be generally assumed that diplogen will always react more slowly than hydrogen As I may partly be responsible for this view,* I should like to point out that this is not always correct Lower reactivity of diplogen compared with hydrogen results mainly from two causes (1) the existence of zero point energy, and (2) the quantum mechanical leakage of particles through energy barriers Whilst the leakage through the barrier is always

* Cremer and Polanyi, 'Z phys Chem,' B, vol 19, p 443 (1932) See also Eyring 'Proc Nat Acad Sci Wash,' vol 19, p 78 (1933)

greater for the hydrogen than for the diplogen atoms, the effect of the zero point energy may occasionally favour the reverse ratio I will confine myself to one special case, as the general treatment will be published shortly by Bawn and Ogden Compare the reaction of a free hydrogen and a diplogen atom, in the initial state the atoms possess no zero point energy and their energies will be equal. However, at the top of the barrier there will be a zero point energy present,* and this will be greater for the complex reacting with the hydrogen atom than for that reacting with the diplogen atom. The effect of the zero point energy at the top of the barrier is, therefore, to increase the activation energy of the hydrogen atoms to a greater extent than that of the diplogen atoms

Professor E K RIDEAL, F R S I cannot do more, in the time available, than give you a very brief résumé of the work which has been carried out by Drs L and A Farkas during the last few months. They had been occupied, when in Germany, in Professor Haber's laboratory in Berlin and Dr Bonhoeffer's laboratory in Frankfurt, with experiments on the ortho-para hydrogen conversion, and it did seem possible that the thermal conductivity methods used for studying the ortho-para hydrogen system might be applicable to the diplogen-hydrogen system The only method we have had of estimating the quantity of diplogen in hydrogen has been that of converting it into water and determining the density, a laborious process and one requiring at least several milligrams, whereas with the thermal conductivity method 0 002 milligram is all that is necessary

The experimental arrangement was a slight modification of that described in a recent publication by Dr A Farkas for the sensitive measurement of ortho-para hydrogen composition This method is based on the different slopes of the specific heat curves for the two hydrogen isotopes H_2 has at 80° K a specific heat of 3 cal /mol which rises to 5 cal /mol at room temperatures, whereas the specific heat of D_2 (and also that of HD) does not alter much over this temperature range and is about 5 cal /mol The actual determination of the hydrogen diplogen concentration was carried out by measuring the temperature of an electrically heated wire stretched in the hydrogen at about 0 04 mm. pressure The difference in the temperatures of the wire which were reached when pure H_2 and pure D_2 were placed in the conductivity cell amounted to about 20° C corresponding to a change of 6 ohms in the resistance of the wire The calibration was effected by the samples of water of different

* Eyring and Polanyi, ' Z. phys. Chem ,' B, vol. 13, p. 279 (1931)

D content   We have to thank Dr Harteck for having performed the very tedious process of concentrating to its last stages our heavy water

The next point was to study the equilibrium $H_2 + D_2 \rightleftharpoons 2HD$ If the hydrogen and diplogen mixture is heated on a catalyst, in fact on a nickel wire, that equilibrium is rapidly established   The formation of HD from H_2 and D_2 effected a rise of approximately 1 ohm in the resistance value of a 50% mixture, of H_2 and D_2 and this 1 ohm corresponds to the establishment of an equilibrium when 50% HD is formed and 25% H_2 and 25% D_2 disappeared
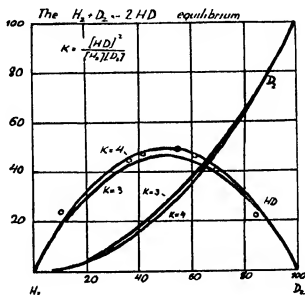
Fig 1

By making suitable mixtures of hydrogen and diplogen and bringing them to equilibrium, one can find the equilibrium constant   In fig 1 are the experimental values, and one can see that the equilibrium constant lies between 3 and 4, the curves correspond to the theoretical values   The first point that has been established here is that, in accordance with theory, the equilibrium constant does not change much above room temperature and up to 600°, and, secondly, that the equilibrium constant is very close to 4, as was also to be anticipated by theory

The next point to consider is how this equilibrium is established   We have seen that on catalysts it can be established very readily at quite low temperatures   How is it established in the homogeneous gas phase at high tempera-

ture ? It was found that there was no reaction at all in quartz under 600° C
At higher temperatures, however, a reaction took place, and samples could be
removed and analysed and we can get the order of the reaction

Fig 2 shows the reciprocal time of half change as a function of the pressure
at 725° C The order of the reaction given by this curve lies between 3/2
and 2

There are two possible mechanisms for this reaction We can first of all
imagine a molecular reaction $H_2 + D_2 \rightleftarrows 2HD$, and secondly an atomic
reaction giving $H + D_2 \rightleftarrows HD + D$, $D + H_2 \rightleftarrows HD + H$, where H and D
are formed by the thermal dissociation of H_2 and D_2. The velocity of the
molecular reaction will be proportional to the square of the pressure (p^2) and
of the other proportional to $p^{3/2}$ From the velocity of the reaction at different
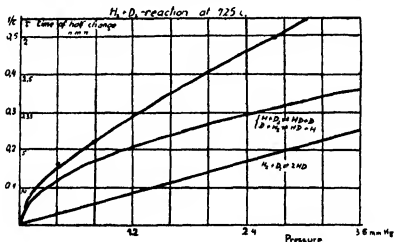
Fig 2

temperatures, it is possible to split up the curve into two corresponding to
each of the above reactions and to get the variation of the collision efficiency
with the temperature, and from that what is called the energy of activation
It is found that for the $p^{3/2}$ reaction, the one going through the atoms, the
energy of activation is 50,000 + 7,000 calories, i e , 57,000 calories, where
50,000 calories are used up for the thermal formation of the H and D atoms
That is in good agreement with the result obtained for the thermal para-
hydrogen reaction which proceed according to the reaction $H + H_2 \rightarrow H_2 + H$
The molecular interchange reaction has an energy of activation of the same order,
that is, between 50,000 and 60,000 calories.

Drs Farkas have also examined the reaction with water

Table I —D_2 + H_2O-reaction.   1 mm. D_2 + 17 mm. H_2O

Temperature	D-content after 2 hours reaction.	Collision efficiency
°C	%	
500	98	2 10⁻¹⁴
600	90	2 10⁻¹²
675	76	9 10⁻¹²

From the data of Table I one can show that the energy of activation of the reaction is again of the order of 60,000 calories

One can analyse the gas mixture from time to time and find out how these particular reactions are proceeding We have two possible reactions, H_2O + D_2 = D_2O + H_2, and H_2O + D_2 = DHO + HD and it is found that the ratios of the velocities of these two reactions are of the order of 1 3

It is also interesting to note that the collision efficiency, extrapolated to room temperature, is about 10⁻⁴⁸, which indicates very clearly that the so-called Oliphant reaction does not proceed directly, but proceeds probably through a catalyst, as shown by Dr Polanyi

Some rather interesting things were discovered in the examination of the effusion of hydrogen diplogen mixtures through a fine nozzle, as the effusion may cause a very great change in the composition of the gas

In Table II are shown the changes in the composition of the residual gas when the pressure p_0 (several hundredths of a millimetre) is diminished to a pressure p

Table II

p_0/p	% D_2 observed	% D_2 calculated
1	47	—
1 5	50 7	50 7
2 0	53 0	53 0
3 25	56 0	57 8

The observed results are in very good agreement with the values calculated on the basis of the theoretical equation

$$\frac{\left(\frac{H_2}{H}\right)^{\circ}}{\left(\frac{D_2}{D}\right)^{\circ}} = \left(\frac{p_2}{p}\right)^{s-1}$$

where "s" the separation factor, is the ratio of the molecular velocities, i e , $\sqrt{2}$

The diffusion of the two isotopes in their passage through palladium, which is one of the best methods of purifying hydrogen, was also studied

If one starts with hydrogen and diplogen mixtures the equilibrium between all three is readily established   The rate of diffusion is temperature exponential, and proportional to the expression $e^{\frac{16000}{RT}}$, where 16,000 cals is the activation energy for the diffusion   If we analyse the hydrogen diplogen of the diffused material and compare it to the hydrogen diplogen ratio of the original material $\frac{(H/D) \text{ diff}}{(H/D) \text{ orig}}$ we find a very interesting thing   This ratio at low temperatures is relatively high, i e , 1 5 at 160° C , while as the temperature rises the ratio gets closer and closer to unity , in other words, the diplogen, as it were, remains behind, and the light hydrogen passes through more freely   The expression for the ratio as a function of the temperature is given by $e^{\frac{830}{RT}}$ where 830 calories, represents the difference in activation energy for some process in the diffusion It is remarkable that the observed 830 calories is very close to the energy difference in the zero point energies for the two substances

This observation suggested that one should be able to separate hydrogen and diplogen in those chemical reactions in which the velocity whatever the energy of activation happened to be, is sensitive to changes in the energy of activation of ca 1000 calories   For example, if one takes metals and dissolves them in water or dilute acids one finds the energy of activation for the process is extremely small   One would therefore anticipate that one could obtain, coming off in the gas, a mixture of hydrogen and diplogen, but that the ratio of hydrogen to the diplogen should be much higher than in the water itself That in fact occurs, and I have here a few tentative figures for the analysis of gas coming off from a 30% hydrogen-diplogen water   If one takes zinc, for example, with a slight quantity of sulphuric acid, and dissolves that in this water, one finds that the ratio of hydrogen to diplogen in the effluent gas is 3 5 to 1 , in other words, one has almost the separation that is found by electrolysing   Other metals are not so effective   For calcium it is 1 5 to 1, for sodium 1 2 to 1, and for aluminium 2 to 1   There is a number of other possible methods of effecting this separation by chemical means , I have simply shown this one because it is very simple, and possibly lends itself to technical application

As I said before, this is just a very brief summary of the work that the two Drs. Farkas have been doing since they came from Germany

Professor R H FOWLER, F R S Personally, I have been interested in trying to understand how it is that electrolysis separates the hydrogen and the diplogen in such a way that over very wide ranges of hydrogen-diplogen concentration in the water that you are electrolysing you get a rate of evolution of hydrogen and diplogen which is some factor, Q, times the ratio of their concentrations in the water I have been trying to satisfy myself, for example, by general arguments that the ideas put forward by Dr Polanyi which are probably right, represent the only possible way of talking about that separation In doing that, I tried to avoid as far as possible all reference to details of the mechanism, and merely to see what was required to get such a constant evolution rate independent of the concentration ratio in the solution; at the same time recognizing that you have a *steady* process of electrolysis going on, so that you have no accumulations in the water of hydrogen or other substance anywhere except in the evolved gas at the expense of the solution in general

The point that I wish to make is this If you consider the whole electrode system where the process is going on, hydrogen is being fed into that by various processes, by the current carrying process, for example, from the solution in general, and is being evolved in gas bubbles, and those two things must take place at the same rate From a simple argument such as that you can, I think, get a certain control over your theories which it is well worth while to develop at some length I do not propose to do that now, I shall merely indicate the sort of arguments employed

For example if diffusion in your liquid were negligible and your only hydrogen carrying process was the actual current transported by the hydrogen ions then, no matter what your electrode processes might be, the ratio of the rates of evolution of the hydrogen and diplogen would be just Q times the ratio of the concentrations, where Q is simply the ratio of the mobilities—that and nothing else Now, that is not true, and what is happening is that atomic diffusion in the neighbourhood of the electrode prevents the building up which would be required by that result, and actually the boundary there is kept by diffusion at a fair sample in H/D ratio of the whole liquid in bulk, in spite of the transport of H and D to the electrode

If you go further into the process and consider the exchange of hydrogen between the electrode itself and the boundary layer of the liquid, you have a deposition of hydrogen on the electrode from the boundary layer, this deposition is a current-carrying process, controlled by the over-potentials, which may be different for the H and D, and that by itself could give rise to a ratio of rates of evolution of the two gases of the observed form, provided this

deposition is the only process effective in exchanging hydrogen and diplogen
between the solution and the electrode   The factor Q is then just the ratio
of the rates of deposition at the given concentration and under the given
conditions of the electrolysis   That would be true no matter how the atoms
after deposition reacted to become gas molecules , but, as Dr Polanyi pointed
out in his interesting experiments, that is not the only process of exchange
The current-carrying process is not the only process of exchange of hydrogen
between the liquid and the electrode, and other conditions come in which must
be taken into account   When you take those other conditions into account,
of course, it may very well happen, and will happen at low current densities,
that the current carrying process is trivial, and you still have your equilibrium
set up between the adsorbed hydrogen and the hydrogen in the water , and
then it matters very much what happens later on   The process which controls
the evolution will then depend on the rate at which the adsorbed hydrogen
react atoms in pairs to form the evolved gas

When you trace that through you find that a certain condition has to be
satisfied between the efficiency of interaction of HD, HH and DD, but a
relationship which is likely to be true, and, if that is true, you then still get a
ratio of rates of evolution of the form QH/D over an infinite concentration
range, but your factor Q may depend here not merely on the overpotential
factors but also on a collision-efficiency factor between the adsorbed hydrogens
The question therefore seems to me still open as to what part of the observed
Q comes from one or other of those processes   This is not the place to go into
such a special point more deeply , I merely wish to point out that such questions
do arise and will need further interesting discussion as the facts become better
known   such discussion will inevitably lead to a better understanding of the
whole phenomenon

Mr R P BELL   I have a very short report to make on some experiments
carried out by Mr Wolfenden and myself on the effect of different factors on
the electrolytic fractionation of water   We determined the concentration of
diplogen by measurements of specific gravity, independent determinations by
different observers agreeing to within 1 part in 100,000   Water of known
diplogen content was electrolysed under different conditions to a known
fraction of its original volume and the concentration of diplogen in the final
product determined by a specific gravity determination   We have expressed
the efficiency of separation by the factor α in the equation

$$d \log D = \alpha d \log H,$$

i e , our α is the same as Professor Fowler's Q.

Our first experiments deal with the effect of varying the cathode metal, and the results are given in Table I

Table I —Effect of Cathode Metal

$$D/H = 0\ 1\% \to 0\ 3\%$$

Electrode	Electrolyte	α
Ni	1% NaOH	0 22
Ni	8% NaOH	0 20
Pt	1% NaOH	0 19 } ±0 05
Cu	1% NaOH	0 19

The estimated possible error in the value of α is 0 05 , this, however, refers to the absolute values, and the differences between the values in a series should be correct to about 0 02 Within the experimental error, exactly the same efficiency was obtained using nickel, platinum and copper as cathodes In one experiment the initial caustic soda concentration was 8%, and hence the final concentration was something like 40% It has been reported that the separation becomes much less efficient in concentrated alkali This is not confirmed by our results, the efficiency being just the same as in dilute solutions

Table II shows the result of experiments on the effect of temperature and of current density

Table II —Effect of Temperature and Current Density

I $D/H = 0\ 25\% \to 0\ 5\%$

Electrolyte	Temperature	α
2% NaOH	100°	0 27 } ±0 05
2% NaOH	10°	0 24

II $D/H = 0\ 05\% \to 0\ 15\%$

Electrolyte	Current density	α
1% NaOH	10 amp /cm²	0 18 } ±0 05
1% NaOH	0 08 amp /cm²	0 27

It will be seen that there is practically no difference between the efficiencies at 10° and 100° There does appear to be a slight difference in α in the two current

density experiments, but it is doubtful whether it is greater than the experimental error   These experiments need repeating with greater accuracy

These are the experimental results which I wish to report, and I think that the most interesting point is that the separation is much less sensitive to different variables than one would have expected   It has been suggested that the separation is in some way connected with over-voltage phenomena   If this is so, one would expect some change in efficiency on changing the nature of the cathode metal ; actually nickel, platinum and copper were found to be equally efficient   The absence of any temperature effect is also unexpected, though it may be that the processes taking place in the neighbourhood of the cathode are not much affected by the temperature of the bulk of the electrolyte

Our average value for the efficiency α was about 0 2, agreeing with the value found by Lewis   Dr Hartock's results also appear to indicate about the same efficiency

Mr J D BERNAL   Through the kindness of Lord Rutherford, I was able to get some of the 91% heavy water   This was put into a small capillary, and a single crystal of ice was made and photographed *   The resulting cell measurements showed a slight, but I think, genuine difference from the values for ordinary ice taken under similar circumstances and with the same camera   The a axis was 4 50 A for heavy ice as compared with 4 52 A for ordinary ice, and the c axes 7 36 and 7 39 A respectively   The difference is small, and amounts in specific volume to a little over 1%, but it is very interesting to note that, if this result is correct, the volume difference is in the opposite sense to the volume difference for water   The apparent molecular volume of heavy water is slightly greater than that of ordinary water , the apparent molecular volume of heavy ice is slightly smaller than that of ordinary ice

I think I can give a theoretical reason for that being so, and at the same time point out that there are two quite different reasons why diplogen compounds should differ from ordinary compounds.   One has already been mentioned the difference between the zero point energies.   The other is the difference which is a pure mass effect, due to the double mass of the diplogen in the water, and that affects the whole nature of the water in this quite simple way   The nature of the difference of the so-called polymers of the water is really determined by the orientation, by the regular or irregular arrangement of the molecules.†   The moment of inertia of the heavy water is about twice that of

* The photographs were taken and analysed by Miss H Megaw
† Bernal and Fowler, 'J Chem. Phys ,' vol I, p 55 (1933)

ordinary water, and therefore it is in general a slower rotator, so that at the same temperature heavy water should be more ice-like , that is, its co-ordination number should be lower, giving it a larger volume   That is what you get in the actual waters , you do get a larger volume for the heavy water On the other hand, with ice, where the rotation is completely suppressed and all the atoms are in regular positions—suppressed, that is, but for a small number of rotators to account for the large dielectric constant—you get a smaller volume

All the properties of heavy water fit in with this hypothesis   The most interesting is the relation of surface tension and viscosity   The viscosity of heavy water is definitely 30% to 50% larger than that of ordinary water, whereas the surface tension of heavy water is actually only 0 8 of the surface tension of ordinary water   Here you have two phenomena both associated with polymerization and going in different directions   The abnormally large viscosity of heavy water is not a translatory but a rotary viscosity   The ease with which an object can be moved through water depends on the degree of spontaneous rotation of the molecules   That will be small for heavy water and therefore you have higher viscosity   On the other hand, the surface tension of water depends on the force between the molecules and is not directly affected by the rotation and therefore you would expect it to be the same or somewhat smaller for heavy water   It is possible to construct a theory for these effects, but I cannot go into it here

The differences due to this mass effect will be very apparent in certain compounds where the other effect may not be so noticeable, and particularly where the possibility of the mobility of the hydrogen ion is concerned, especially in acids   I think the general theory of the mobility of the hydrogen ion depends, at any rate in the form of which Professor R H Fowler and I have worked it out, very much on the mass, and the difference in mobility shown by the hydrogen ion is about 50% greater than could be accounted for by a normal viscosity effect

Dr W JEVONS   Spectroscopic investigations in connection with the hydrogen isotope have not been reviewed in this discussion, beyond Lord Rutherford's opening remarks on Urey, Brickwedde and Murphy's original observation and measurement of the weak Balmer lines of D (*i e*, H²) which accompanied the much stronger corresponding lines of H (*i.e.*, H¹), and Hertz's conspicuous success in obtaining D in such a high state of purity that the line spectrum showed no trace of the Balmer lines of H and the molecular spectrum

consisted of band-lines of D_2 with no trace of those of H_2 and DH. I therefore venture to draw attention to the significance of the spectroscopic results so far secured

These measurements of the Balmer lines of D, and Ballard and White's subsequent measurement of six lines of the Lyman ultra-violet series of D, constitute the only examples of an observed electronic isotopic effect which is given directly by Bohr's well-known expression for the Rydberg constant for one-electron atoms, H, He$^+$, Li$^{+\,\prime}$, Be^{+++},   (For atoms with two or three electrons, such as Li$^\prime$ and Li, the observed isotopic effects are, of course, less simple in theory, the theory has been given by Hughes and Eckart)

Turning now to band-spectra of diatomic molecules we have so far records of the H isotope effect in three well-known band systems of HCl, H_2 and OH —

(i) It is now well known that in the infra-red HCl absorption band near $\lambda 3 46 \mu$ each strong line of the more abundant molecule HCl^{35} has, on the low-frequency side of it, a weaker line of the less abundant molecule HCl^{37}, that is to say there are two overlapping bands arising from the Cl isotope effect Hardy, Barker and Dennison have observed near $\lambda 4 8 \mu$ the corresponding pair of bands due to DCl, with a similar duplex structure arising from the Cl isotope effect, no less than 19 lines of the molecule DCl^{35} and 17 lines of the rarer molecule DCl^{37} being measured   The vibrational displacement is very large (DCl − HCl, $\delta\nu = -805$ cm^{-1}), the coefficient $\rho = 1$ being very much greater than for any other observed isotope effect   The deduced mass ratio is H D · 1 00778 2 0137, in close agreement with the mass spectrograph determination made earlier by Bainbridge, namely, 1 00778 2 01363 (on the chemical scale O = 16)   The estimated abundance ratio H D = 35000 1, has been superseded by Bleakney and Gould's result, 5000 1   The ratio 6000 1 quoted by Lord Rutherford is presumably a still later and closer estimate

(ii) Using a gas mixture consisting of about 25% of H_2, 50% of DH and 25% of D_2, Miss M Ashley and Professor G N Lewis have obtained 21-foot grating spectrograms, and identified and measured several hundreds of new lines   Many of these lines have been arranged into P, Q and R branches of DH and D_2 bands which correspond to the α bands ($3p\ ^2\Pi \to 2s\ ^2\Sigma$) of H_2 The large isotopic displacements observed are in satisfactory agreement with those calculated from H_2 data, and include, not only the usual vibrational and rotational displacements, but also very considerable electronic displacements, the latter amounting to as much as 2 4 cm^{-1} for DH — H_2 Alternating line intensities are observed in the bands of the homonuclear molecule D_2,

but not, of course, in those of the heteronuclear molecule DH The alternations in the D_2 bands are such that, without reasonable doubt, the spin quantum number for the D nucleus (diplon) is 1, which is twice that of the H nucleus (proton)

(iii) In the 0, 0 band of OH, $^2\Sigma \rightarrow {}^2\Pi$, at λ 3064 the hydrogen isotope effect has been reported, though somewhat tentatively, by Miss K Chamberlain and H B Cutter, who observed and measured several new lines in the positions computed for lines of the $^2R_{21}$ branch of the corresponding band of the isotopic molecule OD   This result is confirmed and greatly extended in a detailed investigation by Johnston and Dawson, who have identified and analysed large portions of the 0,1, 1,0 and 2 0 bands as well as the above branch of the 0,0 band   The observed displacements include pronounced isotope effects on the spin-doubling in the $^2\Pi$ state in addition to the larger vibrational and rotational displacements. It may reasonably be expected that this investigation will lead to a very exact value of the H D mass ratio, and also reveal yet unobserved isotope effects on the Λ-type doubling in the $^2\Pi$ state and the spin-doubling in the $^2\Sigma$ state

Lord RUTHERFORD, O M , F R S   I am sure you will all agree that we have had a most interesting meeting, and I regret that lack of time does not allow many speakers to contribute to our discussion   At the moment, only a few scientific men in the country have even a cubic centimetre of heavy water for experimental purposes   I hope this difficulty will soon be removed and that our industrial friends will help us to obtain supplies of the new water at a reasonable price   The cost of making the new water in places like Cambridge where the cost of power is high, is almost prohibitive   If a further discussion is held again, say, in six months' time, new information is likely to be available on the biological as well as on the chemical physical side

Before closing the discussion, I am sure you would like me to say a word on the points raised by Professor Soddy in his communication   As you all know, Professor Soddy was the discoverer of isotopes in the radioactive bodies and coined this name because the radioactive elements appeared to occupy the same place in the periodic table, and to be inseparable by chemical methods Much water has flowed under the bridge since he made that discovery and we now speak of the isotopes of an element not as inseparable bodies but as consisting of atoms which have the same nuclear charge but different masses   I think no one will doubt that heavy hydrogen has the same nuclear charge as hydrogen with one electron circulating round the nucleus, and from this point

of view is properly to be regarded as an isotope of hydrogen   I, of course,
quite understand the reason of Professor Soddy's difficulties   The name
isotope was first applied to atoms of the heavy radioactive elements differing
only slightly in mass, chemically indistinguishable and very difficult to separate
even by diffusion   The name is now given to the atoms of heavy hydrogen
which can be readily separated from ordinary hydrogen and shows some very
distinctive properties   This contrast is due to the fact that in hydrogen the
masses of the isotopes vary in the ratio of 1 to 2, and are thus readily separated by
diffusion or by processes like electrolysis where the mass plays a large part
Even the radioactive isotopes could be partially separated by diffusion methods
but owing to the small difference in their masses the process would be a slow and
tedious one

I hope that I have been able to convince Professor Soddy that in using the
word isotope for heavy hydrogen we are not contradicting the essential ideas
involved in his first use of the word

The Kelvin-Poincaré Problem of Stellar Evolution

By V V NARLIKAR, formerly Isaac Newton Student at Cambridge, Professor
at the Hindu University, Benares

On Dynamical Evolution

By Sir JOSEPH LARMOR F R S

Summary

The evolution of a rotating liquid mass with an assigned angular momentum
about a central axis has been sketched by Poincaré in his celebrated memoir
on a rotating liquid mass (Acta Math," 1885) The liquid continually
contracts so as not to violate the principle of degradation of mechanical energy
which we take for the criterion of the trend of evolution For the sake of
mathematical simplicity we make the assumption that the contraction permits
the liquid to be always homogeneous. Initially a sphere with a "small"
angular velocity about a diameter, the liquid mass acquires greater and greater
velocity as it contracts with constant momentum and passes through the stable

Maclaurin and Jacobian forms. This is the order up to the critical Jacobian ellipsoid, if for conserved momentum the total mechanical energy becomes continually smaller so that the principle of degradation of energy is not contradicted. The next type in the succession, a pear-shaped figure, is unstable, and so it is presumed that a cataclysm involving tumultuous change sets in at this stage. In view of the slowness of the evolution it is perhaps to be expected that the cataclysm would be smooth in its earlier stages. We examine the general features of these earlier stages and show that contraction subject to degradation of energy permits the Darwin-Poincaré pyriform solution, unlike that of Jeans. The former seems to have been found to be stable while the latter, the more developed pear, has been shown by Jeans to be unstable. Without discussing the cataclysm further, we pass next to a series of double-figure configurations (both components spherical), which is characterized by two parameters, λ the mass-ratio and r the separating distance. In the diagram of the course of evolution which summarizes the investigation all the configurations are brought in. If the cataclysm ends in such a smooth state of fission, we must have $\lambda < \frac{1}{2} \cdot 4$ which is in keeping with the observation of double stars. As regards the earlier stages, the Maclaurin spheroid shrinks in every direction, but not the Jacobian ellipsoid.

1 Introduction

The historically famous problem of gravitating liquid masses is discussed here from a point of view which has not received due attention, as Lord Kelvin published a brief statement of results, without proof *. As discussed here the problem is this : given a mass M of a homogeneous liquid rotating uniformly like a rigid body, with a fixed angular momentum μ, what will be its course of evolution, if it slowly contracts so as always to remain homogeneous ? Owing to the recent progress of astrophysics the interest in this form of the problem is now mainly historical. Nevertheless, there is a good reason for presenting these considerations, as Sir George Darwin, who had this problem in view, had to leave it undiscussed ; for the question of the stability of the pear-shaped figure still needed attention when he died, and when the last word was said in this connection, the interest in the problem of evolution had evaporated.

There is also another reason, equally good. The current idea about the origin of the binaries is essentially that held by Darwin and Poincaré †. But

there does not seem to be on record a model of evolution, in conformity with the old or the new ideas of astrophysics, which would support this current view, or otherwise It may therefore be worth while developing fully the Kelvin-Poincaré stellar model

2 An Account of several Successions of Figures of Equilibrium.

Let us take a rectangular set of axes O-xyz fixed in space. O is the centre of a homogeneous liquid sphere of mass M, radius a_0 and density ρ_0 Let a spin ω_0 be given about the axis OZ, being small enough for a spheroidal form to be possible We will suppose that the mass is contracting, owing to cooling, and that the contraction is so slow that whatever form the mass assumes it is always homogeneous As the system remains isolated, the angular momentum μ as well as the mass M must remain constant Throughout this paper the liquid will be supposed to be homogeneous We will consider a succession of figures of equilibrium all of which have the same mass M and angular momentum μ When tables are constructed for the densities, angular velocities, etc , corresponding to these figures, it should be possible to derive a sequence of configurations characterizing the course of evolution With this end in view we proceed to explore the three well-known types of configurations, the Maclaurin spheroid, the Jacobian ellipsoid, and the binary configuration

2 (a) The Maclaurin Spheroid

Consider a typical Maclaurin spheroid with semi-axes a, a, c, density ρ and angular velocity ω Let

$$c = a \cos \gamma, \quad \frac{\omega^2}{2\pi\rho} = \chi, \quad e = \sin \gamma \tag{1}$$

Here e is the eccentricity of the spheroid , χ and γ are parameters connected by the relation[*]

$$\chi = \cot \gamma \left[\gamma \left(3 + \cot^2 \gamma \right) - 3 \cot \gamma \right]$$

For the mass and the angular momentum we have

$$M = \frac{4}{3} \pi a^3 \rho \cos \gamma, \quad \mu = \frac{2}{5} M a^2 \omega \tag{2}$$

Solving (1) and (2) for a, ω, and ρ we obtain

$$a = \frac{25}{6} \frac{\mu^2}{M^3} \frac{\cos \gamma}{\chi}, \quad \omega = \frac{18}{125} \frac{M^5}{\mu^3} \left(\frac{\chi}{\cos \gamma} \right)^2, \quad \rho = \frac{2}{5^4 \pi} \frac{3^4}{\mu^6} \frac{M^{10}}{\mu^6} \frac{\chi^3}{\cos^4 \gamma}$$

* Thomson and Tait, vol. 2, p 771 (1883)

The kinetic energy is

$$T = \frac{1}{2}\,\mu\omega = \frac{9}{125}\,\frac{M^5}{\mu^2}\left(\frac{\chi}{\cos\gamma}\right)^2$$

The potential energy is

$$W = -\frac{4}{5}\,\pi a^2 \rho M = -\frac{18}{125}\,\frac{M^5}{\mu^2}\,\frac{\gamma\chi}{\sin\gamma\cos\gamma}$$

We will denote the expressions

$$\left(\frac{\chi}{\cos\gamma}\right)^2 \qquad \frac{\gamma\chi}{\sin\gamma\cos\gamma} \qquad \frac{9}{125}\,\frac{M^5}{\mu^2}\,,$$

by the symbols η, ϵ, and A respectively The total energy E is then A $(\eta - 2\epsilon)$ There is one and only one Maclaurin spheroid corresponding to each value of γ, subject to the inequalities $0 < \gamma < \frac{1}{2}\pi$ Taking typical values of γ in this region the quantities a, ϵ, ω, ρ, T, W, and E are now calculated and the results are set out in Tables I (a), I (b), and IV (a).

It does not appear that the total energy E has been tabulated up till now, and it is an affair of some trouble, a column for momentum can readily be added to the tables, as it is equal to Iω, while T is $\frac{1}{2}$Iω^2, thus E can be graphed against density ρ subject to μ constant, and the evolution is towards diminishing E on this graph.

2 (b) The Jacobian Ellipsoid *

The semi-axes of a Jacobian ellipsoid may be expressed as a, $b = a\cos\beta$, $c = a\cos\gamma$, β and γ being subject to $0 < \frac{1}{2}\pi$, also $54°\ 21'\ 27'' < \gamma < \frac{1}{2}\pi$ A Jacobian ellipsoid does not exist for $\gamma < 54°\ 21'\ 27''$ β and γ are connected by the relation

$$\sin^2\gamma\cos^2\gamma\int_0^\gamma \frac{\tan^2\phi}{(1-\kappa^2\sin^2\phi)^{3/2}}\,d\phi = \cos^2\beta\int_0^\gamma \frac{\sin^4\phi}{(1-\kappa^2\sin^2\phi)^{3/2}}\,d\phi,$$

where κ is defined by $\sin\beta = \kappa\sin\gamma$

For the Jacobian ellipsoid to be determinate there must be a relation between χ, β, and γ It is

$$\frac{\omega^2}{4\pi\rho} = \frac{1}{2}\chi = \cot\beta\cot\gamma\csc^2\beta\,(1+\cos^2\beta)\,(F-E)$$
$$-\frac{\kappa^2}{\kappa'^2}\,E\cot^2\beta\cot\gamma\csc\beta + \frac{\cot^2\beta\cot^2\gamma}{\kappa'^2},$$

where $\kappa'^2 = 1 - \kappa^2$ while

$$E = \int_0^\gamma (1-\kappa^2\sin^2\phi)^{\frac{1}{2}}\,d\phi \quad \text{and} \quad F = \int_0^\gamma (1-\kappa^2\sin^2\phi)^{-\frac{1}{2}}\,d\phi.$$

* Sir G H Darwin 'Collected Papers,' vol 3, p 123

Since the mass M and the angular momentum μ are assigned we may write

$$M = \frac{4}{3}\pi a^2 \rho \cos\beta \cos\gamma, \qquad \mu = \frac{M}{5} a^2(1 + \cos^2\beta)\,\omega,$$

and solving these for a, ω, ρ,

$$a = \left\{\frac{5\mu}{M(1+\cos^2\beta)}\right\}^{\frac{1}{2}} \frac{2\cos\beta\cos\gamma}{3M_f}, \qquad \omega = \left\{\frac{3M\chi}{2\cos\beta\cos\gamma}\right\}^{\frac{3}{2}}\left[\frac{H(1+\cos^2\beta)}{5\mu}\right]^{\frac{3}{2}},$$

$$\rho = \frac{2}{5^3\pi}\frac{3^4}{\mu^6}\frac{M^{10}}{\mu^6}\left[\left(\frac{\chi}{\cos\beta\cos\gamma}\right)^4 \frac{1}{\chi}\left(\frac{1+\cos^2\beta}{2}\right)^6\right],$$

$$T - A\left[\frac{(1+\cos^2\beta)^2}{8}\left(\frac{\chi}{\cos\beta\cos\gamma}\right)^2\right],$$

$$W = -1\left[\frac{(1+\cos^2\beta)^2}{4}\frac{2F\chi}{\sin\gamma\cos\gamma\cos\beta}\right]$$

Defining η and ε by $T = A\eta$ and $W = -2A\varepsilon$, we have $E = A(\eta - 2\varepsilon)$
Choosing typical values of γ, the quantities a, ω, ρ, etc , are calculated for the
corresponding ellipsoids and Tables II and IV (b) are constructed *

2 (c) The Binary Configuration

The mass M is supposed to be separated into two detached portions M_1
and M_2 rotating like one connected rigid body It is convenient to express
M_1 and M_2 in the forms $\dfrac{M\lambda}{1+\lambda}$ and $\dfrac{M}{1+\lambda}$ respectively $(\lambda \gg 1)$ Let ρ be the
density, the masses being so far apart that they may be regarded as spherical,
with radii a_1 and a_2 and r the distance between the centres As the spheres
rotate and revolve with the same angular velocity ω

$$\frac{M}{r^2} = \omega^2 = 2\pi\rho\chi,$$

$$a_1^2 = \frac{3M\lambda}{4\pi\rho(1+\lambda)}, \qquad a_2^2 = \frac{3M}{4\pi\rho(1+\lambda)}, \qquad \mu = M^{5/3}\omega^{-1/3}\zeta,$$

where

$$\zeta = \frac{2}{5(1+\lambda)^{5/3}}\left[\chi^{5/3}\left(\frac{3}{2}\right)^{5/3}(1+\lambda^{5/3})(1+\lambda)^{1/3} + \frac{5}{2}\lambda\right],$$

$$T = \frac{M^2}{2\mu^2}\zeta^2,$$

$$W = -\frac{4}{5}\pi a_1^2\rho M_1 - \frac{4}{5}\pi a_2^2\rho M_2 - \frac{M_1 M_2}{r}$$

$$= -\frac{M^{5/3}}{\mu^2}[f_1(\lambda) + \chi^{1/2}f_2(\lambda)],$$

---

* The values of F and E needed to complete these computations were taken from Table
IX of the second volume of Legendre's "Traite des Fonctions Elliptiques."

where

$$f_1(\lambda) = \frac{\lambda}{(1+\lambda)^2} \quad \text{and} \quad f_2(\lambda) = \frac{2}{5}\left(\frac{3}{2}\right)^{2/3} \frac{1+\lambda^{5/3}}{(1+\lambda)^{5/3}}$$

It is clear that χ must be very small for the masses to be nearly spherical under their mutual attraction. An upper limit on χ is obtained, taking into account the liability to tidal disruption and partial secular instability. Let us put $r = a\psi$ where a is given by $\frac{3M}{4\pi\rho} = a^3$. Since $\frac{M}{r^3} = \frac{M}{a^3\psi^3} = \omega^2$ we have $\omega^2\psi^3 = \frac{4}{3}\pi\rho$ or $\chi = \frac{2}{3\psi^3}$. For the reasons given by Jeans* $\psi \leq 2.5$ roughly. Thus $\chi \leq 10^{-2} \times 4.268$, say, χ_0.

A rotating mass cannot break up into two spheres unless χ is less than χ_0.

According to the notation followed so far we may write

$$T = A\eta \quad \text{and} \quad W = -2A\varepsilon,$$

where

$$\eta = \frac{125}{18}\zeta^3 \quad \text{and} \quad \varepsilon = \frac{125}{18}\zeta^2[f_1(\lambda) + \lambda^{4/3}f_2(\lambda)]$$

Let us put

$$B = \frac{M^{10}}{\mu^6}\frac{2.3^4}{5^4\pi}, \quad D = \frac{50}{3}\frac{\mu^2}{M^5}$$

Then the numerical values given in the tables for energy, density, and length are A^{-1}, B^{-1}, D^{-1} times their actual values respectively. The binary configurations are characterized by two independent parameters λ and χ subject to the conditions $\lambda \gg 1$, $\chi > \chi_0$. For $\chi = \chi_0$ and some values of $\lambda > 1$, Table III is constructed.

3. The Kelvin-Poincaré Evolution

Fig 1, in which the total energy with its sign changed, i.e., $-E$, is plotted against χ, is the diagram of the gradual succession of configurations as χ increases, but the actual evolution is as infra. The course of evolution starts at O, marches along the thick line OA until it is diverted at A to pursue the other thick line up to E. At this point a cataclysm begins to develop which ultimately comes to an end in the neighbourhood of the binary configuration P that has nearly the same energy for the same μ and ρ. The details are as follows.

The line OABCD represents the Maclaurin spheroids. The thick line OA represents the secularly stable spheroids; AC are secularly stable if the figures

are constrained to be figures of revolution, and C is the limit due to Bryan*
who showed that the range CD are not "ordinarily" stable   Incidentally,
A is the critical spheroid from which the ellipsoidal series starts   The thick
line AE represents the succession of secularly stable ellipsoids, the other
Jacobian ellipsoids being stable only if constrained to remain ellipsoidal
From E branches off the "pear-shaped" series which, however, is not shown in

Fig 1

the diagram as these figures are unstable   Although very little is known of
the cataclysm that starts at the stage E the binary configuration is considered
to be its outcome   We have therefore inserted in the diagram discrete binary
configurations as represented by the thick dotted lines.   The central feature
of the evolution is the principle of degradation of energy.

* 'Phil. Trans.,' A, vol 190, p. 187 (1887)

It is natural to expect that in the initial smooth stages of the cataclysm the pear-shaped figure, although unstable, may develop   The following independent analysis, however, indicates that Jeans' figure, unlike the less-developed Darwin-Poincaré " pear," has no place in the evolution

Since the liquid is not supposed to have become turbulent in such early stages we may consider the density ρ, the total energy E, and the angular momentum μ to be the same for the critical ellipsoid and the initial forms of the changing pear   In our notation

$$T + W = E, \quad 2T = \mu\omega, \quad \omega^2 = 2\pi\rho\gamma, \quad I\omega = \mu,$$

I being the moment of inertia about the axis of rotation   By logarithmic differentiation we obtain for constant μ, if ρ be unchanged,

$$2 \frac{dI}{I} + \frac{d\chi}{\chi} = 0$$

But this is not satisfied by the Jeans' pear (*loc cit*, p 101) for which

$$\frac{d\chi}{\chi} = 0\ 05227\ e^3, \quad \frac{dI}{I} = -\ 0\ 09378\ e^3,$$

where e is a small parameter, so that it is not in the evolutionary succession

This shows that the pear-shaped forms cannot arise in the early smooth stages of the cataclysmic transitions unless perhaps some of the implied restrictions relating to constancy of μ, and E are removed   We may examine whether the density slightly increases   Let then the density of the ' pear " be $\rho + d\rho$, ρ being that of the critical ellipsoid   The total mass and the form of the figure remaining the same, the moment of inertia $I + dI$ is replaced by

$$(I + dI)\left(1 - \frac{2}{3}\frac{d\rho}{\rho}\right) \text{ which is } I + dI - \frac{2}{3}\frac{I}{\rho}d\rho, \text{ to the first order   We have}$$

from the conservation of angular momentum

$$I\omega = \left(I + dI - \frac{2}{3}\frac{I}{\rho}d\rho\right)(\omega + d\omega),$$

giving

$$\frac{dI}{I} + \frac{d\omega}{\omega} = \frac{2}{3}\frac{d\rho}{\rho}$$

Also as

$$\omega^2 = 2\pi\rho\chi, \quad \frac{d\rho}{\rho} = 2\frac{d\omega}{\omega} - \frac{d\chi}{\chi}.$$

Thus

$$\frac{1}{3}\frac{d\rho}{\rho} = 2\frac{dI}{I} + \frac{d\chi}{\chi},$$

so that for Jeans' pear $d\rho/\rho = -0.40587e^2$, which means expansion On the other hand, the formation of the Darwin-Poincaré pear* demands contraction, which is more natural, since for the latter

$$\frac{d\mathcal{A}}{\gamma} = -0.144306\, e^2, \quad \frac{d\Pi}{I} = 0.157786e^2,$$

and hence

$$\frac{d\rho}{\rho} = 0.513798\, e^2$$

If the cataclysm carries over the quantities E, ρ, and μ all practically unchanged from the critical ellipsoid, the binary configuration P is reached The ratio of masses of the pair of bodies corresponding to P is 3.37 The dotted curves in fig 1 are the equi-density curves, the one passing through P corresponding to the density of the critical ellipsoid In view of the principle of the degradation of energy, the conclusion seems inevitable that the ratio of masses (λ) after fission in this model of evolution cannot exceed 3.4 Thus, by the way, is remarkably in agreement with observation for double stars

Lastly, consider the process of contraction geometrically if the contraction is due to cooling of the fluid it might perhaps be expected to proceed uniformly in all directions , then every figure should be wholly within the space occupied by the preceding, instead of bulging in parts Consider first the spheroids

Let r be the radius vector to the surface of a Maclaurin spheroid, drawn from the centre, making an angle θ with the plane of the equator Then we have

$$\frac{1}{r^2} = \frac{\cos^2\theta}{a^2} + \frac{\sin^2\theta}{c^2}$$

The contraction δr in the direction (θ) as the matter passes to the consecutive stage is given in terms of the principal contractions δa, δc by

$$\frac{\delta r}{r^3} = \frac{\delta a \cos^2\theta}{a^3} + \frac{\delta c \sin^2\theta}{c^3}.$$

Since

$$a = p\,\frac{\cos\gamma}{\gamma}, \quad c = p\,\frac{\cos^2\gamma}{\gamma},$$

where p is a constant,

$$-\frac{\delta a}{a^2} = \frac{1}{p^2}\,\frac{\gamma\sin\gamma\,\delta\gamma + \cos\gamma\,\delta\chi}{\cos^2\gamma}\,\chi, \qquad \frac{\delta c}{c^3} = \frac{1}{p^2}\,\frac{2\chi\sin\gamma\,\delta\gamma + \cos\gamma\,\delta\chi}{\cos^3\gamma}\,\chi$$

It can be shown from Tables I (a) and I (b) that $d\chi/d\gamma > 0$ from $e = 0$ to

* Darwin, loc cit., p. 380

$e = 0\ 93$ Hence up to this point $-\dfrac{\delta a}{a^3} < \dfrac{\delta c}{c^3}$ Also $\dfrac{d}{d\theta}(\delta r) = 0$ when $\theta = 0$ and $\tfrac12 \pi$ This shows that the minimum contraction is in the equatorial plane and that its value is $\delta a/a^3$ The maximum expansion is along the axis of rotation and its value is $\delta c/c^3$ δa and δc have been shown to be positive later on All this is quite in keeping with the cooling hypothesis, for the heat generated inside the surface will be conducted more rapidly in the direction of the shortest radius vector, and the subsequent radiation and cooling would produce the maximum contraction in this direction

Table I (a) — Maclaurin Spheroids

$e = \sin\gamma$	$\chi = \dfrac{\omega^2}{2\pi\rho}$	ρ	$T = \eta$	ϵ	$\tfrac14 W$	$2\epsilon - \eta = -E$
0 1	$10^{-2} \times 2\ 361$	$10^{-4} \times 1\ 34$	$10^{-6} \times 3\ 63$	$10^{-3} \times 2\ 37$		$10^{-1} \times 4\ 7$
0 15	$10^{-2} \times 5\ 253$	$10^{-4} \times 2\ 86$	$10^{-5} \times 4\ 00$	$10^{-3} \times 6\ 34$		$10^{-2} \times 1\ 26$
0 2	$10^{-2}\ 1\ 169$	$10^{-4} \times 1\ 69$	$10^{-4} \times 1\ 40$	$10^{-3} \times 1\ 19$		$10^{-2} \times 2\ 37$
0 25	$10^{-2} \times 1\ 589$	$10^{4} \times 5\ 75$	$10^{-4}\ 2\ 69$	$10^{-3} \times 1\ 65$		$10^{-3} \times 3\ 29$
0 3	$10^{-2} \times 2\ 43$	$10^{-4} \times 1\ 73$	$10^{-4}\ 6\ 47$	$10^{-3} \times 2\ 588$		$10^{-3} \times 5\ 111$
0 35	$10^{-3} \times 3\ 516$	$10^{-3} \times 4\ 73$	$10^{-3}\ 1\ 25$	$10^{-3} \times 3\ 61$		$10^{-4} \times 7\ 11$
0 4	$10^{-3} \times 4\ 356$	$10^{-3} \times 1\ 17$	$10^{-3}\ 2\ 25$	$10^{-3} \times 4\ 59$		$10^{-2} \times 9\ 56$
0 5	$10^{-2}\ 6\ 90$	$10^{-4} \times 5\ 84$	$10^{-3}\ 6\ 34$	$10^{-3} \times 8\ 37$		$1\ 61$
0 6	$10^{-1}\ 1\ 007$	$10^{-3} \times 2\ 49$	$10^{-2}\ 1\ 58$	$10^{-1} \times 1\ 35$		$10^{-1} \times 2\ 54$
0 7	$10^{-1} \times 1\ 387$	$10^{-3} \times 1\ 027$	$10^{-2}\ 3\ 77$	$10^{-1} \times 2\ 15$		$10^{-1} \times 3\ 93$
0 75	$10^{-1} \times 1\ 597$	$10^{-2}\ 2\ 13$	$10^{-2}\ 5\ 83$	$10^{-1} \times 2\ 73$		$10^{-1} \times 4\ 88$
0 8	$10^{-1} \times 1\ 812$	$10^{-2}\ 4\ 58$	$10^{-2}\ 9\ 117$	$10^{-3} \times 3\ 499$		$10^{-1} \times 6\ 088$

Table I (b) — Maclaurin Spheroids

$e = \sin\gamma$	$\chi = \dfrac{\omega^2}{2\pi\rho}$	ρ	$T = \eta$	$\epsilon - \tfrac14 W$		$2\epsilon - \eta = -E$
0 81	0 18597	$10^{-2} \times 5\ 43$	0 1005	0 3696		0 6387
0 81267*	0 18712	$10^{-2} \times 5\ 678$	0 1031	0 3748		0 6465
0 82	0 19039	$10^{-2} \times 6\ 42$	0 1103	0 3808		0 6690
0 85	0 2029	0 1085	0 1484	0 4602		0 7721
0 9	0 2203	0 396	0 2556	0 6290		1 0024
0 91	0 2225	0 372	0 2880	0 6740		1 0600
0 92	0 2241	0 477	0 3275	0 7225		1 1175
0 93	0 2247	0 591	0 3736	0 7857		1 1974
0 94	0 2239	0 827	0 4307	0 8530		1 2737
0 95	0 2211	1 139	0 5021	0 9340		1 3659
0 96	0 2160	1 636	0 5945	1 032		1 4685
0 97	0 2063	2 518	0 7300	1 158		1 5961
0 98	0 1890	4 396	0 9012	1 323		1 7447
0 99	0 1551	9 44	1 21	1 587		1 9650
1	0	∞	$\left(\dfrac{\pi^2}{4}=\right)2\ 435$	$\left(\dfrac{\pi^2}{4}=\right)2\ 435$		$\left(\dfrac{\pi^2}{4}=\right)2\ 435$

* Critical spheroid

Table II —Jacobian Ellipsoids

ε=sin γ	γ	β	$\chi = \dfrac{\omega^2}{2\pi\rho}$	μ	T = η	$\dfrac{\epsilon}{-\frac{1}{4}W}$	$\dfrac{2\epsilon - \eta}{-E}$
	° ′ ″	° ′ ″					
0 81287	54 21 27	0 0 0	0 18712	10⁻⁵ × 5 678	0 1031	0 3748	0 6465
0 81915	55 0 0	14 15 0	0 187	10⁻⁵ > 5 6906	0 10315	0 3751	0 6471
0 8388	57 0 0	28 30 0	0 186	10⁻⁵ × 5 935	0 1052	0 3798	0 6545
0 866	60 0 0	40 54 0	0 18120	10⁻⁵ ≠ 6 858	0 1115	0 3964	0 6814
0 9054	65 0 0	54 46 0	0 16590	10⁻¹ × 1 133	0 1271	0 4599	0 7828
0 93850*	69 49 0	64 2? 30	0 14200	0 25?	0 18946	0 5817	0 9739
0 9397	70 0 0	64 4? 0	0 14094	0 2646	0 1932	0 5900	0 9868
0 9659	75 0 0	72 36 0	0 1072	0 9	0 3105	0 855	1 3605
0 984	80 0 0	79 10 0	0 06614	4 499	0 5601	1 564	2 7589
0 9962	85 0 0	84 52 0	0 025860	76 45	1 404	2 633	3 862
1	90 0 0	90 0 0	0	∞	∞	∞	∞

* Critical ellipsoid

Table III —Double Figure Configurations

$$\lambda = \chi_0$$

λ	ρ	1 - η	ε	$2\epsilon - \eta = -E$
1	0 699	0 1608	0 6080	1 228
2	0 3913	0 1292	0 6046	1 08
3	0 183	10⁻² × 8 834	0 4780	0 8688
4	0 093	10 ² × 6 297	0 3915	0 7200
5	0 05108	10 ² × 4 709	0 3287	0 6103
6	0 03188	10⁻² × 3 861	0 2841	0 5297
7	0 02088	10 ² × 2 985	0 2490	0 4681
8	0 0145	10 ² × 2 487	0 2226	0 4204
9	0 01055	10⁻² × 2 212	0 2018	0 3824
10	0 007951	10⁻¹ × 1 842	0 1848	0 3512
100	10⁻⁴ × 1 678	10 ¹ × 2 675	10 ¹ × 5 458	0 1065
1000	10⁻⁵ × 8 374	10⁻² × 1 899	10⁻³ × 4 867	0 08545
∞	10⁻⁵ × 7 771	10⁻³ × 1 82	10⁻³ × 4 286	0 08351

In the preceding we took for granted that δa, δc, the contractions in a, c respectively, are positive Table IV (a) shows that this is actually so Table IV (b) for the axes of ellipsoids shows that b and c decrease so that b/c tends to unity as the material contracts On the other hand, a gradually increases from 0 7785 to 0 845 and then decreases to nothing Such a gradual increase and decrease might tend to produce heterogeneity, but we suppose that there is time for the densities to be equalized

Lastly, I should like to express my thanks to Sir J Larmor, who pointed out the historical interest of the problem and made many valuable suggestions and criticisms while this work was being carried out

Table IV (a) —Maclaurin Spheroids

e	a = b	c	e	c' = b	c
0 1	105 3	105	0 81267	0 7785	0 4536
0 15	39 54	39 05	0 85	0 649	0 3419
0 2	21 11	20 65	0 9	0 4946	0 2260
0 25	15 23	14 71	0 91	0 4657	0 1931
0 3	9 81	9 37	0 92	0 4368	0 1713
0 35	7 02	6 61	0 93	0 409	0 150
0 4	5 36	4 82	0 14	0 3811	0 130
0 5	3 14	2 72	0 95	0 3528	0 1077
0 6	1 99	1 59	0 96	0 3243	0 09084
0 7	1 36	0 92	0 97	0 2945	0 07155
0 75	1 04	0 684	0 98	0 2633	0 05244
0 8	0 8280	0 4968	0 99	0 2272	0 03305
0 81	0 7887	0 4623	1	0 1462	0

Table IV (b) —Jacobian Ellipsoids

$r = \sin \gamma$	$r' = \sin \beta$	$e'' = \sqrt{\dfrac{b^2 - c^2}{b}}$	a	b	c
0 81267*	0	0 81267	0 7785	0 7785	0 4536
0 819	0 246	0 806	0 7905	0 766	0 4534
0 839	0 478	0 784	0 819	0 720	0 446
0 8660	0 6547	0 7500	0 845	0 638	0 432
0 9063	0 8168	0 6807	0 827	0 477	0 349
0 93859†	0 90183	0 6024	0 7454	0 3221	0 2572
0 9397	0 9042	0 5991	0 7369	0 3190	0 253
0 9659	0 9542	0 5014	0 6077	0 1817	0 1578
0 9843	0 9822	0 3822	0 4806	0 0886	0 080
0 9962	0 9960	0 2313	0 2970	0 02058	0 02589
1	1	0	0	0	0

* Critical spheroid   † Critical ellipsoid

Addition   December 18, 1933

"On Astronomical Evolution by Dissipation of Dynamical Energy"

By Sir Joseph Larmor

The object of the analysis in this paper, as stated in the beginning, is to set out in more systematically developed view the Kelvin succession of events in his historical problem, and especially to illustrate the general theory of dynamical evolution. For the dynamics of the planetary system, now so accurately developed, is concerned with the residual cyclic motions, which persist after non-cyclic features have been smoothed away in course of ages

by frictional forces, tidal, and other influences   In the present illustration it
is the trend of an energy-diagram that determines the course of the evolution

In a material system in pure dynamics the variables are a set of co-ordinates
typified by q with their component velocities q and momenta p which are
$\partial T/\partial q$ Here T is the kinetic energy which is a function of the variables q
with coefficients functions of q there is a potential energy W so that $T + W$
is total energy which as was known in early days, is conserved in an isolated
frictionless system   But of these variables there may be a set of co-ordinates
of type ψ which do not appear in the expressions for T and W with velocities ψ
and momenta $\partial T/\partial \psi$ or Ψ These momenta are conserved being cyclic in
type, and the velocities related to them can be eliminated from T by means of
the set of equations $\partial T/\partial \psi$ Ψ' The Lagrangian generalized dynamics, as
developed into cyclic co-ordinates by Routh Kelvin, and Helmholtz replaces
the Lagrangian function $L = T - W$ by a modified function L' which is
$\tau_2 + \tau_1 + \tau_0$ where the terms are of the second degree, first degree, and degree
null, in the remaining velocities of type q, with coefficients involving the q and
also the Ψ which are now constants of the motion   The equations of motion
are then of the form

$$\frac{d}{dt}\left(\frac{\partial L'}{\partial q}\right)\quad \frac{\partial L'}{\partial q}\quad F_q,$$

where F_q is the extraneous force, in addition to the force involved in W, acting
on the co-ordinate q The time-rate of gain of energy of the system is $\Sigma F_q q$
which works out into the complete differential expression dE/dt where
$E = \tau_2 - \tau_0$, in which the first order terms τ_1 which alone would change sign
on reversal of the motion even though the cyclic momenta have not been
reversed have disappeared   The expression L' is equal to $T - W - \Sigma \psi \partial T/\partial \psi$
in which the variables ψ have been eliminated by introducing the constants Ψ
instead of them   All the equations of motion are expressed from L' alone
and it might be hastily presumed that the course of evolution by dissipation
would depend on the change of the time-gradient of the effective Action, which
is L' But that is not so, although L' by its n equations determines the course
of motion completely   The energy that comes into the system is the change
in E, and it is E that is subject to dissipation within the system by frictional
agencies not involved in W Then the course of a steady evolution, as in the
discussion above is to be presented as one of continual fall of E subject to
conserved cyclic momenta   If the co-ordinates are cyclic so that q are not
involved in the energy the form of E is static varying with the co-ordinates q
alone, and the steady so-called secular states of the system are those for which

E is minimal   We can represent the course of this evolution graphically   Let the variables q represent Cartesian co-ordinates in a hyperplane of the same number of dimensions, and imagine an ordinate E drawn at each point of it A set of hypersurfaces each of constant energy E is obtained, and the bottom points represent the steady states of the system   The hypersurfaces of constant E will now take successive forms owing to change by internal dissipation, in simple cases changing an internal parameter   On this succession of hypersurfaces there will be continuous sets of lowest points which trace out curves of smooth evolution   the highest points and cols of saddle shape will represent unstable positions, impermanent but of change initially slow   It is very unlikely that two of these curves of evolution will meet and cross each other, unless there is one co-ordinate q, when the space is a plane with co-ordinates E, q A general principle was advanced by Poincaré on graphical grounds that when a curve of stability meets and crosses one of the other set of curves, those of slowly changing unstable forms, their condition as to stability interchanges, this is the normal course of crossing, for two curves of stability cannot come together unless by way of a curve of summits of the other kind which lies between them   The principle predicted that the pyriform figure is stable   but the result now seems to be accepted, after Jeans, that the pyriform states are initially unstable, in opposition to the Poincaré* criterion   This may be because a real crossing point is very seldom reached, as the number of independent variables for a fluid mass is not finite, for Poincaré himself appears to arrive at an infinite series of transitions (cf Lamb's account) by a Lamé analysis of the normal forms of vibration of the fluid mass   Thus the mode of lapse into static states is determined by a set of equations equal in number to the effective co-ordinates, of which the equation of energy is only one, yet one which is involved along with all the others in the Action Principle and its characteristic function L'   Our evolutionary criterion is far less complete, is merely one for the gradual rough trend of steady evolutionary states, without detail as to the transition which remains unexplored   This general criterion of trend, the only one there is, prescribes total energy falling away for conserved cyclic momenta

* Correction of Poincaré's original investigation (1885) was soon made by Schwarzschild in a discussion which is difficult of access   A very complete historical account was given at an early stage by H Lamb, 'Hydrodynamics,' ed 1895 and ed 1932, where he reproduces some numerical tables from Kelvin and Darwin which ought to agree with those worked out and applied above   There is an account by von Zeipel in the Poincaré Memorial Volume of "Acta Mathematica"   A formal treatise by L. Lichtenstein is announced which may provide closer detail

But the main point is to assert the essential limitation of most of these evolutionary discussions. The subject originated with W. Thomson's formulation of the Dissipation of Energy on the basis of the formal Carnot doctrine, at first without the illustrations from statistical atomic theory which made it so natural. He was soon deflected from the development of his thermodynamic doctrine of Available Energy by the obvious problems of dissipation presented on a vast scale by astronomical systems. If with Kelvin, and Helmholtz, and Waterston even earlier, the availability that is inevitably dissipated is taken to be in part the energy of gravitational collocation of the bodies concerned, a problem is presented of which a very striking analytical exemplification has been prepared gradually by the elegant mathematical work of Jacobi and Kelvin and Poincaré. But this criterion of dissipation confined to energy purely mechanical is only valid, on the Carnot-Kelvin doctrine, under limitation of the system to uniformity and constancy of temperature and of state during its evolution. If the state is liable to change but restricted to constant temperature, it is a different entity, Thomson's Available Energy as distinct from total energy, that is the subject of dissipation. If the temperature can change also, the formulation of a criterion is more complex. It is the special merit of the Clausius procedure by introduction of an Entropy inherent in the system- an offshoot from the Carnot-Kelvin temperature theory, which was later put into illustrative relation with the doctrine of probabilities of molecular states, and has now become a foundation postulate in its own right in these quantal days, specified as an assumed definite function of state and configuration and temperature for every system—that it has covered the ground in a more direct manner, because Entropy trends upward without limitation except such as arises from abstraction of the rather indefinite entity experienced as heat. Entropy may be transferred, but cannot diminish *as a whole.* Any precise definition of heat must indeed be by way of Entropy or of Available Energy. Thus for a gaseous star subject to its immense changes of temperature on shrinkage, the gravitational energy by itself has little to do with the secular course of evolution, except as the merest illustration. In the abstract hydrodynamical problem that fascinated Jacobi, Helmholtz, Poincaré, mainly on Kelvin's initiative, it is, however, reduced to an affair of structureless fluid, of unchanging density and therefore also unchanging temperature, so that as it happens the criterion of falling gravitational energy does apply, as indeed under such limitations it could not help doing. If these conditions were not satisfied, though abundance of types of nearly steady state might be worked out, and their ranges of dynamical stability marked,

there would be no practicable general criterion, so long as discussion by Entropy or Available Energy is unmanageable, of trend of change as in fact governed by dissipation of availability, to decide how far the crowd of possible solutions even belonged to the same linear evolutionary succession, except by presumptions derived from comparisons regarding the ordinary dynamical stabilities of the separate states that have been usually employed Following Poincaré it was commonly held that these questions, which belong really to a pure *topology* of the various linear series of steady secular states and the transitions where they meet, could be readily settled by a principle of exchange of stabilities , though it appears somewhat mysterious that a consideration of linear topological grouping alone should settle a definite dynamical stability where there may be many degrees of freedom involved, obvious or latent , indeed, for the special example now on hand, in the transition from the Jacobian to the pyriform secular figures, actual discrepancy appears to have been encountered A final remark may not be superfluous, that this doctrine of dissipation, which is wider than any atomic scheme, does not stand in any relation to the principle of Least Action, which belongs to reversible dynamics , though Boltzmann, Clausius, Burbury, and others at one period tried hard to connect it up with the foundations of the principle of Carnot.

The feature that has invited close attention to the special Kelvin problem of evolution is its asymmetric character Starting with the Maclaurin oblate spheroids, becoming more oblate as they lose energy (E) while momentum is conserved, the series continues as Jacobi ellipsoids with loss of the axial symmetry, and then, as is suggested, it passes on into lopsided forms, the pyriform bodies of Poincaré and Darwin, which may gradually develop a constriction and finally separate into two masses of the type of the actual double stars without that hint from the heavens such irregular forms might hardly have been thought of as arising in the course of evolution One notes that the conserved momentum G being $I\omega$, can readily be inserted in the tables The total energy E does not appear to have been previously examined at all The Maclaurin stability is found to persist, but only for axial disturbance, beyond the point of bifurcation into Jacobi forms, up to the limit determined by G H Bryan Possible initiation towards a nebular ring-structure is perhaps also not quite improbable, *cf* the astronomical phenomena of *Novæ* , the mathematical theory was explored long ago (*cf* Lamb, § 376) showing as is natural that for a ring of fluid type the period of rotation would be about the same as for meteoric bodies such as are required for stability of

the Saturnian rings. The tendency to such incipient ring-structure of compressible non-uniform types may well be held to have some persistence before breaking up into parts flying off tangentially, in arrangement more or less symmetrical with regard to the axis, after the manner of the wings of the spiral nebulæ The observed rotational velocities $e\ q$, of the Andromeda nebula, are not inconsistent with such an origin The fundamental contrast with the very peculiar but dynamically well-founded lopsided type of evolution towards a double star is connected by Jeans ("Cosmogony") with this expansile tendency of the outer parts

The subject matter of this discussion developed itself some years ago for class lectures at Cambridge on the general theory of Energy The discrepancy of stabilities, as independently determined, with the Poincaré criteria has persisted The Poincaré series of configuration (cf Lamb's discussion, § 377) are series with changing G, the series of an actual evolution are of G necessarily constant but changing E The argument has regard on one side to unrestricted continuous change expressible in terms of differentials of first and second orders, so that stabilities as regards the various co-ordinates can be discussed for each energy state independently of one another, in contrast to the turbulent transitions, necessarily largely undetermined and mixed up, in the path of secular evolution The suspicion here arising would in effect be whether the use of the same differential symbol in discussing ordinary dynamical stability on a given energy-level, and in representing the undetermined frictional transition to the other energy surfaces, is not analogous to the ancient ambiguity between differentials and variations in the variational calculus, which was brought out and surmounted by the notation and procedure of Lagrange

A very remarkable actual fact may here be relevant An arresting feature of the astronomical landscape is the presence of open groups of stars, all of them, though far apart, with the same velocity towards the same direction, in the case of the Ursa Major cluster the Sun happens to lie within the group, so that its stars appear all over the sky These groups cannot have been for long time within our stellar system, else their equality of velocities would have been deranged They must have come in from the outside more empty space, and are perhaps merely passing across—though our own system is itself presumably scattering The stars of each group travel together like a solid body, but as one which has acquired no rotation comparable with its translatory motion The problem of the origin of the group thus arises A solution that suggests itself is that the group has broken off from a much larger

cosmic system, for which rotational motion as a whole would be translatory motion for a local group in it For example, it may have been shed off from an arm of a spiral nebula, when it was in position on the nebula internal gravitational disturbance was compensated, while after it has broken off, on its journey across space with its initial velocity, it need not have had time to cumulate much disturbance The group could not have come from a very distant nebula for yet another reason its velocity would be excessive and in the wrong direction If this be tenable, the velocities being of suitable order, the empty cosmic spaces would be inhabited by such relatively small isolated stellar groups as well as by isolated single stars

A general key is indicated above in the sharp distinction between differentials and variations, introduced into analysis by Lagrange, which made general dynamics a possibility in connexion with his Calculus of Variations For a given form of the energy function E the stabilities of the system may be explored by the *differential* dynamical theory, adjacent forms of E differ by the coefficients in its analytic form having received *variational* change In general there would be as many types of variation as there are co-ordinate variables But if we assert limitation of the modes of variation to one kind, expressed by one parameter λ (*cf* Lamb, § 377) we can draw a series of graphs of E as a function of λ alone, thus of two-dimensional character, and the Poincaré theory of intersections with interchange of stabilities acquires a footing But this limited variation is hard to conceive in general and makes a large call on previous special knowledge of the system. Such knowledge is available in the very special problem of rotating perfect fluid It recognizes the actual existence of a plurality of states, while it has to *postulate* that they are not a mere unrelated assemblage of self-subsisting forms, but express an actual mode of progress in the evolution of the system as a linear series This means that it will not branch off into other modes except where this one becomes unstable, and such ordinary instability is sufficiently explored by neglecting slow dissipation, in the hydrodynamic problem by neglecting viscous terms in the equations. Here the Jacobi series is an example they are stable from their beginning as a branch from the Maclaurin series until a place where a pyriform series branches off, it was found by Poincaré (Lamb, § 380) that afterwards complete change of character arises, that there are an infinite number of bifurcations each originating a branch series, a remarkable transition which perhaps derives from the abstract simplicity of ideal fluid systems

The general theory gets a foothold only when we have an assurance in advance that there is a definite linear order of succession of states, that the evolutional variation of E depends (somehow) on only one parameter λ. In the Kelvin hydrodynamic problem the restriction that is tacitly imposed, involving this result, is that in each stage the system is to be moving like a solid body, implying an evolution of extreme slowness, the general possibilities of freedom would be far wider than this

---

The Emission of Electrons under the Influence of Chemical Action
Part II —Some General Conclusions and a further Study of the
Case of Carbonyl Chloride

By A K DENISOFF, University of London, King's College, and O W
RICHARDSON, F R S, Yarrow Research Professor of the Royal Society

§ 1 *Some General Conclusions*

We have now investigated this effect on the sodium potassium alloy K_2Na for 22 different gases With 15 of these the emission has been found to be sufficiently large for the distribution of kinetic energy among the emitted electrons to be determined, using the reacting gases at pressures of the order of 10^{-3} mm of mercury

As a result of these experiments we have been led to some general conclusions, the most important of which we propose to state, very briefly, at the outset They are —

(1) The energy distribution is not in general of the Maxwellian type as the earlier evidence had tended to indicate We expressed a suspicion of the correctness of this view on p 49 of our previous paper * The later experiments have confirmed that suspicion

(2) The distribution curves all rise from a small value at zero energy (V = 0) to a maximum at a certain energy (V = V_m) and fall away to zero as the energy is increased further to V = E_0 In this statement zero is to be understood to mean zero within the limits of our experimental error

---

* 'Proc Roy Soc,' A, vol 132, p 22 (1931) This paper contains references to earlier publications.

(3) The *actual* maximum energy E_a of the emitted electrons is ultimately reached rather gradually and is difficult to determine precisely The experimental plots, in fact, show a ' tail " similar to that observed in the photoelectric effect There is a *practical* maximum energy E_m obtained by disregarding the tail, 99 9% of the emitted electrons have energies less than E_m in the case of $COCl_2$

(4) The distribution curves for energies $> V_m$ and $< E_m$ can all be represented quite closely by the equation

$$N(V)\,dV = Ae^{-k(1-\tfrac{V}{m^c})}dV, \tag{1}$$

where A, k, and c are constants The constant c has a value very close to 2 for the more energetic and very close to 1 for the less energetic reactions For the most energetic reactions the equation (1) covers approximately the whole range of emitted electrons from $V = 0$ to $V = E_m$, for these reactions the distribution curves, if we disregard the "tails," are almost symmetrical about $V = V_m$

Equation (1) is inconsistent with the existence of a maximum energy E_a such as is referred to under (2) It should be remembered, however, that equation (1) is not a theoretical equation It is a convenient empirical way of representing some of the facts

(5) For chlorine compounds (for other substances we have not sufficient data) there is a simple relation between the maximum energy E_m of the emitted electrons and the energy of dissociation D of the chlorine compound referring to the corresponding reaction responsible for E_m It is

$$E_m + D = \text{constant} \tag{2}$$

(6) At low pressures the electron emission is proportional to the pressure of the reacting gas In most gases it rises to a very sharp maximum and then falls, as has been described in Part I for $COCl_2$ However, this is not completely general , in COS, for example, the rate of rise of emission with increasing pressure steadily diminishes to zero, so that the emission at higher pressures reaches a constant value independent of the pressure

(7) If we define the electronic yield Y of the reaction as the limiting value at $p = 0$ of the emission divided by the pressure p, the yield is greatest for the more energetic and least for the less energetic reactions For Cl_2, for example, the maximum number of electrons emitted for each chlorine atom taking part in the reaction is about $1\ 5 \times 10^{-6}$ whereas for $SOCl_2$ the corresponding

quantity is about $1\,5 \times 10^{-6}$ The contraction in the yield is very large
compared with the contraction in the chemical energy E_c (see below), as this
quantity diminishes   If we plot $\log Y$ against $E_c^{\,1}$ the points tend to group
themselves about a straight line

(8) A fair account of the facts, at any rate so far as the reactions which
involve the formation of alkah-halogen bonds are concerned, can be derived
from the following hypothesis   as a result of the collision of a molecule of
the chemically active gas with the metal surface a stable polar chemical bond
is formed   At the instant of formation the bond consists of a free negative
ion, which is one of the atoms of the gas molecule, and one of the positive ions
of the metal, which is chemically bound to other atoms of the metal   The
kinetics of the heterogeneous change for polyatomic gas molecules may either
be that the two active atoms of the gas molecule simultaneously enter into the
reaction with the metal, or it may be that only one atom enters into the reaction
at the instant of collision with the metal, it depends upon the strength of the
bonds between the atoms of the gas molecule and upon the orientation of the
molecule at the instant of collision   As we are concerned with the formation
not of a diatomic alkah-halogen molecule (or alkah-pseudohalogen molecule)
but of only one chemical bond of a large cluster, for example, $Cl^- - K^+$ $-$ Rest
of the metal, there will be no quantum restrictions for the stabilization of the
nascent bond   The stabilization of the bond may occur by the excess energy
being dissipated among a number of the adjacent metal atoms by the ordinary
mechanism of the heat conductivity of metals   The energy of the reaction
will be thus transformed into heat   However, since in the chemical process
of formation of a *polar bond* from neutral atoms, or molecules, a *spontaneous
re-arrangement of the electronic system* of the nascent bond is involved, the
stabilization of the bond may also occur spontaneously under the mechanism
of a three-body collision with one of the free metallic electrons   In this case
all the energy of the reaction goes off as kinetic energy of the electron which is
thus enabled to escape from the metal surface   These escaping electrons
constitute the electronic spectrum which is the principal subject of the investi-
gation

On the basis of this hypothesis we can give an explanation of the empirical
energy distribution function given by equation (1)   The analysis shows that
the observed form of the distribution function can be qualitatively accounted
for by the form of the function expressing the probability of the collisions of
the second kind for electrons having different velocities (the de-excitation
function).

Furthermore, on the basis of this hypothesis, relation (2) receives a very simple interpretation   It is

$$E_m = E_0 - \phi,\tag{3}$$

where E_0 (*cf* § 6) is the energy of the corresponding elementary chemical reaction responsible for E_m, and ϕ is the work function of the metal   This is true within the limits of accuracy of our estimation of E_0 This relation is general, at any rate so far as we have been able to find the data to test it   *The equation (3) is similar to the fundamental law of photoelectricity*

The evidence which has led us to these conclusions, as well as to some others which will appear in due course, is set forth in this paper and others which will follow it

Much of this paper will be devoted to an account of further experiments with $COCl_4$. This gas has been chosen for a particularly detailed investigation because it gives an emission of a suitable magnitude, it is convenient to experiment with and we have had more experience in manipulating it than the other gases to be dealt with later

§ 2 *The High Energy Part of the Electronic Spectrum from Carbonyl Chloride*

As we have stated already, the results of the experiments described in Part I indicated a possible deviation from the Maxwell distribution of energy for the emitted electrons with high velocities   Further consideration led us to attach much more importance to this point, particularly in view of the great deviation from the Maxwell distribution in the region of low velocities which had been observed in all the previous researches   We therefore decided to investigate this question carefully and in detail

We have to bear in mind that for the determination of the energy distribution among the electrons, the characteristic curves   electron current i, as a function of the retarding field V, were employed   For a Maxwell distribution

$$i = i_0 (1 + \sigma V) e^{-\sigma V},\tag{4}$$

where i_0 is the electron saturation current, and $\sigma = e/kT$ This relation held, within the limits of experimental error, in the range of values $i/i_0 \simeq 0\ 1$ to $i/i_0 \simeq 5 \times 10^{-4}$ Commencing with $i/i_0 \simeq 0\ 1$ and going up to $i/i_0 = 1$, a great deviation from the above relation was observed   In view of the small values of the electron current at large retarding fields, and consequently

large relative error of measurement, determinations were made only down to $s/s_0 \approx 5 \times 10^{-4}$

The purpose of the present experiment consisted mainly in the determination of the energy distribution among the electrons in the region of higher velocities Taking into consideration the experience obtained from the previous work, it was possible to improve upon the accuracy in the measurement of the electron currents, and by such means it was possible to increase the range of measurements and reach a value of s/s_0 so low as 1×10^{-6} For this, it was essential that the following conditions should be fulfilled —

(1) Sufficiently high electron saturation current   This limits the range of gas pressure within which the determinations can be made

(2) High constancy of gas pressure during the whole period of the experiment In Part I it was established that the contact potential difference was a function of the gas pressure, and it was the inconstancy of the gas pressure which mainly determined the error of measurements in obtaining the characteristic curves

(3) It was necessary to add a suitable system of capacities, connected in parallel with the electrometer, which would make it possible to vary the sensitivity of the measuring apparatus quickly

Determinations were made on the same alloy, of the composition approximately K_2Na, as in Part I and with the same sample of phosgene   The description of the apparatus, and the procedure used in the measurements are the same as there described

The previous work on the electrons in the range $s/s_0 = 5 \times 10^{-4}$ to $s/s_0 = 0$ 1 had led to the conclusion that the distribution of energy among the electrons follows Maxwell's law   The average energy corresponding to such a distribution was determined[*] by the use of a graph expressing the relation between σV and V_1, where σV is taken from the equation $s = s_0 (1 + \sigma V) e^{-\sigma V}$, and V_1 is the experimental scale of potential $V = V_1 + K$, where K is the contact potential difference between the alloy and the outer electrode   For a Maxwell distribution this graph is a straight line, the slope of which is equal to $\sigma = e/kT$.   On such a graph the deviations from the Maxwell distributions are easily seen as a departure from rectilinearity

Five characteristic curves $s/s_0 = f(V_1)$, obtained under different phosgene pressures from $1\ 5 \times 10^{-3}$ mm. to 3×10^{-4} mm , served as data for the

* O W Richardson and M. Brotherton, 'Proc Roy Soc,' A, vol 115, p 20 (1927)

present analysis The maximum of electron saturation current i_0 is at about 5×10^{-5} mm , at a pressure of $1\ 5 \times 10^{-5}$ mm , i_0 was about 25% and at 3×10^{-4} mm about 50% of the maximum saturation current Thus the observations were made in the most interesting range of pressures, where the important changes in the surface conditions of the alloy occur A further decrease, or increase, in pressure would inevitably have led to a further decrease of saturation current, and in consequence the relative accuracy of the measurements would have been insufficient

The time T of the drop in all experiments was 25–26 seconds The time of exposure $dt = 25$ seconds The maximum diameter of the drop was about 4 mm and the drops had a regular spherical shape The maximum saturation current under such conditions was equal to $(i_0)_{max} = 1\ 70 \times 10^{-8}$ amp

Figs 1 and 2 show the above-mentioned graphs $\sigma V = F(V_1)$

The curves III, V, and II, fig 1, are shifted to the right relative to curve I by $0\ 3$, $0\ 8$, and $1\ 8$ volts respectively The experimental points for curve I are indicated by crosses, the others by circles Table 1 shows separately the results for one of the curves (curve IV, fig 2) For the purpose of comparison with the results of the previous experiments, a dotted straight line is drawn for each curve This line is so placed that the points of the curve in the range of values of σV from 3 to 8 would have given the best coincidence with the dotted line The slope of this straight line, σ, has a value of about $5\ 5$, i e , practically the same value as in the previous determinations Generally, the curves of the previous research, which have been obtained in the range of σV between 3 and 8, completely coincide with the present curves.

We wish to draw attention to the following features of these curves —

(1) The great similarity of all the curves among themselves Within the limits of experimental error they coincide with one another

(2) The slope of the curves continuously increases as σV increases This can also be seen from Table I In column 3 are given the ratios of each preceding value (i') of the current to the one following (i), for every $0\ 1$ volt With an increase in the retarding field (V_1) the ratio i'/i systematically increases The slope, which has the value about $5\cdot5$ has a local character and has been obtained because the observations were limited to values of σV below about 8

From this we arrive at the following important conclusion *The fundamental distribution of energy among the electrons is not according to Maxwell's law*
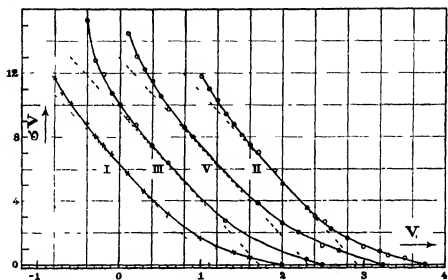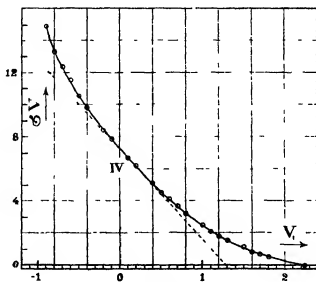
Fig 1

Fig 2

Curve I	.	$p = 2\ 2 \times 10^{-5}$ mm, $t_0 =$	64×10^{-19} amp
Curve II		$p = 1\ 4 \times 10^{-5}$ mm, $t_0 =$	42×10^{-19} amp
Curve III		$p = 2\ 0 \times 10^{-4}$ mm, $t_0 =$	102×10^{-19} amp.
Curve IV		$p = 5\ 0 \times 10^{-5}$ mm, $t_0 =$	138×10^{-19} amp.
Curve V		$p = 2\ 7 \times 10^{-4}$ mm, $t_0 =$	36×10^{-19} amp

The above evidently solves the question as to the reality of the deviations from the linear relationship in the region of low velocities, which have been observed in all previous researches   We can see now that the results of the previous experiments also indicated deviations from the linear relationship in the region of high velocities   Such deviations can be seen, for example, in fig. 10, p 48 of Part I, and also in the paper by Richardson and Brotherton (*loc cit*, pp 25–26, Table IV and fig 2)

Table I

Volts V₁ (C P D = −2 24)	i/i_0	i'/i (at $V_1' - V_1 = 0\ 1$)	σV
+2 1	0 954	–	0 338
2 0	0 933	1 02	0 431
1 9	–	–	–
1 8	0 894	–	0 550
1 7	0 831	1 07	0 728
1 6	0 791	1 05	0 846
1 5	0 687	1 14	1 13
1 4	–	–	–
1 3	0 543	–	1 54
1 2	0 472	1 15	1 77
1 1	0 379	1 24	2 10
1 0	0 304	1 26	2 45
0 9	–	–	–
0 8	0 176	–	3 19
0 7	0 120	1 48	3 68
0 6	0 0878	1 36	4 07
0 5	0 0603	1 46	4 54
0 4	0 0371	1 6	5 10
0 3	–	–	–
0 2	0 0147	–	6 21
0 1	0 00956	1 5	6 71
0	–	–	–
−0 1	0 00950	–	7 84
0 2	0 00212	1 7	8 40
0 3	–	–	–
0 4	0 000613	–	9 78
0 5	0 000304	2 0	10 54
0 6	0 000132	2 3	11 45
0 7	0 0000583	2 3	12 34
0 8	0 0000241	2 4	13 29
0 9	0 0000053	4 6	14 91

In the experiments of Richardson and Brotherton a very interesting fact was observed, namely, the difference between the apparent contact potential, as determined from the properties of the chemically emitted electrons, and from the photoelectric measurements   In the greater number of experiments the difference was about 0 6 volt, and this fact is difficult to explain on the assumption of a Maxwell distribution of energy among the electrons   With a

Maxwell distribution the straight line representing the relationship between
σV and V_1 should intersect the V_1 axis at $V = 0$, $i\,e$, at $V_1 = -K$, as
$V = V_1 + K$, where K is the contact difference of potential   As the straight
line on figs 1 and 2 assumes, with the new interpretation, the significance of an
accidental tangent there is no reason to expect the intercept on the V_1 axis,
between the slope line and the origin, to represent the contact potential
difference

The observed difference between the photoelectric and the chemical zero
can thus be considered as a confirmation of the present conclusion that the
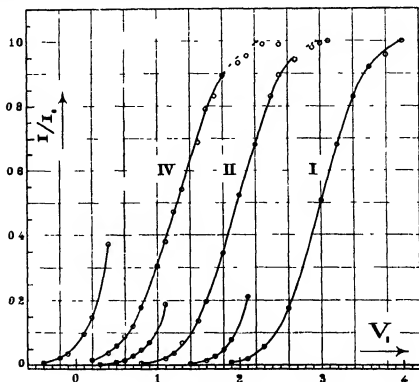distribution of energy is not Maxwellian

Fig 3

Fig 3 shows three characteristic curves $i/i_0 = f(V_1)$ which have been
selected because the measurements they represent were taken with the utmost
care   In each case the smaller currents against the higher retarding potentials
are shown separately to the left of the main curve   For these extensions of
the main curve the ordinates have one-tenth of the value shown on the scale

The curves correspond to the following pressures   Curve I, $p = 2\ 2 \times 10^{-5}$ mm , curve II, $p = 1\ 4 \times 10^{-5}$ mm., curve IV, $p = 5\ 0 \times 10^{-5}$ mm   Curve IV corresponds to the actual V_1 axis, curves II and I are shifted to the right from IV by 1 and 2 volts respectively   It is important to note that in spite of the different pressures under which they have been obtained and the different surface conditions of the alloy resulting therefrom the curves have a very constant shape   The same thing is shown by the curves in Part I throughout the whole range of pressures from 10^{-7} to 10^{-3} mm   The slope of the middle part of the curves is almost a straight line   This fact distinguishes them very strongly from thermionic curves and shows a similarity with photo-electric ones

Fig 4 shows the corresponding differential curve $\Delta\ (i/i_0) = \phi\ (V_1)$, at $\Delta V = 0\ 1$ volt   It represents the distribution of total energy among the
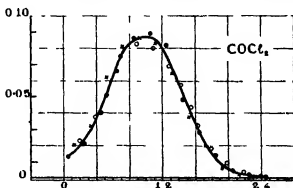

Fig 4

emitted electrons   The points marked ● are derived from fig 3, curve I, those marked × from fig 3, curve II, and those marked ○ from fig 3, curve IV   As the value of the contact potential difference is not known, we do not yet know the exact position of the zero on the V_1 axis, since $V = V_1 + K$ and when $V = 0$, $V_1 = -K$ This point has been determined by experiments with mixtures of gases, which will be described in a later paper   These experiments show that the point of departure of the curves, such as those in fig 3, from the saturation value i_0 corresponds to the value $V = 0$ within the limits of experimental error   The curves in fig 3 have all been drawn to fit this experimentally determined zero   The experimental points show some systematic deviation from the curve, but it is doubtful if this exceeds the experimental error which is greatest in this part of the curve (see § 4, p 62)

The curves in fig 3 give the following values for the contact potential difference and for the maximum electron energy E_m —

Curve I   K = $-2\ 0\ \pm 0\ 1$ volts, $E_m = 2\ 5 \pm 0\ 1$ volts

Curve II   K = $-1\ 9_6 \pm 0\ 1$ volts, $E_m = 2\ 5 \pm 0\ 1$ volts.

Curve IV   K = $-2\ 2_4 \pm 0\ 1$ volts, $E_m = 2\ 6 \pm 0\ 1$ volts

Average value for $E_m = 2\ 5_2 \pm 0\ 1$ volts

If N (V) dV denotes the proportion of the whole of the emitted electrons, which have energies within the range eV to $e(V + dV)$, the distribution function N (V) for $COCl_2$ satisfies the equation

$$N (V) = Ae^{-k(V - V_m)^2}, \qquad (5)$$

where A and k are constants, to within the degree of accuracy of the experimental data, or nearly so, except in the very high and very low energy parts of the spectrum We can test this as follows, taking logarithms of (5) we have

$$\log_{10} A = \log N (V) + \frac{k}{2\ 30_3} (V - V_m)^2 \qquad (6)$$

Thus the right-hand side of (6) should be a constant quantity for all values of V When the data of fig 4, for example, are subjected to this test the result is Table II In this table the value of k, $2\ 303 \times 1\ 087$, has been determined

Table II —Test of the equation N (V) = Ae$^{-k(V - V_m)^2}$ for $COCl_2$

V (volts)	0 2	0 4	0 6	0 8	1 0	1 2	1 4	1 6	1 8	2 0
$(V - V_m)^2$	0 64	0 36	0 16	0 04	0	0 04	0 16	0 36	0 64	1 0
$\log_{10}$ N (V)	2 301	2 562	2 796	2 917	2 937	2 906	2 771	2 525	2 176	3 756
$\frac{k}{2\ 30_3}$ (V - $V_m)^2$	0 696	0 391	0 174	0 044	0	0 044	0 174	0 391	0 696	1 087
$\log_{10}$ A	2 997	2 953	2 970	2 961	2 937	2 950	2 945	2 916	2 872	2 843

by subtracting the values of $\log_{10}$ N (V) at V − $V_m = 0$ and V − $V_m = 1$, and thus eliminating A It will be seen that the values of $\log_{10}$ A in the last line of Table II, which are the sums of the quantities in the two preceding lines in the same column, vary very little over a range of V of 1 8 volts The mean of these values of $\log_{10}$ A is $\bar{2}\ 924$ It is probable that a more accurate value of this empirical constant will be given by the value of $\log_{10}$ N (V) at which it is a maximum This is $\bar{2}\ 937$ These two values do not differ much It is possible that the average of them, $\bar{2}\ 930$, will be more correct

than either If we use this average value to re-determine k in combination with the data for $V = 1\ 0$ and $V = 2\ 0$ volts we find

$$k = 2\ 30_2 \times 1\ 15_2 = 2\ 65_2 \text{ volt}^{-2}$$

Equations (5) and (6) are only to be regarded as *empirical* equations which express the experimental data with a fair degree of accuracy In all probability they do not represent the correct mathematical form of the distribution function Nevertheless, they have a certain degree of practical utility It will be noticed that equation (5) makes the distribution function completely symmetrical about the line $V = V_m$ That the actual distribution function for $COCl_2$ is very nearly symmetrical about this line is one of its most striking features

The extent of the deviation of the actual distribution functions from a Maxwell distribution is shown in fig 8 In this figure the circles represent the experimentally determined values whilst the crosses give the values of the Maxwell distribution function $N(V) = 0\ 775\ V^2 e^{-2}\ ^{2V}$ which fits the experimental data from $V = 0$ to a little beyond $V = V_m$ It is at once seen that after passing the maximum the actual electron density becomes smaller and very rapidly enormously smaller than that which would be given by a Maxwell distribution formula

§ 3 *Influence of the Geometry of the Electrodes on the Experimental Energy Distribution Curves*

The experiments described so far were all made with small drops of the alloy at the centre of a platinum cylinder $4\ 2$ cm long and $2\ 0$ cm. in diameter, as described in Part I Inasmuch as we are only concerned with the distribution of total kinetic energy the shape of the surrounding negative electrode is of no account provided it completely surrounds the small source For this particular case the results are the same as for a small source at the centre of a charged sphere, where the geometry permits an easy calculation of the details of the motion of the electrons In the actual experiment it is not possible to use a surrounding electrode with a completely closed surface as it is necessary to have openings for the tube to admit the alloy and for the escape of the drops. The presence of these apertures introduces an element of uncertainty into the analysis of the data which it is necessary to remove

For concentric spherical electrodes it is possible to estimate the errors introduced by the finite size of the central electrode and by the apertures in the outer electrode The problem of the application of spherical condensers

to energy distribution analysis has, in fact, been considered in detail by Lukirsky [*] The error introduced by the finite radius of the inner sphere is equal to the square of the ratio of its radius to that of the outer sphere Thus in the experiments of Richardson and Brotherton (loc cit), where a sphere of 3 8 cm diameter was used and the drops had a radius of 0 3 to 0 4 cm, the error from this source would not exceed 1% For concentric spheres, since all the trajectories are radial, the proportion of the electrons which escape through the apertures is simply the proportion which the solid angle subtended at the centre by the apertures bears to 4 π With Richardson and Brotherton's electrode this would amount to about 2% This error will be somewhat affected by the distortion of the radial field caused by the presence of the apertures, but it is not believed that this effect will be of much importance in the present experiments

With electrodes of other shapes it is much more difficult to estimate the errors which may be introduced by the presence of apertures We have considered two problems,[†] (1) a narrow emitting plane strip of indefinite length lying in the middle of a coplanar conducting strip of the same indefinite length and width 2l, opposite to an opposing parallel plane electrode of the same dimensions, 2l × ∞, at a distance b, and (2) a small emitting source treated as a portion of a cylinder of radius a placed at the centre of a co-axial cylinder of radius b and length 2l In each the emitting electrons are endowed with a Maxwell distribution of kinetic energy

It might be thought that problem (1) would be very simple It is easy enough to obtain an integral, which expresses the number of electrons which escape through the aperture, but it is not integrable in finite terms, and we have not been able to find any series expansion for it which is of any practical use However, it has one simple property Every element of the integral is real and positive By the artifice of multiplying the integrand by a certain factor which is positive and greater than unity throughout the domain of integration we can reduce it to a very simple integral which must have a value greater than that of the first integral In this way we can show that the proportion of the emitted electrons which escape through the apertures between the planes must be less than

$$\frac{2}{\sqrt{\pi}} \sqrt{\frac{Ve}{kT}} \exp\left(-4\,\frac{l^2}{b^2}\,\frac{Ve}{kT}\right) \tag{7}$$

except when Ve/kT is small, let us say appreciably less than unity   In (7) V is the opposing potential difference, e the electronic charge and k Boltzmann's constant   For any useful values of l/b, such as would correspond to the dimensions of apertures used in actual experimental arrangements, (7) is a very small quantity   It is zero when $Ve/kT = 0$, has a single maximum value $\dfrac{1}{2\pi e}\dfrac{b}{l}$ when $\dfrac{Ve}{kT} = \dfrac{b^2}{8l^2}$ and approaches zero with great rapidity as Ve/kT increases in the direction of $+\infty$

In problem (2) it is possible to write an integral which expresses the number of electrons which escape from the ends of the cylinder   But the integral involves the smallest real root of a transcendental equation which so far has resisted all efforts to contract an infinite series which forms part of it   However, by a graphical method, it is possible to show that with the dimensions of the cylinder used in the present experiment the error in the experimental distribution function caused by the electrons which escape from the aperture is always very small for values of V at which the deviation from the Maxwell distribution, as shown, for example, in fig 8, becomes appreciable

The foregoing considerations make it highly improbable that the deviations from the Maxwellian distribution at high energies can arise from the effects of apertures in the surrounding electrode or from the finite size of the source However, it is not possible to make calculations for the precise structure of electrodes and resulting distribution of electric field used in the present experiments so that the reality of the deviations cannot be regarded as completely established by these arguments

We can obtain some further evidence bearing on this question by considering some of the older experiments   In 1921 it was proved by one of us[*] that, within the limits of experimental error, the substitution for a spherical electrode of a cylindrical one of approximately the same form as the cylinder used in the present experiments did not alter the form of the characteristic curves Again, if we compare the results obtained by Richardson and Brotherton (*loc cit*) when using a spherical electrode with those got with the cylinder in Part I and in the present experiments there is no appreciable difference in the range in which they overlap   However, this evidence is also not entirely conclusive because in the 1921 experiments the accuracy of measurement was far below what it is now, and in the experiments of Richardson and Brotherton the amount of overlap in the high energy region where the deviations occur is very slight

* Richardson ' Phil Trans,' A, vol 222, p 1 (1921)

§ 4 *Experiments with a Spherical Electrode.*

In order to remove any uncertainty, resulting from the considerations set out in § 3, as to the reality of the deviations from the linear σV V₁ plots, we decided to repeat the experiments using a spherical platinum electrode, with the same refinements and precision as had been attained with the cylinder, and extending well into the high energy region   With a spherical electrode, as we have pointed out, the disturbing effects of apertures and finite size of drops can be ascertained with sufficient certainty and shown to be unimportant

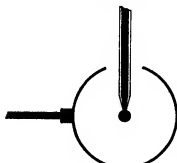The electrode used was a seamless pure platinum sphere about 2 75 cm. in diameter with two circular apertures each 1 00 cm in diameter Fig 5 represents exactly the actual size of the spherical condenser   It also indicates approximately the maximum size of the drops This depends somewhat on the time T of a drop The first experiment was performed with T = 2 minutes 30 seconds and the maximum diameter *d* was about 0 4 cm   In other experiments T was about 10 seconds and *d* about 0 3 cm With this value of *d* the ratio between the diameters of the sphere and the drop is 27 5/3 = 9 2 and the error introduced by the finite size of the source is thus about 1%   The combined error arising from this and from the apertures lies in the neighbourhood of 3–5%

Fig 5

The sphere was thoroughly cleaned with benzene, caustic soda, nitric acid, and distilled water , it was then placed in a quartz tube and evacuated for many hours at 1000° C   In the actual experiment the spherical electrode was used without a heating arrangement and for that reason the pressure of the active gas was not allowed to exceed 5 × 10⁻⁵ mm   At such low pressures the behaviour of the outer electrode, as regards variations of the contact potential difference, was the same as that with the cylindrical electrode with a heating arrangement   Thus it is important because changes in the contact potential difference affect the experimental determination of the characteristic curves and it is necessary to understand and allow for these effects

As a result of a large number of observations on a variety of reactive gases we can sum up the effects of these gases on the contact potential difference between the alloy and the platinum electrode as follows

At very low pressures the variation of the contact potential difference is determined mainly by adsorption of the active gas on the platinum surface. This effect is quite reversible The active gas is electronegative and it reduces, when adsorbed, the work function of platinum, so that the contact potential difference is less than in a good vacuum At the lowest pressures, of the order 10^{-6} mm, the equilibrium conditions result in the formation of a mono-molecular layer on the platinum surface and the effect of the gas in reducing the work function of the platinum is then the greatest With increase of pressure the equilibrium conditions allow the metal surface to be covered with a layer more than 1 molecule thick and this will reduce the effect of the first layer of molecules The contact potential difference will thus show an increase with pressure (maximum about 0 5 volt, see Part I, figs 3 and 4, pp 36–37) When the pressure of the active gas exceeds 5×10^{-5} mm., the vigour of the chemical reaction with the alloy is increased so much that it may cause individual molecules of the alloy, or the reaction products, to evaporate and condense on the platinum surface This is shown by the fact that, even if the exposure to the gas at these higher pressures lasts only a short time, a thin layer can be noticed on the inner side of the platinum electrode after the apparatus has been taken to pieces In this respect, apparently, water vapour gives the greatest effect When such layers are present complicated permanent, or semi-permanent, changes in the contact potential difference may occur of the type described by Richardson and Brotherton (*loc cit*, pp 39–41) as hysteretic effects. It is probable that an essential feature of the mechanism of these effects is the presence on the platinum of a layer of reaction products which insulates it from the electrons and thus forms a condenser of very high capacity

Three independent experiments were carried out with the spherical electrode, the σV V_1 plots of which are given in fig 6 Experiment 1 (marked 2 in fig 6) Time of drop $T = 2$ minutes 30 seconds, time of exposure $dt = 60$ seconds, pressure $p \sim 2 8 \times 10^{-5}$ mm, saturation current $i_0 = 3 7 \times 10^{-10}$ amp Experiment 2 (1 in fig 6) $T = 7$–8 seconds, $dt = 30$ seconds, $p \simeq 1 7 \times 10^{-5}$ mm, $i_0 = 3 8 \times 10^{-9}$ amp Experiment 3 (3 in fig 6) $T = 9 5$ seconds, $dt = 35$ seconds, $p \approx 4 7 \times 10^{-6}$ mm., $i_0 = 9 2 \times 10^{-9}$ amp Curves 2 and 3 in fig 6 are shifted to the right relative to curve 1 by 0 2 and 1 2 volts respectively It will be seen that the results of all three experiments are consistent with each other and, within the limits of experimental error (maximum 5%), the plots can be very well superimposed on each other and on those obtained with the cylindrical electrode This is shown on curve 2 of

fig 6 where the crosses represent the experimental points of curve II, fig 1, which was obtained with the cylinder

This proves that the apparatus with the cylindrical electrode does give the correct energy distribution in the spectrum of the emitted electrons

As the cylinder is more conveniently adapted to heating and we thus avoid troublesome changes in the contact potential difference, we have used it in preference to the sphere in most of the other experiments
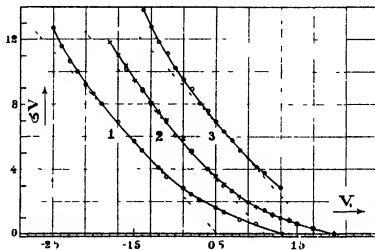

Fig 6

The actual characteristic curves corresponding to 1 and 2 in fig 6 are shown as 1 and 2 respectively in fig 7 where curve 2 is shifted to the right relative to curve 1 by 1 0 volt   In each the high energy part is shown separately from the rest with the vertical scale magnified ten times   The irregularity of the points in the neighbourhood of $s/s_0 = 1$, which is particularly noticeable in curve 1, fig 7, is due to small changes in the contact electromotive force which occur during the experiment, coupled with the fact that the absolute error of measurements is greatest in this part of the curve   It is impossible to determine the exact course of this part of the curve with anything like the certainty which is attained in the high energy part, on the left-hand side

Figs. 8 and 9 show the energy distribution curves $\Delta (s/s_0) / \Delta V = N (V)$ for $\Delta V = 0$ 1 volt corresponding to curves 1 and 2 respectively of figs 6 and 7   The points, which are measured from fig 7, are shown as circles   In fig 8 the crosses represent the Maxwell function 0 775 $V^2 e_0^{-2 \frac{3}{2} V}$ which fits the low energy part of the curve   The deviation of the high energy part from this function is very striking   The crosses in fig 9 are the corresponding data got

in one of the experiments with the cylindrical electrode, and shown as solid dots in fig 4
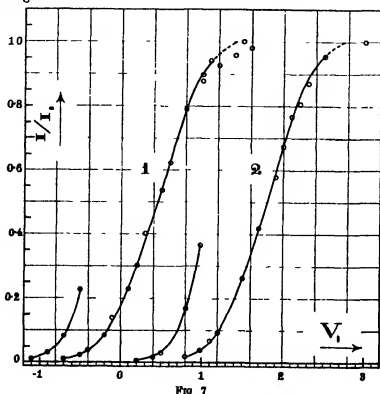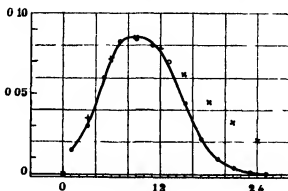

Fig 7

Fig 8

Particular attention was paid to ascertaining whether small accelerating electric fields have any real effect in increasing the electron emission. It will be remembered that the measurements with the cylindrical anode in

Part I gave a negative answer to that, but there were some elements of un-
certainty arising from the geometry of the cylindrical electrode It will be
seen from Table III that the electron current (in arbitrary units) remains
constant within 3% with accelerating fields up to + 6 volts The current
was saturated at about + 1 8 volts These results were obtained in the
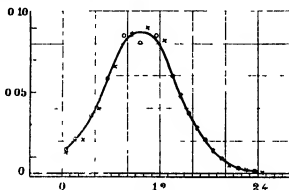course of the experiment 1 of figs 6, 7, and 9

Fig 9

Table III —Test of Effect of Accelerating Field on Saturation Current

Volts V_1	+2 0	+3 0	+4 0	+5 0	+6 0
Current i	195	194	199	195	196

§5 The Low Energy Part of the Spectrum, the Determination of the True Zero on the Volt Scale and of the Maximum Energy

In this section we outline very briefly the conclusions we have reached on
these questions It is impossible at this stage to give the reasons for them
adequately as they depend very largely on an accumulation of evidence which
has been got from the investigation of gases other than $COCl_2$ and which will
be described in the papers to follow

At the end of Part I we expressed a suspicion that the deviations from
linearity of the σV V_1 plots in the low energy part of the spectrum, s e,
near $V = 0$, were a real feature of the energy distribution and not due to
secondary complicating causes tending to prevent the attainment of saturation,
as had hitherto been supposed. We are now quite convinced that these
deviations are real They are found to persist unchanged, as we mentioned in
Part I, over an enormous range of variation of different experimental con-

ditions The former straight lines are now only tangents to a curve which is continuous from $V = 0$ to the highest values of V for which measurements can be made, but which happens to be nearly a straight line over a considerable range. The curious conflict found by Richardson and Brotherton (*loc cit*) between the voltage zero when determined photoelectrically and when determined from the σV V_1 plots on the old interpretation now disappears In fact, we now know where the true voltage zero is It coincides with the photoelectrically determined zero and with the point at which the current *begins* to drop from the saturation value In this respect we are back at the position reached in 1921 * The σV plots have to reach this value of V_1 at $\sigma V = 0$ and they approach it by means of the continuous curve found experimentally and not by means of a straight line which leads somewhere else Other facts which make it quite certain that the deviations of the linear plots near $V = 0$ are real are derived from experiments with gases other than $COCl_2$. The shapes of these " feet " are found to be characteristic of the different gases , in some gases they are even absent and the σV plots are linear down to $V = 0$, to within the limits set by the errors of measurement.

We therefore conclude that the diagrams such as figs 4, 8, and 9 represent the true distribution of energy among the emitted electrons, to the limits of accuracy set by the experimental measurements.

The reason we are so sure that the true voltage zero coincides with that determined photoelectrically and with the voltage at which the current begins o fall from the saturation value is because we have devised a new experimental method of attacking this problem which confirms those determinations This method depends on experiments with mixtures of different gases and will be described in a later paper The reason why this position was abandoned previously is because in the older experiments, owing to the difficulties created by changes in the contact potential difference, the point of departure from saturation could not be determined with sufficient accuracy to enable a decision to be made as to which of the two zeros then measured experimentally was the correct one

Although we can state quite definitely, as we have done above, that the deviations from linearity of the σV V_1 plots in the low energy part of the spectrum are a real feature of the energy distribution and not due to secondary complicating causes tending to prevent the attainment of saturation, it is necessary to point out that sometimes such secondary factors preventing the attainment of saturation did exist in the *immediate* neighbourhood of the

* Richardson, *loc cit*

actual zero   These distortions of the extreme low energy part of the electron spectrum were observed only at pressures higher than 10^{-5} mm, and it seems that the higher the pressure the more readily they appear   Curve 1 of fig 7, obtained at a pressure of $1\cdot7 \times 10^{-5}$ mm, gives a good idea of the magnitude of these distortions   The effect can be explained by a greater change in contact potential difference at higher pressures during the experiment   By all indications, such distortions existed in some greater magnitude in the higher pressure experiments of Richardson and Brotherton (cf fig 1, p 25, of their paper)   They have probably played an important role in making it much more difficult to give a correct interpretation of the difference between the chemical and photoelectric zeros

An analysis of the energy distribution curves, such as I, II, and IV of fig 4, and the curves of figs 8 and 9, shows that the curves do not plunge into the volt axis very sharply in the neighbourhood of the maximum energy, not nearly so sharply as they do in the case of the photoelectric effect   However, the detailed investigation of the high energy part of the electron spectrum (see § 2) has proved quite definitely that the distribution curves do *not* approach the volt axis *asymptotically*   This can be very well seen, for instance, from curve III of fig 1 and curve IV of fig 2   with increase of the energy V the tangent of the curves approaches a value equal to infinity   It follows from this that the *actual* maximum energy E_a can be estimated from the $\sigma V \ V_1$ plots and could be defined as the value of V_1 corresponding to $\sigma = \infty$ There is some reason, however, for dealing with the " *effective* " maximum energy rather than with the actual maximum energy E_a This effective maximum energy E_m will be defined as the value of V_1 at which the energy distribution curve *practically* touches the volt axis   Below we give the values of E_m, obtained from the energy distribution curves, and the corresponding values of s/s_0

Fig 4, curve I $E_m = 2\cdot5$ volts, $s/s_0 = 0\cdot0008$
Fig 4, curve II $E_m = 2\cdot5$ volts, $s/s_0 = 0\cdot0006$
Fig 4, curve IV $E_m = 2\cdot6$ volts, $s/s_0 = 0\cdot0006$
Fig 8, curve 1 $E_m = 2\cdot5$ volts, $s/s_0 = 0\cdot0006$
Fig 9, curve 2 $E_m = 2\cdot5$ volts, $s/s_0 = 0\cdot0005$
Average value for $E_m = 2\cdot5_5$ volts

The values of E_a, obtained from the $\sigma V \ V_1$ plots are —
Fig 1, curve III $E_a = 3\cdot0$ volts, $s/s_0 < 0\cdot000005$
Fig 2, curve IV $E_a = 3\cdot1$ volts, $s/s_0 < 0\cdot000005$
Average value for $E_a = 3\cdot0_5$ volts

It will be seen from this that the values of E_a are about 0·5–0·6 volt higher than E_m, but the electron current at $V = E_m$ is already less than 1/1000 of its saturation value and, as can be seen from the σV V_1 plots, it falls down very quickly at $V > E_m$, so that there is every reason to treat the part of the distribution curve at $V > E_m$ as a "tail" caused by some secondary factors. With many other gases it was even impossible to obtain the ratios i/i_0 at $V > E_m$ because of the small absolute value of i_0, and thus it was impossible to find the actual maximum energy E_a.

It may be pointed out that the values of E_m can be approximately estimated also from σV V_1 plots. As can be seen from figs 1, 2, and 6, at $V = E_m$ the curves turn sharply to the right from the tangent indicated in the diagrams. According to this method the curves III and V of fig 1 (these curves were obtained in the investigation of the extreme high energy part of the electron spectrum and because of the lack of the middle points it was impossible to plot differential curves for those data) give the following values of E_m : —

Fig 1, curve III $E_m = 2$ 4 volts, $i/i_0 = 0$ 0010

Fig 1, curve V $E_m = 2$ 5 volts, $i/i_0 = 0$ 0007

§ 6 *The Relation between the Maximum Energy of the Emitted Electrons and the Energy of the Reaction.*

In the reaction between $COCl_2$ gas and K_2Na alloy we are concerned with the formation of a polar chemical bond between the Cl atom, which on the ground of our experimental results we can assume to be simultaneously liberated from the rest of the molecule and converted into a negative ion, and one of the positive K, or Na, ions of the metal, which is chemically bound to other atoms of the metal It is important to realise that the energy of the formation of the bond will be dissipated, among a number of the adjacent metal atoms, in a very short time, of the order of 10^{-15} seconds, because of the normal heat conductivity of the metal * On the other hand, the time required for an adiabatic formation of a bond is of the order of at least 10^{-13} seconds Therefore, the energy developing during an adiabatic formation of the bond will be practically wholly dissipated to the adjacent metal atoms by the time the incident molecule first reaches the equilibrium position corresponding to the maximum negative potential energy of the nascent bond We thus arrive at an important conclusion that *the observed chemical electron emission can only*

---

* Langmuir, 'Phys. Rev.,' vol. 8, p. 149 (1916), 'J Amer Chem Soc,' vol 38, p 2233, (1916)

be a result of a spontaneous rearrangement of the electronic system of the nascent bond

The experimental evidence on the spectra of alkalihalide molecules,[*] as well as the results of theoretical considerations of non-adiabatic chemical processes,[†] lead to the conclusion that the formation of a stable alkalihalide molecule in the normal state from the two neutral atoms is an essentially non-adiabatic process   That is, if we consider the reverse process of dissociation it is necessary for the alkalihalide molecule in the ground state to absorb a light quantum to give dissociation into normal atoms   It is pointed out, however, that the chemical transformation may be concerned with a quantum transition which involves no change of the character of the electronic term, since in the case of alkalihalides the ground state (which gives dissociation into ions) and the first excited state (which gives dissociation into normal atoms) may both be $^1\Sigma$-terms   If we accept that, in our case of the heterogeneous formation of the polar bond, the process of formation is, in principle, analogous to that in the case of the alkalihalogen molecules, it will follow that the chemical electron emission has as its basis a pure quantum effect

As the amount of energy liberated in most chemical reactions between a gas and a metal is of the order of a few volts, it will be safe to conclude that no chemical electron emission from a metal can be observed during an adiabatic heterogeneous chemical transformation, which does not involve a spontaneous rearrangement of the atomic electrons, such as, for example, the condensation of metal atoms on the surface of their own metal

So far as we are only concerned in giving an energy account of the chemical process it is not necessary to know exactly the actual mechanism of the formation of the polar bond, but we have to know the initial and final states of the system. Because of the short time of de-excitation of the polar bond formed the final state of the transformation will be that which corresponds to the instant of formation of the bond   It is evident that a direct comparison of the maximum energy of the emitted electrons with the chemical energy calculated merely on the basis of thermodynamical arguments under equilibrium conditions will be wrong

The exact theoretical calculation of the energy of the heterogeneous chemical transformation, corresponding to the instant of the formation of the polar bond, even in our comparatively simple case would be quite hopeless. It

   * Sponer, "Molekülstruktur," p 105, Leipziger Vorträge (1931)
    † London, ' Z Physik,' vol 46, p 455 (1928), and vol 74, p 143 (1932)

would be necessary to determine the distance between the ions of the polar bond at the instant of its formation and to calculate the effect of the adjacent metal atoms upon the bond considered. Neither of these two factors can be estimated accurately. We should like, therefore, to put forward an approximate method which will enable us to estimate the order of magnitude of the amount of energy liberated at the chemical transformation. One great simplification which can be introduced in the heterogeneous change considered is that the problem of interaction between alkali and halogen atoms may be simply reduced to an electrostatic problem of interaction between point charges. In fact, the ions constituting the chemical bond have electronic systems like inert gases, and it is easy to show that at the interatomic distances involved, the deformation (polarization) of the ions of the bond by each other, or by the positive ions and free electrons of the metal, will be small. Therefore, their electric fields will be those due to point charges $\pm e$ at the centre of each.

Consider first the simpler case of the combination of a neutral atom of K, for example, with a neutral atom, let us say, of Cl at the instant when the electron jumps from the K to the Cl atom at the distance r between their centres. We can represent this process by—

K		Cl		K	Cl		K	Cl
◯	+	◯	→	◯	◯	→	⊕	⊖
← ∞ →							← r →	
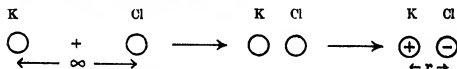
Let us denote the overall energy liberated in this process by (E_s). Now consider the following reverse process, by an alternative route—

K	Cl		K		Cl		K		Cl	Electron
← r →			← ∞ →				← ∞ → ← ∞ →			
⊕	⊖	→	⊕	+	⊖	→	⊕	+	◯	+ ⊖

∞

◯

K
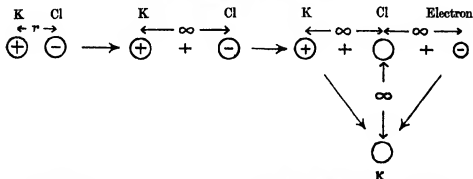
The dissociation of $K^+Cl^-_{(r)}$ into K^+ and Cl^- requires energy e^2/r, the neutralization of Cl^- requires energy A_{Cl} (the electron affinity of Cl) and the neutralization of K^+ supplies energy I_K (the ionization potential of K). It follows that

$$(E_s) = e^2/r + A_{Cl} - I_K \qquad (8)$$

or, in words, the energy liberated instantaneously in the reaction is equal to the mutual potential energy of the two ions at the instantaneous distance r plus the electron affinity of the negatively charged atom minus the initial negative energy of the displaced electron This result is exact and will apply to any reaction of this type (except that, in general, the expression for the potential energy of the ions will be more complicated than $-e^2/r$)

Now consider in what ways the actual heterogeneous reaction will differ from this homogeneous reaction In the first place there will be a certain distance r_1 characteristic for the heterogeneous reaction We shall assume a normal collision diameter and put r_1 equal to the sum of the radii, $r_{Cl} + r_K$, of the neutral halogen atom and of the "neutral atom" of the metal For the latter quantity we shall take one-half of the closest distance between atoms in the metal For the $Cl^- - K^+$ bond we may take $r_{Cl} = 1\ 07 \times 10^{-8}$ cm.* and for $r_K = 2\ 25 \times 10^{-8}$ cm.,* then $r_1 = r_{Cl} + r_K = 3\ 32 \times 10^{-8}$ cm. This distance is probably larger than the equilibrium distance of a normal KCl molecule by about $0\ 5 \times 10^{-8}$ cm In the second place the displaced electron is no longer in the ground state of the K atom , it is in one of the states occupied by the free electrons in the metal Adopting Sommerfeld's theory the minimum negative energy of an electron (at $0°$ K.) will be $\phi = W_a - \mu$ (where ϕ is the work function of the metal, W_a is the total height of the potential barrier and μ is the energy associated with the highest possible state occupied by the free electrons) and this will have to replace I_K in equation (8) There is, however, another difference According to fig 10, which gives a schematic representation of the chemical bond at the instant of formation, an essential difference between this and that of a free molecule is that the negative Cl ion is subject not only to the attraction of the positive K ion, but also to that of the whole mass of metal to the right-hand side of the plane $x = x_0$ Since the negative charge is, in effect, in the plane $x = x_0 + r_{Cl}$, and if we make the further assumption that the field of force to the left of the plane $x = x_0$ is determined by the mirror image of the charge, the final negative energy of the pair of ions will be increased by the amount $\dfrac{e}{4}\left(\dfrac{1}{x_0 + r_{Cl}}\right)$, where the parameter x_0 is determined by the relation $\phi = \dfrac{1}{4}\dfrac{e^2}{x_0}$ Thus we obtain finally

$$E_s = \frac{e^2}{r_1} + \frac{e^2}{4}\left(\frac{1}{x_0 + r_{Cl}}\right) + A_{Cl} - \phi \qquad (9)$$

* Landolt-Börnstein, 'Physikalisch-Chemische Tabellen,' 1924–1931

This formula will only be approximately true, as the distortion of the electron distribution in the metal by the K^+ ion which combines with the Cl^- ion will come into play at these small distances. This would tend to make the expression $\dfrac{e^2}{4}\left(\dfrac{1}{z_0 + r_{\mathrm{Cl}}}\right)$ too large. However, there are other uncertain elements which come in at these distances, arising from our ignorance of the precise form of the electron potential energy distribution as we cross the surface of the solid, and it is probable that, in fact, equation (9) is very little in error. In particular, it is fairly certain that it is less incorrect than the combined inaccuracies of the data to which it is applied.
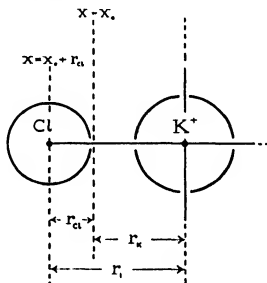

Fig. 10

Since the actual initial state is the gaseous ($COCl_2$) molecule, and not the free (Cl) atom, it is necessary to take into account the energy of the corresponding dissociation of ($COCl_2$). Dissociation of the gaseous molecule will occur simultaneously with the electronic rearrangement of the nascent polar bond, on account of the weakening of the bond connecting the Cl atom to the rest of the $COCl_2$ molecule which is caused by the electron transference. It is well known[*] that in the photochemical decomposition of molecules both the dissociation energy D and the energy of electron transference ε have to be included in the photochemical equation $h\nu = \varepsilon - D$, thus showing that

---

[*] *Cf* Franck, 'Naturwiss,' vol. 19, p 217 (1931).

dissociation occurs *simultaneously* with the electronic rearrangement We have been able to establish, from a comparative study of a large number of different reactions, that in the case of $(COCl_2)$ the energy of dissociation D of the process $(COCl_2) = (CO) + 2(Cl) - D$ is equally distributed between the two Cl atoms This shows that two Cl atoms of the $(COCl_2)$ molecule normally enter into the reaction with the metal simultaneously

Relation (9) will then take the form

$$E_c = \frac{e^2}{r_1} + A_{Cl} + \frac{e^2}{4}\left(\frac{1}{x_0 + r_{Cl}}\right) - \phi - \tfrac{1}{2}D \qquad (10)$$

The electron affinity A_{Cl} of the (Cl) atom can be derived from the grating energy of the alkali halogen crystals, it is $A_{Cl} = 3\ 8\ \pm 0\ 3$ volts * (A more accurate determination of the electron affinity has been made only for the iodine atom, by the method based on the thermal equilibrium at high temperature of CsI vapour)

It may be pointed out that the energy of the reaction E_c can be put in a direct connection with the thermochemical data if we make use of the relation between the grating energy U_{KCl} and the electron affinity A_{Cl} This relation is†

$$U_{KCl} = Q_{KCl} + \tfrac{1}{2}D' + I_K + S_K - A_{Cl},$$

where Q_{KCl} is the heat of the reaction $\tfrac{1}{2}(Cl_2) + [K] = [KCl]$ at $0°$ K, D' is the heat of dissociation of Cl_2, I_K is the ionization potential of the (K) atom, S_K is the heat of sublimation of [K] at $0°$ K   Now,

$$U_{KCl} = M_{KCl} + S_{KCl} \approx \frac{e^2}{r_0} + S_{KCl},$$

where M_{KCl} is the energy of the process $(Cl^-) + (K^+) = (KCl)$, which is approximately equal to e^2/r_0, r_0 being the equilibrium interatomic distance of the (KCl) molecule in the normal state, and S_{KCl} is the heat of sublimation of [KCl] at $0°$ K   We thus obtain

$$E_c = (Q_{KCl} + \tfrac{1}{2}D') + (I_K - \phi) - (S_{KCl} - S_K) + \tfrac{1}{4}\left(\frac{e^2}{x_0 + r_{Cl}}\right) - e^2\left(\frac{1}{r_0} - \frac{1}{r_1}\right) \qquad (11)$$

Taking for $\tfrac{1}{2}D = 1\ 83$ volts, and for the work function of the K_2Na alloy $\phi_{k_2Na} = 2\ 5 \pm 0\ 1$ volts (Richardson, *loc cit*), and therefore $x_0 = 1\ 44 \times 10^{-8}$ cm , we obtain, according to relation (10),

$$E_c = 4\ 34 + 3\ 8 + 1\ 44 - 2\ 5 - 1\ 83 = 5\ 2_5 \text{ volts}$$

---

* van Arkel and de Boer, "Chemische Bindung als elektrostatische Erscheinung," p 63 (Leipzig, 1931)

† *Ibid*, p. 56

with uncertainty at least ± 0.3 volt The calculation according to relation (11) gives practically the same value for E_s, it is less only by 0.1 volt

We obtain the maximum possible value for the energy of the emitted electrons if we consider the de-excitation of the nascent chemical bond by collision of the second kind with an electron of maximum energy μ inside the metal (at $0°$ K) This will be equal to

$$(E_o - \phi_{K, Na})_{max} = 2.7_5$$

It may at once be seen that the calculated value of the maximum energy of the emitted electrons is of the same order of magnitude as the observed, which lies between 2.5_5 and 3.0_5 volts

Since the potential energy of the bond $Cl^- — K^+$ is in inverse proportion to the distance r_1 between the centres of the ions and therefore it is sufficient if the distance is decreased by about 10% ($\Delta r_1 \approx 0.4 \times 10^{-8}$ cm) to give an increase of energy equal to 0.5 volt, it seems to be natural to assume that the observed unsharp limit for the maximum energy (the "tail") is a result of the uncertainty of the collision diameter On the one hand, as gaseous molecules take part in the reaction the collision diameter will depend upon the orientation of the molecule at the instant of collision It is hardly probable, however, that the fact that the $COCl_2$ molecule contains two Cl atoms plays any important part, for the same unsharp upper limit of energies of the emitted electrons was observed, as we shall show in a later paper, also for $(NOCl)$ On the other hand, the collision diameter will depend upon the electron atmosphere of the metal Since the metal is at ordinary room temperature there exists a more or less sharp limit for the maximum kinetic energy of the free electrons in the metal, and we may expect that there will be a more or less abrupt outer limit for the electron atmosphere of the metal, at which most of the halogen molecules will undergo chemical transformation However, there may be some halogen molecules which will penetrate this electron boundary and thus will undergo transformation at a shorter distance from the metal

There are two more factors which will act in the same direction of giving an unsharp character for the distance r_1, and therefore for the upper limit of energies of the emitted electrons One factor is the thermal agitation of the alloy atoms (ions), the K_2Na alloy used in the experiments is quite a mobile liquid at room temperature Another is that the composition of the metal is not homogeneous This latter fact may turn out to be rather important and not only because of the different size of the positive K and Na ions (the

radius of the Na^+ ion is less by about 0.3×10^{-8} cm), but also because of the possible difference in the character of the interatomic forces of the two bonds $Cl^- - K^+$ and $Cl^- - Na^+$.

We might also expect some part of the tail to be caused by the kinetic energy of the partners at the three-body collision, $i.e.$, the gas molecule, the metal atom and the free electron. In particular, the estimation of this temperature effect of the free electrons, on the basis of the Fermi-Dirac distribution function for the electrons inside the metal at 300° K, shows that its contribution to the tail can be appreciable, but only at $V - E_m < 0.2$ volt.

In concluding we should like to take this opportunity of acknowledging our indebtedness to the Department of Scientific and Industrial Research for a grant which has made it possible to carry out these investigations.

Summary

This paper starts by summarizing some general conclusions we have reached from experiments on the reaction between K_2Na and 22 different gases. These include —

(1) The energy distribution is not in general of the Maxwellian type.

(2) The distribution curves all rise from a small value at zero energy ($V = 0$) to a maximum at a certain energy ($V = V_m$) and fall to zero at a certain maximum energy ($V = E_m > V_m$).

(3) These curves have a "tail," like that in the photoelectric effect, and E_m is approached rather gradually. A practical maximum energy E_m is obtained by disregarding the tails. About 99.9% of the electrons have energies below E_m ($E_m > E_m > V_m$).

(4) The distribution curves for energies $> V_m$ and $< E_m$ can all be represented quite closely by $N(V)\,dV = As^{-k(V-V_m)^c}dV$, A, k and c constants. For the most energetic reactions this equation is a fair approximation from $V = 0$ to $V = E_m$.

(5) For the Cl compounds $E_m + D =$ constant, where D is the dissociation energy of the relevant reaction.

(6) At very low pressures the electron emission is proportional to the pressure. It usually rises to a sharp maximum at a quite low pressure and then falls.

(7) The yield of electrons diminishes rapidly as the available chemical energy diminishes.

(8) The facts can be accounted for on the view that in the formation of the polar bond, which involves a spontaneous rearrangement of the electronic systems of the atoms concerned, the bond is stabilized spontaneously by a three body collision with a free metallic electron which carries away all the reaction energy The effect is thus a quantum phenomenon This view gives a reasonable account of the energy distribution It also allows of a simple interpretation of the equation $E_m + D = \text{constant}$ It is $E_m = E_e - \phi$, where E_e is the energy of the corresponding elementary chemical reaction responsible for E_m and ϕ is the work function of the metal *This relation appears to be general and is similar to the fundamental law of photoelectricity*

A more refined and detailed experimental investigation than has hitherto been carried out with phosgene is then given This is followed by a discussion of the low energy part of the spectrum, the determination of the true zero on the volt scale and of E_m and its relation to E_e

The last section confirms the equation $E_m = E_e - \phi$ for the particular case of $COCl_2$

The Structure and Formula of 12-Phosphotungstic Acid.

By J. F. KEGGIN, Ph D

(Communicated by W. L. Bragg, F R S —Received June 14, 1933 —Revised November 27, 1933)

[PLATE 1]

1 Introduction

This acid belongs to a large class of compounds known as the heteropolyacids, of which the structures and exact formulæ have long been a subject for speculation The heteropolyacids are compounds in which one atom of such elements as P, Si, As, B, Al, etc , is combined with a number of atoms of an element such as W or Mo, together with a relatively large number of atoms of oxygen In addition to the elements mentioned, it has been shown that the oxides of a considerable number of other elements show a tendency to form heteropolyacids All formulæ proposed indicate a relatively large number of atoms in the molecule, and a complex structure In spite of the complexity of the molecule, many of these acids are quite stable, and form stable salts with practically all metals The best known compounds of this group are the silicotungstic, silicomolybdic, phosphotungstic and phosphomolybdic acids, in which one atom of silicon or phosphorus is combined with a number of atoms

of tungsten or molybdenum. Mixed acids are also known in which a number of tungsten atoms are replaced by molybdenum atoms, or *vice versa* The heteropolyacids are classified according to the ratio of the numbers of the two types of cations present

Throughout the whole class of heteropolyacids, those acids which have the same cation-cation ratio tend to be isomorphous and have similar properties

These acids have several outstanding properties, the following apply more especially to the 12-acids, though several of the other types of acids are very similar —

(1) They form crystals containing large amounts of water of crystallization

(2) They are usually very soluble in solvents containing oxygen in the molecule*—in water, ether, alcohols, alcoholic esters, ketones, aldehydes, etc, but not in such solvents as benzene which contain no combined oxygen Ether will extract these acids from aqueous solution, forming a system of three layers, with ether on top, an aqueous layer next and at the bottom a saturated solution of the acid in ether It has been suggested† that a loose compound of the oxonium type is formed with ether This property is used in the preparation and purification of the heteropolyacids

(3) They are readily reduced‡ by common reducing agents such as nascent hydrogen, H_2SO_3, etc

(4) Perhaps the most remarkable property is the ability of these acids to form insoluble precipitates, often crystalline, with many substances, which substances often have large molecules With the alkaloids bulky precipitates are formed, the standard method of estimating nicotine makes use of this property They have been suggested as antidotes in cases of alkaloid poisoning Albumen, peptones, etc, also give precipitates with these acids, which are used in their separation They give precipitates with substances containing urea, and with amino-acids form crystalline compounds § With basic dyes they give extremely insoluble lakes which are remarkably stable and fast to light

The present work is concerned with 12-phosphotungstic acid

* Scroggie, 'J Amer Chem Soc,' vol. 51, p 1057 (1929)
† Rosenheim and Jaenicke, 'Z. anorg Chem.,' vol. 100, p 319 (1917)
‡ Wu, 'J Biol Chem.,' vol. 43, p 189 (1920)
§ Drummond, 'Biochem J,' vol. 12, p 5 (1918)

2 *Brief Review of the Literature with Reference to the Constitution of the*
12-heteropolyacids

The heteropolyacids were first discovered by Berzelius[*] in 1826   Among
the more important of the earlier workers on these compounds, De Marignac,[†]
Scheibler,[‡] Sprenger,[§] Soboleff,[||] Kehrmann,[¶] Parmentier,[**] and Copaux[††]
may be mentioned   Most of these workers suggest $H_3PW_{12}O_{40}$, and
$H_4SiW_{12}O_{40}$ as the empirical formulæ of the anhydrous 12-phosphotungstic
and 12-silicotungstic acids, as a result of dehydration experiments

In 1908, Miolati and Pizzighelli,[‡‡] and later Rosenheim and co workers,[§§]
suggested $H_7[P(W_2O_7)_6]nH_2O$ and $H_8[Si(W_2O_7)_6]nH_2O$ as the formulæ of these
acids, as a result of titration experiments   This type of formula is known as
the Miolati-Rosenheim formula, and is now considered as the classical formula

In 1913 W and D Asch[||||] suggested a structure for the 12-acids, in which
the molecule consists of two hexito rings   This gave $H_8SiW_{12}O_{42}nH_2O$ as
the formula for 12-silicotungstic acid

Pauling,[¶¶] in an attempt to explain the properties of the 12-heteropolyacids,
proposed, on theoretical grounds, the first three-dimensional structural
formula in which the positions of the atoms and the exact manner of co-
ordination were indicated   After reviewing the literature, he decided that the
12-phospho-acids are three-basic and the 12-silico-acids are four-basic   Also
that the 12-acids and their salts show a marked tendency to crystallize with
cubic symmetry, which indicates a highly symmetrical molecule   The proposed
molecule is a co-ordinated structure in which 12 tungsten atoms, each sur-
rounded by an octahedron of 6 oxygen atoms, are linked in a continuous shell,
by sharing oxygen atoms, round a central PO_4 or SiO_4 tetrahedral group.
Each WO_6 octahedron shares three oxygen atoms with neighbouring WO_6
octahedra   In the complete acidic anion there are 18 oxygen atoms, each

[*] ' Pogg Ann.,' vol 6, p 369 (1826)

[†] ' C. R. Acad. Sci Paris,' vol 55, p 888 (1862)

[‡] ' Z. Naturwiss Halle,' vol. 40, p 298 (1872)

[§] ' Bull. Soc. Chim. ' vol. 36, p 221 (1881)

[||] ' Ber deuts. chem. Ges ' vol 12, p 16 (1896)

[¶] ' Ber deuts. chem. Ges ' vol 20, p. 1811 (1887)

[**] ' C R. Acad. Sci. Paris,' vol. 92, p 1234 (1881)

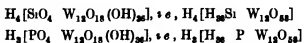[††] ' Ann. Chim. Phys.,' vol. 7, p 118 (1906) , ' Bull. Soc Chim.,' vol. 3, p. 101 (1906).

[‡‡] ' J Pract. Chem.,' vol. 77, p 417 (1908)

[§§] Rosenheim and Pinsker, ' Z anorg. Chem.,' vol 70, p 73 (1911), Rosenheim and
Jaenicke, ' Z anorg. Chem , vol. 100, p. 304 (1917), vol. 101, p. 247 (1917).

[||||] " The Silicates in Chemistry and Commerce," London, vol 15, p. 78 (1913)

[¶¶] ' J Amer Chem. Soc ,' vol. 51, p. 2868 (1929)

shared between two tungsten atoms, thus having their charges completely satisfied   Each of the remaining 36 oxygen atoms is linked to 1 tungsten atom only, and takes up a hydrogen atom to satisfy its charge, giving 36 OH groups as an outer shell   The symmetry is of the cubic point group T_d This gives the formulæ

$$H_4 [SiO_4   W_{12}O_{18} (OH)_{36}], \, i \, e \, , H_4 [H_{36}Si   W_{12}O_{58}]$$
$$H_3 [PO_4   W_{12}O_{18} (OH)_{36}], \, i \, e \, , H_3 [H_{36}   P   W_{12}O_{58}]$$

Thus this type of molecule cannot exist for the dehydrated forms of the 12-acids reported, with oxygen contents less than 58

Scroggie and Clark* attacked the problem of the structure of 12-silicotungstic acid both by chemical and X-ray methods

The acid dried at 100° C was examined by X-rays using the powder method They obtained lines corresponding to a body-centred cube of edge = 12 16 A By density measurements they found that the unit cell contained two molecules   No attempt was made to work out the positions of the atoms, or to get further details from this photograph   Their work showed that 12-silicotungstic acid is 4-basic   The acid dried at 100° C they represent by $4H_2O   SiO_2   12WO_3   4H_2O$, $\, i \, e \, , H_{16}   SiW_{12}O_{46}$

This form of the acid they found to be very persistent, and very strong dehydrating conditions were necessary to remove more water   They succeeded in dehydrating to $2H_2O   SiO_2   12WO_3$, $\, i \, e \, , H_4SiW_{12}O_{40}$, and found that this apparently was the anhydrous acid, as the removal of any further oxygen caused the acid to change its physical and chemical properties completely, indicating a breakdown of the molecule   From these results they proposed a molecule for 12-silicotungstic acid which gave the formula of 12-silicotungstic acid as $H_4 [H_{12}SiW_{12}O_{46}]$

M and E Kahane† studied the dehydration of 12-phosphotungstic acid and came to the conclusion that the dehydrated acid has a formula of the type $H_nP   W_{12}O_{40}$ As the classical Rosenheim-Miolati formula and also Pauling's proposed formula have more than 40 oxygen atoms in the molecule, they consider these formulæ incompatible with their results for dehydrated forms of the acid, and further, consider it unlikely that there should be a different molecule for more highly hydrated forms of the acid.

A large number of hydrates of the 12-acids and their salts have been described by many workers   Representing the 12-acids by the typical formula

* ' Proc. Nat. Acad. Sci. Wash ,' vol. 15, p. 1 (1929)

† ' Bull. Soc Chim.,' vol. 49, p. 557 (1931).

$H_nRM_{12}O_n$, including water of crystallization to avoid confusion, hydrates have been described where n = 40, 44, 46, 58, 58½, 61, 62, 65, 68, 69, 69½, 70, 70½

In addition to the normal 12-acids which have been discussed, so-called iso-12-acids have been reported in the cases of 12-silicotungstic and 12-borotungstic acid The cation-cation ratio is reported to be still 1-12, but the properties of these iso-12-acids differ from those of the normal 12-acids , the iso-acids and their salts crystallize in more complex forms with different amounts of water of crystallization, etc Iso-12-silicotungstic acid was first reported by De Marignac,[*] who also prepared its salts Copaux[†] and Rosenheim[‡] have also studied these iso-12-acids The iso-12-acids are thought to be isomeric forms of the normal 12-acids The literature, however, is not very definite concerning these iso-acids Rosenheim, in his proposed formula, attempts to account for their existence by assigning different properties to different atomic positions in his molecule, whilst Pauling suggests that they may be explained by assuming condensation of two molecules of the normal 12-acid to form the molecule of the iso-12-acid, which would then contain 24 tungsten atoms and 2 silicon or boron atoms

3 Discussion of Literature

The literature concerning the 12-heteropolyacids is very large and much confusion exists owing to uncertainty as to the correct formula of the molecule Many formulæ have been suggested which differ widely The classical chemical formula attributes a basicity of 7 to the 12-phospho-acids and a basicity of 8 to the 12-silico-acids, but the experimental evidence for this is not conclusive Only in very rare cases have salts been reported in which this number of hydrogen atoms have been replaced, e g , some Ag and guanidine salts, and even for these salts it is more normal to have only 3 and 4 hydrogens replaced instead of 7 and 8 respectively The salts in which 7 and 8 hydrogens are replaced are only prepared with difficulty The electrometric evidence supporting these high basicities again cannot be considered conclusive Practically all salts reported support the formulæ which treat with 12-phospho-acids as 3-basic and the 12-silico-acids as 4-basic, and modern workers tend to consider these basicities as correct Also the reactions of the 12-acids indicate a structure of MO_6 octahedra rather than one of MO_4 tetrahedra For example,

---

[*] 'Ann. Chim. Phys ,' vol. 3, p 5 (1864)
[†] 'Ann Chim. Phys.,' vol. 17, p 217 (1909)
[‡] Rosenheim and Jaenicke, ' Z anorg. Chem.,' vol. 101, p 235 (1917)

the MoO_4 group is not usually highly coloured, whereas 12-phosphomolybdic acid is of a bright orange colour, which colour is a characteristic of the MoO_6 group Again, the fact that these acids are very susceptible to reduction would seem to suggest MO_6 groups rather than MO_4 groups

References to hydrates are meaningless unless the formula used for the acid is given Some workers tend to treat different hydrates of the same type of acid as distinct acids, describe them as coming out of the same solution together, with differing crystalline forms, and from these differing crystals prepare salts which they declare to differ according to the hydrate of the acid used Some of these statements are due possibly to the use of impure heteropolyacids , great care must be taken in preparing the 12-acids to ensure that no 9-acid is present Throughout all the published work, however, there appears to be general agreement that the hydrate of the 12-acids which crystallizes out of saturated aqueous solution at room temperature is of the type $H_nRM_{12}O_{70}$, though some workers suggest $H_nRM_{12}O_{69}$, and also that when salts of these acids are dehydrated, the lowest form of the anion is $RM_{12}O_{40}$, removal of more oxygen results in a complete change of properties There is also much evidence that when 12-acid is dehydrated the lowest form is $H_nRM_{12}O_{40}$ In fact several formulæ have been proposed which are based on these facts, the molecule being represented as $H_nRM_{12}O_{40}$

4 The Results of the Present Work

A General Account of the Structure of the Molecule of 12-phosphotungstic Acid, with its Formula, as found by X-ray Analysis [*]—The derivation of this structure is given in a later section of this paper The molecule of 12-phosphotungstic acid has the formula $H_3[PW_{12}O_{40}]$ The phosphorus atom is at the centre of a group of 4 oxygen atoms arranged with their centres at the corners of a regular tetrahedron as in fig 1 Each tungsten atom is approximately at the centre of a group of 6 oxygen atoms, the centres of which are at the corners of a distorted octahedron, as in fig 2

The complete acidic anion $PW_{12}O_{40}^{-3}$ is a co-ordinated structure of point group symmetry T_d, consisting of a central PO_4 tetrahedron, surrounded by 12 WO_6 octahedra as a shell, linked together by shared oxygen atoms. The 12 WO_6 octahedra are arranged in four groups. Each group consists of 3 WO_6 octahedra round a trigonal axis, so that the co-ordinates of the 3 tungsten atoms are of the type $(a \ a \ b) \ (a \ b \ a) \ (b \ a \ a)$, with two co-ordinates

equal, referred to the rectangular axes of cubic symmetry, with origin at the centre of the central phosphorus atom Fig 3 shows the arrangement for one group of 3 WO$_6$ octahedra relative to the PO$_4$ tetrahedron Considering first only this one group of three octahedra, there is 1 oxygen atom shared in
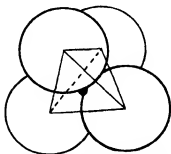

Fig 1 —Four oxygen atoms arranged with centres at the corner of a tetrahedron with a phosphorus atom at the centre
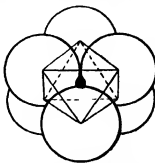
Fig 2 —Six oxygen atoms arranged with centres at the corners of an octahedron, with a tungsten atom at the centre

common between the 3 WO$_6$ octahedra and the central PO$_4$ tetrahedron and each octahedron shares two other oxygen atoms, one with each of the two neighbouring octahedra Thus each octahedron has two edges shared, one
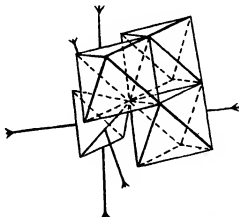

Fig 3 —The arrangement of one group of three WO$_6$ octahedra relative to the central PO$_4$ tetrahedron.

with each of the two neighbouring octahedra Fig 4 shows this arrangement exploded outwards for simplicity The arrows indicate the corners which coincide when in their correct positions as shown in fig 3

Four such groups of 3 WO_6 octahedra are arranged round the central PO_4 tetrahedron in tetrahedral symmetry, so that each oxygen atom of the PO_4 tetrahedron is now an oxygen atom already shared between 3 WO_6 octahedra Fig 5 shows the arrangement with two groups of 3 WO_6 octahedra   For a
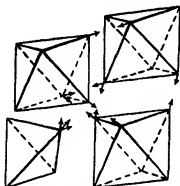

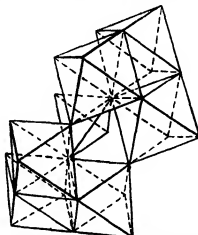
Fig 4 —Exploded diagram of the arrangement shown in fig. 3

Fig 5 —The arrangement of two groups of 3 WO_6 octahedra relative to the central PO_4 tetrahedron.

diagram of the complete acidic anion, in order to avoid confusion, each group of 3 WO_6 octahedra is represented in outline as a solid as in fig 6, which is a representation of the 3 octahedra in fig 3   The complete acidic anion is shown

Fig 6 —Simplified representation of the 3 WO_6 octahedra shown in fig.3

in fig 7, the central PO_4 tetrahedron being shown complete   It will be seen that each WO_6 octahedron, besides sharing 2 oxygen atoms with octahedra in its own group of three, also shares 2 oxygen atoms with octahedra in other groups   In the complete acidic anion, each WO_6 octahedron consists of 1 oxygen atom shared between 3 WO_6 octahedra and 1 PO_4 tetrahedron, 4 oxygen atoms shared between 2 WO_6 octahedra, and 1 oxygen atom unshared with other polyhedra   Also, two edges of each WO_6 octahedron are shared with edges of two other octahedra.

This anion has the formula $PW_{12}O_{40}$ [3]   Hence the molecule of 12-phosphotungstic acid has the formula $H_3PW_{12}O_{40}$ This might be written $H_3[PO_4(WO_3)_{12}]$, to indicate a central PO_4 tetrahedral group surrounded by 12 WO_6 octahedra, each of which is WO_3 in effect   But perhaps

the best form of expression is $H_3[P (W_3O_{10})_4]$, to indicate a modified PO_4^{-3} tetrahedral group, in which each of the 4 oxygen atoms has been replaced by
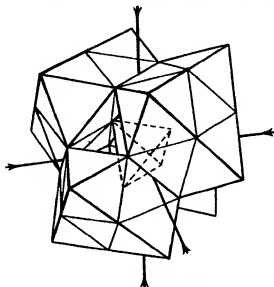
FIG 7 —The complete anion $PW_{12}O_{40}$.

a $W_3O_{10}^{-2}$ group, each $W_3O_{10}^{-2}$ group consisting of 3 WO_6 octahedra sharing oxygen atoms with other octahedra   This formula agrees with the mass of chemical evidence

Co-ordinates of Atoms, and Interatomic Distances—The oxygen atoms fall into four groups, which will be called O_1, O_2, O_3 and O_4 The positions of these types of oxygen atoms are indicated in fig 8, which represents the left-hand octahedron in fig 3   The O_1 oxygen atoms are shared between 3 WO_6 octahedra and 1 PO_4 tetrahedron   The O_2 oxygen atoms are shared between 2 WO_6 octahedra   The O_3 oxygen atoms are also shared between 2 WO_6 octahedra   The O_4 oxygen atoms are unshared with other polyhedra   The O_1–O_3 edges are shared between 2 WO_6 octahedra

FIG 8.—The left-hand octahedron in fig 3, showing the position of the four types of oxygen atoms

The atoms are referred to the rectangular axes of cubic symmetry, with origin at the centre of the central phosphorus atom

The co-ordinates of the atoms are —
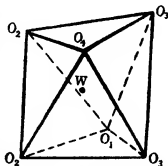
1 P atom at $(0, 0, 0)$

4 O_1 atoms at $(a\ a,\ a,)\ (a,\ \bar{a},\ \bar{a}\ )\ (\bar{a},\ a,\ \bar{a},)\ (\bar{a},\ \bar{a},\ a,)$

$$\text{where } a = 0\ 99\ A$$

12 O_2 atoms at $(\bar{b},\ b,\ c)\ (\bar{b},\ \bar{b},\ \bar{c})\ (b\ \ b,\ \bar{c})\ (b,\ \bar{b}\ \ c)$

$(\bar{b},\ c,\ b)\ (\bar{b},\ \bar{c},\ \bar{b})\ (b,\ c,\ \bar{b})\ (b,\ \bar{c},\ b)$

$(\bar{c},\ b,\ b)\ (\bar{c},\ \bar{b},\ \bar{b})\ (c\ \ b\ \ \bar{b})\ (c,\ \bar{b},\ b)$

$$\text{where } b - 0\ 97\ A\ ,\ c = 2\ 84\ A$$

12 O_3 atoms at $(d,\ d,\ e,)\ (d,\ \bar{d},\ \bar{e}\ )\ (\bar{d},\ d,\ \bar{e}\ )\ (\bar{d},\ \bar{d},\ e,)$

$(d,\ e,\ d,)\ (d,\ \bar{e},\ \bar{d},)\ (\bar{d},\ e,\ \bar{d},)\ (\bar{d},\ \bar{e},\ d,)$

$(e,\ d,\ d,)\ (e,\ \bar{d},\ \bar{d},)\ (\bar{e},\ d,\ \bar{d},)\ (\bar{e}\ \ \bar{d}\ \ d\ )$

$$\text{where } d = 1\ 49\ A\ ,\ e - 3\ 54\ A$$

12 O_4 atoms at $(\bar{f},\ g,\ g,)\ (\bar{f},\ \bar{g},\ \bar{g},)\ (f,\ g,\ \bar{g},)\ (f,\ \bar{g},\ g\ )$

$(\bar{g},\ f,\ g,)\ (\bar{g},\ \bar{f},\ \bar{g},)\ (g\ \ f,\ \bar{g},)\ (g,\ \bar{f},\ g\ )$

$(\bar{g},\ g,\ f,)\ (\bar{g},\ \bar{g},\ \bar{f})\ (g,\ g,\ \bar{f})\ (g,\ \bar{g}\ \ f,)$

$$\text{where } f = 0\ 1\ A\ ,\ g - 3\ 79\ A$$

12 W atoms at $(h,\ k,\ k,)\ (h\ \ \bar{k},\ \bar{k},)\ (\bar{h}\ \ k,\ \bar{k},)\ (h,\ \bar{k},\ k,)$

$(k,\ h,\ k,)\ (k,\ \bar{h},\ \bar{k},)\ (\bar{k},\ h\ \ \bar{k}\ )\ (\bar{k},\ \bar{h},\ k,)$

$(k,\ k,\ h,)\ (k,\ \bar{k},\ \bar{h}\ )\ (\bar{k},\ k\ \ \bar{h},)\ (\bar{k},\ \bar{k},\ h,)$

$$\text{where } h = 0\ 07\ A\ ,\ k = 2\ 495\ A$$

The interatomic distances are as follows —

The PO_4 tetrahedron in the centre is undistorted   All edges (O_1-O_1 distances) are 2 80 A

The WO_6 octahedra are distorted   The shared edges (O_1-O_2 distances) are 2 65 A   The O_1-O_4 distances are 2 70 A   The O_2-O_3 distances are 2 90 A.   The O_3-O_4 distances are 2 65 A   The O_2-O_2 distances are 2 61 A   The O_2-O_4 distances are 3 10 A   The O_4-O_2 distances are 2·80 A.

The tungsten atom is 2 34 A distant from the O_1 oxygen atom, 1 85 A distant from the O_2 and O_4 oxygen atoms and 2 0 A distant from O_3 oxygen atoms

5 *Discussion of this Structure*

From a consideration of the forces acting in this structure, these distances and the distortions are seen to be quite logical The average crystal radii of the P, W, and O atoms may be taken as equal to 0 34 A , 0 62 A , and 1 35 A respectively The tungsten atoms have a major effect in determining the structure, and the positions of the oxygen atoms will be to a large extent governed by them. The tungsten atoms repel each other, and tend to distribute themselves in the most uniform manner possible where their potential energy is lowest Neglecting the very small displacement (0 07 A) of these atoms from the ideal positions, the reasons for which will be dealt with later, in this structure this distribution is realized , the 12 tungsten atoms are arranged on a sphere with the most uniform distribution possible, each tungsten atom being equidistant (3 53 A) from four neighbouring tungsten atoms They may also be regarded as being at the centres of the edges of a regular octahedron, or at the centres of the edges of a cube The oxygen atoms then form distorted octahedra round these tungsten atoms in such a manner as to give this distribution for minimum potential energy of the tungsten atoms most closely The edge of a PO_4 tetrahedron is normally about 2 6 A. In this case the edge is lengthened to 2 8 A, as 3 tungsten atoms act in opposition to the central phosphorus atom and tend to pull the oxygen atoms of the PO_4 group outwards The tungsten atoms are not at the centres of the octahedra Mutual repulsion tends to make the sphere on which they lie be of as large a radius as possible, and in this structure this effect is considerable Hence the distance of the tungsten atoms from the inner O_1 oxygen atoms is relatively large (2 34 A) as compared with their distances from the other oxygen atoms Also, in order to reach positions of minimum potential energy, the tungsten atoms are displaced from the centres of the octahedra so as to be nearer the O_2 oxygen atoms (1 85 A. distant) than the O_3 oxygen atoms (2 0 A distant) In agreement with this displacement, the O_2–O_3 distances are lengthened to 2 90 A and the O_3–O_3 distances and the shared edges, (O_1–O_3 distances) are shortened to 2 65 A.

The formula $H_3PW_{12}O_{40}$ agrees with the large mass of evidence already mentioned, which gives this formula for the anhydrous acid

This structure has some remarkable features It appears that some of the principles determining the structure of complex ionic crystals as formulated by Pauling[*] are not strictly obeyed Each of the 4 oxygen atoms of the type O_1

which form a tetrahedron round the central phosphorus atom, is shared between 1 phosphorus and 3 tungsten atoms. According to Pauling's "electrostatic valence principle," where the electrostatic valence bonds of the cation act in a roughly symmetrical manner and are neutralized by the immediate neighbouring anions, this implies that each O_4 oxygen atom has a force of $+ 4\frac{1}{4}$ acting upon it, if the phosphorus atom has charge of $+ 5$ and the tungsten atom a charge of $+ 6$. Again, there is an outer shell of 12 O_4 oxygen atoms, each of which is directly connected with only 1 tungsten atom. According to the above principle each of these oxygen atoms has a force of $+ 1$ acting upon it. This structure may be considered in two ways. (A) If the bonds of the cations act in a roughly symmetrical manner, then this complex anion has a region of large positive potential at its centre, surrounded by a region of negative potential as a shell, which, by action through a distance across intervening atoms, gives a total charge of $- 3$, or (B) the electrostatic valence bonds of the cations do not necessarily act in a symmetrical manner, the directions of their action being determined by the positions of the unsatisfied anions.

The properties to be expected from this structure agree well with the known properties of 12-phosphotungstic acid.

This acidic anion would be expected to be stable, as the tungsten atoms are practically in positions of minimum potential energy, and the whole structure is compact and tightly bound together.

These acidic anions are complete structural units in themselves, and when packed together in a crystal are not strongly linked to each other, and should thus be relatively easy to separate. Thus the acid would be expected to be highly soluble.

Also any crystalline structure formed by the packing together of these anions would be expected to contain a relatively large amount of water of crystallization. For these anions are large, roughly spherical units, and, when arranged even in close packing, will still leave a considerable volume of unoccupied space. Water of crystallization will tend to pack in these spaces so as to make the whole structure more homogeneous, and as oxygen atoms are very small compared with these acidic anions, there is always room for a relatively large amount of water.

This anion also explains why numerous hydrates are formed by the acid. As the atoms are arranged in a fairly uniform manner, and the charge is small for such a large group of atoms, this anion may be considered as a large, practically spherical, unit, with a fairly uniform charge distribution over its

surface Such a unit has no strong directional forces which would tend to make one type of packing more probable than any other arrangement. Thus it is to be expected that quite a number of arrangements would exist. Also, as these units are so uniform in shape and charge distribution, they will tend to pack in simple arrangements which explains the tendency for the hydrates to be cubic, despite the complexity of the anion.

The tungsten atom, by reason of its small size, may be surrounded by a tetrahedron of oxygen atoms, as well as by an octahedron, as in this structure Thus the reduction of the present arrangement should not be difficult.

The marked tendency of these acids to combine with large organic molecules to form insoluble precipitates is possibly connected with the large, shell-like region of negative potential surrounding the anion

The basicity of three for this structure agrees with that found by most chemical workers Also the oxygen content of the molecule—40 atoms of oxygen—agrees exactly with the results obtained for the anhydrous acid by many workers on the dehydration of the acid and its salts.

6 *Experimental*

The preparation of the acid used in this work was that described by Wu *
It was found that if no HCl was added during the last ether extraction, the product was pure 12-phosphotungstic acid, though the omission of HCl reduces the yield

The colourless octahedra which crystallize from aqueous solutions at room temperatures are extremely unstable, and commence to lose water and to break down to a white powder immediately on drying Thus, though by taking precautions against loss of water an apparently good photograph of this hydrate was obtained, this photograph was not used in this case owing to the uncertainty introduced by the instability of the crystal The structure of this hydrate, however, has since been determined

Dehydration of the Acid —In order to obtain a more definite photograph, a more stable hydrate was sought It was assumed that the hydrate which crystallizes out of saturated aqueous solution at room temperature in colourless octahedra was of empirical formula either $H_7PW_{12}O_{70}$ or $H_5PW_{12}O_{69}$ This was the only assumption made as regards the formula, and losses of water on dehydration were calculated on the first formula Whether H_7 or H_3 is

taken as the basicity is immaterial, owing to the large molecular weight of the acidic anion

In order to find the loss in weight, it was necessary to weigh this unstable hydrate To do this with as little error as possible, large crystals were grown, of dimensions of the order of 1 cm These crystals were taken out of the solution, dried quickly with filter paper, put in a closely stoppered bottle and weighed immediately By using large crystals, surface action had a relatively small effect and it was found possible to repeat results quite accurately

This unstable hydrate was allowed to reach constant weight in the open at about 70% RH 15 6 mols of water were lost An X-ray photograph of this product showed a mixture with no distinct lines

Drying over $CaCl_2$ at atmospheric pressure and room temperature was next tried The acid reached constant weight with a loss of 22 5 mols of water On standing in the open this product took up only 0 5 mols of water, which was probably due to surface adsorption, and indicated that this product is fairly stable This gave a photograph with sharp lines On drying over P_2O_5 in vacuo, the weight was practically constant with a loss of 23 5 H_2O On prolonged drying, however, over a period of several days, the weight continued to fall very slowly, until after about a week, 24 mols of water were lost After this period the acid commenced to turn brown on the surface, indicating that disintegration of the molecule had commenced For losses of water ranging from 22 5 mols to 23 5 mols the product gave identical sharp lines but after losses of more than 23 5 mols of water the lines commenced to broaden, and after a loss of 24 mols of water the lines were distinctly blurred, which indicates the beginning of a change in the crystal structure There is a definite structure in this range, but the number of molecules of water present is not definitely fixed by the above results The water content of this hydrate will be considered later

X-ray Technique—The X-ray photographs were taken by the powder method in a camera of the modified Debye-Scherrer type as described by Bradley and Jay * The specimen to be photographed is in the form of a powder rod Owing to the chemical activity of this acid, and its variable water content, the normal method of preparing the powder rod, by fixing the powder to a hair with adhesive, was not used In order to avoid the possibility of change, the powder was packed into a fine capillary of Lindemann glass, which was sealed, mounted in the camera and used as a specimen This glass

has a low absorption for X-rays, being composed of lithium and beryllium borates

The observed intensities of reflection were obtained by measuring the blackening of the powder photograph by means of a Cambridge microphotometer designed by Dobson * The figures for blackening were then converted into intensity values by means of a calibration curve for the emulsion used, in which exposure is plotted against blackening The intensity measurements were then plotted against distance along the film, and an integrated value of the intensity of each line was obtained by determining the area under the curve and above the base line of general blackening

The structure investigated in this work was that of the dehydrated 12-phosphotungstic acid discussed before, which gave sharp lines The acid actually photographed was the product obtained by dehydrating the octahedral crystals over P_2O_5 *in vacuo*, with a loss in weight corresponding to loss of 23 5 mols. of water

CuK_α radiation was used A typical powder photograph of this hydrate is shown in Plate 1

7 *Determination of the Lattice*

The values of Σh^2 for the lines were found to be all even numbers, except for two very faint lines corresponding apparently to $\Sigma h^2 = 33$ and 41 These two lines were neglected at first, as it was thought that they were due to slight impurity An arrangement of lines where Σh^2 corresponds to consecutive even numbers is a characteristic of the body-centred cubic arrangement. Also, as lines where $\Sigma h^2 = 28$, 60, 92, etc , which are theoretically impossible, were missing from the photograph, it was assumed, at first, that this structure was a body-centred cubic arrangement It was found later that this was not quite the true arrangement The effect of the modification necessary, is, however, extremely small This will be considered later The value of "a," the length of the edge of the unit cube, was now calculated for each line The results are given in Table I

The usual practice of comparing the observed $\sin^2\theta$ with the calculated $\sin^2\theta$ is unnecessary here

By plotting these values of "a" against $\cos^2\theta$, and extrapolating to $\cos^2\theta = 0$,† the true value of the edge of the unit cube was found to be 12 141 ± 0 005 A

* ' Proc Roy Soc.,' A, vol. 104, p. 248 (1923)

† ' Proc Phys. Soc.,' vol. 44, p. 563 (1932)

The density of this hydrate was determined by the displacement of benzene, using a density bottle, and was found to be 5 6   The density calculated for two molecules of $H_3PW_{12}O_{44}$ in a cube of side 12 14 A is 5 55   This agrees well with the experimental value   For a body-centred cubic arrangement, this implies that there is an anion at each corner of the unit cube and one at the centre, all anions being equivalent for this symmetry

Table I

Σk^2	" a " in A	Σk^2	" a " in A	Σk^2	" a " in A
2	11 665	60	—	118	—
4	11 827	62	12 113	120	—
6	11 891	64	—	122	12 139
8	11 937	66	12 115	124	—
10	11 955	68	12 118	126	12 141
12	11 961	70	12 122	128	—
14	12 004	72	12 122	130	—
16	12 007	74	12 121	132	12 147
18	12 027	76	—	134	12 145
20	12 035	78	12 124	136	—
22	12 040	80	—	138	12 147
24	—	82	12 125	140	—
26	12 052	84	—	142	12 147
28	—	86	12 129	144	—
30	12 069	88	—	146	—
32	12 080	90	12 130	148	—
34	12 079	92	—	150	12 147
36 36	12 078	94	12 127	152	12 143
38	12 075	96	—		
40	12 083	98	12 130		
42	12 083	100	12 129		
44	12 085	102	12 129		
46	—	104	—		
48	12 093	106	12 134		
50	12 101	108	—		
52	12 106	110	12 132		
54	12 099	112	—		
56	12 101	114	—		
58	12 111	116	12 135		

The above, together with the observed intensity values, were all the data available, as no single crystal data could be obtained

The problem was now to locate the atoms in the structure by use of the above data

8   Location of the Tungsten Atoms

As the scattering power of a tungsten atom for X-rays is much greater than that of either an oxygen or a phosphorus atom, it was possible to locate the 12 tungsten atoms quite accurately, by neglecting all other types of atoms at first, and considering the agreement between the observed intensities and the

intensities calculated for the 12 tungsten atoms only It was assumed that there were 12 tungsten atoms in each molecule of the acid, and that the anions were arranged in body-centred cubic packing

The simplest way to arrange groups of 12 tungsten atoms to agree with body-centred cubic symmetry, is to arrange them in the manner already given in the section describing the structure of the anion, each group of 12 tungsten atoms having point group symmetry T_d In this arrangement the positions of the atoms are defined by only two variables, and it is thus possible to represent atomic positions on a graph When such groups of atoms are arranged with body-centred packing, the space group is T_d^3 From a consideration of the observed intensities it was possible to impose very rough limits for the calculated intensities which would be consistent with those observed on the film In this way curves defining areas of possible atomic positions could be drawn on a graph for each reflection This was done for a large number of reflections until only a small area of possible positions for the tungsten atoms was left
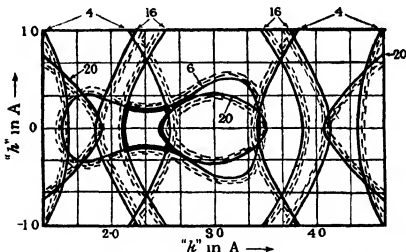
Fig 9 —Curves locating the final small area of possible positions for the tungsten atoms. The final area is heavily outlined

Fig 9 shows the location of the final area of possibility This area is shown heavily outlined, and the reflections used for this location are shown The areas on the shaded sides of the curves are areas of forbidden co-ordinates for the tungsten atoms The area left gives possible co-ordinates for the tungsten atoms between the limits $h = 2$ 155 A $\rightarrow 2$ 51 A , $k = 0$ 185 A $\rightarrow 0 \rightarrow - 0$ 185 A Thus the possible variation of h or k is not more than about 0 36 A The location is

surprisingly definite, even though the limits of possible intensities imposed were quite rough, owing to the large allowances made for the possible effect of atoms other than tungsten In spite of this, a sufficient number of sensitive lines, for which the intensity varies very rapidly for small changes in the atomic co-ordinates, were found to give this small final area of possibility A similar method was used by W L Bragg and Warren* in work on the silicates The mean location is $h = 0$, $k = 2$ 33 A

To get a still more accurate location of the tungsten atoms, the intensities of many lines were now worked out for sets of co-ordinates in this area, still considering only the tungsten atoms By considering the best general agree ment between observed and calculated intensities, it appeared that the most probable co-ordinates for the tungsten atoms are $h = 0$, $k = 2$ 495 A The general agreement for these co-ordinates is reasonably good for all lines

9 The Structure of Co-ordinated Oxygen Polyhedra agreeing with these Tungsten Co-ordinates

It was assumed that the oxygen atoms would be arranged round the phos phorus and tungsten atoms with their centres at the corners of polyhedra, the cations being roughly at the centres of these polyhedra, as is usual for structures of the complex ionic type

The crystal radii of the phosphorus tungsten and oxygen atoms are usually taken as equal to 0 34 A , 0 62 A , and 1 35 A respectively

The positions of the tungsten atoms were fixed, and to agree with symmetry a phosphorus atom must be at the centre of each group of 12 tungsten atoms An arrangement of oxygen polyhedra around these fixed atoms had now to be found which would fulfil the following conditions —

(1) The distances between the centres of neighbouring oxygen atoms in the structure must be within the limits 2 50 A to 3 10 A

(2) The acidic anions must pack in a cube of side = 12 14 A so that the distances between the centres of neighbouring atoms in adjacent anions are of the correct dimensions There must be two anions in each cube

(3) The number of hydrogen atoms necessary to give a neutral structure, i e, the basicity of the acid, must be reasonable, preferably 3 or 7 to agree with the bulk of chemical evidence

(4) The stability of the acid suggests that the polyhedra should be well linked together by sharing oxygen atoms

* 'Z. Kristallog ,' vol. 69, p 168 (1928).

Many arrangements were tried with various types of polyhedra, but the conditions imposed were found to be very stringent, and condition 1 alone eliminated decisively all arrangements other than the anion which was found to be correct and which has been described This structure was found to fulfil all the other conditions, and gave the formula of the molecule as $H_3PW_{12}O_{40}$ It is interesting to note that in none of the structures tried was a basicity of 7 indicated for this acid

10 *The Arrangement of these Anions in the Structure of the Hydrate Investigated*

The symmetry of this anion is essentially tetrahedral, and in considering the orientation of the anions it is convenient to refer to the orientation of the central PO_4 tetrahedron The O_a oxygen atoms are above a base, and the O_b oxygen atoms are above an apex of this central tetrahedron

The structure which has been described for the anion of 12-phosphotungstic acid is very symmetrical At first it was thought that the anions were packed
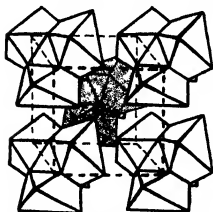
FIG 10 —True body centred arrangement
($T_d{}^3$)
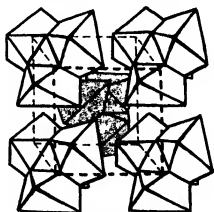
FIG 11 —Arrangement $O_h{}^4$

in a body-centred cubic arrangement, as all the lines on the powder photograph indicated this type of packing, with the exception of two very faint lines corresponding to $\Sigma h^2 = 33$ and 41, which were at first neglected as being due to impurity In this arrangement the orientation of all anions is identical, the anions being arranged base to apex right through the structure This arrangement is shown in fig 10 The space group for this arrangement is $T_d{}^3$, and no reflections for which Σh^2 is odd are possible

On further consideration, it was realized, however, that an arrangement where the anions were base to base and nose to nose in the structure would differ only slightly from the true body-centred arrangement This arrangement is shown in fig 11 The space group here is O_h^4, and the only difference between this packing and the previous body-centred packing is that the anion in the centre of the cube is inverted Thus, if the tungsten co-ordinates are actually $h = 0$, $k = 2$ 495 A , there will be no change at all in the arrangement of the tungsten atoms, and as the oxygen arrangement is also fairly symmetrical, the change in the oxygen lattice will not be great Thus it is to be expected that the photographs for these two types of arrangement would be very similar

For the O_h^4 arrangement, lines where Σh^2 is odd are possible, but only oxygen atoms contribute to these reflections if $h = 0$ for the tungsten atoms Hence these lines will be very weak

The intensities of reflection for both arrangements were calculated, and compared with the observed intensities, in order to decide which arrangement is correct An attempt was also made to find positions for the molecules of water of crystallization

The True Body-centred Arrangement (T_d^3) —In this arrangement the distance between the centres of neighbouring oxygen atoms of adjacent anions is 2 7 A , which is reasonable Here the O_3 oxygen atoms of one anion touch the O_6 oxygen atoms of the adjacent anion

It is impossible to pack six molecules of water* in this structure to agree with symmetry.

A possible arrangement giving seven molecules of water per molecule of acid may, however, be suggested A molecule of water may be placed at the centre of each face of the unit cube—at $b\ o\ o$, $o\ b\ o$, $o\ o\ b$, $\bar{b}\ o\ o$, $o\ \bar{b}\ o$, $o\ o\ \bar{b}$, where $b = 6$ 07 A This gives three molecules of water per molecule of acid The centres of water molecules in such positions are 3 2 A from the centres of neighbouring oxygen atoms in the cube face, and 3 3 A from the centres of neighbouring oxygen atoms in a direction perpendicular to the cube face These water molecules have thus considerable freedom of motion The other four molecules of water might be arranged between the acidic anions, on the trigonal axes of the cube, in tetrahedral symmetry, in positions aaa, $a\bar{a}\bar{a}$, $\bar{a}a\bar{a}$, $\bar{a}\bar{a}a$, where $a = 3$ 28 A Here, however, the centre of each water molecule is only

---

* The term "water molecule" is used here in a general sense to indicate those oxygen atoms which could be removed as water without affecting the chemical properties of the acid. No attempt is made to define the positions of the hydrogen atoms

2 57 A distant from the centres of six neighbouring oxygen atoms The distance is somewhat small

The Arrangement $O_h{}^4$ —In this arrangement, where the two adjacent anions are base to base the oxygen atoms of the anion do not touch, being about 3 5 A apart There is, however, just room for a molecule of water in the hollow left here between the anions, which would hold them apart The water—O_2 oxygen distance is 2 9 A The positions of these four water molecules are $a\overline{a}a$, $\overline{a}aa$, $a\overline{a}a$, $aa\overline{a}$, where $a = 3\ 03$ A This arrangement contributes two molecules of water per molecule of acid Where the two adjacent anions are apex to apex, the O_3 oxygen atoms of one anion touch the O_4 oxygen atoms of the neighbouring anion, the distance between their centres being 2 85 A There is no room for a molecule of water between the anions here

Three more water molecules may be placed, as before, at the centres of the faces of the unit cube This gives, in all, five molecules of water per molecule of acid for this arrangement

11 *Comparison of the Intensities of Reflexion Calculated for these two arrangements with those observed on the Photograph*

The intensities of reflection for these two arrangements were now calculated and compared with the observed intensities The results are given in Table II

For the $O_h{}^4$ arrangement, the tungsten atoms were first considered to have co-ordinates $h = 0$, $k = 2\ 495$ A With such co-ordinates the tungsten atoms do not contribute to reflections where Σh^2 is odd It was found that, though lines 33 and 41 were the strongest of the odd lines, they were not quite strong enough to account for the observed intensities It was found, however, that if the tungsten atoms were shifted a very small distance (0 07 A) to have co-ordinates $h = 0\ 07$ A , $k = 2\ 495$ A , so that these atoms began to contribute to the odd lines, the effect was greatest on lines 33 and 41, and gave calculated values which agreed with the observed intensities

The third column in Table II gives the calculated intensities of reflection when the tungsten atoms only are considered The values for lines where Σh^2 is odd refer only to the $O_h{}^4$ arrangement, as for the $T_d{}^2$ arrangement the values for these reflections are zero As the calculated intensities for tungsten atoms only, for reflections where Σh^2 is even, are practically identical for the two arrangements, the values given in this column for these reflections refer to both arrangements

Table II.

Σh^2	hkl	Calculated intensities 12 tungsten atoms only for both arrangements	Calculated intensities for T_d^2 arrangement		Calculated intensities for O_h^4 arrangement	Observed intensities
			For $PW_{12}O_{40}$	For $PW_{12}O_{40}$ $7H_2O$	For $PW_{12}O_{40}$ $5H_2O$	
1	100	28	—	—	—	—
2	110	0 4	46	43	43	43 5
3	111	—	—	—	0 6	Absent
4	200	12	13 5	14 5	12 5	12
5	210	—	—	—	—	—
6	211	12	11 5	13	13	12
7		—	—	—	—	
8	220	32 5	42 5	29	32 5	34 5
9	300 221	0 3	—	--	0 2	Absent
10	310	28	24	26	26	26 5
11	311	0 2	—	—	0 7	Absent
12	222	87	99	97	101	112
13	320	—	—	—	—	—
14	321	3 5	4	3 2	1	4 1
15		—	—	—	—	
16	400	40	47 5	44 5	42 5	45 5
17	410 322	0 01	—	—	0 2	Absent
18	330 411	22	18 5	18	18 5	21 5
19	331	0 5	—	—	0 7	Absent
20	420	22 5	17	18	18	13
21	421	0	—	—	0 07	Absent
22	332	116	111	108	109	101
23		—	—	—	—	
24	422	0 02	1	3 1	2	?
25	500 430	—	—	—	—	—
26	510 431	82	62 5	62 5	62	55 5
27	511 333	1 0	—	—	1 6	·
28		—	—	—	—	
29	520 432	0 2	—	—	1 1	?
30	521	34 5	17	18 5	18 5	16
31		—	—	—	—	
32	440	15	14	18	16 5	14
33	441 522	1 2	—	—	1 8	Just visible
34	530 433	6 1	6 3	7 8	6	5 9
35	531	0 5	—	—	0 35	Absent
36	600 442	15 5	16 5	17	16	16 5
37	610	—	—	—	—	—
38	611 532	39	45	46 5	46	45
39		—	—	—	—	
40	620	14 5	15	10 5	11 5	14

X-Ray powder photograph of 12-phosphotungstic acid over P_2O_5 *in vacuo* $H_3PW_{12}O_{40} \cdot 5H_2O$ (Cu Kα radiation) (a_0 in $a = 12\ 14$ Å)

Table II—(continued)

Σh²	hkl	Calculated intensities 12 tungsten atoms only for both arrangements	Calculated intensities for T_d^3 arrangement		Calculated intensities for O_h^5 arrangement	Observed intensities
			for $PW_{12}O_{40}$	for $PW_{12}O_{40}\ 7H_2O$	For $PW_{12}O_{40}\ 5H_2O$	
41	521 640 443	2 8	—		4 15	4
42	541	27	29	27 5	27 5	29
43	533	0 06	--		0 35	Absent
44	622	5 6	6 4	6 2	6 8	7 2
45	630 542	0 25	—		0 5	Absent
46	631	2 1	1 6	1 9	1 9	?
47	—	—				
48	444	1 9	4	5 2	4 7	5 2
49	700 632	0 1			0 2	Absent
50	710 550 543	98 3	111	112	111	105
51	551 711	1			0 8	Absent
52	640	5 6	9 4	8 9	9 6	8 4
53	720 641	0 2	—		0 8	Absent
54	721 633 552	12 5	14	14	14	11
55	—	—				
56	642	5	6 7	4	4 3	5 8
57	722 544	0 26	--		0 0	Absent
58	730	13 5	10	10 5	10 4	10
59	731 553	0 45			0 6	Absent
60	—	—				
61	650 643	0 1	—		0 3	Absent
62	732 651	117	120	116	118	130
63	—	—				
64	800	0 16	0 1	0 01	0 2	Absent
65	810 740 652	0 35	—		1 8	?
66	811 741 554	47 5	51	51	51	58
67	733	0 04	—		0 2	Absent
68	820 644	11	12 2	12 5	12 8	12 8
69	821 742	0 4	—		0 95	Absent
70	653	11	11 9	12 3	12 4	12 1
71	—	—				
72	822 660	33	41	46	45	43

All intensities are reduced to the same scale to make comparison simpler A temperature factor $e^{-B\sin^2\theta}$ was applied to the calculated values, where B = 2 0 In calculating these intensities the usual corrections were made for 0 and absorption

No correction was made for the possible effect of motion of the three water molecules in the faces of the cube   Motion would tend to decrease the effect of these molecules on the intensity

12 Discussion of Results

Considering the intensities calculated for the tungsten atoms only, for the lines where Σh^2 is even the agreement with the observed intensities is quite good   This applies to both arrangements   For the odd lines given by the O_h^4 arrangement, the agreement for tungsten atoms only is also reasonable When the oxygen atoms are included, however the agreement is much better, for both arrangements   From a consideration of the agreement for the even lines only, it is difficult to decide which arrangement is better, as the differences are very small, though the O_h^4 arrangement would appear to be slightly better

For the odd lines, however, which are given only by the O_h^4 arrangement, the agreement is also good   In the numerical scale used here to represent intensity values, where strong lines have values in the region of 100, the lower limit of visibility is in the region 1 to 2   Thus line 33 is just visible, and line 41 is distinctly visible   From the calculations it appears that lines 27, 29 and 65 of the odd lines might also be visible, and when looked for could just be detected, though normally they would not be noticed   All the other odd lines were invisible

This agreement of the odd lines, in addition to a slightly better agreement for the even lines for the arrangement O_h^4, appears to prove decisively that the anions are arranged in this manner, and not in the body-centred cubic arrangement T_d^3

This agreement for the odd lines provides a very sensitive check on the correctness of the proposed structure   For, with 45 oxygen atoms present, it is highly probable that any error in their location would give calculated values for the intensity of some odd reflections which would be well above 2 on this scale, as the effect of the oxygen atoms can be quite large   This is well shown in the various intensity values calculated for lines 2, 26 and 30 in the table

Thus there are only five molecules of water per molecule of acid in this partially dehydrated acid   This is of particular interest, as later work on the structure of the so-called 30 hydrate of this acid indicates that the octahedral crystals contain only 29 molecules of water per molecule of acid   Most workers have described a loss of 24 molecules of water per molecule of acid when the octahedral crystals are dehydrated to the stable hydrate investigated here   In the present work sharp lines were not obtained for losses of water of more than 23 5 molecules per molecule of acid, but it is highly probable that a certain amount of moisture is adsorbed on the surface of the fine powder   This water, though not actually in the structure, would tend to decrease the loss in weight   Thus a water content of $5H_2O$ for this hydrate may be said to agree with experimental results

The author wishes to thank Professor W L Bragg, F R S , for his stimulating interest in the work, which was carried out in the Physical Laboratories of the University of Manchester , also Dr A J Bradley for his helpful discussion

13 Summary

The structure of the molecule of 12-phosphotungstic acid has been found by X-ray analysis, using the powder method   The formula of the acid is $H_3[P (W_3O_{10})_4] nH_2O$ The anion consists of a central PO_4 tetrahedral group surrounded by 12 WO_6 octahedral groups as a shell, linked together by shared oxygen atoms   The symmetry is T_d The positions of the atoms are given   This structure has some unusual features   In the partially dehydrated acid investigated, which contains five molecules of water per molecule of acid, these acidic anions pack together with cubic symmetry, the edge of the unit cube being 12 $14_1 \pm 0 005 A$ symmetry $O_h{}^4$ There are two molecules of acid in the unit cube   This formula agrees with the bulk of chemical evidence

The structure was worked out rigorously from experimental results   The method used is described   From the observed intensities of reflection the positions of the heavy tungsten atoms were found, in this first stage the effect of all other types of atoms being neglected   A graphical method was used   This preliminary location of the tungsten atoms was surprisingly definite

A structure of co-ordinated oxygen polyhedra was then found which would give these tungsten positions and also fulfil all other conditions   The com-

parison of observed intensities and those calculated for the complete acid anion is given The agreement is good and proves the correctness of the structure

A brief summary of the properties of the 12-heteropoly acids, and the more important papers in the literature relating to their constitution, is given and discussed

The structure found in the present work is described

This structure is discussed and its bearing on the properties of the acid is considered

The preparation of pure 12-phosphotungstic acid is given and its dehydration described

The experimental X ray technique is described briefly

The method of locating the tungsten atoms is described and the conditions to be fulfilled by the structure are given Two types of arrangement of these anions in the unit cube were found to be possible These are discussed

The problem of the positions of the molecules of water of crystallization for both types of arrangement is discussed

The comparison of observed and calculated intensities is given, and discussed

A General Proof of Certain Fundamental Equations in the Theory of Metallic Conduction

By H. Jones and C. Zener, Wills Physical Laboratory, University of Bristol

§ 1 Introduction

In the modern theory† of electronic conduction the electrons are considered, when the thermal motion of the lattice is neglected, as moving in a periodic potential with the property

$$V(x + la, y + ma, z + na) = V(x, y, z)$$

The wave equation for an electron in this field is

$$\left\{ \frac{h^2}{8\pi^2 m} \nabla^2 + E_K - V \right\} \psi_K = 0 \tag{1}$$

Bloch has shown that this equation has solutions of the form

$$\psi_K = e^{iK \cdot R} U_K(R),$$

where U_K has the periodicity of the lattice.

The quantity $(h/2\pi) K$ has properties analogous to the momentum of free electrons. In particular, the statistical weight of an element of volume in K space is independent of K, so that the number of electrons per unit volume of K space is constant for all values of K having energy below the surface of the Fermi distribution. This surface, which is, of course, identical with a surface of constant energy, is spherical only in the special case of free electrons (fig. 1).

The average velocity of an electron in state ψ_K is

$$v_K = \frac{h}{4\pi m i} \{ \psi^*_K \operatorname{grad} \psi_K - \psi_K \operatorname{grad} \psi^*_K \} / [\psi_K \psi^*_K], \tag{2}$$

where $[\psi_K \psi^*_K]$ denotes the average value of $\psi_K \psi^*_K$ for all points of space. In the special case of free electrons ($U_K = \text{const}$) v_K is related to K by the equation

$$v_K = (h/2\pi m) K$$

† Initiated by F. Bloch, ' Z. Physik,' vol. 52, p. 555 (1928)

For the more general case the relation

$$\mathbf{v_K} = \frac{2\pi}{h} \, \text{grad}_K \, E_K \tag{I}$$

has been suggested, and proved in certain particular cases † One purpose of this paper is to give a general proof (§ 3)

Secondly, we investigate the effect of uniform electric and magnetic fields upon the Fermi distribution Kikuchi and Nordheim‡ have shown that if $f(\mathbf{K}, t)$ is the Fermi distribution function, then if we take an electron with a wave function

$$\psi(x, y, z, t) = \iiint q(\mathbf{K}, t) \, \psi_{\mathbf{K}}(x, y, z) \, dK_x \, dK_y \, dK_z \tag{2A}$$

which satisfies the initial condition

$$|q(\mathbf{K}, 0)|^2 = f(\mathbf{K}, 0)$$

then for all later times

$$\frac{\partial f}{\partial t} = \frac{\partial}{\partial t} |q|^2$$

In the presence of an electric field $\mathbf{F}$, $|q(\mathbf{K}, t)|^2$ will be determined by the wave equation

$$\frac{h}{2\pi i} \frac{\partial \psi}{\partial t} - \frac{h^2}{8\pi^2 m} \nabla^2 \psi = V\psi + e\mathbf{F} \cdot \mathbf{R}\psi \tag{3}$$

In the case of free electrons it is easy to show that $\mathbf{F}$ produces a translation of constant velocity $(2\pi/h) e\mathbf{F}$, that is

$$\frac{\partial}{\partial t} |q|^2 = -\frac{2\pi}{h} e\mathbf{F} \cdot \text{grad}_K |q|^2 \tag{II}$$

and various attempts§ have been made to give a general proof In §4 we show that (II) is a direct consequence of (3), provided the excited bands (§ 2)

---

† Bloch, *loc cit*, gave a proof of I in the limiting case of tightly bound electrons

Peierls, 'Z Physik,' vol 53, p 255 (1929), gave a general proof with the assumption that U_K varies very slowly with $\mathbf{K}$

‡ 'Z. Physik,' vol 60, p 652 (1930)

§ Bloch, *loc cit*, gave a proof where $|q(\mathbf{K})|$ has the form of a Gauss error function, and in which the excited bands were neglected

Peierls, *loc cit*, attempted a general proof The unsatisfactory points in his proof are specifically noted in § 4

Peierls, 'Ergebn Exak. Naturwiss,' vol 11, p 279 (1932), has pointed out that the principle of conservation of energy, combined with I, requires that the average of a wave packet in $\mathbf{K}$ space have the velocity $(2\pi/h) e\mathbf{F}$

are ignored Further, we shall show that when F is so small that the probability that the electron makes transitions from one band to another is negligible,† then (II) is true, provided perturbed ψ_K's are taken in (2A) which bear the same relation to the unperturbed wave functions as the Stark effect functions do to the unperturbed functions of an atom

The energy and velocity of these perturbed wave functions are still related by (I)

In the presence of a magnetic field no velocity can be associated with a stationary state ψ_K, in analogy with there being no unique relation between velocity and momentum in classical mechanics Nevertheless, if a wave packet be represented by

$$\psi\,(x, y, z, t) = e^{i\lambda\,(\mathbf{R}\,\,t)} \iiint g\,(\mathbf{K}, t)\,\psi_K\,dK_x\,dK_y\,dK_z \qquad (4)$$

the gauge invariance‡ of the wave equation may be so used that the average velocity [v] of the wave packet is

$$\frac{2\pi}{h} \iiint (\mathrm{grad}_K\,E_K)\,|g|^2\,dK_x\,dK_y\,dK_z \qquad (5)$$

We then find (§ 5) that $|g\,(\mathbf{K}, t)|^2$ satisfies the equation

$$\frac{\partial}{\partial t}\,|g|^2 = \frac{\pi e}{hc}\,\mathbf{H}\ \ (\mathbf{v}_K + [\mathbf{v}]) \times \mathrm{grad}_K\,|g|^2 \qquad (III)$$

for an interval of time short in comparison to the period of the Larmor precession Thus when $|g|^2$ is such a sharp function of K that [v] becomes identical with the velocity $\mathbf{v}_{K\,(t)}$ at the centre of the wave packet, the wave packet $|g|^2$ moves along a surface of constant energy with the velocity $(2\pi e/hc)\,\mathbf{v}_{K\,(t)}\,\diagup\,\mathbf{H}$

§ 2 *Properties of the Eigenfunctions*

The properties of ψ_k essential for the analysis of the following paragraphs may be derived from a general consideration of the differential equation (1) It will be sufficient to analyse the one dimensional wave equation

$$\left\{\frac{h^2}{8\pi^2 m}\frac{d^2}{dx^2} - V + E_k\right\}\,\psi_k = 0 \qquad (6)$$

with

$$V\,(x + na) = V\,(x) \qquad (7)$$

---

† Zener, communicated to the Royal Society
‡ Pauli, ' Handbuch d. Physik,' 2nd ed., vol 24/1, p 110 (1933)

It may be shown by a variety of methods† that the solutions which remain everywhere finite have the form

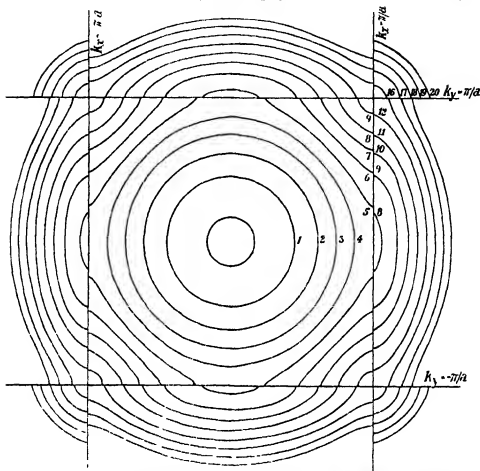$$\psi_k = e^{ikx} U_k(x),$$ (8A)

FIG 1 —The curves represent the contours of the energy in the plane k_x, k_y for the special case when the potential is $V_0 (\cos 2\pi x/a + \cos 2\pi y/a)$ with $V_0 = 4$ electron volts and $a = 2\ 5\ \text{Å}$. The numbers by the contour lines give the energy in electron volts.

where U_k has the same periodic properties as V, $i\ e$,

$$U_k(x + na) = U_k(x)$$ (8B)

† (1) Floquet's theory, Whittaker and Watson, "Modern Analysis," p 412   (2) Group theory, Bloch, loc. cit   (3) An expansion of ψ_k in a series of exponential functions shows that only those terms combine which differ by the factor $\exp(2\pi i n x/a)$ Any sum of such terms will thus have the form (8)

Since ψ_k, ψ^*_k, ψ_{-k}, have the same eigenvalues E_k, a linear relation must exist between these three functions   Inspection shows that this relation can only be

$$\psi^*_k = \psi_{-k} \tag{9}$$

The case in which

$$V = V_0 \cos (2\pi x/a) \tag{10}$$

V_0 being a constant, has received special investigation   One result† of particular importance to us is that two distinct solutions having the periodicity $2a$ cannot have the same eigenvalue   Thus if $\psi_{n\pi/a}$ and $\psi_{-n\pi/a}$ have the same eigenvalues, this theorem implies that

$$\psi_{-n\pi/a} = \psi_{n\pi/a} \tag{11}$$

Moreover, the energy as a function of k has discontinuities at $k = n\pi/a$, the two solutions on each edge of the energy discontinuity having an equal claim to the notation ψ_k

By employing the double suffix (N, K) we shall avoid this ambiguity in notation   The label N may assume the values

$$N = 0, 1, 2, \ldots,$$

and K has the range

$$\pi/a < K < \pi/a \tag{12}$$

The relation between the old suffix k and the new suffixes N, K is given by

$$k = K \pm \frac{2\pi}{a} N, \quad k \gtrless 0 \tag{13}$$

These relations do not specify N and K uniquely when $k = n\pi/a$ We need the additional condition that ψ_K is to be a continuous function of K in the closed interval (12)

Since $\exp(2\pi i N x/a)$ has the periodicity of the lattice   it will be convenient to include this factor in U_k We shall thus write

$$\psi_{N,K} = e^{iKx} U_{N,K}$$

where

$$U_{N,K} = e^{\pm 2\pi i N x/a} U_k, \quad K \gtrless 0$$

Equation (11) now becomes,

$$\psi_{N,-\pi/a} = \psi_{N,\pi/a} \tag{14}$$

We may thus regard K as a cyclic variable, the end points of the interval (12) being equivalent

† Ince, " Ordinary Differential Equations," p 177, Longmans, Green & Co (1927)

The convenience of this notation is illustrated by the perspective energy diagram in fig 2

It is of interest to note that equation (9), together with (11), show that $\psi_{n\,0}(x)$, and $\psi_{n\,\pi/a}(x) = \psi_{n\,-\pi/a}(x)$ are real functions and hence are associated with a zero average velocity

In the above analysis of the eigenfunctions of (6) we have assumed the special potential (10) The authors are aware of no rigorous proof† for a more general potential The following argument, however, indicates that
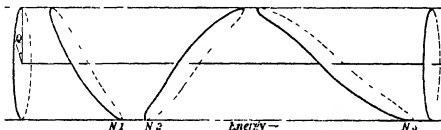

Fig 2 —This figure shows diagrammatically the dependence of energy upon N and K
$Q - aK$

the conclusions embodied in equations (12), (13), and (14), are of general validity

Any periodic potential having a physical significance may be represented by the sum

$$V(r) - \sum_{\nu=1}^{M} C_s \cos 2\pi s x/a,$$

where M is a finite number Let $\psi^{(0)}_{n\,k}$ be the eigenfunctions when all the C's are zero except C_1 Keep C_1 fixed and let all the other C's have finite but arbitrarily small values Let the new eigenfunctions be $\psi^{(1)}_{n\,k}$ These new functions may be expressed by means of the perturbation theory in terms of the $\psi^{(0)}_{n\,k}$'s Since the expansion will be uniformly convergent, the $\psi^{(1)}_{n\,k}$'s will be continuous functions of k in the interval (12), and

† A general proof has been given by M. J O Strutt, " Lamé'sche-Mathieusche- und Verwandte Funktionen in Physik und Technik," pp 22-23, Springer (1932) His proof however, implicitly assumes that the indefinite integral $\int (\psi_{n\,\pi/a})\ ^2 dx$ has not the period of $2a$ This assumption needs to be justified, particularly since Strutt's method shows that the indefinite integral $\int (\psi_{n\,\pi/na})^{-2} dx$, with $n > 1$, must have the period $2na$ in order that $\psi_{n\,\pi/na}$ and its complex conjugate be two distinct solutions, each with period $2na$

will, of course, satisfy (14)   They will thus have the same properties as the $\psi^{(0)}_{n\,k}$'s   As we now continuously increase the coefficients, it appears improbable that the $\psi^{(1)}_{n\,k}$'s will not remain continuous functions of l The conclusions obtained for the special potential (10) are thus valid for a general periodic potential, with $C_t \neq 0$

This analysis may at once be applied to the three dimensional wave equation (3), provided V is separable in the form $V = V(x) + V(y) + V(z)$ The solutions will be labelled by N and K, where N stands for (l, m, n), l, m, n assume all positive integral values, and where K stands for the vector (K_x, K_y, K_z), with $-\pi/a \lessdot K_x, K_y, K_z \lessdot \pi/a$ Moreover $\psi_{N\,K}$ is a continuous function of K such that

$$\psi_{N\,K} = e^{i\mathbf{K}\cdot\mathbf{R}} U_{N\,K}(x, y, z),\tag{15}$$

where $U_{N\,K}(x, y, z)$ has the same periodicity as $V(x, y, z)$ and

$$\left.\begin{aligned}
\psi_{N\,-\pi a\,K_y\,K_z} &= \psi_{N\,\pi a\,K_y\,K_z} \\
\psi_{N\,K_x\,-\pi a\,K_z} &= \psi_{N\,K_x\,\pi a\,K_z} \\
\psi_{N\,K_x\,K_y\,-\pi a} &= \psi_{N\,K_x\,K_y\,\pi a}
\end{aligned}\right\}\tag{16}$$

Brillouin[†] has shown that a similar grouping occurs when V may not be so separated   The construction of the closed intervals from the initial K space becomes, however, more complicated

§ 3 *Proof of* (1)

The second subscript N need not be introduced in this paragraph

In what follows we shall use the vector operators ∇_K ∇_R defined as follows

$$\nabla_K = \partial/\partial K_x, \quad \partial/\partial K_y, \quad \partial/\partial K_z$$

$$\nabla_R = \partial/\partial x, \quad \partial/\partial y, \quad \partial/\partial z$$

We shall also use the operator L_K defined by

$$L_K = \frac{h^2}{8\pi^2 m}\nabla^2 + E_K - V$$

Further, the volume integral over a unit cell will be denoted by $\int_c \quad d\tau$

In this notation the wave equation (1) for the eigenfunctions becomes

$$L_K \psi_K = 0\tag{17}$$

[†] "Quantenstatistik," p 287, Springer (1931)

Since this equation is true for all $\mathbf{K}$, we can operate on it with $\nabla_{\mathbf{K}}$ Remembering that $\psi_{\mathbf{K}} = e^{i\mathbf{K} \cdot \mathbf{R}} U_{\mathbf{K}}$, we obtain

$$(\nabla_{\mathbf{K}} E_{\mathbf{K}}) \psi_{\mathbf{K}} + iL_{\mathbf{K}} \mathbf{R}\psi_{\mathbf{K}} + L_{\mathbf{K}} [e^{i\mathbf{K} \cdot \mathbf{R}} \nabla_{\mathbf{K}} U_{\mathbf{K}}] = 0 \qquad (18)$$

It is clear that

$$L_{\mathbf{K}}\mathbf{R}\psi_{\mathbf{K}} = (h^2/4\pi^2 m) \nabla_{\mathbf{R}}\psi_{\mathbf{K}}$$

Hence (18) becomes

$$(\nabla_{\mathbf{K}} E_{\mathbf{K}}) \psi_{\mathbf{K}} + (h^2/4\pi^2 m) i\nabla_{\mathbf{R}}\psi_{\mathbf{K}} + L_{\mathbf{K}} [e^{i\mathbf{K} \cdot \mathbf{R}} \nabla_{\mathbf{K}} U_{\mathbf{K}}] = 0 \qquad (19)$$

If we multiply (19) by $\psi^*_{\mathbf{K}}$, and integrate over a unit cell, we obtain

$$(\nabla_{\mathbf{K}} E_{\mathbf{K}}) \int_c \psi^*_{\mathbf{K}} \psi_{\mathbf{K}} \, d\tau + \frac{ih^2}{4\pi^2 m} \int_c \psi^*_{\mathbf{K}} \nabla_{\mathbf{R}}\psi_{\mathbf{K}} \, d\tau + \int_c \psi^*_{\mathbf{K}} L_{\mathbf{K}} [e^{i\mathbf{K} \cdot \mathbf{R}} \nabla_{\mathbf{K}} U_{\mathbf{K}}] \, d\tau = 0$$

The last term may be shown to vanish identically, for since the integrand has the same periodicity as the lattice, we obtain, on integrating twice by parts with respect to x, y, z,

$$\int_c \psi^*_{\mathbf{K}} L_{\mathbf{K}} [e^{i\mathbf{K} \cdot \mathbf{R}} \nabla_{\mathbf{K}} U_{\mathbf{K}}] \, d\tau = \int_c [e^{i\mathbf{K} \cdot \mathbf{R}} \nabla_{\mathbf{K}} U_{\mathbf{K}}] L_{\mathbf{K}} \psi^*_{\mathbf{K}} \, d\tau$$

But since $L_{\mathbf{K}}$ is a real operator $L_{\mathbf{K}} \psi^*_{\mathbf{K}}$ vanishes identically by (17)

We now have

$$\frac{h}{2\pi m i} \int_c \psi^*_{\mathbf{K}} \nabla_{\mathbf{R}} \psi_{\mathbf{K}} \, d\tau \Big/ \int_c \psi^*_{\mathbf{K}} \psi_{\mathbf{K}} \, d\tau = \frac{2\pi}{h} \nabla_{\mathbf{K}} E_{\mathbf{K}}$$

But the left member of this equation is equivalent to the definition (2) of $\mathbf{v}_{\mathbf{K}}$ For integration by parts gives

$$\int_c \psi^*_{\mathbf{K}} \nabla_{\mathbf{R}} \psi_{\mathbf{K}} \, d\tau = - \int \psi_{\mathbf{K}} \nabla_{\mathbf{R}} \psi^*_{\mathbf{K}} \, d\tau$$

Hence

$$\int_c \psi^*_{\mathbf{K}} \nabla_{\mathbf{R}} \psi_{\mathbf{K}} \, d\tau = \tfrac{1}{2} \int_c \{\psi^*_{\mathbf{K}} \nabla_{\mathbf{R}} \psi_{\mathbf{K}} - \psi_{\mathbf{K}} \nabla_{\mathbf{R}} \psi^*_{\mathbf{K}}\} \, d\tau$$

$$\tfrac{1}{2} V_0 \{\psi^*_{\mathbf{K}} \nabla_{\mathbf{R}} \psi_{\mathbf{K}} - \psi_{\mathbf{K}} \nabla_{\mathbf{R}} \psi^*_{\mathbf{K}}\}$$

where V_0 is the volume of the unit cell

We have thus established relation (I)

§ 4 Proof of (II)

In this section we prove relation (II) directly from the wave equation (3) Using the notation introduced in § 2, we may expand the solution of this equation as[†]

$$\psi(x, y, z, t) = \sum_N \iiint_{-\pi/a}^{\pi/a} g_N(\mathbf{K}, t) \psi_N \kappa(x, y, z) \, dK_x \, dK_y \, dK_z \qquad (20)$$

[†] Peierls, loc. cit, represented the wave packet by a summation over the discrete set of quantum numbers obtained by specifying periodic boundary conditions. This summation

The $\psi_{N,\,K}$ are the eigenfunctions of the unperturbed equation (1) They will be taken to be normalized to a unit cell, so that

$$\int_c \psi^*_{N'\,K'}\,\psi_{N\,K}\,d\tau = \delta_{N'\,N} \tag{21}$$

where, as in the previous section,

$$\int_c d\tau \text{ denotes } \iiint_0^a dx\,dy\,dz$$

In order to obtain the wave equation for the q_N (K, t), we substitute the expansion (20) into equation (3), multiply by $\psi^*_{N'\,K}$, and integrate over all co-ordinate space The integrals are evaluated in the appendix Denoting by H″ the operator

$$H'' = H_0 - iF\,(R + i\nabla_K), \tag{22}$$

where H_0 is the Hamiltonian for the unperturbed lattice, and writing

$$(N\,|H''|N')_K = \int_c \psi^*_{N'\,K}\,H''\psi_{N'\,K}\,d\tau,$$

we obtain

$$(\frac{h}{2\pi}\frac{\partial}{\partial t} + iF\cdot\nabla_K)q_N\,(K,\,t) = -i\sum_N (N\,|H''|N')_K\,q_{N'}\,(K,\,t) \tag{23}$$

For further reduction we must use the Hermitian property of the operator H″ The Hermitian property of all the components of H″ except $eF\cdot i\nabla_K$ is obvious The property for $i\nabla_K$ is established by operating upon equation (21) with $i\nabla_K$ We obtain at once the desired relation

$$(N\,|i\nabla_K|N')_K = (N'\,|i\nabla_K|N)^*_K$$

We now multiply (23) by g^*_N (K, t), and add the resulting equation to its conjugate complex We obtain

$$\left(\frac{h}{2\pi}\frac{\partial}{\partial t} + eF\cdot\nabla_K\right)|g_N|^2 = i\sum_N \{(N\,|H''|N')_K\,g^*_N g_N - (N'\,|H''|N)_K\,g^*_N\,g_N\}$$

is intrinsically more difficult to handle than an integral Peierls completed his analysis by using the following approximations. In the sum

$$\overset{G/2-1}{\underset{s\,=\,-G/2}{\Sigma}}\,\alpha\,\exp 2\pi s\,(k-k')\,\alpha/G = G\cos\pi\,(k-k')\,(e^{2\pi i(k-k)/G} - 1)^{-1}$$

he replaced the oscillating numerator, $\cos\pi\,(k-k')$, by unity In calculating the sum

$$\sum_L C\,(k)\,(e^{2\pi i(L-k)/L} - 1)^{-1}$$

he assumes that C (k) is very small except when $|L - k'| \ll G$, which is certainly not true of the Fermi function in actual metals

Since the bracketed expression in the right member is antisymmetric with respect to an interchange of N and N', the right member vanishes when we sum over N   We are left with

$$\left(\frac{h}{2\pi} \frac{\partial}{\partial t} + eF \cdot \nabla_K \right) \sum_N |g_N|^2 = 0 \qquad (24)$$

The solution of this equation is, of course,

$$\sum_N |g_N(K, t)|^2 = G\left(\frac{hK}{2\pi} - eFt \right)$$

where G is an arbitrary function of its argument   The function $\sum_N |g_N(K, t)|^2$ thus moves with the uniform velocity $2\pi eF/h$.

Suppose now that *initially* the electron is definitely in one band so that all the $g_N(K)$ vanish except, say, $g_1(K)$ Then if we assume that also after time t the other bands may be left out of account,† only g_1 will remain in the summation of (24), and we have immediately relation (11)

The upper bands affect the problem in two different ways   The wave function $\psi_{N\,K}$ will become perturbed *as soon as* the field is put on, in the same way that an atomic function is perturbed by an electric field   We may reasonably expect that the effect will be given by a first order perturbation calculation, as for a free atom   The wave function may be expanded in terms of all the $\psi_{N\,K}$, but this does *not* mean that the electron actually gets into the excited band   On the other hand, there is a probability, which increases with time, that the electron will make a transition from one band to the next   This transition has been discussed by Zener (*loc cit*) and is always negligible in metals

Consider the equation

$$H'' \psi''_{N\,K} = E''_{N\,K} \psi''_{N\,K},$$

where, as in (22),

$$H'' = H_0 - eF (R + i\nabla_K)$$

Let $\psi''_{N\,K}$ be the solution of this equation which is obtained when $eF \cdot (R + i\nabla_K)$ is treated as a small perturbation   The first order perturbation calculation‡ gives

$$\psi''_{N\,K} = \psi_{N\,K} + \sum_N' \frac{(N \mid eF \cdot (R + i\nabla_K) \mid N')_K}{E_{N\,K} - E_{N\,K}} \psi_{N\,K}$$

---

† This was tacitly assumed in the restricted proof of Bloch, *loc cit*, and in the attempted general proof of Peierls, *loc cit*.

‡ The higher order approximations will not be given by the customary formulæ, since the operator ∇_K in H'' does not commute with the expansion coefficients.

or, omitting the common factor $e^{i\mathbf{K} \cdot \mathbf{R}}$,

$$U''_{\mathbf{v} \mathbf{K}} = U_{N \mathbf{K}} + \sum_{N}{}' \frac{(N \mid e\mathbf{F} \cdot (\mathbf{R} + i\nabla_{\mathbf{K}}) \mid N')_{\mathbf{K}}}{E_{\mathbf{v} \mathbf{K}} - E_{N \mathbf{K}}} U_{\mathbf{v} \mathbf{K}}$$

These approximate functions will not form exactly a complete orthogonal set. Nevertheless, if the electron is initially in the Nth band, we may expect that ψ as represented by the expansion

$$\psi(x, y, z, t) = \iint \int_{\pi}^{\pi} g''_{N}(\mathbf{K}, t) \psi''_{\mathbf{v} \mathbf{K}}(x \ y, z) \, dK_x \, dK_y \, dK_z$$

will differ inappreciably from the exact ψ until transitions to the adjacent bands become important.

We now substitute this expansion into the wave equation (3), multiply by $\psi''^{*}_{N \mathbf{K}}$, and integrate over all co-ordinate space. Using the orthogonality relation

$$\int \psi''_{\mathbf{v} \mathbf{K}} \psi''^{*}_{\mathbf{v} \mathbf{K}} \, d\tau = \delta_{\mathbf{v} \mathbf{v}}$$

and the integrals in the appendix, we obtain

$$\left(\frac{h}{2\pi} \frac{\partial}{\partial t} + e\mathbf{F} \cdot \nabla_{\mathbf{K}} \right) g''_{N}(\mathbf{K}, t) = iE''_{\mathbf{v} \mathbf{K}} g''_{N}(\mathbf{K}, t)$$

We thus obtain

$$\left(\frac{h}{2\pi} \frac{\partial}{\partial t} + e\mathbf{F} \cdot \nabla_{\mathbf{K}} \right) |g''_{N}(\mathbf{K}, t)|^2 = 0$$

and so

$$|g''_{N}(\mathbf{K}, t)|^2 = G'' \left(\frac{h}{2\pi} \mathbf{K} - e\mathbf{F}t \right)$$

Neglecting transitions between bands, the action of the electric field has thus two distinct effects. Firstly, it polarizes the individual "atomic" functions $U_{N, \mathbf{K}}$. Secondly, it produces a uniform translation of $|g''_{N}|^2$ in $\mathbf{K}$ space.

It is of interest to note that the expression for the polarized "atomic" functions becomes, when the lattice constant is increased indefinitely, identical to the usual expression for the polarized wave functions of isolated atoms. For large values of the lattice constant $\psi_{\mathbf{v} \mathbf{K}}$ becomes independent of $\mathbf{K}$ apart from a constant factor, in the region where $\psi_{\mathbf{v} \mathbf{K}}$ is non-vanishing. The second term in the perturbation thus becomes negligible.

It is also of interest to note that the velocity $v''_{N, K}$ associated with a polarized wave function $\psi''_{N, K}$ is related to the energy $E''_{N, K}$ by a relation analogous to (I), that is

$$v''_{N, K} = \frac{2\pi}{h} \operatorname{grad}_K E''_{N, K}$$

When we utilize the Hermitian property of the operator H'' the proof follows that given in § 3 for equation (I)

§ 5 Investigation of (111)

In this section we investigate the motion of a wave packet in a lattice under the influence of a magnetic field H Since the equations which we obtain are valid only for short intervals of time, it would not be profitable to introduce the excited states   Hence in place of representing the wave packet by the sum

$$\psi (x, y, z, t) = \sum_N \iiint_{-\pi/a}^{+\pi/a} g_N (K) \psi_N dK_x \, dK_y \, dK_z,$$

which we would do, of course, if we were to be exact, we shall take only one term of this sum, and so shall omit the suffix N Hence the wave packet will be represented by

$$\psi (x, y, z, t) = \iiint_{-\pi/a}^{+\pi/a} g (K) \psi_K \, dK_x \, dK_y \, dK_z \qquad (25)$$

We shall take ψ to be normalized, i e,

$$\int \psi^* \psi \, d\tau = 1$$

The function ψ must satisfy the wave equation

$$\left\{ \frac{1}{2m} \left(\frac{h}{2\pi i} \nabla - \frac{e}{c} \mathbf{A} \right)^2 + \mathbf{V} + \frac{h}{2\pi i} \frac{\partial}{\partial t} \right\} \psi (x, y, z, t) = 0 \qquad (26)$$

The only condition which the vector potential $\mathbf{A}$ must satisfy is

$$\operatorname{curl} \mathbf{A} = \mathbf{H}$$

The general solution of this equation may be written as

$$\mathbf{A} = \tfrac{1}{2}\mathbf{H} \times \mathbf{R} + \nabla f,$$

where f is an arbitrary function of $\mathbf{R}$ and of t The scalar potential $\mathbf{V}$ is then given by

$$\mathbf{V} = \mathbf{V}_0 - \frac{e}{c} \frac{\partial f}{\partial t},$$

where $\mathbf{V}_0$ is the periodic potential due to the lattice

The arbitrariness of f will be used to simplify the expression for the average velocity [v] of the wave packet. This average velocity is given by

$$[v] = \frac{h}{4\pi m i} \int \{\psi^* \nabla \psi - \psi \nabla \psi^*\} \, d\tau - \frac{e}{mc} \int A \psi \psi^* \, d\tau$$

Now if we choose

$$A = \tfrac{1}{2} H \times (R - [R]),\qquad(27)$$

where

$$[R] \quad \int \psi^* R \psi \, d\tau,$$

then clearly

$$\int A \psi \psi^* \, d\tau = 0,$$

and the average velocity becomes

$$[v] = \iint\int_{-\pi/a}^{\pi/a} v_K \, |g(K)|^2 \, dK_x \, dK_y \, dK_z,$$

where v_K is defined by (2). In order to write A in this form, we must take

$$f = - \tfrac{1}{2} R \quad H \times [R] - \tfrac{1}{2} H \quad R \times [R]$$

Then since

$$\frac{\partial}{\partial t} [R] = [v],$$

the scalar potential becomes

$$V = V_0 - \frac{e}{2c} H \quad R \times [v] \qquad (28)$$

Taking the vector and scalar potentials to be given by (27) and (28), we substitute the expansion (25) into (26), multiply by ψ^*_K, and integrate over all co-ordinate space. We obtain, using (A6), (A7),

$$\frac{\partial}{\partial t} g(K) = -\frac{2\pi i}{h} E_K g(K) + \frac{2\pi i}{h} \left(\frac{a}{2\pi}\right)^3 \int \left(\iiint_{-\pi/a}^{\pi/a} g(K') \psi^*_K \right.$$

$$\times \left\{ \frac{h}{2\pi i} \frac{e}{2mo} H \quad (R - [R]) \times \nabla + \frac{e}{2c} H \quad R \times [v] \right.$$

$$\left. - \frac{e^2}{8mc^2} [H \times (R - [R])]^2 \right\} \psi_K \, dK'_x \, dK'_y \, dK'_z \right) d\tau. \qquad (29)$$

We have, of course, utilized the fact that the ψ_K are eigenfunctions of

$$\{(h^2/8\pi^2 m) \, \nabla^2 + E_K - V_0\} \, \psi_K = 0$$

We multiply equation (29) by g^* (K), and add the resulting equation to its conjugate complex   The integrals are evaluated by the method outlined in the appendix   Neglecting terms in H^3, we obtain

$$\frac{\partial}{\partial t}|g|^2 = \frac{2\pi}{h}\frac{e}{2c}\mathbf{H}\cdot(\mathbf{v_K} + [\mathbf{v}])\times\nabla_K|g|^2 \tag{30}$$

We now consider the terms which have been neglected in (30)   In their evaluation, we need to know the phase of g If we neglect powers of H greater than the second, we may take

$$g = |g|\,e^{2\pi i E_K t/h}$$

We separate the terms in H^2 into those that are also present for free electrons, and those that vanish for free electrons   The former may be written as

$$\frac{2\pi}{h}\frac{e^2}{4mc^2}(\mathbf{H}\times\nabla_K)\cdot\{\mathbf{H}\times(\mathbf{v_K}t - [\mathbf{R}])|g|^2\}$$

If $|g(\mathbf{K})|^2$ is a sufficiently sharp function of K, the variation of $\mathbf{v_K}$ may be neglected in comparison with the variation of $|g|^2$ This term then becomes

$$\frac{2\pi}{h}\frac{e^2}{4mc^2}\{\mathbf{H}\times(\mathbf{v_K}t - [\mathbf{R}])\}\cdot\{\mathbf{H}\times\nabla_K|g|^2\} \tag{31}$$

The origin of co-ordinates may be so chosen that $[\mathbf{R}] = 0$ at $t = 0$ We then observe that the ratio of (31) to the right member of (30) is approximately $(eH/2mc)\,t$, $i\,e$, ωt, where ω is the Larmor precession frequency   Hence (31) may be neglected only for an interval of time t such that $\omega t \ll 1$

Those terms in H^2 which vanish for free electrons reduce to

$$\frac{2\pi}{h}\left(\frac{2\pi}{a}\right)^3\frac{e^2}{4mc^2}\{\mathbf{H}\times\Big|\int_c U^*_{K}\mathbf{r}\nabla_K U_K\,d\tau\Big)\}\cdot\{\mathbf{H}\times\nabla_K|g|^2\}$$

This may, of course, always be neglected in comparison to the right member of (30) when H is sufficiently small

Summary

In the modern literature of the theory of metallic conduction certain equations which are true for free electrons are assumed to remain valid when the potential

is periodic At best proofs have been given only for particular cases In this paper general proofs are given for these equations These equations give (I) the relationship between the velocity and energy of a stationary state, (II) the effect of a constant electric field upon a wave packet, (III) the effect of a constant magnetic field upon a wave packet

Appendix

Let $\phi(k, x)$ be a continuous function of its arguments having the periodic property

$$\phi(k, x + a) = \phi(k, x)$$

Then

$$J \equiv \int_{-\infty}^{\infty} \left\{ \int_{k_1}^{k_2} e^{i(k-k)x} \phi(k, x) \, dk \right\} dx$$

$$= \frac{2\pi}{a} \int_0^a \phi(k', x) \, dx, \quad k_1 < k' < k_2 \qquad (A1)$$

When $\phi(k, x)$ is independent of x, this integral reduces to the Fourier Integral The proof of (A1) which we give below in fact follows closely the ordinary proof† of the Fourier Integral

The integral

$$\int_{k_1}^{k_2} e^{i(k-k)x} \phi(k, x) \, dk$$

represents a wave packet in x space, and so vanishes at $x = \pm \infty$ Hence we may write

$$J = \operatorname*{Lim}_{n \to \infty} \int_{-na}^{na} \int_{k_1}^{k_2} e^{i(k-k)x} \phi(k, x) \, dk \, dx$$

The order of these finite integrations may now be interchanged Now

$$\int_{-na}^{na} e^{i(k-k)x} \phi(k, x) \, dx = \sum_{s=-n}^{n-1} e^{i(k-k')sa} q(k)$$

$$= \frac{2s \sin(k - k') na}{e^{i(k-k')a} - 1} q(k),$$

where

$$q(k) = \int_0^a e^{i(k-k)x} \phi(k, x) \, dx$$

We thus have

$$J = \operatorname*{Lim}_{n \to \infty} \int_{k_1}^{k_2} \frac{2s \sin(k - k') na}{e^{i(k-k')a} - 1} q(k) \, dk$$

† Courant and Hilbert, "Methoden der Mathematischen Physik," vol. 1, pp. 54–55, Berlin (1924).

If k' were outside the interval $k_1 < k < k_2$, integration by parts would show that $J = 0$ Hence J may be written as

$$J = \lim_{n \to \infty} \int_{k-\epsilon}^{k+\epsilon} \frac{2i \sin (k - k') na}{e^{i(k-k')a} - 1} \, q(k) \, dk$$

where ϵ is arbitrarily small   We now make ϵ so small that $q(k)$ may be replaced by $q(k')$, and $\exp i (k - k') a$ by $1 + i (k - k') a$

We thus have finally

$$J = (2/a) q(k') \lim_{n \to \infty} \int_{-\epsilon}^{\epsilon} \frac{\sin n\xi}{\xi} \, d\xi = \frac{2\pi}{a} \int_0^a \phi(k', x) \, dx$$

The generalization of (A1) to three dimensions gives

$$\int \left\{ \iint e^{i(\mathbf{K} - \mathbf{K}) \, \mathbf{R}} \, \phi(\mathbf{K}, \mathbf{R}) \, d\mathbf{K} \right\} d\tau = \left(\frac{2\pi}{a} \right)^3 \int_c \phi(\mathbf{K}', \mathbf{R}) \, d\tau, \qquad \text{(A2)}$$

where

$$\int \quad d\mathbf{K} \quad \text{denotes} \quad \iint\int_{-\pi/a}^{\pi/a} \quad d\mathbf{K}_x \, d\mathbf{K}_y \, d\mathbf{K}_z,$$

$$\int \quad d\tau \quad \text{denotes} \quad \iint\int_{-\infty}^{\infty} \quad dx \, dy \, dz,$$

and

$$\int_c \quad d\tau$$

represents an integration over a unit cell, and $\mathbf{K}'$ is restricted to the range $-\pi/a < \mathbf{K}_x', \mathbf{K}_y', \mathbf{K}_z' < \pi/a$

The second formula which we need is the orthogonality relation

$$\int_c \psi^*_{N, \mathbf{K}} \, \psi_{N \, \mathbf{K}} \, d\tau = 0, \quad N' \neq N \qquad \text{(A3)}$$

This is proved by the usual procedure of subtracting

$$\psi^*_{N, \mathbf{K}} \, (H_0 - E_{N, \mathbf{K}}) \, \psi_{N, \mathbf{K}} = 0$$

from

$$\psi_{N, \mathbf{K}} \, (H_0 - E_{N, \mathbf{K}}) \, \psi^*_{N \, \mathbf{K}} = 0$$

and integrating over a unit cell   Integration by parts then gives (A3)

In the following applications of these two formulæ to the integrals occurring in the text, $\psi_{N, \mathbf{K}}$ will be taken as normalized over a unit cell

The simplest of these integrals follows directly

$$\iint h(\mathbf{K}) \, \psi^*_{N, \mathbf{K}} \, \psi_{N, \mathbf{K}} \, d\mathbf{K} \, d\tau = \delta_{N, N} \left(\frac{2\pi}{a} \right)^3 h(\mathbf{K}') \qquad \text{(A4)}$$

In the next two integrals we must first replace $\mathbf{R}\exp(\imath\,\mathbf{K}\,\mathbf{R})$ by $-\imath\nabla_{\mathbf{K}}\exp(\imath\,\mathbf{K}\,\mathbf{R})$, and integrate by parts with respect to $\mathbf{K}_x$, $\mathbf{K}_y$, $\mathbf{K}_z$. Use is made of the cyclic character of $\mathbf{K}$ (equation (16))

$$\left(\frac{a}{2\pi}\right)^3 \iint q_N(\mathbf{K})\,\psi^*_{\searrow\ \mathbf{K}}\,\mathbf{R}\psi_{\mathbf{V}\ \mathbf{K}}\,d\mathbf{K}\,d\tau = \imath\nabla_{\mathbf{K}}g_N(\mathbf{K}')\,\delta_{\searrow,\,N}$$
$$+\int_c \mathbf{U}^*_{\searrow,\,\mathbf{K}}\,\imath\nabla_{\mathbf{K}}\mathbf{U}_{\mathbf{V}\ \mathbf{K}}\,d\tau\,g_N(\mathbf{K}') \qquad (A5)$$

$$\left(\frac{a}{2\pi}\right)^3 \iint q_N(\mathbf{K})\,\psi^*_{\searrow\ \mathbf{K}}\,\mathbf{R}\times\nabla_{\mathbf{R}}\psi_{\searrow\ \mathbf{K}}\,d\mathbf{K}\,d\tau$$
$$\int_c \psi^*_{\mathbf{V}\ \mathbf{K}}\,\nabla_{\mathbf{R}}\psi_{\searrow\ \mathbf{K}}\,d\tau\times\imath\nabla_{\mathbf{K}}q_N(\mathbf{K}')$$
$$-\left\{\iint_c \psi^*_{\mathbf{V}\ \mathbf{K}}\,\nabla_{\mathbf{R}}e^{\imath\mathbf{K}\ \mathbf{R}}\times\imath\nabla_{\mathbf{K}}\mathbf{U}_{\mathbf{V}\ \mathbf{K}}\,d\tau\right\}g_N(\mathbf{K}') \qquad (A6)$$

Finally, in the following integral we first replace $\mathbf{R}^2\exp(\imath\mathbf{K}\ \mathbf{R})$ by $-\nabla_{\mathbf{K}}^2\exp(\imath\mathbf{K}\ \mathbf{R})$, and integrate by parts twice with respect to $\mathbf{K}_x$, $\mathbf{K}_y$, $\mathbf{K}_z$

$$\left(\frac{a}{2\pi}\right)^3 \iint q_N(\mathbf{K})\,\psi^*_{\searrow\ \mathbf{K}}\,|\mathbf{R}|^2\,\psi_{\searrow\ \mathbf{K}}\,d\mathbf{K}\,d\tau = -\nabla_{\mathbf{K}}^2 q_N(\mathbf{K}')$$
$$-2\{\nabla_{\mathbf{K}}g_N(\mathbf{K}')\}\int_c \mathbf{U}^*_{\mathbf{V}\ \mathbf{K}}\,\nabla_{\mathbf{K}}\mathbf{U}_{\searrow\ \mathbf{K}}\,d\tau$$
$$-q_N(\mathbf{K}')\int_c \mathbf{U}^*_{\mathbf{V}\ \mathbf{K}}\,\nabla_{\mathbf{K}}^2\mathbf{U}_{\mathbf{V}\ \mathbf{K}}\,d\tau \qquad (A7)$$

A Photoelectric Spectrophotometer using Dual Electrostatic Compensation

By LEONARD A. WOODWARD, B A, Ph D, Massey Scientific Research Fellow of University College, Nottingham

I Introduction

The photometer here described is suitable for the purpose of measuring extinction coefficients of substances in solution, more particularly in the ultra-violet region The method employed is a purely electrical one, and does not involve the use of any mechanical devices (sectors or wedges, etc) for the quantitative variation of light intensity Errors due to fluctuations of the light source are eliminated by the use of two photoelectric cells, while the simultaneous electrostatic compensation of both cells does away with the necessity of measuring or controlling times of exposure The actual observations are of (i) a resistance plugged into a resistance box, and (ii) an electro-meter deflection The former gives the approximate result and the latter the correction to be applied

II Description of Apparatus and Method

The source of light is a vertical mercury vapour lamp, running at about $3\frac{1}{4}$ amps and about 100 volts terminal voltage The light from this source is condensed upon the slit of a double quartz monochromator by a suitable cylindrical quartz lens with its axis vertical By means of the double quartz monochromator,* which has auxiliary dispersing prisms rotated by means of wave-length drums, any desired wave-length emitted by the source can be selected and allowed to enter the photoelectric photometer

In the figure, which is purely diagrammatic, the exit slit of the double mono-chromator is shown at S After having been collimated by a quartz lens L, the beam of monochromatic light (shown dotted) is incident upon an inclined quartz plate Q, which is partially platinized by sputtering A fraction of the light is reflected at the plate and enters one of the photoelectric cells P_a, which we will call the comparison cell A fraction of the light is transmitted by the plate Q and passes on to the other photoelectric cell P_m, which we will call the measuring cell Between Q and the measuring cell can be introduced the

* Made by Messrs. Bellingham & Stanley, Ltd.

quartz-ended absorption vessel A containing the liquid whose absorption is under investigation.

The photoelectric cells are both of the vacuum type. Their cathodes are connected together and maintained at a negative potential by means of a battery B_1, the positive end of which is earthed. The voltage of B_1 is more
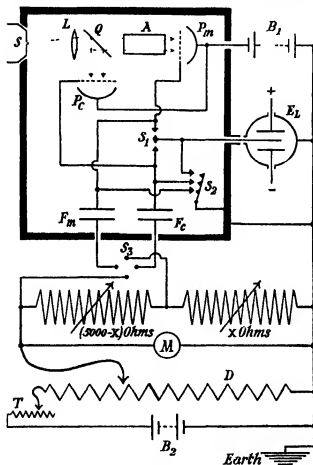
FIG 1

than sufficient to ensure saturation of the cells, so that the photoelectric current is in each case directly proportional to the incident light intensity. The cathode metal is sodium, which gives a sufficient response down to a wave-length of 2500 A. The envelopes of the cells are made entirely of quartz and the distance between anode and cathode seals ensures high insulation *

* Cells specially made by Otto Pressler, of Leipzig.

The rest of the apparatus, to be described and discussed in detail below, provides a means of measuring the ratio of the photoelectric current given by the measuring cell to that given by the comparison cell. Since both cells have a linear response, this ratio is proportional to the ratio of the corresponding incident light intensities. Errors due to fluctuations of the light source are eliminated, for such fluctuations alter the intensities of both beams in the same ratio. The determination of the extinction coefficient of a substance in solution involves the measurement of the ratio of the intensity I_0 incident upon the solution to the intensity I transmitted by it. When the absorption vessel A is filled with the solution, the measured ratio of the current given by the measuring cell to that given by the comparison cell is kI/I_s, where I_s is the intensity of the beam falling upon the comparison cell and k is a constant involving the sensitivities of the two cells. This ratio having been determined, the solution is replaced by pure solvent and the corresponding ratio kI_0/I_s is measured. Division of the second ratio by the first then gives the required quantity I_0/I. This procedure eliminates the effects due to the absorption vessel and the solvent. It will be noted that the properties of the reflector Q and the sensitivities of the photoelectric cells do not enter into the final result, provided only that they remain constant over the duration of the determination.

Now as to the method of measuring the ratio of the photoelectric currents. The anodes of the two photoelectric cells are connected respectively to poles of a switch S_1, by means of which either the one or the other may be put into connection with the needle of the Landemann electrometer E_L.[*] The earthing switch S_2 permits of the earthing of both the anodes and the electrometer needle together. In the actual apparatus S_1 and S_2 are constructed as one unit, so designed as to operate without the generation of charges which would disturb the electrometer needle. The contacts are all gold-plated and are gently pressed together without friction. The arrangement for applying the necessary voltages to the plates of the Landemann electrometer has been omitted from the figure for the sake of clarity. The anode of the comparison cell P_c is further connected to one plate of the screened induction condenser F_c, while the anode of the measuring cell P_m is likewise connected to one plate of the similar screened induction condenser F_m. These are specially constructed cylindrical air condensers[†] (approximate capacity 16 cm.) An earthed metal casing (shown by a heavy line in the figure) encloses the whole of the apparatus

[*] F. A. and A. F. Landemann and Keeley, 'Phil. Mag.,' vol 47, p. 578 (1924)

[†] See Campbell and Ritchie, "Photoelectric Cells" (1929), fig 30, p 126.

so far described and screens it from external influences The switches S_1 and S_2 are manipulated by suitable controls projecting through the casing The short lead to the electrometer needle is screened by an earthed metal tube The whole of the insulation of the anode systems (switches, induction condensers, etc.) to which the needle may be connected is of amber, with the exception of the photoelectric cells which are of quartz

The plates of the induction condensers which are not wired to the photo-electric cells are connected through a change-over switch S_3 to the double potentiometer arrangement shown in the lower part of the figure This consists of a sliding potentiometer D fed by a battery B_2, the slider being connected to one end of a second potentiometer formed by two standard variable resistance boxes, marked X ohms and (5000 — X) ohms in the figure The sum of the resistances of the boxes is kept constant (actually equal to 5000 ohms)

The method is as follows By means of the switch S_1 the electrometer needle is put into connection with one or other of the photoelectric cells, the switch S_2 being closed Switch S_3 is now opened so as to insulate both cell anodes, and the beam of monochromatic light is switched on by opening a shutter (not shown in the figure) The photoelectric currents given by the two cells begin to charge up their respective anode systems negatively, and the electrometer needle begins to move as a result of the rise of the negative potential of the system of which it forms a part This needle movement is compensated, i e, the needle is kept at its original zero position, by moving the slider of the potentiometer D, which applies a positive potential to the induction condenser concerned and maintains the needle potential at its original zero value by electrostatic induction * When the slider of D has been moved along the whole extent of its traverse, the light is cut off by closing the shutter

Now during the whole operation positive potentials have been applied to *both* induction condensers simultaneously, the ratio of these potentials being determined by the ratio of the resistances of the boxes For a certain value of this ratio, not only will the current from the one photoelectric cell have been exactly compensated, but also the current from the other cell Under these conditions, therefore, there will be no throw of the electrometer when, after the light has been cut off, the switch S_1 is moved over into its other position If the resistance ratio has not this correct value, a throw of the electrometer needle will be observed on thus moving over the switch S_1 Hence we have the possibility of finding by trial the correct value of the resistance ratio giving

* *Cf* Campbell and Ritchie, *loc cit*, p 114.

simultaneous exact compensation of both photoelectric currents   In practice
this lengthy process of trial is rendered unnecessary by a method to be described
later

Let C_1 and C_2 be the capacities of the induction condensers connected to the
photoelectric cells giving the greater current and the lesser current respectively
If the total voltage applied from the potentiometer D is V, the magnitude of
the charge on the first condenser will be C_1V and that on the second condenser
$C_2VX/5000$, where X/5000 is the value of the ratio of the resistance of the one
box to the total resistance of both boxes, as indicated in the figure   These
charges are equal to the time integrals of the respective photoelectric currents
over the duration t of the operation   Hence when dual compensation is
effected,

$$- C_1V = i_1t \quad \text{and} \quad - C_2VX/5000 = i_2t,$$

where i_1 and i_2 are the respective average photoelectric currents   Hence

$$\frac{i_2}{i_1} = \frac{C_2}{C_1} \cdot \frac{5000}{X}$$

The capacity ratio C_1/C_2 is a constant, and hence the determination of X gives
a measure of the ratio of the photoelectric currents, which is the quantity
required in the measurement of extinction coefficients (see above)

It should be noted that, since the two compensation operations are simul-
taneous, the time t is necessarily exactly the same for both and vanishes from
the final result   Thus the determinations do not involve the control or
measurement of times of exposure   Also the method is essentially a complete
null method   The potential of both the anode systems and of the electro-
meter needle is kept throughout practically at earth, so that leakage troubles
are reduced to a minimum.   Moreover, the voltage across both the photo-
electric cells remains practically constant throughout and the greatest possible
constancy of behaviour is thus ensured, although with vacuum cells at
saturation the advantage of this is small

In actual practice it is found impossible to cut off the light at the precise
moment at which the slider of the potentiometer D has been brought to the
end of its travel   Thus the electrometer needle usually shows a slight de-
flection after the light is cut off   To correct this small lack of compensation
before moving over the switch S_1, use is made of the small trimming rheostat
T, which is provided with lead-screw motion to allow of rapid operation   A
small touch on this rheostat suffices to correct the compensation before changing

over S_1 to the other system to see how nearly the dual compensation has been effected

According to what has been said so far, the determination of a photoelectric current ratio would involve a lengthy series of trials with different resistance ratios until the correct value was arrived at by a process of " bracketing " Actually, however, a method is adopted whereby the correct resistance ratio is determined directly An approximately correct value is first found by trial—this can be done quite rapidly—and then the electrometer deflection on changing over switch S_1 is observed From these data the correct resistance ratio can at once be calculated

Let us denote by the subscript 1 the quantities associated with the photo-electric cell P_1 (either P_o or P_m) which gives the greater current under the conditions considered Quantities associated with the other cell P_2 we designate by the subscript 2 At the correct resistance ratio for dual compensation, which we will take as 5000/X, the quantities of charge Q_1 and Q_2 given respectively by the two cells P_1 and P_2 during the time of compensation would be $- Q_1 = C_1 V$ and $- Q_2 = C_2 V X / 5000$, where V is the total potentiometer voltage applied Now consider an actual measurement in which a slightly incorrect value $(X + \Delta X)$ is used instead of X Let the experimental procedure always be to compensate the system 2 by manipulation of the potentiometer slider and then, after cutting off the light, to switch over to system 1 (This is a necessary stipulation, as the procedure affects the considerations—see below) At the incorrect setting $(X + \Delta X)$ we have

$$- Q'_2 = C_2 V \frac{X + \Delta X}{5000} = - Q_2 \left(1 + \frac{\Delta X}{X}\right)$$

Since the time of illumination of both photoelectric cells is necessarily the same, it follows that

$$- Q'_1 = - Q_1 \left(1 + \frac{\Delta X}{X}\right) = C_1 V \left(1 + \frac{\Delta X}{X}\right) \tag{1}$$

Thus the compensation of system 1 is imperfect, and on switching over the electrometer needle to this system from the perfectly compensated system 2 (after cutting off the light) an electrometer deflection will be observed Tests showed that the electrometer used gave a linear voltage response over the range of measurement, so that the observed deflection of n scale divisions corresponds to a needle potential of n/k, where k is the voltage sensitivity (We regard k as a positive constant, s e , we make the sign of n the same as that of the needle potential) The magnitude of the charge resident in the

induction condenser is now $C_1 [V - (n/k)]$, while that in the condenser formed by the needle system and the rest of the apparatus, is $Z_1 (n/k)$, where Z_1 is the corresponding capacity   The net charge on the whole needle system is the photoelectric charge Q'_1, since the photoelectric cell is the only source   Hence taking account of signs, we have

$$-Q'_1 = C_1 \left(V - \frac{n}{k}\right) - Z_1 \frac{n}{k},$$

which together with (i) gives

$$\Delta X = -\frac{X}{C_1 Vk}(C_1 + Z_1) n \qquad (ii)$$

From this we see that the absolute error in ΔX for a given error in the reading of n is directly proportional to X, i e, the relative error is the same for all values of X Thus advantage is not obtained when the procedure is to compensate the cell P_1 giving the greater current and then to switch over to the cell P_2, for then a similar calculation shows that a given error in the reading of n corresponds to the same absolute error in ΔX for all values X, i e, the relative error increases as X decreases

The correct resistance X is calculated from the value R actually used by means of the equation

$$X = \frac{R}{1 - \frac{(C_1 + Z_1)n}{C_1 Vk}}, \qquad (iii)$$

which is obtained from (ii) by substituting $\Delta X = R - X$ The value of V is read off from the voltmeter M (see figure) with the slider D at the end of its travel   Of course the slight readjustments of the trimming rheostat T cause corresponding changes in V However, on account of the smallness of the resistance of T relative to that of D, the variations of V are only of the order of 1%, and since they produce errors in X of the second order of smallness, they are quite negligible   Thus V may be taken as constant throughout a run   The constant k of the electrometer is determined directly   Finally, considerations similar to those given above show that the remaining quantity $(C_1 + Z_1)/C_1$, which is a constant of the apparatus, can be determined once and for all as the ratio of the electrometer deflections in the following independent cases (i) a certain voltage is applied to the needle direct, (ii) the needle being insulated, at zero potential and connected to system 1, the same voltage is applied to the induction condenser of capacity C_1 Thus the value of the constant $K = (C_1 + Z_1)/(C_1 Vk)$ can be determined and the correct values of X required in the extinction coefficient determinations can be calculated from

equation (III) in the form $X = R/(1 - Kn)$ In actual observations the deflection n is always small and the quantity Kn is always small relative to unity Thus the method is a true null method for the cell P_1 and approximately a null method for the cell P_2

III *Test of Apparatus and Method*

In order to obtain an idea of the performance of the apparatus, three test runs were carried out with an N/15 aqueous solution of potassium nitrate In each run determinations were made at seven different wave-lengths in the ultra-violet The runs were performed on different days and with different samples of solution, so that the accuracy obtained is the over-all accuracy of the whole procedure, including beside the actual measurement the cleaning and filling of the absorption vessels, etc It is known* that Beer's law is obeyed up to concentrations greater than that used The molecular extinction coefficients ε given in Table I are calculated from the formula

$$\varepsilon = \frac{1}{cd} \log_{10} \frac{I_0}{I},$$

where c is the concentration in mols per litre, d the thickness of the solution in centimetres, and I_0 and I the incident and transmitted intensities respectively Here $c = 1/15\,000$ and $d = 2\,000$

Table I —Determinations of Molecular Extinction Coefficients of KNO_3

λ in mμ	313	302	297	289	280	265	254
ε (run I)	5 38	7 19	6 85	5 72	3 75	1 60	3 63
ε (run II)	5 38	7 21	6 88	5 67	3 77	1 56	3 56
ε (run III)	5 39	7 17	6 92	5 66	3 82	1 62	3 57
ε (mean)	5 38	7 19	6 88	5 68	3 78	1 59	3 59
% error (run I)	0	0	−0 4	+0 7	−0 8	+0 6	+1 1
% error (run II)	0	+0 3	0	−0 2	−0 9	−1 9	−0 8
% error (run III)	+0 2	−0 3	+0 4	−0 35	+1 1	1 9	1−0 6
ε (von H and E)	5 26	6 93	6 84	5 61	3 68	1 56	3 59

The first row of Table I gives the wave-length in mμ of the light used. The next three rows contain the results of the three independent runs, while in the fifth row is given the means of the values obtained The next three rows

* von Halban and Eisenbrand, ' Z phys., Chem ,' vol 132, p 401 (1928)

contain the percentage differences from the mean value. Since the errors of the method are due to small random changes in the apparatus, these figures give an idea not only of the reproducibility but also of the accuracy of the determinations. Thus in the table they are called errors.

The bottom row of the table contains the values of ε taken from the data of von Halban and Eisenbrand* upon the nitrate ion in dilute solution, which are reproduced here for the sake of comparison. The agreement with the mean values given in the fifth row of Table I is fair, but these mean values are definitely somewhat higher than the corresponding values given by von Halban and Eisenbrand.

It is seen from Table I that the maximum percentage deviation from the mean in the present determinations is almost always under $\frac{1}{2}\%$ for the higher values of ε. At the lower values of ε the maximum error becomes greater, but is nowhere more than 2%. Since ε is proportional to log (I_0/I), the percentage error in ε corresponding to a given percentage error in the experimental determination of I_0/I is greater at small values of I_0/I than at larger values. This accounts for the greater percentage errors at the last three wave-lengths in Table I, and particularly at $\lambda = 265$ mμ. The corresponding errors in the measurements of I_0/I are actually about the same throughout (nowhere greater than 1·3%). In the determination of extinction coefficients it is clearly of advantage for the sake of accuracy to choose (when possible) the concentration and thickness of liquid so as to avoid values of I_0/I near to unity. With the apparatus here described, the limits of error in the determinations are then about $\pm \frac{1}{2}\%$.

This performance could probably be improved by the introduction of suitable modifications. Thus, referring to equation (iii), we see that the sensitivity can be increased (a) by increasing the compensating potential V, and (b) by using an induction condenser of greater capacity C_1, thereby decreasing the value of the quantity $(C_1 + Z_1)/C_1$. In (a) the possible increase of sensitivity is in principle unlimited; in (b) $(C_1 + Z_1)/C_1$ approaches the limiting value unity as C_1 approaches infinity. It should be noted, however, that in both (a) and (b) the increase of sensitivity is only obtained at the cost of lengthening the time required in compensation. Moreover, at higher sensitivities the value of R used must approximate more closely to the correct value X, otherwise the method is no longer approximately a null method. In the actual determinations quoted above the time of compensation was usually about $\frac{1}{4}$ minute,

* *Loc. cit.*, Table I, p. 406.

and the accuracy obtained was considered satisfactory for the particular purpose for which the arrangement was set up

The apparatus and method described above are to be used for investigating the ultra-violet absorption of certain extracts from blood sera   The writer wishes to express his thanks to the Nottingham Branch of the Imperial Cancer Campaign for a grant covering the cost of the apparatus

Summary

A new type of photoelectric photometer is described, suitable for the measurement of extinction coefficients of substances in solution, more particularly in the ultra-violet region   Errors due to fluctuations of the light source are eliminated by the use of two photoelectric cells, while the simultaneous electrostatic compensation of both cells by means of one and the same potentiometer system does away with the necessity of measuring or controlling times of exposure   No devices for the quantitative variation of light intensity are required   The quantity measured is the ratio of the compensating potentials, and the actual observations are of a resistance and an electrometer throw   The method is tested by a series of determinations of the molecular extinction coefficient of potassium nitrate in dilute solution   The results show that the error in the measurement of I_0/I does not exceed 1 3%, which corresponds, under the conditions of experiment, to a maximum error of about $\frac{1}{2}$%, in the determination of extinction coefficients

[*Note added in proof*, January 2, 1934]—Subsequent work with the instrument has shown that the approximation (III) above, though otherwise sufficiently accurate, becomes inadequate when R is small relative to 5000   It is then no longer permissible to neglect the small induction effect of system 1 upon system 2   The equations $-Q_1 = C_1V$ and $-Q_2 = C_2VX/5000$ remain unaltered, but if c is the small capacity between the two systems during compensation, we have

$$- Q'_2 = \frac{C_2VR}{5000} + cv = -Q_2\left(\frac{R}{X} + \frac{5000cv}{C_2VX}\right), \qquad (\text{IV})$$

where v is the small potential of system 1 at the end of the compensation operation and before switching over   Hence instead of (I) we obtain

$$- Q'_1 = -Q_1\left(\frac{R}{X} + \frac{5000cv}{C_2VX}\right) = C_1V\left(\frac{R}{X} + \frac{5000cv}{C_2VX}\right) \qquad (\text{V})$$

At this stage

$$- Q'_1 = C_1 (V - v) - cv - y_1 v, \qquad \text{(vi)}$$

where y_1 is the capacity between system 1 and its earthed surroundings   In changing over switch S_1 a charge $-c_s v$ is transferred from system 2 to system 1, c_s being the small capacity between system 1 and the switch arm.   As a result of the switch-over system 1 assumes a potential n/k (the corresponding electrometer throw n being observed), while system 2 assumes a potential p by induction   We now have

$$- (Q'_1 - c_s v) - C_1 \left(V - \frac{n}{k} \right) + c \left(p - \frac{n}{k} \right) - z_1 \frac{n}{k}, \qquad \text{(vii)}$$

where z_1 is the new value corresponding to y_1 Also for system 2,

$$(C_2 + c + z_2) p = c \left(\frac{n}{k} - v \right), \qquad \text{(viii)}$$

c being the same in both positions of the switch

Elimination of Q_1, Q_2, Q'_1, Q'_2, v and p from these equations gives an expression for the required quantity X in terms of constants of the apparatus and the observed quantities R and n The result becomes identical with (iii) if we put $c = c_s = 0$, while for $n = 0$ it reduces to $X = R$ Without reproducing the expression we may note that for any particular value of X it gives (as did the simpler treatment) a linear relationship between n and R   This is confirmed by experiment, and X may be conveniently determined by observing the electrometer throws for two different values of R and interpolating linearly to zero throw

Changes in the Raman Spectrum of Sulphuric Acid on Dilution

By L. A. WOODWARD, B.A., Ph.D.,* and R. G. HORNER, B.A., Physics
Department, University College, Nottingham.

Introduction

The results of previous workers upon the Raman effect of sulphuric acid show a considerable lack of agreement, due no doubt in part to the intensity of the accompanying continuous background and the apparent diffuseness of certain of the lines. Thus both Nisi† and Woodward‡ found that change of the concentration of the acid greatly modified the appearance of the spectrum, influencing both the positions and the relative intensities of the lines. Woodward gave photometer curves of the spectra for concentrations ranging from 100% to 25% by volume, and attributed the observed intensity changes to the successive stages of ionization of the acid. The lines $\Delta\nu = 910$ and 1140 cm^{-1} (approximate values), which were strong in the 100% acid, became weaker and shifted somewhat as the concentration decreased; while a new line $\Delta\nu = 1046$ cm^{-1} made its appearance and increased correspondingly in intensity. At low concentrations this last line became double, a companion appearing at 982 cm^{-1}. The frequencies 910 and 1140 were regarded as characteristic of the H_2SO_4 molecule, 1046 of the HSO'_4 ion, and 982 of the SO''_4 ion. Other diffuse lines also showed frequency shifts. Bell and Fredrickson,§ however, whose measurements were made not only with a prism spectrograph but also with a grating, failed to find any appreciable shifts of the lines with dilution. Moreover, they stated that on their plates the 1046 line gave no indication of becoming double at low concentrations, but merely grew more diffuse. The findings of other workers are referred to in the discussion of our results (see below).

In view of the conflicting nature of the above evidence regarding the two stages of ionization of the acid, it was thought desirable to repeat the investigations using a higher dispersion than that employed by Woodward (*loc. cit.*),

the object of the work being to obtain more conclusive photometer curves of the spectra The curves we have actually obtained not only give a clear picture of the intensity changes involved, but have also been used in a rational method of wave-length determination, the adoption of which has made it possible for us to propose a somewhat more detailed interpretation of the spectra than has hitherto been attempted

Apparatus

A modified form of Wood's well-known arrangement was used. In order to obtain comparable spectra it was essential that the alignment of the Raman tube and spectrograph should remain undisturbed throughout the series of exposures The apparatus was therefore designed so as to permit of changing the liquid without in any way altering the position of the tube

The main cylindrical part of the tube was surrounded with a thin water-jacket for cooling, and sloped at a small angle to the horizontal At the upper end and immediately in front of the spectrograph slit was a plane window, and at the highest point of the tube a small air vent which could be tightly closed The lower end of the tube was of the usual tapering horn-shape The horn pointed downwards so that its end was the lowest point The tube was filled and emptied from this end, which was attached to the middle of a relatively narrow vertical tube fitted with externally ground stoppers top and bottom Thus observation vessel was made entirely of glass, the window being fused on No grease was used on the ground stoppers

The source of illumination was a 15-inch Cooper-Hewitt glass mercury lamp equipped with an automatic starting device whereby it could be switched on without being touched This lamp was mounted close and parallel to the Raman tube, so that lamp and tube lay along the focal axes of a cylindrical chromium-plated mirror of elliptical cross-section closely surrounding them both The water cooling maintained the liquid under investigation at a temperature between 20° and 25° C during the exposures

The spectrograph was a Hilger constant-deviation instrument with a dispersion of about 40 A. per millimetre in the region investigated (Compare 150 A per millimetre in the same region given by the spectrograph used by Woodward (loc cit) in obtaining his photometer curves) Every precaution was taken to avoid stray light, screens and diaphragms being interposed at suitable points In addition the whole instrument was enclosed in a blackened box from which only the collimator projected. The end of the collimator

carrying the slit was further surrounded by another blackened compartment totally enclosing the slit and the window of the Raman tube.

Both spectrograph and Raman tube were firmly mounted upon a single heavy base, the whole assembly being set up so as to slope at the small angle to the horizontal necessary for the proper functioning of the mercury lamp Screw adjustments were provided for the important process of aligning the tube coaxially with the collimator This was accomplished conveniently by sighting the inside of the tube from the focal plane of the spectrograph camera (*Schlüssellochperspektive*) After careful alignment everything was firmly clamped in position and not disturbed in any way throughout the whole series of experiments

Materials

The solutions were made up from the pure acid (B D H "Pure 100%") and dust-free distilled water from a special still Precautions were taken to exclude dust and, for the 100% acid, moisture Following previous example, the concentrations used were 100%, 90%, 75%, 50%, 25%, and 10% by volume

The photographic plates used (backed "Double-X-Press") were prepared by Messrs Ilford, Ltd, from an experimental emulsion They combined a high gamma with a low inertia for the spectral region under consideration (4400–4600 A.), and proved markedly superior to any other type of plate tested They were developed in complete darkness for a uniform time of 4½ minutes, using a pyro-soda developer

Experimental Method

Preliminary exposures were taken with the 75% acid (which previous experiments had shown suffered most from background) in order to find the most suitable slit width and exposure time Photometric measurements of the plates obtained showed that the ratio of the intensity of the Raman lines to that of the continuous background was practically constant for different slit widths over the range investigated (5 to 33 μ) This result provides proof that the "lines" cannot be strictly monochromatic (see also below) As wide a slit as was compatible with the desired detail was therefore chosen (actual width 25 μ) As is to be expected, it was found that for a given slit width the height of the lines above the background on the photometer curve increased with decrease of exposure time, provided that the background was not under-exposed

In spite of the comparatively small numerical aperture of the spectrograph camera (1 9), the exposure times required were quite short   In order to obtain spectra of approximately comparable density, the exposure times for the different solutions were made inversely proportional to the volume concentrations. The most suitable exposure time for the 75% acid was first found by trial to be 10 minutes, and the others were then adjusted accordingly (viz, $7\frac{1}{2}$, $8\frac{1}{3}$, 10, 15, 30 and 75 minutes for the 100%, 90%, 75%, 50%, 25% and 10% solutions respectively)   A shutter between the prism and camera objective was used for making the exposures, before each of which the mercury lamp was allowed to run for at least half an hour so as to attain a steady state

The plates obtained were passed through a projection-type photoelectric microphotometer, electrometer readings being taken every 0 01 mm of plate The resulting photometer curves, which were plotted on a very large scale, are shown (much reduced) in fig 1 Each plate was traversed from the 4339 to the 4916 A mercury lines, but for the sake of clarity the full traverse including the mercury lines is reproduced only in the case of the 100% and 10% acids In no case was the broadening of the exciting line 4358 A sufficient to affect seriously the neighbouring 4339 A line, which was always well separated

It was concluded that the position of a line, as defined by its point of maximum intensity, could be determined with considerably greater accuracy from its shape in the photometer curve than by the adjustment of the cross-wires of a travelling microscope. Moreover, in using the photometer curves, due allowance could be made for the effect of the slope of the continuous background and the proximity of other diffuse lines upon the position of the line under consideration   Each spectrum was already provided with two satisfactory fiducial marks—the blue mercury line 4339 A and the dark green mercury line 4916 A. These were not over-exposed on any plate   They always appeared on the photometer curves as narrow lines with almost vertical sides , and their width corresponded exactly to the theoretical value for a monochromatic line, as calculated from the known widths of spectrograph and photometer slits (see below)   No actual measurements upon the plates were necessary   The photometer curves were carefully plotted on millimetre graph paper using a very large scale and, when the true point of maximum intensity of a line had been decided upon, its position was read off directly   A dispersion curve on the same scale was constructed from the photometer curve of a mixed copper arc and mercury spectrum, photographed by means of a very small reflecting prism introduced between the spectrograph slit and the window of the Raman tube The smooth dispersion curve passed exactly through every
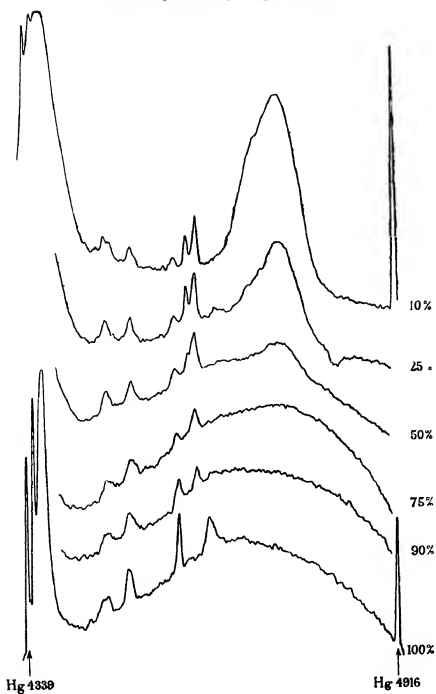
10 %

25 .

50%

75%

90%

100%

Hg 4339

Hg 4916

Fig 1

reliable known point, and the accuracy obtained with it was greater than that
with which the positions of the lines could be determined   All the plates,
including the comparison spectrum, were taken without disturbing the setting
of the apparatus.   In actual fact, although the plate-holder of the camera was
necessarily moved each time, the distance on the plates between the two
fiducial mercury lines was constant to within 1 part in 2000 (actual measure-
ments   11 160, 11 155, 11 157₅, 11 160, 11 155, 11 160, and 11·160 mm
on the 100%, 90%,   , 10% acid and comparison plates respectively)   Hence
the readings taken from the different photometer curves could be immediately
transferred to the single dispersion curve and the wave-lengths obtained
directly   For conversion to wave-numbers use was made of Kayser's " Tabelle
der Schwingungszahlen "   The estimated error in the determination of the
wave-length of a sharp line is less than $\pm$ 0 2 A (corresponding to $\pm$ 1 cm.$^{-1}$)
Owing to the diffuseness of the Raman lines and the presence of the background,
the Δv-values given below vary in accuracy between this and $\pm$ 5 cm $^{-1}$ or
more, and the probable error is given for each line individually

Experimental Results and Discussion

For convenience of comparison, the photometer curves of figs 1 and 2
have been arranged above one another so that their wave-length scales coincide
to within 0 2 A   Fig 1 is a small-scale reproduction showing the general
shape of the curves.   It will be seen that the continuous background is in the
form of a band extending from about 4400 to about 4900 A.   In studying the
curves this background must not be confused with the well-known Raman band
of water, which is much narrower and stands out most markedly in the most
dilute acids (see below)   The behaviour of the background is interesting
Its intensity at first increases as the concentration of the acid is reduced from
100%,* but then drops off again in a striking manner   At 10% acid the
background has become negligible, although the exposure time is ten times
longer than for the 100% acid   Thus indicates clearly that the background
cannot be wholly due to Rayleigh scattering of the continuous spectrum of the
mercury lamp in this region ,   for the intensity of the classically scattered
mercury lines is observed to increase regularly with the exposure time   Our
curves would thus seem to lend support to the view of Placzek and van Wijk†
that the background consists mainly of a true continuous Raman effect due to
vibrations of molecular complexes.

* It must be remembered that the exposure time increases in proportion to the dilution
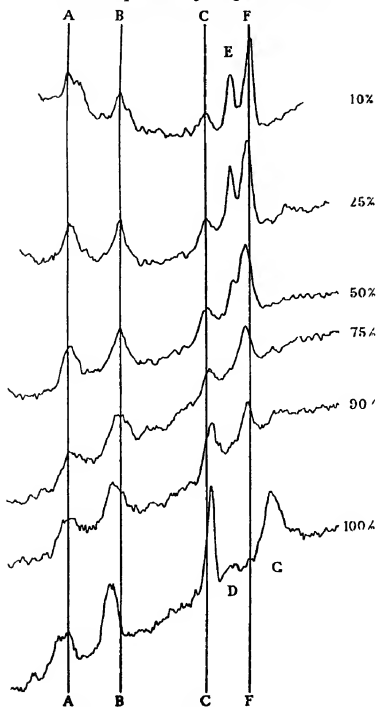† ' Z. Physik,' vol. 70, p. 287 (1931)

Fig 2.

The characteristically unsymmetrical Raman band of water, excited by 4047 A, begins to show at 75% acid and increases rapidly in intensity as we pass to greater dilutions At no stage is there any indication of its splitting into two separate components in the manner observed in the case of nitric acid (see Woodwood, loc cit)

Fig. 2, on a rather larger scale, shows the Raman lines (all excited by 4358 A) in more detail The vertical lines drawn right down the figure pass through points of the same wave-length on the different curves For convenience of discussion the Raman lines have been lettered A to G It will be seen at once that the curves provide clear evidence in support of the general conclusions of Woodward (loc cit) The line F, supposed characteristic of the HSO_4' ion, is completely absent in the 100% acid, but appears strongly in the 90% and increases in intensity with dilution Already at 50% its companion E, ascribed to the SO_4'' ion, has made its appearance, while in the lower concentrations it is stronger and quite clearly separated from the HSO_4' line The strong line G and the weak line D of the pure acid (the latter not very marked on the photometer curve, but visible on the plate) vanish rapidly on dilution, they are ascribed to the H_2SO_4 molecule The line D has not been found by previous workers

In addition to the intensity changes outlined above, an apparent general wave-length shift of the lines with dilution is to be observed The lines A, B, and F appear to move to longer wave-lengths as the acid concentration is reduced, while C shows the reverse behaviour (compare Nisi and Woodward, loc cit) Such shifts have also been noted by Specchia,* who states, however, that all the lines are displaced to longer wave-lengths On the contrary, Bell and Fredrickson (loc cit), using a grating, failed to find any appreciable changes of wave-length with dilution, except for a possible extremely small shift in the single case of λ 4470 (B)

Our results would seem to leave no doubt as to the reality of the displacements under consideration It appears difficult, however, to explain shifts of the observed magnitudes as due to alterations of the vibrational frequencies by intermolecular forces dependent upon the concentration In this connection we may refer to some measurements of Embirikos† upon the frequency of the strongest line of the sulphate ion in salt solutions For lithium and magnesium sulphates he found that this frequency increased with increase of concentration For the latter salt he gave the values 985 7 cm $^{-1}$ for 1 N solution and 995 7

cm $^{-1}$ for 2 N solution We have carefully repeated the measurements upon this salt over an extended concentration range, but find no evidence whatever for a frequency shift of the magnitude reported by Embirikos Our results are given in Table I, from which it is seen that the frequency of the line is independent of the concentration within the limits of error of our measurements

Table I - Frequency of Strongest SO''₄ Line in Solutions of Magnesium Sulphate

Concentration of $MgSO_4$	$\Delta \nu$ (obs) in cm.$^{-1}$
1 25 N	982 ± 2
2 55 N	982 ± 2
5 1 N	981 ± 2

Returning now to the photometer curves for sulphuric acid given in fig 2, it is seen on closer inspection that the wave-length shifts of the lines B and C are not gradual and uniform, but occur entirely in the region of 75% acid The $\Delta \nu$-values, as determined from the points of maximum intensity of the lines, are given in Table II Both lines are relatively sharp and of practically constant frequency both at the high and the low concentrations, but broaden and become intense in the intermediate stages The broadening occurs on the

Table II --Frequencies of Points of Maximum Intensity of B and C

Acid concentration	Line B (in cm $^{-1}$)	Line C (in cm $^{-1}$)
%		
10	⎧ 596 5	⎧ 896
25	⎨ 594 5	⎨ 894 5
50	⎩ 594 5	⎩ 896
75	590	903
90	563	⎧ 909 5
100	555 5	⎩ 910

side towards which the frequency is apparently changing, thus giving rise to the intermediate values given in Table II These facts would suggest that in each of B and C we are dealing with two independent frequencies of practically constant value In each the one which is predominant at 100% rapidly diminishes in intensity with dilution, while the other becomes correspondingly more intense, the former would naturally be regarded as characteristic of the H_2SO_4 molecule, the latter of the HSO'_4 ion Actually it was found that for all the apparent

intermediate frequencies recorded in Table II the shape of the broadened line in the photometer curves is indeed consistent with an analysis into two relatively narrow, symmetrically shaped components having the practically constant frequencies found in the most concentrated and most dilute acids respectively The idea here proposed is illustrated diagrammatically in fig 3, which is a tentative line scheme of the spectra   The vertical lines in the diagram represent relatively narrow components or lines of practically constant frequency (except for the line F—see below), and the course of the intensity changes is indicated for each by corresponding variations in height

The " line " A is slightly more complicated   Comparison with the widths of B and C shows at once that A is relatively broad throughout the whole range of concentrations   It must either be a diffuse band or it must consist of more than one component frequency   In the light of what has been said above about the lines B and C, the nature of the changes of shape of A with dilution (see fig 3) suggests an analysis into three symmetrically shaped and relatively narrow components of practically constant frequency   These are represented diagrammatically in fig 3, which also shows qualitatively the intensity trend of each Thus the behaviour of A is explicable on the view that it is made up of a central component of approximately constant intensity at all concentrations, a second component of lower frequency, which dies away from 100% to 75% acid, and a third of higher frequency which first appears at the intermediate concentrations and becomes stronger with dilution   This explanation finds support in the fact that on the photographic plate for the 100% acid the line A appears to the eye to be double (contrast effect) *

As to the line E it was found that, after correction for the influence of the neighbouring line F, a constant value of $\Delta \nu$ was obtained within the estimated limits of error

The line F, however, seems to be an exception to the rule of practically constant frequency   It shows a frequency shift greater than the estimated maximum error of determination (see Table III below, which gives the measured values for all the lines or proposed components)   A real displacement of F towards higher frequency in the lowest concentrations seems established It may be noted that this line has a peculiar unsymmetrical shape and an excessive breadth at intermediate concentrations   This may perhaps mean

---

* This double appearance is also noted by Médard in a paper ('C R Acad. Sci. Paris,' vol. 197, p 582 (1933)) on the Raman effect of 100% sulphuric acid, published since the conclusion of our experiments and the writing of this account. His experimental findings are everywhere in harmony with our own
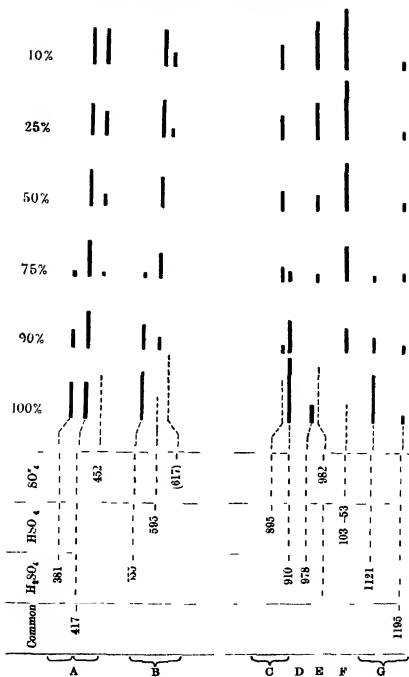
Fig. 3.

Table III — Observed Frequencies (in cm^{-1})

	A			B			C		D	E	F	G	
10%	—	418 ±5	454 ±8	—	596.5 ±2	(617)	896 ±5	—	—	983 ±2	1053 ±2	—	—
25%	—	(418)	450 ±6	—	594.5 ±2	—	894.5 ±3	—	—	981 ±3	1043 ±3	—	—
50%	—	(414)	(451)	—	594.5 ±3	—	896 ±5	(910)	—	(985)	1036 ±4	—	—
75%	(381)	417 ±5	—	(565)	(595)	—	(894)	—	—	—	1035 ±4	—	—
90%	(381)	(414)	—	(565)	(595)	—	(896)	909.5 ±3	—	—	—	—	—
100% –	381 ±5	417 ±5	—	565.5 ±2	—	—	—	910 ±3	978 ±4	—	1038 ±4	1121 ±7	(1196) ±15
Mean values	381	417	453	565.5	595	(617)	895.5	910	978	983	1036 to 1033	1121	(1196)

that we are dealing with more than one component, but the evidence is too slight to justify further discussion

The strong line G (1121 cm^{-1}) in the spectrum of the 100% acid rapidly disappears on dilution In the photometer curve it is seen to be definitely broadened on the long-wave side, and we find that this broadening can be interpreted as due to the overlap of a weak diffuse line with its centre at about 1195 cm.$^{-1}$ Although this line does not show up on the photometer curves (except perhaps feebly in the 25% curve), it is actually visible by eye on all the plates except those for 90% and 75% acid which suffer most from background

The Δν-values given in Table III are those of the lines or components referred to in the above discussion Those components not unambiguously defined by some part of the smoothed photometer curves are placed in brackets, because of their uncertainty they have not been used in reckoning the mean values

Usually the course of the intensity changes with dilution, fig 3, indicates the molecular species (H$_2$SO$_4$, HSO$_4'$, or SO$_4''$) of which any given line is characteristic Thus the frequencies 381, 555, 910 (strong), 978 (weak) and 1121 cm^{-1} are present in the pure acid, but die out by 75% They are therefore presumably characteristic of the H$_2$SO$_4$ molecule (The frequency 978 here referred to must not be confused with the fortuitously almost equal frequency 982, which appears only in the most dilute solutions and is characteristic of the SO$_4''$ ion) The lines 595, 895, and 1036–1053 cm^{-1} are not present at all in the pure acid, but appear and rapidly become stronger on dilution, reaching maximum intensity in the neighbourhood of 25% acid This is the behaviour to be expected of lines characteristic of the HSO$_4'$ ion Nisi (*loc cit*) described the last of these frequencies (the strongest) as present in the pure acid (compare also Fadda[*]) Since even a small addition of water suffices to bring out this line (by 90% acid it is already strong), probably this discrepancy is to be explained as due to traces of water in the supposedly 100% acid of Nisi Returning to our own results, the lines 452 and 982 cm^{-1}, although present in the 50% acid, and possibly even in the 75%, do not become markedly appreciable until the acid content has been reduced to 25%, and are strongest in the lowest concentrations This behaviour naturally supports the view that these lines are characteristic of the SO$_4''$ ion These allocations of the different frequencies are indicated beneath the line scheme of fig 3.

The above views as to the origins of the different lines find confirmation in the Raman spectra of solutions of normal and acid sulphates A large number

of workers* agree in giving the following frequencies as characteristic of the SO'_4 ion 452, 617, 982 (strong), and 1106 Of these 982 appears as a strong separate line (E) and 452 as a component of A in the most dilute acids Inspection of the 10% photometer curve at the point corresponding to 617 (namely, just on the long-wave side of B) gives faint indications of the presence of this frequency also Then of the frequencies 595, 895, and 1036–1053 (strong), which we regard as characteristic of the HSO'_4 ion, the first and the last have been observed by Woodward (loc cit) in a solution of $KHSO_4$, where they were accompanied by the SO'_4 ion frequency 982 owing to the partial ionization of the HSO'_4 ions.

There still remain two lines of our spectra as yet unassigned—a moderately strong one at 417 cm.$^{-1}$ and a doubtful diffuse one of very low intensity at about 1195 Since the intensities of both these lines appear to remain approximately constant at all dilutions, they cannot be regarded as characteristic of any one of the species H_2SO_4, HSO'_4, or SO'_4 in particular Their behaviour is, however, consistent with their being common to all three In this connection it is suggestive that approximately the same two frequencies occur in the Raman spectra† of other compounds whose formulæ may be written with two oxygen atoms linked to hexavalent sulphur, viz, sulphuryl chloride (408, 1182), chlorsulphonic acid (410, 1183), dimethyl sulphite (410, 1200) and diethyl sulphite (410, 1204) Moreover, these two frequencies seem to be the only ones common to all these molecules

In conclusion, we should like to make it clear that our analysis of the more diffuse Raman lines of sulphuric acid into relatively narrow components of practically constant frequency is put forward with some reserve While its correctness as an interpretation cannot be regarded as conclusively proved, it is nowhere in conflict with observed fact and the weight of supporting evidence makes it highly plausible It should be noted that our view does not exclude the possibility of relatively small frequency shifts (of the order of ± 5 cm^{-1}) with dilution Another point to be observed is that even the proposed components (like the simple Raman "lines") are only approximately monochromatic Each of them is broader than the theoretical value to be expected from the known widths of the spectrograph and photometer slits This would be 0 18 mm of plate, and the mercury line 4916 A, although more intense than any of the Raman lines, does indeed possess this breadth The Raman components, on the contrary, have an average breadth of about 0 30 mm of

---

* See, for example, the collected data in Kohlrausch, " Der Smekal Raman-Effekt "
† Matossi and Aderhold, ' Z. Physik,' vol. 68, p 683 (1931)

plate   The excess corresponds to an actual line breadth of about 5 Å or 25 cm[1]   This result is in harmony with the conclusions from the preliminary experiments with various slit widths (see above), which give 8 cm[1] (corresponding to the widest slit used) as a lower limit for the breadth of the Raman lines

Summary

Microphotometer curves of the Raman spectra of sulphuric acid are reproduced for concentrations ranging from 100% to 10%   The intensity changes of certain of the lines give a clear picture of the two stages of ionization of the acid   Thus on dilution the frequencies 910, 978, and 1121 cm^{-1} (characteristic of the H_2SO_4 molecule and present in the pure acid) rapidly vanish, while the frequency 1036 (characteristic of the HSO'_4 ion and absent in the pure acid) makes its appearance and increases in intensity   At 50% acid another frequency 982 (characteristic of the SO''_4 ion) appears and subsequently becomes stronger   Other diffuse lines are found to change somewhat in frequency with dilution , but it is shown that their behaviour is consistent with an analysis into relatively narrow components of practically constant frequency, ascribable to the different molecular species present   On this view the characteristic frequencies come out as H_2SO_4, 581, 555 5, 910, 978 and 1121 , HSO'_4, 595, 895 5 and 1036 , SO''_4, 452 and 982 , while 417 and 1195 cm^{-1} are common   The inherent breadth of the lines is found to be about 25 cm[1]   Reference is also made to the behaviour of the continuous background.   Measurements on solutions of magnesium sulphate give no evidence for a variation of the sulphate ion frequency 982 with concentration

A Comparison of Experiment and Calculated Wave-Profiles and Wave-Resistances for a form having Parabolic Waterlines

By W C S WIGLEY

Introduction

It has been found possible to calculate the wave-resistance of simple three dimensional forms, and a number of such results have been obtained[*] which on the whole have shown good agreement with actual measurements when the forms are such as not to violate the assumptions on which the calculations are founded But the calculation of wave-profiles is at present limited to two dimensional forms having infinite draft Hence for the purpose of this research two models were made, at the William Froude Laboratory one of the maximum draft possible under mechanical limitations, with vertical sides and a flat bottom, the other having the greatest draft and displacement which would allow of the measurement of its resistance over the desired range of speeds, but with vertical sides for only half its draft and being then rounded off in vertical section to an edge at the keel The first model (No 1254) was used to measure wave-profiles which were compared with those calculated for infinite draft, the second model (No 1302) was used for the comparison of measured and calculated resistances

It was impossible to use the first model for this purpose as the added resistance due to eddying round the sharp corners at the bilges would render quite meaningless any calculation of the frictional resistance which must be subtracted from the measured force to find the wave-resistance Its wave-resistance was, however, calculated in order to show the similarity in shape between the calculated resistance curves of the two models Fig 1 shows perspective sketches of these models and the equations of their surfaces appear below (equations (1) and (7) respectively)

List of Symbols used throughout the Paper

L = total length of model,

l = length of curved entrance or run,

$2a$ = length of parallel body,

$2b$ = maximum beam,

d = draft,

c = speed of advance,

ρ = density of water, taken as 1 94 foot lb sec units in calculations,

g = acceleration due to gravity, taken as 32 2 in calculations,

$\kappa = g/c^2$,

ζ_w = surface elevation due to wave-system,

ζ_l = surface elevation due to "non-wave" portion of the disturbance caused by the motion of the form,

R_w = resistance due to wave-making,

H_0 = Struve's function of order zero,

Y_0 = Bessel's function of the second kind and of order zero
$\left.\right\}$ (G N Watson's definitions)

P_n and Q_n represent certain functions defined as they occur in the paper

Model 1254

Model 1302
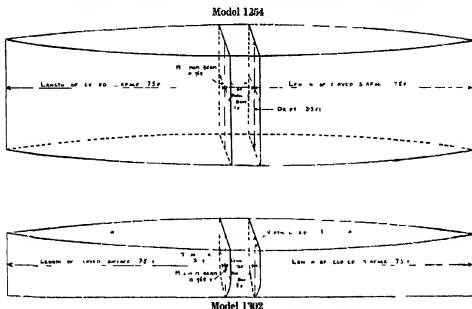
FIG 1 —*Sketch of under water forms of models 1254 and 1302*

Foot-pound-second units and Cartesian axes were used throughout the calculations ; Ox being in the direction of motion, Oy vertically downwards, and Oy at right angles to the other two axes The origin of co-ordinates is amidships, in the centre line and in the plane of the undisturbed water surface, except that in equation (2) (to avoid negative values of the arguments of

certain functions) the origin has been taken at the bow and Ox reversed in
direction

The calculations of resistances and wave-profiles are made on the following
assumptions, by the methods either of Michell or of Havelock —

(1) The usual assumption in dealing with wave motion that the wave
height is small compared with the other lengths occurring in the problem
and that the velocities due to the wave motion are small compared with the
other velocities involved   For ship waves this means that the wave height
is small compared with the length and draft of the ship, and the velocities due
to the wave motion are small compared with the ship's speed   It is also
assumed that the angle made by the tangent plane to the side of the form with
the vertical median plane of the ship is small

(2) It is assumed that the effects of turbulence and viscosity can be neglected

(3) In comparing calculated resistances with those of models in the tank,
it is necessary also to assume that the alteration in the trim and sinkage of
the hull during motion does not alter the effective wave-making form sufficiently
to affect the wave motion appreciably   When wave-profiles alone have been
compared this question does not arise, since the models were rigidly attached
to the tank carriage and not allowed to trim or sink.

Measurement of Wave-Profiles

The model (No   1254) used for the wave-profile measurements had water
lines with the equation

$$\left\{ \begin{array}{ll} y = b \left\{ 1 - \overline{[x-a/l]^2} \right\}, & \text{from } x = a \text{ to } x = l + a \\ y = b, & \text{from } x = -a \text{ to } x = +a \\ y = b \left\{ 1 - \overline{[x+a/l]^2} \right\}, & \text{from } x = -a - l \text{ to } x = -a \end{array} \right\}, \quad (1)$$

where

$$l = 7\ 5,$$
$$b = 0\ 484,$$
$$a = 0\ 5$$

The draft of the actual model was 3 5 feet, with 0 5 feet of necessary free-
board.   This gave a total depth of 4 0 feet, which was the maximum vertical
dimension of a model which could be lifted into the Yarrow tank *

* The dimensions of the cross-section of the Yarrow tank are 30 feet wide by 12¼ feet
deep.

For the purpose of the measurement of the wave profiles this model was rigidly attached to the travelling carriage of the Yarrow tank, and was towed through the water at a series of speeds from 3 5 to 10 8 feet per second

A network of vertical and horizontal lines had been previously marked on one side of the model, the horizontal lines being $\frac{1}{4}$ inch apart, and the verticals normally 1 foot apart, but placed more nearly together near the ends of the model During experiments at each speed the height of the water surface at each vertical was observed, the closer spacing near the ends of the model enabling more accurate observation where the slope of the water surface was greatest

Two wooden beams were clamped to the carriage, forming extensions of 20 feet aft and 6 feet forward respectively of the centre line of the model Each of these beams carried, at intervals of 1 foot, pointers sliding vertically which were adjusted during each experiment so that their pointed ends just touched the water surface By this means the wave-profile could be plotted for a distance corresponding to the length of the beams Additional pointers were again fitted where the slope of the wave-profile was steepest, *i e*, near the bow and stern of the model Owing to a very slow, long and persistent wave which is always set up in the tank during experiments, errors of measurement of $\pm$ 0 05 inch are unavoidable Once an experiment has been made at one of the higher speeds, changes of this order in the water level are known to last for some 24 hours, and it is therefore impracticable to wait for their cessation

Calculation of Wave-Profiles

Calculations were made for a form as given by equations (1) but having infinite depth using a formula given by Havelock[†] for the wave-profile of any two-dimensional form of infinite draft The profile actually given by the formula is that along the centre line of the form (the axis of x), but the error involved in using this formula to find the profile on the curved surface of the model (which is of the same order as those introduced by the assumption that the angle is small between the tangent plane to the side of the form and the median plane) can be neglected For this particular form the expressions for the " wave " and " non-wave " portions of the profile become respectively

$$\zeta_w = (8b/\pi\kappa l) \left[P_0 \{\kappa x\} + P_0 \{\kappa (x - 2l - 2a)\} - (1/\kappa l)(P_0^{-1} \{\kappa x\}\right.$$
$$\left. - P_0^{-1} \{\kappa (x - l)\} + P_0^{-1} \{\kappa (x - l - 2a)\} - P_0^{-1} \{\kappa (x - 2l - 2a)\}\right], \quad (2A)$$

$$\zeta_t = (- \ 2b/\pi a d) \, [Q_0 \, \{\kappa x\} + Q_0 \, \{\kappa \, (x - 2l - 2a)\} - (1/\kappa l) \, (Q_1 \, \{\kappa x\})$$
$$- \ Q_1 \, \{\kappa \, (x - l)\} + Q_1 \, \{\kappa \, (x - l - 2a)\} - Q_1 \, \{\kappa \, (x - 2l - 2a)\}] \qquad (2\text{B})$$

In these expressions the origin has been moved to the bow, and the positive
direction of x is now astern. The functions P_0 and P_1 are supposed to be
zero for negative values of their arguments, and for other values to be defined
by the equations

$$\left. \begin{array}{l} P_0 \, (u) = \displaystyle\int_0^{\pi/2} \sin \, (u \sec \phi) \; d\phi \\[2mm] P_0^{\;1} \, (u) - 1 = P_1 \, (u) = 1 - \displaystyle\int_0^{\pi/2} \cos \phi \; \cos \, (u \sec \phi) \, d\phi \end{array} \right\} \qquad (3\text{A})^*$$

The functions Q_0, Q_1 are defined, for positive values of the arguments by the
equations

$$\left. \begin{array}{l} Q_0 \, (u) = \dfrac{\pi}{2} \displaystyle\int_0^u \{H_0 \, (t) - Y_0 \, (t)\} \, dt \\[3mm] Q_1 \, (u) = \displaystyle\int_0^u Q_0 \, (t) \; dt \end{array} \right\} , \qquad (3\text{B})$$

where H_0 is Struve's function and Y_0 the Bessel function of the second kind,
both of order zero, and by the convention that $Q_0 \, (-u) = Q_0 \, (u)$ and
$Q_1 \, (-u) = -Q_1 \, (u)$ for negative values of the argument.

Detailed calculations of the wave heights have been made for this form from
equations (2) for seven speeds covering a range which corresponds with possible
ship speeds. These speeds are given in Table I, with the value of the non-
dimensional speed unit used in this paper, the (P) speed unit commonly used
in shipbuilding work in this country and the so-called Froude number $(c/\sqrt{gl})$
which is in common use abroad

Table 1

c	$c/\sqrt{gl}$	(P)	$c/\sqrt{gl}$, → (Froude number)
4 22	0 272	0 562	0 193
5 45	0 351	0 726	0 250
6 74	0 433	0 897	0 308
7 95	0 512	1 059	0 364
9 18	0 592	1 225	0 421
10 42	0 675	1 399	0 480
10 70	0 694	1 434	0 494

* For further particulars, series, and asymptotic expansion of these functions, see
Havelock, 'Proc Roy Soc,' A, vol. 108, pp 81, 82 (1925), vol 103, pp 577–579 (1923)
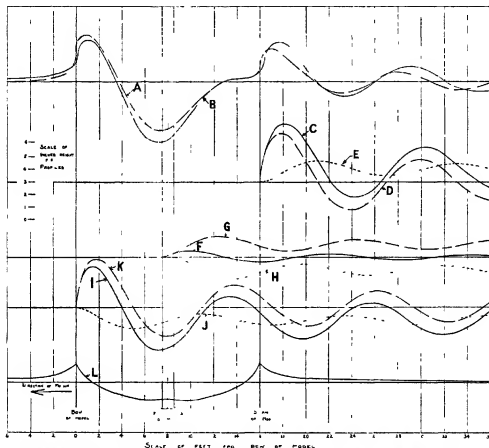
FIG 3.—Model 1264. Analysis into components of calculated wave-profile Speed 7 95 feet per second, $c \sqrt{gl} = 0\ 512$

A   Observed wave profile

B   Total calculated wave-profile $\zeta_w + \zeta_l$ given in (2a)

C   Total stern wave profile given by terms $(8b/\pi d) [P_0^{-1} \{ x(x - 2l - 2l) \} + (1\ 'd)\ P_0^{-1} \{ x(x - 2l - 2l - 2u) \}]$ in (2a)

D   Profile of wave system commencing at stern due to stern angle given by term $(8b/\pi d)\ P_0^{-1} \{ x(x - 2l - 2l) \}$ in (2a)

E   Profile of wave system commencing at stern due to curvature of form given by term $(8b/\pi e^{2l})\ P_0^{-1} \{ x(x - 2l - 2l - 2u) \}$ in (2a)

F   Sum of profiles of forward and after shoulder wave systems given by term $(8b/\pi e^{2l}) [P_0^{-1} \{ x(x - l) \} - P_0^{-1} \{ x(x - l - 2u) \}]$ in (2a)

G   Profile of wave-system commencing at forward shoulder and due to curvature of form, given by term $(8b/\pi e^{2l})\ P_0^{-1} \ x(x - l)\}$ in (2a)

H   Profile of wave-system commencing at after shoulder and due to curvature of form, given by term
$(- 8b/\pi e^{2l})\ P_0^{-1} \{ x(x - l - 2u) \}$ in (2a)

I   Total bow wave profile given by term $(8b/\pi d) [P_0 \{ xx \} - (1/'d) P_0^{-1} \{ xx \}]$ in (2a)

J   Profile of wave-system commencing at bow and due to curvature of form, given by term $(- 8b/\pi e^{2l})\ P_0^{-1} \{ xx \}$ in (2a)

K   Profile of wave-system commencing at bow due to bow angle given by term $(8b/\pi d)\ P_0 \{ xx \}$ in (2a)

L   Profile of symmetrical disturbance $= \zeta_l$, given in (2b)
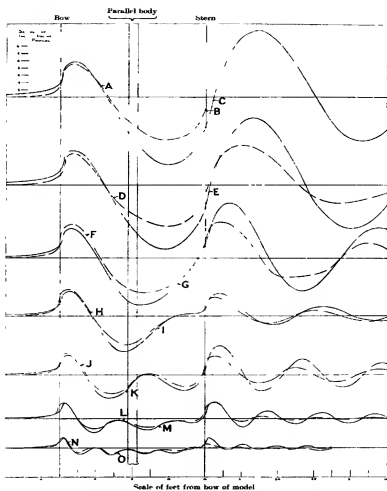
Scale of feet from bow of model

Fig 2.—Model 1254   Comparison of calculated and observed wave profiles

A Broken line is observed wave profile at 10 78 feet per second ($c/\sqrt{gl} = 0$ 694)   (No experimental values of wave height are available aft of the point marked B for this speed)
C Full line is calculated wave profile at 10 78 feet per second ($c/\sqrt{gl} = 0$ 694)
D Broken line is observed wave profile at 10 50 feet per second ($c/\sqrt{gl} = 0$ 675)
E Full line is calculated wave profile at 10 50 feet per second ($c/\sqrt{gl} = 0$ 675)
F Broken line is observed wave profile at 9 29 feet per second ($c/\sqrt{gl} = 0$ 592)
G Full line is calculated wave profile at 9 29 feet per second ($c/\sqrt{gl} = 0$ 592)
H Broken line is observed wave profile at 7 95 feet per second ($c/\sqrt{gl} = 0$ 512)
I Full line is calculated wave profile at 7 95 feet per second ($c/\sqrt{gl} = 0$ 512)
J Broken line is observed wave profile at 6 74 feet per second ($c/\sqrt{gl} = 0$ 433)
K Full line is calculated wave profile at 6 74 feet per second ($c/\sqrt{gl} = 0$ 433)
L Broken line is observed wave profile at 5 46 feet per second ($c/\sqrt{gl} = 0$ 351)
M Full line is calculated wave profile at 5 46 feet per second ($c/\sqrt{gl} = 0$ 351)
N Broken line is observed wave profile at 4 22 feet per second ($c/\sqrt{gl} = 0$ 272)
O Full line is calculated wave profile at 4 22 feet per second ($c/\sqrt{gl} = 0$ 272)

The actual and the calculated wave-profiles for each speed are shown in fig 2. It will be seen that along the side of the form the chief peculiarities of the observed profiles are well reproduced by calculation The observed bow wave is generally a little higher than the calculated, except at the highest speeds, whereas the stern wave is generally lower Ahead of the form the disturbance is never so high as calculated, while aft of the form the disturbance (as would be expected) dies away much more quickly particularly at the slow speeds than it would in a perfect fluid

Examination of the first equation (2) shows that the wave profile may be divided into six components, two originating at the bow, two at the stern, and one at each end of the parallel body, that is, at the forward and after shoulders The two terms involving the function P_0 are the same as would occur to produce bow and stern wave-systems in a form composed of straight lines having the same angle at bow or stern This bow wave is decreased and this stern wave increased by the terms

$$- (1/\varkappa l) \ P_0^{-1}(\varkappa x) \quad \text{and} \quad (1/\varkappa l) \ P_0^{-1}\{\varkappa (x - 2l - 2a)\},$$

respectively, which may be considered as representing additional wave-systems due to the curvature of the form starting at bow and stern respectively Owing to the presence of an extra factor $\varkappa$ in the denominator, these terms increase more rapidly with the speed than the terms in P_0, and their effect is therefore much greater at the higher speeds The other two terms,

$$(1/\varkappa l) \ P_0^{-1}\{\varkappa (x - l)\} \quad \text{and} \quad (- 1/\varkappa l) \ P_0^{-1}\{\varkappa (x - l - 2a)\}$$

represent wave-systems starting at the beginning and end of the parallel body, they also are of little importance at low speeds, owing to the factor $\varkappa$ in their denominator, and since they are equal in amplitude and opposite in phase and separated only by the length of parallel body—which corresponds, as the speed increases, to less and less difference in phase between them - their combined effect does not grow greatly with speed, and they are never of very great importance

These statements are consistent with the known experimental facts, that the wave-making of a parabolic form is largely concentrated at the ends, and that it is an efficient form for low speeds, where the two terms mentioned in the second place above are of no great importance In order to exhibit the relative importance of these terms, fig 3 has been drawn showing their respective sizes for $c = 7\ 95$ ft per sec $(c/\sqrt{gl} \approx 0\ 512)$ To see the relative importance at any other speed it should be noted that the two systems depending on the bow and stern angles respectively will increase in height as the square of the

speed, while the remaining four systems will increase in height as the fourth power of the speed, and the wave-lengths of all the systems will increase in proportion to the square of the speed

From what has been written above it will be seen that the total bow wave-profile is given by the equation

$$\zeta_{B_{w}} = (8h/\pi\kappa l) [P_0 \{\kappa x\} - (1/\kappa l)\ P_0^{-1} \{\kappa x\}], \qquad (4)$$

and that the crests and troughs of the bow wave-system will therefore occur at positions given by values of x such that

$$\delta\zeta_{B_{w}}/\delta x = 0,$$

or, differentiating,

$$Y_0 (\kappa x)/P_0 (\kappa x) = -2c^2/\pi g l, \qquad (5)$$

since $d\ P_0 (u)/du = -\pi\gamma_0 (u)/2$ and $d\ P_0^{-1} (u)/du = P_0 (u)$ Curves of the function $Y_0 (u)/P_0 (u)$ have been plotted and with them aid the values of x satisfying equation (5) for a series of values of c have been calculated A similar equation, with only the sign changed, holds for the stern wave system , curves showing the position of the crests and troughs of the waves of the two systems over a range of speeds have been calculated and plotted in fig 4 on a base of $c/\sqrt{gl}$

From these curves the speeds of coincidence in the crests and troughs of these systems can be seen , the relation of these to the maxima and minima of wave resistance will be discussed at a later stage in the paper

Calculation of Resistance for the Form of Great Draft

The wave resistance of this form was calculated by the use of Havelock's result, which in the notation of this paper is given by the equation

$$R_w/c^2 = [64\rho b^2/\pi\kappa^3 l] [\{1/3 + 1/\kappa^2 l^2\} + \{P_3 (p_2)/2 - P_4 (p_1)/p + P_5 (p_1)/2p^2\} \\ - \{P_4 (p)/p - P_5 (p)/p^2 - P_4 (p_2)/p + P_5 (p_2)/2p^2)\}], \qquad (6)$$

in which, for brevity, p has been written for κl, p_1 for $2 (l + a)\kappa$ or $l\kappa$, p_2 for $(2a + l)\kappa$ and p_2 for $2a\kappa$, whilst

$$\left.\begin{array}{l} P_3 (u) = \displaystyle\int_0^{\pi/2}\ \cos^3 \phi\ \ \cos (u \sec \phi)\ \ d\phi \\[2mm] P_4 (u) = \displaystyle\int_0^{\pi/2}\ \cos^4 \phi\ \ \sin (u \sec \phi)\ \ d\phi \\[2mm] P_5 (u) = -\displaystyle\int_0^{\pi/2}\ \cos^5 \phi\ \ \cos (u \sec \phi)\ \ d\phi \end{array}\right\}\ *$$
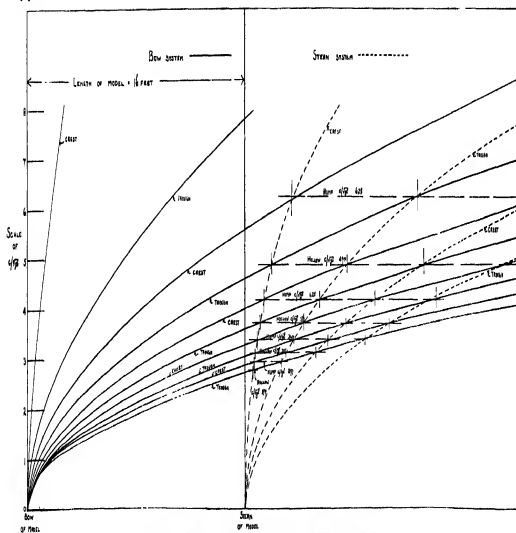
* See footnote * on p. 148.

Fig. 6.—Model 2254. Positions of crests and troughs of bow and stern wave systems at various speeds

Of the three terms of equation (6) in twisted brackets the first clearly represents the steady increase of wave making resistance with speed, apart from any question of interference between the wave-systems The second, depending directly on the total length of the form, represents the interference between the bow and stern systems Each of the terms in the third bracket represents some form of interference between the systems at the ends of the parallel body and the bow and stern systems, or between the systems at the ends of the parallel body themselves These terms have not been considered separately because in this form their total effect is comparatively small

Fig 5 gives curves showing these three components, and also a curve of the total value of R_w/c^2 Owing to the great increase of this quantity with speed, the scale of the lower portions of the curves had to be exaggerated as shown in the diagram It is clear that the main peculiarities of the total curve of R_w/c^2 are due to the component corresponding with the second term in twisted brackets on the right-hand side of equation (6), and are therefore due to interference between the waves of the bow and stern systems It is therefore of interest to compare the speeds of coincidence of crests and troughs of

Table II—Values of $c/\sqrt{gl}$ Corresponding to certain Phenomena

	Model 1254			Model 1302		Maximum or minimum of R_w/c^2
		Calculated values of $c/\sqrt{gl}$ for maxima and minima of		Values of $c/\sqrt{gl}$ for maxima and minima of total R_w/c^2		
Calculated values of $c/\sqrt{gl}$ for wave coincidences between bow and stern systems	Bow and stern interference component of R_w/c^2	Total R_w/c^2	Calculated	Measured	
Crest with crest 0 63	0 09	0 85	0 75	0 80	Maximum
Crest with trough 0 49	0 51	0 64	0 61	0 52	Minimum
Crest with crest 0 42	0 44	0 44	0 44	0 44	Maximum
Crest with trough 0 37	0 38	0 38	0 38	0 38	Minimum
Crest with crest 0 34	0 34	0 34	0 34	0 35	Maximum
Crest with trough 0 31	0 31	0 31	0 31	0 31	Minimum
Crest with crest 0 30	0 30	0 30	0 30	0 30	Maximum

these systems, as calculated in the last section of the paper, with the corresponding speeds of maximum and minimum values of R_w/c^2 This comparison appears in Table II, which also includes for reference the calculated and measured maxima and minima for the shallower model 1302, experiments on this model and the corresponding calculations are described later

It will be seen that the wave-coincidences agree quite well with the maxima and minima of R_w/c^2, excepting at the highest speeds where the maxima and minima of R_w/c^2 always occur at a higher speed than that of the wave-coincidences—seriously so in the last maximum   Further, the main discrepancy

FIG 5A.—Parabolic model of infinite draft model 1254   Separation of wave resistance into components. $c/\sqrt{gl} < 0\ 675$

is between the last maximum of total R_w/c^2 and the last maximum of the interference component of R_w/c^2 This latter difference is due entirely to the term $1/c^{3/2}$ in the first term in the bracket on the right-hand side of equation (6)   this term varies as c^4, and therefore delays the maximum of the R_w/c^2

curve by causing the function to continue to increase after the interference term has actually begun to decrease The difference between the highest maximum of the component and the corresponding wave coincidence is due to the factor $1/\kappa^2 l^2$ outside the bracket, which acts in a similar way Naturally the effects of these factors are only sensible for large values of c, and their influence has been checked by separate calculations which confirm the remarks made above It is noteworthy that the distance from the first crest of the
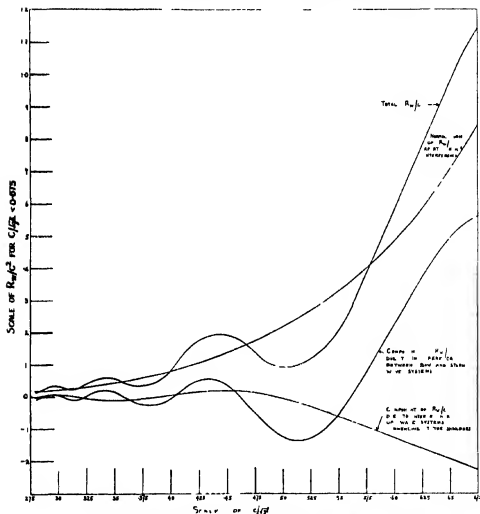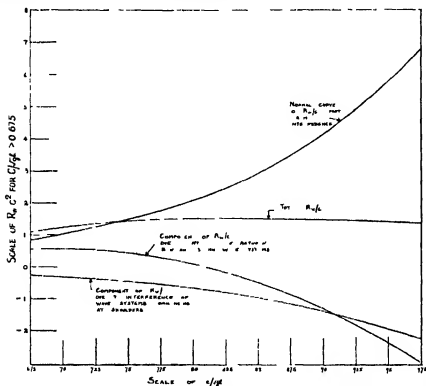

Fig 5B —Parabolic model of infinite draft model 1254 Separation of wave resistance into components $c/\sqrt{gl} > 0.675$

bow wave to the first crest of the stern-wave, as shown in fig 4, increases from a value equal to the length of the model ($= 16$ feet) at very slow speeds to a value of just over 20 feet at $c/\sqrt{gl} = 0.80$, where l is, as above, the length of the curved surface of the bow or stern of the form ($= 7.5$ feet) Owing to the delay in the higher maxima of R_w/c^2, for reasons which are stated above this distance if deduced from the calculated resistances would appear to increase more than it actually does Thus Havelock (*loc cit*) has calculated the apparent value of this distance from the resistance of a model, like No 1254 but without

parallel, whose length was 160 feet he finds this distance—equal to $Z + \lambda/2$ in his notation—to increase from 166 feet at the slowest speeds to 260 feet at $c/\sqrt{gl} = 0\ 72$

Measurement of Resistance of Shallow Model

It has been shown that the calculated components of the wave-profiles for this form are related to the maxima and minima of the calculated curves of R_w/c^2, and that these calculated components add up to form a complete wave-profile which, generally speaking, has the same peculiarities of shape as the wave-profile actually measured with model 1254 It remains to show that the calculated resistance curve agrees in the same way with a measured resistance curve As explained earlier, the sharp corners at the bilge of model 1254 would render resistance measurements with this model of very doubtful interpretation Since it is known that draft has very little influence on the shape of resistance curves,* a model, No 1302, was constructed having the equation

$$
\left.
\begin{aligned}
y &= b\left\{1 - \overline{[x - a/l]^2}\right\} && \text{from } z = 0 \text{ to } z = 1 \\
y &= (b/3)\{4 - z^2\}\{1 - \overline{[x - a/l]^2}\} && \text{from } z = 1 \text{ to } z = 2
\end{aligned}
\right\}
\begin{aligned}
& \text{from } x = l + a \\
& \text{to } x = a
\end{aligned}
$$

$$
\left.
\begin{aligned}
y &= b && \text{from } z = 0 \text{ to } z = 1 \\
y &= (b/3)(4 - z^2) && \text{from } z = 1 \text{ to } z = 2
\end{aligned}
\right\}
\begin{aligned}
& \text{from } x = a \\
& \text{to } x = -a
\end{aligned}
$$

$$
\left.
\begin{aligned}
y &= b\left\{1 - \overline{[x + a/l]^2}\right\} && \text{from } z = 0 \text{ to } z = 1 \\
y &= (b/3)\{4 - z^2\}\{1 - \overline{[x + a/l]^2}\} && \text{from } z = 1 \text{ to } z = 2
\end{aligned}
\right\}
\begin{aligned}
& \text{from } x = -a \\
& \text{to } x = a
\end{aligned}
$$

$$(7)$$

where a, b, l have the same values as for model 1254 described above, i e, 0 5, 0 484, and 7 5 feet respectively The form of this model is shown in fig 1, it is the same as model 1254 for 1 foot depth, but then tapers off in a parabolic curve to a knife edge keel at 2 feet depth, the waterlines at any section are similar parabolic arcs joined by 1 foot of parallel body amidships It will be seen from the equation that there is a slight vertical angle or knuckle at $z = 1$, but this was rounded off in the actual model on the sections near amidships, where alone it was sensible The resistance of this model was measured in the Yarrow tank, using the ordinary resistance dynamometer, over a range of speeds from $c = 4\ 0$ to $c = 12\ 3$ ft per sec Since the dynamometer is only capable of measuring 49 lbs. resistance, added pulls of 10 and 20 lbs

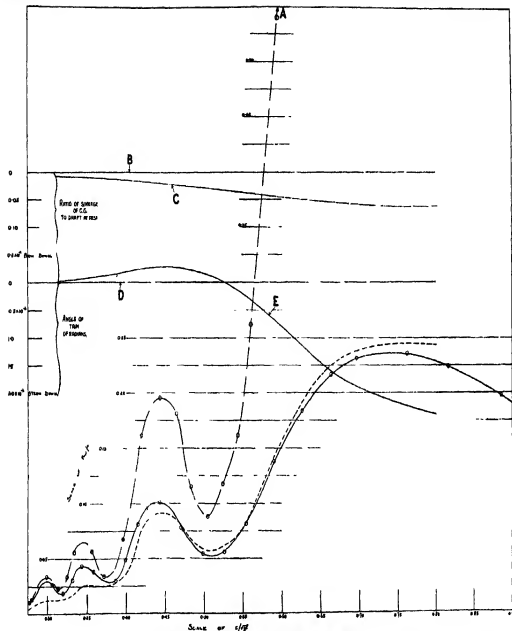* See Havelock, 'Proc. Roy Soc,' A, vol 108, pp. 582 et seq (1925).

Fig 5.—Resistance of parabolic models Nos. 1354 and 1302.

A. Curve rises to maximum value of R_w/c^2 = 1·52 at $c/\sqrt{g}$ = about 0·79. B. Zero line for sinkage curve. C. Curve of sinkage of C.G (plotted as proportion of draft at rest). D. Zero line of trim curve. E. Curve of angle of trim.

Key to Resistance Curves.

— · — Calculated curve of R_w/c^2 for model of infinite draft with vertical sides—approximately Model 1354—load water line same as Model 1302.

· · · Observed curve of R_w/c^2 for Model 1302. Frictional resistance subtracted as calculated by Froude using surface as actually wetted during motion.

— 0 — Calculated curve of R_w/c^2 for Model 1302.

were provided as required by cords attached to the model and tensioned by the necessary weights   The speed of advance was measured, as usual, by the aid of an electric contact which opened momentarily at intervals of 20 feet travel, and of a clock recording half-seconds   In addition the trim and bodily sinkage of the model due to its motion were recorded during each experiment, in order to estimate the actual violation of the third assumption mentioned above   The actual measured speeds and resistances are given in Table III

Table III —Model 1302   Mean Temperature 55 7° Fahrenheit

Speed	Resistance	Speed	Resistance	Speed	Resistance
4 04	3 507	6 71	13 00	9 22	40 11
4 21	3 827	6 87	13 56	9 26	39 20
4 29	4 025	6 96	14 26	9 46	41 84
4 46	4 389	7 08	14 54	9 59	43 00
4 57	4 650	7 21	14 62	9 74	35 83
4 74	5 064	7 32	14 85	9 71	36 49
4 84	5 211	7 47	14 93	9 92	39 37
4 97	5 450	7 54	15 04	10 14	40 18
5 04	5 713	7 67	15 24	10 20	42 61
5 17	6 165	7 81	15 62	10 25	42 69
5 32	6 541	7 93	15 80	10 47	46 44
5 58	7 291	7 98	16 17	10 56	46 59
5 69	7 579	8 18	17 04	10 67	48 82
5 81	7 706	8 23	17 40	10 73	49 25
5 98	8 015	8 43	19 01	11 04	52 15
6 04	8 587	8 46	19 41	11 21	54 94
6 24	9 238	8 70	21 77	11 81	59 65
6 32	10 14	8 79	22 61	12 04	62 71
6 49	11 04	8 93	24 57	12 28	64 74
6 56	11 99	8 96	25 14		

The frictional resistance was calculated from the data of Froude,[*] a correction being made when the temperature differed from the standard value of 55° F used by Froude   The area of wetted surface assumed in the calculation exceeded the actual wetted surface of the model when at rest by an amount varying from $1\frac{1}{4}\%$ at the lowest speed to $5\frac{1}{4}\%$ at the highest, to allow for the additional surface wetted during motion   This correction was the same as had been measured on a model of similar dimensions used previously   Since the correction is in any case only an approximation, the added error due to this procedure is not of importance

When the frictional resistance as thus calculated is subtracted from the measured resistance, the measured wave resistance R_w is found , and in fig 6

* 'Trans Inst Naval Arch ,' vol. 29, p 304 (1888)

is shown the curve of R_w/c^2 as measured for this model The values of the measured angle of trim (in radians), and of the measured sinkage of the C G of the model (expressed as a fraction of the draft) are also shown in this figure

Calculation of Resistance for Shallow Model

The resistance of this form has also been calculated by the use of the expression found by Michell* for the wave-resistance of a form obeying the assumptions quoted at the beginning of this paper For a form having the equation $y = f(x, z)$ this expression is as follows —

$$R_w = (4\rho g^2/\pi c^4) \int_1^\infty (I^2 + J^2) (\lambda^2/\sqrt{\lambda^2 - 1}) \ d\lambda$$

where

$$I = \int_0^\infty \int_{-\infty}^{+\infty} f'(x, z) \ e^{-\lambda^2 g z/c^2} \cos(\lambda g x/c^2) \ dx \, dz$$

$$J = \int_0^\infty \int_{-\infty}^{+\infty} f'(x, z) \ e^{-\lambda^2 g z/c^2} \sin(\lambda g x/c^2) \ dx \, dz$$

(8)

where $f'(x, z) = \delta \{f(x, z)\}/\delta x$

For model 1302, having the equation (7) above, a simple integration shows that

$$J = -(1024/225 \ \theta^2) \{\sin \theta - \sin (\theta/16)$$
$$- (15 \ \theta \ \cos \theta/16) \{3\psi^2 - 2e^{-\psi} (\psi + 1) + 2e^{-2\psi} (2\psi + 1)\}/3\psi^3$$

$$I = 0,$$

where

$$\theta = 8\lambda g/c^2, \qquad \psi = \lambda^2 g/c^2,$$

and hence

$$R_w/c^2 = 11 \ 98 \int_1^\infty \{F_1 (\psi) \ F_2 (\theta)/\lambda^3 \sqrt{\lambda^2 - 1}\} \ d\lambda,$$

(9)

where θ and ψ are as above, and

$$F_1 (\psi) = \{1 - 2e^{-\psi} (\psi + 1)/3\psi^3 + 2e^{-2\psi} (2\psi + 1)/3\psi^3\}^2,$$
$$F_2 (\theta) = \{\sin \theta - \sin \theta/16 - (15 \ \theta \ \cos \theta/16)\}^2/\theta^4$$

The functions F_1 and F_2 have been calculated and plotted on a large scale , it is thus a simple matter to calculate the value of the integrand on the right-hand side of the equation (9) for a number of values of λ at each speed Hence the value of the integral has been obtained by Simpson's rule, care being taken

* 'Phil Mag,' vol 45, p. 113 (1898)

that a sufficient number of values was used to ensure accuracy in the final result The apparent infinity at the lower end of the range of integration was avoided by the usual method of assuming that to the order of accuracy required

$$\int_{1}^{1\,001} \{F_1(\psi)\ F_2(\theta)/\lambda^3\sqrt{\lambda^2-1}\}\,d\lambda = \tfrac{1}{2}\left\{\left[\frac{F_1(\psi)\ F_2(\theta)}{\lambda^3}\right]_{\lambda=1\,001}\right.$$
$$\left. + \left[\frac{F_1(\psi)\ F_2(\theta)}{\lambda^3}\right]_{\lambda=1\,000}\right\}\int_{1}^{1\,001}\frac{d\lambda}{\sqrt{\lambda^2-1}}$$

the right-hand side of this equation being easily calculated At the upper end of the range of integration the approximate integration was at each speed carried out sufficiently far to ensure that $F_1(\psi)$ had attained to within 2% of its maximum value of unity The rest of the integral can be expanded in inverse powers of θ_0, and the first two terms of the result are given by the equation

$$\text{Correction to integral} = (225\kappa^2/320\theta_0^4)\,(1 - 2\sin 2\theta_0/\theta_0),$$

where θ_0 is the value of θ up to which the approximate integration has been carried out

Table IV — Calculated R_K/c^3 for Model 1302

$r/\sqrt{gl}$	R_K/c^2	$r/\sqrt{gl}$	R_K/c^3
0 186	0 0049	0 443	0 1013
0 222	0 0086	0 471	0 0766
0 251	0 0085	0 499	0 0540
0 277	0 0105	0 526	0 0561
0 306	0 0265	0 554	0 0820
0 310	0 0178	0 590	0 1379
0 342	0 0303	0 627	0 1840
0 343	0 0435	0 663	0 2164
0 358	0 0377	0 697	0 2315
0 387	0 0303	0 762	0 2355
0 399	0 0490	0 815	0 2234
0 415	0 0816	0 886	0 1974
0 428	0 0954		

The curve of R_K/c^2 as thus calculated is shown in fig 6 compared with the curve for the same quantity as derived from the model experiments, it will be seen that there is general agreement The actual calculated values of R_K/c^3 are also given in Table IV The curve of R_K/c^3 as calculated for model 1254 by the method described above is also shown on the diagram, and it will be seen that apart from amplitude the positions on a speed base of the maxima and minima of all three curves are in good agreement These are

tabulated in the last two columns of Table II, they have been derived from curves drawn on a much larger scale than can be reproduced here

It appears from Table II and from inspection of all the relative curves in fig 6 that the main features of the wave-making of all the shallower three-dimensional model are the same as those of the model of infinite draft, and accordingly must originate in interference of similar wave systems to those relating to that form and described above As might be expected, the resistance at the higher speeds (corresponding to larger waves) is very much larger for the model of infinite draft, whereas at slower speeds the difference is not so great It is known that the depth to which the shape of a form affects the wave-making varies, at any rate approximately as the length of the wave generated, and thus is supported by the foregoing observation

General Conclusions

The maxima and minima of the resistance curves have been shown to originate in interference between the bow and stern component wave-systems, this being calculated definitely for the model of infinite draft, and inferred from the similarity of the resistance curve for the shallower three-dimensional model It is noted that the higher speed maxima of the resistance curves tend to occur at higher speeds than would be produced from the speeds of coincidence of the wave-systems, and the reason for this is given

This general result is in contrast with that obtained previously from a model[*] having sections composed of straight lines meeting at angles at the shoulder, in the latter shoulder wave-making was of primary importance

It is hoped to make further experiments with models of different shapes, and in this way to obtain some definite relation between form and wave-profile Particularly it is proposed to investigate a form with hollow water-lines, since straight and convex lines have now been dealt with Until this has been done it is not wise to draw any general conclusions regarding the wave-making properties of forms not yet investigated, since it is clear that in different forms the relative importance of different portions of the form will vary greatly

Summary

The several effects of the various geometrical features of a body on the form of the waves it generates when moving on the surface of water, and on the resistance it experiences, are of theoretical as well as practical interest to

shipbuilders. It is now possible to investigate this influence, for simple forms, by approximate methods of calculation, in this paper an investigation is described for a form having parabolic waterlines, where possible the results of calculation are compared with actual measurements made in the Alfred Yarrow tank at the William Froude Laboratory

It is found that there is a general agreement between measurement and calculation The main difference between the parabolic forms dealt with here and straight line forms previously investigated is that the ends of the former contribute more largely to the wave resistance

No conclusions can be drawn concerning the wave making effects with other shapes until further experiments and calculations have been made

---

Study of Electrolytic Dissociation by the Raman Effect   II —Nitrates

By I. RAMAKRISHNA RAO, M A, Ph D, Andhra University, Waltair

(Communicated by O W Richardson, F R S—Received October 18, 1933)

1 *Introduction*

In the first part* of these investigations by the author, the possibility of studying electrolytic dissociation by the Raman effect has been described with special reference to nitric acid   Accurate quantitative estimation has since† been made of the degree of dissociation in the acid by measuring the intensities of Raman lines corresponding to the dissociated NO^-_3 ions at various concentrations   The results thus obtained indicated that the dissociation in nitric acid is progressive between the concentrations 1–16 N and not complete as has been assumed for highly dilute solutions

A comparison of the values of the degree of dissociation obtained from this method with those calculated from conductivity measurements revealed a large discrepancy which was attributed to the uncertainty of the latter   The degree of dissociation cannot be directly evaluated from the values of electrolytic conductivity, which depend upon a number of factors such as viscosity of the solution, mobility of the ions, etc, as there is much uncertainty as to the dependence of conductivity on such factors   With Raman spectra, however,

---

* 'Proc Roy Soc,' A, vol 127, p 279 (1930).

† 'Proc. Acad. Sci, Amst.' vol. 33, p. 632 (1930).

the number of molecules or ions is directly proportional to the intensity of the Raman lines corresponding to them. Hence a comparison of the number of molecules or ions at one concentration with that in another is made by simply comparing the intensities of the lines corresponding to them in the Raman spectra taken with the respective concentrations The accuracy of the method is that attainable in the intensity measurements Thus we have in this method a reliable means of measuring electrolytic dissociation, and another advantage is its applicability to concentrated solutions, for which at present no theory has been fully developed In order to determine whether electrolytes are completely dissociated even in concentrated solutions, a systematic study of different electrolytes is being undertaken The results for nitrates will be described in this communication

2 *Raman Spectra of Nitrates in the Crystalline State and in the State of Solution*

The applicability of the Raman effect to the determination of electrolytic dissociation consists in the fact that the undissociated molecules give rise to a set of Raman lines which are in entirely different positions from those arising from the dissociated ions In nitric acid, for example, it is found that the lines with Raman frequencies equal to 953, 1120, 1306 cm $^{-1}$ attributed to the undissociated molecules are different from those with $\delta\nu = 725, 1049$, and 1357 cm $^{-1}$ corresponding to the NO$^{-}_3$ ions The latter set of lines are found to be common to solutions of all nitrates, the former being entirely absent from them. With dilution of the acid the lines with $\delta\nu = 953, 1120$, and 1306 cm $^{-1}$ progressively diminish in intensity, while the other set actually increase in intensity up to a certain dilution and then diminish, a phenomenon similar to the variation of electrolytic conductivity with dilution, which has been explained as being caused by dissociation of the electrolyte

To determine whether there is a similar change in the Raman spectra with undissociated to dissociated nitrates, such spectra are taken with crystals as well as solutions of these salts Table I contains the results of measurements of Raman frequencies in the two different states

There are three generalizations which can be deduced from this table Firstly, the frequencies in the crystalline state are different for different kations Secondly, for the same kation, the frequency in the solid state is higher than for the solution, with the exception of ammonium and possibly potassium nitrates And thirdly, the frequencies of all nitrates in solution are identical

All the three frequencies given in Table I are well known to be due to inner vibrations of the nitrate radical Leaving alone the two fainter lines with mean $\delta\nu = 726$ and 1390 cm $^{-1}$, the intense line 1049 cm $^{-1}$ is attributed to the inactive vibrations of the three oxygen atoms symmetrically with respect to the nitrogen atom Any change in the above frequency can be brought about only by a change in the distances of the oxygens from the nitrogen atom This can be accomplished by imposing upon this group a strong electric field This is perhaps what happens in the crystalline state

Table I – Raman frequencies in cm $^{-1}$ of nitrates in crystals and solutions

Kation	w_3		w_2		w_1	
	Crystal	Solution	Crystal	Solution	Crystal	Solution
Lithium*	728	—	1080	1050	1391	—
Sodium	726 (1)	721 (1)	1071 (10)	1049 (10)	1389 (1)	1361 (1)
Potassium	711 (1)	730 (1)	1051 (10)	1049 (10)	1359 (1)	1357 (1)
Ammonium	709 (1)	728 (0)	1043 (10)	1050 (10)	—	1361 (0)
Magnesium	—	—	1059 (10)	1049 (10)	—	—
Calcium	—	722 (0)	1064 (10)	1049 (10)	—	—
Strontium	—	720 (0)	1054 (10)	1049 (10)	—	1355 (0)
Barium	—	—	1049 (10)	—	—	—
Lead*	—	—	1045	—	—	—

* The values for the crystalline state for these two substances are taken from Gerlach (Ann Physik ,' vol 5, p 196 (1930))

X-ray analysis has revealed that different nitrates crystallise in different forms and belong to different systems of symmetry Thus the relative disposition of the kations and anions is different for different crystals

Sodium nitrate has hexagonal crystals, which appear to have the rhombohedral symmetry of the calcite group Its structure may be pictured as a sodium chloride grouping in which the nitrate groups replace the chlorine atoms, and which has been compressed along a trigonal axis normal to the plane of the nitrate groups Thus the sodium atoms are symmetrical with respect to the nitrate groups and form an ionic lattice, in which no single sodium ion can be exclusively attached to any single nitrate ion If the nitrogen atom is supposed to occupy the centre of the nitrate group, it can be concluded from the above that the nitrogen and sodium atoms are uniformly distributed in the space lattice But the plane containing the oxygen atoms is not thus situated The nitrogen atom is not exactly in the above plane, but is slightly

outside it as is revealed by X-ray study Thus owing to the electrostatic
field arising out of the kations there may be a further displacement of the
nitrogen atom with respect to the plane containing the oxygen atoms, which
would not have taken place if there was no such field The change in the
nitrate frequencies may be due to this displacement Since the nitrates
with different kations belong to different systems of symmetry the relative
disposition of the kations and the anions will be different Hence the dis-
position of the resultant electrostatic field with respect to the plane of the
oxygen atoms in the nitrate group may be different Thus the displacement
of the nitrogen atom from its mean position, and hence its distance from each
of the oxygen atoms, will be slightly different for different crystals, and conse-
quently the internal frequencies will differ

For crystals belonging to the same type of symmetry, as with calcium,
strontium, barium, and lead nitrates, in which the relative disposition of the
kations and the anions is the same, there is a gradual diminution in frequency
from the lighter to the heavier elements This regular change may be explained
as follows The heavier elements, having a larger ionic volume, are at
greater distances from the anions, and hence the resultant electrostatic field,
to which the anion is subject, is smaller in intensity thus resulting in a smaller
displacement of the nitrogen atom

The equality of the Raman frequency in solutions of all nitrates indicates
the identity of this radical in all of them This can occur only if it is present
in the completely dissociated condition If there were undissociated molecules,
the kation with which the nitrate group is in combination should give rise
to a strong electrostatic field (much stronger than in the ionic lattice of the
crystal) involving a change in the distance of the nitrogen with respect to the
oxygens As the different kations of the same valency, which have the same
charge, are of different diameters, they should be at different relative distances
from the centre of the nitrate group Hence the displacement of the nitrogen
atom from the centre of the group should be different Hence the Raman
frequency also should change from one nitrate to another

In order to detect whether there are even faint lines in positions different
from that of the strong line $\delta \nu = 1049$ cm $^{-1}$, very long exposures with solu-
tions of ammonium and sodium nitrates of concentrations 12 N and 8 N
respectively were given Though the above line gave as much density on the
photographic plate as some of the strong mercury lines, no trace of any
additional line could be seen though the concentrations were nearly the highest
possible, thus giving confirmatory evidence of the identical nature of the nitrate

ion in solutions of all nitrates, and consequently of their complete dissociation in solution

If it is assumed that there is complete ionization, the anions and kations are uniformly distributed in space, with the result that there are nearly as many anions surrounding a nitrate group as there are kations. Thus the resultant electrostatic field, if there be one at all, is negligible compared to that present in the crystalline state. Also the nitrate groups, on account of their freedom of movement, are oriented in all possible directions with respect to the neighbouring ions and hence there is no possibility of any displacement of the nitrogen ion with respect to the plane containing the oxygen atoms. Hence the frequency of the nitrate ion is undisturbed by the neighbouring ions.

Other evidence for the hypothesis of complete dissociation is obtained from nitrates containing water of crystallization. Magnesium and strontium nitrates containing respectively six and four molecules of water of crystallization have shown in the solid state lines of very small Raman frequencies which belong to the outer vibrations. Though they are very strong in the crystalline state they are entirely absent in solution. This shows that the complex group containing the six H_2O molecules and the two NO_3 groups are completely disrupted in solution, so that they are no longer intact to produce the outer vibrations.

3 *Variation with Concentration of the Raman line of Sodium Nitrate*

On lines similar to the study of dissociation in nitric acid, the variation, with concentration, of the intensity of the Raman line with $\delta v = 1049$ cm.$^{-1}$ for sodium nitrate has been investigated. Raman spectra with 6 0, 4 8, 3 6, and 2 4 N concentrations are taken under identical conditions of illumination, temperature, time of exposure, etc., so that any variation in the intensity of the Raman line can only be due to variation in the number of radicals giving rise to it. The intensity of the Raman line at 4226 λ due to excitation by the 4047 line of the mercury arc spectrum is given in Table II

Table II — Intensity of the 1049 cm.$^{-1}$ Raman line at different concentrations

Concentration C	Intensity I_o	I_o/C	$I_o/C + 1/6 \, o/8 \, 0$
6 0 N	3 9	0 65	100
4 8 N	2 9	0 61	94
3 6 N	2 2	0 61	94
2 4 N	1 6	0 67	103

The first column contains the molal concentration, the second the intensity of the Raman line, the third the ratio of the intensity to concentration, and in the fourth column are given the ratios of the values of I_s/C to the corresponding value for 6 0 N taken as 100

4 *Discussion of the Results*

The values in the last column are constant to within the degree of accuracy that is attainable in intensity measurements   There is no progressive change and if the slight variation owing to the inaccuracy in the intensity determination is neglected they are fairly constant   This is an indication that the number of NO $_3$ ions at any concentration is proportional to the concentration There is no evidence of any other change taking place as was found for nitric acid, wherein the diminution in intensity is much less than that in proportion to concentration   The above is therefore a clear evidence for the complete dissociation of sodium nitrate even at high concentrations

The results from conductivity data lead to a different conclusion   In Table III is shown the degree of dissociation calculated from both the formulæ

$$\alpha = \frac{\Lambda_c}{\Lambda_0}$$

where Λ_c and Λ_0 are the equivalent conductivities at concentrations c and 0 respectively as well as

$$\alpha = \frac{\Lambda_c \eta_c}{\Lambda_0 \eta_0}$$

where η_c and η_0 are the viscosities

Table III – Degree of dissociation in sodium nitrate from conductivity data

Concentration c	Equivalent conductivity Λ_c	$\dfrac{\Lambda_c}{\Lambda_0}$	Viscosity η	$\dfrac{\Lambda_c \eta_c}{\Lambda_0 \eta_0}$
0 0 N	105 33	100	1 00	100
0 1 N	87 24	82 8	1 00	82 8
0 2 N	82 28	78 1	1 01	78 0
0 5 N	74 05	70 3	1 02	71 7
1 0 N	65 86	62 5	1 04	65 0
2 0 N	54 5	51 8	1 15	59 7
1 0 N	46 0	43 7	1 27	55 5
4 0 N	39 2	37 2	1 40	52 1

The values of the degree of dissociation calculated from both the formulæ indicate that the dissociation in sodium nitrate progressively increases with increasing dilution

This discrepancy can be explained by the fact that the Raman effect method is direct involving no uncertainties, the only assumption made is that the intensity of the Raman line is proportional to the number of NO^-_3 ions giving rise to it, which seems to be quite legitimate. The conductivity formula however, is uncertain as has already been pointed out.

The sources of evidence for the hypothesis of complete dissociation of nitrates are the following –

(1) All nitrates in solution give rise to exactly the same Raman line, though in the solid state they reveal different lines. This shows that the nature of the radical corresponding to this line is identical in all of them in the state of solution, which cannot be so unless they are completely dissociated.

(2) Raman spectra even with saturated solutions of nitrates taken with very long exposures did not show any trace of additional lines which can be attributed to undissociated molecules.

(3) In some nitrates containing water of crystallization, e g , magnesium and strontium, the external frequencies which are revealed by the solid state are entirely absent in solution. This indicates that the molecular aggregates are completely disrupted in solution.

(4) Measurements of the variation of intensity of the 4226 λ line of sodium nitrate with concentration have revealed a direct proportionality between the two, this should occur only if the substance is completely dissociated even at high concentrations.

Summary

Raman frequencies of nitrates in the crystalline state and in the state of solution are given. While in the former state the frequencies are different for different nitrates, in the latter they are identically the same. This is taken as an indication of the complete dissociation of nitrates in solution. Spectra with large concentrations of sodium and ammonium nitrates, taken with very long exposure, did not reveal even the slightest trace of any additional line due to undissociated molecules. Determination of the variation of intensity of the NO^-_3 line of sodium nitrate with concentration has shown that the ratio of intensity to concentration is constant, indicating the exact proportionality between number of NO^-_3 ions and concentration. It is therefore concluded that the study of the Raman effect leads to the hypothesis of complete dissociation of nitrates even at high concentrations.

The Theory of the Structure of Ethylene and a Note on the Structure of Ethane †

By W. G. PENNEY, 1851 Exhibition Senior Research Student, Trinity College, Cambridge

There are two fairly distinct methods of attempting the solution of the structure of polyatomic molecules One is associated principally with the names Hund and Mulliken, while the other owes its development chiefly to Heitler, London, Slater and Pauling The former of these, which following Van Vleck,‡ we shall denote as the H-M procedure, allows the electrons to be fed, one at a time, into a self-consistent field possessing the symmetry of the nuclear framework Each energy level can absorb two electrons on account of the spin degeneracy, and the levels are filled in succession until all of the electrons have been used up In contrast, the H-L-S-P method is based on the idea of electron pairs The spin of an electron on one nucleus is coupled with that of another electron on another nucleus to give a resultant spin or zero, and the pair then form a saturated bond Pairing occurs between the spins in such a way as to give a maximum bonding energy, and the number of free spins capable of being paired with electrons on other atoms constitutes the valency of an atom While the two modes of attack, when carried to a complete solution, are equivalent, they often bear little resemblance to each other, to the approximation to which they are generally tractable It is therefore important, when considering any problem of valency, to make calculations both ways, and if the results agree, one can feel fairly sure of their accuracy It is the principal aim of the present paper to attempt such an attack on the ethylene molecule $CH_2\cdot CH_2$ In addition, some interesting results will be given on the ethane molecule $CH_3\cdot CH_3$

Pauling§ and Slater‖ have suggested rather tentatively that with ethylene the four valence electrons on the C nuclei are arranged with tetrahedral symmetry, just as they are in the methane molecule This would make the H C H angle 109 5°, and the two pairs of electrons comprising the double bond,

similar In order to get the maximum overlapping, and hence presumably the least energy, all six nuclei must lie in one plane We shall discuss this model in some detail and show that by a slight redistribution of the bonds an even more stable arrangement is possible Mulliken[†] has proposed essentially the same type of double bond as we employ, but he did not make any detailed calculations to establish the point If the HCH angles are made right Hückel[‡] has also considered the ethylene molecule, and he concluded that it is the π–π bonds which prevent free rotation about the C–C joint We shall establish this point in much greater detail than he did, and prove at the same time that if one of the CH₂ groups is rotated, the position of minimum energy is attained when all six nuclei lie in one plane

There is one position of the nuclei, " the right-angled model," that appears at first sight more stable than any other If the HCH angles are made right angles and the HCH planes parallel, it is possible to have a pure *p*-bond between each H and its C atom, and for the double bond one pure *s*-*s* and one pure *p*-*p* bond The criterion that the most stable configuration is that with the most overlapping would seem to favour this arrangement However, a closer examination shows that there are other arrangements which involve a large amount of hybridization,[§] sufficient to render them even more stable than the somewhat curious model just described

One can obtain very simply a rather entertaining result on the ethane molecule It is that there is free rotation about the C–C joint, both in the H–M and the H–L–P S approximations, provided interactions between any two hydrogen atoms and between any hydrogen atom and the distant carbon atom, are neglected

We proceed to give these ideas more exact formulation

The H-L-P-S Approximation for Ethylene.

Our computations are based on the well-known formula of perfect pairing

$$W = Q + \sum_i J_{ii} - \tfrac{1}{2} \sum_{i \neq k} J_{ik}, \qquad (1)$$

where W is the energy of the configuration apart from atomic terms, Q is the Coulomb energy, and the J are defined as the diatomic two-electron integrals

$$J = \iint \psi^* (a_1) \, \psi^* (b_2) \, \mathrm{H} \psi (b_1) \, \psi (a_2) \, dv_1 \, dv_2 \qquad (2)$$

---

† 'Phys Rev,' vol. 43, p 279 (1933)

‡ 'Z Physik,' vol. 60, p 423 (1930)

§ When wave functions *f* and *g* from two different families have nearly equal energies, they may " hybridize," so that the functions to be taken are $af + bg$ and $cf + dg$

Here a_1 represents the co-ordinates of electron 1 relative to the nucleus a, and H is the Hamiltonian operator The summation is over all pairs (i, k), $a - \frac{1}{2}J_{ca}$ term arising from any two not coupled to zero spin, $i e$, not forming a bond, and a J_{ii} from each pair forming a bond Our calculations bring out very clearly the importance of *hybridized* wave-functions , by allowing some $2s$ wave-function to be mixed in with the various $2p$ wave-functions, still retaining the aggregate carbon configuration $2s(2p)^3$, the bonds are made very much stronger In consequence, the molecule constructed with them gains enormously in stability As is usual, we shall neglect the $(1s)^2$ shell of carbon, the int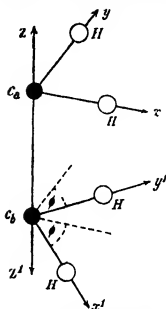eraction between any two hydrogen atoms, and the interaction between any hydrogen atom and the distant carbon atom Furthermore, we shall ignore the presence of the higher quantum orbits of both C and H in the expansion of the complete wave-function in terms of the unperturbed C and H wave-functions

It is necessary to introduce two kinds of exchange integrals, the C which have four suffixes, and the N which have two These integrals are exhibited in (4) The C arise from two electrons which are always on one of the other carbon nuclei Two of the suffixes define the initial state and two the final With the integrals N there is always one electron on a hydrogen nucleus and one on a carbon nucleus Two suffixes are sufficient here to define the integral since it is assumed that an electron on a hydrogen nucleus is always in a $(1s)$ state

We consider now several plausible arrangements of the ethylene molecule Since the " right angle " model is by far the simplest algebraically, we start with it

The Right-angle Model —Let us arrange the model so that the C-C line is vertical , denote the upper C nucleus by C_a and the lower by C_b Take as the axis of z the upward drawn line through the two carbon nuclei, and as the x and y axes, the lines joining C_a to its two H companions, such that $(x \ y, z)$ is an orthogonal, right-handed system of axes,

Fig 1 – The figure illustrates the right angled model The bonds between the C and H atoms are pure $2p\sigma$ and the double bond is made up of one (s, s) and one (σ, σ) band The energy of the configuration does not depend on ϕ

of origin C_a The lower CH_2 group may be specified by the left-handed system (x', y', z'), of origin C_b, where z' is taken in the opposite sense to z Denote by ϕ the angle between the x and the x' axes

The choice of wave-functions is as follows —

$$
\left.
\begin{array}{llll}
\psi\,(\mathrm{H_1}) & , & \psi_a\,(2p\sigma_x) & , & \psi\,(\mathrm{H_3}) & , & \psi_a\,(2p\sigma_y) \\[4pt]
\psi\,(\mathrm{H_2}) & , & \psi_b\,(2p\pi_x) & , & \psi\,(\mathrm{H_4}) & , & \psi_b\,(2p\sigma_y) & , \\[4pt]
\psi_a\,(2s) & , & \psi_b\,(2s) & , & \psi_a\,(2p\pi_z) & , & \psi_b\,(2p\sigma_z) & ,
\end{array}
\right\} \quad (3)
$$

where members of a pair with balancing spins are separated by a comma, and pairs are separated by semi-colons   Here ψ (H) is simply the wave-function of the ($1s$) state of H   By ψ_a ($2p\sigma_x$) we mean that this is a $2p$ wave-function on the C_a nucleus, x being the axis of quantization and σ denoting that m_l is zero with reference to this axis   This wave-function clearly has the form $xf(r_a)$.   There are, however, two π wave-functions, corresponding to $m_l = \pm 1$ respectively, and these may be taken in either real or complex form   We prefer the real form and take ψ_a ($2p\sigma_x$) $= \psi_a$ ($2p\pi_x$), which has the form $xf(r_a)$, and ψ_a ($2p\sigma_x$) $= \psi_a$ ($2p\pi_x$) which has the form $yf(r_a)$ The equality signs are a consequence of the fact that a $2p$ wave-function which is of the σ type with reference to one axis of quantization is of the π type when referred to an axis of quantization perpendicular to the former   The notation π and π' is to remind ourselves that there are two types of π wave-functions.

Neglecting the atomic and Coulomb parts of the energy, we obtain on using (2) and (3) in (1) —

$$
W = -\, C_{aaaa} - C_{bbbb} + C_{xxxx} + 2C_{abab} + 2C_{xxxx}
$$
$$
+\, C_{xxxx} + C_{xaxa} - 4\mathrm{N}_{aa} + 4\mathrm{N}_{xx} + 2\mathrm{N}_{xx}
$$

where

$$
\left.
\begin{array}{l}
C_{a\beta\gamma\delta} = -\tfrac{1}{2} \displaystyle\int\!\!\int \big\{ \psi_a\,(\alpha_1)\,\psi_b\,(\beta_2)\,\mathrm{H}\,\psi_b\,(\gamma_1)\,\psi_a\,(\delta_2) \\[4pt]
\hspace{3.5cm} +\, \psi_a\,(\delta_1)\,\psi_b\,(\gamma_2)\,\mathrm{H}\,\psi_b\,(\beta_1)\,\psi_a\,(\alpha_2) \big\}\,dv_1\,dv_2 \\[10pt]
\mathrm{N}_{a\beta} = -\tfrac{1}{2} \displaystyle\int\!\!\int \big\{ \psi_\mathrm{H}(s_1)\,\psi_a\,(\alpha_2)\,\mathrm{H}\,\psi_c\,(\beta_1)\,\psi_\mathrm{H}\,(s_2) \\[4pt]
\hspace{3.5cm} +\, \psi_\mathrm{H}\,(s_1)\,\psi_a\,(\beta_2)\,\mathrm{H}\,\psi_c\,(\alpha_1)\,\psi_\mathrm{H}\,(s_2) \big\}\,dv_1\,dv_2 \\[10pt]
\mathrm{H}/e^2 = \dfrac{1}{r_{a1}} + \dfrac{1}{r_{b1}} - \dfrac{1}{\mathrm{R}} - \dfrac{1}{r_{12}}, \; \mathrm{H}'/e^2 = \dfrac{1}{r_{a1}} - \dfrac{1}{r_{\mathrm{H}2}} - \dfrac{1}{r_{12}}
\end{array}
\right\} \quad (4)
$$

Here, for example, ψ_a (α_1) means the wave-function of electron 1 on the a nucleus in a quantum state α The minus sign has been inserted into the

definition of the integral C to make certain of the more important integrals positive   Subscripts π and π' only occur together, and the primes denote that the π and π' wave-functions have their axes of symmetry perpendicular to each other   It may be remarked here that any integral C with one or three π suffixes, or any integral N with one π suffix vanishes, as can be seen very simply from the symmetry properties of the wave-functions

The angle ϕ does not appear in the expression for the energy, and hence within the limits of our approximation there is free rotation about the C-C
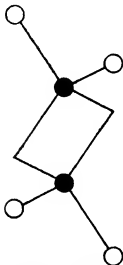
FIG 2 —The figure illustrates an ethylene molecule built on tetrahedral wave functions (Slater and Pauling's original suggestion)   This arrangement is not as good as that shown in fig 3
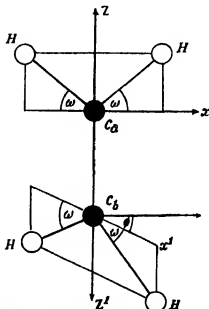

FIG 3 —The figure illustrates the ω model   When $\phi = 0$ we have " plane ethyl ene " and when $\phi = \pi/2$, " perpendi cular ethylene "   The angles ω and ϕ are to be chosen to make the energy a minimum

joint   We postpone a discussion of the signs and relative magnitudes of the various integrals till later

The Slater-Pauling Model —Next in order of simplicity is the Slater-Pauling model   The reader will probably understand immediately from the figure the way that the various atoms are disposed in this particular arrangement Each C atom has four tetrahedral valence arms, two of which point away symmetrically from the remote C nucleus, and are saturated with H atoms

The four remaining valence arms are coplanar and constitute the double bond It is seen that all six nuclei lie in one plane and that the HCH angle has the tetrahedral value 109 5° The appropriate carbon wave-functions are

$$(3/4)^{\frac{1}{2}} \, [\psi \, (2p, \sigma_i) + (1/3)^{\frac{1}{2}} \, \psi \, (2s)],$$

where $\psi \, (2p, \sigma_i)$ means that the $2p$ wave-function is directed along one of the four tetrahedral lines radiating from the C nucleus

After some manipulation, the energy is found to be

$$W = 5 \, (C_{xxxx} + C_{xxxx})/16 + C_{xxxx}/4 + C_{xxxx} + 5 \, (2C_{xxxx} + C_{xxxx} + C_{xxxx})/8$$
$$- 3 \, (2C_{xxxx} + 2C_{xxxx} + C_{xxxx})/8 - 3 \, (2C_{xxxx} + 2C_{xxxx} + C_{xxxx})/8 + 3 \, (C_{xxxx})$$
$$+ C_{xxxx})/4 + 3 \, (C_{xxxx} + C_{xxxx} + C_{xxxx})/2 - 5N_{xx}/2 + \tfrac{1}{2}N_{xxx} + 4N_{xx} - 3 \, (3)^{\frac{1}{2}} \, N_{xx}$$

where the integrals are defined by equation (4) As before, Coulomb and atomic energies have been omitted We shall return to this formula later

The ω-Model —We now discuss the arrangement which we believe to be the one actually realized in nature It is assumed that the plane of either CH_2 group contains the other C nucleus The model then has two angular parameters ω and ϕ whose values are to be chosen so that the energy has its minimum value The choice of directed wave-functions for this model has been given by Van Vleck *(loc cit)* Construct on the nucleus C_a a right-handed system of axes (x, y, z) with $C_a z$ pointing away from C_b and with the x-z plane containing H_1 and H_2 Construct on the C_b nucleus a similar system of axes (x', y', z'), these, however, being left-handed with H_3 and H_4 lying in the x'-z' plane Denote by ϕ the angle between the x and the x' axes, and by ω any of the four equal angles $H_1 C_a x$, $(\pi - H_2 C_a x)$, $H_3 C_b x'$, $(\pi - H_4 C_b x')$

The directed wave-functions are as follows —

$$\psi \, (H_1), \quad \psi \, (H_2), \quad \psi \, (H_3), \quad \psi \, (H_4),$$
$$\psi_a \, (2p, \sigma_y), \quad \psi_b \, (2p, \sigma_{y'}),$$
$$(1 + \cos 2\omega)^{-\frac{1}{2}} \, [\psi_a \, (2p, \sigma_i) + (\cos 2\omega)^{\frac{1}{2}} \, \psi_a \, (2s)], \quad i = H_1 \text{ and } H_2$$
$$(1 + \cos 2\omega)^{-\frac{1}{2}} \, [\psi_b \, (2p, \sigma_k) + (\cos 2\omega)^{\frac{1}{2}} \, \psi_b \, (2s)], \quad k = H_3 \text{ and } H_4 \qquad (5)$$
$$[k \, (\omega)]^{\frac{1}{2}} \, [- \operatorname{cosec} \omega \cos 2\omega \, \psi_a \, (2p, \sigma_x) + (\cos 2\omega)^{\frac{1}{2}} \, \psi_a \, (2s)],$$
$$[k \, (\omega)]^{\frac{1}{2}} \, [- \operatorname{cosec} \omega \cos 2\omega \, \psi_b \, (2p, \sigma_{x'}) + (\cos 2\omega)^{\frac{1}{2}} \, \psi_b \, (2s)],$$

with

$$1/k \, (\omega) = \operatorname{cosec}^2 \omega \cos^2 2\omega + \cos 2\omega$$

Proceeding exactly as before, one can obtain the expression for the energy
After collecting terms and rejecting some which vanish from symmetry pro-
perties, we find that

$$
\begin{aligned}
W - C_{xxxx}\,(1 - 3\cos^2\phi/2) + C_{xxxx}\,(1 - 3\sin^2\phi/2) + 2C_{xxxx} + 2C_{xxxx} + C_{xxxx} \\
+ \tfrac{1}{2}\,(-11 + 12\sec^2\omega - 3\sec^4\omega)\,C_{xxxx} + \tfrac{1}{2}\,(-2 + 6\sec^2\omega - 3\sec^4\omega)\,C_{xxxx} \\
- 3\tan^2\omega\sec^2\omega\cos 2\omega\,(C_{xxxx} + C_{xxxx} + C_{xxxx}) \\
+ 6\sin\omega\sec^4\omega\,(\cos 2\omega)^{\frac{1}{2}}\,[\cos 2\omega\,C_{xxxx} \\
+ \sin^2\omega C_{xxxx}] + (2 - 3\sec^4\omega)\,N_{xx} + (-1 + 3\sec^4\omega)\,N_{xx} + 4N_{xx} \\
- 6\sec^2\omega\,(\cos 2\omega)^{\frac{1}{2}}\,N_{xx}
\end{aligned}
$$

As usual the atomic and Coulomb terms are omitted   These are presumably
the same for all models   the atomic terms need not concern us, but we give
now the expression for the Coulomb energy Q

$$
\begin{aligned}
Q = D_{xxxx} + D_{xxxx} + 2D_{xxxx} + 2D_{xxxx} + 4D_{xxxx} \\
+ 4D_{xxxx} + 2D_{xxxx} + 4M_{xx} + 4M_{xx} + 8M_{xx},
\end{aligned}
$$

where

$$
D_{a\beta\gamma\delta} = \tfrac{1}{2}\iint\{\psi_a\,(\alpha_1)\,\psi_b\,(\beta_2)\,H\psi_a\,(\gamma_1)\,\psi_b\,(\delta_2)
$$
$$
+ \psi_a\,(\gamma_1)\,\psi_b\,(\delta_2)\,H\psi_a\,(\alpha_1)\,\psi_b\,(\beta_2)\}\,dv_1\,dv_2,
$$

$$
M_{a\beta} = \tfrac{1}{2}\iint\{\psi_H\,(\eta_1)\,\psi_a\,(\alpha_2)\,H'\psi_H\,(s_1)\,\psi_a\,(\beta_2)
$$
$$
+ \psi_H\,(s_1)\,\psi_a\,(\beta_2)\,H'\psi_H\,(\eta_1)\,\psi_a\,(\alpha_2)\}\,dv_1\,dt_2,
$$

and H is defined by (4)   Notice that D and M, unlike C, have no minus sign
in their definition

A brief explanation of why the angle ϕ does not appear in the expression
for the energy of the right-angled model while it does in that of the ω-model,
may be given here   The essential point is that with the right-angled model
there are no π-π bonds, and when the summation $- \tfrac{1}{2}\Sigma_iJ_i$ for interactions
between bonds is made, the dependence of W on ϕ disappears   With the
ω-model, however, there is a π-π bond, and as the contribution to the energy
from a bond has a coefficient $+1$ (compared with $-\tfrac{1}{2}$ for electrons in different
bonds), the angle ϕ still remains explicitly in W

We have now expressions for the energy of three plausible models   The
important question arises as to the signs and magnitudes of the various
integrals   We devote a special section to a discussion of this point

Discussion of Signs and Magnitudes of Various Integrals—There are three possible ways of determining the size and approximate magnitude of most of the integrals appearing in our equations. The simplest is the criterion of maximum overlapping. This would tell us, for example, that C_{ssss} is positive and quite large, N_{ss} is negative and fairly small, and so on. The second possibility is from the work of Bartlett and Furry[†] on the Li_2 and Be_2 molecules. We can obtain some very useful information from the tables given in their papers. The third possibility is from the celebrated figure given by Mulliken[‡] for the behaviour of the energy levels of various diatomic molecules as the internuclear distance is decreased from large distances to small. On the whole, the three methods agree fairly well, and fortunately, those integrals whose sign is doubtful are small, and not of much consequence.

Bartlett and Furry in their work use conjugate complex wave functions $(x \perp iy)f(r)$ while we use the real wave-functions $xf(r)$ and $yf(r)$. It is therefore necessary to get the transformation scheme from their integrals to ours. This is obtained without much trouble by the use of simple trigonometric identities.

$$C_{ssss} = -I_{10}, \quad C_{sese} = J'(ss, 00), \quad JC_{ssss} = -J'(ss, 11)$$

$$C_{ssss} = J'(s1, s1), \quad C_{ssss} = -I_{11}, \quad C_{ssss} = -I_6$$

$$C_{ss\,ss} = -t_2/2, \quad C_{ssss} = -I_2 - t_2/2, \quad C_{ssss} = \tfrac{1}{2}\,[J'(ss, s0) - J'(ss, 0s)]$$

The remainder of our integrals do not occur in the expressions for those energy levels which were calculated.

Perhaps the most interesting integrals are C_{ssss} and $C_{ss\,ss}$, since it is the relative magnitude of these two which determines whether the angle ϕ is zero or $\pi/2$, i.e., whether "plane" or "perpendicular" ethylene is the more stable. According to Bartlett and Furry t_2 is small and positive, while I_2 is much larger in magnitude and negative in sign. As a consequence, the π-π bonds are bonding. This agrees with Mulliken's figure. The criterion of maximum overlapping does not give very definite information on the sign and magnitude of these two integrals, but our conclusions seem very reasonable when this test is applied to them. We therefore have obtained the important result that plane ethylene is more stable than perpendicular. If C_{ssss} were negative and larger in absolute magnitude than $C_{ss\,ss}$, the π-π bonds would

---

[†] J. H. Bartlett, jr., 'Phys. Rev.,' vol. 37, p. 507 (1931); Furry and J. H. Bartlett, jr. *ibid.*, vol. 38, p. 1615 (1931); vol. 39, p. 210 (1932)

[‡] 'Rev. Mod. Phys.,' vol. 4, p. 40 (1932)

be anti-bonding if coupled to zero spin, but then, of course, we would couple them to a spin of unity   For the dependence of W on ϕ we then find

$$C_{x x x x} (1 + \tfrac{1}{2} \cos^2 \phi) + C_{x x \cdot x x} (1 + \tfrac{1}{2} \sin^2 \phi),$$

and once again the plane model is the more stable   The fact that ethylene is not paramagnetic rules this case out

One can substitute the numerical value of $C_{x x x x}$ as calculated by Bartlett (*loc cit*), to evaluate the dependence of the energy W on ϕ It is found that $W = 3I_2 \cos 2\phi/4$ Taking an effective nuclear charge of unity and an inter-nuclear distance of 8 gives 0 176 volts as the total variation with ϕ For $R = 6$, the figure is 0 376 volts   These values seem rather low, especially as the latter is, in a way, an upper limit   Dr Sutherland has kindly informed the writer that from data (not yet published) on the infra-red spectrum of ethylene, he has concluded that there is a fundamental twisting frequency of about 750 wave-numbers (1/10 volt)   Eucken and Parts† have observed independently a similar value from their work on specific heat determinations When allowance is made for the half-quantum zero point energy, it is seen that a lower limit for the depth of the trough is about 1/6 volt ‡

According to overlapping considerations $C_{x x x x}$ is large and positive, and one would expect it to be the greatest of all the integrals   Mulliken (*loc cit*.) has it large and positive, but Bartlett has it negative   This gives him $(\sigma_g)^2 \Sigma_g^{-}$ for the ground state of a molecule formed from two similar atoms, each with a single $2p$ electron, an incorrect result   The reason has been elucidated by Stehn,§ who concluded that the Heitler-London first order perturbation theory would give very poor results for any state involving a σ_u electron There seems little doubt therefore, that $C_{x x x x}$ is positive and large

The integral $C_{x x x}$ is positive by all three methods, and in magnitude is fairly large   One would expect all of the integrals $C_{x y x y}$, $C_{x x x x}$, and $C_{x x x y}$ to be positive, and of about equal magnitude, somewhere between that of $C_{x x x x}$

† ' Z. Phys. Chem.,' B, vol. 20, p 184 (1933)

‡ [*Note added in proof, January* 10, 1934 —Applying the results of Koenig on eigen values in periodic fields of potential (' Phys Rev ' vol 44, p 657, 1933), we find that in order to account for a fundamental twisting frequency of 750 cm $^{-1}$, it is necessary to have $C_{x x x x} \approx 0\ 7$ v e   This gives about 1 v e for the difference of energy between plane and perpendicular ethylene   According to Pauling and Wheland (' Jour Chem Phys.,' vol 1, p 362, 1933), $C_{x x x x}$ is about $1\frac{1}{2}$ v e   Chemical evidence on the heat of activation of various compounds derived from ethylene seems to favour the former of these estimates   The calculations will be described in a note to the Physical Society of London]

§ ' Phys Rev ,' vol 42, p 582 (1932)

and that of C_{ssss} Now the choice of relative phase of the $2s$ and $2p$ wave-functions is still at our disposal and we can therefore take C_{ssos} and C_{ooos} as negative Since N_{so} is of a type similar to $-C_{ssos}$, N_{so} will be positive, a circumstance very favourable to the ω-model Summing up, we have approximately

$$C_{xxxx} > -C_{oosx} > C_{ssoo} = C_{soxo} = C_{ooxx} > -C_{ssso} > C_{ssss} > 0,$$

where the equality signs are not to be taken too seriously, but are probably satisfied fairly well

We consider next those integrals with two π-subscripts Both C_{ssxx} and C_{soxx} are almost certainly negative and small, but the remainder seem very uncertain However, they are not capable of affecting our results to any extent and so we do not trouble about them There still remain the integrals involving two H and two C wave-functions These are well known (Van Vleck, *loc cit*), N_{xo} and N_{ss} are positive and N_{xx} negative We have already chosen N_{so} positive

$$N_{so} > N_{ss} > 0 > N_{xx}$$

Comparison of Energies of Different Models —Using the results of the previous sections, we can make a critical comparison of the different models For the ω-model there are two parameters ω and ϕ, but we shall, of course, take $\phi = 0$ throughout, for reasons already explained The best value of ω is probably a small one, perhaps about $25°$ To facilitate comparison with the Slater-Pauling model, however, let us take for ω the tetrahedral value $\sin \omega = (1/3)^{\frac{1}{2}}$ By doing this the hydrogen energies N in the ω-model are made exactly equal to those in the Slater-Pauling model, and the comparison is simplified accordingly We find for the difference in energy

$$W = -\left[3\left(C_{ooss} + C_{ssss}\right)/16 - 3\left(C_{ssss} + C_{ooss}\right)/4 + 3\left(C_{ssss} + C_{soss} + C_{ssoo}\right)/4 + 3C_{ssss}/4\right] + 3\left[\left(C_{ssss} + C_{ssss} + C_{ssss} + C_{ssss} + C_{ssss} + C_{ssss}\right) - 2\left(C_{ssss} + C_{soss} + C_{ssss}\right)\right]/4$$

The terms in the first bracket all favour the ω-model The terms in the second bracket are doubtful, but in any case nearly cancel each other out We conclude that even with this value of ω, the ω-model is more stable than the Slater-Pauling model A few words may well be spent in explaining what the difference really is between the Slater-Pauling model and the ω-model with $\phi = 0$ and ω the tetrahedral value The difference is solely in the double bond The ω-model has a strong (s, σ) bond along the C-C axis and a weak

(π-π) bond perpendicular to this axis The Slater-Pauling model has two equivalent bonds which are not very strong because they are too much inclined to the C-C axis

Let us now compare the ω-model with the right angle model For convenience take $\omega = 90°$ We find

$$W_{\omega=90} - W_F = [5C_{xxxx}/6 + 4C_{xxzz}/3 + 2 \ (2)^{\frac{1}{2}} (2C_{xxyy} + C_{xzxz})/3 - 3C_{xxxx}/2$$
$$- 2 \ (C_{yzyz} + C_{xyxy} + C_{xzxz})/3] + [2 \ (N_{xx} - N_{xz}) - 4 \ (2)^{\frac{1}{2}} N_{yz}]$$

There does not seem any doubt that this quantity is negative, so that the ω-model is the more stable of the two An even more convincing proof can be obtained by taking, for example, cotan $\omega = 3$, but the expressions for the energy are rather too long to print It should be noticed that it is the hybrid terms which gain the day for the ω model

The H-M Approximation for Ethylene

It is possible to make calculations on the ethylene molecule by the H-M method The secular determinants for the various models are readily set up , the difficulty is to solve them The assumptions that we shall make and the general procedure that we shall adopt are very similar to those described by Van Vleck (loc cit) We give only the barest minimum description of these and refer the reader to Van Vleck's paper for further details A certain number of interesting results can be obtained without much trouble, but others need a very complete examination before their validity is established The trouble is briefly this the magnitudes of the differences of the binding energies of carbon and hydrogen as they appear in the perturbation problem are only about equal to those of some of the resonance integrals If, therefore, one tackles the problem by perturbation theory, there are difficult questions of convergence, and on this account one may obtain quite the wrong result In addition, there is the further complication that not even the order of the roots is known for certain There are in all twelve electrons to be established in the molecule, so that allowing for spin-degeneracy, the lowest six of the twelve roots of the secular determinant are required Two are undoubtedly much lower than the rest, and four higher, but the order of the remaining eight, of which four are needed, is somewhat uncertain According as to which four are considered lowest, so the degree of the " ionic-ness " of the resulting molecule is varied If one assumes, for example, what is certainly not so, that those four of the eight are much the lowest which are built up on carbon root approximations, then the molecule is very ionic and the majority of the

charge is around the two carbon nuclei, leaving the hydrogen nuclei very bare
All one can do in a situation such as this is to consider different variations in
the order of the roots which may correspond to physical reality, to make
plausible assumptions for the relative magnitudes of the resonance integrals
and to examine how the stability of the molecule changes as these various
factors are changed By such a process we attempt to show that plane ethylene
is the most stable

The same general method of attack is to be adopted as was employed in
the H-L P-S approximation, that is, we shall endeavour to discover which of
several possible models is the most stable From symmetry arguments, it
is very reasonable to suppose that the plane of one CH_2 group and the plane
of the other CH_2 group are either (a) coincident, or (b) perpendicular, or (c)
parallel, and that the two hydrogens in either CH_2 group are equivalent and
symmetrically situated with respect to the C atom We could decide between
(a) and (b) by minimizing the energy with respect to the azimuth ϕ, and, in
fact, we set up the secular determinant in a way that would permit this. It
turns out, however, that the determinant is so much simplified by putting
$\phi = 0$ or $\phi = \pi/2$, that it is worth our while to make these substitutions
directly and compare the roots in the two cases To get the best results
from (c) when it is agreed that H-H repulsions are to be neglected, one would
naturally take the HCH angle as $\pi/2$ In other words, (c) is the analogy of our
old right-angle' model We now wish to prove that (a) is better than (c)
This must be accomplished by a suitable choice of the angle $\omega = (\pi - HCH)/2$,
the best value of which we believe to be small It should be noticed that
there is no point in introducing a case (d), based on tetrahedral wave-functions,
because this would only give us the same secular determinant in another guise,
and would change neither the roots nor the final wave-functions.

The molecular wave-functions for the ethylene molecule are to be taken as
linear combinations of the twelve wave-functions

$$\psi(1s, H_i), \quad (i = 1, 2, 3, 4)$$

$$\psi(2s, C_j), \quad \psi(2p\sigma_x, C_j), \quad \psi(2p\tau_y, C_j), \quad \psi(2p\sigma_z, C_j), \quad (j = 1, 2)$$

suitably centred around their appropriate nuclei The axes of quantization
(x, y, z) may be conveniently taken as an orthogonal set with the z axis corre-
sponding with the C-C line These wave-functions are solutions of the
equations

$$[\nabla^2 + (8\pi^2 m/h^2)(W_k{}^0 - V_c)]\,\psi(2k, C) = 0 \qquad (k = s \text{ or } p),$$

$$[\nabla^2 + (8\pi^2 m/h^2)(W^H - V_H)]\,\psi(1s, H) = 0,$$

where V_H and V_C are suitable " self-consistent field " potential energies of an electron in the field of an H and C atom respectively   For the convenience of the reader we redefine Van Vleck's integrals, which have one suffix or none, and some of our own, which have two —

$$B = \int \psi (1s, H_4)^2 V_C \, dv, \qquad C_k = - \int \psi (2k_t, C)^2 V_H^t \, dv,$$

$$D_H = - \int \psi (2s, C) \, \psi (2\sigma_t \, C) \, V_H^t \, dv,$$

$$Q_k = - \int \psi (1s, H_t) \, \psi (2k_t, C) \, V_H^t \, dv,$$

$$R_k = - \int \psi (1s, H_t) \, \psi (2k_t, C) \, V_C \, dv,$$

$$T_k = \int \psi (1s, H_t) \, \psi (2k_t, C) \, dv,$$

$$M_{kk} = - \int \psi_a (k_a, C) \,^2 V_C^b \, dv, \qquad S_{kl} = \int \psi_a (k_b, C) \, \psi_b (l_a, C) \, dv,$$

$$D_C = - \int \psi_a (2s, C) \, \psi_a (2\sigma_b, C) \, V_C^b \, dv,$$

$$N_{kl} = - \int \psi_a (k_b, C) \, \psi_b (k_a, C) \, \{ V_C^a + V_C^b \} \, dv$$

$$(b)$$

Here k and l represent π, σ, ϵ The suffix on k or l denotes the axis of spatial quantization   Once again a and b refer to the carbon nucleus, and s to the hydrogen nucleus, which is under consideration   Notice that T and S are non-orthogonality parameters whereas the rest of the integrals are energy parameters.

The ω-model —We shall now set up the secular determinant for the ω-model There are two possible ways of obtaining it   Either very simple wave-functions may be employed and the determinant so obtained reduced by the application of some elementary transformations, or suitable wave-functions may be taken to give the required determinant immediately   The former is the natural line of attack, but on account of the difficulties of printing we adopt the latter method of approach, thereby avoiding the necessity of printing the secular determinants more than once

Let us adopt a system of axes similar to that we used before , a right-handed set (x, y, z) on the upper nucleus C_a and a left-handed set (x', y', z') on the lower nucleus C_b The x-axis and the x'-axis are taken parallel, and

z and z' are taken collinear but of opposite sense   We denote by ω any of the four equal angles $(\pi - \text{HCH})/2$, and by ϕ the azimuth of H_1 as measured from $C_a z$ Then the azimuth of H_2 is naturally $(\pi + \phi)$ The azimuth of H_3 we maintain as zero, and the azimuth of H_4 as π Consider the following twelve wave-functions, arranged in two sets of six ---

(1) $[\psi_a (2s) + \psi_b (2s)]/(2)^{\frac{1}{2}}$,

(6) $[\psi_a (2s) - \psi_b (2s)]/(2)^{\frac{1}{2}}$,

(2) $[\psi_a (2p\sigma_z) + \psi_b (2p\sigma_z')]/(2)^{\frac{1}{2}}$,

(5) $[\psi_a (2p\sigma_z) - \psi_b (2p\sigma_z')]/(2)^{\frac{1}{2}}$,

(3) $[\psi (H_1) + \psi (H_2) + \psi (H_3)$
$\qquad + \psi (H_4)]/2$,

(4) $[\psi (H_1) + \psi (H_2) - \psi (H_3)$
$\qquad\qquad\qquad - \psi (H_4)]/2$,

(7) $[\psi_a (2p\sigma_x) + \psi_b (2p\sigma_x)]/(2)^{\frac{1}{2}}$,

(12) $[\psi_a (2p\sigma_x) - \psi_b (2p\sigma_x)]/(2)^{\frac{1}{2}}$,

(8) $[\psi_a (2p\sigma_y) + \psi_b (2p\sigma_y)]/(2)^{\frac{1}{2}}$,

(11) $[\psi_a (2p\sigma_y) - \psi_b (2p\sigma_y)]/(2)^{\frac{1}{2}}$,

(9) $[\psi (H_1) - \psi (H_2)]/(2)^{\frac{1}{2}}$,

(10) $[\psi (H_3) - \psi (H_4)]/(2)^{\frac{1}{2}}$

On calculating the matrix elements $\big| \psi_a H \psi_\beta$, where α represents any one of the upper six and β any one of the lower six wave-functions, H being the Hamiltonian, it is found that the integral is zero   In other words, this choice of wave-functions has factorized the secular equation of order twelve into two each of order six   Moreover, the first of these sixth order equations again factors into two cubics   It is convenient, in the arrangement of these equations, to number the rows and columns to correspond with the way the wave-functions are numbered   The two (s, σ) cubics may be written together in the form

$\mathbf{F}_\pm$	a	b
a	$\mathbf{G}_\pm$	c
b	c	$\mathbf{H}$

where

$$\mathbf{F}_\pm = \mathbf{W}_s^c - 2\mathbf{C}_s \pm \mathbf{N}_{ss} - \mathbf{M}_{ss} \pm \mathbf{S}_{ss}\mathbf{W} - \mathbf{W},$$

$$\mathbf{G}_\pm = \mathbf{W}_p^c - 2\left(\sin^2 \omega\, \mathbf{C}_x + \cos^2 \omega\, \mathbf{C}_z\right) \pm \mathbf{N}_{\sigma\sigma} - \mathbf{M}_{\sigma\sigma} \pm \mathbf{S}_{\sigma\sigma}\mathbf{W} - \mathbf{W},$$

$$\mathbf{H} = \mathbf{W}^{\text{H}} + \mathbf{B} - \mathbf{W}, \qquad a = \mathbf{N}_{s\sigma} - \mathbf{S}_{s\sigma}\mathbf{W} - 2\sin \omega\, \mathbf{D}_{\text{H}} + \mathbf{D}_{s},$$

$$b/(2)^{\frac{1}{2}} = -\mathbf{Q}_s - \mathbf{R}_s + \mathbf{T}_s\mathbf{W}, \qquad c/(2)^{\frac{1}{2}} = -\sin \omega\, (\mathbf{Q}_\sigma + \mathbf{R}_\sigma - \mathbf{T}_\sigma\mathbf{W})$$

The sixth order (π, π) equation does not factorize with a general value of ϕ It is

$$
\left|
\begin{array}{cccccc}
J & p & s & r & p & q \\
p & K & t & 0 & -q & p \\
s & t & H & 0 & t & s \\
r & 0 & 0 & H & 0 & r \\
p & -q & t & 0 & K_1 & p \\
q & p & s & r & p & J
\end{array}
\right|
\qquad (7)
$$

where

$$
J_1 = W_p{}^c - \cos^2\omega\,(1 + \cos^2\phi)\,C_\sigma - (1 + \sin^2\omega - \cos^2\omega\cos^2\phi)\,C_\pi
$$
$$
+ N_{\pi\pi} - M_{\pi\pi} \pm S_{\pi\pi}W - W,
$$
$$
K_1 = W_p{}^c - \cos^2\omega \sin^2\phi C_\sigma - (2 - \cos^2\omega \sin^2\phi)\,C_\pi
$$
$$
+ N_{\pi\pi} - M_{\pi\pi} \pm S_{\pi\pi}W - W,
$$
$$
H = W^H + B - W, \qquad p = \cos^2\omega \cos\phi \sin\phi\,(C_\sigma - C_\pi)
$$
$$
q = \cos^2\omega \sin^2\phi\,(C_\sigma - C_\pi) \qquad L_1 = Q_\pi + R_\pi - T_\pi W,
$$
$$
r = - L \cos\omega \qquad s = r\cos\phi, \qquad t = r\sin\phi
$$

Two results are immediately clear In the first place, there is a decided hybridization of s and σ wave-functions, but no hybridization of s and π or of σ and π wave-functions While this does not agree with the H-L-S-P viewpoint, represented by (5), there is no cause for alarm, since it is the type of contrast continually arising between the two methods The second result is, that as far as the dependence of the energy on ϕ is concerned, we can confine our attention to the second of these determinants, since ϕ does not occur in the first We do have to decide, however, which roots must be taken out of the one determinant and which out of the other

Let us for the present confine our attention to the second of these determinants If we put $\phi = 0$, two of the roots, viz , K_1, separate out completely, and one easily reduces the remaining quartic to two quadratics, which can be solved exactly

$$
\left|
\begin{array}{cc}
J_- & r\,(2)^{\frac12} \\
r\,(2)^{\frac12} & H
\end{array}
\right|
\qquad
\left|
\begin{array}{cc}
J_1 & r\,(2)^{\frac12} \\
r\,(2)^{\frac12} & H
\end{array}
\right|
\quad \text{with } \phi = 0
$$

If we put $\phi = \pi/2$ in the determinant, there is again considerable simplification and it factorizes immediately into two identical cubics

J_-	r	q
r	H	$-r$
q	$-r$	J_π

with $\phi = \pi/2$, $J_+ = K_+$.

The question of the determination of the roots of this cubic now arises. One is tempted to use perturbation theory, but unfortunately the results by this method are not satisfactory. In the first place the ordinary formulæ must be modified to allow for the presence of the off-diagonal elements in W. Fortunately, these are already of second order, a circumstance which allows the roots to be obtained to the fourth order without too much extra complication. One can assume that the carbon roots are a good way below the hydrogen, and thus expand in powers of $r/(J - H)$, etc., taking for the four required roots those built on J_-, K_-, J_+, K_+. Alternatively, one can assume that the H roots are much lower than the C, and again the expansion can be made in powers of $r/(J - H)$. This time, however, only the two H roots are required from this determinant, and from the (s, σ) determinant are to be taken the other two H roots and the lowest two C roots. With either approximation, one finds that it is not until the fourth order terms are included that there is any difference between $\phi = 0$ and $\phi = \pi/2$. Even then, the fourth order terms practically balance out, leaving a residual of equivocal sign. Although this is rather a troublesome state of affairs, it is really due to our having limited the size of the various parameters sufficiently to render the perturbation approximation valid. The difference between the energies of plane and perpendicular ethylene can hardly be calculated as a fourth order term, although it may be rather small.

As a last resource, it was decided to try numerical values in the equations and to examine the rotational stability in this way. The roots are not very difficult to obtain numerically once the values of the various quantities have been specified, and a simple addition of roots decides immediately between $\phi = 0$ and $\phi = \pi/2$. We have tried wide ranges of values in the different parameters, and it seems probable that with values corresponding roughly to those in the actual molecule $\phi = 0$ is the best arrangement. However, the rather amusing result is obtained that for a highly ionic molecule perpendicular

ethylene is very slightly more stable than plane ethylene   We give now a few
illustrative examples.   For the angle ω we assume a value 30°, for the non-
orthogonality parameters $T_σ = 0\ 25$, $S_{ss} = 0\ 20$, and   for   the   various
energy parameters, in volts

$$H - W_s{}^C + M_{πx} = 1, \quad N_{πx} = 3, \quad Q_σ + R_σ = 2\ (3)^{\frac{1}{2}}, \quad C_σ = \tfrac{1}{2}, \quad C_π = -1/6,$$

$$N_{sd} \text{ and } N_{σx} \text{ equal and each 5 volts.}$$

Later calculations must decide whether these values are anywhere near the
truth or not   More important for our present purpose are the ratios of the
various energies, and these should not be too inaccurate   The roots are to
be taken as follows   two C and one H from the $(s, σ)$ determinants and one C
and two H from the $(π, π)$ determinants   It is found that with this very non-
polar molecule, plane ethylene is at least $1\tfrac{1}{2}$ volts better than perpendicular
ethylene (we cannot give the exact figures without specifying the $(s, σ)$ deter-
minants exactly)   Thus is almost certainly too large a difference †

If we take $H + M_{πx} - W_p{}^C = 10$ volts, and leave all the other quantities
the same, we get a very ionic molecule with most of the charge around the C
nuclei.   This tame perpendicular ethylene is about 1/25 volt better than plane
ethylene   If we take $H + M_{πx} - W_p{}^C = 3$, and reduce $N_{σx}$ to 1 volt, we
still have a fairly ionic molecule, and it turns out that perpendicular ethylene
is 1/16 volt better than plane   With $H + M_{πx} - W_p{}^C = 2$ and $N_{σx} = 2$,
perpendicular ethylene is 0 28 volt more stable than plane   By increasing
$N_{σx}$ or decreasing $H + M_{πx} - W_p{}^C$ beyond these values, however, plane
ethylene soon becomes more stable than perpendicular   This is caused by the
root K_+ of the plane configuration becoming positive, and an H root for it
can then be taken from the $(s, σ)$ determinant   The above calculations can
be very easily modified where the hydrogen roots are below the carbon, and
one obtains the same conclusions as before, that for a molecule which is not
too highly ionic, plane ethylene is more stable than perpendicular.   While
it cannot be said that our calculations by the H-M method decide definitely
in favour of $φ = 0$, they do at least reveal how great will be the difficulties
of making exact computations of the energy difference between plane and
perpendicular ethylene by this method.   One would certainly expect the
variation of the energy with $φ$ to be very much more than in the very sym-
metrical ethane molecule, where it is only the H-H repulsions that give any-
thing of total amount 1/60 volt ‡   Probably the true situation is somewhere

† Perhaps not after all   See footnote, p 174
‡ Eyring, ' J Amer Chem Soc,' vol. 54, p. 319 (1932).

between our numerical examples one and four, perhaps a little nearer to one If this is so, then plane ethylene is better by a fraction of a volt, but it is not fair to claim that we have proved this.

We have now to examine the dependence of the energy on ω This problem also is too complicated for even an approximate solution, but one can see in a rough sort of way that a fairly small positive value can be given The one term in our approximation that decides that ω is to be positive is c, just as in the H-L-P-S approximation it was the analogous terms C_{sss} and $C_{sss'}$. The (s, σ) determinants have terms in $\sin \omega$, and the roots would have their best values with $\omega = \pi/2$, but the (π, π) determinants have terms only in $\cos \omega$ and the roots here would like to have $\omega = 0$ Since the diagonal elements in the former determinant are more widely separated than those in the latter, and since the former has only one root strongly affected by ω while the latter have two, it is plausible that the best value of ω is a small one It is not obvious at first sight why ω is not actually zero, but numerical calculations again elucidate the point and show that ω may be small but is not zero

We have finally to consider the stability of the ω-model compared with that of the right-angled model Once again the situation is such that until some more information is available on the magnitudes of the various quantities appearing in the equations no satisfactory answer can be given The author was not successful in discovering a transformation which completely eliminated the appearance of ϕ from the secular equation of the right-angled model, but the dependence of the roots on ϕ is obviously less than it is in the ω-model Little is lost, therefore, by putting $\phi = 0$ directly, and the equation then factorizes into two quadratics and two quartics While it seems likely that the roots are not as favourable as those of the ω-model, the argument is so incomplete that we do not give it The conclusions of the H-L-P-S approximation on this point must be accepted.

THE ETHANE MOLECULE

Calculations very similar to those made on ethylene can be made on ethane It is a relatively simple matter to write down expressions for the energy, but there is no advantage in doing so, since there can be no doubt of the approximate structure of the molecule, and that is all our calculations can give There is, however, one interesting result which we shall obtain, namely, that both in the H-L-P-S and the H-M methods of approximation there is free rotation of the

CH_3 groups around the C-C axis, provided interactions of any H atom with the distant C and H atoms are neglected

The choice of directed wave-functions suited to this example is that given by Van Vleck (loc cit) for a pyramidal model of methane We arrange three H atoms around each C atom, symmetrically with regard to the C-C axis The angle HCC, which we denote by θ, and the angle φ, by which we denote the azimuth around the C-C axis of one CH_2 group with respect to the other, then specify the ethane molecule, apart from scale factors The wave-function of an electron on a C nucleus, entering into a bond with an electron on the other C nucleus, is given by

$$\psi_L = (1 - 2 \cot^2 \theta)^{\frac{1}{2}} \psi (2p, \sigma_c) - 2^{\frac{1}{2}} \cot n \, \theta \psi (2s),$$

while any of the three electrons on the C nucleus forming bonds with the electrons of three adjoining H atoms, is given by

$$\psi_H = (2 \, \csc^2 \theta/3)^{\frac{1}{2}} \psi (2p, \sigma_H) + (1/3 - 2 \cot^2 \theta/3)^{\frac{1}{2}} \psi (2s),$$

where σ_c and σ_H mean that the electrons are σ electrons when viewed along the C-C and the C-H lines respectively

We do not attempt to calculate the energy and then minimize it with respect to θ The principal integral, however, is probably $C_{\sigma\sigma\sigma}$ and one would therefore make its coefficient rather larger than it is with tetrahedral wave functions In other words, the angle θ is probably smaller than the tetrahedral angle and the three C-H lines radiating from each C nucleus must enclose a slightly larger solid angle than they do in methane The effect of the H-H steric repulsions will be to increase this angle still further

Let us now consider how the angle φ appears in the expression for the energy Clearly, the energy must have trigonal symmetry expressed by the relation

$$W (\phi) = W (\phi + 2\pi/3) = W (\phi + 4\pi/3)$$

In the expression for W by the H-L-S-P approximation, the angle φ can appear only in a limited number of ways It can conceivably arise as $\cos^2 \phi$, $\sin^2 \phi$, $\cos \phi \sin \phi$, $\cos \phi$ and $\sin \phi$, each term with different coefficients But with each term must arise two others obtained by increasing φ by $2\pi/3$ and $4\pi/3$ respectively Performing the simple addition, it is easily verified that W is independent of φ That is, there is free rotation of the CH_3 groups around the C-C axis, to the approximation we have considered When one allows for the H-H interactions, φ will appear implicitly in the H-H exchange integrals,

because the distance between an H atom of one CH_2 group and an H atom of the other depends on ϕ

We consider now the situation as viewed from the H-M viewpoint The molecule as defined above by the angles θ and ϕ has sufficient symmetry to induce considerable factorization of the secular determinant There are two types of resonance terms, those between a carbon atom and the hydrogen members of its group, and those between two carbon atoms We agree to neglect resonance terms between any two hydrogen atoms and between any hydrogen atom and the distant carbon atom Let us take the C-C axis vertical and choose a right-handed system of axes (x, y, z) about the upper nucleus C_a, and a left-handed system (x', y', z') about the other nucleus C_b We make x' parallel to x, y' parallel to y, and z' pointing in the opposite direction to z The choice of carbon wave-functions which practically diagonalizes the carbon-carbon interaction is

$$\left. \begin{aligned} \psi_a\,(2s) &\pm \psi_b\,(2s) \\ \psi_a\,(2p,\,\sigma_z) &\pm \psi_b\,(2p,\,\sigma_z) \end{aligned} \right\} \tag{8}$$

$$\left. \begin{aligned} \psi_a\,(2p,\,\sigma_x) &\pm \psi_b\,(2p,\,\sigma_x) \\ \psi_a\,(2p,\,\sigma_y) &\pm \psi_b\,(2p,\,\sigma_y) \end{aligned} \right\} \tag{9}$$

We have now to define the location of the hydrogen atoms Suppose the lower three to be kept fixed, one of them lying in the $x'z'$ plane We can write the wave-functions for these as

$$\psi_b\,(H,\,0) \qquad \psi_b\,(H,\,2\pi/3) \qquad \psi_b\,(H,\,4\pi/3)$$

Similarly, if we denote the azimuth of one of the three upper H-atoms by ϕ, the wave-functions of these can be written

$$\psi_a\,(H,\,\phi), \qquad \psi_a\,(H,\,\phi + 2\pi/3), \qquad \psi_a\,(H,\,\phi + 4\pi/3)$$

We are now in a position to write down the secular determinant but it will have such a form that its independence of ϕ is by no means obvious We introduce the trigonal wave-functions

$$\Psi_1 = [\psi_a\,(H,\,\phi) + \psi_a\,(H,\,\phi + 2\pi/3) + \psi_a\,(H,\,\phi + 4\pi/3)]/(3)^{\frac{1}{2}},$$

$$\Psi_2 = [2\psi_a\,(H,\,\phi) - \psi_a\,(H,\,\phi + 2\pi/3) - \psi_a\,(H,\,\phi + 4\pi/3)]/(6)^{\frac{1}{2}},$$

$$\Psi_3 = [\psi_a\,(H,\,\phi + 2\pi/3) - \psi_a\,(H,\,\phi + 4\pi/3)]/(2)^{\frac{1}{2}},$$

with similar definitions for Ψ_4, Ψ_5, and Ψ_6, which refer, of course, to the H-atoms on the C_b nucleus. We now take the combinations

$$\Psi_1, \qquad \Psi_6, \tag{10}$$

$$\left.\begin{array}{cc} \cos\phi \ \Psi_2 - \sin\phi \ \Psi_3, & \sin\phi \ \Psi_2 + \cos\phi \ \Psi_3 \\ \Psi_4, & \Psi_5, \end{array}\right\} \tag{11}$$

It is easily verified that the secular determinant is independent of ϕ, and furthermore that it factorizes directly into a determinant of order six, involving wave-functions (8) and (10), and one of order eight involving wave-functions (9) and (11). Additional factorization is obvious, and one obtains without any difficulty the twice repeated quadratics and the cubics

$$\begin{array}{|cc|} \hline P, & \alpha \\ \hline \alpha & H \\ \hline \end{array} \qquad \begin{array}{|ccc|} \hline Q_{\pm} & \beta & \gamma \\ \hline \beta & R_{\pm} & \delta \\ \hline \gamma & \delta & H \\ \hline \end{array}$$

$P_{\pm} = W_s{}^C + N_{ss} - M_{ss} - 3\cos^2\omega \ (C_s - C_s)/2 - 3C_s - W \pm WS_{ss}$,

$\alpha = (3)^{\frac{1}{2}}\cos\omega \ (Q_\sigma + R_\sigma - T_\sigma W)$, $H = W_{11} + B - W$,

$Q_{\pm} = W_s{}^C \pm N_{ss} - M_{ss} - 3C_s - W \pm WS_{ss}$,

$R_{\pm} = W_s{}^C \pm N_{ss} - M_{ss} - 3 (\sin^2\omega \ C_s + \cos^2 \omega C_s) - W \pm WS_{ss}$,

$\beta = -N_{ss} + S_{ss} W + 3\sin\omega \ D_{11} - D_C$, $\gamma = -(3)^{\frac{1}{2}} (Q_\sigma + R_\sigma - T_\sigma W)$

$\delta = (3)^{\frac{1}{2}} (Q_\sigma + R_\sigma - T_\sigma W)$

We do not attempt the solution of these equations, but it is instructive to exhibit their form. We see that there is considerable hybridization of the $2s$ and the $2p\sigma_x$ wave-functions, but that the initial $2p\pi_z$ wave-functions do not acquire any $2s$ wave-function in the approximation we have considered.

If we insert terms to allow for the interactions between an H and a distant C atom, the secular determinant is much more complicated. Either correction alone is sufficient to spoil the dependence on ϕ, and one has to develop the roots to a high perturbation approximation before this type of integral appears with a coefficient depending on ϕ. In the H-L P-S approximation there is, of course, no dependence on ϕ at all, and it is only the H-H interactions which give anything. Eyring (loc. cit.) has considered this problem and shown that

the most stable position is $\phi = 0$, although the fluctuation in energy as ϕ is varied amounts to only 1/60 volts (0 4 kg cal per mol)

Calculations are now in progress on the N_2O_4 molecule to determine which is the most stable one of the three models that have been proposed † Experimental evidence is largely in favour of the one similar in shape to the ethylene ω-model discussed at some length in the present paper, but it is as well to have the additional check of theoretical computations An effort is also being made to extend the calculations of Hückel‡ on the benzene ring, by taking account of the bonds in the plane of the ring as well as those perpendicular to it

A considerable part of the work described in this article was performed at the University of Wisconsin The author wishes to express his deepest appreciation to Professor J H Van Vleck for invaluable guidance and stimulus so readily offered at all times He also wishes to thank the Commonwealth Fund for the award of a Fellowship which made possible his stay in the United States of America

SUMMARY

Calculations have been made to determine the structure of the ethylene molecule Two modes of attack are employed, that of electron pairs and that of molecular orbitals The two methods give consistent results It is shown that the most stable arrangement has all six nuclei coplanar, with a large HCH angle, perhaps about 130° The energy needed to rotate one of the CH_2 groups through $\pi/2$ about the C-C axis is quite small, probably about $\frac{1}{4}$ volt

Similar calculations on the ethane molecule show that it is only the H-H repulsions that prevent the free rotation of the CH_2 groups about the C-C axis.

† Mellor, "Treatise on Inorganic Chemistry," vol 8, p 646

‡ E. Hückel, ' Z Physik,' vol 70, p 204 (1930) , vol 72, p 310 (1931)

Free Paths and Transport Phenomena in Gases and the Quantum Theory of Collisions II. The Determination of the Laws of Force between Atoms and Molecules

By H S W Massey, Ph D, Senior 1851 Exhibitioner, Trinity College, Cambridge, and C B O Mohr, Ph D Trinity College Cambridge, 1851 Exhibitioner, University of Melbourne

The quantum theory has provided a means of calculating the interaction energies of two atoms by a perturbation method It appears that the short range interaction forces are due mainly to electron exchange phenomena between the two atoms, while the van der Waals forces arise from mutual polarization effects * The theory gives the first of these forces in the first approximation, while the van der Waals forces appear only in the second approximation At large distances, where the interaction is small, it is somewhat surprising that the first approximation is not sufficient, and one is led to doubt the accuracy of the method when applied at distances at which the first and second approximations give comparable results At these distances the mutual potential energy is comparable with the mean kinetic energy of a gas atom at ordinary temperatures, and it is therefore clear that a study of gas-kinetic collision phenomena should provide a satisfactory test of the validity of the perturbation method in this region It is the object of this paper to carry out a number of calculations with this aim in view

In a previous paper† the quantum theory of collisions was applied to gas-kinetic collisions, and it was shown that, although the classical theory can be used with accuracy to determine the law of force from viscosity and diffusion phenomena associated with heavy gases, it cannot be applied with safety to hydrogen and helium The method to be used in such cases was given, and it was also shown that the existence of a definite total collision area—a feature of the quantum theory of scattering by a centre of force, the potential of which falls off more rapidly than r^{-3} at large distances—provides a further means of determining the law of force As this collision area can now be directly measured with accuracy by molecular ray experiments, the range of applica-

* Vide Lennard-Jones, ' Proc Phys Soc,' vol 43, p 461 (1931)

† Paper I, ' Proc Roy Soc,' A, vol 141, p 434 (1933)

ability of this method is considerably greater than that of methods based on transport phenomena

In this paper we first consider the interaction of two helium atoms Using the interaction energy given by Slater,[*] the viscosity of helium is computed using the method described in paper I, and it is found by comparison with experiment that although Slater's field is fairly satisfactory, it is not completely accurate The modifications necessary to improve it are indicated, and the possibility of further test by measurement of free paths is then discussed Next, the interaction of a helium atom and a helium ion is considered by calculating the mobility of helium ions in helium, taking account of electron transfer processes. In this case it is possible to devise a method of calculating the interaction energy which should be quite accurate, but it is found that the final value for the mobility, calculated with this field, is not in agreement with experiment The reason for this discrepancy is not clear Finally, the calculation of free paths for various laws of force between gas atoms is carried out in order to provide material for molecular ray investigation of the inter-actions

§1 *The Interaction of Two Helium Atoms and the Viscosity of Helium*

The interaction of two helium atoms has been calculated by Slater (*loc cit*), who obtains

$$\{7 \ 7e^{-2 \ 43\rho} - 0 \ 68\rho^{\ 6}\} \times 10^{-10} \ erg, \tag{1}$$

where ρ is the nuclear separation in units of a_0 Margenau[†] has given a second expression

$$\{7 \ 7e^{-2 \ 43\rho} - 0 \ 68\rho^{\ 6}(1 + 7 \ 9\rho^{-2} + 30\rho^{-4})\} \times 10^{-10} \ erg, \tag{2}$$

which takes account of dipole-quadrupole and quadrupole quadrupole inter-action terms These two forms are illustrated in fig 1

The viscosity of helium is given by

$$\eta = \frac{5}{(J^3 M^2)} \left(\frac{2\pi}{J M}\right)^{3/2} \frac{1 + \varepsilon}{\pi R_{11}} \tag{3}$$

where

$$J = 1/2 \ \kappa T, \tag{4}$$

M is the mass of a gas atom, and κ is Boltzmann's constant The quantity R_{11} is defined by

$$R_{11} = \frac{1}{2} \int_{-\infty}^{\infty} v^7 Q_\eta(v) \ e^{-J J v^4} dv \tag{5}$$

---

* 'Phys Rev,' vol. 32, p 349 (1928)

† 'Phys Rev, vol 38, p 747 (1931)

where Q_η is the viscosity cross-section, given by

$$Q_\eta = 2\pi \int_0^\pi I(\theta) \sin^2 \theta \, d\theta \qquad (6)$$

The angular distribution function $I(\theta)$ has been defined in paper I, and is such that if a stream of N atoms per unit area per second is incident on an atom
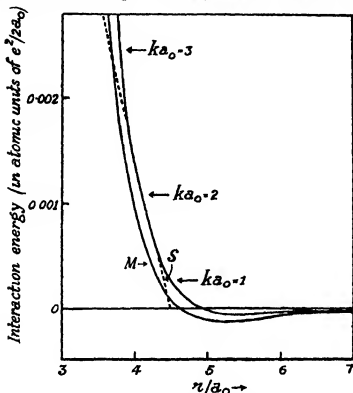

FIG 1 —Calculated Interaction Energy of Two Helium Atoms   S– that due to Slater-Kirkwood.   M—that due to Margenau-Slater.   ------ form of the field

$$\sigma \left(\frac{1}{r^4} - \frac{1}{r_0^4} \right), \quad r < r_0$$

supposed held at rest, the number of incident particles deflected per second between the angles θ and $\theta + d\theta$ is

$$2\pi NI(\theta) \sin \theta \, d\theta \qquad (7)$$

$I(\theta)$ is given, on the quantum theory of collisions, by the expression*

$$I(\theta) = \frac{1}{2k^2} \left| \sum_n (4n+1)(e^{2i\delta_{2n}} - 1) P_{2n}(\cos \theta) \right|^2, \qquad (8)$$

* Allowance has been made for the identity of the colliding particles

where

$$k = \pi M v / h \tag{9}$$

corresponding to the velocity v and the reduced mass $M/2$ of a pair of colliding atoms, each of mass M. The phases δ_n are obtained from the asymptotic form of the solution of

$$\frac{d^2 u}{dr^2} + \left\{ k^2 - \frac{8\pi^2 M}{h^2} V(r) - \frac{n(n+1)}{r^2} \right\} u = 0, \tag{10}$$

which is zero at the origin, this asymptotic form being

$$u \sim \sin\left(kr - \tfrac{1}{2}n\pi + \delta_n\right) \tag{11}$$

It was shown in paper I how δ_n may be calculated if V is known, by using in the appropriate region methods of approximation due to Jeffreys and to Born for the solution of the equation (10) If we apply this method to the potential (1), we obtain the values, Table I, for Q_v as a function of the velocity

Table I—Viscosity Cross-sections for Helium, using Slater's Field

$k a_\sigma$	8/9	2/3	4/3	2	4	6
Viscosity cross-section (in units of a_o^2)	46 8	46 0	45 3	41 7	37 5	32 0

Using these values in the appropriate formulæ, viz (3) and (5), one finally obtains the values given in Table II for the viscosity of helium at different temperatures they are compared with the experimental values

Table II—Viscosity of Helium at Various Temperatures

Absolute temperature	Experimental value (in micropoise)	Quantum theory (Slater's field)
294 5	199 4	213
203 1	156 4	165
88 8	91 8	96
20 2	35 03	43
15 0	29 46	36

It will be seen that Slater's field gives values for the viscosity which are about 6 % too large at the higher temperatures, while the calculated values are unlikely to be in error by more than 3 % At lower temperatures, however,

the discrepancy is more marked, being of the order of 22 %. This indicates too small a range for the interaction of the two atoms, as the viscosity varies inversely as the viscosity cross-section   Better agreement would be obtained by diminishing the attractive part of Slater's field   Referring to fig 1, we see that Margenau's field is likely to give even less correct values for the viscosity at low temperatures, a result which is confirmed by a detailed calculation *   These results are to be expected, since the quantum theory includes the possibility of some penetration of the incident waves into the region excluded on the classical theory   At low temperatures it is just possible that some of the discrepancy may be due to the use of the Maxwell-Boltzmann statistics instead of the Bose-Einstein statistics in forming the general equations for viscosity †

In view of the interest of these results, it is important to obtain an independent check on the accuracy of the values of Q_η calculated by the method used To do this, the following method of calculating the phases δ_n was also used for certain chosen values of k Suppose we write

$$V \sim V_0 + v_1,$$ (12)

where v_1 is small compared with V_0.   Then equation (10) may be written

$$\frac{d^2(ru)}{dr^2} + \left\{ k^2 - \frac{8\pi^2 M}{h^2} V_0 - \frac{n(n+1)}{r^2} \right\} (ru) \quad \frac{8\pi^2 M}{h^2} v_1\, ru$$ (13)

Let us suppose V_0 is chosen so that the equation

$$\frac{d^2(ru_0)}{dr^2} + \left\{ k^2 - \frac{8\pi^2 M}{h^2} V_0 - \frac{n(n+1)}{r^2} \right\} (ru_0) = 0$$ (14)

can be solved analytically to obtain two independent solutions, one of which is zero at the origin and has the asymptotic form

$$ru_0 \sim a_n \sin(kr - \tfrac{1}{2}n\pi + \eta_n)$$ (15)

Since u_0 must represent the sum of an incident plane wave and a scattered spherical wave, we have

$$a_n = e^{i\eta_n} i^n (2n+1) k^{-1}$$ (16)

---

* It would seem that the above results are in contradiction to the results of paper I, where the quantum mechanics of the hard sphere model was seen to give larger cross sections than the classical theory   This model has special properties, however, in view of the fact that the wave function of the incident atom must vanish at the boundary of the struck atom, giving a maximum density outside the boundary   For a non-rigid particle, there is some penetration of the incident waves inside the boundary, and the wave function is nearly at a maximum at the boundary

† Uehling and Uhlenbeck, ' Phys Rev,' vol. 43, p 552 (1933)

We may now obtain a further approximation by substituting this solution for ru_0 on the right-hand side of (15), and solving the resultant equation We then obtain* for the asymptotic form of the function ru

$$ru \sim a_n \sin (kr - \tfrac{1}{2}n\pi + \eta_n) + e^{\frac{1}{2}i\pi}(2n+1) e^{ikr} \int_0^\infty \frac{8\pi^2 M}{k^2 h^2 \sigma_n^2} v_1 r u_0^2 \, dr$$

$$\simeq k^{-1}(2n+1) \left[i^n \sin (kr - \tfrac{1}{2}n\pi) + \tfrac{1}{2}i(1 - e^{2i(\eta_n + \sigma_n)}) e^{ikr}\right], \quad (17)$$

where

$$\sigma_n = - \int_0^\infty \frac{8\pi^2 M}{k h^2 \sigma_n^2} v_1 r^2 u_0^2 \, dr, \qquad (18)$$

since σ_n must be small compared with unity The phase δ_n will be given by

$$\delta_n = \eta_n + \sigma_n \qquad (19)$$

Applying this method to the interaction V, the form adopted for the potential V_0 was

$$V_0 = C\left(\frac{1}{r^2} - \frac{1}{r_0^2}\right), \qquad r < r_0,$$

$$= 0, \qquad r > r_0, \qquad (20)$$

with the constants C and r_0 chosen to make the phase σ_n quite small With this form for V_0 the equation (14) has the solution

$$ru_0 = D_n J_{\nu + \frac{1}{2}}(\lambda r) + E_n J_{-\nu - \frac{1}{2}}(\lambda r), \qquad r < r_0,$$

$$= A_n J_{n + \frac{1}{2}}(kr) + B_n J_{-n - \frac{1}{2}}(kr), \qquad r > r_0, \qquad (21)$$

where

$$\lambda^2 = k^2 + \frac{8\pi^2 M}{h^2} \frac{C}{r_0^2},$$

$$\nu (\nu + 1) = n (n + 1) + \frac{8\pi^2 M}{h^2} C \qquad (22)$$

Since ru_0 must vanish at the origin, E must be zero The ratio of the constants A, B, D is then determined by the conditions at the boundary $r = r_0$, namely, that u and its derivative be continuous across the boundary Then η_n is given by

$$\eta_n = \arctan (-)^{n+1}\left(\frac{B_n}{A_n}\right)$$

With appropriate choice of the velocity v for the calculation, it was possible to arrange that the numerical values of the Bessel functions could be obtained from the very meagre tables available Having obtained η_n in this way, σ_n

* Massey. 'Proc Roy Soc,' **A**, vol. **137**, p. 447 (1932)

was then calculated from the formula (22) by numerical integration   The form of V_0 used is shown by the broken curve in fig 1, and it was found that the phase shift σ produced by the difference v of the Slater field from the field V_0 was seldom more than 0 1 radian.   In Table III the values obtained by this method for $ka_0 = 2$ using the Slater field are compared with those obtained using the methods of approximation due to Jeffreys and Born.   It is seen that when the phase is greater than unity, it is given by Jeffreys's method with considerable accuracy   Phases less than, say, 0 1 will be given quite accurately by Born's method   There will generally be only one even phase lying in the intermediate region, and it can be obtained quite accurately by careful interpolation

Table III —Phases for $ka_0 = 2$

------	Accurate calculation	Jeffreys's approximation	Born's approximation.
δ_0	7 63	7 63	—
δ_2	4 90	4 90	—
δ_4	2 70	2 72	—
δ_6	1 17	1 08	—
δ_8	0 27	0 07	1 6
δ_{10}	−0 07	−0 25	−0 07

As the evidence from viscosity indicates a certain inaccuracy in Slater's field, it would be of interest to check these conclusions by measurement of the free paths of helium atoms by molecular ray methods.   Therefore, the value of the total cross-section Q for the Slater field was calculated for various velocities of impact from the formula

$$Q = \int_0^\pi I(\theta) \sin\theta \, d\theta$$
$$= 8\pi k^{-2} \sum_n (4n+1) \sin^2\delta_{2n} \qquad (23)$$

The values obtained are shown in fig. 2 for various values of ka_0 and the corresponding effective temperatures   It will be seen that definite maxima and minima appear in the curve,[*] their occurrence is in no way dependent on the form of the field of interaction, as we saw in paper I that they occurred in the hard sphere model.   The effect is due to the presence of a small number of terms only in the series (23) at low velocities, and the fact that only the even

---

[*] This is not to be confused with the ordinary Ramsauer effect, which cannot occur with a repulsive field.

phases appear owing to the identity of the colliding particles Oscillations of this nature do not occur in the effective cross-section Q_η for viscosity, for the formula for Q_η consists of two series of terms of opposite sign, so that such oscillations occur together and tend to cancel out It will be difficult to confirm the occurrence of the oscillations shown in fig 2, owing to the necessity of using homogeneous beams of atoms, but the marked increase in the cross-section at low temperatures should be observed It will be noticed that the
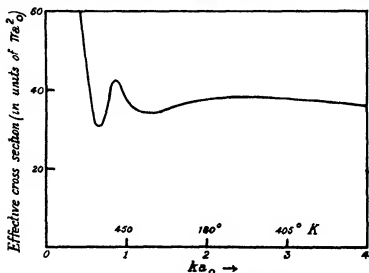
Fig 2 —Effective cross section for the collision of two helium atoms

collision radii corresponding to the cross-section shown in fig 2 are nearly $\sqrt{2}$ times the classical closest distance of approach, showing that the result obtained for the rigid sphere model in paper 1 holds also for this type of field

§ 2. *The Motion of Helium Ions in Helium The Mobility and the Interaction*
$$He^+ - He$$

The mobility of ions in a gas is given by

$$k = eD/\kappa T,\tag{24}$$

where e is the charge on the ion, and D is the coefficient of diffusion of the ions in the gas This coefficient is given by

$$D = \tfrac{3}{8}\pi^{1/2}\left(\frac{M_1 + M_2}{jM_1M_2}\right)^{7/2}\frac{1}{\nu_1 P_{12}}\frac{1}{1 - \varepsilon_0},\tag{25}$$

where M_1, M_2 are the masses of the ion and atom respectively, v_1 the number of atoms per cubic centimetre, and P_{12} is given in terms of a diffusion cross-section Q_D by the formula

$$P_{12} = 2 \int_{-\infty}^{\infty} V^2 Q_D \exp \left\{ - \frac{M_1 M_2}{M_1 + M_2} V^2 \right\} dV \qquad (26)$$

Q_D is defined in terms of the angular distribution $I(\theta)$ for collisions between an ion and an atom by

$$Q_D = 2\pi \int_0^\pi I(\theta) \sin^2 \tfrac{1}{2}\theta \sin \theta \, d\theta. \qquad (27)$$

To calculate $I(\theta)$ requires a knowledge of the interaction energy between He^+ and He, and we must take into account the possibility of charge transfer from the ion on impact   We will consider the interaction first

The quantum theory of the interaction of He^+ with He introduces the feature of level splitting due to nuclear symmetry   A helium ion and a helium atom, both in their ground states at infinity, can react in two different ways according as the wave function representing the combined system is symmetric or anti-symmetric in the nuclear co-ordinates   The first of these possibilities gives rise to a potential energy which has a deep minimum (2 5 volts) at a nuclear separation of 2 $1a_0$, and which only changes to a repulsion at still smaller distances, while the second gives rise to a repulsive interaction, which changes sign only at large distances as a result of the effect of the polarization interaction   The first approximation in the theory, therefore, which neglects the polarization, gives rise to two potential energy functions $v_s(r)$, $v_a(r)$ Making the usual approximation, we then take for the complete interaction at large distances for the two cases

$$V_s(r) = v_s(r) - C/r^4,$$
$$V_a(r) = v_a(r) - C/r^4 \qquad (28)$$

The theory necessary for the evaluation of v_s, v_a has been given by Majorana,[*] and by Pauling,[†] who also calculated the potential energy out to a distance $4a_0$. At this distance the energy is of the order of 0 3 volt, showing that the calculation must be extended to much larger distances   This was first done by extending the range of the above-mentioned calculations.   It is important to use unperturbed wave functions for the helium atomic electrons which are accurate

* 'Nuovo Cimento,' vol. 8, p. 22 (1931)

† 'J Chem. Phys,' vol. 1, p. 56 (1933)

at the large distances involved. Rosen,* in discussing the technique of this type of calculation, gives the wave function

$$u = 3\ 20\ e^{-1\ 48r/a_0}, \tag{29}$$

where r is measured in A, as accurately representing the charge density of helium at these distances This wave function was used whenever the overlap of charge densities at large nuclear separations was involved in the integrals concerned The constant C, given from the known polarizability of the helium atom, has the value $2\ 34 \times 10^{-44}$ in c g s units The resulting form of the potential functions V_s, V_a is shown in fig 3
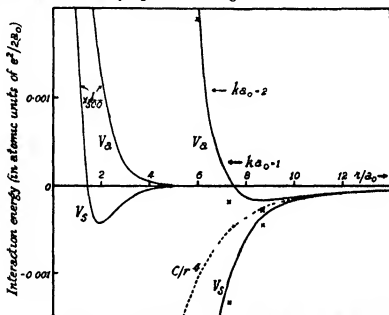
Fig 3 —Calculated interaction energies of a helium ion and a helium atom
Full line curves calculated by method of Majorana Pauling Crosses give points calculated by the method of Hylleraas

We must now consider the possibility of charge transfer on collision After a collision has taken place between a helium atom and a helium ion, it is impossible to distinguish in any way between a scattered ion and a struck atom which has lost an electron, and account of this must be taken in the quantum theory of the collision. This theory has already been discussed by Massey and Smith,† and it is found that the function $I(\theta)$ must take the form

$$I(\theta) = \tfrac{1}{4} \left| f_s(\theta) + f_a(\theta) + f_s(\pi - \theta) - f_a(\pi - \theta) \right|^2 \tag{30}$$

* 'Phys. Rev.,' vol. 38, p 255 (1931)
† 'Proc Roy Soc,' A, vol. 142, p. 142 (1933) .

Here $f_e(\theta)$, $f_a(\theta)$ are the functions

$$\frac{1}{2ik}\Sigma\,(e^{2i\beta_n}-1)\,(2n+1)\,P_n\,(\cos\theta),$$

$$\frac{1}{2ik}\Sigma\,(e^{2i\gamma_n}-1)\,(2n+1)\,P_n\,(\cos\theta),\qquad(31)$$

where the β_n, γ_n are the phase shifts produced by the fields V_s, V_a respectively

Since

$$P_n\,(\cos\theta) = (-)^n\,P_n\,(\cos\overline{\pi-\theta}),$$

we see that $I(\theta)$ given by (30) has the same form as for the collision of two neutral atoms, viz,

$$\tfrac{1}{2}\,|\,f(\theta) + f(\pi-\theta)\,|^2,$$

with

$$f(\theta) = \frac{1}{2ik}\Sigma\,(e^{2i\delta_n}-1)\,(2n+1)\,P_n\,(\cos\theta),$$

where the even phases δ_{2n} are calculated for the field V_s, and the odd phases δ_{2n+1} for the field V_a. Then we have, from equation (26) of paper I,

$$Q_D = 2\pi k^{-2}\Sigma_n\{(2n+1)\sin^2\delta_n - 2\,(n+1)\cos(\delta_n - \delta_{n+1})\sin\delta_n\sin\delta_{n+1}\},$$

$$= 2\pi k^{-2}\Sigma_n\{(2n+1)\sin^2\delta_n - 2\,(n+1)\,(\tfrac{1}{4}\sin 2\delta_n\sin 2\delta_{n+1} + \sin^2\delta_n\sin^2\delta_{n+1})\},\quad(32)$$

where $\delta_n = \beta_n$ for n even, and $\delta_n = \gamma_n$ for n odd   The calculation of the phases proceeds in just the same way as in § 1, but we are now concerned with a large number of terms owing to the big range of the potentials V_s, V_a and the calculation of Q_D must be simplified in the following way

The series (33) is broken up into two parts, thus

$$Q_D = Q_D^1 + Q_D^2,$$

where

$$Q_D^1 = 2\pi k^{-2}\sum_{n=0}^{m},$$

$$Q_D^2 = 2\pi k^{-2}\sum_{n=m}^{\infty}.\qquad(33)$$

For a particular value of k, the value of m is so chosen that β_n rapidly becomes very large as n decreases to values less than m, while γ_n also becomes large, but not nearly so large as β_n Hence sin δ_n oscillates rapidly in the region $0 < n < m$, also, since $\delta_{2n} = \beta_{2n}$, $\delta_{2n+1} = \gamma_{2n+1}$, sin δ_{2n} and sin δ_{2n+1} will be independent functions.   We can therefore replace $\sin^2\delta_n$ and sin $2\delta_n$ in

expression (32) by their mean values of $\frac{1}{2}$ and 0 respectively   We thus have[*]

$$Q_D{}^1 = 2\pi k^{-2} \sum_0^m \tfrac{1}{2}n$$

$$= \tfrac{1}{2}\pi k^{-2}(m^2 + m) \tag{34}$$

For values of n greater than m, the series (32) may be summed directly to give the value of $Q_D{}^2$ as n increases, a point is reached where $\beta_n \sim \gamma_n$ and the series begins to converge quite rapidly

Values of Q_D are so obtained for different values of k, and are then used in formula (26) in order to take account of the Maxwellian distribution of velocities   Substitution in relations (25) and (24) then gives the value of the mobility at the required temperature   The final result of the calculation is that $k = 12$ cm./sec per volt/cm at 760 mm Hg and 20° C   This is to be contrasted with the most recent value, 21 4, obtained by Tyndall and Powell [†]   This discrepancy might at first sight seem surprising, in view of the fact that Hassé[‡] obtained nearly the experimental value by using classical theory and an assumed field based on the interaction of two helium atoms   He takes a single interaction energy

$$V_n = v_n - C/r^4, \tag{35}$$

where v_n is the interaction energy (1) between two helium *atoms*   Reference to figs 1 and 3 shows that this potential cannot be correct, and it has no justification in quantum theory, as the effect of nuclear symmetry extends the range of the potentials v_i, v_e beyond that of v_n Since a larger range interaction means a smaller mobility, it is to be expected that the mobility calculated above will be smaller than that calculated by Hassé   A check on the method given above for the calculation of the mobility was made by computing the mobility for the field V_n used by Hassé , the value 24 was then obtained, in fair agreement with the value 26 deduced by him from classical theory §   Moreover, the quantum theoretical calculation indicates an unvarying value of 24 for the mobility, provided that the fields v_i and v_e fall off sufficiently rapidly   thus if v_i and v_e have become small compared with the polarization

---

[*] If the fields V_i, V_e fall off rapidly at the point r_0, we have $m \sim kr_0$ and then equation (34) merely corresponds to the fact that at not too low velocities quantum and classical theory both give $Q_D = \frac{1}{2}\pi r_0^2$ for a hard sphere of radius r_0.

[†] 'Proc Roy Soc ,' A, vol. 134, p 125 (1931)

[‡] 'Phil. Mag ,' vol 1, p 139 (1926)

§ Hassé and Cook ('Phil. Mag.,' vol. 12, p 554 (1931)) have deduced values of 21 and 19 7 on the arbitrary assumption that the probability of charge transfer at any gas-kinetic collision is one-half, in an attempt to take into account exchange processes.

term C/r^4 at a distance less than $6a_0$, whatever their value inside this point, the mobility is determined entirely by the polarization field beyond the point $6a_0$, and a value of 24 for the mobility is obtained

However, it is important to obtain as much information as possible about the interaction in order to trace the discrepancy It might well be that the formula (28), derived by a perturbation method, is inaccurate in the intermediate region where the two terms are comparable in magnitude Another method was therefore used to calculate V_s and V_a which should give accurate results The method is that used by Hylleraas[*] for calculating exactly the interaction of a hydrogen atom and a proton Reference to the papers of Pauling and Majorana shows that at the distances at which we are concerned the interaction energy terms V_s and V_a arise almost entirely from a single electron and the possibilities of nuclear interchange In short, we may treat the interaction of He and He as a two-centre problem involving a single electron, but with an effective nuclear charge of Z instead of 1 where Z is taken as 1 5 (the value 1 45 leads to the correct polarization at large distances, while the value 1 48 is used in the wave function (29)) Now Hylleraas has shown that the interaction energy for different nuclear separations r is given by $Z^3 f(r/Z)$, so that we have merely to carry out Hylleraas' calculations for hydrogen for much greater nuclear separations, and then convert the values to those for helium by taking $Z = 1$ 5 in the expression $Z^3 f(r/Z)$ For V_s we have $n = 1$, $l = 0$, $m = 0$, and for V_a $n = 2$, $l = 1$, $m = 0$ in Hylleraas' calculations [†] The computations must be carried out with high accuracy, as the energies V_s, V_a are very small compared with the total energy The resulting values obtained for H_2^+ for various distances are given in Table IV in units of $e^2/2a_0$—the atomic unit of energy (13 53 volts), and in fig 3 the corresponding values (denoted by a X) for He_2^+ are shown, together with the curves which were obtained with the use of the formula (28) based on the perturbation method, and which were used in obtaining the mobility

It will be seen that the agreement is very satisfactory, and makes it improbable that any serious error can arise in the above calculations from inaccuracy in the form of V_s and V_a It is difficult to see where the error lies, and it would be of great interest to obtain further experimental values over a considerable temperature range, if this should be possible It would also be of great

---

[*] 'Z Physik,' vol 71, p 739 (1931)

[†] It may be useful here to mention that there are a few minor misprints in Hylleraas paper In particular, it is obvious that a term $-2\sqrt{C}$ has been omitted in printing the first term of the infinite determinant (28)

value to measure the free path of helium ions in helium under gas-kinetic conditions The cross-section effective in the collision of a helium ion with a helium atom was calculated for the above interaction by methods similar to those used in calculating the mobility cross-section A value of $10\ 3 \times \sqrt{2}a_0$ $= 14\ 6\ a_0$ was obtained for the collision radius for a velocity corresponding to a temperature of 20° C

It is interesting to note the effect of charge transfer in determining the values obtained above The potentials V_a and V_s taken separately give values of 25 and 12 respectively for the mobility, as compared with the value 12 obtained if the fields V_a and V_s are combined, in the manner already

Table IV - -Interaction Energy of H and H^+ for Different Nuclear Separations

r/a_0	V_a	r/a_0	V_s
3 3760	0 1886	2 9523	−0 1582
5 1682	0 0392	4 9810	−0 0495
7 0842	0 00706	7 0293	−0 0107
		8 0371	−0 00455
9 0533	0 00084	9 0430	−0 00199
11 0412	−0 00008	11 0386	−0 00059
13 0349	−0 00032	13 0344	−0 00020

shown, to take account of charge transfer In the latter case, the mobility is mainly determined by the field V_s, which is larger in magnitude inside a distance $8a_0$ than the field V_a, while the field beyond $9a_0$ contributes comparatively little For the collision cross-section, however, the effect of taking charge transfer into account is seen, on calculation, to be quite small

§ 3 *Calculation of Cross-Sections for Various Laws of Force*

In considering the collision of helium atoms, the effect of the attractive van der Waals potential could be neglected except at quite low temperatures, but for all other gases and vapours the attractive field plays an important and usually predominant part —at least in the calculation of free paths The asymptotic form of the attractive potential is known to be $V \sim -C\,r^{-6}$, and the constant C is usually so large that, for reasons we shall see, the repulsive field cannot affect the result We shall now calculate the collision cross-section for a potential of the form $-Cr^{-s}$ The total cross-section Q is given by

$$Q = \frac{4\pi}{k^2} \sum_n (2n + 1) \sin^2 \delta_n,$$ (36)

and in all the cases of interest a large number of terms n are required in this series. However, the summation may be carried out in much the same way as the calculation of Q_D in § 2

The phases δ_n are given by Jeffreys's approximation in the form*

$$\delta_n = \int^\infty \left(k^2 - \frac{n\ n+1}{r^2}\right)^{\frac12} dr - \int^\infty \left(k^2 - \alpha V - \frac{n\ n+1}{r^2}\right)^{\frac12} dr, \quad (37)$$

where the lower limits of integration are the zeros of the respective integrands, and α is written for $8\pi^2 Mh^{-2}$　For large n we have

$$\delta_n \simeq \int \left(k^2 - \frac{n\ n+1}{r^2}\right)^{\frac12} \left(1 - 1 + \frac{\frac12 \alpha V}{k^2 - \frac{n\ n+1}{r^2}}\right) dr$$

$$= \int \frac{\frac12 \alpha V}{\left(k^2 - \frac{n\ n+1}{r^2}\right)^{\frac12}} dr, \quad (38)$$

a result which is also given by Born's formula, as may be shown† by using the asymptotic expression for the Bessel function for n large　Jeffreys's approximation may therefore be used for all values of n

Now if $\alpha V = - C/r^2$, we have for large n,

$$\delta_n \simeq \frac12 C \int_s^\infty \frac{1}{r^2 \left(k^2 - \frac{n\ n+1}{r^2}\right)^{\frac12}} dr$$

$$= \frac12 \frac{C}{k} \int_s^\infty \frac{1}{r^{s-1}(r^2 - a^2)^{\frac12}} dr,$$

where $a = (n + \frac12)/k$　On integration we easily obtain

$$\delta_n = \frac{C}{2ka^{s-1}} f(s)$$

$$= \frac{Ck^{s-2}}{2(n + \frac12)^{s-1}} f(s), \quad (39)$$

---

* The formula given here is slightly different in form to that given in paper I　The present form is much more convenient and accurate when used for the computation of phases

† Massey and Smith, loc. cit

where

$$f(s) = \frac{s-3}{s-2}\frac{s-5}{s-4}, \quad \frac{1}{4}\frac{\pi}{2}, \quad s \text{ even},$$

$$\frac{s-3}{s-2}\frac{s-5}{s-4}, \quad \frac{3}{4}, \quad s \text{ odd},$$

$$1, \ s = 3, \quad \frac{\pi}{2}, \quad s = 2 \tag{40}$$

The use of more exact methods in a number of cases showed that this formula holds quite accurately if δ_n is less than 0·5, and then sin $\delta_n \simeq \delta_n$. Hence, if m is that value of n for which $\delta_n = 0 \cdot 5$, we have for the contribution to the cross-section Q from $n > m$

$$\frac{4\pi}{k^2}\sum_{n=m}^{\infty}(2n+1)\sin^2\delta_n \simeq \frac{8\pi}{k^2}\sum_{n=m}^{\infty}\frac{C^2}{4}\frac{k^{2s-4}}{(n+\frac{1}{2})^{2s-3}}f^2$$

$$\simeq 2\pi C^2 k^{2s-6}f^2\int_{m}^{\infty}(n+\frac{1}{2})^{-2s+3}\,dn$$

$$= \frac{2\pi C^2 k^{2s-6}}{2s-4}f^2\,(m+\tfrac{1}{2})^{-2s+4}f^2$$

$$= \frac{4\pi}{s-2}\frac{(m+\frac{1}{2})^2}{k^2}\delta_m^2, \text{ using (39),}$$

$$= \frac{\pi}{s-2}\frac{(m+\frac{1}{2})^2}{k^2}, \tag{41}$$

since by definition $\delta_m = 0 \cdot 5$. Now the contribution to the total cross-section Q from $n < m$ is given approximately—using the method of §2—by

$$2\pi\frac{m^2}{k^2} \tag{42}$$

The total cross-section Q is therefore nearly equal to

$$\pi\left(2 + \frac{1}{s-2}\right)\frac{(m+\frac{1}{2})^2}{k^2},$$

since m is large, and using (39) with the fact that $\delta_m = 0\cdot5$, we obtain finally

$$Q = \pi\frac{2s-3}{s-2}f^{2/(s-1)}\left(\frac{C}{k}\right)^{2/(s-1)} \tag{43}$$

The accuracy of this formula was investigated more carefully by breaking the summation (36) into three parts instead of two. Particular values of s, C, and k were chosen, and for each the phases were determined in the intermediate region by numerical integration using Jeffreys's formula (37), the

summation (36) then being carried out in this region by direct calculation The contribution to Q from the region of quite large and quite small phases was determined as before The results indicated that the formula (43) should give the total cross-section accurate to within about 5%

The relation (43) shows that the collision cross-section is proportional to $(C/v)^{2/(s-1)}$, where v is the velocity of the colliding particles Now classical theory predicts for the intensity of the scattering at any particular angle the same dependence on the velocity and the law of force * On classical theory, however, the total cross-section tends to larger and larger values as smaller and smaller deviations are taken into account in the measurements, whereas quantum theory gives the perfectly definite value (43)

Let us now apply the formula to the determination of the mean free path in argon at room temperature The average kinetic energy of the atoms then corresponds to $k = 10/a_0$ Now the attractive van der Waals force between the atoms has the value $31\ 8 \times 10^{-10}\ (r/a_0)^{-s}$ erg,[†] so that we have $s = 6$, $C = 5\ 5 \times 10^6/a_0^5$ Substituting in (43) we obtain $Q = 365\ \pi a_0^2$, and hence a collision radius of 19 1 a_0 for a pair of colliding argon atoms This corresponds to the collision of two rigid spheres, each of diameter 19 1 $a_0/\sqrt{2} = 13\ 5\ a_0$

Again, for water vapour at room temperature, the attractive force is effectively that between two dipoles, and from the dipole moment of the water molecule we deduce $C = 960/a_0^2$, $s = 3$, while $k = 6\ 7/a$ Substitution in (43) gives $Q = 4\ 30\ \pi a_0^2$ As for argon, this value has not been averaged over the Maxwellian distribution of velocities

It is thus possible, with the use of formula (43), to interpret immediately experimental results obtained by molecular ray methods It is important in making these measurements that the angular resolution of the apparatus be sufficient to give accurate values The method of ensuring this was discussed in paper I, and although the considerations introduced there were illustrated by reference to the rigid sphere model, the same considerations apply to the above cases where r_0 is given by $r_0 = \sqrt{(Q/2\pi)}$ ‡ In the foregoing we have not taken into account the repulsive field, but its effect can be neglected if the zero of the interaction energy falls appreciably inside the point r_0, a condition satisfied for most atoms Thus for argon $r_0 = 13\ 5\ a_0$, whereas the zero falls at about $7a_0$

---

* Darwin, ' Phil. Mag,' vol. 27, p 499 (1914)

† Lennard-Jones, ' Proc Phys Soc,' vol 43, p 461 (1931)

‡ It should be noted that in paper I, and in the present paper, r_0, for the collision of two rigid spheres, is the *sum* of the classical radii of the two spheres

Summary

It has been shown in a previous paper that it is important to use the quantum theory of collisions for the determination of the laws of interaction between atoms at large distances from observations of transport phenomena and free paths. In the present paper, the form and magnitude of the inter-action energy between two helium atoms is discussed in terms of observations of the viscosity of helium at different temperatures. The interaction between a helium atom and a helium ion is considered with reference to the mobility of helium ions in helium. Finally, formulæ are obtained which facilitate the determination of the law of force between atoms at large distances by direct measurements of free paths.

Studies on Gas-Solid Equilibria. Part V.—Pressure-concentration Equilibria between Silica Gel and (1) Oxygen, (2) Nitrogen, (3) Mixtures of Oxygen and Nitrogen, determined isothermally at 0° C.

By Bertram Lambert and David H. P. Peel

Experiments carried out on the adsorption of (1) pure oxygen and (2) pure nitrogen by a sample of silica gel, at 0° C., and at pressures up to 1 atmosphere, have shown that the adsorption is directly proportional to the pressure in each experiment.

The pressure-concentration isothermals are reproducible, completely reversible, and linear (except for a slight divergence at low pressures) throughout their whole length, there is therefore no sign of the silica gel approaching saturation with either oxygen or nitrogen at atmospheric pressure.

The study of the adsorption by the *same* silica gel from *mixtures* of oxygen and nitrogen (at 0° C. and within a total pressure range of 1 atmosphere) appeared, therefore, to offer a good opportunity of obtaining information, under simple conditions, on the problem of adsorption from binary gas mixtures.

The silica gel used was a sample from the same batch as that employed in the previous parts of these investigations.

A satisfactory study of adsorption from a binary gas mixture will involve measurements giving —

(1) Accurate and reproducible pressure-concentration isothermals for each of the *pure gases* in contact with the adsorbent ,

(2) Accurate and reproducible isothermals for *mixtures*, showing the *partial pressures* of the components plotted against the amounts adsorbed at equilibrium

It is, of course, essential that the intrinsic adsorptive power of the adsorbent should undergo no variation during the whole course of the investigation

The determination of the partial pressures of a binary gas mixture in equilibrium with a solid adsorbent requires an accurate knowledge of the composition of the gaseous phase at equilibrium   A sample of the equilibrium gas mixture must be withdrawn from the adsorption system and, if this sample is to represent the true equilibrium gas phase, it must be withdrawn without disturbing the equilibrium at the surface of the solid   This gas sample must then be measured and analysed by a method which ensures a uniformly high degree of accuracy

The necessity for high accuracy in this operation is obvious when it is pointed out that errors at this stage are magnified many times in applying the results of the analysis to the determination of the true partial pressures in the equilibrium gas phase and to the amounts of each separate gas adsorbed at equilibrium

The difficulties of technique inherent in an investigation of this kind are probably responsible for the lack of reliable published data on the subject of adsorption from gas mixtures

The experimental difficulties have now been overcome completely and the application of a technique accurate at *all* stages has enabled reliable and repeatable results to be obtained for the adsorption from mixtures of oxygen and nitrogen by a sample of silica gel

The experimental procedure adopted in this investigation may be summarized as follows —

A known weight (*in vacuo*) of the activated silica gel was placed in an all-glass, sealed apparatus consisting of five parts, separated, where necessary, by stop-cocks —

(A) *The calibrated gas-volume burette* for the accurate measurement of the gases to be introduced into or withdrawn from the adsorption system

(B) *The distributor vessel* to enable the measured volumes of gases to be introduced into the adsorption system and also to enable samples of gas to be withdrawn from the adsorption system for subsequent measurement and analysis

(C) *The adsorption system*—a vessel consisting of two compartments, one containing the solid adsorbent and the other (from which the sample of equilibrium gas mixture is withdrawn) separable from the first by means of a magnetically-operated internal valve, by this means it was possible to remove a sample of the true equilibrium gas phase without disturbing the gases adsorbed on the solid adsorbent

(D) *The mercury manometer* for the measurement of equilibrium pressures This was attached to the adsorption system (gel compartment), the mercury being brought to a fixed point on this side of the manometer so that the volume of the adsorption system was invariable

(E) *The gas analyser* used in conjunction with (A) for the analysis of the sample of equilibrium gas mixture after withdrawal from the adsorption system.

The adsorption system was maintained, throughout the whole period of each experiment, at 0° C by surrounding it with a large Dewar vessel (with drainage tube) filled with broken ice

The gas-volume burette and the manometer were surrounded by water jackets maintained at a temperature of 20° C ($\pm$ 0 01°) Gas volumes could be read to 0 001 c c and pressures to 0 02 mm. of mercury by methods described below

The gas analyser was capable of giving uniformly reliable analyses of oxygen-nitrogen mixtures, the error being less than 0 1% in samples of 6 to 8 c c

The whole apparatus was thoroughly evacuated by means of a mercury vapour pump while the silica gel was heated for several hours at 150° C The residual pressure in the apparatus after this and all subsequent evacuations was less than 10^{-4} mm. of mercury as measured by a McLeod gauge

After the regular procedure of " washing out " the apparatus,* the volume (free gas space) of the adsorption system at 0° C was determined by the

---

* A regular procedure was followed *before* the introduction of any gas or gas mixture into the adsorption system After thorough evacuation, during the last hour of which the silica gel was heated at 150° C, the cold system was " washed out " twice with the gas (or gases) to be used, the system being thoroughly evacuated and the silica gel heated for 1 hour at 150° C after each of these operations

introduction of measured volumes of pure helium, the pressure on the manometer being read after each addition, until the final pressure was about 1 atmosphere   The separate values thus obtained for the free gas space of the adsorption system did not vary more than 0 02% Careful preliminary experiments carried out over a range of temperatures and pressures had shown that the adsorption of helium by silica gel at 0°C was negligible

The true volume of the adsorption system being now known, after the usual preparation, measured volumes of oxygen and nitrogen were introduced and the (total) equilibrium pressure read off on the manometer   It was found, contrary to expectation, that the attainment of equilibrium between the silica gel and mixtures of oxygen and nitrogen was rapid and a pressure read within half an hour of the introduction of the gases into the adsorption system underwent no change over a period of several days   Nevertheless, 12 hours was allowed after the introduction of gas before the equilibrium pressure was read on the manometer

The gel compartment of the adsorption system with the attached manometer was then shut off from the rest of the adsorption system (by closing the magnetically-operated internal valve) and a sample of the equilibrium gas phase withdrawn into the distributor vessel This sample of the true equilibrium gas phase was now measured accurately in the gas-volume burette before transference to the analyser In the analyser the measured sample of mixed gases was submitted to the action of red-hot pure iron (electroplated on a platinum spiral which could be electrically heated—details of the manipulation are given below) The oxygen having been completely removed by this process, the residual nitrogen was transferred back to the gas-volume burette for measurement

These operations, all conducted within a sealed glass apparatus in which the gases could be transferred from one part to another by means of mercury, made it possible to get accurate and reliable values for—

(1) the volume (free gas space) of the adsorption system ,

(2) the volumes of each separate gas added to the adsorption system ,

(3) the total pressure of the mixed gases in equilibrium with the gel at 0° C ,

(4) the composition of the gaseous phase at equilibrium

It was thus possible to calculate the exact amounts of each gas adsorbed from a mixture of oxygen and nitrogen and the exact partial pressures of each of the gases in equilibrium with the gel under these conditions.

Experiments were conducted within the total pressure limits of 1 atmosphere and the results showed a high degree of repeatability   Accurate and reproducible isothermals could be drawn showing values of the equilibrium partial pressures of oxygen and nitrogen plotted against the amounts of each separate gas adsorbed   A comparison of these isothermals with those for pure oxygen and pure nitrogen shows how the adsorption of each gas is affected by the presence of the other

The apparatus used in this work is shown diagrammatically in fig 1   For the purpose of this description it is conveniently divided into five sections as in the introduction above , the five sections are designated by the letters A, B, C, D, E, both in the diagram and in the description
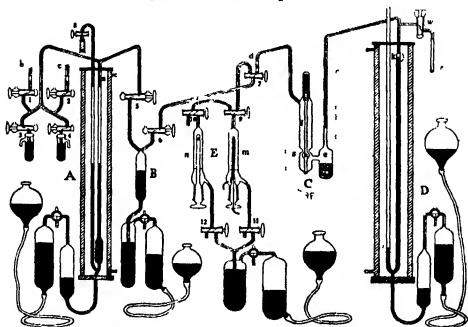
Fig 1

(A) *The Calibrated Gas-volume Burette*

This was of the type generally used when gas volumes are measured at atmospheric pressure , it consisted of a measuring limb and a balancing limb connected together and attached, at the bottom end, to a mercury reservoir   The graduated part of the measuring limb had the same internal diameter (5 mm) as the balancing limb , meniscus corrections were thus avoided and

gas contained in the measuring limb was at atmospheric pressure when the mercury levels in the two limbs were brought to the same height, with the balancing limb open to the air

The burette was mounted vertically in a jacket fitted with plate-glass windows back and front   It was maintained at a temperature of 20° C ($\pm$ 0 01°) by the rapid circulation through the jacket of water from a large constant-temperature bath, the thermostatic control of the bath being adjusted from time to time to compensate for alterations in the room temperature

The capacity of the measuring limb of the burette was 12 c c and it was graduated every 0 02 c c   It was very carefully calibrated at 20° C by the weighed mercury method

The burette was read by means of a reading microscope fitted with a micrometer scale in the eye-piece   The magnification of the microscope was adjusted so that 20 micrometer scale divisions exactly covered the space between the centres of two adjacent graduation marks when the burette was viewed through the microscope, volume readings could therefore be made to 0 001 c c , or less, by estimation   The reading microscope was mounted on a carriage which moved vertically, by rack and pinion action, on an accurately-machined steel bar fixed to the front of the jacket, the microscope carriage was also provided with a true horizontal movement which was brought into action after locking the carriage in a given vertical position

This precision reading device attached to the burette jacket was found to be much superior to a cathetometer, there was a complete freedom from all detectable errors in reading the position of the mercury meniscus on the etched burette scale and gas volume readings could be repeated with certainty to less than 0 001 c c   Reflected light effects were removed from each mercury meniscus by a black ebonite shroud surrounding the glass tube and brought to a position about 1 mm. above the mercury level, this enabled the mercury meniscus to be viewed as a black silhouette when illuminated by a suitably diffused light placed behind the water jacket

The mercury reservoir was connected to the burette by glass tubing and its position was thus fixed   The alterations of pressure necessary to work the reservoir were obtained by compressing or rarefying the air in contact with the mercury by means of an external mercury compressor as shown in the diagram   The movable compressor-reservoir was carried in a cradle moving in a long vertical slide and a fine adjustment was provided so that the levelling of the mercury in the burette limbs could be carried out satisfactorily to within 0 02 mm. The T-stop-cock between the burette reservoir and the

mercury compressor allowed of variations in the amount of air in the intervening air-buffer and so permitted the application of a wide range of positive and negative pressures to the mercury in the burette reservoir. This method of working a mercury reservoir was found to be very satisfactory and was used on all those employed throughout the apparatus.

The upper ends of the burette limbs were made of capillary tubing of 1 mm. bore, and the zero mark of the burette was an etched line *a* on the capillary part of the measuring limb. The balancing limb terminated in a stop-cock 8 opening to the air through a protecting tube containing soda-lime and active charcoal granules. Above the zero mark the capillary tubing branched at a Y-junction, one side being connected with the distributor vessel B (through the stop-cock 5) and the other with the oxygen and nitrogen storage vessels (through stop-cocks 1 and 2), the gas storage vessels were connected by capillary tubing, the oxygen storage vessel being sealed on at *b* and the nitrogen storage vessel at *c*. Stop-cocks 3 and 4 communicated with the open air through mercury cups with side-tubes as shown. All connecting tubes were made of 1 mm. bore tubing.

With suitable pressure adjustments on the mercury reservoirs of the burette and the distributor vessel, the system of stop-cocks allowed the complete removal of all gas and its replacement by mercury in the capillary connections between these vessels and the gas storage vessels; stop-cocks 1 to 5 being then closed, reduction of the pressure on the burette reservoir, followed by the opening of stop-cock 1 (or 2), allowed gas to be drawn from the oxygen (or nitrogen) storage vessel into the burette. Finally, the opening of stop-cock 3 (or 4) and the application of pressure (by means of a hand-bellows) to the mercury in the attached mercury cup, allowed the oxygen (or nitrogen) left behind in the connecting tube to be pushed into the burette (and above stop-cock 1 (or 2)) and the mercury level to be adjusted at the zero mark *a* on the burette.

A suitable volume of pure oxygen or nitrogen could thus be transferred from its storage vessel to the burette without introducing any impurity or leaving any traces behind in the connecting tubes. The mercury levels could then be adjusted so as to bring the gas to atmospheric pressure and its volume accurately measured. All measured volumes of gases were reduced to standard temperature and pressure.

(B) *The Distributor Vessel*

This consisted of a cylindrical glass bulb (of about 30 c.c. capacity) provided, at its lower end, with a mercury reservoir to which a wide range of positive

and negatve pressures could be applied by the method described under A , the upper end terminated in a Y-junction, of capillary bore, connecting it on one side with the gas-volume burette A (through stop-cock 5) and on the other side with either the adsorption system C or the gas analyser E (through stop-cock 6 and the appropriate limb of the three-way stop-cock 7) All the connecting tubes were made from capillary tubing of 1 mm. bore and all the stop-cocks had accurately-fitting stoppers with the same bore

By suitable adjustment of pressures on the mercury reservoirs concerned, it was possible to transfer gas completely—following it with mercury and avoiding the trapping of bubbles of gas—(1) from the distributor vessel B to the gas-volume burette and vice versa , (2) from the distributor vessel B to the gas analyser E and vice versa , (3) from the distributor vessel B to the adsorption system C In this last operation the mercury following the gas was stopped at the fixed mark d which was one of the two limits defining the volume of the adsorption system

The distributor vessel was also used to remove gas from the adsorption system , after the gas thus removed had been transferred to the burette for measurement, the gas left in the tubes and stop-cocks between the distributor vessel and the adsorption system was pushed back into the latter section and the mercury again brought to the fixed mark d

(C) The Adsorption System.

This section of the apparatus consisted of two compartments—referred to, throughout this description, as the gel compartment and the gas compartment. The gel compartment e contained the silica gel which was in the form of small granules , it was attached to the manometer D by capillary tubing and to the gas compartment f by tubing of wide (1 cm.) bore The upper end of the gas compartment was connected, by capillary tubing, with the distributor vessel B (through the stop-cocks 7 and 6)

A magnetically operated internal valve which served, when required, to close the connection between the two compartments was made from light glass tubing blown into a bulb at h and widened at the top so as to enclose a hollow soft-iron cylinder It was sealed at both ends and rested loosely in the gas compartment which was shaped at its upper end so as to hold the valve in an approximately vertical position.

When the valve was resting in its normal position, as it is shown in the diagram, the gel and gas compartments were open to one another and there

was no interference with the easy diffusion of gas throughout both compartments The application of an electromagnet at the top of the gas compartment caused the valve to rise and the bulb h to be held in close contact with a ground seating g on a constricted part of the gas compartment With the valve in this position, the connection between the two compartments was closed The valve readily fell away from the ground seating when the electromagnet was switched off and so restored the open connection between the two compartments When the valve was closed, gas could be withdrawn from the top section of the gas compartment into the distributor vessel B without appreciably affecting the pressure indicated by the manometer in the gel compartment

In the experiments with gas mixtures, the use of this device ensured that a sample of gas (for the determination of the partial pressures of the two constituents) could be withdrawn without disturbing the equilibrium at the surface of the silica gel during the actual withdrawal operation and that the sample withdrawn was really representative of the true equilibrium gas phase

The adsorption system was maintained at 0° C , throughout each experiment, by surrounding it with a large Dewar vessel filled with broken ice , the Dewar vessel was constructed with a drain-tube through the bottom

The volume of the adsorption system was the gas space between the two fixed points d and k each defined by a mercury meniscus A "dead-space" correction was made, throughout the work, for the very small fraction of the volume which was outside the ice-bath

(D) *The Mercury Manometer*

This consisted of a long U-tube of internal diameter 8 mm. throughout, one limb being connected to the adsorption system by a short length of capillary tubing, the other limb being open to the air through a protecting tube containing soda-lime and active charcoal granules. The bottom of the U-tube was connected to a mercury reservoir to which a wide range of positive and negative pressures could be applied by the method described under A.

A pressure reading on this manometer involved three operations (1) adjusting the pressure on the mercury reservoir so as to bring the mercury level to the fixed position k in the limb connected to the adsorption system ; (2) measuring the exact difference in height between the mercury levels in the two limbs , (3) reading the standard barometer The necessary temperature corrections were made so as to bring all pressure measurements to values expressed in millimetres of mercury at 0° C

The manometer was mounted in a jacket made with machined sides and base of duralumin and having plate-glass windows back and front Inside the jacket, and immediately behind the manometer, there was mounted a thick plate-glass scale This scale was made by the Société Genevoise and guaranteed to be accurate (to within 5 microns) at 20° C over the whole length of 800 mm. It was graduated in millimetres and the graduation marks were of an even thickness of 0 05 mm. The manometer and scale were maintained at a temperature of 20° C ($\pm$ 0 01°) by the method described under A.

A high-precision reading device was mounted on the front of the manometer jacket, this was similar to that fitted on the gas-volume burette except that two reading microscopes were used The magnification of the microscopes was adjusted so that 25 micrometer (eye-piece) scale divisions exactly covered the space between the centres of two adjacent millimetre graduations, when the graduated scale was viewed through the microscopes. Direct readings could therefore be made to 0·04 mm., or less, by estimation.

In setting up this section of the apparatus, great care was exercised to ensure that all the essential parts were quite rigid and vertical

When each mercury meniscus was properly shrouded and suitable illumination provided behind the manometer jacket (vide supra), it was possible—using the vertical and horizontal movements of the microscope carriages—to read very accurately the position of each mercury meniscus on the graduated glass scale For a given pressure in the adsorption system, the vertical distance between the two mercury levels could be measured with certainty to less than 0 02 mm No meniscus correction was necessary as each mercury meniscus was in tubing of the same bore

Accurate *barometer* readings were necessary for the calculation of equilibrium pressures and also of gas volumes. These were made on a standard Fortin barometer and the usual temperature corrections made to reduce the readings to 0° C Independent readings were made on a U-tube barometer set up and read like the manometer described above This barometer was made from Pyrex glass, thoroughly " baked out " *in vacuo* and filled by distilling pure mercury into it. The readings of the two barometers, corrected to 0° C , agreed to within 0 02 mm.

(E) *The Gas Analyser*

This was used in conjunction with the gas-volume burette for the accurate analysis of the samples of equilibrium oxygen-nitrogen mixtures.

After a sample of equilibrium gas mixture had been withdrawn from the adsorption system and transferred to the burette, the gas remaining in the connecting tubes and stop-cocks between the distributor vessel and the adsorption system was pushed back into the latter, the mercury level adjusted again at the fixed mark d and the stop-cock 7 closed. The measured volume of oxygen-nitrogen mixture was then transferred, via the distributor vessel, to the gas analyser E.

In one part, m, of the gas analyser, the oxygen-nitrogen mixture was submitted to the action of red-hot, pure iron (electroplated on a spiral of platinum wire which could be heated electrically). This resulted in the conversion of the oxygen into iron oxide and its complete removal from the gaseous phase. Small traces of carbon dioxide and water vapour were necessarily produced in this operation since the oxygen-nitrogen mixture contained grease vapour owing to its passage through grease-lubricated stop-cocks; these impurities were removed from the residual nitrogen in another part, n, of the gas analyser, where it was left for 12 hours in contact with a Pyrex glass rod o coated with a thin layer of fused potash. The pure nitrogen was finally transferred back to the burette, its volume determined and the composition of the original mixture calculated.

The accuracy of this technique was thoroughly tested by analysing oxygen-nitrogen mixtures of known composition—made from measured volumes of the pure gases withdrawn from the storage vessels. The difference between the known composition of a mixture and that determined as above, was always less than 0.1% even when the total volume of gas analysed was only 6 to 8 c.c.

The detailed construction of the gas analyser is clearly shown in the diagram. The three-way stop-cocks 9, 10, 11, 12, arranged as shown, and the large mercury reservoir (to which a wide range of positive and negative pressures could be applied) made it possible to transfer the whole of the gas to where it was required for the various operations, and to follow it by mercury so avoiding the trapping of gas bubbles in the connecting tubes and stop-cocks.

The pressure arrangements attached to the mercury reservoir also made it possible to produce a Torricellian vacuum in either of the vessels m or n, so that dissolved air could be completely removed from the mercury and adsorbed gas from the iron-coated platinum spiral. Since this spiral had to be reduced—by heating it in a stream of pure, dry hydrogen and then cooling it in the gas—before each analysis, it had to be heated to bright redness several times, *in vacuo*, in order to remove the adsorbed hydrogen. The dissolved or adsorbed

gas thus removed was pushed out by mercury through the open limb of stop-
cock 10

The arrangement of the stop-cocks 9, 10, 11, 12, made it possible—by
the use of the appropriate open limbs of the last three—(1) to reduce the iron-
coated platinum spiral by heating it in a current of pure, dry hydrogen and
cooling it in the gas stream , (2) to renew the potash on the Pyrex rod o by
removing it at the ground junction, dipping it in molten potash and cooling
it, after replacement, in a stream of pure dry nitrogen After such operations
and the subsequent removal of dissolved and adsorbed gases, as described
above, the whole system could be filled with mercury and left ready to receive
a measured volume of gas for analysis.

Each stop-cock used in the construction of the apparatus was carefully
chosen so that mercury could be passed through it without trapping small gas
bubbles. Each stopper had a bore of the same diameter (about 1 mm.) as
the capillary tubes sealed on to the stop-cock barrels and the openings of these
tubes coincided exactly with the ends of the capillary passage through the
stopper The stop-cocks were lubricated with Ramsay stop-cock grease
(previously boiled in vacuo) and, after the stoppers had been turned many
times in both directions, the excess grease accumulated in the bore was washed
out with carbon tetrachloride , air was then drawn through the bore for several
hours.

Great care was taken to ensure that the gases used in these experiments
were of the highest possible purity Before filling with gas, each storage
vessel was thoroughly evacuated, heated and " washed out " several times
with the gas to be stored in it Each gas storage vessel contained a supply
of pure phosphorus pentoxide with which the gas was left in contact for several
weeks before use

The nitrogen was made by heating pure sodium azide (purified by several
recrystallizations) in a wide tube directly sealed to the storage vessel No
purification of this gas was necessary

The oxygen was made by the electrolysis of a saturated solution of barium
hydroxide (purified by many recrystallizations). The electrolytic cell was
similar in design to that used by Lambert,* but air was kept out of contact
with the electrolyte in the cell reservoir by means of a buffer of oxygen Since
traces of hydrogen must be contained in electrolytic oxygen, owing to the
solubility of this gas in the electrolyte, the oxygen was purified by circulating
it over a red-hot platinum spiral and pure phosphorus pentoxide for 20 hours

The stop-cocks of the purifying and storage vessel were lubricated with glacial phosphoric acid Gas drawn from this vessel was passed through a narrow U-tube immersed in liquid air to remove traces of water vapour taken up by the oxygen in its passage through the stop-cock lubricated with phosphoric acid

The *helium* used for the measurement of the free gas space of the adsorption system was made from thorianite and purified by circulating it for many hours over large quantities of active charcoal cooled to liquid air temperature The 100% helium supplied, in sealed glass tubes, by the British Oxygen Company, was also used and found to be quite satisfactory for the purpose

The pressure-concentration equilibria between the silica gel and (1) pure nitrogen, and (2) pure oxygen were first determined Two independent experiments were carried out with each gas, the adsorption system being evacuated and the silica gel heated for 1 hour at 150° C between each experiment

The results are given in Tables I and II The weight (*in vacuo*) of the silica gel used in the experiments was 9 8812 gm. Amounts of gas adsorbed by this weight of gel are given in cubic centimetres at standard temperature and pressure ; equilibrium pressures are expressed in millimetres of mercury at 0° C

These results are plotted in fig 2

The results show quite clearly that the equilibria between (1) silica gel and nitrogen, (2) silica gel and oxygen are completely reversible and reproducible over the whole pressure range and that the adsorption, in each experiment, is proportional to the pressure except over the lower range of pressures It is noticeable that the amount of nitrogen adsorbed is over 10% more than the amount of oxygen adsorbed at the same pressure

Adsorption from Oxygen-Nitrogen Mixtures

Two separate and independent experiments were carried out on the adsorption shown by the silica gel when exposed to *mixtures* of oxygen and nitrogen, the adsorption system being thoroughly evacuated, and the silica gel heated for 1 hour at 150° C, between the two experiments

Mixtures containing approximately equal quantities of the two gases were used throughout and the partial pressures of the two gases in the adsorption system were never far apart. The gases were mixed in the adsorption system —the oxygen being introduced before the nitrogen—in the determination of each " ascending " equilibrium point.

B Lambert and D H P Peel.

Table I—Silica Gel—Nitrogen Equilibria at 0° C

No	Volume of nitrogen adsorbed	Equilibrium pressures	Volume adsorbed / Pressure
1	1 937	78 15	0 025
2	3 738	151 73	0 025
3	5 798	238 30	0 024
4	7 921	337 39	0 024
5	10 133	421 42	0 024
6	12 318	517 25	0 024
7	14 614	617 55	0 024
8	16 858	716 43	0 024
9	16 050	680 72	0 024
10	13 437	564 63	0 024
11	11 117	463 97	0 024
12	8 777	363 39	0 024
13	6 402	262 96	0 024
14	4 201	170 73	0 025
15	2 127	85 58	0 025
16	0 457	18 09	0 025
17	2 480	100 42	0 025
18	5 249	214 93	0 024
19	7 728	318 85	0 024
20	10 322	430 11	0 024
21	12 922	542 40	0 024
22	15 292	647 02	0 024
23	16 754	713 21	0 024
24	17 911	763 49	0 024
25	15 324	648 53	0 024
26	12 438	521 17	0 024
27	9 463	392 62	0 024
28	6 840	281 83	0 024
29	4 228	171 78	0 025
30	2 886	116 63	0 025
31	1 311	52 69	0 025

The equilibrium points are numbered in the order in which they were obtained

First experiment { "Ascending" points—Nos. 1 to 8
{ "Descending" points—Nos. 9 to 16

Second experiment { "Ascending" points—Nos. 17 to 24
{ "Descending" points—Nos 25 to 31

The adsorption system was completely evacuated between the first and second experiments.

About 12 hours were allowed for the establishment of equilibrium after the addition (or withdrawal) of gas, although careful experiments had shown that the equilibrium (total) pressure was reached in half an hour and showed no subsequent alteration over a period of several days.

The results of the two experiments are given in Tables III and IV The equilibrium points are numbered in the order in which they were obtained, each oxygen point in Table III being obtained in the same experiment as the nitrogen point designated by the same number in Table IV. The amounts of gas adsorbed by the gel (9 8812 gm) are given in cubic centimetres at standard temperature and pressure, and the equilibrium partial pressures are given in millimetres of mercury at 0° C The results are given in two tables so as

Table II —Silica Gel—Oxygen Equilibria at 0° C

No	Volume of oxygen adsorbed	Equilibrium pressures.	Volume adsorbed / Pressure
1	1 512	68 65	0 022
2	3 206	147 76	0 022
3	5 055	234 97	0 022
4	6 914	333 30	0 021
5	8 925	420 29	0 021
6	10 966	519 33	0 021
7	12 486	592 95	0 021
8	14 042	669 65	0 021
9	15 339	724 87	0 021
10	16 331	783 00	0 021
11	14 543	694 16	0 021
12	13 341	635 49	0 021
13	12 109	574 17	0 021
14	10 504	495 88	0 021
15	8 890	417 97	0 021
16	7 381	339 30	0 021
17	5 536	257 15	0 022
18	3 703	169 71	0 022
19	2 296	104 20	0 022
20	1 386	61 97	0 022
21	0 440	18 18	0 024
22	2 369	105 37	0 022
23	4 633	215 61	0 021
24	6 833	319 16	0 021
25	8 900	420 24	0 021
26	10 981	520 15	0 021
27	12 659	602 24	0 021
28	14 602	698 02	0 021
29	14 036	669 58	0 021
30	11 321	537 51	0 021
31	8 778	413 46	0 021
32	6 497	301 20	0 021
33	4 298	199 30	0 022
34	2 096	96 56	0 022
35	0 665	29 51	0 022

The equilibrium points are numbered in the order in which they were obtained

First experiment { "Ascending" points—Nos 1 to 10
{ "Descending" points—Nos. 11 to 21

Second experiment { "Ascending" points—Nos 22 to 28.
{ "Descending" points—Nos 29 to 35

The adsorption system was completely evacuated between the first and second experiments

to show clearly how the adsorption of each gas is affected by the presence of the other

In Table V the results are arranged so as to show how the added amounts of the oxygen and nitrogen adsorbed at the twelve equilibrium points compare with the sum of the amounts of these gases when adsorbed singly at the same pressures. It is clear that the total amount of gas adsorbed by the silica gel from mixtures of oxygen and nitrogen is slightly less than the sum of the separate amounts of the pure gases adsorbed singly at the same pressures.
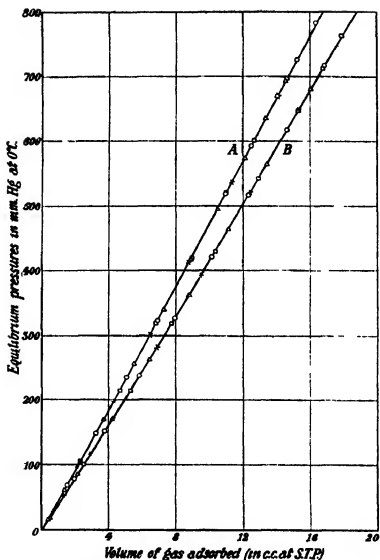
Fig 2 —Curve A oxygen, curve B nitrogen.

First experiments with each gas　　$\begin{cases} \text{" Ascending " points—O} \\ \text{" Descending " points—} \triangle \end{cases}$

Second experiments with each gas　　$\begin{cases} \text{" Ascending " points—} \boxdot \\ \text{" Descending " points—} \times \end{cases}$

The results are plotted in figs. 3 and 4, along with the isothermals for the pure gases, so as to show how the adsorption of each gas is affected by the presence of the other

Table III —Silica Gel—Oxygen Equilibria (in presence of Nitrogen)

No	Partial pressure of oxygen	Volume of oxygen absorbed (mixture).	Volume of oxygen absorbed from pure oxygen at same pressure	Change in adsorption of oxygen due to the presence of nitrogen
1	59 45	1 345	1 326	+0 019
2	118 02	2 789	2 585	+0 204
3	170 48	4 109	3 709	+0 400
4	223 81	5 288	4 835	+0 453
5	107 53	2 787	2 360	+0 427
6	209 12	5 095	4 520	+0 575
7	286 50	6 920	6 148	+0 772
8	355 05	8 443	7 522	+0 921
9	330 73	7 939	7 075	+0 864
10	308 81	7 380	6 607	+0 773
11	287 89	6 916	6 170	+0 746
12	265 77	6 420	5 715	+0 705

Table IV —Silica Gel—Nitrogen Equilibria (in presence of Oxygen.)

No	Partial pressure of nitrogen	Volume of nitrogen adsorbed (mixture).	Volume of nitrogen adsorbed from pure nitrogen at same pressure	Change in adsorption of nitrogen due to presence of oxygen
1	59 50	1 346	1 485	−0 139
2	118 65	2 602	2 936	−0 334
3	172 39	3 701	4 238	−0 537
4	226 34	4 885	5 533	−0 648
5	113 36	2 339	2 780	−0 441
6	214 17	4 583	5 243	−0 660
7	296 32	6 339	7 200	−0 861
8	365 01	7 831	8 837	−1 006
9	342 00	7 393	8 385	−0 992
10	318 83	6 835	7 739	−0 914
11	297 10	6 372	7 219	−0 847
12	274 30	5 879	6 679	−0 800

First experiment   " Ascending " points—Nos. 1 to 4
Second experiment { " Ascending " points—Nos. 5 to 8.
                     " Descending " points—Nos 9 to 12.

After the above experiments had been completed the adsorptive power of the gel for each of the pure gases was re-determined. It was found that the intrinsic adsorptive power of the gel for pure oxygen and pure nitrogen had undergone no change whatever ; equilibrium points were obtained which fell exactly on the originally-determined isothermals.

The accuracy of the technique employed in this work and the reproducibility of the results in separate, independent experiments, seem to leave no doubt that, with the sample of silica gel used, the adsorption of oxygen from mixtures
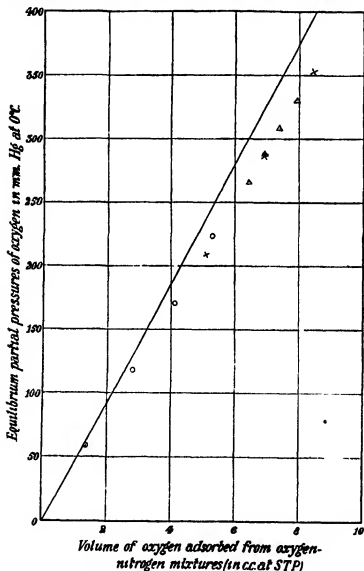
Fig. 3.—Pure oxygen isothermal.

of oxygen and nitrogen (at approximately equal pressures) is markedly higher than it is from pure oxygen. The adsorption of nitrogen is, on the other hand, definitely lower than it is from pure nitrogen. Although the silica gel showed

a greater adsorption from pure nitrogen than from pure oxygen (at corresponding pressures) this order is reversed when the gel is placed in contact with mixtures of approximately equal volumes of the two gases.
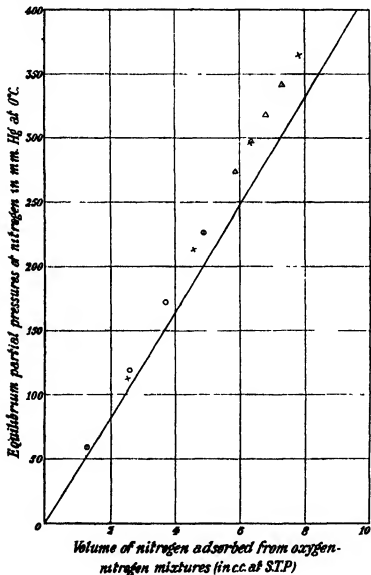
Fig. 4.—Pure nitrogen isothermal.

A discussion of these results is postponed until data are obtained for the adsorption by the same sample of silica gel from other binary gas mixtures.

Table V —Silica Gel—Oxygen-Nitrogen Equilibria at 0° C

No	Oxygen		Nitrogen		Totals.		Change on mixing
	Volume O_2 adsorbed, mixture	Volume O_2 adsorbed, single gas	Volume N_2 adsorbed, mixture	Volume N_2 adsorbed, single gas	Total gas adsorbed, mixture	Total gas adsorbed, singly	
1	1 345	1 326	1 346	1 485	2 691	2 811	−0 110
2	2 759	2 585	2 602	2 936	5 361	5 521	−0 130
3	4 109	3 709	3 701	4 238	7 810	7 947	−0 137
4	5 288	4 835	4 885	5 533	10 173	10 368	−0 195
5	2 787	2 360	2 339	2 780	5 126	5 140	−0 014
6	5 095	4 520	4 583	5 243	9 678	9 763	−0 085
7	6 920	6 148	6 339	7 200	13 259	13 348	−0 089
8	8 443	7 522	7 831	8 837	16 274	16 359	−0 085
9	7 939	7 075	7 293	8 285	15 232	15 359	−0 128
10	7 380	6 607	6 825	7 739	14 205	14 346	−0 141
11	6 916	6 170	6 372	7 219	13 288	13 389	−0 101
12	6 420	5 715	5 879	6 679	12 299	12 394	−0 095

First experiment   " Ascending " points—Nos. 1 to 4

Second experiment { " Ascending " points—Nos. 5 to 8
                  { " Descending " points—Nos. 9 to 12

Summary

(1) An accurate technique is described for the study of adsorption by solid adsorbents from binary gas mixtures.

This technique has been applied to the investigation of the adsorption by silica gel at 0° C. from mixtures of oxygen and nitrogen when these gases are present in approximately equal quantities

(2) An investigation of the adsorption of the *separate* gases at 0° C. has shown that, in each experiment, the adsorption is directly proportional to the pressure, except for a very slight divergence at pressures below 100 mm. The pressure-concentration isothermals show a complete reversibility over the whole range of pressures studied (up to 1 atmosphere), and they are reproducible throughout in separate independent experiments.

The adsorptive power of the silica gel is greater, at corresponding pressures, for pure nitrogen than for pure oxygen.

(3) A study of the adsorption at 0° C. from *mixtures* of approximately equal quantities of these pure gases has yielded remarkable results :—

(a) The adsorptive power of the silica gel for oxygen is, in the presence of nitrogen actually greater (up to 15%) than when oxygen alone is present

(b) On the other hand, the adsorptive power of the gel for nitrogen is less in the presence of oxygen than when nitrogen alone is present

(c) The total amount of gas adsorbed from the mixture is always slightly less than the sum of the separate amounts of the pure gases absorbed singly at the same pressures

---

The Theory of Alloys in the γ-Phase

By H. Jones, Lecturer in Theoretical Physics, Wills Physical Laboratory, University of Bristol

(Communicated by A. M. Tyndall, F.R.S.—Received November 9, 1933.)

1 Introduction

Binary alloys in the γ-phase according to Endo† and Bernal‡ have especially large diamagnetic susceptibilities It appears also that the Hall coefficients§ may be much greater for the alloys in this phase than for either of the constituent pure metals It will be shown that it is possible to relate these properties to the crystal structure of the alloys, and to the fact that the composition within the γ-phase follows the Hume-Rothery‖ electronic rule For alloys in this phase the rule states that there are 21 loosely bound, or valency electrons, to every 13 atoms A reason will also be shown to exist for this rather odd ratio of the number of approximately free electrons to the number of atoms

The remainder of this section gives a summary of results already known which we shall require

The wave-function of an electron moving in the periodic field of a lattice is of the form¶

$$\psi_k = e^{\frac{2\pi i}{a}(k \cdot r)} u_k(r), \tag{1}$$

---

† 'Sci. Rep. Imp. Univ. Tokyo,' vol 14, p 479 (1925)

‡ 'Trans. Faraday Soc.,' vol 25, p 367 (1929)

§ Richards and Evans, ' Phil. Mag.,' vol 13, p 201 (1932)

‖ "The Metallic State," p 328

¶ Bloch, ' Z. Physik,' vol 52, p 555 (1929)

where u_k (r) is periodic with the period of the potential field, and the three components of k are the numbers used to specify a state The γ-structures are based on a cubic lattice, so that it will be sufficient only to consider crystals with cubic symmetry a is then the length of the side of a unit cell

It is convenient to regard k_x, k_y, k_z as plotted along three rectangular axes, so that every state of an electron in the lattice is represented by a point in k space   The energy of a state associated with a point in k space may be determined to a first approximation by perturbing free electrons with the lattice field   For free electrons the energy is

$$E_k^{(0)} = \frac{h^2}{2ma^2} |\mathbf{k}|^2 \tag{2}$$

Since the momentum of a free electron is hk/a, and since owing to spin there are two states per h^3 of phase space, it follows that the number of states per
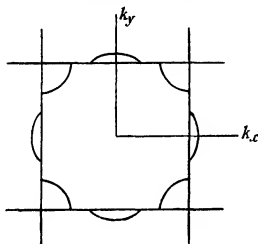
FIG 1

unit volume of k space is 2N/8 where N is the total number of atoms in the crystal and 8 the number per unit cell   Hence the density of states per atom in k space is 2/8

It is a well-known result of the theory that the effect of the lattice field is to introduce planes in k space across which the energy changes discontinuously †   For example, for a two dimensional cubic lattice the energy is discontinuous across the sides of a square as shown in fig 1   The curved line is a line of constant energy , such a line will represent the boundary between states which

† Brillouin, " Quantenstatistik,' chap 8

are occupied and states which are unoccupied. Such a boundary is sharply defined at low temperatures. In a three dimensional lattice it forms a surface in k space which for convenience is usually referred to as the surface of the Fermi distribution.

The equations to the planes across which the energy may change discontinuously are given by the conditions

$$E_{k+n}^{(0)} - E_k^{(0)} = 0, \tag{3}$$

where n stands for the three integers (n_1, n_2, n_3) each of which may be positive, negative, or zero. These planes, viz.,

$$n_1 k_x + n_2 k_y + n_3 k_z + \tfrac{1}{2}(n_1^2 + n_2^2 + n_3^2) = 0 \tag{4}$$

lie parallel in k space to the set of parallel planes in the crystal associated with the Miller indices (n_1, n_2, n_3).

If the potential of the lattice field be expressed in the form

$$V = \Sigma_n V_n e^{\frac{2\pi i}{a}(n, r)} \tag{5}$$

the discontinuity in the energy on crossing the plane (n_1, n_2, n_3) in k space is given to the first approximation by

$$\Delta E_n = 2\epsilon |V_n| \tag{6}$$

This approximation to the energy gap becomes more accurate as the energy of the state corresponding to the point $(\tfrac{1}{2}n_1, \tfrac{1}{2}n_2, \tfrac{1}{2}n_3)$ in k space increases, $i\,e$, as $\tfrac{1}{2}n$ increases, because the greater the energy the more nearly do the wavefunctions of the states approximate the plane waves.

2. *The Relative Magnitudes of the Fourier Coefficients of the Potential*

As any crystal with cubic symmetry can be built up of interpenetrating simple cubic lattices, the potential may be written

$$V = \sum_n \left\{ \sum_{\tau=1}^{s} A_{n\tau} e^{2\pi i (n, u_\tau)} \right\} e^{\frac{2\pi i}{a}(n, r)}, \tag{7}$$

where $A_{n\tau}$ are the coefficients of the potential for a simple cubic lattice composed of atoms of a type denoted by τ, and $a\,.\,u_\tau$ is the displacement of the atom τ from the origin of the unit cell.

If $\phi_\tau(r)$ be the potential due to a single atom of the type τ we have by definition of the $A_{n\tau}$

$$\sum_m \phi_\tau(r - ma) = \sum_n A_{n\tau} e^{\frac{2\pi i}{a}(n, r)}$$

Hence

$$A_{n\tau} = \frac{1}{a^3} \int \phi_\tau(r) \, e^{-\frac{2\pi i}{a}(n \cdot r)} \, dv \qquad (8)$$

This integral is just the well-known atomic scattering factor for electrons,[†] and if the charge distribution surrounding an atom be assumed spherically symmetrical, it may be put in the form

$$A_{n\tau} = \frac{e}{a\pi^2 n^2} (Z - f_n), \qquad (9)$$

where f_n is the atomic scattering factor for X-rays taken at the value of its argument $\frac{\sin \theta}{\lambda} = \frac{n}{2a}$ and Ze is the nuclear charge

If we write

$$\theta_\tau = 2\pi \, (n, \, u_\tau)$$

then, since the coefficients $A_{n\tau}$ are real, we obtain by comparing (5) and (7)

$$|V_n|^2 = (\sum_\tau A_{n\tau} \cos \theta_\tau)^2 + (\sum_\tau A_{n\tau} \sin \theta_\tau)^2 \qquad (10)$$

θ_τ is just the phase difference between the origin of the unit cell, and the atom τ when the crystal is reflecting X-rays from the planes $(n_1, \, n_2, \, n_3)$ in the first order

Thus if the crystal structure and the atomic scattering factor are known from X-ray data it is always possible to obtain ΔE_n, the discontinuity of the energy across any given plane in k space, to the accuracy given by the perturbation method   Although the absolute values of ΔE_n obtained in this way may not be very accurate, one may expect to obtain satisfactory values of the relative energy gaps for the different planes

In the special case when the atoms forming the crystal have nearly the same atomic number, so that the atomic scattering factors may be taken to be equal, a simple approximate formula may be given for the energy gap across a given plane —

$$\Delta E_{n_1 n_2 n_3} = \frac{2e^2}{\pi^2 n^2 a} (Z - f_n) \, S_{n_1 n_2 n_3}, \qquad (11)$$

where

$$`S_{n_1 n_2 n_3} = \{(\sum_\tau \cos \theta_\tau)^2 + (\sum_\tau \sin \theta_\tau)^2\}^{\frac{1}{2}}$$

is the structure amplitude, which largely determines the relative intensities of the X-rays reflected by the crystal planes $(n_1, \, n_2, \, n_3)$

[†] Mott and Massey, " Theory of Atomic Collisions," chap VII, Mott, 'Leipziger Vorträge,' p 63 (1930)

Even for those alloys for which there is a considerable difference between the atomic numbers of the constituent atoms, there will be a close similarity between the relative intensities of the X-rays reflected by the different sets of planes (n_1, n_2, n_3) and the energy gaps across the corresponding planes in k space   The reason for this is that it is known that the X-ray reflection spectra of the three alloys Cu-Zn, Ag-Zn, Au-Zn are very similar, and that the relative intensities reflected from the different planes are principally determined by the values of $(S_{n_1 n_2 n_3})^2$ Hence, since for given n the difference between the values of $(Z - f_n)$ for two different atoms is smaller than the difference between the values of f_n, it follows that the energy gaps will depend on $S_{n_1 n_2 n_3}$ to an extent at least as great as the extent to which the X-ray reflections depend upon $(S_{n_1 n_2 n_3})^2$ Therefore, as the X-ray reflections for the three alloys are very similar, it follows that the energy gaps across the same planes in k space for the different alloys will also be approximately equal

3 *Alloys with the γ-structure*

Bradley and Thewlis[†] have made a detailed examination of the structure of the alloys Cu-Zn, Ag-Zn, and Au-Zn in the γ-phase, based upon the X-ray measurements made by Westgren and Phragmen[‡]   These measurements show that of the crystal planes with small indices only the set {411} and the set {330} give rise to strong X-ray reflections   We deduce, therefore, that the first planes in k space, outwards from the origin, across which the energy shows an appreciable discontinuity are those lying parallel to the sets {411} and {330}, and whose perpendicular distance from the origin is, in each case accord ing to equation (4), $3/2\sqrt{2}$ A perspective drawing of the zone marked out in k space by these planes is given in fig 2   The polyhedron has 36 faces and is very symmetrical   The ratio of its volume to that of the inscribed sphere is $5\sqrt{2}/2\pi$, $i\,e\,,1\,12$ The volume is equal to 45, and since there are 2/8 states per atom, the zone must contain 90 states per unit cell, and the inscribed sphere very nearly 80

For the alloy Cu-Zn Westgren and Phragmen (*loc cit*) give for the value of the lattice constant $a = 8\,86$ A , therefore with $n = \sqrt{(18)}$ one finds $n/2a =$ $0\,239\,10^8$, the value of the atomic scattering factor f for Cu at $(\sin\theta)/\lambda =$ $0\,239\,10^8$ may be interpolated from the data given by James and Brindley[§] and is found to be $19\,9$ Bradley and Thewlis (*loc cit*) give for the square

† ' Proc Roy Soc ,' A, vol 112, p 678 (1926)

‡ ' Phil Mag ,' vol 50, p 331 (1925)

§ ' Phil Mag ,' vol 12, p 81 (1931)

of the structure amplitude $S^2_{411} = 31\ 7$ and $S^2_{330} = 78\ 3$ Thus using equation
(11) we obtain the approximate values of the energy gaps across the planes
(411) and (330) in k space

$$\Delta E_{411} = 0 \cdot 93 \text{ electron volts}$$

$$\Delta E_{330} = 1\ 46 \text{ electron volts}$$
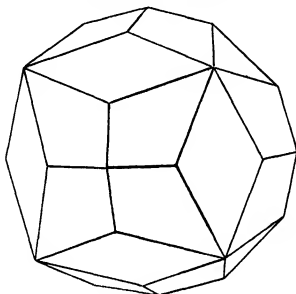
Fig 2

These values are probably an over-estimate due to the approximations involved
in the perturbation calculation which gives (6)

Within the γ-phase the formulæ for the alloys Cu-Zn, Ag-Zn, Au-Zn are
Cu_5Zn_8, Ag_5Zn_8, Au_5Zn_8, and there are 52 atoms per unit cell   If the number
of loosely bound electrons contributed by each atom is given by the valency,
i e., Cu 1, Zn 2, Al 3, Sn 4, and so on, then throughout the whole set of alloys
with the γ-structure there are as Hume-Rothery points out just 21 loosely
bound electrons to every 13 atoms at a composition in the neighbourhood of
the centre of the phase   Thus there are 84 electrons per unit cell , we have
seen that the zone is nearly spherical, contains 90 possible states, and that the
inscribed sphere contains 80 , hence the surface of the Fermi distribution
must lie at all points very close to the surface of discontinuity in the energy.
This is the distinguishing feature of alloys with the γ-structure

If the energy of the states associated with the points lying along a line in k
space through the origin, and perpendicular to a plane of discontinuity, is

plotted against the distance from the origin, a curve of the form shown in fig 3 is obtained   The dotted line represents the energy of free electrons   Although from the present standpoint it is impossible to say anything about the actual value of the binding energy of the metal, it can be seen from fig 3 that the effects of the energy gaps, considered by themselves, will be to give an additional contribution to the negative energy, when the surface of the Fermi distribution lies just within or just touching the boundary of a zone in k space   Thus with the structure characteristic of the γ-phase we may expect the composition of the centre of the phase to correspond with somewhat less than 90 loosely
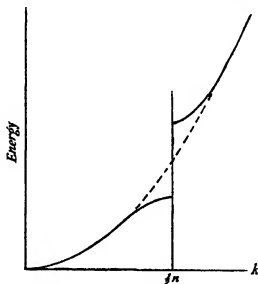
Fig 3

bound electrons per unit cell of 52 atoms   For, on account of the smallness of the energy gaps, 90 electrons per unit cell would cause an overlapping into the second zone, and the energy minimum must occur just before this happens   The Hume-Rothery rule gives 84 electrons

4 Diamagnetism

Let κ be the distance in k space measured normal to a plane across which the energy is discontinuous   For the discussion of the diamagnetism we require the value of $\partial^2 E/\partial \kappa^2$, see, for example, equation (12)   It is easy to find the values of $\partial^2 E/\partial \kappa^2$ at the origin, and by an elementary perturbation calculation, at either side of a plane of discontinuity   At the origin the value is simply

h^2/ma^2, which if the electrons were entirely free would be the value at all points in k space. The first approximation to the energies of states associated with points which lie close, on either side, to a plane of discontinuity, $i\,e$, for which k is nearly equal to $\frac{1}{2}n$, are given by the roots of the equation

$$\begin{vmatrix} \frac{h^2}{2ma^2}\,|\,n-k\,|^2 + V_0 - E, & V_n \\[2mm] V^*{}_n \quad , & \frac{h^2}{2ma^2}\,|\,k\,|^2 + V_0 - E \end{vmatrix} = 0$$

Hence by use of (6) we obtain

$$\left(\frac{\partial^2 E}{\partial k^2}\right)_{k=0} = \frac{h^2}{ma^2}\left(1 - \frac{4E_{\frac{1}{2}n}{}^{(0)}}{\Delta E_n}\right)$$

$$\left(\frac{\partial^2 E}{\partial k^2}\right)_{k=0} = \frac{h^2}{ma^2}\left(1 + \frac{4E_{\frac{1}{2}n}{}^{(0)}}{\Delta E_n}\right),$$

where $E_{\frac{1}{2}n}{}^{(0)}$ is the energy of a free electron at the point $\frac{1}{2}n$, and ΔE_n is the jump in the energy across the plane. Thus with the estimated values of ΔE_n given for the alloy Cu_5Zn_8 the magnitude of $\partial^2 E/\partial k^2$ in the immediate neighbourhood of the planes {411} will be 37 times its value for free electrons, and in the neighbourhood of the planes {330} 24 times. This may easily be seen by reference to fig 3

Recently Peierls[†] has examined the diamagnetic susceptibilities of electrons in metals. He finds three terms which contribute to the susceptibility. For the most important of these terms he gives a formula which for metals at low temperatures may be written

$$\chi = -\frac{2m^3\mu^2}{3\hbar a}\iint\left(\frac{\partial E}{\partial n}\right)^{-1}\left\{\frac{\partial^2 E}{\partial k_x{}^2}\,\frac{\partial^2 E}{\partial k_y{}^2} - \left(\frac{\partial^2 E}{\partial k_x\,\partial k_y}\right)^2\right\}\,dS, \qquad (12)$$

where the integration is over the surface of the Fermi distribution. m is the mass of the electron, and μ its magnetic moment. $\partial E/\partial n$ is the rate of change of E along the normal to the surface over which the integration is taken. This formula was obtained for a special case corresponding to the Bloch limiting case of tight binding. Since, however, the formula reduces for free electrons just to Landau's[‡] formula it appears justifiable to use it in intermediate cases.

In general the magnitude of $\dfrac{\partial^2 E}{\partial k_x{}^2}\,\dfrac{\partial^2 E}{\partial k_y{}^2}$ will be much greater than the magni-

† 'Z Physik,' vol. 80, p 763 (1933)
‡ 'Z. Physik,' vol 64, p. 629 (1930)

tude of $\left(\dfrac{\partial^2 E}{\partial k_x \, \partial k_y}\right)^2$ at all points on the surface over which the integration is taken Hence, when the surface of the Fermi distribution lies close to a surface of energy discontinuity χ may be expected to have a value many times greater than the value given by free electrons.

The experiments of Endo (*loc cit*) show that the alloys Cu-Zn and Cu-Sn have a remarkable maximum in the diamagnetic susceptibility for compositions which lie within the γ-phase Fig 4 is a reproduction of Endo's
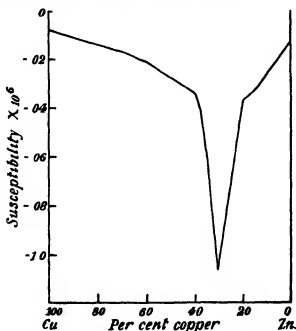
FIG 4

curve showing the diamagnetic susceptibility as a function of the composition of the alloy Cu-Zn

Hall Effect

The following theoretical formula for the Hall coefficient has been obtained†

$$R = \frac{a^3}{2e} \frac{\displaystyle\iint \left(\frac{\partial E}{\partial n}\right)^{-1} \left\{\left(\frac{\partial E}{\partial k_x}\right)^2 \frac{\partial^2 E}{\partial k_y^2} - \frac{\partial E}{\partial k_x} \frac{\partial E}{\partial k_y} \frac{\partial^2 E}{\partial k_x \, \partial k_y}\right\} dS}{\left[\displaystyle\iint \left(\frac{\partial E}{\partial n}\right)^{-1} \left(\frac{\partial E}{\partial k_y}\right)^{-1} dS\right]^2},$$

† Jones and Zener (*in course of publication*)

where in this case the integration is taken over that part of the surface of the Fermi distribution where it is not in contact with a surface of discontinuity

It can be seen that if the surface of the Fermi distribution lies in the main just within the boundary of the zone the Hall coefficient will be large and positive, i.e., of the same sign as for zinc, whilst if it lies just outside the boundary it will be large and negative

By slightly varying the composition of an alloy the number of loosely bound electrons may be varied slightly without changing the structure of the phase For the γ-structures a small change in the number of loosely bound electrons would change the surface of the Fermi distribution from lying just within to just outside the boundary of the zone (cf fig 1) For these alloys therefore it may be expected that the Hall coefficient will change for small variations in the composition from large positive to large negative values as the composition varies in the direction of increasing number of loosely bound electrons The experimental curves given by Evans and Richards (loc cit) do appear to behave in this way

It is a pleasure to express my thanks to Dr C Zener and Professor N F Mott for discussions on various points

Summary

The zones of allowed energies for the loosely bound electrons in alloys with the γ-structure are examined It is shown that the lowest group of energy levels is almost completely filled by the number of loosely bound electrons given by the Hume-Rothery rule, and a reason for the existence of this rule is discussed In addition it is shown that large diamagnetic susceptibilities may be expected for alloys in this phase, and that the Hall coefficient should change from large positive to large negative values as the composition varies through the phase in the direction of increasing number of loosely bound electrons

Some Experiments on the Production of Positive Electrons

By J. Chadwick, F R S, P M S Blackett, F R S, and G P S Occhialini

[Plates 2–5]

§ 1 Introduction

This paper describes work carried out during the last year on the production of positive electrons, or positrons * by various radiations. Although it is probable that the positrons found in conjunction with cosmic rays have their origin in the interactions of some penetrating radiation with matter, these experiments gave no direct information about their mode of origin. In order to throw light on this and to have a method of studying their properties more closely it was necessary to seek a means of producing positrons under easily controlled conditions.

Our first experiments directed to this end were those which showed that the radiation from beryllium bombarded by polonium α-particles, a radiation consisting of γ-rays and neutrons, could eject positrons from lead. A preliminary notice of these results was given by us in a letter to 'Nature '† Almost at the same time Meitner and Philipp‡ and Curie and Joliot§ reported the same effect.

We next proceeded to see whether positrons were produced by the high energy γ-rays emitted by thorium C", and our first results were reported by Chadwick in the Bakerian lecture‖ last year. By this time Curie and Joliot had shown that the positrons produced by the beryllium polonium radiation were mainly due to the γ-rays, rather than the neutrons, and first Anderson ¶ then Curie and Joliot** and Meitner and Philipp†† reported the production of positrons by the γ-rays of thorium C". It was pointed out by Blackett and

---

* The name ' positron ' for a particle of about electronic mass and positive charge was suggested by Anderson, and it seems to be coming into general use. The negative electron will still be called, as usual, an electron

† Chadwick, Blackett, and Occhialini, 'Nature,' vol 131, p 473 (1933)

‡ 'Naturwiss,' vol 21, p 286 (1933)

§ 'C R Acad Sci Paris,' vol 196, p 1105 (1933)

‖ 'Proc Roy Soc,' A, vol 142, p 1 (1933)

¶ 'Science,' vol 77, p 432 (1933)

** 'C R Acad Sci Paris,' vol 196, p 1581 (1933)

†† 'Naturwiss,' vol 24, p 468 (1933)

Occhialini* that the Dirac theory of the electron led to the view that a pair of electrons of equal mass and opposite sign may be produced when γ-rays of high energy are absorbed in matter   If m is the mass of either electron then the combined kinetic energies of the particles will be

$$E_2 = h\nu - 2mc^2 \tag{1}$$

and this will also be the maximum kinetic energy which the positron can acquire †   Since the mass of the electron is equivalent to an energy of 511,000 electron volts the total kinetic energy of the pair (or the maximum energy of the positron) produced in this way by the thorium C'' γ-ray of $h\nu = 2\ 62 \times 10^6$ e volts will be $1\ 60 \times 10^6$ e volts   Anderson and Neddermeyer‡ have, in fact, measured the energies of the two particles for several pairs and they have found that their total kinetic energy does not appreciably exceed this value , and Curie and Joliot and Meitner and Philipp have measured single positrons with energies up to about this value   The preliminary results of our own measurements, quoted in the Bakerian lecture, also led to the same conclusion A survey of these results has recently been given by Blackett §

It is clearly of the greatest importance to establish the above relation thoroughly, for upon it largely depends the experimental evidence that the positron is created, simultaneously with an electron, by some interaction of a γ-ray with matter, and, moreover a value for the mass of the positron can be deduced from it   The experiments were therefore continued until about 4000 tracks of electrons and about 400 tracks of positrons had been obtained, giving a body of evidence sufficient to justify quantitative conclusions

§ 2 Experiments with the γ-rays of Thorium Active Deposit

The expansion chamber used in these experiments was the one made by Blackett and Occhialini for the study of cosmic rays   The chamber had an internal diameter of 13 cm and the piston travelled horizontally   The chamber was filled with oxygen, to a pressure of about 1 7 atmospheres   The chamber was placed between two coils which served to establish a magnetic field with its lines parallel to the axis of the piston   The strength of the field was in most experiments about 800 gauss , in others, 400 and 600 gauss   The tracks

---

were photographed by means of two cameras, one with its axis along the axis of the piston, the other at an angle of 20° to this

In the first series of experiments, the source of thorium active deposit, of about 1/50 mg γ-ray activity, was placed outside the chamber in a lead cylinder The γ-radiations, filtered through 1 cm of lead, passed through the glass walls of the chamber and fell on a target of lead, 2 cm square and 1 mm thick, attached to the inside wall

In order to avoid any possibility that a negative electron moving towards the lead target should be counted as a positron, a thin metal plate, of aluminium or of copper, was placed across the middle of the chamber so as to intercept the path of the particles, following the arrangement used originally by Anderson The particle must lose energy in passing through the plate and its track must therefore show a greater curvature on the emergent side than on the incident side The direction of motion, and therefore the sign of the charge of the particle, can then be definitely known In this series some 1200 tracks were obtained about 50 of which could with certainty be ascribed to particles carrying a positive charge The ionizing power of these particles and the loss of energy in passing through the plate were both consistent with the view that the particles had a mass about the same as that of the negative electron Occasionally positive electrons were observed from the glass walls of the chamber, and also from the plate of copper across the chamber

In a second series of experiments the source of thorium active deposit was placed inside the chamber The deposit was obtained on a wire about 5 mm long and this was surrounded by a closed cylinder of lead of 3 mm wall The lead cylinder was fixed to the top plate of the expansion chamber With this arrangement, the source occupied a very small volume and the chance that a negative electron produced in a remote part of the chamber should be bent so as to hit the lead cylinder was very small It seemed no longer necessary to place a metal plate across the chamber in order to identify the sign of the charge in the particle, and the plate was therefore omitted, as its presence interfered with the accurate measurement of the curvature of the tracks

About 700 pairs of photographs were taken in this series of experiments giving more than 4000 tracks of negative and positive electrons

The curvature of the tracks was measured by superimposing over the image of a track a transparent scale with circles of different radii marked on it. This method is not a very accurate one, but it does serve to avoid errors due to any departure of the track from a true circle such as might be caused by small nuclear deflections Experience has shown that such deflections are difficult

to recognize and may cause serious errors   This method enabled the energy of a particle to be determined with a probable error of about 4%   A further source of error was present because no attempt was made to correct for the actual position of the track in the chamber   On this account the true magnification of the different tracks varied as much as 3% from the mean   Nor, when calculating the energy of the particle from the track curvature, was any correction made for the fact that a track might not lie exactly in the plane normal to the magnetic field   This error was, however, small since only those tracks were selected for measurement the planes of which, as revealed by comparison of the two stereoscopic photographs were within a small angle to the plane normal to the field   Clearly it would have been desirable to improve the accuracy of the measurements by taking all these sources of error into account, but we considered that the great labour was not justified for a preliminary survey of the phenomena, and we preferred to select from the photographs those tracks which were most suitable for measurement

The results of the measurements of the curvatures of the tracks are shown in fig 1   Curve 1 gives the data for all the positrons with energies greater than 0.5×10^6 volts which were suitable for accurate measurement, and curve 2 for the electrons with energies above 1×10^6 volts, selected from about one-tenth of all the photographs   In each curve the number of tracks within an energy range of 200,000 volts is plotted against the mean of the energy range   It must be pointed out that these curves do not represent the energy distributions of the electrons as they are ejected by the γ-radiation, for the thickness of the lead absorber in which the electrons arise is greater than the maximum range of the fastest particles   Thus electrons of all energies from zero to the maximum must be present, whatever the original distribution may be   No detailed interpretation of the curves of energy distribution is possible owing to the complexity of the experimental conditions

The γ-radiation emitted by thorium active deposit consists of (1) the soft radiation of thorium B, with energies up to 300,000 volts , (2) the radiation from thorium (C + C'), mostly of energies below about 700,000 volts but with two weak lines of 1 6 and 1 8 million volts , (3) those of thorium C'', some of low energy up to 600,000 volts and the strong line of 2 62 million volts   If we restrict our examination of the electrons to those of high energy then only the γ-rays of 1 6 and 1 8 million volts, associated with the thorium C C' transformation, and that of 2 62 million volts, arising from the Th C'' Pb transformation, are concerned   The first two rays are of weak intensity and, although twice as many atoms transform from Th C to C' as from Th C'' to Pb,

about 70% of the quanta of high energy must be contributed by the line of 2 62 million volts   The end portions of the curves of fig 1 must then be due mainly to the action of this γ-ray   It seems reasonable for a first approximation to assume that the maximum energy of the particles is given by the intercept on the energy axis of the steep portion of the curve, as drawn in fig 1
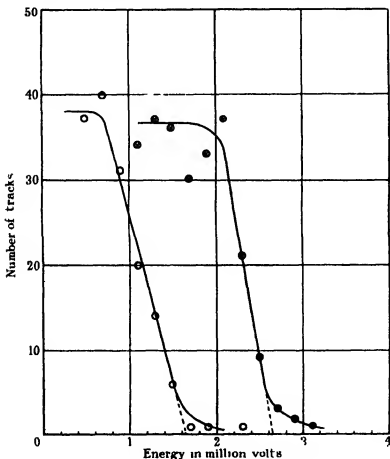
FIG 1 — O Positrons , ⊗ electrons

The end point as thus defined will be too high by a quantity somewhat greater than the mean error of measurement *

* The effect of the errors of measurement in the track curvatures is to increase the slope of the end part of the curves of fig 1   Suppose, for example, that the energy distribution is uniform up to a maximum energy E_0 (see fig. 2)   If each energy determination is subject

The measured end points for the positron and for the electron curves are $1\ 63 \times 10^6$ volts and $2\ 62 \times 10^6$ volts respectively, with estimated probable errors of about $1\frac{1}{2}\%$ The calculation given in the note shows that these values should be about 5% high   We thus get for the corrected values of the maximum energies of the positron and electron the values

$$E_2 = (1\ 55 \pm 0\ 03) \times 10^6 \text{ volts}$$

$$E_1 = (2\ 49 \pm 0\ 04) \times 10^6 \text{ volts}$$
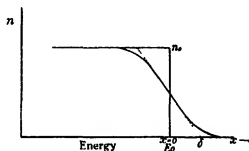
Fig 2

The value found for E_2 is sufficiently close to the value of $1\ 60 \times 10^6$ volts given by equation (1) above to provide very strong support to the hypothesis that a γ-ray produces a negative electron at the same time as a positive electron and that the two have equal masses

It is conceivable, however, that in contradiction to Dirac's theory the mass m_2 of the positron is not exactly equal to the mass of the electron   If we rewrite (1) in the form

$$m_2 c^2 = h\nu - E_2 - m_1 c^2, \tag{2}$$

to an error, the probability of which is given by the Gaussian error law, then the true distribution curve ($n = n_0$ for $x < 0$ and $n = 0$ for $x > 0$) is transformed into the curve

$$n(x) = \frac{n_0 h}{\sqrt{\pi}} \int_{y=-\infty}^{y=0} e^{-h^2(y-x)^2}\, dy$$

Since $n(x) = \frac{1}{2}n_0$, when $x = 0$, the value of the energy at which the number of particles passes through half value gives the true end point E_0 The tangent to the distribution curve at this midpoint cuts the x axis at a value δ given by $\delta = \sqrt{\frac{\pi}{2}}$ $\mu = 1\ 25\,\mu$, where μ is the R.M S error of the observations   For this special case the quantity δ must be subtracted from the observed end point to give the true value of E_0.   Since the R.M S error of the energy determination was estimated at about 4%, the end point should be about 5% too high

Fig. 3

Fig. 4

Fig. 5

Fig. 6

Fig. 7

Fig 8　　　　　　　　　　　　　Fig 9

and introduce the observed value of E_2 and the known value of $h\nu$ we obtain

$$m_2 = (1\ 10 \pm 0\ 06)\ m_1$$

A preferable procedure, which reduces the error introduced by any small consistent error in the absolute values of the measured energies, is to use the observed value of E_1 rather than the value of $h\nu$. The majority of the observed electrons are recoil electrons, which have a maximum energy of $2\ 39 \times 10^6$ volts. The photo-electrons are probably about 10% of the recoil electrons and mostly come from the K shell, the contributions of the L and other shells being quite small. It is very probable therefore that the end point of the electron curve as we have defined it will correspond to the maximum energy of the photo electrons from the K shell, that is,

$$E_1 = h\nu - \omega_e, \tag{3}$$

where ω_e is the binding energy of the K shell.

From (2) and (3) we get

$$m_2c^2 = E_1 - E_2 + \omega_e - m_1c^2$$

Since $\omega_e = 0\ 09 \times 10^6$ volts, we obtain

$$m_2 = (1\ 02 \pm 0\ 10)\ m_1$$

This calculation gives probably the most accurate determination of the mass of the positron which is yet available.

It will be noticed that both curves of fig 1 show a tail, particularly marked for the electron curve. Such a tail is due in part to errors of measurement, possibly caused by unrecognized deflections in the tracks but it may also be partly due to the presence of a small amount of γ-radiation of energy greater than $2\ 62 \times 10^6$ volts.* The presence of a few cosmic ray tracks passing through the source may perhaps contribute to these tails, the vertical type of cloud chamber, such as we used, is sensitive to cosmic radiation.

§ 3 *Yield of Positive Electrons*

In the first series of experiments the number of positive electrons obtained in 360 pairs of photographs was 50, compared with 1200 negative electrons. In the counting of the positive electrons an over strict criterion was adopted

---

* Dr Ellis informs us that the nuclear level system proposed by Mott and himself for the thorium C'' γ-rays suggests a radiation of $h\nu = 3\ 2 \times 10^6$ e. volts.

The yield of positive electrons, about 4% of the negatives, obtained from this series is certainly much too low

In the second series, in which the source of γ-rays was inside the expansion chamber, all tracks which started from the lead cylinder and which showed a positive curvature were counted as positrons   A corresponding criterion was taken for the negative electrons   Two counts were made, in the first all particles of energy greater than about 200,000 volts were counted, and in the second only those of energy greater than 400,000 volts   The first gave 323 tracks of positrons and 3563 tracks of negative electrons   The ratio of positive to negative electrons is thus about 9%, and may be slightly greater, for some positive tracks which could not be traced to their origin in both photographs of the stereoscopic pair were rejected as doubtful   The second count gave a similar proportion

The actual production of positrons in the lead absorber must be greater than this observed ratio, owing to the fact that the energy of the positives is less than that of the negatives and a greater fraction will be unable to escape from the absorber   A rough estimate of the correction to be applied for this absorption can be made in the following way

Consider the production of secondary electrons in a thick layer of matter by a homogeneous γ-ray, and assume that all the secondary electrons are emitted directly forwards with the same energy E_0 Then the number which emerge from the absorber with energies greater than E_1 will be proportional to $\alpha\,(R_0 - R_1)$, where αdx is the chance of production of a secondary electron in a layer of thickness dx and R_0 and R_1 are the ranges in the absorbing material of electrons of energy E_0 and E_1 Thus in this case the ratio of the observed number N' of positrons to the number N of electrons both with energies greater than E_1, will be

$$\frac{N'}{N} = \frac{\alpha'}{\alpha}\,\frac{R'_0 - R'_1}{R_0 - R_1},$$

where α', R'_0, R'_1 refer to the positrons   It is here assumed that positive electrons have the same range as negative electrons of the same energy   From the known data on the ranges of β-particles we find the following data -

$$E_0 = 2\cdot39 \times 10^6 \text{ volts}^* \qquad R_0 = 1\ 12 \text{ gm /sq cm}$$
$$E'_0 = 1\cdot60 \times 10^6 \text{ volts} \qquad R'_0 = 0\ 67 \text{ gm /sq cm}$$
$$E_1 = 0\cdot2 \times 10^6 \text{ volts} \qquad R_1 = 0\ 04 \text{ gm/sq cm.}$$

* One must take here the value for the recoil electrons since these are in great majority

Taking the observations in which all particles with energies greater than 200,000 volts were counted, N'/N was 9%, whence $\alpha'/\alpha = 15\%$. This calculation is very rough for several factors have been neglected. For example, no account has been taken of the angular distribution of the particles. It is possible that the positrons are emitted mainly within small angles of the direction of the γ-ray, and the above correction for escape will then be over-estimated. It seems likely that the probability of production of a positron in the lead absorber is from 12 to 15% of the probability of the production of a recoil electron.

Now the γ-radiation passing through the lead consists, as we have already described, mostly of γ-rays of low energy with three γ-rays of energy 1·6 1·8, and 2·62 million volts. If the Dirac theory of the production of positive electrons is correct then the positive electrons can be due only to γ-rays of energy greater than $1·02 \times 10^6$ e volts. Further, it seems probable, both from theory and from such experimental information as is available, that the probability of production increases rapidly with the energy of the γ-ray. Thus the positrons observed in our experiments must be due almost entirely to the γ-ray of 2·62 million volts, while the other radiations present take part in the production of the recoil electrons. It is only possible to make a very rough estimate of the proportion of the negative electrons which are produced by the γ-ray of 2·62 million volts; it seems likely that this fraction is between 0·5 and 0·7, under the conditions of our experiments. We thus arrive at the conclusion that the probability of the production of a positron by the γ-ray of 2·62 million volts in lead may be as high as 20 to 30% of the probability of the production of an electron by the normal processes of scattering and photoelectric absorption.

§ 4 *Experiments with a β-ray Source*

In some experiments a thin aluminium wire coated with thorium active deposit was enclosed in a glass tube, about 0·1 mm thick, and placed in the centre of the expansion chamber. With this arrangement the majority of the β-rays emitted by the active deposit could escape through the glass tube. The source was of much weaker activity than in the previous experiments, about 15 electron tracks being observed on the average in each expansion. A few tracks of positrons were also observed; in all 24 tracks among 2000 tracks due to electrons. The energy of the positrons was never greater than $1·4 \times 10^6$ volts. A rough calculation based on the results of the previous sections shows that it is unlikely that these positrons could be due to the action of

γ-rays in the metal of the wire or in the glass walls of the tube   Moreover, in some experiments the active deposit was obtained on a platinum wire instead of aluminium   If the positrons were produced in the wire, a much greater proportion should have been found in this case, but the proportion remained sensibly the same   Some photographs were taken in which a thin platinum cylinder was placed round the source tube to test whether the β-particles could produce positrons in passing through the platinum   No increase in the proportion of positives could be noticed   It seems probable therefore that these positive electrons have their origin in the radioactive atoms themselves, possibly by an internal conversion of a γ-ray or perhaps by an interaction of a β-particle in its escape through the nuclear field

It may be pointed out that these results indicate that a bare source of thorium active deposit provides the most powerful source of positive electrons which is yet known   This is indeed evident from the experiments of Thibaud[*] who has succeeded in obtaining from a radiothorium source a pencil of positive electrons sufficiently intense to give a good trace on a photographic plate, and to offer the possibility of measuring the ratio e/m of the charge to the mass

§ 5   Experiments with the Radiations Excited in Beryllium, Boron, and Fluorine

The arrangement of the source and target in these experiments was similar to that in the first series with the thorium γ rays   A capsule containing a polonium source and a piece of beryllium was placed outside the expansion chamber close to the wall, and on the inside wall was fixed a target of lead, 2·5 cm square and 2 mm thick   The lead target was thus exposed to the γ-rays and neutrons liberated from the beryllium under the bombardment of the α-particles from the polonium, and also to the γ-rays emitted by the polonium itself   Since the γ rays of polonium have a maximum energy of only 1 million volts, no confusion can arise if observations are restricted to electrons of energy greater than this amount   This fact was confirmed in control experiments in which the polonium alone was used as a source, and in these experiments no positive electrons were observed [†]   In most photographs a metal plate was placed across the middle of the expansion to intercept the paths of the positive electrons and to show unambiguously their direction of motion   In all the photographs with a lead target 203 negative electrons were

obtained and 66 positive electrons, a proportion of the latter of about 32%. In some experiments the lead target was removed so that the electrons observed came from the glass wall of the chamber. In this case the proportion of positrons was much less, being only of the order of 4%.

The measurements of the curvature of the tracks showed that the end point of the positron curve was at about 4×10^6 volts, and the end point of the electron curve at about 5×10^6 volts. These results are similar to those already published by Curie and Joliot.[*] They are consistent with the view that the positrons are produced by a γ-ray of about 5×10^6 e volts.[†] Some electron tracks, 10 in all, were observed which had energies greater than 6×10^6 volts but their curvatures were too small for accurate measurement. The evidence is too meagre to decide whether these tracks are due to a γ-radiation of high energy emitted from the beryllium or whether they are cosmic rays passing accidentally through the lead target.

Two sets of observations were made in which the beryllium in the source capsule was replaced first by boron then by calcium fluoride. With boron 11 positrons and 27 electrons were observed in 122 photographs; a proportion of about 40%. The radiation from boron bombarded by polonium α-particles consists partly of neutrons and partly of γ-radiation, the maximum energy of which appears to be about 3×10^6 volts.[‡] The energy of the radiation is thus not very different from that of the strong line of the thorium radiation, and we should expect the efficiency of production of positrons in the two cases to be about the same. It seems very probable, therefore, that some of the positive electrons observed from boron must be attributed to the action of neutrons. This conclusion is supported by the observations made with fluorine, in which 12 positrons and 31 electrons were found in 139 photographs. As far as is known no γ-radiation is emitted from fluorine bombarded by polonium α-particles with energy greater than about 1 million electron volts. It appears then that the positrons observed in this case must also be attributed to the action of neutrons. It is probable that the production of positrons by neutrons is an indirect effect. It is known that the passage of neutrons through lead is accompanied by the emission of γ-radiation, due perhaps to an excitation or a disintegration of the lead nucleus in a neutron collision. This γ-radiation, if of sufficient energy, will in its absorption in the lead produce positive electrons, possibly also by a type of internal conversion in the escape from the excited nucleus.

* 'J. Phys. Rad.,' vol. 8, p 494 (1933)

† *Cf* Becker and Bothe, 'Z. Physik' vol 76, p 421 (1932)

‡ *Cf* Becker and Bothe, *loc cit*

§ 6   Conclusions

It has been shown that when γ-rays of high energy are absorbed in matter positive electrons as well as negative electrons are ejected.   The observations of the energies of the positrons ejected by the γ-rays of thorium C'' are consistent with the view that an electron is always produced at the same time as a positron   This is confirmed to some degree by the observation that occasionally pairs of tracks occur, one positively curved in the magnetic field, the other negatively, which are almost certainly due to the simultaneous production of a pair of electrons of opposite sign (see figs 5, 6, Plate 3)   This event was, however, seldom observed   Presumably, under the conditions of our experiments in which the particles originated in a thick lead absorber, one or other of a pair was generally absorbed or scattered before emerging from the target   On the hypothesis that an electron is always produced at the same time as a positron the measurements lead to the result that the mass of the positron is the same as that of the electron

It has been tacitly assumed that the pair of particles is produced in the atom rather than inside the nucleus   This view is supported by a consideration of the frequency of production of the positrons   In the case of beryllium radiation passing through lead, one pair is produced for rather less than two electrons produced by the normal scattering process   Assuming for this radiation the value of the scattering coefficient given by the Klein-Nishina formula for $h\nu = 5 \times 10^6$ e volts, we find that the effective cross section for the production of a positron is rather more than 3×10^{-24} cm^2 This is distinctly larger than the area of cross-section of the lead nucleus

Again, the results of § 3 gave a ratio of about 25% for the absorption of the thorium C'' γ-rays by the production of positrons to the absorption by normal processes   From the total absorption coefficient of this radiation in lead, $0 \cdot 46$ cm^{-1}, we obtain for the area of cross-section of the lead atom for the production of a positron the value $2 \cdot 8 \times 10^{-26}$ cm^2 Recently Heitler and Sauter[*] have calculated the cross section for the production of positrons from Dirac's theory   They find a value of $2 \cdot 6 \times 10^{-26}$ cm^2 for the case considered here   The good agreement, though to some extent fortuitous on account of the corrections applied to the experimental results, gives strong support to the validity of the theoretical calculations, particularly to the assumption that the positrons produced by the interaction of γ-rays with matter have their origin (mainly at least) in the field around the nucleus rather than inside it

* ' Nature,' vol 132, p 892 (1933)

It may be that positrons produced by other agencies may arise from the nucleus itself, Curie and Joliot have found that positrons are produced when aluminium and boron are bombarded by α-particles, and they suggest that these are ejected from the disintegrating nucleus

A necessary consequence of the production of the positron is its subsequent disappearance, for general experience shows that the positron has no permanent existence. If a quantum can interact with an atom to produce a pair of electrons of opposite sign, then the reverse process, in which a positron and an electron combine under the influence of an atom to produce radiation must also be possible. The positron cannot exist for more than a very short time in matter of ordinary density. We might then expect to observe the annihilation of a positron by the sudden disappearance of its track in the cloud chamber. This event has unfortunately not yet been observed with certainty. A few photographs have been obtained in which it appears that the positron has disappeared when still possessing a large amount of energy but it is not possible to be quite certain that the track has not merely passed out of the field of view or out of the illumination. Examples of this disappearance are shown in fig 6, Plate 3, and fig 10, Plate 5

It was suggested by Blackett and Occhialini that the creation of positrons might account for the ' anomalous " absorption of high energy γ-rays, and that the radiations arising from the annihilation of the positrons might correspond to the secondary radiations which accompany the anomalous absorption. This question has been discussed at some length in a recent paper by Gray and Tarrant * They come to the conclusion that the creation and disappearance of positrons cannot account for all their experimental results, more particularly for those on the secondary radiations. Here we wish only to point out that the results of § 3 show that the extra absorption due to the production of positrons by the γ-ray of thorium C" is just sufficient to account for the anomalous absorption. It may be that we have over-estimated the corrections to be applied to the observations and that the creation of positrons is not so frequent as we have suggested, but at least a large part of the anomalous absorption, if not all, must be attributed to this process.

* ' Proc Roy Soc ,' A, vol 143, p. 706 (1934).

Summary

The emission of positive electrons has been observed under different experimental conditions   (1) from a lead target exposed to the γ-rays of thorium active deposit , (2) directly from a source of thorium active deposit , and (3) from a lead target exposed to the radiations (γ-rays and neutrons) emitted by beryllium, boron, and fluorine when bombarded by polonium α-particles   The measurements of the energies of the positrons ejected from lead by the thorium γ-rays support the view that a positron and an electron are produced simultaneously by the interaction of a γ-ray and an atom, and that the mass of the positron is the same as that of the electron   The positron and electron are probably created in the electric field outside, rather than inside, the nucleus   The observations show that when γ-rays of high frequency pass through lead an appreciable fraction (about one-fifth for a γ-ray of $h\nu = 2\ 6 \times 10^6$ volts) of the energy absorbed is used in this process of creating a positron and an electron

DESCRIPTION OF PLATES.

The magnification is approximately the same in all photographs, and about 0 8

PLATE 2

FIGS 3 and 4 – The source was thorium active deposit inside a lead cylinder of 3 mm wall   Magnetic field 740 gauss   Negative particles travelling to the right are bent downwards   On both photographs tracks of positrons, ejected from the lead by γ-rays, can be seen   The α track in fig 4 is due to contamination

PLATE 3

FIG 5 —Source of radiation, calcium fluoride bombarded by polonium α particles, outside the chamber   The photograph shows a pair of tracks from the lead target , the upper track is due to an electron, the lower to a positron   Both particles have energies of about half a million volts

FIG 6 —Source of radiation, beryllium + polonium   The positron of this pair has an energy of 2 8 × 10⁶ volts   The track does not pass through the aluminium plate (0 90 mm thick)   The positron may have been annihilated while still possessing great energy, or it may merely have been deflected in such a way that it did not emerge from the plate

FIG 7 —Source was thorium active deposit in a thin glass tube, so that the β-rays could emerge   Two sharp β-ray tracks are seen, and one positron track travelling downwards

PLATE 4

In all four photographs, figs 8–11, the source of radiation was beryllium + polonium.

FIG 8 — An electron of energy 3 9 × 10⁶ volts passes through the aluminium plate, 0 33 mm thick.

Fig 9 —A positron passes through an aluminium plate, 0 33 mm thick, its energy on the upper side is $1\ 02 \times 10^6$ volts, on the lower side $0\ 7 \times 10^6$ volts

PLATE 5

Fig 10 —A positron track ends suddenly in the gas The positron has probably been destroyed, but it is possible that it has merely passed out of the illumination

Fig 11 —A positron passes through a copper plate, 0 25 mm thick, its energy on the upper side is $3\ 2 \times 10^6$ volts, on the lower side $2\ 6 \times 10^6$ volts

The Influence of Pressure upon the Flame Spectra of Hydrogen and Carbonic Oxide

By William A. Bone, D Sc , F R S and F G Lamont, M Sc

Some time ago, as a new development in high-pressure technique, apparatus was installed in our laboratories for the study of continuous flames at high pressures, and recently it has been adapted for spectrographic work The present paper deals with observations on the influence of increasing pressure up to 100 atmospheres on the flame-spectra of hydrogen and carbonic oxide, and various mixtures thereof, burning in oxygen

Experimental

Apparatus--Experience with the apparatus employed in previous experiments on the formation of nitric oxide in continuous high-pressure flames of carbonic oxide in oxygen-nitrogen atmospheres* suggested certain improvements which led to the new design shown in elevation and section in figs 1 and 2 It consists of a central combustion chamber $4\frac{1}{2}$ inches internal diameter and 1 inch deep enclosed by a massive ring AA, 12 inches diameter to which are bolted two end plates B and C $3\frac{3}{4}$ inches thick The ring carries the burner, the two inlet connections D and E and two quartz window plugs F and G Each of the cover plates also carries a quartz window plug, H and K, and an outlet connection through which the products of combustion may be led away By employing this method of construction it was possible to reduce the distance between the burner and the quartz windows H and K to less than $\frac{3}{8}$ inch with a corresponding reduction in the absorption effects of the compressed gases in the chamber

The cover plates are secured by six bolts of " Vibrac " steel and are designed to withstand a working stress of 10 tons each, which corresponds, after allowing for that due to tightening, to an internal pressure in the chamber of 300 atmospheres The joints are made with Klingerite washers. The body, cover plates, and plugs were constructed of stainless steel (E S C Immaculate 3) to resist the corrosive effects of the hot gases from the flame

The system of valves, gauges, and connections supplying the compressed gases from the respective storage cylinders (100 to 120 atmospheres) to the combustion chamber was similar to those previously employed,* and included two bronze tubes in series, the one packed with activated charcoal for the removal of any traces of iron carbonyl from the compressed carbonic oxide, and the other with purified phosphoric anhydride for drying purposes   Also, a large capacity " trap " was inserted in the outlet pipe of the combustion
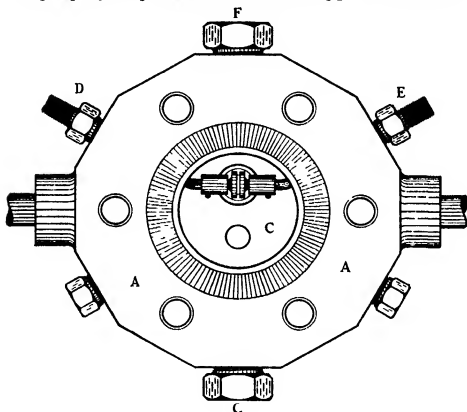
Fig 1

chamber to prevent the release valve becoming blocked by condensed water in experiments with hydrogen flames

The burner was on the " opposed-jet " principle employed in previous work In this case, however, in lieu of the slotted tube surrounding the jets, each of them was fitted with a silica washer, 1 inch diameter and $\frac{1}{16}$ inch thick, by means of which the flame could be maintained more accurately in the form of

* *Loc cit.*, p. 86.

a vertical disc mid-way between the jets without touching either of them
And by carefully focussing a slightly enlarged image of the flame on the slot of
the Hilger E$_2$ quartz-spectrograph employed it was possible entirely to prevent
any continuous " black-body " radiation from the hot silica discs reaching
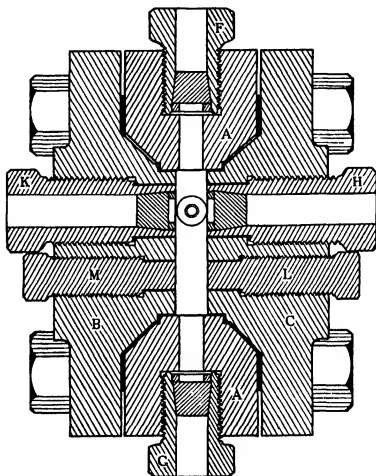
Fig 2

the plate on which the flame spectra were photographed, the images of the
discs falling quite clear of the actual slit

    Procedure —The experimental procedure consisted in maintaining steady
flames of carbonic oxide, hydrogen, or known mixtures thereof, in an atmosphere
of oxygen at each of the selected pressures (1, 10, 30, and 100 atmospheres),
and after focussing them on the slit of the spectrograph in exposing its photo-
graphic plate for a period such that approximately equal amounts of gas were

burnt during each exposure The exposure diminished from 2½ hours for flames at atmospheric pressure down to 2 minutes only for those at 100 atmospheres, the flames being maintained, as nearly as could be, of constant size

Oxygen was employed as the supporter of combustion so as to eliminate any effects of oxides of nitrogen , it was always maintained in excess, namely in approximately equal volumetric ratio to the gas burnt   The combustible consisted first of pure dry carbonic oxide,* and thence through a graded series of CO- H₂ mixtures, namely, 93CO/7H₂, 78CO/22H₂, 50CO/50H₂, 22CO/78H₂, and 7CO/93H₂ finally to pure hydrogen itself, because it was desired to study not merely the influence of pressure upon the flame spectra of hydrogen and carbonic oxide, but also, at each pressure, the effects of successive H₂-additions to the CO-flame, and thus extending Weston's work to higher pressures †

Weston's Observations—It may be recalled how Weston's spectrogram of an undried CO-flame maintained at atmospheric pressure had shown, besides two groups of " steam " (i e , OH) bands, a banded radiation extending from 5000 A in the visible region to 2200 A in the ultra-violet, on which a continuous spectrum was superposed Fowler and Gaydon‡ have recently concluded (in general agreement with and amplification of what was said in Weston's paper) that the banded radiation referred to is due to the direct combination of excited neutral CO molecules with neutral O₂ molecules without dissociation into atoms of carbon and oxygen or molecules of carbon   The superimposed continuous spectrum which Weston showed is also associated with the *direct* oxidation of carbonic oxide in the flame, is due to the emission of unquantized radiation during the combustion

Weston also found that as the carbonic oxide in the burning gas was progressively replaced by hydrogen, both the banded and the continuous parts of the burning CO-spectrum rapidly faded away, until with an equimolecular CO-H₂ mixture they had nearly all disappeared leaving only the " steam lines " visible in the spectrum   What were then termed   steam lines " are now known to be OH bands, and in what follows will be so described

Repetition of Weston's Experiments—As it was thought advisable, for comparative purposes, to include in the present series a repetition of Weston's observations with flames at atmospheric pressure, especially as we contemplated burning much larger quantities of gas, and were using a spectrograph of greater analysing power, than he did

---

* Dried by insertion of a bronze tube (10 inches long) filled with purified phosphoric anhydride.

† 'Proc Roy Soc ,' A, vol 109, pp. 523–524 (1925)

‡ 'Proc Roy Soc ,' A, vol 142, p 369 (1933)

Accordingly in fig 3, Plate 6, are reproduced our spectrograms for $CO-H_2$ flames in oxygen at atmospheric pressure. The CO flame spectrogram shows a continuous radiation extending to circa 2400 A, and superposed upon (i) the banded $CO-O_2$ radiation previously observed by Weston, and (ii) the HO-band at circa 3064 A., the intensity of which is relatively so weak that only the lines near the head are visible. On progressively adding hydrogen to the CO-flame, the continuous radiation rapidly diminished and HO bands became more pronounced until with a pure H_2-flame four of them (with heads at 2608, 2811, 3064, and 3428 A.) were well developed.

Flame Spectra at Higher Pressures —Our spectrograms for flames maintained at 10, 30, and 100 atmospheres respectively are reproduced in figs 4–6, Plates 7 to 9. The principal effects thereon (i) of increasing pressure with each burning medium, and (ii) of successive CO by H_2 replacements at each pressure, are summarised in Table I.

Reviewing the results as a whole we find —

Effects of Pressure (1) *With a Pure CO-Flame* --While the continuous spectrum was (if anything) intensified and completely obliterated the $CO-O_2$ bands as the pressure was increased up to 100 atmospheres, the 3064 HO-bands visible at atmospheric pressure became very faint at 10, and completely faded out at 30 atmospheres and above, indicative of the CO-oxidation becoming increasingly direct with rising pressure

(2) *With a Pure H_2-Flame* the general effect of increasing pressure was to strengthen all the HO-bands, and at 100 atmospheres to produce reversals at the head of the 3064 A band—doubtless owing to the survival of free HO-radicals in the cooler atmosphere surrounding the flame And at the same time the bands did not degrade so rapidly, indicative of a progressive shifting of the energy distributed away from the band-head as the pressure rose Also there was a growing tendency, most marked at 100 atmospheres, to produce a slightly diffused background There was no sign of any H-lines developing

(3) *With $CO-H_2$-Flames* --With corresponding mixture-compositions increasing pressure induced a growing tendency for the HO-bands to become relatively fainter and for the continuous CO-spectrum to become more pronounced, as though the direct oxidation or carbonic oxide was progressively superseding the indirect This is well shown in fig 7, Plate 10 in which the spectra for a 78CO/22H_2 flame at 1, 10, 30, and 100 atmospheres respectively are reproduced. In other words, the effect, first observed by Weston, of successive H_2-additions to a CO-flame at atmospheric pressure are now seen to be counteracted by increasing pressure.

Combustible gas		
CO	H₂	
100	0	
93	7	
78	22	
50	50	
92	78	
0	100	
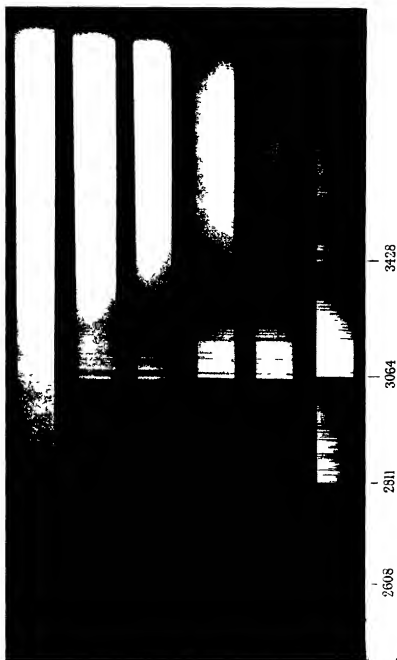
3428 3064 2811 2608
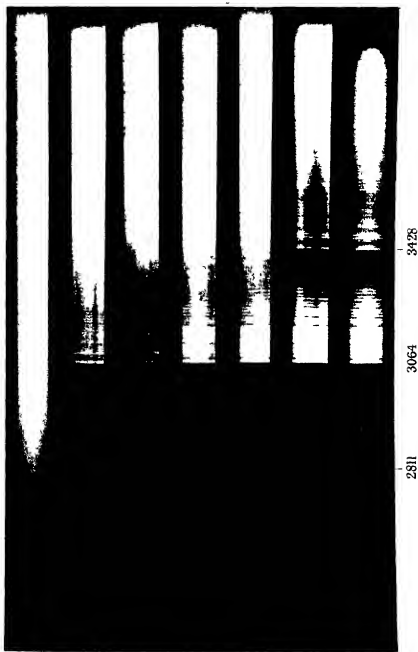
Fig 4 —Spectra of carbonic oxide flame- burning in oxygen at 10 atmospheres pressure

Combustible gas		
CO	H₂	
100	0	
93	7	
78	22	
50	50	
22	78	
7	93	
0	100	

2811 3064 3428

Combustible gas	
CO	H₂
100	0
93	7
78	22
50	50
22	78
7	93
0	100

2608 2811 3064 3428
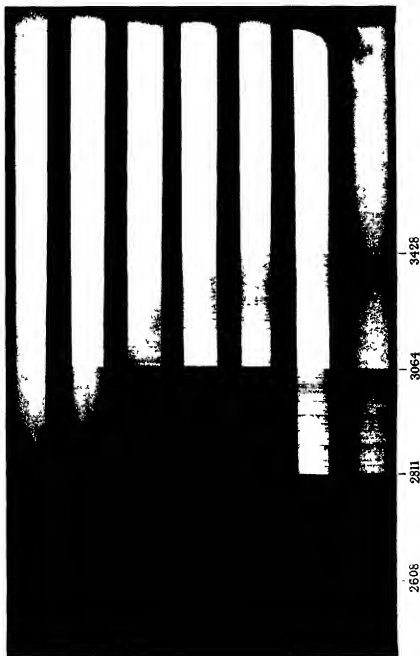
Fig 7.—Spectra of carbonic oxide hydrogen flames burning in oxygen at 30 atmospheres pressure.

Fig 6 —Spectra of carbonic oxide hydrogen flames burning in oxygen at 100 atmospheres pressure

Atmospheres

100

50

10

1

3064

P_{10} 7—2^1CO—2^1H mixture

Table I—Spectra of CO-H₂-O₂ Flames   OH bands observed   0,0 at 3064 A., 1,0 at 2811 A., 2,0 at 2608 A., and 0,1 at 3428 A.

Fuel				Pressure			
CO %	H₂ %	Atmosphere	10 atmospheres	30 atmospheres	100 atmospheres	Effect of pressure on given mixture	
100	0	Strong continuous spectrum extending to far ca 2400 A., 0,0 band visible	Strong continuous spectrum extending to ca 2400 A., 0,0 band faintly visible	Strong continuous spectrum, no OH bands visible	Strong continuous spectrum, no OH bands visible	Little change in continuous spectrum, 0,0 band fades out at 30 atmospheres.	
93	7	Slight reduction in continuous spectrum, 0,0 and 1,0 bands visible	Strong continuous spectrum, 0,0 band clear, 1,0 band visible	Strong continuous spectrum, 0,0 and 1,0 band, 1,0 band very faint	Strong continuous spectrum, 0,0 band visible, 1,0 reversed at head	Reduction of continuous spectrum by addition of H₂, 0,0 band visible to higher pressures. Counteracted by pressure	
78	22	Much less continuous spectrum, 0,0 and 1,0 bands very distinct	Reduced continuous spectrum, 0,0 and 1,0 bands (0,1 vis.) visible	Slightly reduced continuous spectrum, 0,0 band strong, 1,0 band weak	Strong continuous spectrum, 0,0 band faintly visible, reversed at head	Increased continuous spectrum with pressure, 1,0 band fades out above 30 atmospheres	
50	50	Continuous spectrum very much reduced, 0,0 and 1,0 bands very strong, 2,0 and 0,1 bands now visible	Reduced continuous spectrum, 0,0 and 1,0 bands strong, 2,0 and 0,1 bands weak	Reduced continuous spectrum, 0,0 and 1,0 bands strong, 2,0 band weak	Reduced continuous spectrum, 0,0 band strong, 1,0 and 2,0 band reversed, 1,0 band faintly visible	At 1 atmosphere spectrum resembles that of H₂ flame, at 100 atmospheres that of CO flame	
22	78	Very little continuous spectrum, 0,0 and 1,0 bands very strong, 2,0 band weak	More continuous spectrum than at 1 atmosphere, 0,0 and 1,0 bands strong, 2,0 and 0,1 bands weaker	Reduced continuous spectrum, 0,0 and 1,0 bands strong, 2,0 and 0,1 bands weak	Much continuous spectrum, 0,0 and 1,0 band reversed at head, 1,0 and 2,0 bands visible	Decided pressure effect in increasing continuous spectrum and changing intensity of bands	
7	93	Little continuous spectrum, 0,0 and 2,0 bands very strong, 1,0 and 2,0 bands weak	Little continuous spectrum, 0,0 band and 1,0 band strong, 2,0 band weak	Some continuous spectrum, 0,0, 1,0, 2,0 and 0,1 bands all very distinct	Continuous spectrum, 0,0 band reversed at head	Continuous spectrum increased with pressure, intensity of bands reduced	
0	100	No continuous spectrum, 0,0, 1,0, 2,0 and 0,1 bands all very clear	No continuous spectrum, 0,0 and 1,0 bands very strong and do not degrade so rapidly	Bands very heavy	0,0 band reversed at head, slight diffuse background	At higher pressure bands which give non degrade so rapidly	
Effect of varying composition combustible.		Bone-Weston effect well so well marked	Bone-Weston spectrum spec very strong all very clear	Bone-Weston effect not so well marked	Bone-Weston effect no longer evident	Continuous spectrum very strong even with large proportions of H₂ in the fuel	

Speaking generally, although in some of the spectrograms of CO–H₂ flames at atmospheric pressure the banded spectrum of burning carbonic oxide underlying its continuous spectrum is faintly discernible in the original photographic plates, in those obtained at higher pressures it is swamped by the intensity of the continuous spectrum

In conclusion, we desire to acknowledge our indebtedness (i) to Dr D M Newitt for help in connection with the design of the high pressure combustion chamber employed in these experiments, and (ii) to the Government of Northern Ireland for a grant which has enabled one of us (F G L) to devote his whole time to the work

Summary

A new apparatus is described for maintaining continuous flames of combustible gases in air or oxygen at high pressures, and with it has been studied the influence of increasing pressure up to 100 atmospheres upon the flame-spectra of hydrogen and carbonic oxide, and various mixtures thereof, burning in oxygen

(1) *With a Pure CO-flame*.—While the continuous spectrum was (if anything) intensified and completely obliterated the CO O₂ bands as the pressure was increased up to 100 atmospheres, the 3064 HO-bands visible at atmospheric pressure became very faint at 10, and completely faded out at 30 atmospheres and above, indicative of the CO-oxidation becoming increasingly direct with rising pressure

(2) *With a Pure H₂-flame*.—The general effect of increasing pressure was to strengthen all the HO-bands, and at 100 atmospheres to produce reversals at the head of the 3064 A band—doubtless owing to the survival of free HO-radicals in the cooler atmosphere surrounding the flame   And at the same time the bands did not degrade so rapidly, indicative of a progressive shifting of the energy distributed away from the band-head as the pressure rose   Also there was a growing tendency most marked at 100 atmospheres to produce a slightly diffused background   There was no sign of any H-lines developing

(3) *With CO–H₂-flames*.—With corresponding mixture-compositions increasing pressure induced a growing tendency for the HO-bands to become relatively fainter and for the continuous CO-spectrum to become more pronounced, as though direct oxidation of carbonic oxide was progressively superseding the indirect   In other words, the effect, first observed by Weston, of successive H₂-additions to a CO-flame at atmospheric pressure are now seen to be counteracted by increasing pressure

The Supposed Intervention of Steam in Hydrocarbon Combustion

By WILLIAM A. BONE, F R S, and JACK BELL B Sc, A R C S

(Received November 15, 1933)

[PLATES 11-12]

An important issue in connection with the theory of hydrocarbon combustion, needing further discussion, is whether or not the presence of water vapour plays any essential role in the process

H E Armstrong, who originated the hydroxylation theory in 1874, has always insisted that it does, its action (taking the first oxidation stage of methane as a typical example) being supposed as follows —

$$CH_4 + HOH + O_2 = CH_2OH + HO \cdot OH,$$

the hydrogen peroxide so formed participating in the oxidation and regenerating the steam thus - -

$$CH_4 + HO \cdot OH = CH_2OH + H \cdot OH$$
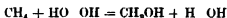
On the other hand, Bone and his co-workers, while maintaining that the oxidation involves successive "hydroxylation" stages, regard the action of the oxygen (whether molecular or atomic) as direct, thus --

$$CH_4 + O \cdot O + CH_4 = 2CH_3OH, \text{ etc }, *$$
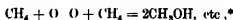
or possibly, in flames, $CH_4 + O = CH_3OH$, etc

As H E Armstrong has recently re-affirmed his view in discussing Bone's experimental results, the time seems opportune for both reviewing the evidence already published and supplementing it by some newly acquired in our laboratories

1 Previous Evidence about Slow Combustion

Previous evidence all relates to non-explosive slow combustion and comprises two somewhat different sets of conditions, which had best be dealt with in the reverse of their chronological order, as follows (A) in the course of recent re-investigations (1930-33) in our laboratories of the slow combustions

_____

* This equation expresses two outstanding facts, namely, (i) that the slow combustion $2CH_4 + O_2$ is much the most reactive of all methane oxygen mixtures, and (ii) that methyl alcohol is the first recognizable product

of methane, ethane, and ethylene,* studies were made of the effects of small additions of water-vapour upon the durations of both "induction" and "reaction" periods of selected P_2O_5-dried hydrocarbon-oxygen mixtures in a quartz vessel at atmospheric pressure and a temperature no higher than was required to give a conveniently measurable rate of reaction in each case The reaction vessel had been thoroughly dried-out by prolonged evacuation at the experimental temperature prior to the admission of the gaseous medium, which was slowly passed in through a metre long column of pure redistilled phosphoric anhydride The drying thus effected, while not severely intensive, would be as thorough as was needed for the purpose in view In the "moist" experiments, 1 or 2% by volume of vapour from "ammonia-free" redistilled water was added to the so-dried medium just as it entered the reaction vessel The observed results are given in Table I

Table I

Mixture employed	Temperature of reaction vessel	Hygroscopic condition	Observed durations of-	
			"Induction" (mins)	"Reaction" (mins)
	°C			
$2CH_4 + O_2$	447	Dry	6 to 7	91 to 98
		Moist, 2%	1 to 4	35 to 36
$C_2H_6 + O_2$	316	Dry	20	70
		Moist 1%	10	25
$C_2H_4 + O_2$	400	Dry	54	50 to 52
		Moist, 1%	56 to 60	50

It is thus seen that while additions of water-vapour to the P_2O_5-dried $2CH_4 + O_2$ and $C_2H_6 + O_2$ (i e, the paraffin-containing) media materially shortened both the induction and reaction periods, they had little or no effect upon the P_2O_5-dried $C_2H_4 + O_2$ (i e, olefine-containing) medium None of the dried media, however, appeared unreactive

(B) In 1906 Bone and Andrew published† the results of a careful study of effects of an intensive P_2O_5-drying (4 to 12 weeks) upon the reactivities of $C_2H_6 + O_2$, $C_2H_4 + O_2$, and $C_2H_2 + O_2$ media at various temperatures between 300° and 500° and pressures between 2 and 3 atmospheres For details of

* 'Proc Roy Soc ,' A, vol 129, p 434 (1930) vol 134, p 578 (1932)

† 'J Chem Soc ,' vol 89, pp 652-659 (1906)

the experimental procedure, the original paper should be consulted ; suffice it now to say that on comparing the behaviour of each *dried* and *undried* medium, when subjected to the same degree and duration of heat, little or no difference could be found between them—the *dry* always reacting quite as fast as (and if anything even slightly faster than) the corresponding undried medium. This evidence was strengthened by the fact that the same drying procedure had caused enormous differences between the percentages of reaction (e g , *nil* and 42, 0 5 and 52, 3 and 40 or 45) in "dry" and "undried" $2H_2 + O_2$ media, respectively, after 15 minutes at 525° This is well illustrated by the results of two such comparative sets of experiments with a $C_2H_4 + O_2$ medium, where the "drying period" extended over 11 weeks The temperature at which the first visible sign of reaction occurred, when the tubes were subsequently heated, was about the same (385°–398° C) in the "dry" as in the "moist" medium ; and after 15 minutes further heating up to a maximum of 430° to 450°, the amounts of reaction were substantially the same in each, as can be seen from Table II

Table II —Results with Moist and 'Dry' $C_2H_4 + O_2$ Media at 430 to 450° and 2 5 Atmospheres for 15 minutes (Bone and Andrew)

State of medium	Percentage contraction on cooling	Percentage composition of gaseous products					
		CO_2	CO	C_2H_4	C_2H_6	H_2	O_2
(1) P_2O_5-dried, 11 weeks	37 0	10 25	45 75	32 65	2 10	1 05	8 20
	37 7	10 25	44 50	28 85	6 35	4 00	6 05
(2) Moist, $H_2O = 2\%$	34 8	10 60	48 4	27 6	4 65	2 70	6 05
	36 1	11 45	50 8	24 85	5 15	3 23	4 50

Two experiments with a 4-weeks P_2O_5-dried $C_2H_2 + O_2$ medium showed in (1) first visible sign of reaction after 27 minutes at 315°, and complete disappearance of oxygen within a further 8 minutes during which the temperature had risen to 415° ($p_2/p_1 = 0$ 672, and gaseous products contained $CO_2 = 19$ 65, $CO = 56$ 65, $C_2H_2 = 22$ 5, $C_2H_6 = 0$ 35, $H_2 = 0$ 85, and $O_2 = nil$ %), while in (2) when the contents of the tube were heated to 520°, they exploded after 2 minutes with shattering effect

Two sets of comparative experiments with "dry" and "undried" $C_2H_4 + O_2$ mixtures, respectively, at temperatures between 415° and 450° left no room for doubt but that reactivity was definitely increased by a 7 weeks

P_2O_5-drying   Ignition finally occurred in both "dry" media, and also in one of the two moist ones

Although the experimental conditions precluded any estimation of the effects of the intensive drying on the length of the "induction period" in each case—which would in any case be extremely short—there could be no doubt about the P_4O_5-drying having (if anything) rather increased than diminished the reactivities of all the media examined at the temperatures and pressures concerned

<center>11 New Evidence re Explosive Combustion</center>

Although the evidence regarding slow combustion seemed decisive enough on the point at issue, it was thought desirable to extend the enquiry to explosive combustion, and for this purpose equimolecular mixtures of ethylene or acetylene and oxygen seemed most suitable* inasmuch as on explosion they yield substantially nothing but carbonic oxide and hydrogen, without any discernible carbon separation or steam formation, thus —

$$C_2H_4 + O_2 = 2CO + 2H_2$$
$$C_2H_2 + O_2 = 2CO + H_2$$
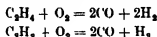
The Experimental Mixtures - The experimental mixtures were made up very accurately over dry redistilled mercury in a large cylindrical gas burette A, fig 2, from stocks of highly purified hydrocarbon and oxygen, each hydrocarbon having previously undergone (i) a thorough chemical purification followed by (ii) two successive liquefactions and fractionational vapourizations of the liquid, the middle third only being reserved in each case , on analysis the compositions of the experimental mixtures were found to be as follows —

$$C_2H_4 + O_2 \quad C_2H_4 = 49\ 8,\ O_2 = 50\ 2\%$$
$$C_2H_2 + O_2 \quad C_2H_2 = 49\ 5,\ O_2 = 50\ 4,\ N_2 = 0\ 1\%$$
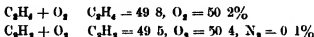
The Explosion Tubes, GG, fig 1, were constructed out of Jena red-line borosilicate glass tubing (internal diameter = *circa* 2 cm), each was 35 cm long, having expanded ends for the reception of the drying-agent, and being fitted mid-way with "swinging" platinum electrodes (1 mm diameter terminating in a bulb 1 5 mm diameter)

Cleaning and Drying of the Explosion Tubes —The elaborate ritual for thoroughly cleaning and drying out the insides of the explosion tubes was that

---

* Experiments on $CH_4 + O_2$ or $C_2H_6 + O_2$ mixture were deemed unsuitable because they would have yielded H_2O on explosion.

followed in previous similar experiments in our laboratories and has been fully described in a former publication. Between the initial and final stages, and again thereafter, the platinum electrodes were electrically ' glowed-out " each time *in vacuo* for 8 hours and then in 2 mm of oxygen for 3 hours, for the elimination of any trace of occluded hydrogen. All other glass apparatus used during the experiments was similarly cleaned and dried.

Final Drying of the Experimental Mixtures.—Finally the clean and dried explosion tubes, GG, into each expanded end of which a quantity of purified and redistilled P_2O_5 had been introduced, were connected through a suitable KOH- and P_2O_5-drying train, CDE, and manometer, F, with the gas burette
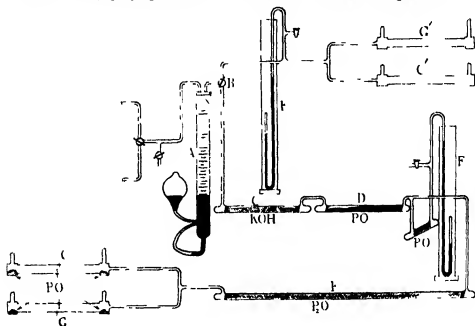
Fig 1

A containing the experimental mixture, as shown in fig 1. An alternative connection was also provided, through the tap B, between the gas burette and the explosion tubes G' G' used in the comparative experiments with the corresponding " moist " mixtures, which were about half-saturated with water vapour at the room temperature (17° to 20°). The actual drying system comprised (i) a 50-cm long tube packed with solid KOH followed in succession by two tubes 50 and 100 cm long respectively, filled with purified and redistilled P_2O_5. All joints throughout the apparatus were of fused glass, the fusion being effected in a dust free and CaCl-dried CO — O_2 blowpipe flame

Before transferring the gaseous mixture from the gas burette A to the explosion tubes, GG, the whole of the intervening apparatus was exhausted down to a pressure of 0 001 mm by means of a Hyvac pump which was kept continually running each time for at least 24 hours Finally the mixture was passed, at a rate not exceeding 1 and sometimes as low as 0 5 c c per minute, from the gas burette, through the "drying system" into the explosion vessels The filling arrangements in the control experiments with the corresponding "undried" mixture were similar to the foregoing, except for the omission of the "drying train," and of P_2O_5 in the explosion tubes concerned

On completion of the filling at room temperature and the selected firing pressure (735 mm and 20° for the $C_2H_4 + O_2$ and 370 mm and 17° for the $C_2H_2 + O_2$ mixture), the tubes were finally sealed off in the blow-pipe at a constriction previously made in the glass for the purpose

The Drying Period—The subsequent 'drying period" always extended over rather more than 300 days during which the expanded ends of each tube were frequently tapped to expose a fresh P_2O_5 surface to the gaseous medium, and at regular intervals of 14 days the main part of the tube between the expanded ends (but not the latter) was heated to about 150° in order to ensure the dispersion of any film of moisture that otherwise might have adhered to the inner walls

Control Experiments—While the drying was in progress, two special control experiments were made as a precaution to ensure that prolonged exposure to the P_2O_5-drying agent employed does not alter the composition of either a $C_2H_4 + O_2$ or a $C_2H_2 + O_2$ mixture—by some preferential absorption of one or other of its constituents In neither case, however, had a 7 months' exposure any appreciable effect upon the composition of the mixture

Photographic Investigations of the Explosions

Two pairs of "dry" and "moist" tubes (the latter for comparison) for each of the two experimental mixtures having been so prepared, and the drying period ended, arrangements were made for firing each pair of tubes in a horizontal position by means of a condenser discharge of 0 06 m f at 1000 volts and photographing the resulting explosion on a film moving vertically, at constant velocity, in one of our Fraser high-speed cameras In this way comparative photographic analyses were obtained of the flame movements throughout each pair of "dry" and "moist" explosions, from which a series of comparative flame-speeds could be calculated, showing precisely what had

been the effect (if any) of the intensive P_2O_5-drying It will, however, suffice to reproduce and analyse the relative photographs for *one* pair only of " dry " and " moist " explosions for each of the two experimental mixtures, and then merely to tabulate, as confirmatory evidence the relative flame speeds observed in the other pair of explosions with each mixture

A *The* $C_2H_4 + O_2$ *Explosions* —(1) The relative photographs for the first pair of " dry " and " moist " explosions (tube internal diameter = 2 0 cm) are reproduced in figs 2 and 3, Plate 11

The film speeds were 33 0 for the ' dry " and 31 8 metres per second for the " moist " explosion, respectively The drying period in the former had been 316 days, and the gaseous pressure in both cases 736 mm On firing the mixtures, in each an explosion ensued instantaneously the flame traversing the mixture much faster than the eye could follow and ultimately filling the whole tube, and while the tube itself always remained intact, its capillary end was fractured by the explosion

The resulting photograph showed that the flame speed had been materially faster and the total duration of luminosity (T D) also shorter in the " dry " than in the " moist " explosion Each photograph shows clearly (i) the flame starting instantaneously from the igniting discharge and thence spreading rapidly and symmetrically towards each end of the tube, (ii) a continuance of luminosity for some time after the flame had completely filled the tube, during which the medium was traversed from end to end by compression waves, and (iii) the production in the central region round the electrodes and also in the flame front itself, of striæ of enhanced luminosity, all of which coalesced just as the advancing flame fronts reached the ends of the tube

Particulars of the flame-speeds deduced from the photographs are as follows —

Average flame speed from source to point	(a) " Dry " explosion (metres per sec)	(b) ' Moist " explosion (metres per sec)
(i) 5 cm. distant	55 6	54 4
(ii) 10 cm. distant	68 8	70 4
(iii) To end of tube	70 0	55 0
	(millisecs)	(millisecs.)
Total duration of luminosity	6 3	7 7

(2) The internal diameter of the tubes used in this pair of explosions was 2 3 cm , otherwise the conditions were precisely the same as previously

Particulars of the flame-speeds deduced from the resulting photographs are as
follows —

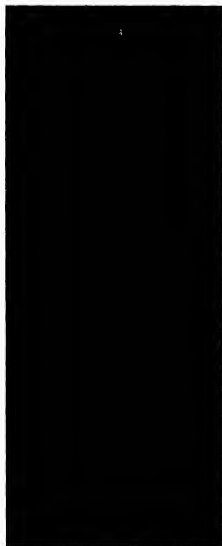| Average flame-speed from ignition to point	(a) "Dry" explosion (metres per sec)	(b) "Moist" explosion (metres per sec)
(i) 5 cm distant	65 0	53 8
(ii) 10 cm distant	89 4	61 7
(iii) End of tube	85 5	60 0

It is thus seen that in each pair of explosions the average flame speed through
the "dry" was decidedly (27%–42%) greater than through the "moist"
medium

B *The* $C_2H_2 + O_2$ *Explosion* —(1) The relative photographs for the first
pair of "dry" and "moist" explosions (internal diameter of tube = 2 0 cm)
are reproduced in figs 4, 5, Plate 12   The drying period in the former had
been 314 days and the pressure in both cases 371 mm.

In each case a deafening report immediately followed the passage of the
discharge, the tube being shattered by the force of the explosion, although it
had remained intact until completely filled with flame

The film speeds were 79 7 for the "dry" and 74 0 metres per second for
the "moist" explosion respectively   The average flame speeds were very
high, namely, 700 and 585 metres per second respectively, or about 20% higher
in the "dry" than in the "moist" medium   The fact that the total duration
of luminosity was apparently greater in the "dry" than in the "wet" ex-
plosion is probably of no particular significance owing to the fracturing of the
tube after the flame had reached its ends

Particulars of the flame speeds deduced from the photographs are   -

Average flame-speed from ignition to point	(a) 'Dry' explosion (metres per sec)	(b) "Moist" explosion (metres per sec)
(i) 5 cm distant	416	333
(ii) 10 cm distant	476	417
(iii) End of tube	700	585

(2) The internal diameter of the tubes used in the second pair of explosions
was 1 8 cm , but otherwise the conditions were the same as previously   Par-
ticulars of the flame-speeds deduced from the resulting photographs are given
in the following table

Fig 2 —" Dry "   Fig 3 —" Moist "

$C_2H_4 + O_2$ explosions
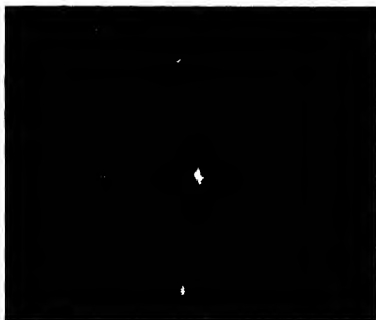
FIG 3 — Moist

($_4$H$_4$ — O$_2$) explosions

FIG 4 — Dry

Average flame-speed from ignition to point.	(a) "Dry" explosion (metres per sec).	(b) "Moist" explosion (metres per sec.)
(i) 5 cm. distant	312	278
(ii) 10 cm. distant	434	385
(iii) End of tube	600	500

It is thus seen that in both cases the flame-speeds were greater in the "dry" than in the "moist" explosions. Another point of interest about the photographs to which attention may be directed is the entire absence of any sign of carbon separation in the flame front, which accords well with the view that the primary reaction is $C_2H_2 + O_2 \rightarrow (C_2H_2O_2) \rightarrow 2CO + H_2$.

Conclusion.

(1) The results as a whole are, we think, decisive against any supposition that in general the combustion of a hydrocarbon is conditioned by the presence and chemical intervention of steam, as H. E. Armstrong supposes, although in certain but not every case of slow combustion it may in some way assist the reaction. Hence we conclude that the oxidation is, in general, direct.

(2) Nor yet do photographs of the $C_2H_4 + O_2$ and $C_2H_2 + O_2$ explosions lend any support to the view (sometimes suggested) that the final production of substantially carbonic oxide and hydrogen only is nearly the resultant of the successive reactions $C_2H_4 + O_2 \rightarrow 2C + 2H_2O \rightarrow 2CO + 2H_2$, and $C_2H_2 + O_2 \rightarrow CO + C + H_2O \rightarrow 2CO + H_2$, for they show neither carbon separation in the flame front, nor yet any sign of carbon-steam reaction behind it.

We desire to thank the Trustees of the Walker Scholarship Fund, the Miners' Welfare National Scholarship Scheme, and the D.S.I.R. for grants which have enabled one of us (J. B.) to participate in the research.

Summary

The paper deals with the question as to whether in hydrocarbon-combustion the oxygen acts directly in hydroxylating the hydrocarbon or only indirectly (as H. E. Armstrong maintains) through the intervention of steam, as, for example —

$$CH_4 + H . OH + O . O = CH_3OH + H_2O_2$$
$$CH_4 + H_2O_2 = CH_3OH + HOH, \text{ etc.}$$
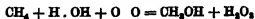
Existing evidence in regard to the effects of P_4O_5-drying upon the slow combustion of typical hydrocarbon-oxygen mixtures is reviewed, and new evidence in regard to its effects upon explosions of $C_2H_2 + O_2$ and $C_2H_4 + O_2$ media is detailed The conclusion is reached that intensive P_4O_5-drying if anything increases rather than diminishes the reactivities of hydrocarbon-oxygen mixtures, both in slow and explosive combustion, and therefore that steam does not intervene, the oxidation being direct

---

The Bending of Marble

By Lord RAYLEIGH, For Sec. R S

(Received December 1, 1933)

[PLATE 13]

§ 1 Introduction

Cut slabs of marble are often noticeably bent An old marble mantelpiece, say 1 5 metres long, will always show a depression in the middle when tested with a stretched thread This depression is often 1 to 2 mm , and I have heard of cases where it is much more My interest in this phenomenon was aroused by a conversation with the late Dr D W Dye, F R S , and a few preliminary experiments were made My first notion was that the marble bent by viscous flow, as a stick of sealing wax will do when loaded in the middle, and I even speculated as to whether it would be possible by the continued application of force to bend a piece double The well-known experiments of Adams and Nicholson[*] on the flow of marble under high pressures seemed at first glance to give this notion some plausibility

Bent pieces of marble were obtained from a local marble merchant, Mr J B Slythe, of Witham. He was not able to say anything definite about their origin, except that they had been in his yard for many years. A bent strip was supported at the ends with the concave side up, and loaded at the middle with as much weight as it was judged safe to put on A suitable index

---

* ' Phil. Trans.,' vol. 195, p. 363 (1901).

was fixed at the middle and observed by a microscope with eyepiece scale There was noticeable motion the first day, but it rapidly diminished in amount from day to day, until it practically ceased after a few weeks. I then reversed it, thinking that if there were a limit to the bending it would at least be possible to restore its original straightness Again, there was noticeable motion at first, but it soon almost stopped, and calculation showed that decades would be required at the least to straighten the piece in this way, even under the favourable conditions of the experiment This made it improbable that the piece could have been bent cold It then seemed that it might have been bent by the application of force while hot A similar experiment was accordingly tried at a higher temperature A strip of new marble was placed on the hot-water pipes, similarly supported at the ends and heavily loaded in the middle It was covered with cotton-wool lagging, and thus maintained at from 45° to 50° C throughout the winter But tests with a spherometer showed that only very slight bending had occurred, and this was nearly all in the first week or two

At this stage it was difficult to know what to think, the more so that Mr Slythe informed me that he had had pieces of marble which would gradually bend under their own weight when leaned against the wall, and would become straight again in course of time, if reversed I eventually succeeded in obtaining a slab, obviously an old mantelshelf, of very marked curvature, which showed this behaviour Careful observations were made on it The length was 182 4 cm, the breadth 15 cm, and the thickness 2 cm It was geometrically supported at the ends, and loaded at the middle with weights amounting to 8 6 kg, and a suitable pointer and mirror glass scale provided The weights were removed for taking readings. The first tests were made with the smooth side up, i e, as used for a mantelshelf In seven weeks the index had sunk 6 1 mm, increasing the *sagitta** of the arc from 16 9 mm to 23 mm. Towards the end of this period the motion had become very slow, though it could still be detected in a week

Having got something near the maximum curvature in this way, the slab was reversed and replaced with the convex (rough) side upwards, in order to straighten it After reversal, when the slab had been allowed to take up its position, most of the concavity of the smooth side had disappeared At first reading the sagitta was only 8 7 mm This great diminution of curvature had taken place immediately under the weight of the slab acting in the reversed

---

* This convenient word for the maximum distance from the chord to the arc is used in Newton's " Principia," and is here revived.

sense Leaving the slab under its own weight the sagitta was further diminished to 6 7 mm. in 5 days The change had become very slow, and the same weights as before (8 7 kg) were put on This resulted in a further change, and eventually the slab, as observed unloaded, became straight, and finally achieved a curvature in the opposite direction (sagitta—2 5 mm.) The motion under the load had then become very slow, amounting to 1 7 mm. in 77 days, and the experiment was discontinued

It is noticeable that this specimen, unlike the previous one, is highly flexible within certain limits, and that these limits are unsymmetrical It can take a much greater concavity on the smooth side (i e , the top side of mantelshelf) than on the rough side This may be regarded as a combination of permanent curvature with flexibility

Finally, a marble strip was brought to me which had been in a wooden shed burnt to the ground in an accidental fire, and which had presumably become considerably heated This had very marked flexibility without permanent curvature

It appears therefore that flexibility and permanent curvature (warping) may appear either combined or separately, and that at all events in some striking cases the specimens which show either have been subjected to a more or less high temperature * It was with this clue that some success was obtained in the further investigation

Preliminary experiments on baking marble in a kitchen oven at about 300° C. showed that marked flexibility resulted from this treatment A demonstration experiment was shown at the Royal Society soirée on June 21, 1933 The strips exhibited were each gripped at one end in a wooden vice, and protruded some 30 cm The thickness was about 8 cm The baked strip could be moved to and fro through a range of 2 cm between stops, by gentle pressure with the forefinger The unbaked strip provided for comparison was rigid

§ 2 *Systematic Observations on Flexure and Expansion, after Baking at Various Temperatures*

For a closer examination apparatus was arranged as in fig 1 The marble was vertical. It was gripped at its upper end in a cast iron vice of special construction, carried on the wall The lower end could be pulled to right or left by the attached threads By this method any complication from the

---

* Mr Slythe was inclined to think that old marble, i e., marble which had been long exposed to the weather, as tombstones and the like, often showed flexibility I have not so far been able to confirm this.

weight of the marble itself is avoided, and the force admits of easy reversal
The threads passed over pulleys working on centres with a minimum of
friction, and carried the scale pans. Weight in one or other of these pans
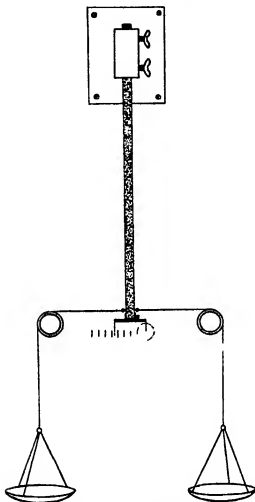provided a known force A brass piece carrying two separate index needles

Fig 1 (¼ actual size)

was clamped to the lower end of the marble quite independently of the attach-
ment for the threads, which latter is not shown in detail One of the needles
is the index for minute movement, and is read by a microscope with eyepiece
scale [Microscope shown by the dotted circle] The other needle is read by

a millimetre scale on mirror glass, and is used for indicating the larger move-
ments. The use of two separate indexes is convenient since the microscope
need not be removed when the millimetre scale is used The microscope is
useful in the early stages of the experiment to examine the small flexure of
unbaked marble, or marble baked at low temperatures

Any shift of the marble in the vice would make the results inaccurate for
the smaller deflections To avoid crushing the marble, strawboard packings
2 5 mm thick were used on either side between it and the iron jaws, which
latter were screwed up "thumb tight" by means of the three thumb screws
[The details are shown in fig 2 The lower thumb screw shown is to be in-
terpreted as representing two, one above, one below, the plane of the diagram]
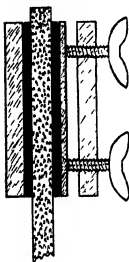
As a test of the reliability of holding, a piece of flat
bar iron of about the same dimensions was set up
instead of the marble, and clamped in the same way
After loading with 1 kilogram, and unloading
again, the original microscope reading was exactly
recovered It is concluded from this that the
method of holding is satisfactory, and that the
strawboard packings are unobjectionable

For baking the marble strips an electrical oven
was constructed An asbestos muffle received the
strip This muffle was wound with resistance wire,
and surrounded with a thick layer of slag wool for
heat insulation The furnace current was increased
a definite amount for each experiment and the
specimen heated for about 20 hours, the tempera-
ture being taken at the end of that time Some

FIG 2 (½ actual size)

hours are required to reach a steady temperature, so that the baking was
not under strictly uniform conditions *

As is known, marble undergoes a permanent increase of length on heating
It was considered desirable for reasons which will appear later to observe the
increment concurrently with the mechanical tests For this purpose fine
scratches were made at the two ends of the marble strip, about 400 mm apart
The marble was laid on a planed iron slab, and a piece of sheet glass laid on
the marble The glass had fiducial lines engraved upon it about 399 mm

---

* It is possible that alternate heating to a given temperature and cooling might have
more effect than continuous heating to the same temperature This point has not been
examined.

apart, thus 1 mm. less than the distance between the scratches on the marble.
The engraved side of the glass was, of course, downwards, and weights were
placed on it to keep the whole flat and steady   The short distance at each
end between the mark on the glass and that on the marble was measured
with travelling microscopes   In this way the small increments of length
were determined   The greater part of the length was taken care of by the
glass standard, its exact absolute value being unimportant

A strip of marble, believed to be from Carrara, was taken, measuring 78 mm
broad, 9 mm thick, and a little over 400 mm long   It was clamped in the
vice, the protruding length being 34 cm   and was carried through a cycle of
changes, being first loaded up to +1000 grams (s e , 1000 grams on the right-
hand pan)   This was taken off 200 grams at a time, with readings at each
step   Weights were then progressively added on the other side to —1000
grams, and so on until two complete cycles had been gone through , the mean
of the two cycles being taken   The discrepancies were small, particularly in
the early stages of the experiment   Having gone through this process with
the marble in its initial condition, it was baked at a determined temperature,
on cooling the increase of length was measured, and the mechanical tests
repeated ,   and so on, increasing the baking temperature each time, until
finally the specimen broke off under the standard force of 1 kilogram.

The readings were always taken as quickly as convenient after loading or
unloading   There is a certain creep following on this, which goes on for a long
time, becoming slower and slower, and perhaps never definitely ceasing   But
the initial movement is the important one, the creep being comparatively
small   In the cyclic tests the creep was ignored, though it probably accounts
for any small outstanding lack of definiteness in the measurements *

The most important part of the results is in the following table.

The total flexure referred to is the difference between the extreme
positions under load   The inelastic flexure is the difference between the
positions on unloading after pulling to the right and left respectively

The small permanent elongation observed after baking at 55° is doubtful
Definite elongation is first observable after baking at 77°, and at this point
the change of mechanical properties also begins to appear

It will be noticed that the inelastic flexure becomes a much larger fraction of
the whole as the baking temperature is increased.   With the load used (± 1

---

* This creep was the subject of observation in my earlier experiments already referred to
I was slow in recognizing that it was of secondary importance, and not the main process of
flexure. Judgment was confused by the existence of permanently warped specimens
see § 4 below

272   **Lord Rayleigh.**

kilogram) it becomes ultimately comparable in amount with the elastic flexure

Temperature of baking, ° C	Permanent elongation, mm	Flexure by ± 1 kilogram		Ratio inelastic total.
		Total mm	Inelastic mm	
Not baked	0	2 3	0 16	0 07
55	0 015 ?	2 2	0 15	0 07
77	0 03	2 6	0 28	0 11
114	0 04	3 1	0 35	0 11
144	0 14	3 9	0 50	0 13
182	0 27	5 5	0 91	0 17
221	0 45	7 7	1 7	0 22
266	0 71	11 0	2 7	0 24
297	0 94	16 0	5 3	0 33
336	1 29	25 8	10 3	0 40
365	1 56	Broke		

While the table gives the flexure, elastic and permanent, due to the full load of ± 1 kilogram, it does not show the effect of a progressive increase or diminution of the load. This is conveniently exhibited by a cyclic hysteresis curve, similar in form to the curve of magnetic induction A selection of three of these stress strain diagrams are shown in fig 3, which illustrate the progressive steepening and still more marked opening out of the diagram as the baking temperature is increased. To avoid confusion only the initial and final conditions, with one intermediate condition, are included

It will be noticed that the marble in its initial condition, as received from the marble merchants, is capable of some inelastic flexure. The amount is small, only 0 16 mm under the standard load, and would not come into evidence without special arrangements, but there is no reason to doubt that it is genuine. Inadequate holding might simulate this effect, but, as already explained, this source of error was tested for and excluded

Other untreated samples of marble show this effect, and sometimes much more conspicuously. A piece closely similar to the one used for the main series of tests gave an inelastic flexure of 0 38 mm under a load of ± 500 grams, it was thus considerably more flexible than the foregoing

I had also a sample of pale grey (dove) marble from Messrs Wilkins, which they had noticed to be flexible. It was untreated by heat, and was as imported from Italy. Unfortunately it broke under the load I applied before any definite tests had been made. Evidently in this specimen mechanical weakness goes with flexibility, as in the heat-treated specimen
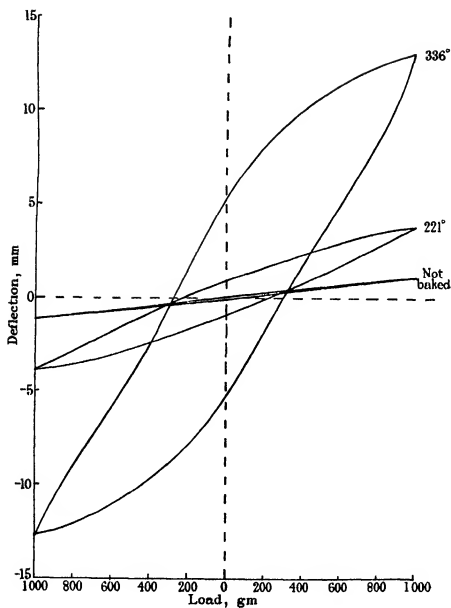
Fig. 3.

These cases of natural flexibility in untreated marble deserve further investigation In particular, it would be important to determine whether the specimen may not have got heated in the process of sawing it up

§ 3 *General Discussion of Flexibility*

The marble used in these experiments consists of calcite crystal grains which, as viewed in a thin section under the microscope seem to fill practically the whole space The size of these calcite grains is about 0 1 mm. and the edges are not infrequently fairly straight It is difficult to make out any very definite evidence of cementing material between the grains, and it seems possible that they are simply adhering by close contact * It would seem at all events that the structure cannot hold together as it does without some adhesion between the grains, for the individual grain have no obvious re-entrant angles, and therefore cannot be held together simply by interlocking

Now calcite is known to expand by heat much more in the direction of the optic axis than in the perpendicular direction. Indeed this is an understatement for in the latter direction the thermal expansion is actually negative † The rhombohedron of calcite may be regarded as derived from a cube by shortening one of the diagonals, the edges which run up to one end of this diagonal becoming obtuse instead of right-angled Thermal expansion tends to reverse this process and to diminish these obtuse angles Mitscherlich found, in fact, that the rhombohedral angle was 105° 4' at 10° C, but was reduced to 104° 56' at 110° C ‡ The actual grains are not, of course, of rhombohedral shape, but their irregular shape similarly alters with temperature, and a grain which fitted accurately into the crystalline mosaic at ordinary temperature is no longer able to do so when the temperature is raised The result of this is a springing apart of the contiguous grains, necessarily involving a partial rupture of the adhesion between them In this way the whole structure is loosened, and progressive loss of mechanical rigidity results The known permanent elongation of marble§ as recorded in the table, p 272, is in accordance with this

---

* Mr F Twyman, F R S , has kindly informed me in answer to a question that it is possible though not easy for the practical optician to put flat calcite surfaces into adhesive optical contact

† Benoit's values for the coefficient of expansion are parallel to axis 2 4963 × 10⁻⁶ and perpendicular to axis − 5 541 × 10⁻⁶ These are in agreement with the earlier work of Fizeau. See Tutton, " Crystallography and Crystal Measurement," vol 2, p 1329

‡ See Tutton, vol 2, p. 1303

§ The permanent expansion of marble is described by Schad, ' Phys Rev ,' vol. 10, p. 74 (1917)

general point of view and may be said decidedly to confirm it for the two effects become sensible at about the same temperature

Two other indications of the general loosening of the structure may be mentioned First, it is found that ink will "run" on marble that has been baked much more freely than on marble in its original condition Fig 4, Plate 13, shows the effect for indian ink, and fig 5, Plate 13, for ordinary writing ink, which flows more freely than indian ink In each of these pictures the marble on the left was baked for 24 hours at 365° C That on the right was a piece of the same, not baked. The lines are ruled with an ordinary drawing pen , to ensure equal treatment a line was drawn on each piece of marble alternately without any refilling or readjustment of the pen throughout The running of the ink is, of course, attributed to the increased porosity of the material (*cf* blotting paper and writing paper)

Secondly, it is noticeable at the higher temperatures, marble is extremely friable, and can easily be crumbled with the help of pliers, or even broken off with the fingers No measurements have been made on the ultimate strength after baking at various temperatures Such measurements would probably not be very definite , but the observations casually made suggest a progressive loss of ultimate strength, proceeding *pari passu* with the elongation and increased flexibility It is this which sets a limit to the temperature of baking (see table, p 272)

At a high enough temperature marble, of course, loses carbon dioxide, and is converted into quicklime I was at one stage disposed to regard this change as conditioning the increased flexibility and tendency to crumble, but the experiments show marked increase of flexibility at temperatures below 150° C , which would seem to be too low a temperature for serious loss of carbon dioxide to take place A special experiment clears up any doubt A strip of marble was weighed as carefully as the rough balance available would allow, baked in the kitchen oven to a high degree of flexibility (temperature not determined), and weighed again The weight was 425 grams No loss of weight was indicated, and the loss, if any, was certainly less than 0 2 gram. It is clear, therefore, that there was no appreciable loss of carbon dioxide

Although the diminished rigidity of marble is generally accounted for on the above lines, more must be said to fill in the details We have to explain not only increased elastic flexure, but also the inelastic flexure which increases in relative importance the more the structure is loosened As to the increased elastic flexure the number of grain-contacts at which the internal stress is

taken must be diminished, and the stress at each increased, producing an increased strain

As regards inelastic flexure, it is natural to turn in the first instance to the example of other crystalline aggregates, and metals are the most obvious. In these, inelastic flexure occurs by the individual crystalline grains changing their shape by the occurrence of slip or twinning on particular crystallographic planes, and the work of Adams and Nicholson[*] indicates that in the flow of marble under stresses of the order of 18,000 lbs per square inch the process is in many respects similar to that in metals But in the present case the extreme forces to which the marble is subjected are only of the order of 450 lbs per square inch.[†]

Both the elastic and the inelastic flexure of baked marble are to most observers very surprising and unexpected effects. Considering the way that they develop together as the baking temperature is raised (table, p 272) it seems probable that they are closely connected For reasons already given, the increased elastic flexure is connected with the loosening of contacts between adjacent grains, and if this is correct for the inelastic also, then any comparison with the metals is altogether wide of the mark It seems that a plausible explanation can be derived if we combine the idea of elastic flexure with that of solid friction The latter is supplied by the motion of the partially loosened grains one over the other When the bending force is removed, this friction prevents complete recovery of straightness, by opposing the elastic force of restitution The more the structure is loosened the greater becomes the friction and the less the elastic restoring force, and we are lead to anticipate the inelastic bending becoming a progressively greater fraction of the total, as observed If the structure is thought of as approaching complete disintegration, the friction would become all important, and the whole bending would approach to being inelastic For obvious reasons we cannot approach very near the extreme case experimentally

According to the point of view explained, the elastic restoring force, and the friction which prevents it from fully asserting itself, are considered to exist alongside of one another in the structure As a rough model which may assist the imagination, consider a hinge working with some friction, and uniting two

---

[*] *Loc cit*, p 372
[†] This figure is derived by treating the bent marble as perfectly elastic, so that the stress is proportional to the distance from the neutral axis This supposition cannot, of course, be exact where Hook's law is not followed, but alternative suppositions, such as that the whole stress due to bending is uniformly taken on an outside skin of 1 5 mm thickness would lead to a similar result

long arms Let these be straightened out, and let a flexible steel lath be tied alongside Then, on bending the model and releasing it again, the friction of the hinge will prevent the full recovery of straightness The effect of baking the marble at a higher temperature will be represented by making the elastic lath thinner This will diminish the force required to bend it, and increase the amount of permanent flexure

It has been pointed out to me that the observed flexure of unbaked marble in the above experiments leads to a value of Young's modulus much less than that found for single calcite crystals These give a value of the modulus between $5\ 8 \times 10^{11}$ and 11×10^{11} according to the direction of the specimen in relation to the crystal axes,[*] whereas the data on p 272 lead to a value of $2\ 6 \times 10^{11}$, and another sample, which I have examined, gave a value of only $0\ 79 \times 10^{11}$ From this it seems clear that the crystals are not firmly united all over as in a metal, and that in fact there is some looseness of structure even in untreated marble The same may indeed also be inferred from the varied behaviour of different samples as regards elastic flexure, and from the fact that they are all to some extent capable of permanent flexure

§ 4 *Warping of Marble*

We have seen in the introduction that some bent specimens of marble are incapable of being completely straightened by the external application of force

Permanent bending or warping may be attributed to unsymmetrical heating The known permanent expansion, if it occurred at one side only, would necessarily have this result To illustrate the matter experimentally, the top surface of a piece of marble was made the bottom of an electric oven, and the under surface was kept cool by immersion in a shallow trough of running water It was found that as expected, the hot side became permanently convex, and the cool one concave The length of one piece used was 40 8 cm., thickness 1 9 cm Heated to 300° C on one side, a marked curvature was developed The sagitta was 1 25 mm. and the radius consequently 16 7 metres

Such bent slabs are not flexible owing to the rigidity of the side that has not been heated They imitate the bent piece of unknown origin which was mentioned in the introductory section, and maintain their curvature when placed with the convex side up and heavily loaded Two such pieces, placed with the concave faces together, are shown in fig 6, Plate 13

[*] Voigt, 'Ann. Physik,' vol 39, p 413, (1890) Quoted by Landolt and Bornstein, Tabellen, vol 1, p. 84

Unilateral heating has already been indicated by Kıestrınger* as a probable cause of the deformation of marble mantelpieces. As we have seen, however, these may become sufficiently baked right through to acquire flexibility In the present experiment, the baking right through is prevented by water cooling, and the curvature is very great compared with that ordinarily seen in mantelpieces.

The curvature developed by unilateral heating is of the order of magnitude to be expected from the permanent expansion on the convex side Let us take the piece above mentioned With length l, expansion dl, and thickness t, we should have

$$\frac{l}{dl} = \frac{r}{t} = \frac{1670}{1\ 9} = 880$$

On the actual length of 40 8 cm this would mean an expansion of 0 465 mm. Actually the expansion of the uniformly baked strip for 300° C was somewhat larger than this, about 1 mm, see table, p 272 Unfortunately the warped piece of marble did not come from the same source as the uniformly baked piece with which it is being compared But even if they had been of identical texture, we must remember that with unilateral heating, while the temperature gradient may be regarded as uniform through the section, the permanent length increases much more rapidly at the higher temperatures (see p 272) Thus the normal expansion (ı e, that which would take place in the absence of constraint) is not able fully to assert itself on the convex side The warped piece is presumably in a state of stress, the convex side being in compression, and the concave in tension

§ 5 *Possible Geological Application*

The possible importance for geology of the permanent change of marble on heating should not be overlooked By examining a laboratory specimen we can determine a limit to the temperature to which it can have been heated since the time when the calcite grains were formed into a compact aggregate as at present. Applying this criterion to the Carrara marble examined, the temperature cannot have risen so high as 77° C, for if this had occurred the specimen should be incapable of showing the elongation and loss of mechanical stiffness which it does show when baked at this temperature But caution is perhaps necessary in applying such conclusions to material which has been at great pressures deep down in the earth's crust.

* "Umschau," vol. 35, p. 436 (1931)
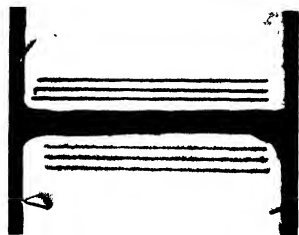
§ 6. *Summary*

Marble which has been baked at a temperature of 100° C or even less has its rigidity diminished This effect becomes increasingly conspicuous up to temperatures of 350° C , when the bending under a given force may become 10 times as great as at first Stress-strain diagrams are given showing hysteresis, the flexure being partly elastic, partly permanent The progressive change of mechanical properties is traced as the baking temperature is increased At the same time the marble becomes permanently elongated, its porosity is increased, as evidenced by the spreading of ink lines ruled on it , and its ultimate strength is diminished.

These results are interpreted as due to the unequal expansion of calcite by heat The expansion is a maximum along the optic axis, and actually negative in the perpendicular direction Thus the shape of each grain changes on heating, and they are no longer able to fit into the initial closely packed mosaic The structure is dislocated and loosened, with increase of volume, and this process is irreversible It is probable that with the moderate forces acting in these experiments, the individual grains are not deformed by slip or twinning, as when metals or marble are caused to flow, but that their elastic deformation, combine with friction in the loosened structure, will account for everything Experiments are described on the warping of marble by unilateral heating, which are also brought under the same general point of view

DESCRIPTION OF PLATE.

Fig 4 —Right Lines on marble in initial condition Left Lines on marble baked at 365° C Indian ink used. Actual size

Fig 5 —The same Writing ink used.

Fig 6 —Two strips of marble warped by heating the (eventually) convex faces to 300° C. and keeping the others at 15° C., water cooled The concave faces are placed together One-third actual size.

The Energies of Alpha and Gamma Rays

By H A. WILSON, F R S, Rice Institute, Houston, Texas.

The energies of disintegration of the radioactive atoms, calculated from the alpha ray energies, may be arranged in pairs having sums which are multiples of 3 85* The following table shows this for the disintegration energies of radium C' The values of the disintegration energies are those given by Rutherford, Lewis, and Bowden† and the unit is 10^5 electron volts

Pairs of Disintegration Energies.   Multiples of 3 85

78 29 +	91 12 = 169 41		3 85 × 44 = 169 40
78 29 +	94 93 = 173 22		3 85 × 45 = 173 25
78 29 +	102 69 = 180 98		3 85 × 47 = 180 95
91 12 +	105 26 = 196 38		3 85 × 51 = 196 35
92 41 +	0 = 92 41		3 85 × 24 = 92 40
94 93 +	105 26 = 200 19		3 85 × 52 = 200 20
96 73 +	99 68 = 196 41		3 85 × 51 = 196 35
96 73 +	103 42 = 200 15		3 85 × 52 = 200 20
100 97 +	107 09 = 208 06		3 85 × 54 = 207 90
102 69 +	105 26 = 207 95		3 85 × 54 = 207 90

The sum of all these pairs is 1825 16, which is equal to $3 \cdot 8506 \times 474$

The following table shows the same thing for pairs of disintegration energies of the other radioactive atoms. The values used are those given by Rutherford, Wynn-Williams, Lewis, and Bowden.‡

Pairs of Disintegration Energies   Multiples of 3 85.

Rn, AcA	55 80 +	75 08 = 130 88		3 85 × 34 = 130 90
Rn, AcCa	55 80 +	67 39 = 123 19		3 85 × 32 = 123 20
RaCa, RaCa₁	56 15 +	55 52 = 111 67		3 85 × 29 = 111 65
RaCa₁, AcCa₁	55 52 +	63 83 = 119 35		3 85 × 31 = 119 35
Ana₁, AcC'	66 65 +	75 81 = 142 46		3 85 × 37 = 142 45
ThA, ThC'	68 97 +	96 61 = 165 58		3 85 × 43 = 165 55
ThC', ThC"	96 61 +	107 41 = 204 02		3 85 × 53 = 204 05
ThC₂₁, ThC'	62 04 +	107 41 = 169 45		3 85 × 44 = 169 40
Po, Ana₁	54 06 +	65 31 = 119 37		3 85 × 31 = 119 35
ThCa	61 64 +	0 = 61 64		3 85 × 16 = 61 60
Ana	69 37 +	0 = 69 37		3 85 × 18 = 69 30

The sum of these pairs is 1416 98, which is equal to 3 8505 × 368   The value 3 8505 agrees almost exactly with the value 3 8506 got from the pairs of radium C' energies.

The following table gives similar pairs of disintegration energies, each pair containing one radium C′ energy and an energy for another atom —

Pairs of Disintegration Energies.   Multiples of 3 85

RaCa	55 52 +	98 44 = 153 96	3 85 × 40 = 154 00
AcC′	75 81 +	78 29 = 154 10	3 85 × 40 = 154 00
AcC′	75 81 +	105 26 = 181 07	3 85 × 47 = 180 95
Ana₁	66 65 +	91 12 = 157 77	3 85 × 41 = 157 85
Ana₁	66 65 +	94 93 = 161 58	3 85 × 42 = 161 70
Ana₁	66 65 +	102 69 = 169 34	3 85 × 44 = 169 40
RaA	61 09 +	96 73 = 157 82	3 85 × 41 = 157 85
ThCa₁	62 04 +	99 68 = 161 72	3 85 × 42 = 161 70
ThC′	96 61 +	84 37 = 180 98	3 85 × 47 = 180 95
ThC′	96 81 +	99 68 = 196 29	3 85 × 51 = 196 35
ThC′	62 04 +	107 41 = 169 45	3 85 × 44 = 169 40
ThCa	61 84 +	92 41 = 154 05	3 85 × 40 = 154 00
Ana	69 37 +	92 41 = 161 78	3 85 × 42 = 161 70

The sum of all these pairs is 2159 91, which is equal to 3 8501 × 561 The sum of all the pairs is 5402 05, which is equal to 3 8504 × 1403   Thus it appears that the above three sets of pairs give values of this constant which differ from the mean value 3 8504 by + 0 0002, + 0 0001, and − 0 0003 respectively, or by less than one part in twelve thousand

The relative values of the disintegration energies are believed to be accurate to about one part in five thousand, but the absolute values may be in error by as much as one part in one thousand.

The constant 3 8504 × 10⁶ electron volts appears to have very exactly the same value for all the radioactive atoms so that it must represent some general atomic property

The gamma ray energies of the different radioactive atoms may also be arranged in pairs having sums which are equal to multiples of a constant which is nearly equal to 3 85   This was shown for radium C′ by the writer in a paper recently communicated to the Royal Society

The relative values of the gamma ray energies for any one substance are known in some cases to about one in one thousand, but the absolute values may be in error by several parts in one thousand

The following table gives the values of the constant, multiples of which are equal to the sums of pairs of the gamma ray energies, for several radioactive bodies —

Substance	Authors of energy determinations	Value of constant
RaC′	Ellis and Skinner, 1924	3 89
RaB	Ellis and Skinner, 1924	3 88
ThB, ThC	Ellis, 1932	3 85
RaC′	Ellis, 1933	3 85
RaB	Ellis, 1933	3 85

It seems probable that the differences between these values and 3 8504 are due to experimental errors in the absolute values   Since the alpha ray energies are believed to be correct to within one part in one thousand it follows that the earlier values of the energies of the RaC′ and RaB rays are too large by about 1%

An exact determination of the energies of any alpha or gamma ray would enable the energies of all the others to be corrected so that the errors in the absolute energies would be no greater than those in the relative energies

A determination of the energies of several beta rays is now in progress in the writer's laboratory, which it is hoped will give the absolute values to within one part in ten thousand

The fact that the alpha and gamma ray energies can be arranged in pairs with sums equal to 3 85n shows that the energies are equal to 3 85$n \pm c_m$, where c_m has a number of different values   It has been shown by the writer[*] that the c's for the alpha rays are approximately equal to the c's for radium C′ It is also found that the c's can be expressed as sums of multiples of the electronic energy levels   The electronic energy levels for the different radioactive atoms do not differ much and the alpha ray energies are not known with sufficient accuracy to enable the small differences between the c's, for alpha rays, due to the differences between the electronic energy levels of the different atoms to be detected

A simple system of energy levels which explains the emission of gamma rays with energies 3 85$n \pm c_m$ is shown in fig 1   Only four values of c_m are shown for simplicity

The fact that the c's are independent of n suggests that the energy levels belong to two separate or only slightly coupled systems and since the c's are related in a simple way to the electronic energy levels it is natural to suppose that the two systems are the nucleus and the electrons as previously suggested by the writer

According to this, then, we have the remarkably simple result that the possible energies of any radioactive nucleus are equal to 3 85n, where $n = 1, 2, 3,$

If a nucleus disintegrates emitting an alpha ray the disintegration energy must be 3 85 $(n - n')$ because the energy before disintegration is 3 85n and 3 85n' after   In the same way when the nucleus emits a gamma ray the energy of the gamma ray will be equal to 3 85 $(n - n')$ The observed energies

include the energy changes of the electronic system $\pm c_m$. The energy transfer may take place, at the moment of emission, between the electrons and the nucleus or between the particle emitted and the electrons. It is impossible at present to distinguish between the two possibilities; in fact, it is doubtful if there is any real difference between them.

The simplest supposition we can make to explain the possible energies $3.85n$ is that the nucleus acts like an elastic sphere which can vibrate with a frequency ν given by $h\nu = 3.85 \times 10^6$ electron volts. The possible energies are then $h\nu (n + \frac{1}{2})$, if we suppose the vibrations are analogous to those of a
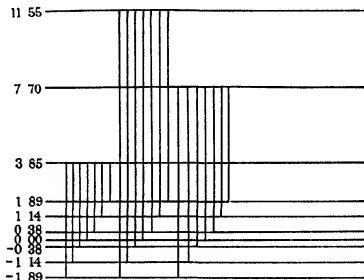
Fig. 1

one-dimensional harmonic oscillator. The frequency must be supposed independent of the mass and charge of the nucleus.

If a nucleus contains only protons and neutrons, then when it emits a beta ray a neutron may be converted into a proton. Possibly a gamma ray splits up into a beta ray and a positron which combines with a neutron. We should expect the beta ray to be emitted with energy $3.85n$ like the alpha and gamma rays and the observed continuous energy distribution of the nuclear beta rays must be attributed to some secondary action such as collisions with the electrons * It may be significant that the average beta ray energy per dis-

---

* The beta rays may either lose energy to or gain energy from the electrons

integration of radium E is about 3 9 × 10⁶ electron volts, which is nearly
equal to 3 85 × 10⁶

Another way of explaining the energies 3 85n is to suppose that 3 85 is the
energy set free when a neutron combines with a proton   The uranium nucleus
may be supposed to contain 119 protons, 119 neutrons, and 27 electrons   The
combination of the protons and neutrons would give energy 119 × 3 85 = 458
This is nearly equal to the total energy emitted in the uranium series of dis-
integrations which is about 45 million electron volts   The change of atomic
weight corresponding to 3 85 × 10⁶ electron volts is 0 00041, and this is a
possible value for the loss of atomic weight when a proton and a neutron
combine to form a deuton, but, of course, the masses of the protons and neutrons
in a nucleus are not equal to their masses in the free state

A theory of nuclear energy differences was suggested by Rutherford and
Ellis [*]   According to this theory there are two main energy levels which, to
explain the energy differences 3 85n ± cₘ, may be supposed here to differ
by 3 85   If there are p_1 alpha particles in the upper level and p_2 in the lower
level, the energy is 3 85p_1 + $f(p_1, p_2)$, where $f(p_1, p_2)$ is a function of p_1 and
p_2 which represents the energy of mutual action between the alpha particles
If n alpha particles drop from the upper to the lower level, the energy change
is

$$3 \ 85n + f(p_1, p_2) - f(p_1 - n, p_2 + n)$$

The differences $f(p_1, p_2) - f(p_1 - n, p_2 + n)$ would then represent the c's
but we should expect these differences to depend on n, whereas the c's in
3 85n ± cₘ are independent of n This theory, therefore, does not seem to
be capable of explaining energy differences 3 85n ± cₘ with c's independent
of n

In a recent paper by Rutherford, Lewis, and Bowden[†] a scheme of
energy levels for the radium C' nucleus is proposed   This scheme gives a large
number of the gamma rays, but it does not seem as well fitted to represent
energy differences equal to 3 85n ± cₘ as the simple scheme suggested
above

The nuclear energy constant 3 85 × 10⁶ electron volts is equal to 6 122 × 10⁷
ergs.   The corresponding wave-length given by 6 122 × 10⁻⁷ = hc/λ is
equal to 3·21 × 10⁻¹⁰ cm   The corresponding wave-number is 3 12 × 10⁹

* ' Proc. Roy. Soc.,' A, vol. 132, p. 667 (1931)

† ' Proc Roy Soc.,' A, vol. 142, p. 347 (1933)

It seems clear that this constant represents some fundamental atomic quantity, the nature of which is as yet uncertain

Summary

It is shown that the energies of disintegration of the radioactive atoms may be arranged in pairs having sums equal to multiples of $3\ 8504 \times 10^6$ electron volts This constant must, therefore, represent some general atomic property, the nature of which is as yet uncertain

---

Two New Properties of Mathematical Likelihood.

By R A Fisher, F R S

1 *Introductory*

To Thomas Bayes[*] must be given the credit of broaching the problem of using the concepts of mathematical probability in discussing problems of inductive inference, in which we argue from the particular to the general; or, in statistical phraseology, argue from the sample to the population, from which, *ex hypothesi*, the sample was drawn Bayes put forward, with considerable caution, a method by which such problems could be reduced to the form of problems of probability His method of doing this depended essentially on postulating a *priori* knowledge, not of the particular population of which our observations form a sample, but of an imaginary population of populations from which this population was regarded as having been drawn at random Clearly, if we have possession of such *a priori* knowledge, our problem is not properly an inductive one at all, for the population under discussion is then regarded merely as a particular case of a general type, of which we already possess exact knowledge, and are therefore in a position to draw exact deductive inferences

To the merit of broaching a fundamentally important problem, Bayes added that of perceiving, much more clearly than some of his followers have done, the logical weakness of the form of solution he put forward Indeed we

[*] ' Phil. Trans.,' vol. 53, p 370 (1763)

are told that it was his doubts respecting the validity of the postulate needed for establishing the method of inverse probability that led to his withholding his entire treatise from publication   Actually it was not published until after his death

If a sample of n independent observations each of which may be classified unambiguously in two alternative classes as " successes " and " failures " be drawn from a population containing a relative frequency x of successes, then the probability that there shall be a successes in our samples is, as was first shown by Bernoulli,

$$\frac{n\,!}{a\,!\,(n-a)\,!}\,x^{a}\,(1-x)^{n-a} \tag{1}$$

This is an inference, drawn from the general to the particular, and expressible in terms of probability   We are given the parameter x, which characterizes the population of events of which our observations form a sample, and from it can infer the probability of occurrence of samples of any particular kind

If, however, we had a priori knowledge of the probability, $f(x)\,dx$, that x should lie in any specified range dx, or if, in other words, we knew that our population had been chosen at random from the population of populations having various values of x, but in which the distribution of the variate x is specified by the frequency element $f(x)\,dx$ of known form, then we might argue that the probability of first drawing a population in the range dx, and then drawing from it a sample of n having a successes, must be

$$\frac{n\,!}{a\,!\,(n-a)\,!}\,x^{a}\,(1-x)^{n-a}\,f(x)\,dx\,, \tag{2}$$

since this sequence of events has occurred for some value of x, the expression (2) must be proportional to the probability, subsequent to the observation of the sample, that x lies in the range dx The postulate which Bayes considered was that $f(x)$, the frequency density in the hypothetical population of populations, could be assumed a priori to be equal to unity

As an axiom this supposition of Bayes fails, since the truth of an axiom should be manifest to all who clearly apprehend its meaning, and to many writers, including us, it would seem, Bayes himself, the truth of the supposed axiom has not been apparent   It has, however, been frequently pointed out that, even if our assumed form for $f(x)\,dx$ be somewhat inaccurate, our conclusions, if based on a considerable sample of observations, will not greatly be affected , and, indeed, subject to certain restrictions as to the true form of $f(x)\,dx$, it may be shown that our errors from this cause will tend to zero as the

sample of observations is increased indefinitely   The conclusions drawn will depend more and more entirely on the facts observed, and less and less upon the supposed knowledge *a priori* introduced into the argument   This property of increasingly large samples has been sometimes put forward as a reason for accepting the postulate of knowledge *a priori*   It appears, however, more natural to infer from it that it should be possible to draw valid conclusions from the data alone, and without *a priori* assumptions   If the justification for any particular form of $f(x)$ is merely that it makes no difference whether the form is right or wrong, we may well ask what the expression is doing in our reasoning at all, and whether, if it were altogether omitted, we could not without its aid draw whatever inferences may, with validity, be inferred from the data   In particular we may question whether the whole difficulty has not arisen in an attempt to express in terms of the single concept of mathematical probability, a form of reasoning which requires for its exact statement different though equally well-defined concepts

If, then, we disclaim knowledge *a priori*, or prefer to avoid introducing such knowledge as we possess into the basis of an exact mathematical argument, we are left only with the expression

$$\frac{n!}{a!\,(n-a)!}\,x^a\,(1-x)^{n-a},$$

which, when properly interpreted, must contain the whole of the information respecting x which our sample of observations has to give   This is a known function of x, for which, in 1922, I proposed the term " likelihood," in view of the fact that, with respect to x, it is not a probability, and does not obey the laws of probability, while at the same time it bears to the problem of rational choice among the possible values of x a relation similar to that which probability bears to the problem of predicting events in games of chance   From the point of view adopted in the theory of estimation, it could be shown, in fact, that the value of x, or of any other parameter, having the greatest likelihood possessed certain unique properties, in which such an estimate is unequivocally superior to all other possible estimates   Whereas, however, in relation to psychological judgment, likelihood has some resemblance to probability, the two concepts are wholly distinct, in that probability is appropriate to a class of cases in which uncertain inferences are possible from the general to the particular, while likelihood is appropriate to the class of cases arising in the problem of estimation, where we can draw inferences, subject to a different kind of uncertainty, from the particular to the general

The primary properties of likelihood in relation to the theory of estimation have been previously demonstrated * In the following sections I propose to exhibit certain further properties arising when the functional properties of the specification of the population fulfil certain special, but practically important, conditions

2 The Distribution of Sufficient Statistics

The essential feature of statistical estimates which satisfy the criterion of sufficiency is that they by themselves convey the whole of the information, which the sample of observations contains, respecting the value of the parameters of which they are sufficient estimates This property is manifestly true of a statistic T_1, if for any other estimate T_2 of the same parameter, θ, the simultaneous sampling distribution of T_1 and T_2 for given θ, is such that given T_1, the distribution of T_2 does not involve θ, for if this is so it is obvious that once T_1 is known, a knowledge of T_2, in addition, is wholly irrelevant, and if the property holds for all alternative estimates, the estimate T_1 will contain the whole of the information which the sample supplies

This remarkable property will be possessed when

$$\frac{\partial}{\partial \theta} \log L,$$

where L is the likelihood of θ for a given sample of observations, is the same function for all samples yielding the same estimate T_1, for on integrating the expression above with respect to θ, it appears that $\log L$ is the sum of two components, one a function only of θ and T_1, and the other dependent on the sample but independent of θ If

$$f(T_1, T_2, \theta) \, dT_1 \, dT_2$$

is the frequency with which samples yield estimates simultaneously in the ranges dT_1 and dT_2, it follows that

$$f(T_1, T_2, \theta) = \phi_1(T_1, \theta) \; \phi_2(T_1, T_2),$$

where the first factor involves T_1 and θ only, and the second does not involve θ The distribution of T_2 given T_1 will therefore be

$$\phi_2(T_1, T_2) \, dT_2 \Big/ \int \phi_2(T_1, T_2) \, dT_2$$

---

* Fisher, ' Proc Camb Phil Soc,' vol 22, p 700 (1925)

the integral being taken over all possible values of T_2, and in this expression the parameter θ is seen not to appear

The condition that $\partial L/\partial \theta$ should be constant over the same sets of samples for all values of θ, which has been shown to establish the existence of a sufficient estimate of θ, thus requires that the likelihood is a function of θ, which, apart from a factor dependent on the sample, is of the same form for all samples yielding the same estimate T The sufficiency of sufficient statistics may thus be traced to the fact that in such cases the value of T itself alone determines the form of the likelihood as a function of θ If a conventional value such as unity is given to the maximum likelihood for any sample, the likelihood is thus expressable as a function of θ and T only, if T is the sufficient estimate We shall use this property in obtaining a general form for the sampling distribution of sufficient statistics

2 1 It will help if we take an illustrative example of this problem. Let the element of frequency in a distribution be given by

$$\frac{1}{\theta!} x^\theta e^{-x} dx$$

where the variate x can take any real value from 0 to ∞, and θ is an unknown parameter greater than -1 Consider the problem of estimating θ from a sample of n values of x

If L is the likelihood of any possible value of θ,

$$\log L = - n \log \theta! + \theta S (\log x) - S (x),$$

and this is maximized for variations of θ, when $\theta = T$, where

$$F (T) = \frac{1}{n} S (\log x),$$

and $F (T)$ is the first differential of the logarithm of the factorial function This is the equation of estimation by the method of maximum likelihood It will be observed that apart from a constant factor the likelihood is expressible as a function of θ and T only, that is

$$L = A \exp \{-n \log \theta! + n \theta F (T)\}$$

so that T is evidently a sufficient estimate

2 2 The sampling distribution of our estimate must evidently be derived from that of the mean of the logarithms of the several values of x in the sample Now the mean value of

$$\frac{x^\theta}{e^x} \log x$$

18

$$\int \frac{1}{\theta!} x^{\theta + \frac{u}{n}} e^{-x} dx = \frac{\left(\theta + \frac{u}{n}\right)!}{\theta!}$$

By the familiar process of expanding the multiple integral in a product of single integrals, the mean value over all samples of

$$e^{u \frac{1}{n} \Sigma (\log x)} = e^{u \cdot \mathcal{F}(T)}$$

is

$$M = \frac{\left\{\left(\theta + \frac{u}{n}\right)!\right\}^n}{\{\theta!\}^n}$$

and this is the characteristic function of

$$\mathcal{F}(T)$$

from which its distribution may be inferred

To determine the probability function knowing the characteristic function M (u) we may use the property of the sine integral

$$\int_0^\infty \frac{\sin u}{u} du = \frac{\pi}{2},$$

writing kt for u it appears that

$$\frac{1}{\pi} \int_0^\infty \sin kt \frac{dt}{t} = \frac{1}{2}$$

when k is positive, and $-\frac{1}{2}$ when k is negative, or that

$$\frac{1}{\pi} \int_0^\infty \{\sin (x - a) t - \sin (x - b) t\} \frac{dt}{t}$$

where $b > a$, is unity when $b > x > a$, and zero when x is less than a or exceeds b.

Consequently the Stieltjes integral

$$\int_a^b df(x) = \frac{1}{\pi} \int_0^\infty \frac{dt}{t} \int_{-\infty}^\infty \{\sin (x - a) t - \sin (x - b) t\} df(x),$$

writing

$$\sin (x - a) t = \frac{1}{2i} \left(e^{it (x-a)} - e^{-it (x-a)}\right)$$

gives us

$$\int_a^b df(x) = \frac{1}{2\pi} \int_0^\infty \frac{dt}{it} \{e^{-iat} M (u) - e^{iat} M (-u) - e^{-ibt} M (u) + e^{ibt} M (-u)\},$$

where $f(x)$ is the probability function of the variate x, and M is its characteristic function

We may note that M (ut) and M $(-ut)$ must be conjugate quantities, which may be written R $\pm$ tI, then

$$- e^{-ibt}\,M(ut) + e^{ibt}\,M(-ut) = 2iR \sin bt - 2iI \cos bt$$

so that the integral takes the real form

$$\frac{1}{\pi} \int_0^\infty \frac{dt}{t} \{R(\sin bt - \sin at) - I(\cos bt - \cos at)\}$$

Where the probability function is differentiable so that

$$df(x) = y\,dx$$

then

$$df(x) = y\,dx = \frac{dx}{2\pi}\int_0^\infty \{e^{-ixt}\,M(ut) + e^{ixt}\,M(-ut)\}\,dt$$

$$= \frac{dx}{\pi}\int_0^\infty \{R\cos(tx) + I\sin(tx)\}\,dt$$

2 4 For the sufficient statistic T, the sampling distribution will therefore be given by

$$df = \frac{dF(T)}{2\pi}\int_{-\infty}^\infty e^{-itF(T)}\,M(ut)\,dt\;,$$

but

$$e^{-itF(T)}\,M' = \frac{L(\theta)}{L\left(\theta + \dfrac{ut}{n}\right)}.$$

hence the distribution may be directly inferred from the nature of the likelihood function in the form

$$df = \frac{F(T)}{2\pi}\,dT\int_{-\infty}^\infty \frac{L(\theta)}{L\left(\theta + \dfrac{ut}{n}\right)}\,dt$$

or

$$\frac{n}{2\pi}F(T)dT\int_{-\infty}^\infty \frac{L(\theta)}{L(\theta + ut)}\,dt$$

where $F(T)$ stands for the second differential coefficient of log (T')

We may illustrate the use of this formula by deriving the limiting forms for extreme values of θ

Near the limit $\theta \to -1$ the general expression

$$\frac{ud\,(F(T))}{2\pi}\int_{-\infty}^\infty \frac{(\theta + ut)\,!}{\theta\,!^n}\,e^{-intF(T)}\,dt$$

may be rewritten, substituting

$$T = -1 + e^{-s}$$
$$\theta = -1 + e^{-\gamma},$$

and, since, as will be apparent, when γ is large, all important contributions will arise from small values of t, the limiting form of our distribution is

$$\frac{ne^s\,dq}{2\pi}\int_{-\infty}^{\infty}\left(1 + \frac{it}{1+\theta}\right)^{-n} e^{ints^2\theta}\,dt$$

Writing t for te^γ we then have

$$\frac{n\,dq}{2\pi}\,e^{(g-\gamma)}\int_{-\infty}^{\infty}(1 + it)^{-n}\,e^{ints(g-\gamma)}\,dt$$

and writing z for $1 + it$

$$e^{-nu}\,\frac{n\,du}{2\pi i}\int z^{-n}\,e^{nzu}\,dz$$

where u stands for $e^{g-\gamma}$, and the integral is taken from $1 - i\infty$ to $1 + i\infty$ or in an open contour passing counter clockwise to the right of the singularity, $z = 0$ Writing ζ for nuz we have

$$\frac{n\,(nu)^{n-1}\,e^{-nu}\,du}{2\pi i}\int \zeta^{-n}\,e^{\zeta}\,d\zeta,$$

where the integral does not now involve the variate u, and is evidently $2\pi i/(n-1)$! The distribution now appears as

$$\frac{1}{(n-1)\,!}\,n^n\,u^{n-1}\,e^{-nu}\,du,$$

in which $e^{g-\gamma}$ may be substituted for u.

The probability integral in this case is given by the χ^2 distribution for $2n$ degrees of freedom. Thus if a sample of 10 had been taken, we have 20 degrees of freedom, and the 5% values are at $\chi^2 = 10\ 851$ and $31\ 410$ [*]   Putting $nu = \frac{1}{2}\chi^2$ the 5% values of u are 0 5426 and 1 5705, whence those of $g - \gamma$ can be obtained, showing that in 90% of samples g will lie between $\gamma - 0\ 6110$ and $\gamma + 0\ 4514$ For given g, therefore, the fiducial probability is 5% that γ exceeds $g + 0\ 6110$, or falls short of $g - 0\ 4514$

At the upper limit where $\theta \to \infty$ we may write

$$T = g^2, \quad \theta = \gamma^2,$$

----

* "Statistical Methods for Research Workers," Table III

and since $g - \gamma$ remains finite for finite values of the probability function

$$\log \frac{T}{\theta} = \frac{2(g - \gamma)}{\gamma}$$

and tends to zero   The general expression for the distribution, which is

$$\frac{nd\left(F(T)\right)}{2\pi} \int_{-\infty}^{\infty} \frac{(\theta + it)!^n}{\theta!^n} e^{-int f(1)} dt,$$

tends to the limiting form

$$df = -\frac{n\,dT}{2\pi T} \int_{-\infty}^{\infty} (t)^{int} e^{-\frac{nt^2}{2t}} T^{-int} dt$$

or substituting for T and θ

$$df = \frac{n\,dg}{\pi g} \int_{-\infty}^{\infty} e^{-2int (g - \gamma)/\gamma} e^{-nt^2/2\gamma^2} dt$$

$$= \sqrt{\frac{2n}{\pi}} e^{-2n(g - \gamma)^2} dg$$

showing that g tends in the limit to be normally distributed about the population value γ with variance $1/4n$ The 5% points of the distribution of g are therefore $\gamma \pm 1\ 645/\sqrt{4n}$, and for a given g the 5% points of the fiducial distribution of γ are $g \pm 1\ 645/\sqrt{4n}$ *

2 5   The interest of this form lies in the possibility of generalizing it for all sufficient statistics   For, let the equation of maximum likelihood have a solution

$$\phi(T) = A$$

where A is a symmetric function of the observations not involving the parameter θ The expression for $\partial/\partial\theta \log L$ must have been of the form

$$C\left\{A\psi'(\theta) - \phi(\theta)\ \psi'(\theta)\right\}$$

where the possible factor C, if not a constant, must be a function of the observations which is expressible as a function of A, if the likelihood is to be expressible as a function of θ and T only

The expression for $\log L$ then must be of the form

$$CA\psi(\theta) - C\int \phi(\theta)\,d\psi(\theta) + B$$

---

* "Statistical Methods for Research Workers," Table I

where B is a function of the observations only   That C a symmetric function of all the observations must be merely the number n in the sample appears from the fact that log L is the sum of expressions involving each observation singly   Hence

$$CA = S(X), \qquad B = S(X_1),$$

where X, X_1, are functions of the individual observations x The likelihood is now the product

$$e^{-n\int \phi(\theta)d\psi(\theta)} e^{\psi(\theta)\ S(X)} e^{S(X_1)}$$

and

$$\frac{L(\psi)}{L(\psi + ut)} = e^{-utS(X)} e^{nF_1(\psi + ut) - nF_1(\psi)}$$

where $F_1(\psi)$ is written for $\int \phi\, d\psi$

But the frequency function of the variate X was given by

$$e^{-F_1(\psi)} e^{\lambda\psi} e^{\lambda_1} \frac{dx}{dX} dX,$$

hence its characteristic function is

$$M(ut) = e^{F_1(\psi + ut) - F_1(\psi)}$$

while that of $S(X)$ is the nth power of this expression, hence the probability that $S(X)$ lies between S_0 and S_1 is

$$\int^{S_1} df = \frac{1}{2\pi} \int_0^\infty \frac{dt}{ut} \left\{ e^{-utS_0} M^n(ut) - e^{utS_0} M^n(-ut) - e^{-utS_1} M^n(ut) + e^{utS_1} M^n(-ut) \right\}$$

$$= \frac{1}{2\pi} \int_0^\infty \frac{dt}{ut} \left\{ \frac{L(\psi, S_0)}{L(\psi + ut, S_0)} - \frac{L(\psi, S_0)}{L(\psi - ut, S_0)} - \frac{L(\psi, S_1)}{L(\psi + ut, S_1)} + \frac{L(\psi, S_1)}{L(\psi - ut, S_1)} \right\}$$

this being the general expression for the probability of any sufficient statistic falling within assigned limits , S_1 and S_0 being the limits of the known function $n\phi$ (T) of the sufficient estimate T

2 6 The property that where a sufficient statistic exists, the likelihood, apart from a factor independent of the parameter to be estimated, is a function only of the parameter and the sufficient statistic, explains the principal result obtained by Neyman and Pearson in discussing the efficacy of tests of significance   Neyman and Pearson introduce the notion that any chosen test of a hypothesis H_0 is more powerful than any other equivalent test, with regard to an alternative hypothesis H_1, when it rejects H_0 in a set of samples having

an assigned aggregate frequency ε when H_0 is true, and the greatest possible aggregate frequency when H_1 is true

If any group of samples can be found within the region of rejection whose probability of occurrence on the hypothesis H_1 is less than that of any other group of samples outside the region, but is not less on the hypothesis H_0, then the test can evidently be made more powerful by substituting the one group for the other Consequently, for the most powerful test possible the ratio of the probabilities of occurrence on the hypothesis H_0 to that on the hypothesis H_1 is less in all samples in the region of rejection than in any sample outside it For samples involving continuous variation the region of rejection will be bounded by contours for which this ratio is constant The regions of rejection will then be required in which the likelihood of H_0 bears to the likelihood of H_1, a ratio less than some fixed value defining the contour

The test of significance is termed uniformly most powerful with regard to a class of alternative hypotheses if this property holds with respect to all of them This evidently requires that the contours defined by the ratio of the likelihood of H_1 and H_0 shall be the same as those defined by the ratios of the likelihood of any two hypotheses in the class If, therefore, T' is a statistic defining these contours, and θ_1, θ_2, , are variable parameters defining the hypothetical populations, the likelihood of any hypothesis must be expressed in the form

$$L = Af(T', \theta_1, \theta_2,)$$

where A is a factor independent of the parameters

The method of estimation by maximum likelihood, when applied to the form above, will yield equations for θ_1, θ_2, , etc

$$\phi_1(T', \theta_1, \theta_2,) = 0,$$
$$\phi_2(T', \theta_1, \theta_2,) = 0,$$

where

$$\phi_s = \frac{\partial}{\partial \theta_s} \log f,$$

and the solutions of these will give estimates of θ_1, θ_2, , which we may designate T_1, T_2, , in the form

$$T_1 = \psi_1(T')$$
$$T_2 = \psi_2(T'), \text{ etc}$$

It is evident, at once, that such a system is only possible when the class of hypotheses considered involves only a single parameter θ, or, what comes to

the same thing, when all the parameters entering into the specification of the population are definite functions of one of their number In this case, the regions defined by the uniformly most powerful test of significance are those defined by the estimate of maximum likelihood, T For the test to be uniformly most powerful, moreover, these regions must be independent of θ, showing that the statistic must be of the special type distinguished as sufficient Such sufficient statistics have been shown to contain all the information which the sample provides relevant to the value of the appropriate parameter θ It is inevitable therefore that if such a statistic exists it should uniquely define the contours best suited to discriminate among hypotheses differing only in respect of this parameter , and it is surprising that Neyman and Pearson should lay it down as a preliminary consideration that " the testing of statistical hypotheses cannot be treated as a problem in estimation " When tests are considered only in relation to sets of hypotheses specified by one or more variable parameters, the efficacy of the tests can be treated directly as the problem of estimation of these parameters Regard for what has been established in that theory, apart from the light it throws on the results already obtained by their own interesting line of approach, should also aid in treating the difficulties inherent in cases in which no sufficient statistic exists

3 A Second Class of Parameters for which Estimation need Involve no Loss of Information

In the case of sufficient statistics the likelihood function is, apart from a constant factor, the same for all sets of observations which yield the same estimate by the method of maximum likelihood A second case, of somewhat wider practical application, occurs when, although the sets of observations which provide the same estimate differ in their likelihood functions, and therefore in the nature and quantity of the information they supply, yet when samples alike in the information they convey exist for all values of the estimate and occur with the same frequency for corresponding values of the parameter

The nature of the correspondence may be stated as follows If x_1, , x_n stands for a sample of n values of a variate x, the distribution of which is conditioned by a parameter, θ, then for any value of θ, there will be a definite probability

$$p(x, \theta)$$

of the occurrence of a variate less in value than x.

If, therefore, we take any other value of the parameter, say ϕ, there will, with continuous variates, always exist a series of observational values, y, corresponding to the original series x, such that

$$p(y, \phi) = p(x, \theta)$$

The samples x and y will, however, only correspond in the sense required for our present purpose if corresponding to any possible value, θ, a value, ϕ, can be found so that the relationship above holds for all values of x If, in fact, the equation were solved for y, in the form

$$y = f(x, \theta, \phi)$$

it is required that f shall be of the form

$$f(x, \theta, \phi) = F(x, \Omega) \tag{3}$$

where Ω is a function of θ and ϕ, independent of the observations, and such that for any possible values of θ and Ω there exists a corresponding value of ϕ Stated symmetrically it is required that some function of x and y can be equated to a function of θ and ϕ

The typical case of such a relationship occurs in parameters of location If the distribution of the variate x involves a parameter θ, such that the frequency with which x falls in any element dx of its range is a function of $(x - \theta)$, then θ may be called a parameter of location   In such a case the functional relationship (3) may be written

$$x - y = \theta - \phi$$

and is clearly of the form required

Let us take an example in which there is no sufficient estimate, and in which the loss of information in estimating the unknown parameter even by the method of maximum likelihood is considerable The distribution of x is a double exponential curve, the probability of x falling in the range dx, being

$$\tfrac{1}{2} e^{-|x-\theta|} dx$$

The logarithm of the likelihood is

$$-S|x-\theta|,$$

and this increases when θ is increased only if more observations are greater than those less than θ The likelihood is therefore maximized if the number of observations is odd, by equating θ to the median observation , if the number

of observations is even the likelihood is constant when θ has any value between the two central observations

For a sample of an odd number, $n = 2s + 1$ of observations, the sampling distribution of the median is determinate, and the loss of information, if we use the median as an estimate, unsupplemented by the ancillary information which the sample contains, may be calculated. For, if the central observation lies at a distance u from the centre of the distribution, u being supposed positive, then the s highest values observed must each have fallen in a region comprising only

$$\tfrac{1}{2}e^{-u}$$

of the total frequency, while the s lowest values have fallen in the remaining region comprising

$$1 - \tfrac{1}{2}e^{-u}$$

of the total Finally, the probability of the median itself falling in the range du is

$$\tfrac{1}{2}e^{-u}\,du,$$

so that compounding the independent probabilities into which the event has been analysed we have

$$df = \frac{(2s+1)!}{(s!)^2} \cdot (\tfrac{1}{2}e^{-u})^s\,(1 - \tfrac{1}{2}e^{-u})^s\,\tfrac{1}{2}e^{-u}\,du$$

as the probability of the median having a positive sampling error, u As s is increased without limit we may write

$$u\sqrt{n} = t,$$

and the distribution tends to the limit

$$df = \frac{1}{\sqrt{2\pi}}\,e^{-\tfrac{1}{2}t^2}\,dt$$

The amount of information derivable from a large sample of n thus tends to equality with n, as the size of the sample is increased   Since the information supplied by the independent observations is additive,[*] each must supply one unit, and a sample of $2s + 1$ observations must contain $2s + 1$ units of information   The quantity elicited by using the median, i e, by replacing the $2s + 1$ observations from the distribution

$$df = \tfrac{1}{2}\,e^{-|x-\theta|}\,dx,$$

* Fisher, 'Proc Camb Phil Soc' vol 22, p 700 (1925)

by a single observation from the distribution

$$df = \frac{(2s+1)!}{(s!)^2\, 2^{2s+1}} e^{-s|u-\theta|} (2 - e^{-|u-\theta|})^s\, e^{-|u-\theta|}\, du,$$

may be calculated from the mean value of

$$\left(\frac{d}{d\theta} \log \frac{df}{du}\right)^2,$$

or of

$$\left(s - \frac{se^{-|u-\theta|}}{2 - e^{-|u-\theta|}} + 1\right)^2.$$

When s exceeds unity the average values may be evaluated from the consideration that

$$\int_0^\infty \frac{(2s+1)!}{(s-1)!\,(s+1)!\, 2^{2s+1}} e^{-(s-1)u} (2 - e^{-u})^{s-1}\, e^{-u}\, du$$

represents the probability that at least $s+2$ observations have positive, and only $s-1$ observations negative, deviations, and may therefore be equated to

$$\tfrac{1}{2} - \frac{(2s+1)!}{s!\,(s+1)!\, 2^{2s+1}}$$

The mean value of $e^{-|u-\theta|}/(2 - e^{-|u-\theta|})$ is therefore found to be

$$\frac{s+1}{s}\left(1 - \frac{(2s+1)!}{s!\,(s+1)!\, 2^{2s}}\right)$$

Similarly, the mean value of $e^{-2|u-\theta|}/(2 - e^{-|u-\theta|})^2$ is

$$\frac{(s+1)(s+2)}{s(s-1)}\left(1 - \frac{(2s+1)!}{s!\,s+1!\, 2^{2s}} - \frac{(2s+1)!}{(s-1)!\,(s+2)!\, 2^{2s}}\right)$$

The amount of information provided by the median of $2s+1$ observations is therefore

$$(s+1)^2 - 2s(s+1)\,\frac{s+1}{s} + s^2\,\frac{(s+1)(s+2)}{s(s-1)}$$

$$+ 2(s+1)^2\,\frac{(2s+1)!}{s!\,(s+1)!\, 2^{2s}} - \frac{s(s+1)(s+2)}{s-1}\,\frac{(2s+1)!}{s!\,(s+1)!\, 2^{2s}}$$

$$- \frac{s(s+1)(s+2)}{s-1}\,\frac{(2s+1)!}{(s-1)!\,(s+2)!\, 2^{2s}}$$

or

$$\frac{(s+1)(2s+1)}{(s-1)} \left\{ 1 - \frac{(2s)\,!}{(s\,!)^2\, 2^{2s-1}} \right\}$$

In the special case, $s = 1$, the general method fails, and a direct integration yields the value

$$12 (\log 2 - \tfrac{1}{2}),$$

which is the limit to which the general expression tends as $s \to 1$

The median is an efficient estimate in the sense of the theory of large samples, for the ratio of the amount of information supplied to the total available tends to unity as the sample is increased   Nevertheless, the absolute amount lost increases without limit   As s increases, this amount lost,

$$2s + 1 - \frac{(s+1)(2s+1)}{s-1} \left\{ 1 - \frac{2s\,!}{(s\,!)^2\, 2^{2s-1}} \right\},$$

may be replaced by

$$\frac{2(2s+1)}{s-1} \left(\frac{s+1}{\sqrt{\pi(s+\tfrac{1}{4})}} - 1 \right)$$

approximately, or by $4(\sqrt{s/\pi} - 1)$ Thus with $s = 314$, for a sample of 629 observations, the loss of information is near to 36 units, or the value of about 36 observations

It is a matter of no great practical urgency, but of some theoretical importance, to consider the process of interpretation by which this loss can be recovered   Evidently, the simple and convenient method of relying on a single estimate will have to be abandoned   The loss of information has been traced to the fact that samples yielding the same estimate will have likelihood functions of different forms, and will therefore supply different amounts of information   When these functions are differentiable successive portions of the loss may be recovered by using as ancillary statistics, in addition to the maximum likelihood estimate, the second and higher differential coefficients at the maximum.   In general we can only hope to recover the total loss, by taking into account the entire course of the likelihood function

In our particular problem the curve of likelihood is a succession of exponential arcs, having n discontinuities at the values of the n observations of the sample, the exponent changing by -2, as each observation is passed in a positive direction   For the same value of our estimate, the median observation, this function will have very different forms according to the length of the intervals which separate the median from its successive neighbours   Any samples, however, in which these $n - 1$ intervals are the same will have the same

likelihood function. More explicitly the likelihood of the parameter having a value ϕ as judged from the series of observations y_1, , y_n will be equal to the likelihood of its value being θ as judged from the series x_1, , x_n, if

$$x - y = \theta - \phi$$

for each pair of observations in the pair of samples

We may specify the configuration of a sample by a series of positive non-decreasing numbers a_1, , a_s representing the positive deviations from the median of the s largest observations, and a second series of positive non-decreasing numbers a'_1, , a'_s, representing the excesses of the median over the s smallest observations, so that if T is the median value the n observations are represented by $T - a'_s$, , $T - a'_1$, T, $T + a_1$, , $T + a_s$.

The probability of occurrence of any series of observations, the true centre of the distribution being θ,

$$L\,dx_1, \quad , dx_n$$

may now be written

$$n\,!\;L\;\frac{\partial\,(x_1 \quad x_n)}{\partial\,(T,\,a_1 \quad a_s,\,a'_1 \quad a'_s)}\,dT\,da_1 \quad da_s\,da'_1 \quad da'_s,$$

$$= n\,!\;L\;\;dT\,da_1 \quad da_s\,da'_1 \quad da'_s,$$

where, if, for example, θ lies between $T - a'_p$ and $T - a'_{p-1}$

$$L = \frac{1}{2^n}\,e^{-(2p-1)\,(T-\theta)-S'_1\,(s+e)+\Sigma\,(s_1+\ \ +s_{p-1})}$$

Given the configuration of the sample, therefore, the probability that T lies in a range dT, between the limits $\theta + a'_{p-1}$ and $\theta + a'_p$ is

$$df = \frac{1}{A}\,e^{\Sigma\,(s_1+\ \ +s_{p-1})}\,e^{-(2p-1)\,(T-\theta)}\,dT$$

of which the integral between these limits is

$$\frac{1}{(2p-1)\,A}\,e^{\Sigma\,(s_1+\ \ +s_{p-1})}\,(e^{-(2p-1)\,\theta\,a'_{p-1}} - e^{-(2p-1)\,\theta\,a'_p}),$$

and A is equal to the sum of all such integrals

$$1 - e^{-a'_1} + \tfrac{1}{3}\,(e^{-a_1} - e^{2a_1 - 3a_1}) + \tfrac{1}{5}\,(e^{2a_1 - 3a_1} - e^{3a_1 + 2a_1 - 5a_1}) +$$
$$+ 1 - e^{-a_1} + \tfrac{1}{3}\,(e^{-a_1} - e^{2a_1 - 3a_1}) + \tfrac{1}{5}\,(e^{2a_1 - 3a_1} - e^{3a_1 + 2a_1 - 5a_1}) +$$

Apart from the details of the analysis, however, it is apparent that *if attention is confined to samples having a given configuration the sampling distribution of*

T for a given θ is found from the likelihood of θ for a given T, the probability curve in the first case being the mirror image of the likelihood curve in the second

To evaluate the amount of information supplied by this distribution we must evaluate the mean square of

$$\frac{d}{d\theta} \log \frac{df}{dT}$$

Now, if T lies between $\theta + a'_{s-1}$ and $\theta + a'_s$,

$$\log \frac{df}{dT} = -(2p-1)(T-\theta)$$

so that in this case

$$\left(\frac{d}{d\theta} \log \frac{df}{dt}\right)^2 = (2p-1)^2,$$

and the amount of information supplied by our estimate, *in conjunction with a specification of the configuration of the sample from which it was obtained*, is

$$\frac{1}{A} \{ 1 - e^{-a_1} + 3(e^{-a_1} - e^{2a_1(-3a_1)}) + 5(
\\ + 1 - e^{-a_1} + 3(e^{-a_1} - e^{2a_1-3a_1}) + 5(\qquad \}$$

This value will differ greatly from sample to sample. Thus, if a_1 and a'_1 were both large, so that the median lies in a considerable range otherwise unoccupied by observations, the amount of information approaches unity, at the other extreme if a_s and a'_s were both so small that e^{-a_s} is near to unity, then

$$A \to 2/(2s+1),$$

and the amount of information rises to $(2s+1)^2$, or n^2

To find the average value of the amount of information derivable from the median, in conjunction with the configuration of the sample, we may note that the probability for a given configuration that $s + p$ observations shall exceed, and $s - p + 1$ fall short of the true value is

$$\frac{1}{(2p-1)A} (e^{2a_1+2a_1+ \quad -(2p-1)a_{p-1}} - e^{2a_1+2a_1+ \quad -(2p-1)a'_p})$$

and that the amount of information is obtained by multiplying this probability by $(2p-1)^2$ and adding for all values of p

The average information for all configurations may, therefore, be found from the total probability for all configurations that exactly $s + p$ observations

shall exceed the true value, since the probability of exceeding θ is $\frac{1}{2}$ independently for each observation, the probability is

$$\frac{1}{2^n} \frac{n!}{(s+p)!\,(s-p+1)!}$$

and this, multiplied by $(2p-1)^2$, and added for all values of p, will give the average amount of information. The probabilities are the terms of the expansion of

$$(\tfrac{1}{2} + \tfrac{1}{2})^n,$$

and $(2p-1)$ is twice the deviation from the mean corresponding to each value of p. The variance of the binomial is well known to be exactly $\frac{1}{4}n$, and the average amount of information used is consequently found to be exactly n, equal to the total amount known to be contained on the average in the sample.

The process of taking account of the distribution of our estimate in samples of the particular configuration observed has therefore recovered the whole of the information available. This process will seldom be so convenient as the use of an estimate by itself, without reference to the configuration, for instead of replacing the n observations by a single value, we now have to take account of all their values individually. Actually, indeed, in this case only the central group of values matters greatly, but in general the theoretical process illustrated here uses the available information exhaustively, only at the expense of abandoning the convenience of disregarding all properties of the sample beyond the best estimate it can provide. The reduction of the data is sacrificed to its complete interpretation.

The frequency distribution, which makes this complete interpretation possible, is the mirror image of the likelihood function. Thus if T_1 is the estimate (the median) derived from the actual sample observed, and L $(\theta - T_1)$ is the likelihood derived from this sample of any value of θ, then the sampling distribution of T for any value of θ, in samples of the same configuration is given by

$$df \propto \text{L} \, (\theta - \text{T}) \, d\text{T}.$$

This is an extremely simple derivation of the sampling distribution of the estimate of maximum likelihood from the form of the likelihood function.

4 *The Simultaneous Estimation of Location and Scaling*

In a very frequent class of cases not only the origin but the scale of the distribution is also represented by a parameter to be estimated from the observations. The frequency element is then of the form

$$f(\xi)\, d\xi,$$

where

$$\xi = \frac{x - \theta_1}{\theta_2}$$

In such cases it is obvious that the sample of values ξ in relation to any values α_1 and α_2 of the parameters corresponds in the sense of section 3 to the sample of values of x in relation to the values $\theta_1 + \alpha_1\theta_2$ and $\theta_2\alpha_2$, and a double series of samples exists corresponding to any sample observed

The samples will have all the same configurations in the sense that supposing any two observations of the sample, such as the lowest and the lowest but one in value, have values a, $a + b$ then the other members of the sample will be

$$a + bt_p, \qquad p = 1, \qquad , n - 2,$$

where the $n - 2$ values of t_p specify the configuration, and are the same for all samples of which the configuration is the same

The frequency element

$$L dx_1, \qquad dx_n,$$

giving the frequency with which the n observations fall within assigned values, may then be replaced by

$$L \frac{\partial (x_1, \quad x_n)}{\partial (a, b, t, \quad t_{n-2})} da \, db \, dt, \qquad dt_{n-2},$$

where the Jacobian is simply

$$\begin{vmatrix} 1 & 0 & 0 & & 0 \\ 1 & 1 & 0 & & 0 \\ 1 & t_1 & b & & 0 \\ & & & & \\ & & & & \\ 1 & t_{n-2} & 0 & & b \end{vmatrix}$$

or b^{n-2} The simultaneous frequency distribution of a and b is therefore given by

$$df \propto L b^{n-2} \, da \, db$$

Now, it is evident that the estimates of θ_1 and θ_2 from such a sample will be

$$T_1 = a + \lambda b,$$
$$T_2 = \mu b,$$

where λ and μ depend only on the configuration of the sample Hence

$$\frac{\partial\,(\mathbf{T_1},\,\mathbf{T_2})}{\partial\,(a,\,b)} = \begin{vmatrix} 1 & 0 \\ \lambda & \mu \end{vmatrix} = \mu$$

and the distribution of these estimates in samples of the same configuration will be

$$df \propto \mathrm{L}\,\mathbf{T_2}^{n-2}\,d\mathbf{T_1}\,d\mathbf{T_2}, \tag{4}$$

where in L, $\mathbf{T_1} + u_p\mathbf{T_2}$ is substituted for x_p, $p = 1$, , n, the n values of u being known for the configuration observed

If, therefore, we choose to take into account not merely the sampling distribution of our estimates for samples of all configurations, distributions which will involve, apart from the parameters of the population, only these two statistics, but rather the special simultaneous distribution for the particular configuration observed, we may obtain this special distribution directly from the form of the likelihood function

Since, moreover, the whole course of the likelihood function is taken into account, it is, from this point of view evident that no information can be lost An independent analytical proof of this is as follows , it is equally applicable to information in respect of θ_1 and of θ_2.

The information respecting θ_1 contained in a single observation from the distribution (4) is numerically equal to the average value of

$$\left(\frac{\partial}{\partial\theta_1}\log \mathrm{L}\right)^2$$

for all values of $(\mathbf{T_1} - \theta_1)$ from $-\infty$ to ∞, or, otherwise, to the average value of

$$\left\{\frac{\partial}{\partial\theta_1}\mathrm{S}\,(\log f)\right\}^2$$

where $f(x - \theta_1)$ is the frequency of an observation falling in the range dx The average for all values of $\mathbf{T_1}$ is, for any particular observation, the average for all values of x Now the average value of

$$\frac{\partial}{\partial\theta_1}\log f$$

is zero, for

$$\int_{-\infty}^{\infty}\frac{\partial}{\partial\theta_1}\log f\;f\,dx = \int_{-\infty}^{\infty}\frac{\partial f}{\partial\theta_1}\;dx$$

which is zero, since the total frequency is unity, independent of θ_1 But the average value for all values of $(\mathbf{T_1} - \theta_1)$ and for all configurations including

variations of T_2, is the average value for all possible samples   We may apply this principle to the expression

$$S^2 \left(\frac{\partial}{\partial \theta} \log f \right)$$

when all the values of x are independent   Then the average value of the square of the sums of n terms, independent and all having a mean value zero, is n times the mean square of each of them, or n times the mean value of

$$\left(\frac{\partial}{\partial \theta_1} \log f \right)^2$$

for all values of x from $-\infty$ to ∞, which is, by definition, the amount of information supplied by a sample of n observations. Hence the average amount of information respecting θ_1 supplied by (4) for all configurations is the entirety of that supplied by the data

With respect to θ_2, we require the average value of

$$S^2 \left(\frac{\partial}{\partial \theta_2} \log f \right)$$

for all values of T_2 from 0 to ∞ The average of this for all configurations and for all values of T_1, again reduces to the mean value of

$$n \left(\frac{\partial}{\partial \theta_2} \log f \right)^2$$

for all values of x from $-\infty$ to ∞, and so to the average amount of information contained in a sample of n observations

Summary

(I) Reasons are given for the use of mathematical likelihood in problems of inductive inference

(II) When a statistic exists, satisfying the criterion of sufficiency, the likelihood function involves only that statistic

(III) An example is given of a sufficient statistic, and its sampling distribution is expressed in terms of the likelihood function

(IV) This property is generalized for all cases of simple estimation, where a sufficient statistic exists

(V) It is shown that these cases and only these supply tests of significance of the kind termed by Neyman and Pearson " uniformly most powerful " with regard to a class of alternative hypothesis

(VI) Where no sufficient statistic exists the precision of estimation may in general be enhanced by the use of ancillary statistics A class of cases is defined and illustrated in which the totality of the ancillary information supplied by the observations may be utilized

(VII) This process gives a very simple derivation of sampling distributions, in which there is no loss of information, even for small samples.

The Electrical Condition of Hot Surfaces during the Adsorption of Gases Part V —The Charging up of Hot Surfaces

By J C Stimson, Imperial College of Science and Technology

Introduction

The investigation into the electrical condition of hot surfaces has consisted mainly of measurements of (a) the steady equilibrium potentials acquired by such surfaces when heated in a vacuum or in contact with various gases, and (b) the rates at which these potentials build up after earthing The previous communications of this series* have dealt with the steady potentials exhibited by gold, silver, nickel, platinum, carbon, and copper surfaces under varying conditions During the course of these experiments the rates of attainment of the steady potentials were also observed and recorded, and are described below The results with the silver sheet, however, have been omitted for reasons which have already been given. Certain general regularities in the results have been distinguished, whereby much light is thrown on the nature and mechanism of the processes taking place at the interface between solid and gas phases It has now been found possible to advance a more complete explanation of the changes occurring on the surfaces and which give rise to their electrical charging up as observed in these researches It also gives information, which is of fundamental importance, on the subject of the role played by hot surfaces in heterogeneous catalytic reactions.

---

* ' Proc Roy Soc.,' A, vol. 116, p 379 (1927), vol 120, p 235 (1928), vol 124, p 356 (1929), and vol. 132, p 192 (1931)

Experimental

The apparatus employed has been described for the most part in sufficient detail in the earlier communications   The addition of a number of multi-vane variable air condensers, each of 0 001 microfarad capacity in parallel to the surface-electrometer-earth system made it possible to vary the capacity of any surface to earth within suitable limits   The condensers, connecting leads, and switches were completely enclosed in an earthed metallic shielding as a protection against spurious electrical effects from external sources.   The
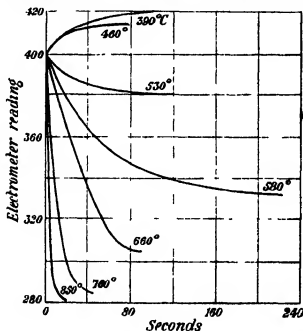
Fig 1

condensers were calibrated against a Dubilier standard condenser, while the capacities of the surface-electrometer systems were determined by the method of mixtures, one of the variable air condensers serving as a sub-standard

The Rate of Charging Up —The rates of charging up of the surfaces were calculated from the observed electrometer readings at suitable time intervals starting from zero potential, i e., at the moment of re-insulation of the surface-electrometer system after earthing   The general type of the curves connecting the readings of the electrometer with time is shown in fig 1   These were obtained in the course of experiments with the nickel sheet in contact with oxygen at a constant capacity of 1020 cm (Part II, Series C, and the present paper, Series B), and they represent the general characteristics of the manner in

which the hot surfaces charge up to the equilibrium potentials   The slope of
such curves gives a measure of the current (i) flowing from the surface at any
instant, and can be calculated by the equation

$$i = C \; dv/dt, \tag{1}$$

where C is the capacity of the surface-electrometer system, dt is the interval
of time between two electrometer readings, and dv is the corresponding incre-
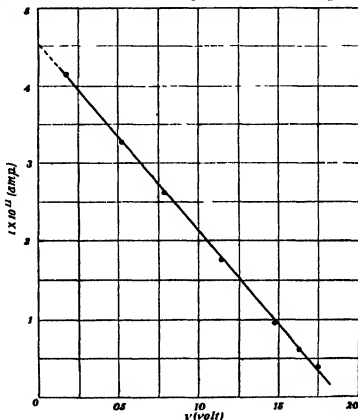
Fig 2

ment of potential   The current thus obtained was taken to correspond to
the potential at the middle of the time interval   This method of calculation
was also used by Richardson and Brown[*] in their experiments on the kinetic
energy of electrons and positive ions emitted from hot bodies by measuring
the rate of charging up of a neighbouring electrode.   Values calculated in
this way using equation (1) for the nickel surface in contact with oxygen at
580° C, from the charging up curve given in fig 1, have been plotted in fig 2

* 'Phil Mag,' vol 16, p 353 (1908), vol 17, p. 355 (1909), and vol 18, p 649 (1909)

The relationship between the momentary current flowing from the surface (i) and the potential of the surface at the same time (v) is very nearly linear, and can be represented by an equation of the general type

$$i = i_0 - av,   (2)$$

where i_0 is the value of i when $v = 0$, i e, the instantaneous value of the current flowing from the surface at the moment of insulation from earth, and a is a constant equal to the slope of the straight line   These calculations have been applied to a large number of the experimental results and the approximately linear relation between the current from the surface at any time during the charging up process and the mean potential of the surface during the same time has always been obtained   Richardson and Brown also found that there was a tendency for the current to be a linear function of the potential, especially after a long period of heating in a vacuum, or at a high temperature   The current flowing from the surface is zero when its potential has reached the limiting value, V, under the given experimental conditions.

The rates of charging up in Series A to E recorded below have been expressed as values of i_0, i e, the instantaneous maximum current flowing from a surface just as it is insulated from earth   Two methods were employed in this investigation for the evaluation of i_0 (a) the straight line obtained by plotting i against v in the manner outlined above was extrapolated to the axis of i to give the value of i_0, (b) it could also be calculated from I the average or mean rate of charging up to a potential equal to half the limiting value (V/2)   It can be shown that

$$I = CV/2t = \tfrac{1}{2}i_0,$$

where t is the time in seconds required to attain half the limiting potential, in volts, in an electrometer system of capacity C, in farads   The values of i_0 are independent of the actual capacity of the surface-electrometer systems as the rate of increase of potential on the surface was always found to vary inversely with capacity

As the rate of charging up of a surface in any given experiment can be expressed in the form of an equation of the first degree, it follows that it has been completely and fully represented in terms of the equilibrium potential, V, and the maximum rate of charging up, i_0

Equation (2) can be rewritten in the form

$$C   dv/dt = a (V - v),$$

where C is the capacity of the surface-electrometer system, V is the final

steady value of the surface potential, and v is the momentary potential at any time t By integrating and re-arranging terms this becomes

$$v = \mathrm{V}\,(1 - e^{-at/C})$$

The fact that the variation with time of the potential acquired by a surface could be represented by a function of this form has also been indicated by independent work in these laboratories *

Experimental Results

It has been repeatedly confirmed throughout the course of this investigation that the magnitude of the steady surface potential in contact with a gas was independent, within the limits of experimental error, of the gaseous pressure between 100 mm and atmospheric pressure In a similar way it has been found that within this range the rate of charging up of a surface to the steady potential characteristic of the given experimental conditions does not depend on the pressure The results given below have been confined to experiments with single gases, as those with reacting mixtures require more detailed examination especially in connection with their rates of interaction

Series A Experiments with the Gold Sheet – The surface potential results of this series of experiments have been previously described in Part I (Series C) The rates of charging up, as expressed by t_0, for this surface are recorded against temperature up to 850° C (*in vacuo* and in contact with hydrogen, oxygen, argon, carbonic oxide, and nitrogen) in fig 3 The dotted portion of the oxygen curve is that over which the potential was changing from a positive to a negative value and where it is very difficult to obtain reproducible results

On admitting a gas into contact with the heated gold sheet when it was exhibiting the appropriate *in vacuo* surface potential, it has been shown that the latter gradually gave place to the potential characteristic of the particular gas during a period of time which was dependent on the nature of the gas It has also been found that this change is accompanied by a gradual and similar alteration in the rate of charging up, while removal of a gas by evacuation produces the same type of change in the reverse direction This behaviour has been confirmed in the experiments with the other surfaces, the appropriate change in the rate of charging up always accompanying such an alteration in the experimental conditions

Series B Experiments with the Nickel Sheet —The variations in the rates of charging up of the nickel sheet with temperature, corresponding to the surface

* Bradford, " Dissertation, Ph D ," London (1931)

potentials determined in Part II (Series C, D, and F), are given in fig. 4 The curves recorded are for hydrogen, *in vacuo*, carbonic oxide, oxygen, argon, and nitrogen

Series C Experiments with the Platinum Sheet—The results correspond to the surface potential experiments described in Part III (Series A, B, and C) In the experiments with the platinum sheet heated only to a maximum tempera-
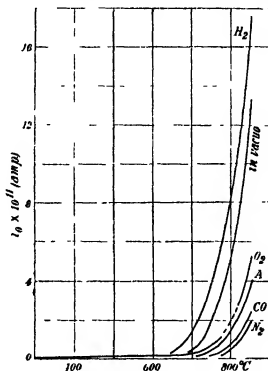
Fig 3.

ture of 500° C the values of i_0 were very small, even at 500°, thus hydrogen (1), 0 04 $\times$ 10^{-11} amp , *in vacuo*, 0 33 $\times$ 10^{-11} amp , and hydrogen (2), 0 04 $\times$ 10^{-11} amp. In the series up to 660° the rates of charging up at 660° were *in vacuo* (1), 0 79 $\times$ 10^{-11} amp , hydrogen, 0 80 $\times$ 10^{-11} amp , oxygen, 0 76 $\times$ 10^{-11} amp , and *in vacuo* (2), 2 00 $\times$ 10^{-11} amp Similar measurements were carried out during the series of experiments up to 850° and are recorded in fig 5

Series D Experiments with the Carbon Rod—The rates of charging up of the carbon rod corresponding to the potential measurements recorded in Part IV (Series A) are plotted against temperature in fig 6 Most of the values

of i_0 have been given only over the lower part of the temperature range (up
to 90×10^{-11} amp.), as at higher temperatures the increases were so very
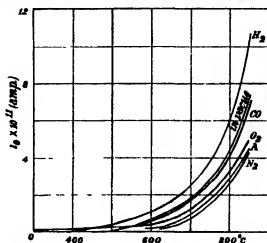
Fig 4
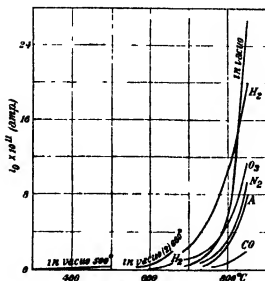
Fig 5

rapid that i_0 was, for the most part, beyond the limits of accurate experi
mental measurement.

Series E. Experiments with the Copper Sheet.—The rates of charging up in
the following experiments, already described in Part IV (Series B), with the

copper sheet are recorded in fig 7   in vacuo and hydrogen up to 520°,   in vacuo and hydrogen up to 660°, and in vacuo, hydrogen, nitrogen, and carbonic oxide up to 850°

Series F   Experiments on the Rate of Leak of a Potential applied to a Hot Surface —A large number of experiments have been carried out with the surfaces so far examined under various conditions of temperature and gas pressure, in which the rate of leak of an applied potential was determined   The
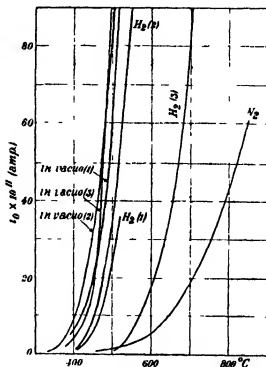
Fig 6

experimental procedure was as follows   The potential of the surface-electrometer system was brought to a known positive or negative value whereupon it was left insulated while electrometer readings at suitable time intervals were observed   It was found that the potential of the system always changed in a gradual and uniform manner, from the applied value to that characteristic of the surface under the given experimental conditions. The rates at which applied voltages of + or − 1, 2, and 4 volts leaked away from a heated gold gauze in contact with oxygen, recorded in fig 8, illustrate the general nature of these changes
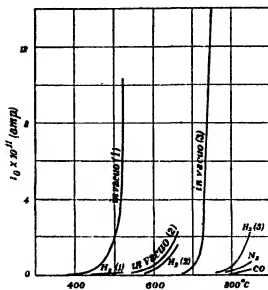
Fig 7
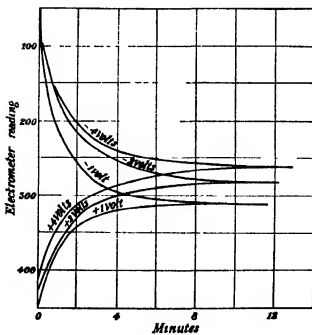
Fig 8

Bangham and Lewis* have investigated the effect of gases on the electrical charges developed by heated metals, and have found, in experiments similar to those described in this series, that the mode of approach to the equilibrium potential was widely different according to whether equilibrium value was approached from the positive or from the negative side   In the latter method, they found that the rate of change was a highly sensitive function of the momentary potential ; in the former it was markedly insensitive, the rate being nearly uniform   It has not been found possible, during the course of the present investigation, to reproduce Bangham and Lewis' results ; in fact, smooth and regular changes of the type shown in fig 8 have been obtained in every experiment so far carried out   It might be suggested that Bangham and Lewis had not been entirely successful in overcoming all the experimental difficulties to be met with in measurements of this nature

Discussion of the Results

The most important facts revealed by a study of the rates of charging up of the various surfaces are as follows —

(a) When the rates of charging up, expressed as values of t_0, for the gold, nickel, and platinum surfaces at 850° C are tabulated as in Table I, it is seen that they fall naturally into a group exhibiting certain well-defined features

Table I —(Multiplied by 10^{11})

Surface	H_2.	in vacuo	O_2	A	CO	N_2.
Platinum	20 00	26 67	11 27	8 00	2 00	9 33
Gold	17 60	13 33	5 33	4 03	2 53	2 00
Nickel	10 60	7 36	5 00	4 53	7 07	4 32

This shows that the rates of charging up for the platinum sheet were larger throughout than those for gold or nickel except in contact with carbonic oxide where the order was completely reversed   It is quite reasonable to suspect that the low rate for platinum under these conditions is probably connected with the well-known poisoning effect of carbonic oxide on platinum catalysts,† whilst the higher rate for nickel in contact with carbonic oxide is associated with the method of attachment of these molecules to the surface as indicated in Part II   For the gold and nickel sheets, beyond the fact that the rates in

* 'J Chem Soc ,' p. 1140 (1929)
† Rideal and Taylor, " Catalysis in Theory and Practice," p 133 (1926).

contact with hydrogen and *in vacuo* always exceeded those in contact with other gases, no general regularity seems to exist

(b) In the experiments with the carbon rod the rates of charging up were very large compared with those considered in (a) Thus, with the carbon rod *in vacuo* (3) $i_0 = 93 \cdot 3 \times 10^{-11}$ amp at 500° and was rising extremely rapidly , in contact with hydrogen (3) $i_0 = 86 \cdot 7 \times 10^{-11}$ amp at 700° and was likewise rising rapidly , in contact with nitrogen $i_0 = 62 \cdot 0 \times 10^{-11}$ amp at 850° Even this latter value was nearly seven times greater than the corresponding rate for the platinum sheet The apparent area of the surface of the carbon rod was almost of the same order as that of the metal sheets, but the work of Bowden and Rideal* has shown that its accessible area, *i e*, that which could be reached by a reactant, might be over 300 times its apparent area Furthermore, there are a number of substances present in the type of carbon rod used in this investigation which might have had the effect of increasing the rates of charging up Thus it seems quite likely that the rapid rates of charging up of the carbon rod were due, at least in part, to one or other or both of these causes It has been pointed out in Part IV that previous heat treatment had a profound effect on the values of the surface potentials of the carbon rod *in vacuo*, whereas the rates of charging up seemed to depend very little on heat treatment Thus, in fig 6 the *in vacuo* curves (1), (2), and (3) were very close over the whole temperature range where accurate measurements were at all possible Similarly, the rates of charging up for the carbon rod in hydrogen heated to maximum temperatures of 520° and 660° respectively were very nearly identical Heat treatment at 850°, however, greatly influenced the results, *e g*, at 550° the rate of charging up was reduced from 93·3 to 6 7 × 10^{-11} amp

(c) The rate of charging up of the copper sheet *in vacuo* at temperatures above 750° was extremely high, but in contact with gases, including hydrogen, it was low compared with the other metals At the present time it is not possible to advance any explanation of this behaviour, but it is quite probable that on completion of an investigation now in progress in these laboratories further light may be thrown on this subject

(d) In Part IV it was established that the steady potentials exhibited by surfaces under similar experimental conditions tend to approach to zero as the normalization temperature is raised The results with the platinum and copper sheets in Series C and E indicate that this change is accompanied by a reduction in the rate of charging up, and this can be illustrated by the figures given in Table II.

* 'Proc Roy Soc ,' A, vol 120, p. 80 (1928)

Table II

Surface	Temperature of normalisation	Experimental temperature	$(i_0 \times 10^{11})$
	°C	°C	amp.
Platinum in vacuo	500	500	0 33
	660	500	0 07
	660	660	2 00
	850	660	0 27
Copper in vacuo	520	520	10 33
	660	520	0 13
	660	660	2 24
	850	660	0 05

(e) Figs. 3 to 7 show that the rates of charging up of hot surfaces increase rapidly with temperature It has been found that the logarithm of the rate of charging up of a surface is a linear function of the reciprocal of its absolute temperature This relationship can be expressed by the equation

$$\log i_0 = \log a - b/T, \qquad (3)$$

where a and b are constants. It follows that

$$i_0 = ae^{-b/T},$$

e being the base of the natural logarithms Fig 9 gives the results of plotting values of $\log (i_0 \times 10^{11})$ as ordinates against values of $10^3/T$ as abscissae for the carbon, nickel, platinum, gold, and copper surfaces respectively in contact with hydrogen, and for each $\log i_0$ is seen to be a linear function of $1/T$ The special significance of equation (3) can be seen when it is compared with the Arrhenius equation for the temperature variation of the velocity constant, k, for any reaction

$$\log k = C - A/RT \qquad (4)$$

My thanks are due to the Department of Scientific and Industrial Research for a grant which enabled me to devote my full time to this research, and to Professor G I Finch for his continued interest and assistance

General Summary

The rates at which the steady equilibrium potentials are built up on gold, nickel, platinum, carbon, and copper surfaces after earthing have been studied

under varying experimental conditions The experiments have shown that the rate of charging up of a surface is a linear function of its instantaneous potential The effect of the surface temperature is very marked, the logarithm of the rate of charging up being a linear function of the reciprocal of the
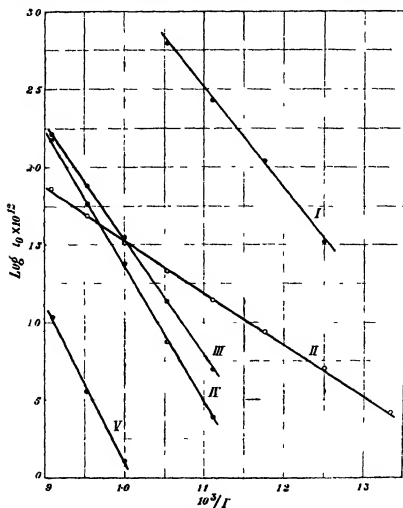
Fig 9

absolute temperature According to the evidence available it is extremely probable that the hot surfaces emit positive electricity over the temperature range investigated (up to 850° C) When heated in a vacuum there is little doubt that the emission consists of positively charged metal ions, while in experiments carried out in contact with gases, the ions are positively charged

G I Finch and B. W. Bradford

atoms or molecules of the gas. With oxygen at low temperatures, however, the ions appear to be negatively charged. The ionic emission is preceded by a partial separation of the atoms of the gas molecules by adsorption with the formation of heteropolar molecules When the free atom of one of the latter can acquire sufficient thermal energy, it is liberated as an ion, the sign of which depends on the orientation of the polarized molecule on the surface

---

The Electrical Condition of Hot Surfaces   Part VI —A Gold Surface Catalysing the Combustion of Carbonic Oxide

By G I Finch and B W Bradford, Imperial College of Science and Technology

(Communicated by Professor W A Bone, F R S —Received July 31—Revised December 15, 1933)

Introduction

A study of the electrical condition of hot surfaces in contact with gases* has revealed the fact that in several important respects a striking parallel exists between such electrical condition and the catalytic properties of the surfaces Thus, it has been found that, whereas at comparatively low temperatures the specific effect of a surface upon the potential it acquires in contact with a gas is highly pronounced, with increasing temperature such specificity tends to disappear until, at a sufficiently high temperature, the value of the surface potential is almost wholly determined by the nature of the gas and is nearly independent of the nature of the surface itself This may be compared with the fact, established by Bone and his co-workers,† that the differences between the catalytic powers of various surfaces, which are often considerable at low temperatures, diminish as the temperature is raised, until they practically disappear Furthermore, it is now well recognized that the catalytic properties of a surface are intimately connected with its structure, and a close parallelism has been observed between the surface potential of a metal and changes in its

* See footnote, p. 307
† 'Howard Lectures, Royal Society of Arts,' 1914

superficial structure brought about by heat treatment * Finally, it has been
found that the electric current which can be drawn from a heated metallic
surface in contact with a gas increases rapidly with increasing temperature,*
an observation which has its parallel in the well-known rapid increase in the
catalytic activity of such a surface with increasing temperature

The present investigation was undertaken with the object of determining the
relationship, if any, between the role played by moisture in promoting the
heterogeneous catalytic combustion of carbonic oxide with oxygen and the
structure of the surface as revealed by its catalytic activity and electrical
condition.

Experimental

In these experiments, moist or dry mixtures of carbonic oxide and oxygen in
their combining proportions were circulated over an electrically insulated,
heated gold gauze surface connected to a Lindemann quadrant electrometer
The reaction velocity, the rate of charging up and the equilibrium potential
of the surface were recorded We have found, *inter alia*, that (i) the structure
of the surface most suitable for the promotion of the combustion of dry carbonic
oxide differed from that required when steam was present, (ii) the reaction
velocity was greater in the presence of steam than otherwise, with increasing
temperature, however, the rates of reaction in the moist and dry systems
converged until in the neighbourhood of 550° C they were nearly equal, and,
finally, (iii) changes in the activity of the surface were paralleled by changes
in the rate of electrical charging

The Apparatus —The combustion of $2CO + O_2$ mixtures in contact with a
heated gold gauze was carried out in one or other of the two circulation systems
shown in fig 1, according to whether the moist or the dry reaction was being
studied The gold gauze, G, was suspended on a quartz rod in the electrically
heated transparent quartz vessel, S, which was joined into the circulation
systems by graded seals at *s* and *s* A gold wire welded to the gauze led out
of the combustion vessel through a quartz side tube, sealed off with sealing wax,
to a Lindemann electrometer The CO_2 absorption and drying tubes were each
5 feet long Fig 1 is self-explanatory so far as the remainder of the apparatus
is concerned All parts of the apparatus were cleaned before assembly with
hot nitric-chromic acid cleaning mixture, and then steamed out with ammonia-
free steam The individual parts of the dry system were further dried and
strongly heated while passing a current of dry oxygen. Precautions were
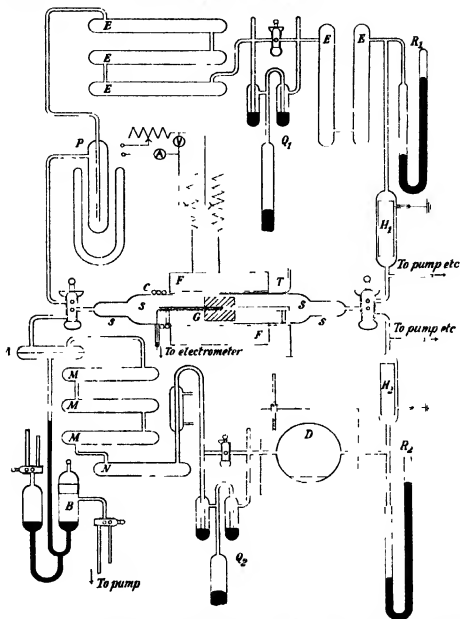
Fig 1 —*SS*—combustion vessel ending in graded quartz to glass seals.   *G*—gold gauze   *C*—water-cooling coil   *T*—thermocouple   *F*—electric furnace, non inductively wound with nichrome over an iron tube which, together with the electrical mid point of the winding, was earthed   *O₁O₂*—dry and moist system circulating pumps respectively   *H₁H₂*—earthed aluminium foils   *MM*—moist system absorption tubes, packed with 1 10 soda lime   *N*—guard tube partially filled with saturated baryta solution   *A*—short absorption tube containing concentrated sulphuric acid to dry gas roughly before removal of CO₂   *B* was a device enabling the spent acid to be replaced without allowing air to enter the apparatus.   *D*—1-litre bulb containing distilled water and surrounded by heat-insulating material, to maintain constant water-vapour pressure in the reaction zone.   *P*—liquid-air cooled trap for removal of CO₂ in dry system   *EE*, etc —drying tubes filled with redistilled phosphoric oxide.   *R₁R₂*—closed-limb mercury manometers.

taken to prevent the ingress of moisture to the dry system during assembly
The purified tap-grease recommended by Baker* was used as lubricant through-
out the apparatus, the grease was thoroughly out-gassed before use

The Circulating Pumps †—In all the experiments to be described below the
rate of circulation was such that the volume of gas, measured at the temperature
and pressure of the apparatus, circulated in unit time was constant   The time
of one complete circuit, whether in the moist or dry system, was 13 minutes
This uniform rate of circulation was obtained by maintaining a constant
oscillation frequency of the mercury piston and controlling its amplitude by
suitable weighting of the plunger

The Gases—Carbonic oxide and oxygen were prepared and purified in the
manner previously outlined ‡   The purity of the gases was verified in two ways
(i) by analysis in a Bone-Newitt apparatus, and (ii) by determining both the
insensitiveness to ignition by a condensed discharge and the dielectric strength§
of a rigidly dried equivalent mixture of the two gases, a procedure which
afforded a stringent test for the absence of hydrogen and hydrogenous gases
The dry system was filled with the equivalent mixture through three tubes 1 m
long, containing redistilled phosphoric oxide

The Gold Gauze—The history and other details of the gold gauze have been
given previously ‖   Since completion of Finch and Stimson's experiments, in
the course of which the gauze was last used, it had been stored for a period of
three years in dry air

Experimental Procedure—The rate of catalytic reaction was determined
first in moist, then in dry, and finally again in moist $2CO + O_2$ experiments
being carried out in each series at several temperatures   The gauze was never
allowed to cool to room temperature during the course of any of these three
main series of experiments and was kept as far as practicable in contact with
the circulating mixture, long periods of stagnation or evacuation being avoided

The range of pressures employed was from 450 mm down to the lowest limit
of effective circulation, approximately 10 mm   The time required for complete
combustion in the case of either of the reaction systems over this pressure
range varied from several weeks at the lowest to less than one hour at the
highest temperatures   Manometer readings were corrected for temperature

---

* 'J Chem Soc,' vol 128, p 1661 (1929)
† *Ibid.*, vol 127, p 2464 (1925)
‡ 'Proc Roy Soc,' A, vol 124, p 303 (1929)
§ 'J Chem Soc,' vol 129, p 1540 (1930)
‖ 'Proc Roy Soc,' A, vol 116, p 379 (1927)

variations, standardized thermometers being placed at different parts of the apparatus for this purpose   An additional correction was made in experiments in the dry system to allow for variation in the level of the liquid air surrounding the carbon dioxide trap   In comparing rates of reaction at different temperatures, a small correction was necessary in order to take into account corresponding changes in the mass of gas contained in the heated zone of the furnace at different temperatures   Differences of volume had also to be allowed for in comparing rates of reaction in the moist and dry systems   The rates of reaction were derived from the mean slopes of the graphs connecting the logarithms of the corrected partial pressures of the dry nitrogen-free gas with time   Samples of the gas entering the reaction vessel were frequently taken and analysed in order to test the efficacy of the CO_2 absorption tubes, and to verify the absence of leaks   In the moist system, tests for the presence of hydrogen were also applied, but this gas was never found

The rate of charging-up of the surface on re insulation after earthing was found to proceed in accordance with the equation $v = A (1 - e^{-Pt})$, where v is the surface potential at the time, t, A, is the final equilibrium, and therefore maximum, value of the surface potential, and P is a constant for given conditions of temperature, gas pressure, and surface activity   Hence, the product PC, where C is the electrical capacity of the surface system, afforded a measure of the rate of charging-up of the surface   In what follows the values of PC are expressed in terms of micro-micro-coulombs per minute per volt

The Results

Fifteen series of experiments were carried out   in the first two, moist (15 mm H_2O) 2CO + O_2 mixtures were circulated over the gold gauze at 245° and 334° respectively, in the next five series, dry mixtures were employed, the temperature range being between 245° and 495°, finally, eight series were carried out in a moist system between 228° and 530°   Throughout, the gauze was never in contact with any gas other than dry or moist 2CO + O_2 mixtures

A fully detailed account of all the experimental results would occupy much space and is hardly necessary in order to elucidate the more important facts It will suffice to give in the first place a broad and general summary of the main experimental results, and then where necessary to set forth in sufficient further detail those results whereby such facts are established which cannot be brought out, or are insufficiently emphasized in the more general summary

The results are set forth in summarized form in Table I and fig 2

Table I

Condition	Series	Temperature °C	Time of heating	Initial stage			Intermediate stage			Final stage		
				l	A_1	PC	l	A_1	PC	l	A_1	PC
Moist	1	245	38 days	0.0062	−0.70	8.0	0.0076	−1.75	5.5	0.0077	−&−	—
	2	334	10 days	0.0230	+0.55	4.5	0.0301	+&−	0.3	0.0295	+1.55	1.4
	3	245	18 days	0.0006	−0.14	0.4	0.0010	−0.15	0.3	0.0012	+0.20	0.3
	4	325	7 days	0.0001	−0.07	1.6	0.0056	−0.09	0.5	0.0056	+0.10	0.5
Dry	5	410	14 days	0.0250	−0.09	1.8	0.0200	−0.19	0.20	0.0260	−0.35	0.24
	6	495	4 days	0.0500	−0.82	38	0.0425	−0.86	36	0.0420	−0.86	34
	7	565	3 days	0.0980	−0.51	275	0.0570	−0.51	185	0.0415	−0.51	150
	8	225	1 day, 2 months cold, 14 days	0.0038	+0.13	0.02	After 2 months 0.0026	−0.26	0.70	After further 14 days 0.0026	+0.20	0.20
	9	228	15 days	0.0039	−3.8	1.3	0.0045	−0.10	2.0	0.0048	+0.50	1.0
	10	317	12 days	0.0120	+0.25	0.50	0.0112	−ve		0.0109	+&−	—
	11	406	9 days	0.0280	+ve		0.0340	−&−		0.0300	−ve	—
Moist	12	464	19 days	0.0070	−0.50	21	0.0592	−0.60	16	0.0379	−0.55	10
	13	530	5 days	0.160	−0.73	120	0.190	−0.75	215	0.122	−0.76	185
	14	470	2 days	0.0660	−0.48	10				0.0560	+0.49	17
	15	373	2 days	0.0225	−0.15	0.49				0.0200	−0.15	0.54
	16	485	1 day	0.0570	+0.46	6.1						

Note.—Values of l, A_1, and PC above refer to a total gas pressure of 100 mm except in Series 3 and 9, in which the pressures were 250 mm and 150 mm respectively.

These results establish the following facts —

(1) On comparing the rates of reaction in the dry and moist systems it will be seen that (a) under similar experimental conditions, the reaction velocities were invariably higher in the moist than in the dry system. With increasing temperature, the difference between the rates observed in the two systems diminished practically throughout the range of temperature covered by the experiments These observations confirm the results obtained by Bone* for the rate of combustion of a P_2O_5-dried $2CO + O_2$ mixture on the surface of the same

Fig 2
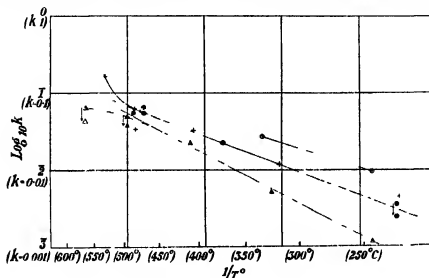
		Series 9 to 13	temperature raised throughout
Moist	{	Series 1 and 2	
		Series 14 to 16, temperature varied.	
Dry	{	Series 3 to 7, temperature raised throughout	
		Series 8(a) and (b)	

specimen of gold gauze at a temperature of 240° C , and give strong support to the suggestion made by that author that at sufficiently high temperatures the reaction of carbonic oxide and oxygen might prove to be independent of the presence of moisture   At the highest temperatures, however, the reaction velocity in the moist system attained what appeared to be an abnormally high value, whereas in the dry system, k showed a similarly abnormal decrease , (b) on changing from the moist to the dry reaction or vice versa, a long period of time elapsed before complete readjustment, i e , normalization of the surface to the

* ' Proc Roy Soc ,' A, vol 112, pp 474-499 (1926)

new conditions, was attained (see Series 3 and 9), (c) after drying, the efficiency of the surface in promoting the moist reaction was found to be permanently impaired (cf Series 1 with 9, or 2 with 10, see also fig 2) The apparent heat of activation of the moist reaction was not, however, altered as a result of drying, and, furthermore, the reduction in the value of k at a given temperature was practically equal to the total reduction in the activity of the surface at high temperatures in the dry system

(2) On maintaining the surface at constant temperature for long periods of time, the catalytic activity did not in general remain constant, thus, (a) when first heated to 245° in the moist system (Series 1), the reaction velocity increased rapidly at first, and then more slowly Table II illustrates the rapid initial rise

Table II

Time after attainment of con stant temperature (hours)	0	0 75	1 42	1 85	2 35	1 17	4 08	4 67
Reaction velocity constant, k	0 00096	0 00235	0 00238	0 00308	0 00368	0 00397	0 00437	

After a further period of 18 hours the observed pressures and times gave a sensibly linear relationship between $\log p$ and t, the value of k being 0 00630 The catalytic activity of the surface continued to increase slowly for 37 days, as shown in Table I (Series 1) (b) At higher temperatures in both moist and dry systems, other effects became evident Thus, in the dry system over the range 300°–400°, the values of k increased slowly with time, whereas, at temperatures above 450°, the values of k at constant temperature fell from the commencement of each series In the moist system, apart from the initial normalization referred to above, a slight decrease in the value of k was observed in Series 2 at 334° and in Series 10 at 317° In Series 11 at 406° a gradual rise occurred similar to that at the same temperature in the dry system (Series 5) At 484° (Series 12), k fell steadily, but, as will be shown later, the fall could not be regarded as of the same nature as that which took place in the dry system At the highest temperature attained in the moist system (Series 13 at 530°), the values of k passed through a maximum.

(3) Slow changes in the value of k at a given temperature were not necessarily accompanied by permanent changes in the catalytic activity of the surface at other temperatures or in different conditions Thus, although the gradual decrease in k at the higher temperatures in the dry system led to an approximately proportional decrease in the catalytic activity in the moist, it also

resulted in increased activity at low temperatures in the dry (see Series 3 and 8) Also, during the experiments in the moist system at 484° (Series 12), the value of k decreased to 60% of its initial value Further changes took place at 530° (Series 13), where, although k attained a maximum, its value at the close of the series was lower than at the commencement In spite of these decreases, on returning to 470° (Series 14), k had practically the same value as at the commencement of Series 12, and at a lower temperature (373° , Series 15) the value of k agreed well with that interpolated between Series 10 and 11, previous to the high temperature treatment Hence it may be concluded that the gradual decrease in k in Series 12 did not entail a permanent decrease in the catalytic activity of the surface at other temperatures.

(4) With few exceptions, on changing from a lower to a higher temperature, the value of k showed a rapid initial increase and, for the reverse temperature change, a rapid initial decrease These effects were, however, sometimes masked to some extent by the occurrence of other changes in the catalytic activity at constant temperature The initial increase on passing from a lower to a higher temperature may be seen in Series 1 , similar effects in Series 3, 4, 5, 9, and 11 may not have been due solely to temperature increase In Series 13 an initial increase was followed by a decrease The reverse effect is clearly shown in Series 8 Thus, immediately on reduction of the temperature from 565° to 228°, the value of k was 0 0036 After cooling at room temperature for some time, k had fallen to 0 0026 The operation of both effects may be seen in Series 14, 15, and 16 Thus, the value of k at 470° on the first day after cooling from 530° was 0 0660, but had fallen by the second day to the normal value of 0 0560 On further cooling to 373°, k followed an analogous course, having the values 0 0225 on the first, and 0 0200 on the second day after such reduction in temperature When the temperature was again increased to 485°, k had the abnormally low value of 0 0570 on the first day

(5) The general facts relating to the electrical condition of the gauze established by the results recorded in Table I are as follows (a) The potentials acquired in the moist system differed from those in the dry at the same temperature (see Series 8 followed by 9, and cf also 1 and 3) , (b) the difference between the potentials in the moist and dry tended to decrease as the temperature was increased

(6) The coefficient of charging rate, PC, did not, in general, remain constant at constant temperature (a) when the temperature of the surface had been increased from a lower value, PC diminished gradually at constant temperature At low temperatures in either system, the fall was rapid at first (see Series 3

and 4), but PC soon attained a practically constant value   At high tempera-
tures, PC fell steadily throughout the period of heating, a decrease parallel
to the decrease in the value of k in the same conditions (see Series 6, 7 and 12)
In Series 13 at 530°, the values of PC and k passed simultaneously through a
maximum   At low temperatures, however, a rise in k was in certain cases
accompanied by a fall in PC (see Series 1, 3 and 4), but these three may all be
regarded as anomalous in some particular   In the only case where PC gradually
rose to constancy (Series 5), it was accompanied by a parallel rise in the value
of k (b) On reduction of the temperature of the surface, PC at first rose
rapidly (see Series 14 and 15)   In Series 8, the value of PC was abnormally
low immediately after cooling to 228° from a higher temperature, after the
surface had been cooled to room temperature, however, and then re-heated to
228°, PC rose to the exceptionally high value, 0 7, but on continued heating
this fell to the normal value of 0 2 for that temperature   (c) For a given
temperature, the value of PC in the moist system was lower after the period of
drying than before   In both moist and dry systems, the value of PC passed
through a maximum at the temperature where the sign of A changed from
positive to negative

Further Experimental Results relating to the Catalytic Reaction

*Variation of the Reaction Velocity with the Gaseous Pressure —*Throughout
the experiments, in either the moist or the dry system, it was found that
during the combustion of a given charge of the gaseous mixture, the rate of
reaction did not accurately follow a unimolecular law, the rate of decrease of
pressure falling off less rapidly than required by such a law   In consequence,
the curves connecting log p and t were not linear except over small ranges of
pressure   The extent of the variation is shown in fig 3, where k (measured by
the slope of the tangent to the log p, t curve) is plotted against pressure

Experiments were carried out on the rate of combination of $2CO + O_2$
mixtures on the surface of a heated gold wire, in order to determine whether
the form of the surface affected the type of variation of k with pressure, with
negative results   It is therefore clear that the effect of pressure cannot be
attributed to the operation of diffusion factors dependent on the use of a
catalyst in the form of gauze

*Effect of Evacuation on the Reaction Velocity —*In either the dry or the moist
system, evacuation resulted in a reduction of the reaction velocity when the
$2CO + O_2$ mixture was subsequently admitted   Such reduction was, however,
only temporary and the surface soon regained its normal state of activity

corresponding to the conditions under investigation The recovery was
complete within three hours at 250° in the moist system, in 24 hours in the dry,
and within a few minutes in either system at 450° or above

Catalytic Combustion on the Walls of the Quartz Vessel —The rates of reaction
in the dry and moist systems between 225° and 650° in the quartz vessel from
which the gold surface had been removed are shown in Table III An important
feature of these results is that they show that the value of k was throughout
higher in the dry than in the moist system
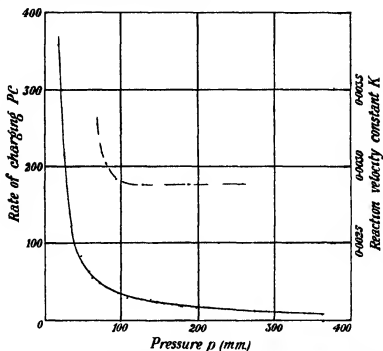
FIG 3 — — — $k \propto p$ (Series 2, 334° C), ——— PC $\propto p$ (Series 5, 495° C)

Table III

Dry System					
Temperature ° C	226	333	457	571	602	—
k	0 0000	0 0000	0 0001	0 0047	0 0063	—
Moist System						
Temperature ° C	225	350	502	550	567	580
k	0 0000	0 0000	0 0001	0 0002	0 0007	0 0012

The Equilibrium Potential of the Surface —For purposes of comparison, the
electrical condition of the surface was examined in the individual gases CO,

O_2 and CO_2, both moist and dry, throughout the temperature range covered by the experiments on reaction velocity, the results being summarized in fig 4

The sign and magnitude of the equilibrium potential of the surface in the reacting mixture varied considerably in the moist system at temperatures below 400° (see Table I)   No such variations were observed with any of the individual gases in the moist, or in the dry in any conditions   The magnitude of A was found to be independent of the gaseous pressure throughout the range covered in the experiments
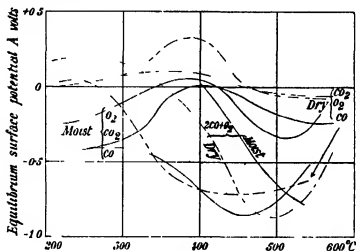
Fig 4

The following facts are evident from fig 4 —

(1) All the curves showing the variation of A with temperature have a general formal similarity

(2) In the dry system   (a) The $2CO + O_2$ curve approximated more closely to the CO curve than to that for O_2 At lower temperatures, the value of A for the mixture had a higher positive value than for either CO or O_2 or their sum, passed through zero at the temperature where the potentials in CO and O_2 began to diverge considerably, became equal to the CO A-value at the temperature where the O_2 A-value was zero, and rose to a higher positive value than CO in the range of temperature in which both CO and O_2 had negative A-values   (b) The CO_2 curve followed the O_2 curve closely throughout, the magnitude of A in CO_2 being, however, uniformly less than in O_2.

(3) In the moist system   (a) The $2CO + O_2$ curve followed the O_2 curve in general form more nearly than that for CO   (b) The CO_2 curve approximated to the CO curve at low temperatures and to the O_2 curve at high temperatures

(4) On comparing the curves for the individual gases in the moist and dry systems respectively, it will be seen that (a) the curves for all three gases were displaced in a negative direction by the presence of moisture , (b) the CO and CO_2 curves were displaced more at low than at high temperatures , and, finally, (c) the O_2 curve was displaced uniformly throughout, and showed signs of a change of form at high temperatures in the moist

(5) The values of A for the reacting mixture $2CO + O_2$ were displaced uniformly in a positive direction by the introduction of water

The Rate of Electrical Charging of the Surface – The rate of charging of the gold surface increased rapidly with decreasing pressure , the type of increase which occurred is shown in fig 5   All values of PC quoted in the present communication refer to a total gaseous pressure of 100 mm

The experiments on the rate of charging (PC) in the reacting mixture, and in the individual gases are summarized in Table IV

Table IV

	Gas	250° C	300° C	350° C	400° C	450° C	500° C	550° C
Moist	O_2	6 5	6 5	7 9	13	32	156	1750
	CO	11	19	33	59	130	500	8000
	CO_2	30	53	100	282	708	2000	6100
	$2CO + O_2$	1 6	1 6	1 6	3 5	7 6	45	216*
Dry	O_2	0 0	1 0	2 0	11 5	42	—	—
	CO	0 8	1 6	5 0	32	400	1510	2510
	CO_2	—	—	0 4	2 5	25	200	1260
	$2CO + O_2$	0 37	0 50	0 45	0 25	1 9	45	180

* At 530°

The following facts are clearly brought out in Table IV —

(1) Increase of temperature was not invariably accompanied by an increased rate of charging   Thus, the value of PC for the dry, reacting mixture $2CO + O_2$ fell from 0 50 to 0 25 as the temperature was raised from 300° to 400°   PC remained constant in the moist mixture while the temperature was raised from 250° to 320°, and in moist O_2 over the

temperature range from 200° to 300°. In all three cases the temperatures were in the neighbourhood of that at which the sign of A changed in the respective systems.

(2) In general, the rate of charging in the moist was much greater than in the dry system, but the differences became less marked as the temperature was increased.
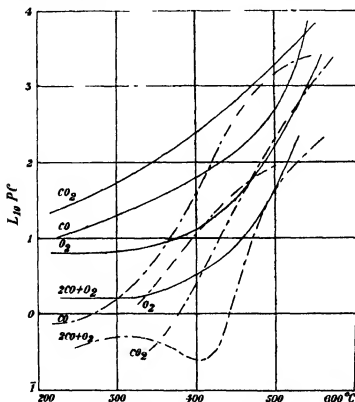
Fig 5 —— Moist series , — — dry series

(3) CO was an exception to the general rule that the rate of charging was greater in the moist than in the dry. Over the range of temperature 420° to 530°, PC was higher in the dry than in the moist, although at higher and lower temperatures the reverse occurred. The PC values for the reacting mixture became identical at 480°, whilst diverging at higher and lower temperatures.

(4) The PC values for O_2 in either system were considerably less than those for CO and CO_2 although greater than those for the reacting mixture $2CO + O_2$

In order to exhibit the effect of moisture on the rate of charging more clearly the graphs of log PC plotted against temperature are shown in fig 5   In addition to those set forth above, the results incorporated in fig 5 establish the following facts —

(1) The slopes of the curves for the individual gases and the reacting mixture in the moist system increase steadily with increasing temperature, while those for the dry system pass through one or more points of inflexion

(2) The mean rate of increase of PC with temperature is throughout higher in the dry than in the moist system, an observation which may be compared with the higher rate of increase of reaction velocity, k, with temperature in the dry, compared with that in the moist system

Variation of Reaction Velocity with Temperature

In fig 2 the values of log k are shown plotted against the reciprocals of the corresponding absolute temperatures   The dry and second moist series give linear relationships over the greater part of the temperature range   In the former series, deviations occur at the higher temperatures where the gradual decrease of activity previously noted took place (Series 6 and 7)   In the second moist series, the points representing Series 9 and 13 both lie above the line joining the remainder of the points   The former may represent a change in the heat of activation at low temperatures, but is more probably to be ascribed to the other changes in the surface brought about by the long period of drying   The latter deviation appears to represent a change in the course of the reaction at the highest temperatures attained   The results for the reaction on the surface of the quartz vessel (Table III) show that it cannot be due to a change from heterogeneous to homogeneous reaction

The slopes of the graphs give values for the apparent heats of activation of 12,000 and 8730 cal per gm mol for the dry and second moist series respectively   The slope of the line joining the points corresponding to the two series of experiments in the first moist series give a value of 8500 cal per gm mol It may therefore be concluded that the period of drying did not change the mechanism of the moist reaction on the gold surface

The apparent heat of activation of a heterogeneous reaction such as that under consideration is a composite quantity, representing not only a true heat of chemical activation, but also additional energy factors connected with the processes of adsorption and desorption on the surface   In the absence of sufficient data relating to the adsorption of CO, O_2 and CO_2 by gold in moist

and dry systems, the differing heats of activation in the moist and dry cannot be taken as direct proof that the mechanisms of the two reactions are dissimilar It cannot be supposed, however, that the presence of moisture would modify the processes of adsorption and desorption of gaseous molecules on the surface and leave the chemical reactions unaffected

Discussion

The results set forth above establish the facts that under the conditions of our experiments the heterogeneous catalytic combustion of carbonic oxide by oxygen in contact with a gold surface approximates more closely to a reaction of the first, than to one of any other order, and that the reaction is not retarded by the presence of carbon dioxide Bone and Andrew* have, however, previously shown that, under conditions similar to those employed by us, neither carbonic oxide nor oxygen are strongly adsorbed by the catalysing surface The conclusion may, therefore, be drawn that the order of reaction found experimentally is also, in fact, the true order, and that the rate of combustion of a $2CO + O_2$ mixture in contact with gold is directly proportional to the concentration of one of the two constituents of the mixture, probably carbon monoxide The fact that k increased with falling pressure can then be reasonably ascribed to an increase in the value of the ratio of adsorbed to free gaseous carbon monoxide

The remarkable deactivating effect of evacuation upon the catalytic powers of the gauze, also previously observed by Bone and Andrew (loc cit), appears to have its parallel in a recent observation by Finch and co-workers† to the effect that the catalytic activity of a sputtered platinum film may be completely destroyed by drying or by evacuation It would seem that drying results in the growth of larger crystal aggregates with consequent closing up and elimination of Smekal cracks The fact that the activity of the previously dried gold surface can be relatively rapidly restored by heating in contact with $2CO + O_2$ strongly suggests that activation of, and interaction between these gases at the surface resulted in a reopening of fresh Smekal cracks

The anomalous increase in the reaction velocities at the highest temperatures in the moist system occurred within the temperature range where the rate of the dry reaction closely approached that of the moist reaction In view of the above considerations this fact suggests that at such temperatures both the dry and moist reaction mechanisms occurred simultaneously and independently,

---

* 'Proc Roy Soc ,' A, vol 109, p 459 (1925)

† 'Proc Roy Soc ,' A, vol 141, p 414 (1933)

and, furthermore, that the nature of surface structure most favourable for promoting the dry reaction differed greatly from that suitable in the combustion of the moist mixture   Thus, on changing from the dry to the moist reaction or *vice versa*, a more or less prolonged period of induction, amounting, in one case, to 28 days, elapsed before the surface had become completely normalized to the changed conditions of reaction   These facts strongly suggest that the mechanisms of the moist and dry reactions differ, and it may be reasonably supposed that in the dry reaction adsorbed oxygen is burnt directly by carbonic oxide, whereas, in the presence of moisture the carbonic oxide reacts with adsorbed steam, the hydrogen thus liberated reacting with adsorbed oxygen

The close connection between the structure and catalytic properties of a surface has been previously recognized by Bone, Langmuir, Rideal, Taylor and others, and the above experiments enable us to discriminate between two processes resulting in profoundly different classes of surface structural change Of these, normalization towards a specified reaction or temperature is one type, the other being a process of sintering whereby the activity of the surface, as measured in terms of the rate of a standard reaction, was permanently impaired

Reaction and temperature normalization of the surface differed in themselves in that normalization at an elevated temperature left the surface in a temporarily abnormally active condition on return to a lower temperature   after sufficiently prolonged promotion of the reaction, however, the activity of the surface returned to the normal value   These facts in conjunction with those previously discussed suggest that heating, or the promotion of either the moist or the dry reaction all lead to the formation of different types of surface structure   Sintering, on the other hand, which must be regarded purely as a temperature effect, produces structural changes deleterious to catalytic action from which complete recovery was not possible under the conditions of our experiments

The electrical properties of the gold gauze in different conditions show clearly that the influence of water cannot be regarded as merely additive, since, if such were so, its effect, as revealed by the values of A and PC, would be the same for the three individual gases as for the reacting mixture, whereas the experiments have shown the effect to be specific   This is particularly in evidence in the values of A for the reacting mixture, in which a positive displacement of potential occurs on introduction of water, contrasted with the negative displacement brought about in all the individual gases   It is clear that, during the progress of chemical reaction, some molecular complex or type of configuration was present on the surface of the metal which was not capable

of being formed by contiguous adsorption of water and either CO, O₂ or CO₂. While this fact alone does not prove that water participated in the reaction, the close relation which was found to exist between the rate of electrical charging and the rate of chemical reaction makes it difficult to resist such a conclusion

Further support for the view that water plays an essential part in the surface reactions may be derived from the observations on the rate of charging. It has been shown that the introduction of water not only changed the general type of functional relationship between the rate of charging and temperature, but that the different gases were not affected to the same extent. In both moist and dry systems, the rate of charging during chemical reaction was considerably less than in any of the individual gases. Since, in general, the energy necessary to ionize a molecule is less than that required to excite it to a state of chemical activity, it may be supposed that the probability of ionization of molecules adsorbed on the gold surface was substantially reduced by the occurrence of chemical reaction. The product of such reaction (CO₂) must, at least for a short time after its formation, have been in a favourable condition for ionization. Of all the individual gases, CO₂ had the lowest rates of charging in the dry, and the highest in the moist. It would, therefore, be anticipated that the differences between the rate of charging in the reacting mixture and that in either CO or O₂ would be less in the moist than in the dry, a conclusion which is borne out by the experiments

In only one case did the rate of charging attain a higher value in the dry system than in the moist, namely, in CO over the temperature range 420° to 530°. This anomaly may be attributed to the occurrence of the water gas reaction in the moist system and a consequent reduction in the rate of charging. The marked resemblance previously pointed out between the electrical properties of the surface in CO and in the reacting mixture over this range of temperature lends further support to the view that oxidation of CO in the moist system takes place indirectly through the intervention of adsorbed water

The experimental results set forth above have shown that, in general, when the surface was fully normalized at a constant temperature, gradual changes in the value of the reaction velocity constant, k, were accompanied by parallel changes in the coefficient of charging rate, PC. When, on the other hand, the surface of the metal was passing through readjustments resulting from changes in temperature, k and PC were no longer parallel. In particular, the rapid initial rise or fall in the value of k following increase or decrease of temperature was usually accompanied by change of PC in the contrary sense, decrease in

rate of charging resulting from increase of temperature and *vice versa* Following the view of structural changes of the surface put forward above, it is clear that the extent to which activation or ionization of molecules adsorbed on the surface occurs must depend upon the simultaneous operation of two factors, definable as accessibility and suitability respectively Sintering of the surface, which has been characterized in the foregoing as an irreversible decrease in catalytic activity, is to be regarded as reducing the accessibility of catalytic surface, and in the present experiments led to decrease of both the rate of chemical reaction and the rate of electrical charging Factors, other than sintering, upon which the catalytic activity of the surface depends, may be classified as suitability factors, distinguishable by the period of time required for their operation which was short compared with the long and gradual process of sintering Two such factors have been elucidated in the present experiments, namely, reaction and temperature normalization Reaction normalization the occurrence of which is seen most clearly in the moist Series 13 undoubtedly affects rate of reaction and rate of electrical charging in the same way The operation of temperature normalization, on the other hand, which is made evident in the behaviour of the surface immediately after increase or decrease of temperature, leads to opposite changes in λ and PC It is therefore clear that while, in general, the rate at which chemical reaction occurs on the surface is parallel to the rate at which the characteristic electrical interface potential is established, the magnitudes of the two rates are determined to some extent by forces which act in contrary directions

We are carrying out further investigations on the nature of these forces

Summary

Previous experimental study of the electrical condition of heated metals having indicated the existence of a striking analogy between such electrical condition and the catalytic properties of the surfaces, a series of experiments with a gold gauze surface was carried out in such a manner that the catalytic and electrical activities of the metal could be simultaneously observed and followed The reaction selected was the heterogeneous combination of carbon monoxide and oxygen , in view of the well-known influence of water on this reaction, series of observations were made in both moist and dry systems, with

the further object of elucidating the function of water in the reaction   The electrical condition of the metallic surface was expressed in terms of the magnitude and sign of the equilibrium potential which it acquired in given conditions, and its electrical activity was measured by the specific rate at which that potential was approached on insulation at zero or other standard potential

In similar experimental conditions, the reaction velocities were invariably higher in the moist than in the dry reaction system ; with increasing temperature, however, the differences between the rates observed in the two systems diminished practically throughout the range of temperature covered by the experiments   Several types of gradual change in the catalytic activity of the surface were observed, some reversible, others permanent   Such changes were ascribed to alterations in the superficial structure of the metal and were correlated with the effects of temperature, evacuation of the catalyst, and the presence or absence of moisture on the surface

In general, throughout the experiments, changes in the rate of electrical charging of the metal followed closely the corresponding changes in the catalytic activity, increasing with rising temperature or with the introduction of water, and undergoing similar variations to the rate of reaction when the surface was maintained at constant temperature   The equilibrium potential of the metal gave further evidence of the close connection between the electrical and catalytic properties of the surface, being affected by the presence of moisture and by the occurrence of chemical reaction   The evidence derived from the electrical properties of the surface indicated that water played an essential part in the changes which occurred in the layer adsorbed on the metallic surface

The Crystal Structure of the Heusler Alloys

By A J BRADLEY, D Sc, Royal Society Warren Research Fellow,
and J W RODGERS, B Sc

(Communicated by W L Bragg, F R S --Received October 4, 1933)

Beginning in the year 1898 Heusler* discovered a series of ferromagnetic alloys the most important containing copper, manganese, and aluminium They are characterized by remarkable magnetic properties, because although composed only of paramagnetic or diamagnetic elements, they become ferromagnetic after suitable heat treatment † Various explanations of this property have been advanced, but it was usually considered to be due to the formation of a series of solid solutions of the type (CuMn)₃Al, in which the proportions of copper and manganese may be varied within fairly wide limits

The Heusler alloys have been repeatedly investigated by means of X-rays Young,‡ using molybdenum radiation examined alloys of two different compositions He found that one was face-centred cubic, while the other was a mixture of face-centred and body-centred cubic structures The mixed alloy was the more magnetic

A more detailed investigation was made by Lew Harang,§ using copper radiation He found three structures, face-centred cubic, body-centred cubic, and a structure similar to that of γ brass, which correspond respectively to the α, β, and δ phases of the copper-aluminium system ‖ They are successively produced by increasing the proportion of aluminium in the alloy Harang did not find it possible to trace any relation between the magnetic properties and the crystal structure, and therefore could not ascribe them to a single lattice These conclusions are not in agreement with recent investigations ¶

Later, Elis Persson investigated these alloys by means of chromium radiation In a preliminary note** he showed that the structure of a ferromagnetic alloy

---

* Heusler, Stark, and Haupt, ‘Verh deuts phys Ges,’ vol 5, p 219 (1903), Heusler and Richarz, ‘Z anorg Chem,’ vol 61, p 269 (1908)

† Take, ‘Inaug disc Marburg’ (1904)

‡ ‘Phil Mag,’ vol 46, p 291 (1923)

§ ‘Z Kristallog,’ vol 65, p 261 (1927)

‖ Jette, Westgren, and Phragmén, ‘J Inst Metals,’ vol 31, p 201 (1924), Obinata, ‘Mem Ryojun Coll Eng,’ vol 31, pp 3, 286, 295 (1929), Bradley and Jones, ‘J Inst Metals,’ vol 51, p 131 (1933)

¶ Krings and Ostmann,‘Z anorg Chem,’ vol 163, p 154 (1927), Heusler, ‘Z anorg Chem,’ vol. 171, p 126 (1928)

** ‘Naturwiss,’ vol 16, p 613 (1928)

corresponding to the formula Cu₂MnAl was body-centred cubic, with the aluminium atoms forming a face-centred superlattice. The structure was therefore like that of Fe₃Si*, or that of Fe₃Al† discovered later. The unit cell is built up of eight small body-centred cubes, and therefore contains 16 atoms, of which four are aluminium, four manganese, and the remainder copper. The aluminium atoms form a face-centred cube with double the dimensions of the small body-centred cube. No attempt was made to find the position of the manganese atoms by means of X-rays.

Potter‡ made an X-ray examination of single crystals using copper radiation. He believed that the Mn atoms occupied special positions like the Al atoms. On account of the resemblance between the magnetic properties of this alloy and nickel, he concluded that its ferromagnetism was due to the manganese atoms being arranged on a face-centred cubic lattice.

In continuation of his earlier researches, Persson§ came to the same conclusion. The series of alloys (CuMn)₃Al is only ferromagnetic when the manganese content exceeds 19% (atomic). Thus it is independent of the arrangement of *aluminium* atoms, which is apparently the same whatever the amount of manganese present, within wide limits. Persson believes that the presence of 19% of manganese is required in order to produce a regular arrangement of manganese atoms.

Persson attempted to find whether the special Cu₂MnAl type of structure was alone responsible for the ferromagnetic properties of the copper-manganese-aluminium alloys. He examined a whole series of alloys of the composition (CuMn)₃ Al, varying the proportions of copper and manganese. An X-ray examination was made after heat treatment of the powdered alloy. In one series of experiments the alloys were quenched in water from a temperature only 50° below the melting point. In another series the alloys were tempered for 350 hours at 210°.

The quenching experiments showed that four different types of structure occurred. Face-centred cubic, body-centred cubic, and " Gamma " structures corresponded to the α, β and δ phases of the copper-aluminium system, and a fourth phase possessed a structure like that of β Mn. Contrary to Haraug Persson concluded that only the body-centred cubic β phase was ferromagnetic, the ferromagnetism of the alloys increasing with the amount of the β phase present

* Phragmén, ' Tekn Tidskrift ' (Stockholm), vol 56, p 81 (1926)

† Bradley and Jay, ' Proc Roy Soc ,' A, vol 136, p 210 (1932)

‡ ' Proc Phys Soc ,' London, vol 41, p 135 (1929)

§ ' Z Physik,' vol 57, p 115 (1929)

The tempering experiments showed that the β phase was decomposed by this form of heat treatment The alloy splits up into two or more phases If the Mn content is less than required for the formation of the alloy Cu_2MnAl, the phases are Cu_3Al with lattice spacing 5 833 A , and Cu_2MnAl with lattice spacing 5 950 A If the Mn content is greater, a structure of the β Mn type with lattice spacing 6 370 A is formed, together with Cu_2MnAl and lattice spacing 5 950 A Maximum ferromagnetism corresponds to the greatest amount of Cu_2MnAl

Whether the alloy is quenched or tempered the lattice spacing of the β body-centred cubic phase never exceeds 5 950 A For quenched alloys the lattice spacing increases linearly with increase of manganese content between Cu_2Al and Cu_2MnAl and ferromagnetism is the greater the greater the lattice spacing

An alloy of the composition $CuMnAl_2$ has the CsCl type of structure and is non-magnetic The property of ferromagnetism is thus associated in a peculiar degree with the special composition Cu_2MnAl The closer the alloy attains to this composition the more marked is its ferromagnetic character Persson concludes that the property of ferromagnetism is due to the nature of the crystal structure of Cu_2MnAl, and is linked up with the mode of distribution of the manganese atoms

The object of the present paper is to fix the position of the manganese atoms in the magnetic alloys by direct experiment, and to test whether a change of structure *without change of composition* will destroy the ferromagnetic character of the alloy This should decide whether structure or composition is the more important condition for ferromagnetism

I Present Experiments

Eight alloys of the approximate composition Cu_2MnAl were prepared by melting together 50 gm. of copper, manganese, and aluminium in slightly different proportions in an alumina lined crucible* in a high frequency induction furnace, under a low pressure of hydrogen In order to remove toring, and to make the alloys homogeneous, they were heated for 6 hours at 750° C in an electric furnace and allowed to cool slowly down to room temperature Drillings were then taken by means of a special drill,† kindly supplied by Mr Gardiner, of Easterbrook Allcard & Co , Sheffield The drillings gave small particles which could be ground in an agate mortar The fine powders so obtained were

---

* Jay, ' J Iron and Steel Inst ,' vol. 125, p 427 (1932)
† Edgar Allen's Stag Major

sieved through a mesh 250 to the inch, and then subjected to further heat treatment

A portion was heated in hydrogen at 500° C for 6 hours, and then allowed to cool slowly down to 300° C over a period of a few hours At this point the current was switched off, and the powders were allowed to cool to room temperature in the furnace X-ray powder photographs of these alloys were taken using radiation from an iron anticathode They show that the bulk of each alloy consists of a phase of the γ brass type* like Cu_9Al_4† and that at least one other phase is present

Very different photographs were obtained from the second portions of the powders These were heated in hydrogen to a temperature of 800° C and after about half an hour quenched by allowing a stream of cold water under pressure to enter the furnace The structure is now body-centred cubic with a superlattice of the typical Heusler alloy type, as described by Persson and Potter These photographs were repeated using radiation from copper and from zinc anticathodes There are differences between the relative intensities of the fainter lines of the three photographs, which we shall explain later

In the alloy selected for detailed investigation the proportions of the ingredients did not correspond exactly to the theoretical values for the composition Cu_2MnAl Analysis‡ of the alloy showed that the approximate composition was Cu 67 5%, Mn 17 5%, Al 15% corresponding to the atomic composition Cu 2 2, Mn 0 65, Al 1 15 The deficit of manganese was therefore made up partly by copper and partly by aluminium This particular alloy was chosen because it was the only one which showed an almost complete change of structure with the two methods of heat treatment After annealing at 500° and slowly cooling down to room temperature, it gave an X ray powder photograph corresponding to the δ copper aluminium structure (Cu_9Al_4), with only a faint trace of lines belonging to another pattern In this state the alloy was found to be practically non-magnetic On the other hand, the same powder after quenching from 800° showed only a body-centred cubic structure with face-centred superlattice The alloy was now strongly ferromagnetic

---

* Westgren and Phragmén, ‘Phil Mag,’ vol 50, p 331 (1925), Bradley and Thewlis, ‘Proc Roy Soc,’ A, vol 112, p 678 (1926)

† Bradley, ‘Phil Mag,’ vol 6, p 878 (1928), Bradley and Jones, ‘J Inst Metals,’ vol 51, p 131 (1933)

‡ The alloys were analysed by Mr J W Cuthbertson of the University, to whom the authors are indebted for his kindness.

The above facts show conclusively that the magnetic properties of the alloy are dependent on the type of crystal structure, as Persson suggested   The composition of the alloy after heat treatment was checked by chemical analysis, and found to be unaltered *   There is therefore no doubt that the ferro-magnetism of the alloy is not a matter of chemical composition but of atomic arrangement

The arrangement of the atoms in the annealed and slowly cooled alloy can be fixed to some extent from a visual inspection of the photograph Its resemblance to the powder photograph of Cu_9Al_4 is extraordinarily close   In Cu_9Al_4, the unit cell is cubic and contains 52 atoms of which 36 are copper
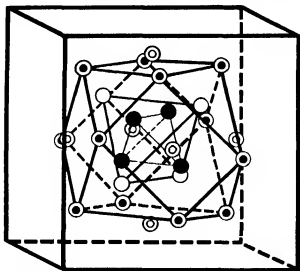
FIG 1 —Annealed Heusler alloy (non magnetic), ● A, ○ B, ◎ C, ◉ D

and 16 aluminium   The copper and aluminium atoms each occupy definite positions in the lattice   From considerations of symmetry the 52 atoms can be divided into eight sets which may be called A_1, A_2, B_1, B_2, C_1, C_2, D_1, D_2 respectively   Four A_1, 4 B_1, 6 C_1, and 12 D_1 constitute a cluster of 26 atoms which are grouped symmetrically around the centre of the cell, fig 1   A second cluster of 26 atoms, not shown in the figure, is grouped symmetrically about each corner of the cell, so that the whole structure would be body-centred cubic, except for the fact that there are more copper atoms and fewer aluminium atoms in one cluster than in the other   The aluminium atoms are concentrated in A_1 and D_2 The copper atoms occupy the remaining positions

* The manganese contents of the quenched and annealed specimens agreed to 0 1%.

The similarity of the powder photographs of the annealed Heusler alloy and that of Cu_9Al_4 shows at once that the atomic co-ordinates are almost identical in the two   Further, it can be concluded that the aluminium atoms again occupy positions A_1 and D_3 The remaining positions are filled chiefly by copper atoms, but about one-fourth of these are replaced by manganese   The formula of the annealed alloy can therefore be written as $(CuMn)_9 Al_4$ The proportions of aluminium are not quite sufficient to satisfy this formula, which may possibly explain the slight admixture of the second phase, shown by the powder photograph   Without a more detailed investigation, it is impossible to say whether the manganese atoms occupy special positions in the lattice, or whether they are mixed up with the copper atoms in a purely random manner, but there is no doubt about the aluminium atoms
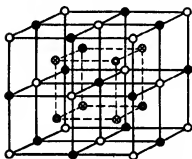
FIG 2 —General type of structure,
O A, ◎ B, ● C, ⊗ D
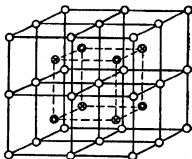
FIG 3 —Quenched Heusler alloy (magnetic), O Cu, ◎ Al, ⊗ Mn

The ferromagnetic quenched alloy has a unit cell containing 16 atoms, fig 2   These consist of four sets of atoms (A, B, C, D) each corresponding to a face-centred cubic lattice   The superlattice lines are caused by the segregation of the aluminium atoms into one of the four sets of positions (say B)   Both Persson and Potter suggest that the ferromagnetism of these alloys is due to the manganese atoms occupying a special position as in fig 3   It was our object to test this hypothesis   The question is whether the manganese atoms are mixed up at random with the copper atoms or whether they keep to their own positions   The difference between the scattering powers of copper and manganese for X-rays is so slight that this might at first sight appear to be a matter of some difficulty, but, in fact, the problem has been solved by means of accurate photometer measurements of powder photographs taken with X-rays of different wave-lengths, making use of the anomalies in atomic scattering

factor which occur when the frequency of the radiation is close to the character-
istic absorption frequency of the element

The powder photographs of the quenched alloys taken with iron, copper,
and zinc radiations were photometered by means of a Cambridge micro-
photometer This instrument employs a null method, the blackening of the
film being balanced against an Ilford wedge Each film was calibrated by
means of a rotating sector wheel, giving 10 uniform increments of intensity
On comparing the blackening of the film corresponding to each of the 10 steps,
it is possible to trace the relationship between intensity and blackness character-
istic of the film   For the films used in the present series of experiments the
blackening curve is practically linear, so that the wedge readings may be
taken as true measures of the intensity, some slight correction being applied
to the strongest peaks where the calibration curve shows a slight departure
from the linear law

Table I—Observed Intensities   Arbitrary Units

Line		Iron Kα radiation λ = 1 934		Copper Kα radiation λ = 1 539		Zinc Kα radiation λ = 1 434	
2h²	hkl	Observed values	Corrected for absorption	Observed values	Corrected for absorption	Observed values	Corrected for absorption
3	111	110	96	119	171	123	158
4	200	330	236	172	198	152	161
8	220	4730	2040	4041	2750	3663	2490
11	311	78	26	92	48 5	67	36
12	222	171	53	71	34 5	49	24
16	400	1181	288	895	342	758	303
19	331	31	6 5	47	15 5	29	10
20	420	272	54	111	35	53	18
24	422	1974	694	2111	503	1616	482
27 { 511 / 333 }		58	8 5	35	8 5	43	11
32	440	2811	349	697	142	497	111
35	531	106	12	47	9	—	—
36 { 600 / 442 }		867	94 5	62	11	—	—

For each line wedge readings were taken at intervals of 0 1 mm., and the
blackening values so found plotted against the distance along the film. The
areas included under the peak curve and above the general level of the back-
ground intensity were computed, and tabulated in Table I Corrections for
the effect of absorption in the powder specimen were made by the method

of graphical integration described by Claassen * The values of the absorption
factor depend on the product of the absorption coefficient (μ) and the radius
of the specimen (r)

As a convenient method of support during the exposure, the specimen is
diluted with Canada balsam and mounted on a hair The effective value of
μr is thereby reduced The appropriate value of μr is most easily obtained
from the following equation —

$$\mu r = \frac{\mu}{\rho} \, m \, \frac{1}{\pi r l}$$

The weight of the specimen (m) was 0 0024 gm., the length (l) 0 49 cm ,
and radius (r) 0 0265 cm The values of μ/ρ were calculated with the help
of Jonsson's tables,† for each of the elements Al, Cu, and Mn with each of the
radiations Fe, Cu, and Zn The results are summarized in Table II

Table II

| Radiation | λ | μ/ρ values | | | | μr |
		Al	Cu	Mn	Cu₂MnAl	Cu₂MnAl
Fe K$_a$	1 934	93 9	100	64	89 5	5 3
Cu K$_a$	1 539	51 2	50 4	285	113	6 7
Zn K$_a$	1 434	41 8	42 6	234	93 6	5 5

Applying these values of μr to the data given by Claassen, the values of the
absorption factor were found for glancing angles 0°, 22½°, 45°, 67½°, and 90°
Curves were then drawn giving the absorption factors for all angles between 0°
and 90°, for each of the three radiations From these curves were obtained
the absorption factors by which the observed intensity values were divided

The corrected intensity values in Table I are proportional to theoretical
intensity values given by the equation

$$I = \frac{1 + \cos^2 2\theta}{\sin^2 \theta \cos \theta} \, p F^2 ,$$

where θ is the glancing angle, p the number of co-operating planes, and F the
structure factor at room temperature With the help of this equation the

* ' Phil. Mag.,' vol 9, p. 57 (1930)

† Jönsson, ' Uppsala Univ Årsskr ' (1928) , Siegbahn, " Spektroscopie der Röntgen
strahlen," Julius Springer, Berlin (1931)

relative F values in Table III were obtained They were reduced to a comparable scale by putting F220 = 100 for each radiation

This table shows some interesting features On account of their smaller intensity, the superlattice lines $\Sigma h^2 = 3, 4, 11, 12, 19, 20, 27, 35, 36$ are easily distinguished from the body-centred lines 8, 16, 24, 32 The superlattice lines themselves may be divided into two series, the odd reflections 3, 11, 19, 27, 35 being definitely weaker than the corresponding even reflections 4, 12, 20, 36 This distinction is to some extent obscured in Table I owing to the complications introduced by the θ factor and the planar factor It is shown better

Table III —Observed F Values for Three Radiations

Line		Iron K_α radiation $\lambda = 1\ 934$		Copper K_α radiation $\lambda = 1\ 539$		Zinc K_α radiation $\lambda = 1\ 434$	
Σh^2	hkl	Relative F values	Differences in neighbouring superlattice lines	Relative F values	Differences in neighbouring superlattice lines	Relative F values	Differences in neighbouring superlattice lines
3	111	15	} −17 {	17	} −8 {	18	} ~ 6 {
4	200	32		25		24	
8	220	100	—	100	—	100	—
11	311	10	} −15 {	11	} −6 {	10	} −5 {
12	222	25		17		15	
16	400	79	—	76	—	75	—
19	331	6	} −12 {	9	} −5 {	8	} −2 {
20	420	18		14		10	
24	422	65	—	60	—	59	—
27	511 333 }	6	—	7	-	8	—
32	440	50	—	47	—	46	—
35	531	4	} −7 {	6	} −2 {	—	—
36	600 442 }	11		8		—	—

by the figures given in Table III for the differences between the F values for neighbouring odd and even lines The table shows that *the distinction between odd and even superlattice lines is far more marked with iron radiation than with copper or zinc radiation* We shall now discuss the explanation of this phenomenon

It will be shown that the differences with different radiations are due to the relation of the atomic scattering factor (f) to the wave-length λ f is usually given as a function of $\sin \theta/\lambda$ which is independent of the wave-length, but this is not strictly correct.

II *The Atomic Scattering Factors of Aluminium, Manganese, and Copper*

It has been shown in a number of experimental investigations[*] that the atomic scattering factor (f) of an element for X-rays depends upon the wave-length of the radiation, or to put the matter more precisely, the atomic scattering factor of an element is depressed by the use of radiation whose frequency lies close to the critical K absorption frequency of the scattering element This fact was to be expected on theoretical grounds, and is analogous to anomalous dispersion in the optical region It has been explained with the help of a combination of classical theory and quantum mechanics by Kallmann and Mark, Kronig, and Prins † According to Coster and Knol,‡ the theory of Prins may be expressed in the following way

The atomic scattering factor f of an element may be regarded as consisting of two components f_K due to the K electrons, and f_R due to the L, M, etc , electrons Now in the present experiments, the factor f_R may as a first approximation be considered as independent of the wave-length, because we are using radiation much harder than the critical L, M, etc , absorption edges

On the other hand, for copper and manganese, the value of f_K is very susceptible to changes in wave-length, since all three radiations used are close to the K absorption edges of these elements

According to Coster and Knol, for radiation on the short wave-length side of the absorption edge, there is a phase-change in the contribution of the K electrons to the atomic scattering factor This may be expressed by writing f_K as a complex quantity, thus

$$f_K = f'_K + \imath f''_K, \qquad (2)$$

where $\imath = \sqrt{-1}$, and f'_K and f''_K are two components with a phase difference of $\pi/2$, the resultant of which is f_K The component f'_K either has the same phase as f_R or differs from it by an amount π The component f''_K has a phase difference $\pi/2$ compared with f'_K and f_R.

* Mark and Szillard, ' Z Physik,' vol 33, p 688 (1925), Armstrong, ' Phys Rev ,' vol 34, p 931 (1929), Wyckoff, ' Phys Rev ,' vol 35, pp 215, 583, 1116 (1930), Morton, ' Phys Rev ,' vol 38, p 41 (1931), Coster, Knol and Prins,' Z Physik,' vol 63, p 345 (1930), vol 75, p 340 (1932), Glocker and Schäfer, ' Z Physik,' vol 73, p 289 (1931), Bradley and Hope,' Proc Roy Soc ,' A, vol 136, p 272 (1932)

† Kallmann and Mark, ' Ann Physik,' vol 82, p 585 (1927), Kronig and Kramers, ' Z Physik,' vol 48, p 174 (1928), Prins, ' Z Physik,' vol. 47, p 479 (1928), Kronig, ' Phys Z ,' vol. 30, p 521 (1929)

‡ ' Z Physik,' vol 75, p 340 (1932), ' Proc Roy Soc ,' A, vol. 139, p 459 (1933)

f'_K is given by the equation

$$f'_K = n_K \left\{ 1 + \frac{\log_e |x^2 - 1|}{x^2} \right\}, \tag{3}$$

where $x = \frac{\lambda_K}{\lambda}$, λ_K being the critical absorption wave-length of the scatterer,

and λ the wave-length of the radiation

f''_K is given by the equation

$$f''_K = \frac{\pi}{x^2} n_K \tag{4}$$

In each of the above equations n_K represents the full effect of the K oscillators away from the region of anomalous scattering   According to Prins the most probable value of n_K is 1 3, though Kronig and Kramers gave 0 86

For radiation on the long wave-length side of the absorption edge there is no change of phase angle, and the expression for f_K therefore simplifies to

$$f_K = n_K \left\{ 1 + \frac{\log_e |1 - x^2|}{x^2} \right\}, \tag{5}$$

where n_K and x have the same meaning as before   Taken as it stands, equation (5), like equation (3), gives values of $f = -\infty$ at the absorption edge, but Glocker and Schäfer have shown how this may be modified by the introduction of damping terms

The change of phase angle on the short wave-length side of the absorption edge was verified qualitatively by the experiments of Coster, Knol, and Prins with zinc blende, and the general nature of the depression of the f values near the absorption edge is well verified by all the experimental work done in this region , but no satisfactory quantitative check has yet been obtained   According to most experimenters, the scattering factor is depressed on the short wave-length side considerably more than is demanded by theory   On the contrary, Bradley and Hope found that the scattering power of iron for copper K_a radiation was very little depressed   Coster and Knol have recently pointed out that a correction must be made to this result to allow for the effect of a change in phase angle   However, this correction does little to bridge the difference from the results of other investigators, as may be seen from the following table

We have chosen what we consider to be the most probable values of the scattering factors of copper and manganese, based on the experimental work of Bradley and Hope   They compared the values of the atomic scattering factor of iron for different radiations at the same value of $\sin \theta / \lambda$ For both

Table IV —The Atomic Scattering Factor of Iron (f_{110})

Radiation	λ/λ_K	Glocker and Schäfer*	Wyckoff †	Bradley and Hope	Calculated from equations (3), (4), (5)
Mo K$_a$	0 41	16 3	(17 1)	16 3	17 2	17 55
Cu K$_a$	0 89	9 4	(11 6)	11 8	16 1 (corrected)	16 3
Ni K$_a$	0 95	8 0	—	10 1	—	—
Co K$_a$	1 01	—	—	—	14 1	12 6
Fe K$_a$	1 10	11 9	(13 5)	13 8	15 7	14 5
Cr K$_a$	1 31	12 7	~		17 2	15 25

* Glocker and Schäfer have recently amended these values, and in a private communication to one of the authors they give values more nearly in agreement with those of Wyckoff   These are given in brackets
† Corrected for temperature factor

cobalt and iron radiations the scattering factor was found to be depressed below that for molybdenum radiation by an amount which was almost independent of $\sin\theta/\lambda$ This is to be expected on theoretical grounds   The depressions are due to changes in the contributions of the K electrons to the atomic scattering factor for different values of λ/λ_K These depend only on n_K which is almost independent of $\sin\theta/\lambda$

For copper K$_a$ radiation, according to Coster and Knol, the difference in scattering factor should be greater as the value of $\sin\theta/\lambda$ increases, owing to the fact that f_K is a complex quantity   However, we may split up the atomic scattering factor into its two components, a real component $(f_R + f'_K)$ and an imaginary component, f''_K which differs in phase by $\pi/2$ At all values of $\sin\theta/\lambda$, $(f_R + f'_K)$ should be depressed by the same amount   It is therefore possible to obtain for each radiation a characteristic value of the depression of the " real " component of the f curve of iron, which is independent of $\sin\theta/\lambda$

The depression in f in the neighbourhood of the K absorption edge is due to a variation in the contribution of the K electrons to the total f value of the atom   Whether we use a combination of classical theory and quantum theory (as Prins has) or a purely wave-mechanical theory,* the variation in the contribution of the K electrons to the total value for the atom is a function of λ/λ_K

It follows from this result that the anomalous dispersion by different elements can be deduced from experiments on one element only, provided the results

* We are indebted to Dr Williams of this University for discussing this matter with us

are expressed in terms of λ/λ_K Experiments are now being undertaken to
test the validity of this generalization, the results of which will be communicated
in due course

In fig 4 the depressions in the observed f values for iron are plotted against
the values of λ/λ_K, λ being the wave-length of the radiations used (Mo, Cu,
Co, Fe, Cr characteristic K$_\alpha$ radiations), and λ_K the wave-length of the K
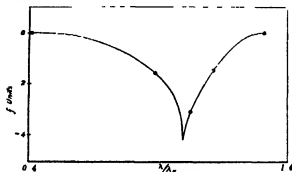
FIG 4 —Depression of f curves in the region of the K absorption edge   ○ Points from
experiments on FeAl (Bradley and Hope) giving the difference between the normal
f values and the values found near the absorption edge   For Cu radiation the value
plotted is not f but $f_K + f'_K$ f''_K is calculated separately from the formula

$$f''_K = \frac{\pi}{g^2}\, n_k$$

absorption edge of iron   The values for molybdenum radiation are taken as
zero   In this figure the values of the depression at some distance from the
absorption edge approach zero, and the biggest values of the depression are
in the immediate neighbourhood of the K edge   Plotted as a function of
λ/λ_K, theory indicates that the values represented on this curve should be
universal   They represent the amounts to be subtracted from the normal f
values where the frequency of the radiation is comparable with the critical
absorption frequency

In order to obtain the value of the atomic scattering factor for a given
element with a given radiation for a given value of sin θ/λ, we first take the
" normal " value of the atomic scattering factor of the element for the required
value of sin θ/λ, and then subtract an amount read off from this curve, fig 4,
to allow for the anomalous effects of the K absorption edge on f_K Then we
calculate the amount of f''_K from equation (4), assuming $n_K = 1$ 3, and intro-
duce a separate term into the calculations to allow for the effect of f''_K when

$\lambda/\lambda_K < 1$ An illustration will show how simple the procedure can be. To find $f_{Mn} - f_{Al}$ for copper K_a radiation we have

$$F = \sqrt{(f_{Mn} \text{ normal} - f_{Mn} \text{ depression} - f_{Al})^2 + f''_K{}^2} \qquad (6)$$

Table V contains the necessary data for the evaluation of this expression, for the Heusler alloy.

Table V —Depression in f Curve, due to Anomalous Dispersion

Scattering elements	λ_K	Zinc K_a radiation $\lambda = 1\ 434$	Copper K_a radiation $\lambda = 1\ 539$	Iron K_a radiation $\lambda = 1\ 934$
Al 13	7 936	0	0	0
Mn 25	1 892	1 0	1 0	3
Cu 29	1 377	2 5	1 5	0

Substituting in equation (6),

$$F = \sqrt{(f_{Mn} \text{ normal} - f_{Al} - 1\ 0)^2 + 2\ 7^2}$$

The normal f curves of aluminium, manganese, and copper were obtained from a paper by James and Brindley * The aluminium values were calculated by Hartree's method of self-consistent fields , for copper an approximate curve was obtained by the same method , for manganese, the Thomas values were used   It was shown by Bradley and Hope that the Thomas curve for iron gave an excellent agreement for molybdenum radiation, and since manganese is the next element to iron and does no differ greatly in atomic volume, it seems fairly safe to use the Thomas curve though, of course, it is probably less accurate than the other two calculated by Hartree's method

It is now possible to understand the differences in the powder photographs taken with zinc, copper, and iron radiations   As Table V shows, the atomic scattering factor of manganese with iron radiation is three units less than normal, whereas that of copper with iron radiation is practically normal Hence the difference in scattering power between copper and manganese is *three units greater* than normal   On the other hand, with zinc radiation the scattering power of copper is depressed more than that of manganese, so that the difference in scattering power between copper and manganese is now 1 5 *units less* than normal   Thus iron radiation emphasizes the difference in scattering power between copper and manganese, whereas zinc radiation

* 'Phil. Mag.,' vol 12, p 81 (1931), 'Z Kristallog.,' vol 78, p 470 (1931).

minimises the difference This fact naturally leads to differences in the intensities of the weaker reflections, where copper and manganese work in opposite directions As we shall see later, the figures given in Table V provide not merely a qualitative explanation, but ultimately give a perfect quantitative explanation of all the observed intensities (Table VII)

On the other hand, if we had used the data of Glocker and Schafer or of Wyckoff, we should have been led to the conclusion that the scattering powers of copper and manganese with iron radiation ought not to be appreciably different from those with copper or zinc radiation The different results obtained with different radiations prove that this is impossible The theoretical expressions (equations (3), (4), and (5)) predict a difference between the scattering powers of copper and manganese for the different radiations employed, but do not explain the observed numerical values as well as our empirical values from the iron-aluminium experiments Possibly more accurate results would be obtained if this theory took account of the variation in the contribution of the L electrons as well as the K electrons The empirical curve, given in fig 4, automatically makes this allowance, and partly for this reason should give accurate f values, if the experiments of Bradley and Hope are a sufficient basis for the curve It is expected that new data will shortly become available, giving more points on the curve

III Possible Structure for the Heusler Alloy

The unit cell contains 16 atoms with the co-ordinates —

A	$0\ 0\ 0,$	$0\ \frac{1}{2}\ \frac{1}{2},$	$\frac{1}{2}\ 0\ \frac{1}{2},$	$\frac{1}{2}\ \frac{1}{2}\ 0$
B	$\frac{1}{4}\ \frac{1}{4}\ \frac{1}{4},$	$\frac{1}{4}\ \frac{3}{4}\ \frac{3}{4},$	$\frac{3}{4}\ \frac{1}{4}\ \frac{3}{4},$	$\frac{3}{4}\ \frac{3}{4}\ \frac{1}{4}$
C	$\frac{1}{2}\ \frac{1}{2}\ \frac{1}{2},$	$\frac{1}{2}\ 0\ 0,$	$0\ \frac{1}{2}\ 0,$	$0\ 0\ \frac{1}{2}$
D	$\frac{3}{4}\ \frac{3}{4}\ \frac{3}{4},$	$\frac{3}{4}\ \frac{1}{4}\ \frac{1}{4},$	$\frac{1}{4}\ \frac{3}{4}\ \frac{1}{4},$	$\frac{1}{4}\ \frac{1}{4}\ \frac{3}{4}$

Symmetry considerations divide the atoms into the four sets A, B, C, D, as shown in fig 2 The problem is to find which of these positions are occupied by copper, aluminium, and manganese atoms respectively The data of Table III point the way to a solution

Three facts must be explained —

(1) The existence of three series of reflections, one strong series of lines [(1) 220, 400, 422, 440], and two weak series of superlattice lines

$$\left[(2)\ \overset{442}{200,\ 222,\ 420,\ 600} \right], \quad \left[(3)\ \overset{333}{111,\ 311,\ 331,\ 511,\ 531} \right]$$

(2) The superlattice lines of series (3) are definitely weaker than those of series (2)

(3) The difference in intensity of the two series of superlattice lines depends on the wave-length of the radiation, being greatest for iron radiation and least for zinc radiation

Let the scattering powers in the four groups be f_a, f_b, f_c, and f_d respectively Then the structure factors for planes of types (1), (2), (3) may be written in the following way —

(1) $f = f_a + f_b + f_c + f_d$
(2) $f = (f_a + f_c) - (f_b + f_d)$
(3) $f = \sqrt{(f_c - f_a)^2 + (f_d - f_b)^2}$

From these equations it may be seen that the presence of reflections of both types (2) and (3) requires one group to be appreciably different in scattering power from the other three Since copper and manganese are not very different in scattering power, this condition is equivalent to a requirement that most if not all the aluminium atoms should be sorted out into one group, say B

If the atoms in groups A, C, D were equivalent in scattering power, reflections of types (2) and (3) would be equally strong This is not so The greater intensity of type (2) reflections shows that the scattering power of D groups is intermediate between those of A and C on the one hand and B on the other This admits of two interpretations either manganese atoms go into D positions, or the aluminium atoms are not completely sorted out into B positions, a minority of the aluminium atoms being found in D positions

The second alternative would be analogous to the iron aluminium alloys* containing a little more than the correct amount of aluminium to satisfy the formula Fe_3Al Here most of the aluminium atoms occupy position B, but a certain proportion move over to position D, leaving B without its full complement of aluminium atoms

To distinguish between the two alternatives, it is necessary to make use of the fact that the intensities of the two sets of superlattice lines differ considerably with different radiations (see Table III) This could not be explained by a partial distribution of aluminium between positions B and D It can, however, be explained by placing manganese atoms in D and aluminium atoms in B This distribution gives structure factors $2Cu - (Mn + Al)$ and $(Mn - Al)$ for types (2) and (3) respectively The difference is $2(Cu - Mn)$ As we have shown in a previous paragraph, the scattering power of copper

---

* Bradley and Jay, ' Proc Roy Soc,' A, vol. 136, p 210 (1932)

exceeds that of manganese more with iron radiation than with copper and zinc radiations With this structure, we should therefore expect that the intensity differences between reflections of type (2) and (3) would be greatest with iron radiation and least with zinc radiation, which is in complete accordance with the facts

The above arguments show that most of the aluminium atoms are in position B and most of the manganese atoms are in position D, but the sorting out of the atoms cannot be complete, because the composition of the alloy does not correspond exactly to the formula Cu_2MnAl In order to decide the exact arrangement, a quantitative test is necessary Before comparing the observed intensities with the calculated intensities for the most probable arrangement, we shall first give calculations for three different arrangements of manganese atoms with the ideal composition Cu_2MnAl It will be seen that the differences between the intensities of the superlattice lines in the three cases are so large that it is possible to be quite sure of the ultimate solution

The three arrangements considered first are —

(ı) Mn in D, Cu in A and C, Al in B
(ıı) Mn and Cu at random in A, C, and D, Al in B
(ııı) Mn in A, Cu in C and D, Al in B

Table VI —Comparison of Observed and Calculated Intensities for Three Different Structures

	Line	Iron K_α radiation $\lambda = 1\ 934$				Copper K_α radiation $\lambda = 1\ 539$			
		Observed with temperature correction	Calculated			Observed with temperature correction	Calculated		
Σh^2	hkl		i	ıı	ııı		i	ıı	ııı
3	111	14	10	27	48 5	33	28	43	59
4	200	36	49	14	5	39 5	51	23	14
8	220	340	354	354	354	600	593	593	593
11	311	4 5	2	10	22	11	9 5	17	26
12	222	9 5	12	J	0 5	8	12	5	3
16	400	57	56	56	56	88	90	90	90
19	331	1 5	1	4	9 5	4	3 5	6	8 5
20	420	11 5	17	4	0 5	10	12	5	2 5
24	422	156	148	148	148	173	167	167	167
27 {	511 333 }	2	1	4 5	11	2 5	3	4	5 5
32	440	97	95	95	95	51	54	54	54
35	531	3 5	5	12 5	30	3 5	3 5	4	5 5
36 {	600 442 }	29	46	10	2	4 5	5	2 5	2

In order to make the observed intensities comparable with the calculated values, they must be reduced to the same scale This process is complicated because the observed values are found at room temperature, whereas the calculated values apply only at the absolute zero of temperature This causes the observed intensities to fall off too quickly with increasing values of $\sin \theta/\lambda$ The observed values should be related to the calculated values in the following way

$$I_{obs.} = I_{calc} \, K e^{-\frac{B \sin^2 \theta}{\lambda^2}},$$

where λ is the wave-length and θ the glancing angle B is a physical constant which is the same for all radiations K is arbitrary and differs for each experiment, depending on the experimental conditions The scales of the observed values are adjusted by choosing values of K and B to give the best measure of agreement between observed and calculated reflections for planes 220, 400, 422, and 440, the values of which are independent of the atomic arrangement It was found that the best agreement between observed and calculated values was obtained by putting B = 3

Table VI includes results from iron and copper radiations The zinc values are not included as the difference in the scattering powers of copper and manganese is too small to give decisive results It can be seen from this table that almost all the observed intensity values of the superlattice lines lie between the calculated values for structure (I) and structure (II) Structure (III) is, therefore, ruled out

The obvious interpretation of this result is that structure (I) is essentially correct, but since there are too few manganese atoms to fill the whole of the D positions some of the manganese has been replaced by copper This has the effect of reducing the difference in scattering power between A and C on the one hand and D on the other The formula for the alloy may be written as $Cu_2(MnCu)Al$ It must, however, be taken into account that there is a small proportion of aluminium atoms in excess This must either replace copper in A and C or manganese in D Good agreement with the observed intensities can only be obtained if it is supposed that the excess of aluminium is equally distributed between positions A, C, and D The most probable atomic distribution is as follows —

A atoms 0 95 copper, 0 05 aluminium

B atoms All aluminium.

C atoms · 0·95 copper, 0·05 aluminium

D atoms 0·3 copper, 0·65 manganese, 0 05 aluminium

The calculated intensities for this structure are compared with the observed values in Table VII The scale has again been fixed to give the best agreement for the strong reflections, which depend only on the composition and not on the manner in which the atoms of different kinds are distributed. The intensities of the superlattice lines are thus obtained on an absolute scale, and the close agreement with the calculated values can therefore be taken as a conclusive proof that both the structure is correct and also that the empirical rule for calculating f values in the neighbourhood of the K absorption edge is reliable

Table VII —Comparison of the Observed and Calculated Intensities for the Most Probable Structure

Line		Iron K_α radiation $\lambda = 1\ 934$		Copper K_α radiation $\lambda = 1\ 539$		Zinc K_α radiation $\lambda = 1\ 434$	
Σh^2	hkl	Observed	Calculated	Observed	Calculated	Observed	Calculated
3	111	15	15	32 5	30	37	40
4	200	37 5	37	38 5	39	39	36
8	220	353	354	587	589	655	647
11	311	5	5	11	11 5	10	11
12	222	10	8 5	8	9	7	8
16	400	59	57	86	87	95	95
19	391	1 5	2	4	4	3	4
20	420	12	12	9 5	9 5	6	7
24	422	161	153	169	164	172	171
27 {	511 333	} 2	2	2 5	3	4	3
32	440	} 101	98	50	52	49	50
35	531	3 5	5 5	3 5	3	—	—
36 {	600 442	} 30	32	4 5	3 5	—	—

In conclusion, the authors thank Professor W L Bragg, F R S, for his kind interest in the work, which was carried out in the Physical Laboratories of the University of Manchester

Summary

In an investigation of the ferromagnetic alloys of copper, manganese, and aluminium an alloy was found which showed an almost complete change of crystal structure due to heat treatment Drillings of this alloy, which had been annealed at 500° for several hours and cooled slowly to room temperature, were found to have the δ type of copper aluminium (Cu_9Al_4) type of structure. The formula may be written as $(CuMn)_9Al_4$, the atoms occupying the same positions as in Cu_9Al_4 The annealed and slowly cooled alloy is non-magnetic, but on

quenching from 800° C it becomes strongly ferromagnetic The structure is now entirely body-centred cubic, with a face-centred superlattice

A quantitative X-ray examination of the ferromagnetic alloy showed the utility of a new method for distinguishing between elements of almost equal scattering power On comparing X-ray powder photographs of the same specimen made with radiations from iron, copper, and zinc anticathodes, it was found that the relative intensities of the weaker reflections varied with the wave-length of the radiation This fact made it possible to distinguish the manganese atoms from the copper atoms, which would not have been possible if results from only one radiation had been available. The difference between the atomic scattering factors of copper and manganese which is very small with zinc radiation becomes fairly large with iron radiation

The ideal structure of the ferromagnetic alloy would be —

Cu	$0\ 0\ 0$	$0\ \frac{1}{2}\ \frac{1}{2}$	$\frac{1}{2}\ 0\ \frac{1}{2}$	$\frac{1}{2}\ \frac{1}{2}\ 0$
	$\frac{1}{4}\ \frac{1}{4}\ \frac{1}{4}$	$\frac{1}{2}\ 0\ 0$	$0\ \frac{1}{2}\ 0$	$0\ 0\ \frac{1}{2}$
Al	$\frac{1}{4}\ \frac{1}{4}\ \frac{1}{4}$	$\frac{1}{4}\ \frac{3}{4}\ \frac{3}{4}$	$\frac{3}{4}\ \frac{1}{4}\ \frac{3}{4}$	$\frac{3}{4}\ \frac{3}{4}\ \frac{1}{4}$
Mn	$\frac{3}{4}\ \frac{3}{4}\ \frac{3}{4}$	$\frac{3}{4}\ \frac{1}{4}\ \frac{1}{4}$	$\frac{1}{4}\ \frac{3}{4}\ \frac{1}{4}$	$\frac{1}{4}\ \frac{1}{4}\ \frac{3}{4}$

In the specimen examined there was a deficit of manganese atoms The alloy was nevertheless homogeneous, some copper taking the place of the missing manganese atoms The aluminium atoms in excess were distributed equally in the positions normally occupied by copper and manganese

The Diffraction of Electrons in the Halogens

By F L Arnot, Ph.D, Lecturer in Natural Philosophy, The University, St Andrews.

Introduction

Although the complete theory of the scattering of electrons by gas atoms must take into account the distortion of the incident and scattered waves by the atomic field, the exchange of electrons between the atom and the incident beam, and the disturbance of the atomic wave functions by the incident and scattered waves, a satisfactory explanation of the diffraction effects observed in the angular distribution of the elastically scattered electrons is obtained simply by considering the distortion of the incident wave by the undisturbed field of the atom * The scattering at large angles will then mainly depend upon the nature of the atomic field at the point in the atom where the potential energy of the incident electrons is equal to their kinetic energy

Now the magnitude and gradient of the field at any point within the atom at a distance r from the centre is determined mainly by the nuclear charge and the screening constants of the electrons within the radius r, and hence the nature of the field at a point well within the outer electron shell will be similar for atoms whose electronic structures differ only in the constitution of the outer shell

Thus, if the energy of the incident electrons is large compared to the ionization energy of the outer electron shell, we should expect that those elements of adjacent atomic number, which differ only in the structure of the outer shell, such as a rare gas and the adjacent alkali metal or halogen, would give similar diffraction patterns

Some experimental evidence for this was recently obtained by Mohr and Nicoll[†] who showed that the angular scattering curves for argon, sulphur and phosphorus were very similar Further evidence is provided by some previous results of mine[‡] for CH_4, N_2, CO and Ne, the diffraction patterns of which are all very similar, as one would expect, since the scattering in these gases is

---

* Except for very slow electrons and for the lightest gases when exchange effects become important

† ' Proc Roy Soc ,' A, vol 138, p 469 (1932)

‡ Arnot, ' Proc Roy Soc ,' A, vol 133, p 615 (1931)

mainly due to the C, N, O and Ne atoms which all occupy the same row of the Periodic Table and differ only in the structure of the outer electron shell

In this paper I present some results for iodine, bromine, bromoform and carbon tetrachloride It will be seen that these results are very similar to those which I obtained some time ago for the rare gases *

Apparatus

The apparatus used in this work, and the experimental procedure adopted, have been fully described in previous papers † It consists essentially of an electron gun producing a narrow homogeneous beam of electrons which can be set at different angles to a system of collecting slits, between which potentials are placed so as to separate the elastically scattered electrons from those which have excited or ionized the atom and from the positive ions so produced

The apparatus was thoroughly baked out, the filament flashed and then run for about 15 minutes until the pressure read on a McLeod gauge fell to about 10^{-5} mm of Hg Mercury vapour was excluded from the apparatus by having a trap on the outlet tube immersed in a mixture of solid CO_2 and alcohol During a run the pumps were kept going and the vapour of the various substances was allowed to flow continuously through the apparatus, being admitted through an adjustable leak The vapour pressure was measured by a Pirani gauge situated in the scattering chamber itself The Pirani gauge was calibrated against the McLeod gauge with air, and it was then assumed that the calibration constant so obtained was approximately correct for the vapours used During a run the pressure was kept constant at a value between 1×10^{-3} and 3×10^{-3} mm, of Hg Over this range of pressure the relation between the scattered current and the pressure is known from previous work* to be linear for argon The linear relationship was again tested in this work with CCl_4 and with $CHBr_3$ and was found to hold, consequently it may be concluded that the results presented here are due to single scattering

The substance in the vapour of which the scattering was to be measured was contained in a small bulb which communicated with the apparatus through a tap and the adjustable leak

Iodine —About a gram of solid iodine was placed in the bulb which was then surrounded with cotton wool and kept at room temperature The vapour pressure behind the leak was thus about 0 15 mm

Bromine —The bulb containing about 1 c c of bromine was immersed in alcohol at a temperature of about $-60°$ C contained in a vacuum flask. The temperature of the alcohol was reduced by adding solid CO_2 until the vapour pressure behind the leak was about 0 3 mm The bromine was supplied by The British Drug Houses, Ltd , and was of their A R standard.

Bromoform —About 1 c c of bromoform was placed in the bulb which was then immersed in a mixture of crushed ice and water giving a vapour pressure behind the leak of about 2 mm The bromoform was supplied by The British Drug Houses, Ltd , as free from alcohol

Carbon Tetrachloride —The bulb containing a few cubic centimetres of CCl_4 and a lump of anhydrous calcium chloride was surrounded with cotton wool and kept at room temperature The vapour pressure in the bulb was thus about 70 mm

The iodine and bromoform were dried by inserting a small glass tube containing P_2O_5 into the bulb containing the substance with its open end above the surface of the substance No drying agent was used with bromine as the vapour pressure of ice at $-60°$ C is negligible compared with the vapour pressure of bromine in the bulb In each experiment during the evacuation of the bulb the substance was frozen with solid CO_2 and alcohol

After completing the work on one substance the apparatus was dismantled and thoroughly cleaned except after doing bromoform, which was the second last vapour to be used When the work on bromoform was completed the bromoform was replaced by bromine, and the apparatus baked out at $400°$ C for about 2 hours After the apparatus had cooled down, and with the filament on, the vapour pressure read on the Pirani gauge was less than 10^{-4} mm The reason for not dismantling the apparatus (and for not renewing the filament) was so as to have the conditions for scattering in bromoform and bromine as identical as possible, so that the magnitude of the scattering in $CHBr_3$ and Br_2 might be truly comparable

Discussion of Results

The results, which have all been reduced to a common pressure and a common value for the intensity of the electron beam, are shown graphically in figs 1 and 2, and the experimental values used in constructing these curves are given in Tables I and II As the results for all electron energies in any one vapour, except carbon tetrachloride, were obtained in a single run on the same day, the values for different energies in the same vapour should be strictly comparable Owing to the precautions taken not to disturb the alignment of

slits and filament between the experiments with bromoform and bromine (see above) the values for these two vapours should also be strictly comparable.

Table I —Carbon Tetrachloride and Iodine

Carbon tetrachloride (CCl₄)							Iodine (I₂)				
V_e	15	30	42	50	84	100	V_e	15	42	80	122
$\theta°$	I_θ	I_θ	I_θ	I_θ	I_θ	I_θ	$\theta°$	I_θ	I_θ	I_θ	I_θ
25	224	103		112		76 0	18			81 0	93 0
30			113		60 0		23			27 5	38 0
35	98 0	76 0	78 5	50 0		25 3	28		52 1	18 0	34 0
40	79 0	57 0		24 9			33		30 5	21 5	41 7
45		23 7	20 5		11 6		38	274	—	23 4	37 9
50				9 4	10 9		43		11 4	23 4	30 3
55	66 5	25 5				9 15	48	155	9 45	17 7	22 5
60		12 7		7 23		10 6	53		9 65		10 6
65	44 0	12 8		7 1	6 20		58	108	10 8	6 85	4 38
70				5 85			63		12 1		
75	31 4	12 0		7 9	5 40		73	68 2	12 0	2 57	4 70
80			10 9	5 60			78		10 9		
85	31 2	15 1		11 3	6 54		83	51 7	9 15	5 41	15 3
90		16 4			6 40		88	40 7	7 50	6 25	18 1
95	33 4	19 6	12 0			5 65	98	35 6	10 6	5 30	7 22
100		16 8			6 00		108	35 3	20 0	6 90	3 22
105	32 3	20 7	12 0			4 82	118	35 6	26 0	10 6	3 40
110		15 0			5 45		128	35 0	22 6	9 90	6 60
115	31 6	17 2		11 3		4 30	138	32 6	14 2	4 99	4 73
120		13 6			4 87		148	39 2	11 5	5 95	5 08
125	32 8	12 8	10 2			6 00					
130		11 0			5 62						
135	39 0	11 6	10 0			9 80					
140		12 1	12 3	11 0	8 62						
145						15 6					
150		13 7	14 3	15 3	14 7						

The curves in figs 1 and 2 have all been displaced in a vertical direction, the ordinate zero for each curve being shown by the short horizontal lines at the side of the curves The curves for 15- and 30-volt electrons in CCl₄ have not been displaced relative to each other, and consequently have a common base line The ordinates of the 15-volt curve in iodine, bromine and bromoform have all been reduced by half The number at the side of each curve represents the energy V_0 of the incident electrons in volts.

In fig 1 some curves for xenon and krypton, taken from an earlier paper,* have been given for comparison. The ordinate values of the xenon curves (which are comparable for the different energies) have been adjusted so that the

* Arnot, 'Proc Roy Soc ,' A, vol. 133, p 615 (1931).

maximum at 90° in the 122-volt curve fits the corresponding maximum in the 122-volt curve for iodine The krypton values, which are also comparable, have been adjusted so that the maximum at 70° in the 80-volt curve fits the corresponding maximum in the 80-volt curve for bromine

Table II —Bromoform and Bromine

Bromoform (CHBr₃)				Bromine (Br₂)				
V_e	15	41	80	121	V_e	15	41	80	121
$\theta°$	I_θ	I_θ	I_θ	I_θ	$\theta°$	I_θ	I_θ	I_θ	I_θ
24	—	—	—	146	24	—	—	144	82 0
29	485	251	110 5	74 0	29	495	220	78 0	36 8
34	—	108	65 5	41 7	34	—	138	34 2	16 6
39	284	129	74 8	30 1	39	285	79 0	16 4	10 4
44	—	73 5	24 3	24 4	44	—	53 1	9 52	8 97
49	221	51 0	22 9	22 5	49	182	30 8	8 77	9 45
54	—	37 9	22 8	20 5	54	—	23 0	10 4	10 2
59	167	28 3	22 7	19 1	59	121	19 6	11 7	10 3
64	—	25 5	19 0	17 2	64	—	19 4	12 2	9 80
69	117	21 5	16 1	13 2	69	90 0	20 1	12 1	7 82
74	—	22 5	14 7	—	74	—	19 3	11 0	6 34
79	76 8	21 0	12 3	6 80	79	75 0	17 7	9 62	3 84
84	—	19 3	—	—	84	—	16 2	—	—
89	66 1	16 8	7 62	4 65	89	65 8	15 0	5 40	—
99	62 5	14 0	6 90	8 02	99	61 4	15 7	2 87	4 00
109	68 2	13 9	9 28	12 0	109	58 7	18 2	3 80	6 00
119	78 0	17 5	12 5	13 2	119	59 0	21 6	5 57	7 96
129	85 7	23 3	15 2	10 3	129	63 4	21 1	6 00	6 30
139	96 7	31 0	15 6	8 59	139	71 5	19 7	4 99	3 64
149	—	28 2	12 6	6 65	149	—	19 9	4 16	2 62

In fig 2 my argon results for 42-, 83- and 124-volt electrons have been reduced so that the maximum at 105° in the 42-volt curve fits the corresponding maximum in the 42-volt curve for CCl₄ As my results extended only to 120° I have used the results of Mohr and Nicoll[*] to extend these curves to 155° The 30-volt curve for argon and the four curves for H₂S are also due to Mohr and Nicoll These five curves have all been fitted separately to the CCl₄ curves at the maxima

* 'Proc Roy Soc,' A, vol 138, p 469 (1932) I have not used their complete curves because their values for different energies are not comparable The extension of the 124-volt curve is not very accurate as it was obtained by interpolation between the ordinate values of Mohr and Nicoll's 150-volt curve and Hughes and McMillen's 100-volt curve ('Phys. Rev.,' vol. 39, p. 585 (1932)).
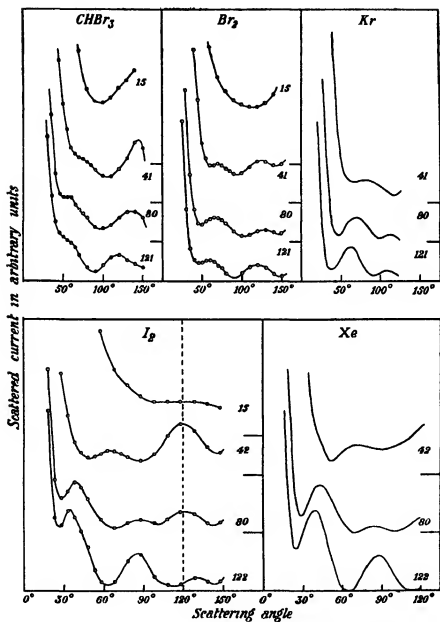
FIG 1 —Angular distribution of elastically scattered electrons in bromoform, bromine
and iodine with curves for krypton and xenon given for comparison

Referring now to the curves for iodine and xenon, and remembering that the xenon curves extend only to 120° (*i e*, up to the broken line in the iodine figure), we notice the remarkable similarity that exists not only in the shape of the curves but also in the relative magnitude of the scattering at the different energies The various maxima and minima occur at approximately the same
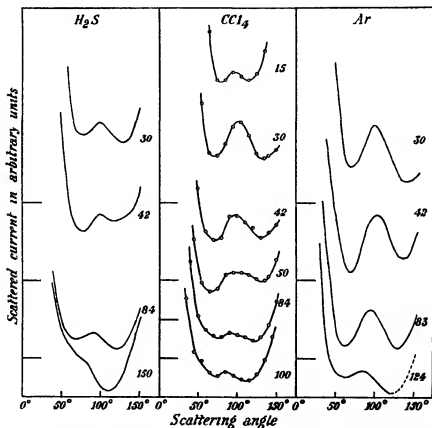
FIG 2—Angular distribution of elastically scattered electrons in carbon tetrachloride, with curves for hydrogen sulphide and argon given for comparison

angle in both sets of curves, but the first minimum in the iodine curves is not quite so pronounced as it is in the xenon curves

The same general similarity is shown by the bromine and krypton curves, but it is not so marked as for those of iodine and xenon

The vapour of iodine and bromine at room temperature consists of diatomic molecules, but Massey and Mohr* have shown that the scattering produced

* 'Proc Roy Soc,' A, vol 135, p 258 (1932)

by a homonuclear diatomic molecule is practically the same as that caused by the two separate atoms These results, therefore, provide further evidence that the scattering produced by atoms that differ only in the structure of the outer electron shell is practically identical for electrons having an energy greater than the ionization potential of the outer shell

It is interesting to notice the remarkable similarity of the bromine curve for 41-volts and the iodine curve for 42-volts In both curves there are maxima at 70° and 120°, the latter being higher than the former The interesting and important point is that these curves in bromine and iodine are so very similar, whereas the two corresponding curves (40-volt curves) in krypton and xenon are not nearly so similar, neither are the curves for higher energies in bromine and iodine or in krypton and xenon so similar

In view of the recent work of Childs and Massey* it might be expected that curves for the same energy in krypton and xenon, or in atomic bromine and iodine would be similar, for they have shown that cadmium gives curves very similar to those found for mercury, which lies in the same column of the Periodic Table They explain this by showing that the outer field of the cadmium atom is similar to that of mercury, since the two outermost shells in the two atoms have respectively the same number of electrons and approximately the same ionization potentials, and the same radii

Table III

Shell	Sub shell	Xenon		Krypton	
		Ionization potential in volts	Radius in A	Ionization potential in volts	Radius in A
K	$1s^2$	33500	0 010	14300	0 015
L	$(2s, 2p)^8$	4800	0 041	1800	0 067
M	$(3s, 3p)^8$	647	0 112	160	0 194
	$3d^{10}$	518	0 146	74 5	0 324
N	$(4s, 4p)^8$	150	0 280	13 94	0 885
	$4d^{10}$	27 4	0 490		
O	$(5s, 5p)^8$	12 08	1 04		

This, however, is not so for xenon and krypton In Table III are given the ionization potentials and the radii (defined as the distance from the centre at which the charge density of the shell electrons is a maximum) for the various

* 'Proc Roy. Soc.,' A, vol. 141, p. 473 (1933)

shells in xenon and krypton The number of electrons in each shell is denoted
by the superscript on the symbol giving the total and azimuthal quantum
numbers of the shell The values (except the ionization potential of the
outer shell for which the experimental value is used) have been calculated by
Slater's rules [*]

It will be seen from the table that the 42-volt electrons in xenon will be
scattered mainly by the field at about the centre of the N shell of 18 electrons
In krypton the 41-volt electrons will be scattered by the field between the N
shell of 8 electrons and the M shell of 18 electrons We should therefore not
expect these curves in xenon and krypton to be very similar The same will,
of course, apply to scattering by atomic iodine and bromine since the fields
of these atoms will be much the same as those for xenon and krypton

In diatomic iodine and bromine, however, the ionization potentials of the
outer shells will be different from those in the atom owing to the redistribution
of the outer electrons Owing to the striking similarity of the 40-volt curves
in iodine and bromine the portion of the field that is mainly effective in scatter-
ing electrons of this energy must be very similar in nature in the two molecules
—far more similar than it is in the atoms

The energies of the inner shells will not be very different from those of the
atom, and hence the scattering curves for fast electrons will be practically the
same as those for the atom

Considering now the curves for bromine and bromoform we see that the
curves for corresponding energies are on the whole of a similar nature, the
main difference being that the first maximum in the $CHBr_3$ curves is not so
pronounced as in the Br_2 curves, while the minimum at about 90° is more
marked in the $CHBr_3$ curves

The theory of the scattering by a molecule of $CHBr_3$ is complicated by the
fact that since the molecule has a permanent dipole moment the scattering
will depend upon the orientation of the axis of the molecular field relative to
the incident and scattered waves [†] However, the general similarity of the
curves given here for $CHBr_3$ and Br_2 shows that the scattering in $CHBr_3$
is mainly due to the relatively heavy bromine atoms constituting most of
the outer portion of the molecule

---

[*] 'Phys Rev,' vol 36, p 57 (1930)

[†] When the molecule has no permanent dipole moment the treatment is considerably
simplified for we can then consider the axis of the molecules to be orientated in random
directions This allows us to average the scattering over all orientations to obtain the
experimental conditions (see Massey, 'Proc. Roy Soc,' A, vol 129, p. 616 (1930))

We can explain the increased prominence of the minimum at 90° in the curves for $CHBr_3$ as being due to a contribution from the carbon atom to the total scattering, for the field of the central carbon atom will be fairly exposed over the portion that is screened only by the light hydrogen atom If we " uncover " more of the field of the central carbon atom by replacing the heavy bromine atoms by relatively light hydrogen atoms we obtain a scattering curve consisting solely of a minimum at 90° as is shown by the results[*] for CH_4.

It is clear from the above considerations that the scattering produced by a complicated molecule such as $CHBr_3$, which would be difficult to obtain theoretically, can be explained qualitatively by simply summing the contributions to the total scattering coming from the separate atoms of the molecule, assuming these scatter independently and paying due regard to the fact that the field of an atom may be effectively screened on one or more sides by relatively heavier atoms Thus it appears that a suggestion which I originally put forward some time ago[*] in explaining the results obtained for the scattering of low energy electrons in methane, namely, that we might be able to examine the structure and field of complex molecules by analysis of the diffraction patterns exhibited in the angular scattering curves, may prove to be of definite value

Since the scattering by bromoform is mainly due to the bromine atoms we should expect that the scattering produced by carbon tetrachloride would be even more truly representative of the scattering by chlorine, for not only has the CCl_4 molecule no permanent dipole moment but also the field of the central carbon atom is now practically completely screened by the four chlorine atoms (assuming the tetrahedral structure of the molecule)

The results given in fig 2 support this conclusion, for we see that the CCl_4 curves are similar to those of argon, and are intermediate in form between those of argon and hydrogen sulphide, just as the position of chlorine in the Periodic Table is intermediate between argon and sulphur The fact that the maximum at about 90° in the CCl_4 curves is not appreciably depressed shows how effective is the screening of the carbon atom by the four chlorine atoms

General Discussion

The elastic scattering of electrons by a spherically symmetrical field is given by[†]

$$I(\theta) = \frac{1}{4k^2}\left|\sum_{l=0}^{\infty}(2l+1)[e^{2i\eta_l}-1]P_l(\cos\theta)\right|^2, \tag{1}$$

---

[*] Arnot, ' Proc Roy Soc ,' A, vol 133, p 615 (1931)

[†] Mott and Massey, " The Theory of Atomic Collisions," chap II

where I (θ) is the scattered intensity at an angle θ, $k = 2\pi/\lambda$, where λ is the wave-length of the incident electrons, and the P_l (cos θ) are Legendre polynomials having the values —

$$P_0 \ (\cos \theta) = 1$$
$$P_1 \ (\cos \theta) = \cos \theta$$
$$P_2 \ (\cos \theta) = \tfrac{1}{2} \ (3 \cos^2 \theta - 1), \text{ etc}$$

The form of these curves is shown in fig 3 (c)

The incident electrons are resolved into beams of different angular momentum $\sqrt{l \ (l+1)} \ h/2\pi$ For each value of l a value of the wave function is found which is zero at the origin and has the asymptotic form

$$\sin \ (kr - \tfrac{1}{2}\pi l + \delta_l),$$

which becomes

$$\sin \ (kr - \tfrac{1}{2}\pi l),$$

in the absence of a scattering field

The phases δ_l in (1) are thus the phase differences between the asymptotic value of the wave function and its value when there is no atom situated at the scattering centre for each of these beams of different angular momentum These phases for the various values of l determine the form of the angular scattering curve

Now δ_l decreases monotonically as l increases, and the series in (1) converges more rapidly the lighter the atom and the lower the energy of the incident electrons Thus to represent the scattering of low velocity electrons by light atoms we require only the first few phases , and when this is so the predominant harmonic in (1) is that for which the corresponding phase has a value most nearly equal to $\pi/2$ This is clearly seen by separating the complex expression (1) into its real and imaginary parts We then obtain

$$I \ (\theta) = \frac{1}{4k^2} \left[\sum_{l=0}^{\infty} \ (2l+1) \ (\cos 2\delta_l - 1) \ P_l \right]^2 + \frac{1}{4k^2} \left[\sum_{l=0}^{\infty} \ (2l+1) \ \sin 2\delta_l P_l \right]^2$$

Thus if $\delta_i \simeq \tfrac{1}{2}\pi$ then the angular scattering curve will be of the form $|P_i \ (\cos \theta)|^2$ For example, for 30-volt electrons in argon the calculated phases are[*] $\delta_0 = 2\pi + 0 \ 885$, $\delta_1 = \pi + 1 \ 689$, $\delta_2 = 1 \ 938$, $\delta_3 = 0 \ 374$, $\delta_4 = 0 \ 159$, and the scattering curve closely resembles the curve $|P_2|^2$

Now as the velocity is increased the number of phases which have an appreciable size and which must therefore be taken into account in (1) increases ;

[*] Holtsmark, 'Z Physik,' vol 55, p 437 (1929) In Table II of his paper δ_l should be replaced by $\delta_l - \pi$

and when there are a large number of phases effective it is difficult to see from the above formula which harmonic (if any) will mainly determine the shape of scattering curve, for the effect of the higher harmonics will be increased by the weight factor $(2l + 1)$ However, even when a large number of terms must be taken into account in (1) it can be shown that the form of the curve at large angles is still due to the lower order harmonics, for all the higher harmonics interfere to form a curve which falls off monotonically to a small value at large angles To see this we write the equation (1) in the form

$$I(\theta) = \frac{1}{4k^2} |\Sigma(2l+1) 2i\delta'_l P_l(\cos\theta) +$$
$$\Sigma(2l+1)[e^{2i\delta_l} - 1 - 2i\delta'_l]P_l(\cos\theta)|^2 \quad (2)$$

Now the first series on the right is just Born's first approximation to the exact formula (1) where δ'_l are the Born phases which for small values are equal to the exact phases δ_l

It is well known that for all atomic fields the scattering given by Born's formula falls off monotonically* to a small value at large angles, and therefore the shape of the scattering curve at large angles will be determined by the second series on the right for all velocities less than that for which the Born approximation is valid , and it is clear that this series will contain only the lower order harmonics for which the phases have a value greater than about 0 5

Thus for electrons of high energy $\delta_l = \delta'_l \ll 1$ for all values of l Then the term in square brackets in (2) is zero, and the scattering curve is given by the Born formula As the energy of the incident electrons is decreased the phases increase, δ_0 first becoming appreciable, then δ_1, then δ_2, and so on , and consequently deviations from Born's formula will be noticeable at large angles through contributions coming in from the first few harmonics Thus when the energy is decreased until $\delta_0 \sim 1$ the term in square brackets becomes effective, and at large angles the scattering curve is of the form $|P_0|^2$ On further decreasing the energy δ_0 increases and passes through the value $\pi/2$ after which its effect on the scattering becomes less marked, but now δ_1 is approaching the value $\pi/2$ and so the scattering curve takes the form $|P_1|^2$

For example, in helium, when the energy of the incident electrons is greater than 500 volts, all the phases are very much less than unity, and the scattering

---

* The first series of harmonics when summed forms a smooth curve since for no value of l does δ'_l become strictly zero owing to the fact that the field of an atom has no finite boundary

curve is given accurately by the Born formula When the energy is reduced to 340 volts the zero order phase increases to the value $\delta_0 = 0.696$ which makes the term in square brackets in (2) appreciable and so gives the scattering curve at large angles the form $|P_0|^2$, i e, the curve remains practically flat instead of falling off uniformly with angle On further decreasing the energy, $\delta_0 \to \pi$ but $\delta_1 \to 0$ and consequently δ_1 never becomes great enough to give the scattering curve* the form $|P_1|^2$ We might, however, expect to find the Born curve changing to the form $|P_0|^2$ and then to the form $|P_1|^2$ in a heavier atom, and this is found to be the case in neon, as an examination of the curves in fig 2 of a previous paper† clearly shows For argon we see from fig 3 (a) of this paper that as the velocity is decreased the scattering curve, which is of the form $|P_0|^2$ at 780 volts, changes to $|P_1|^2$ at about 330 volts, and finally to $|P_2|^2$ at about 80 volts

Now in order that the scattering curve should pass from the Born curve successively through the forms $|P_0|^2$, $|P_1|^2$, $|P_2|^2$, etc, as the energy is decreased, the phases of these lower harmonics must not be too close together in magnitude, for if they are, the contributions coming from these lower harmonics will be comparable, and so the scattering curve will be the result of the superposition of several lower harmonics ‡ For light atoms the lower order phases are probably sufficiently far apart in magnitude (over the range of energies up to that for which the Born approximation is valid) for the form of the curve to pass successively from one harmonic to the next, and the results for helium, neon and argon described above strongly support this view But for heavy atoms such as mercury this may no longer be true, and the scattering curves will then be more complicated

As the energy of the incident electrons is reduced from the value at which the Born approximation is valid all the lower order phases at first increase We have seen how this accounts, with light atoms, for the scattering curve passing successively from the Born curve through the forms $|P_0|^2$, $|P_1|^2$, $|P_2|^2$, etc Now as the energy tends to zero all the phases do not continue to increase In helium δ_0 increases to π, but all the other phases pass through a maximum and then tend to zero as $k \to 0$ In argon $\delta_0 \to 3\pi$, $\delta_1 \to 2\pi$ and the higher phases tend to zero In krypton $\delta_0 \to 4\pi$, $\delta_1 \to 3\pi$, $\delta_2 \to \pi$ and the others tend to zero, and in mercury $\delta_2 \to 2\pi$ and the higher phases tend to zero Therefore, as the energy is decreased from the value at which the Born

---

* The minimum in the curve observed at lower energies is due to electron exchange.

† Arnot, 'Proc Roy Soc,' A, vol 133, p 615 (1931)

‡ I am indebted to Dr C. B O Mohr for drawing my attention to this point

approximation is valid we should expect the scattering curve to take the form of successively higher harmonics down to a certain energy, and then to reverse the order and pass back to the form of the lower harmonics

That this actually does occur is seen by an examination of the curves for argon * We have already seen above that the curve passes successively through the forms $|P_0|^2$ at 780 volts, $|P_1|^2$ at 330 volts, to $|P_2|^2$ at 83 volts It maintains the form $|P_2|^2$ down to 30 volts at which value δ_2 is close to $\pi/2$ On further decreasing the energy the phase δ_2 goes to zero rather rapidly,† and the curve changes back towards the form $|P_1|^2$ At 10 volts the curve has almost precisely the same form as it had at 167 volts

Now for any one atom the phases at first increase as the energy is decreased, and the same will occur if we keep the energy constant and increase the atomic number of the scattering atom We might, therefore, obtain a series of curves by scattering electrons of a constant energy in various gases of *increasing* atomic number which show the same variation in form as curves obtained by scattering electrons of *decreasing* energy in a single gas A series of such curves is shown in fig 3 In fig 3 (a) a set of scattering curves for electrons of decreasing energy in argon is shown , in fig 3 (b) is given a series of scattering curves for 83-volt electrons in various gases‡ of increasing atomic number , and in fig 3 (c) the form of the harmonics $|P_0|^2$ to $|P_5|^2$

We have already described the curves in fig 3 (a), and have explained their change of form from $|P_0|^2$ to $|P_1|^2$ and finally to $|P_2|^2$ as being due to the phases δ_0, δ_1 and δ_2 increasing and passing through the value $\pi/2$ in turn as the energy of the electrons is decreased The same reasoning applies to the curves in fig 3 (b) As the atomic number of the gas is increased the phases δ_0, δ_1 and δ_2 increase and pass in turn through the value $\pi/2$, so giving the curves the form $|P_0|^2$, $|P_1|^2$, and $|P_2|^2$

The agreement between the two sets of curves is very striking, and this together with the internal consistency of each set provides strong evidence in favour of the fundamental correctness of the interpretation of scattering curves as given in this section We see that at large angles the shape of a scattering curve *for any energy up to the energy at which the Born approxi-*

---

* A set of curves for energies from 780 volts to 1 1 volts is given by Mott and Massey in " The Theory of Atomic Collisions," p 135

† Holtsmark,' Z Physik,' vol 55, p 437 (1929)

‡ The curves for sulphur, phosphorus and carbon are due to scattering in H_2S, PH_3 and CH_4 The H_2S and PH_3 curves were obtained by Mohr and Nicoll (loc. cit) , the other curves in fig. 3 are the author's

mation is valid depends upon the first few harmonics, and that in light atoms,
where the phases of low order are well separated in magnitude, the form of the
curve is given approximately over the whole of the above range of energies,
by the harmonic whose associated phase has a value most nearly equal to $\pi/2$

From figs 3 (a) and 3 (b) we see that the order of the phase which determines
the shape of the scattering curve at first increases as the energy is decreased
from the value at which the Born approximation holds, and that it also increases
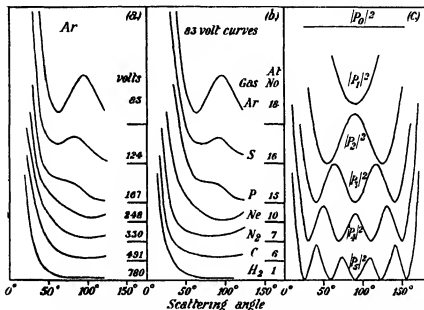
Fig 3 —(a) Scattering curves for electrons of various energies in argon   (b) Scattering
curves for 83 volt electrons in various gases of decreasing atomic number   (c) Form
of the curves $|P_0|^2$ to $|P_4|^2$

with the atomic number of the scattering atom   Thus the phase whose
harmonic gives the form of the curve is the same for fast electrons in a heavy
gas as it is for slow electrons in a light gas   This suggests that we may be
able to determine the shape of the curve from the relation between the radii
of the electron shells of the atom and a certain parameter r_0 dependent upon
the energy of the incident electrons   If r_0 is defined as the distance from
the centre of the scattering field to the point in the field at which the
potential energy of the incident electron is equal to twice its initial kinetic
energy, it is found that r_0 must be approximately equal to the radius of the
same shell for the scattering curve to have the same form in neon, argon
and krypton.

The value of r_0 can be found from the Hartree* curves giving the effective nuclear charge for potential Z_p at various distances r from the centre of the atom   Tables of Z_p for various values of r are given by Holtsmark† for argon and krypton, and by Brown‡ for neon   The values of r_0 for various energies for which scattering curves have been obtained in krypton, argon and neon have been found from curves constructed from these tables   In fig 4 these values of r_0 have been marked on the curves showing the radial distribution of
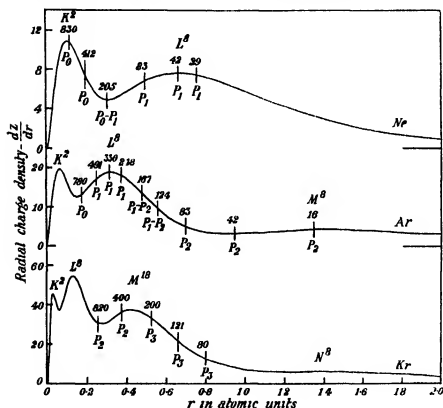
Fig 4 —Showing, for electrons of various energies, the position of the incident electron with respect to the atomic shells when its kinetic energy is equal to half its potential energy in the atomic field

charge in the atoms   For argon and krypton I have used the charge distribution curves for the Cl⁻ ion and the Rb⁺ ion respectively given by Hartree,

* 'Proc Camb Phil Soc,' vol 24, pp 89 and 111 (1928)

† 'Z Physik,' vol 55, p 437 (1929) , vol 66, p 49 (1930)

‡ 'Phys Rev,' vol 44, p 214 (1933)

since Holtsmark does not give values of $- dZ/dr$ These curves should be practically identical with those for argon and krypton

The number at the top of the short vertical line marking the point r_0 at which the kinetic energy of the incident electron is equal to half its potential energy in the atomic field, is the energy of the electron in volts, and below is marked the harmonic giving the approximate form of the scattering curve for electrons of this energy *

We see from fig 4 that, for these three rare gases, when r_0 is approximately equal to the radius of the K-shell the scattering curve has the form $|P_0|^2$, and hence it is δ_0 which most closely approximates to $\pi/2$ When r_0 is equal to the radius of the L shell the curve has the form $|P_1|^2$, and when r_0 is approximately equal to the radius of the M-shell the curve has the form $|P_2|^2$ or $|P_3|^2$

It also appears that we cannot expect the Born approximation to be valid at large angles unless the energy of the electrons is greater than the ionization potential of the K-shell In mercury this potential is given by Slater's rules† as 75 600 volts A rough extrapolation of the phase curves for mercury given by Henneberg‡ shows that δ_0 does not fall to the value $\pi/2$ until the energy is increased to about 135,000 volts

Calculations are in progress to determine the phases and theoretical scattering curves for the halogen atoms and molecules The experimental work is also being continued in other molecular gases and vapours

I wish to thank the Carnegie Trustees for a grant towards the cost of apparatus

Summary

The angular distribution of the elastically scattered electrons in the vapours of iodine, bromine, and carbon tetrachloride has been measured for several different energies of the incident electron beam Diffraction effects are observed in all the curves The curves for iodine, bromine and carbon tetrachloride are similar respectively to the curves previously obtained by the author for xenon, krypton and argon The curves for bromoform show the same diffraction structure as do those for bromine

These results, together with some previous results obtained by the author and other investigators, are then discussed from the theoretical standpoint

---

* $P_1 - P_2$ means that the form of the scattering curve is intermediate between $|P_1|^2$ and $|P_2|^2$

† ' Phys Rev,' vol 36, p 57 (1930)

‡ ' Z Physik,' vol. 83, p. 555 (1933)

Evidence is put forward to show that at large angles the shape of a scattering curve for any energy up to the energy at which the Born approximation is valid depends upon the first few harmonics, and that in light atoms, where the phases of low order are well separated in magnitude, the form of the curve is given approximately, over the whole of the above range of energies, by the harmonic whose associated phase has a value most nearly equal to $\pi/2$

On Metallic Dispersion in the Near Infra-Red

By C HURST, M A , D Phil , Christ Church, Oxford

(Communicated by F A Lindemann, F R S —Received November 9, 1933)

Kronig[*] has recently attempted to derive a quantum theory of dispersion in metallic conductors, using as a basis the Bloch theory of the metallic state , a more rigorous formulation of the same line of thought has been given by Fujioka[†] In particular, Kronig has developed explicit formulæ for the coefficients of reflection and extinction and for the index of refraction of a metal in the so-called " transitional " region of the spectrum, where the period of the incident radiation is comparable with the mean time between two collisions of an electron with the metallic lattice In order to obtain reasonable agreement with the room temperature measurements of Försterling and Fréedericksz[‡] in the near infra-red, it is necessary to assume a value for the electrical conductivity of the metal which is very much less than the value obtained by direct measurement Kronig has suggested that this result may be due to the fact that the optical constants depend upon the properties of a thin surface layer of the metal, in which layer it is possible that the conductivity is diminished on account of boundary imperfections of the metallic lattice It has already been shown, however, that even though this additional hypothesis be allowed, the formulæ in question are not consonant with the results of recent measurements[§] on the high-temperature emissivities of metals in the near infra-red

[*] ' Proc Roy Soc ,' A, vol 124, p 409 (1929) , vol 133, p 255 (1931)
[†] ' Z Physik,' vol 76, p 537 (1932)
[‡] ' Ann Physik,' vol 40, p 201 (1913)
[§] Hurst, ' Proc Roy Soc ,' A, vol 142, p 466 (1933)

The inadequacies of the quantum theory of the transitional region are more readily appreciated when it is realized that the formulæ for the optical constants derived therefrom are identical in scope with the formulæ of the dispersion theory of Drude,* published in 1900 Kronig himself mentions that his formulæ tend, in the limit of zero frequency, to the classical, phenomenological relations which Drude† derived in 1894 , but it does not appear to have been pointed out hitherto that the Kronig formulæ are, in fact, *identical* with, and not merely asymptotic to, those of the later dispersion theory of Drude

In the latter theory, it was imagined that the free electrons in a metal were acted upon by a frictional force, proportional to their velocity, which represented the effect of their collisions with bound electrons and ions If e and m are respectively the charge and mass of an electron, and N is the number of conduction electrons per unit volume, such an assumption leads to equations of the form

$$n^2 - k^2 - \Pi^2 - \frac{4\pi Ne^2 m}{(2\pi m \nu)^2 + b^2}, \qquad nk = \frac{bNe^2}{\nu\{(2\pi m \nu)^2 + b^2\}},$$

for the refractive index, n, of the metal and its absorption coefficient, k, at frequency ν b is the coefficient of the frictional force in the equations of motion of the free electrons, and is connected with the electrical conductivity, σ_0, of the metal by the relation

$$b = \frac{Ne^2}{\sigma_0}$$

In the derivation of the formulæ, Drude assumed that the region of the spectrum under consideration is so far from the free periods of bound electrons and ions that their influence (Π^2) on the index of refraction is constant and on the coefficient of absorption may be neglected

Drude (*loc cit* 1904) himself came to the conclusion that this type of equation, with a constant value of b, would not suffice to represent the dispersion of metals, and pointed out that b might be expected to increase with the frequency, ν, owing to stronger radiation losses at the higher frequencies   To explain the fact that the values of electrical conductivity given by the formulæ were too low, he, like Kronig, suggested a diminished conductivity of the surface layers of the metal Försterling and Fréedericksz compared their experimental results in the near infra-red with those given by the Drude equations, and failed to find agreement ; they, too, put forward the hypothesis of an abnormally low surface conductivity

* ' Phys Z ,' vol 1, p 161 (1900)   ' Ann Physik,' vol 14, p 936 (1904)
† ' Physik des Athers,' 1st Ed., p 574 (1894)

It is one of the great advantages of the modern conduction theory that no distinction need be made between free and bound electrons Accordingly, Kronig (*loc cit*) has applied the Schrodinger dispersion theory to a metal lattice, regarded as a periodic field of potential, and has shown that, for sufficiently high frequencies, when the interaction of the electrons with the lattice may be neglected, the behaviour of an electron in a given stationary state, r, in an elementary cube of side, L, may be replaced, as far as its mathematical behaviour is concerned, by a fictitious system of harmonic oscillators, whose strengths are expressed in terms of the matrix elements of the linear momentum of the electron As far as the near infra-red region is concerned, the most important oscillator (of strength f_r) has a natural frequency zero In other words, the spectrum of an electron, r, consists of the resonance frequency, $\nu = 0$, and a number of discrete absorption lines Since the electrons in the metal are distributed over various stationary states, the equivalent spectrum of the electrons in the cube, in the absence of interaction, consists of the sharp resonance line and practically continuous absorption bands In the visible region of the spectrum, the influence of the bands is predominant, while in the infra-red, the resonance frequency is the more important From about 1 5 μ onwards into the infra-red, the metal may be treated as though it had only the pseudo resonance frequency at $\nu = 0$, and the effect of the interaction of the electrons with the lattice may be introduced by discussing the broadening which this line undergoes thereby Calling δ the half-breadth of the representative line, $\nu = 0$, Kronig obtains the formulæ

$$n^2 = \frac{\sigma_0}{\nu}\left(\frac{\delta}{\sqrt{\nu^2 + \delta^2}} - \frac{\nu\delta}{\nu^2 + \delta^2}\right), \qquad k^2 = \frac{\sigma_0}{\nu}\left(\frac{\delta}{\sqrt{\nu^2 + \delta^2}} + \frac{\nu\delta}{\nu^2 + \delta^2}\right)$$

These equations are, however, identical in content with the Drude equations above (when the term II^2 is omitted), provided that

$$\delta = \frac{b}{2\pi m} = \frac{Ne^2}{2\pi m\sigma_0}, \tag{1}$$

or, since δ is connected with the sum of the strengths, $\Sigma_r f_r$, of the fictitious resonators of frequency zero (where the summation is taken over all stationary states in which there are electrons) by the equation

$$\delta = \frac{\iota e^2}{2\pi m\sigma_0 L^3}\Sigma_r f_r,$$

provided that

$$NL^3 = \Sigma_r f_r$$

Thus the only equation necessary for a complete correlation of the Drude and the Kronig dispersion formulæ is the trivial one expressing the fact that the zero frequency resonators are playing a rôle identical with that of the free electrons of the classical theory

That the results obtained by Kronig for the spectral range in question are precisely the same as those given by the classical treatment is not surprising as soon as it is realized that his method is closely analogous to that employed by Drude Just as it is assumed in the older derivation of the formulæ that the influence of the free periods of the bound electrons and ions may be neglected, it is assumed in the quantum derivation that the contribution of the fictitious oscillators of non-zero frequency to the current induced in the metal by the incident light-wave is of little importance so long as the frequency under consideration is sufficiently low, the only excited electron states which are allowed to occur are therefore those which have slightly higher translational energies in the field-direction than usual Again, when Kronig postulates that the effect of the interaction of the electrons with the metallic lattice is to cause a broadening of the remanent resonance-frequency, he is really making the assumption that the effect of the lattice vibrations is a shortening of the mean life-period of the excited electron states , and, as the electrons in excited states give their energy up to the lattice in the form of vibrational energy, which is ultimately distributed over all frequencies, the result is equivalent to the introduction of a damping factor, connected with the half-breadth of the resonance line by the relation (1)

Just as Drude regarded σ_0 and his damping factor, b, as arbitrary parameters, so Kronig adjusts σ_0 and δ to make the values of n and k derived from the dispersion formulæ fit the experimentally observed values of Försterling and Fréedericksz As would be expected, the value of δ computed for various wave-lengths for any one metal is not constant, but shows a tendency to decrease progressively with increasing wave-length, thus confirming the experience of Drude, already mentioned, concerning the behaviour of the damping factor, b The comparison with experiment given by Kronig is, of course, superfluous, since Försterling and Fréedericksz (loc cit) had already tested, in a slightly different manner, the same dispersion formulæ by means of their results

As has so often occurred in the interpretation of other phenomena, the quantum-mechanical treatment of the problem of metallic dispersion in the near infra-red has proved to be nothing more than a new and rather more pleasing representation, in a different language, of classical concepts Not

until an electron statistics which takes adequate account of the mutual potential energy of the electrons in a metal is developed, does there seem much hope of formulating a theory of the optical properties of metals in the near infra-red which will agree better than the classical theories with experimental data

In conclusion, I should like to thank Professor F A Lindemann, F R S, and Dr F London for their kind and helpful criticisms

Summary

It is shown that the equations for the index of refraction and the coefficient of absorption of a metal in the near infra-red, which have been developed by Kronig on a quantum-mechanical basis, are formally identical with the dispersion equations obtained by Drude in 1900 by classical methods The close analogy between the underlying assumptions of the two derivations is indicated

---

Photographs of Fluid Flow Revealed with an Ultramicroscope

By A Fage, A R C Sc

(Communicated by G I Taylor, F R S—Received November 14, 1933)

[Plates 14–15]

1 *Introduction* —When an intensely bright beam of light from an ultra-microscope is passed through moving water, minute impurities which are always present and which cannot be seen in ordinary light, even with a micro-scope, become visible provided that they are seen against a dark background These illuminated particles reveal the internal motions of the water without any interference with the flow, such as might be caused if extraneous particles or colouring matter were introduced into the water

The ultramicroscope has recently been used to examine turbulent flow in pipes,* and to obtain information on the flow in the wakes behind bluff obstacles † An attempt has now been made to take photographs of some of the views seen when this earlier work was in progress These photographs

---

* Fage and Townend, ' Proc Roy Soc ,' A, vol 135, p 656 (1932) Also ' Aero Res Ctee,' R & M 1474

† Fage, ' Aero Res Ctee,' R & M 1510

are given in the present paper * Photographs of the flow around a long circular cylinder at low Reynolds' number are also given All the photographs, with the exception of those of fig 4 (c) and (d), Plate 14, are of water direct from the main It is perhaps of interest to mention that the number of particles (probably mostly minute air bubbles) in the water appeared to differ appreciably from day to day

2 Photomicrographs of the Brownian movements of ultramicroscopic particles in soap solutions have been taken by Darke, McBain, and Salmon † These authors found that the finer details of the movements were not recorded It appeared doubtful, therefore, whether satisfactory photomicrographs of moving water under a high magnification could be obtained, when, as in the present experiments, the particles in the water moved much faster than those which show the Brownian movement in a stationary fluid Nevertheless, an attempt was made to take photographs with a Leitz photo-micrographic camera Two makes of fast plate were used Ilford Hypersensitive Panchromatic and Ilford Double X-Press Orthochromatic A few streaks made by exceptionally bright particles were recorded, but details of the flow were not portrayed The next steps possible were to increase the intensity of the light beam, or to decrease either the speed of flow or the magnification The last of these steps was the most convenient to take, and it was decided to attempt to obtain photographs at a reduced magnification, and if these were satisfactory to enlarge the negatives A small camera with an $f/3$ lens ($f = 2$ inches) and a Compur shutter was constructed Photographs taken with this camera are given in figs 4–7, Plates 14, 15 The views were taken under a magnification of about 4 to 1 (except those for the prism, magnification 2 to 1) and the prints used for reproduction purposes were obtained from negatives enlarged 2 3 times Ilford Hypersensitive Panchromatic and Ilford Double X-Press Orthochromatic plates ($4\frac{1}{2} \times 6$ cm) were used, and they were found to give closely similar results The exposure times varied from about 1 to 6 seconds

3 *Turbulent Flow in a Pipe*—Photographs of turbulent flow in a square pipe of internal side 1 372 inches at a section situated 57 8 inches from the entry are given in fig 4 The mean rate of flow (U_0) was about 0 7 ft per second The corresponding value of $U_0 m/\nu$, where m is the hydraulic mean

* The photographs were taken in the Aerodynamics Department of the National Physical Laboratory, and permission to communicate them was kindly granted by the Aeronautical Research Committee

† 'Proc Roy Soc ,' A, vol 98, p. 395 (1920–21)

depth, was about 1700 As described in the earlier work,* the illuminated
particles appeared as bright streaks inclined at various angles to the mean
direction of flow, and these streaks appeared to intersect each other, owing to
the persistence of vision The maximum obliquity to the pipe axis of the
streaks at a point in an axial plane XOY normal to a wall of the pipe increased
slowly with the distance y from the axis, and reached a maximum at about
$y = 0\ 8s$, where $2s$ is the side of the pipe The obliquity then fell to zero at

OX = Axis of pipe
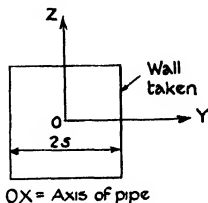
Fig 1

the wall $(y = s)$, so that particles viewed along and very close to the wall
appeared to be moving in laminae parallel to the wall Fig 4 (b) and (c)
illustrate these features of the flow

The maximum obliquity of particles viewed on a plane parallel to a wall
increased continuously as the wall was approached, fig 4 (d) Cerebos salt
was added to the water before taking photographs, fig 4 (c) and (d), to increase
the number of bright particles near the wall, and so to improve the views

The most interesting views seen in the earlier work were obtained when the
microscope (magnification 200) was focused on the inner surface of a wall
Particles within a surface film of about 0 001 inch thick were then in focus
The view obtained showed all the particles to be moving in sinuous paths and
occasionally paths of several wave-lengths were seen It was also observed
that the slowest particles, which were estimated to be about 1/40,000 of an
inch from the surface, often moved in short jerks An attempt was made to
photograph with a Leitz photo-micrographic camera the details of this interest-
ing motion, but without success One of the difficulties experienced was that
the intensity of light falling on the photographic plate from the illuminated

* *Loc cit*, § 1

particles was greatly reduced by the high magnification necessary to obtain the view Moreover, it was found impossible to illuminate a very thin film without illuminating the surface itself and the light scattered from the surface tended to fog the plate A photograph of laminar flow in the pipe is given in fig 4 (a)

4. *Triangular Prism* —Photographs of the turbulent wake behind a long triangular prism are given in fig 5 (a) and (b), Plate 14 These photographs illustrate the work described in the earlier paper (R & M , 1510), which was undertaken to show that at a sufficiently high Reynolds' number the eddying wake behind a very long cylindrical obstacle, mounted with its length normal to the stream eventually settles down to a regime in which the velocity disturbances are three-dimensional, even although the mean flow in planes at right angles to
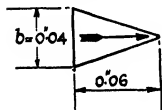
Fig 2

the length tends to be two-dimensional The prism was mounted between the opposite sides of a 1 125 inch water tunnel The dimensions of the triangular cross-section were 0 04 inch (base) and 0 06 inch (height) The photographs were taken at $U_0 b/\nu = 250$ (b = base of section), at a point situated in the middle of the turbulent wake at a distance 35b behind the prism Fig 5 (a)

gives a view of the flow in a plane at right angles to the axis of the prism It is seen that the disturbances are greatest over the central part of the wake, and that these disturbances gradually die away as the outer limits of the wake are approached The maximum deviations of the streaks in the middle of the wake from the direction of mean flow were observed to be about ± 17° Photograph 5 (b) was taken on the plane passing through the axis of the prism and shows that the flow is disturbed along the whole length of the prism The maximum deviations observed in this plane were about ± 23°

5 *Short Circular Cylinder* —Photographs of the flow at the exposed end of a circular cylinder extending from a wall to the centre of the tunnel are given in fig 6, Plate 14 The diameter, D, of the cylinder was 0 04 inch These photographs were taken at a water speed, U_0, of 0 58 ft per second ($U_0 D/\nu = 160$ approx.) Fig 6 (b) shows clearly the traces made by the axial flow of particles into the dead-water region behind the top of the cylinder

6 *Long Circular Cylinder* —The photographs given in fig 7, Plate 15, show the changes with $U_0 D/\nu$ in the flow around a long circular cylinder of diameter 0 04 inch The cylinder was mounted with a small clearance of about 0 01 inch at one end between the walls of the water tunnel The distance between the walls

At axis   At wall

(a)   (b)   (c)

Laminar flow (axis) $y = 0.25s$ $y = 0.25s$, $y = 0.6s$ wall

View on plane XOY
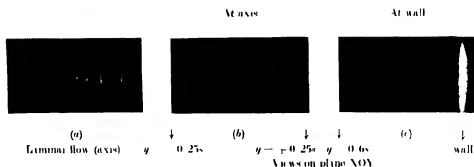
Fig 4 — Turbulent flow in pipe $R_m v = 1700$

Fig 4 — (d) View on plane parallel to wall at $y = 0.9s$ (about)

(a)   (b)

Fig 5 — Flow in the centre of the wake at a point 15b behind triangular prism

(a)   (b)

Fig 6 — Flow at the end of circular cylinder

Views at O on plane XOY

(b)

(c) 21

(d) 27

(e) 32

$\frac{u_0 D}{v}$ 17 7

(a)

(f) 47

(g) 104

(h) 170

(a) Free stream

Views at O on plane XOZ

(i)

(j)

(k)

Fig 7 —Circular cylinder Diameter 0 04 m length 1 12 m

was 1 125 inches   Photograph (a) shows the steady nature of the flow in the
empty tunnel   Photographs (b)–(h) were taken on the median plane XOY at
right angles to the axis of the cylinder at values of U_0D/ν lying within the
range 17 7 to 170   The flow patterns shown in these photographs of tap
water resemble those obtained from experiments of other workers* in which
extraneous particles were introduced into the fluid (air and water)   The
first photograph (b) shows a flow which is obviously not far removed from the
symmetrical laminar type   Fig 7 (c) to (f) show the progressive changes in
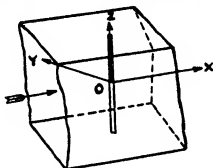
FIG 3

the standing-vortex regime as the value of U_0D/ν is increased in steps over
the range 21 to 47   The gradual increase in the length of the vortices with
Reynolds' number will be noticed   Eventually, the standing vortices are
drawn out to such a length that they break down and give place to a dead-
water region behind the cylinder   Fig 7, photographs f, g, and h illustrate the
sequence in this breakdown

Photographs i, j, and k were taken on the plane XOZ passing through the
axis of the cylinder   Of these photographs j is the most interesting for it
clearly shows that the flow in the standing vortices at $U_0D/\nu = 38$ 0 is of a
spiral character   This spiral motion is associated with an inward flow of
particles from the ends of the cylinder   It will be noticed that the angles of
the spirals become progressively smaller, and eventually zero, as the plane of
symmetry XOY is approached

7 In conclusion, the writer wishes to acknowledge his indebtedness to Miss
V M Emms for assistance in the photographic work

* Nisi and Porter, ' Phil. Mag ' (1923)   Also Nayler and Fraser, ' Aero Res Ctee ,'
R & M. 332 (1917–18)

Summary

The ultramicroscope has recently been used to examine turbulent flow in pipes, and to obtain information on the eddying wake behind a bluff obstacle Photographs are given in the paper of some of the views seen when this earlier work was in progress , also of the flow around a circular cylinder at low Reynolds' number The flows were revealed by the motions of those minute particles in water which became visible in the light beam of the ultramicroscope

---

The Thermal Decomposition of Nitrous Oxide at Pressures up to Forty Atmospheres

By E Hunter

(Communicated by C N Hinshelwood, F R S —Received November 16, 1933)

Nitrous oxide decomposes to nitrogen and oxygen at velocities which can be conveniently measured at temperatures between 600° and 850° C M A Hunter[*] investigated the reaction by streaming the gas through a porcelain bulb in a furnace and measuring the decomposition for different times of passage No attempt was made to determine whether the reaction is homogeneous or heterogeneous The effect of wide variation of pressure was not used to determine its order, since the reaction was followed only over small ranges of decomposition at atmospheric pressure From the velocity of decomposition, however, bimolecular constants were obtained which could be represented by the equation

$$ln\,k = 24\,12 - 31800/T,$$

where k is the bimolecular velocity constant and T the absolute temperature If this equation holds, the activation energy of the bimolecular reaction is 62,040 cal /gm mol

A much more thorough examination of the reaction was made by Hinshelwood and Burk,[†] who measured the rate of reaction by following the pressure increase at constant volume in a silica bulb The reaction was proved to be

[*] ' Z phys Chem ,' vol 53, p 441 (1905)
[†] ' Proc Roy Soc ,' A, vol 106, p 284 (1924)

homogeneous   The initial pressure was varied between 50 and 500 mm Hg, and it was found that the reciprocal of the half-lives when plotted against the initial pressures gave a straight line   True bimolecular reaction requires the straight line $1/t_{\frac{1}{2}} = ka$, where $t_{\frac{1}{2}}$ is the half-life, and k the velocity constant, and a the initial concentration   The line through the experimental points showed a small intercept on the $1/t_{\frac{1}{2}}$ axis for which no explanation was offered at the time   From the variation of the bimolecular constants between 565° and 852° C the activation energy of the reaction was calculated to be 58,450 cal /gm mol   If the reaction were a unimolecular one dependent on immediate decomposition at each activating collision of the molecules the number of molecules reacting per second should be equal to $Z \times e^{-E/RT}$, where Z is the number of molecules colliding per second and E is the activation energy   From the observed rate of reaction at 1000° K a value of 55,000 cal /gm mol was found for the activation energy   The fairly close agreement between the two values of the activation energy, 58,450 and 55,000 cal /gm mol and the manner in which the half-life varied with pressure provided good grounds for believing the reaction to be a simple bimolecular one, dependent only on collisions between the molecules

Further work on the reaction has been published by Volmer and Kummerow,[*] who made velocity measurements at 665° C between 25 and 300 mm Hg   They came to the conclusion that the velocity of reaction was simply that to be expected from the low pressure part of a quasi-unimolecular reaction of the type, which according to the theory of Lindemann[†] may show a half-life independent of pressure over a very wide pressure range and yet exhibit a falling off of velocity at some sufficiently low pressure   Volmer and Kummerow expected to find that the nitrous oxide decomposition would give true uni molecular constants at some sufficiently high pressure   In a paper by Volmer and Nagasako[‡] results at pressures up to 8000 mm Hg were given, and it was claimed that these agreed with the theory of a quasi-unimolecular reaction and showed that the unimolecular constants were practically independent of pressure above a pressure of about 6½ atms   The activation energy was 53,000 cal /gm. mol

Some measurements made by Musgrave and Hinshelwood[§] during a study of the reaction at low pressures are shown in fig 1   The line is almost straight

* 'Z phys Chem ,' B, vol 9, p 141 (1930)
† 'Trans Faraday Soc ,' vol 17, p 598 (1922)
‡ 'Z phys Chem ,' B, vol 10, p 414 (1930)
§ 'Proc Roy Soc ,' A, vol 135, p 23 (1932)

near the origin, but passes through a region of great curvature at about 50 mm
Hg and thereafter straightens out to a line of a much smaller slope than that
near the origin   It is difficult to explain these results on the basis of Volmer's
theory of a simple quasi-unimolecular reaction, since this would give a curve
rising smoothly from the origin finally becoming horizontal, without the marked
change of curvature and straight lines of fig 1   Musgrave and Hinshelwood
were led to the conclusion that the observed reaction was the sum of a uni-
molecular reaction, the line OAB of fig 1, and a bimolecular reaction   The
intercept OC was regarded as a measure of the full extent of the unimolecular
reaction and its variation with temperature gave a value of 50,500 cal /gm
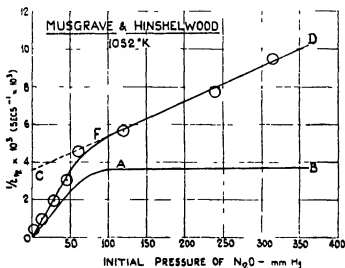
FIG 1

mol for the activation energy of the unimolecular reaction   In the same paper
Musgrave and Hinshelwood gave results which proved that the nitric oxide
formed as a by-product catalysed the reaction slightly

If Volmer's theory of a simple quasi-unimolecular reaction is correct, the
half-life should be almost independent of pressure at all pressures above
approximately 6 atms   On the other hand, Musgrave and Hinshelwood's
theory of two concurrent reactions, one of which is bimolecular, suggests that
the half-life might still be dependent upon pressure even above 6 atms   In
order to discover the true state of affairs velocity measurements at pressures
much greater than 6 atms are needed   Such results are provided by the
present paper, which reports measurements of the velocity of decomposition
of nitrous oxide at pressures as high as 40 atms

Experimental

Apparatus

The reaction was studied at temperatures between 840° and 999° C and at pressures between 0 10 and 40 atms , by measuring the rate of pressure increase of the gas at constant temperature and volume in a silica bulb   Two types of apparatus were used   The low pressure apparatus was designed for work at pressures between 50 and 2500 mm Hg, the high pressure apparatus for work at pressures up to at least 40 atms

(1) *Low Pressure Apparatus* –The apparatus used by Hinshelwood and Burk (*loc cit*) and described by Hinshelwood and Topley* was used for pressures up to 500 mm Hg and was adapted for use at pressures up to 2500 mm Hg by fitting spring-loaded taps to stand the pressure, and by employing a closed manometer for the pressure measurement   This manometer was made from a J-shaped glass capillary tube, 1 mm internal diameter   In the longer limb, dry CO_2-free air was enclosed by a mercury thread, the movement of which in the shorter limb was used to indicate the pressure   The enclosed air was kept at a constant temperature by fitting the longer limb with a water-jacket through which water from a 25° C thermostat was circulated   The manometer was calibrated against an open mercury column and then sealed to the apparatus   The advantage of using a closed manometer of this type is that it entails only a small dead space (1 5 to 2% of the volume of the re action bulb) and only a small correction to the results obtained with it is needed

The nitrous oxide was stored in a glass bulb over mercury at a pressure of about 3000 mm Hg   At pressures up to 2500 mm the highest used with this apparatus, the gas appeared to reach the temperature of the reaction bulb within a second of its entry

A change was made in the method of temperature measurement   In place of a millivoltmeter calibrated in degrees Centigrade, which was found to be liable to changing zero errors, the calibrated platinum-platinum rhodium thermocouple was used in conjunction with a potentiometer which made it possible to control the temperature to $\pm$ 0 3° C

(2) *High Pressure Apparatus* –No apparatus for this type of work at pressures up to 40 atms has been described   Volmer and Nagasako (*loc cit*) used the static method at pressures up to 10 atms   They made little alteration to the apparatus used for normal pressures, the range of which is limited by the strength of the silica bulb

The solution of the present experimental problem seemed to be to have a steel bomb whose walls could be kept at a low, safe temperature, serving as a container for an electric furnace surrounding the reaction bulb There remain the difficulties of keeping the reaction vessel at a uniform and accurately measurable temperature, of keeping down the dead space, and of providing a sufficiently sensitive means of pressure measurement It is believed that these difficulties have been overcome in the apparatus described below, which was designed for use at pressures up to 100 atms

The Bomb, Furnace, and Reaction Vessel A diagram of the steel pressure vessel and its contents is given in fig 2 The bomb A was made of mild steel, the cover plate B of "Vibrac," and the two gave a pressure-tight fitting on the copper ring C by the tightening of eight nuts over the cover plate

It was necessary to have insulated leads into the bomb for the current supplying the furnace and for the thermocouple The chrome-steel glass-insulated cones* which have been in use for some time at Winnington were used For the furnace a single insulated cone was enough, the return being via the steel body of the apparatus The copper wire leads to the furnace were threaded through a length of twin-bore "Vitreoal" tube within the steel pressure tubing D One wire was fastened to the inner terminal of the insulated cone E, the other was connected to the metal at F By using the length of tube D, the cone was kept away from the heat of the furnace, which it was feared might have caused a breakage of the glass, if the cone had been fixed directly into
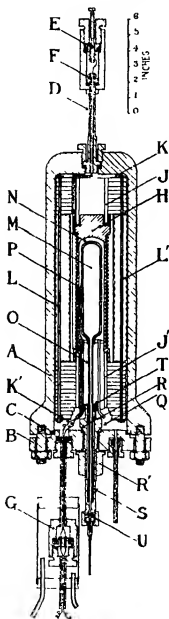
Fig 2

* Welbergen, 'J Sci Instr, vol 10, p 247 (1933)

the body of the bomb The outer part of the cone E was connected through rheostats to the positive lead of a 200-volt D C supply The negative was connected to the steelwork of the apparatus The glass insulation of the cones was much less than a millimetre thick, but care was taken to keep the bomb free from moisture, and it was found that the cone would carry a current of at least 3 amps throughout the pressure range without trouble

For the thermocouple leads into the bomb, two insulated cones set into one plug were needed The platinum and platinum rhodium wires from the hot junction were fixed to the inner terminals of the two cones, and from the outer terminals platinum and platinum-rhodium wires ran to cold junctions with copper, kept at the temperature of melting ice The readings of a couple arranged in such a way are only correct if all the four junctions to chrome steel are at precisely the same temperature Because of this it was not permissible to fix the pressure cones directly into the cover plate B, where they would have been subjected to a temperature gradient along their length, as a result of the dissipation of heat from the furnace The pressure joint was accordingly made in the separate vessel G which was attached to the cover plate by a length of steel tubing along which passed the insulated wires from the hot junction The vessel G was water-jacketed, so preventing the occurrence of any difference in temperature along or between the insulated cones

A connection through the cover plate was made for the entry of the nitrogen used to balance the pressure within the reaction vessel

The furnace was designed to give as even and as steady a temperature as possible in the heating space It was rather a difficult problem because of the necessity of having a lagging which would take up a temperature gradient between the furnace wall at 600° to 900° C, and the inner bomb will which it was hoped to keep below 200° C It was found to be unavoidable that the furnace space would not be much greater than the required volume of a reaction bulb This increased the difficulty of ensuring an even temperature throughout the furnace and reaction bulb, for with the bulb filling most of the furnace space it became important to minimize any tendency for the furnace temperature to fall away at the ends

The tendency for a furnace to show this effect of a serious temperature gradient at its ends is usually due to the efficiency of the endwise lagging of the furnace being much poorer than that of the lagging of the sides In the design of the furnace shown in fig 2 special attention was given to this point The nichrome heating wire, 70 ohms resistance, insulated with porcelain "fish spine" beads, 3 mm in diameter, was wound in a deep helix cut in the

steel tube H   This metallic tube was used for the purpose of giving a good heat conductivity along the length of the furnace which would help to maintain an even temperature   The heating wire was covered with a thin layer of alundum cement, over which was wound sufficient asbestos string to give a diameter which would just fit the bomb   The asbestos was held in place by a jacket of wire-netting   The tube H was supported and prolonged by two lengths of wide " Vitreosil ' tube J and J'   Over these were pressed a sufficient number of discs of asbestos cement board to occupy the space between the ends of the steel furnace tube and the ends of the bomb   The hollow space within the " Vitreosil " tube J was filled up with alundum cement   The whole furnace assembly was made rigid and self-supporting by bolting together two thin steel end-plates K and K', with two lengths of steel tube L and L' screwed at the ends   Tubing was used instead of rod to give a free passage for the gas between the front and the back of the bomb

The reaction bulb M was made of silica and was about 16 cm long with a volume of 110 c c   To promote a rapid equalization of temperature over the whole surface of the silica, the bulb was covered with a closely fitting jacket N, made from sheet silver about $\frac{3}{4}$ mm thick   This jacket was made in two sections, one a test-tube shaped piece covering the whole length of the reaction vessel, the other a hemispherical cap which covered the remainder of the silica surface   The silica bulb was sealed to the silica capillary tube O, round which were arranged three ' Vitreosil ' tubes to pass gas into the furnace space, and a length of twin-bore " Vitreosil ' tube to carry the thermocouple wires, over all these was wound asbestos string to the diameter of the tube J'   The hot junction of the thermocouple was fixed in contact with the mid point of the silver jacket at P, by looping it round a small tang of silver raised from the body of the jacket N   The leads to the junction were kept out of contact with the silver by threading them through 1 mm bore " Pythagoras " refractory tubing

The above type of construction gives a reaction bulb with an outer surface of a good heat conductor, heated in a furnace tube made of a good conductor, surrounded by a considerable thickness of lagging, particularly at the ends , so that the requirements for as even a temperature as possible are fulfilled

One of the earliest difficulties was to find a way of making the joint between the reaction bulb and the steel gas supply pipe   The first attempts were made with butt joints, for which a flange formed on the end of the silica capillary O was held against a flange on the incoming steel tube, with a " Klingerite " washer between   The first joint made in this way was satisfactory,

but after a breakage many attempts to repair the joint were unsuccessful and the principle was discarded   The type of joint finally used was found to be quite satisfactory   It is shown in fig 2   The mild steel tube Q was turned with a cone R, which gave a gas-tight fitting on the cover plate when the nut R′ was tightened   It was found possible to join the silica to the steel by soldering the capillary O to the inside of the tube at a point S, sufficiently remote from the heat of the furnace to avoid softening the solder   From the solder at S to the interior of the bomb there was a clearance of about a millimetre between the silica and the steel   Some support was given to the capillary by the tightly fitting brass sleeve T   The length of the tube Q outside the bomb was cooled by a jet of air to make sure that there would be no softening of the joint S   The steel tube was connected to the gas supply and manometer system by a lens ring joint at U to 0 7 mm bore copper capillary tube, running to a T-piece (G, fig 3)

Pressure Measurement —The half-life, in the decomposition of nitrous oxide, is reached when the pressure is 1 25 times the initial pressure   For an accuracy of 1% a pressure measuring instrument sensitive to 0 25% of its pressure reading would be wanted   Closed gas manometers could not conveniently be used because of the difficulty of achieving this sensitivity and at the same time avoiding a large dead space   A pressure balance* affords the most sensitive and accurate method of measuring pressures of the order of 100 atms , but it could not readily be adapted to follow the pressure change during reaction   It provides a reservoir of fluid at a constant pressure, which can only be changed by changing the load on the balance, an operation which takes an appreciable length of time , while the reaction pressure to be measured would rise smoothly and continuously from the instant of filling the bulb

It seemed best to use sensitive carefully calibrated Bourdon tube gauges Six gauges were obtained and calibrated against a pressure balance   Four of these were Schaeffer and Budenberg gauges with 12-inch dials, two for 100 kg / cm² and two for 50 kg /cm²   The remaining two gauges were Budenberg gauges for 300 lbs /sq inch   With practice it was found possible to read these gauges to 0 05 kg /cm², 0 02 kg /cm², and 0 4 lbs /sq inch respectively, so that they were sufficiently sensitive for the purpose for which they were required

If these gauges had been used connected directly to the gas, the volume of the Bourdon tube, which was several cubic centimetres, would have been a very serious addition to the dead space of the apparatus   The presence of such a

* Michels, 'Ann Physik ,' vol 72, p 285 (1923) , vol 73, p 577 (1924)

large dead space was avoided by filling completely with oil the gauge reading the reaction pressure, and separating the oil from the gas by a mercury buffer The system used is shown in fig 3   The gauge A was connected by steel pressure tubing to a valve B and a pressure vessel C   A Pyrex glass capillary tube D, 1 mm bore, dipped almost to the bottom of this vessel   This capillary
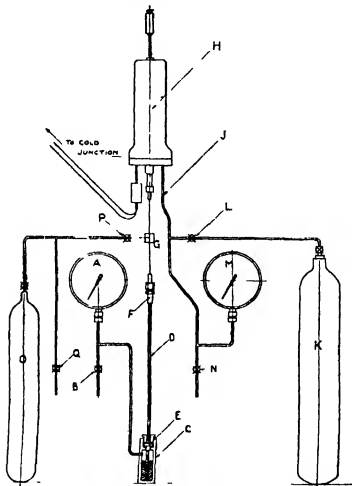
Fig 3

was held by a nut which pressed on a flange E, soldered to the glass   The capillary tube was about a metre long and its upper end was fitted with a soldered-on coupling F, through which it was connected to the reaction bulb, with 0·7 mm bore copper capillary, by way of the T-piece G   The Bourdon tube was evacuated through the valve B, and at the same time the

space over the mercury in the capillary D was evacuated Refrigerator oil was then allowed to run into the gauge through B, filling up completely all the free space and forcing mercury up the capillary tube to a height approximately barometric The valve B was then closed This oil filling made the gauge system so incompressible that a pressure of 80 atms produced a movement of only 40 cm in the mercury meniscus in the 1 mm tube D

General Arrangement of the Apparatus—The complete apparatus is shown in fig 3 The bomb B was held horizontally on a cradle on a bench about 3 feet high Passing through its cover plate was a steel pressure tube J, supplying nitrogen The nitrogen was stored under pressure in the large cylinder K, and the quantity of gas admitted to the bomb was controlled by the fine-adjustment valve L The pressure of gas in the bomb was shown by the gauge M A valve N was fitted for blowing off gas or for evacuating the bomb

The nitrous oxide was stored under pressure in the cylinder O which was connected by steel tubing to a fine-adjustment valve P, leading to the bomb, and a valve Q which was used for blowing off the gas, and for evacuating the reaction bulb The fine-adjustment valve P controlled the quantity of gas entering the reaction bulb and its speed of entry It was connected to the T-piece G by 0 7 mm bore copper capillary tube This T piece was connected by similar tubing to the reaction bulb and the glass capillary D By using this small bore tubing the dead space between the valve P, the reaction bulb, and the mercury meniscus in D was kept below 1 c c

The control valves L and P were placed together at shoulder-level on a panel, with the gauges A and M on either side

Protection against the danger attending a burst of the glass tube D was given by a Triplex glass screen

Temperature Measurement and Control—The Johnson-Matthey platinum platinum rhodium couple which was used had been calibrated against a platinum resistance thermometer up to about 650° C and checked at the salt point (801° C) and gold point (1063° C) The cold junction was kept at the temperature of melting ice, and the e m f of the couple was measured with a Cambridge Scientific Instrument Company ' Workshop potentiometer ' which had been altered to give a tapping for a low resistance external galvanometer The potentiometer dials were set to the required voltage and the current through the furnace was controlled to give no deviation of the galvanometer A change of one microvolt in the couple e m f produced a deflection of 1½ mm By watching the first signs of a deviation and taking steps to correct it immediately by changing the heating current, it was usually found to be

possible to keep the couple reading constant within less than 2 microvolts, which meant a temperature constant to about $\pm$ 0 2° C

Experimental Procedure –After assembling the apparatus the furnace was baked out at the working temperature, and at the same time evacuated through the valve N fig 3, by a " Hyvac " pump with a liquid air trap By doing this a large amount of water and grease was removed from the asbestos lagging, and the danger of shorting the insulated cones by a layer of condensed moisture averted After this evacuation the bomb was always kept filled with nitrogen

To prepare for an experiment the furnace temperature was adjusted to the required value and the reaction bulb evacuated through the valves P and Q Valves P, Q, L, and N were then closed and the valves of the two cylinders N and O were opened By opening simultaneously the fine adjustment valves P and L, the silica bulb was filled with nitrous oxide at the same time as the bomb was filled with nitrogen and during this filling the pressures of the two gases as shown by the gauges A and M were kept equal The filling could be carried out at speeds up to 2 atms per second When the gas pressure for the experiment was reached the two valves P and L were tightly closed One observer began immediately to take readings of the gauge A, and of the height of the mercury meniscus in the capillary D, and a second observer started a stop-watch and noted the pressure readings and the time at which they were taken, and also controlled the furnace temperature A continual light tapping of the gauge was necessary to get the proper reading

As the reaction proceeded the pressure in the bulb shown by the gauge A rose, and it was necessary to adjust the balancing pressure of nitrogen This was best done continuously, by adjusting the valve L to give a steady leakage of gas into the bomb, at a rate corresponding to the rate of increase of pressure in the reaction bulb

After the reaction had been followed for a sufficient length of time, the gas was blown out by opening valve Q and then slowly releasing valves P and N When atmospheric pressure was reached, the reading of the gauge A and the height of the mercury column in D was taken It was then possible to correct the observed readings for the calibration error of the gauge and for the effect of the changing head of mercury in D to obtain the absolute pressures of the gas in the reaction bulb The results of typical experiments are shown in Table 1

When experiments were made at pressures above approximately 25 atms there was a tendency for the furnace temperature to fall slightly during the filling, because of the larger quantities of gas which had to be heated This

fall in temperature was usually less than half a degree, but its effects on the reaction velocity were nullified by starting with the temperature half a degree high

It is important that the time taken to fill the reaction bulb should be short If this filling time is an appreciable fraction of the half life, it becomes difficult to decide the initial pressure and starting time of the reaction from the experimental curve, for some of the gas will be reacting and giving a pressure change, although more gas is still entering the bulb By choosing the working temperature to give half-lives of at least 15 to 20 minutes, the time taken to fill at a speed of 2 atms per second or faster, becomes such a small fraction of the half-life of the reaction that there is no difficulty in fixing the initial pressure within 0 5% and the time zero to a second or two

Good evidence that the time taken by the gas to reach the reaction temperature was very short was provided by the shape of the reaction curves If the gas had remained below the final reaction temperature for some length of time, the experimental pressure time curve would have shown a pronounced change of curvature near the origin, the points being low, gradually rising to the true reaction curve from a steady temperature as the rising temperature of the gas produced a higher pressure Actually the experimental curves showed no such effect

Source of Nitrous Oxide —The nitrous oxide was taken from a cylinder of the pure liquid supplied by the British Oxygen Company marked " for inhalation " The gas was found to be 96 7% nitrous oxide, the remainder being nitrogen and oxygen For many of the experiments in the low pressure apparatus the gas was purified by condensing the nitrous oxide in liquid air and pumping away the permanent gas before evaporating and collecting the pure gas This purified gas gave the same results as the gas taken directly from the cylinder This was also the experience of Hinshelwood and Burk, and of Musgrave and Hinshelwood (*loc cit*) who found that even large quantities of air had no effect on the velocity of reaction except at very low pressures of nitrous oxide, *e g* , 30 mm Hg

For the high pressure apparatus cylinder gas was the only convenient source of supply of large quantities of compressed nitrous oxide, and it was used in all the experiments There was no difficulty in filling the reaction bulb at pressures up to at least 40 atms , since the vapour pressure from liquid nitrous oxide at room temperatures is above 50 atms

Determination of Nitric Oxide in the Reaction Product – The amount of nitric oxide formed as a by-product during the high pressure reaction was

measured in a few instances   The method was one of those used by Musgrave and Hinshelwood   When the half-life had been reached the mixture of nitrous oxide and its reaction products was blown into an evacuated, calibrated 3-litre flask, and the temperature and pressure of the gas were measured   In this mixed gas the by-product was present as nitrogen peroxide formed from nitric oxide and oxygen on cooling   It was converted to nitric acid by admitting about 50 c c of distilled water to the flask and shaking the contents for half an hour   The acid so formed was titrated with centinormal alkali   Control experiments were made to ensure that no soda was removed from the walls of the flask by the shaking with water, and that the original nitrous oxide shaken with water gave no acid   The percentages of nitric oxide found are given in Table VII, the accuracy is probably about 10%

The Temperature and Pressure Ranges Employed —With the low pressure apparatus experiments were made between 75 mm Hg and 2200 mm Hg at temperatures between 999° and 888° K   The half-lives varied between 120 and 10,000 seconds   The high pressure apparatus was used between $\frac{1}{2}$ and 40 kg /cm^2 and 840° and 930° K   with half-lives varying between 10,000 seconds and about 500 seconds

Some attempts were made to carry out experiments at pressures as high as 70 kg /cm^2 To do this it was necessary to warm the supply cylinder to obtain a high enough pressure to fill the reaction bulb, and also to heat the connections to the manometer to prevent the formation of liquid nitrous oxide which would lead to a discrepancy between the observed rate of pressure increase and the true rate of reaction   It becomes necessary to heat the dead space of the system above the critical temperature, 36 5° C, for all experimental pressures much above 40 kg /cm^2, for when the half-life is reached at about 50–60 kg /cm^2 the pressure is sufficient to liquefy the unreacted nitrous oxide in the dead space if this is at room temperature   These experiments above 40 kg /cm^2 were not successful   On a number of occasions the reaction bulb exploded, probably as a result of contamination of the gas with grease forced from the valve packings by the heating   It is possible that the use of valves packed with fibre or white metal might cure the trouble

Three of these experiments, although unsatisfactory from the point of view of temperature control and reaction velocity measurement, have provided some of the data for Table VII, which shows the amount of by-product nitric oxide formed during reaction at different pressures

Table I.—Typical Measurements of the Velocity of Decomposition of Nitrous Oxide at High Pressures

857 8° K			867 7° K			875 0° K		
Time from entry of gas	Thermo couple Millivolts	Pressure Kg /cm²	Time from entry of gas	Thermo couple Millivolts	Pressure Kg /cm²	Time from entry of gas	Thermo couple Millivolts	Pressure Kg /cm²
min sec			min sec			min sec		
0 45	5 400	37 52	0 21	5 750	24 62	0 19	5 601	18 41
1 5	5 395	37 57	0 34	5 750	24 77	0 40	5 600	18 48
1 26	5 395	37 62	0 42	5 747	24 78	1 30	5 599	18 56
1 57	5 395	37 72	1 2	5 747	24 88	2 30	5 600	18 70
2 52	5 400	37 93	1 28	5 753	25 05	3 15	5 599	18 85
3 25	5 401	38 03	2 9	5 753	25 25	4 30	5 599	18 96
4 10	5 400	38 18	2 46	5 752	25 47	5 45	5 600	19 09
5 5	5 400	38 33	3 23	5 752	25 73	6 40	5 600	19 25
6 23	5 400	38 53	4 19	5 749	25 96	7 30	5 600	19 35
7 15	5 400	38 68	5 4	5 750	26 21	8 52	5 600	19 51
8 50	5 397	38 94	5 50	5 749	26 42	10 5	5 600	19 66
10 10	5 400	39 10	7 20	5 750	26 83	12 15	5 599	19 92
11 40	5 400	39 44	8 28	5 750	27 14	13 33	5 601	20 07
12 52	5 399	39 59	9 31	5 750	27 30	15 6	5 601	20 22
13 57	5 399	39 64	10 40	5 750	27 56	16 36	5 600	20 36
15 12	5 400	39 94	11 11	5 748	27 82	18 37	5 602	20 61
16 47	5 400	40 20	12 40	5 750	28 07	19 40	5 602	20 71
18 55	5 401	40 50	13 35	5 749	28 21	20 30	5 601	20 81
19 33	5 399	40 65	14 25	5 749	28 41	21 25	5 600	20 90
21 10	5 402	40 84	16 0	5 748	28 75	22 28	5 598	21 00
23 8	5 402	41 14	17 15	5 750	28 98	23 37	5 600	21 10
24 22	5 397	41 29	18 30	5 750	29 22	25 5	5 601	21 23
26 30	5 400	41 54	19 45	5 750	29 41	26 30	5 600	21 36
28 30	5 399	41 84	21 23	5 750	29 71	28 0	5 600	21 50
30 0	5 402	42 03	22 30	5 752	29 99	29 0	5 599	21 60
31 35	5 400	42 23	23 30	5 750	30 09	30 20	5 598	21 70
33 10	5 403	42 43	25 10	5 750	30 28	32 10	5 600	21 85
37 18	5 402	42 93	26 20	5 747	30 43	33 27	5 600	21 95
38 42	5 402	43 13	27 25	5 750	30 58	34 55	5 597	22 00
40 45	5 400	43 32	28 55	5 747	30 78	37 0	5 600	22 24
41 47	5 399	43 43	29 43	5 750	30 87	39 0	5 597	22 33
43 50	5 401	43 53				40 45	5 603	22 48
46 38	5 402	43 78				42 28	5 601	22 57
47 27	5 400	44 03				43 30	5 600	22 65
48 45	5 403	44 23				44 50	5 601	22 76
49 40	5 402	44 33				46 30	5 602	22 85
51 8	5 400	44 43				47 52	5 600	22 94
53 50	5 400	44 73				49 17	5 600	23 03
55 32	5 403	44 94				51 28	5 600	23 15
58 55	5 403	45 14				54 30	5 600	23 27
60 0	5 400	45 39				56 0	5 602	23 36
62 40	5 402	45 39						
64 45	5 399	45 74						
65 52	5 402	45 84						
67 37	5 400	46 00						
69 48	5 400	46 20						
71 45	5 400	46 35						
74 20	5 400	46 55						
75 30	5 400	46 66						
76 20	5 401	46 74						
78 45	5 398	46 92						
81 5	5 399	47 19						

RESULTS

The Velocity of Reaction at Pressures up to 2000 mm Hg (2 72 kg /cm²)   Low Pressure Apparatus

The results at pressures below 500 mm were obtained with the normal low pressure apparatus ; those above this pressure with the low pressure apparatus fitted with closed manometer

Table II

913 5° K		971° K		996 5° K	
Initial pressure mm Hg	Half life, secs	Initial pressure, mm Hg	Half life , secs	Initial pressure, mm Hg	Half life, secs
180	7350	220	910	228	416
400	4760	390	675	375	317
759	3270	832	494 4	829	231 6
1137	2778	988	436 5	932	207 4
1506	2326	1119	399 3	1049	195
1816	2160	1315	360	1126	182 3
2120	1893	1683	307 5	1208	175
		1896	286 2	1278	178 1
		2002	287 5	1385	166 7
				1460	159 7
				1574	148 6
				1728	142 7
				1853	139 2
				1930	131 4
				1983	129 6
				2026	132 2
				2165	122 2

The Velocity of Reaction at Pressures up to 40 atms   High Pressure Apparatus

Table III —Temperature   614 7° C , 887 7° K   1 kg /cm.² = 0 967 atms

Pressure, kg /cm²	Half life, secs	Pressure, kg /cm²	Half life, secs
0 36*	13,824	10 63	2,415
0 46*	11,394	12 50	2,093
0 54	9,540	12 84	2,123
2 44	4,815	19 20	1,836
3 40	3,490	24 61	1,542
3 97	3,220	26 67	1,560
4 65	2,970	30 40	1,493
5 64	2,835	32 86	1,482
6 76	2,850	36 45	1,459
8 70	2,425	39 56	1,454

* Low pressure apparatus

Table IV —Temperature 644 7° C , 917 7° K   1 kg /cm² = 0 967 atms

Pressure, kg /cm²	Half life, secs	Pressure, kg /cm²	Half life, secs
0 54	3,115	7 24	762
2 21	1,680	9 26	711
3 05	1,240	10 78	663
3 59	1,044	12 20	665
4 64	803	12 85	604
5 80	819		

Table V —Temperature 657 5° C , 930 5° K   1 kg /cm² = 0 967 atms

Pressure, kg /cm²	Half life, secs	Pressure, kg /cm²	Half life, secs
0 52	2,195	6 40	534
2 20	957	7 99	473
2 97	767	9 22	429
3 98	658	11 26	398
5 15	585	12 73	348

Table VI —Change of Reaction Velocity with Temperature and Change of Activation Energy with Pressure at Constant N_2O Concentration

Temperature, ° K	Pressure, kg /cm²	$\log_{10}(1/t_{\frac{1}{2}})$		Activation energy E, cals /gm mol
		Observed	Calculated	
1 Pressure 37½ kg /cm.²				
840 9	37 0	$\bar{4}$ 0545	$\bar{4}$ 054	
857 8	37 4	$\bar{4}$ 383	$\bar{4}$ 386	
866 2	38 1	$\bar{4}$ 544	$\bar{4}$ 546	} 64,900
875 0	37 85	$\bar{4}$ 711	$\bar{4}$ 710	
2 Pressure 18¼ kg /cm.²				
840 9	18 2	$\bar{5}$ 948	$\bar{5}$ 935	
857 8	18 05	$\bar{4}$ 256	$\bar{4}$ 261	
866 2	18 6	$\bar{4}$ 421	$\bar{4}$ 419	} 63,900
875 0	18 4	$\bar{4}$ 5755	$\bar{4}$ 581	
3 Pressure 0 53 kg /cm.², 390 mm. Hg				
904 3	0 536	$\bar{4}$ 2645	$\bar{4}$ 280	
919 6 {	0 524	$\bar{4}$ 542	} $\bar{4}$ 528	
	0 536	$\bar{4}$ 501		
934 7	0 533	$\bar{4}$ 796	$\bar{4}$ 761	} 61,000
951 5	0 546	$\bar{3}$ 0075	$\bar{3}$ 013	
962 5	0 536	$\bar{3}$ 2640	$\bar{3}$ 260	

Table VI —(continued)

Temperature, °K	Pressure, kg/cm²	log₁₀(1/t₁)		Activation energy F cals/gm mol
		Observed	Calculated	

4   Pressure 0 26 kg /cm², 190 mm Hg

Temperature, °K	Pressure, kg/cm²	Observed	Calculated	Activation energy
904.3	0.250	1.095	1.109	
934.7	0.256	1.558	1.542	
951.5	0.252	1.7645	1.770	55,200
	0.265	1.770		
968.5	0.255	1.985	1.994	
985.8	0.258	3.220	3.213	

5   Pressure 0 14 kg /cm², 103 mm Hg

Temperature, °K	Pressure, kg/cm²	Observed	Calculated	Activation energy
904.3	0.147	5.939	5.843	
	0.137	5.900		
919.6	0.137	4.1845	4.160	
	0.137	4.1725		53,750
951.5	0.143	4.540	4.588	
	0.146	4.631		
968.5	0.141	4.790	4.805	
999.0	0.144	3.192	3.175	

6   Pressure 0 10 kg /cm², 73 5 mm Hg

Temperature, °K	Pressure, kg/cm²	Observed	Calculated	Activation energy
916.5	0.10	4.0875	4.050	
934.7	0.10	4.2775	4.298	
951.5	0.10	4.510	4.518	53,000
968.5	0.10	4.750	4.732	
985.8	0.10	4.941	4.941	
999.0	0.10	3.103	3.096	

Table VII —The Amount of By-Product Nitric Oxide formed at various Pressures at 590° C

Initial pressure of N₂O, kg /cm²	11 4	18 2	24 1	33 3	45 3	51 0	63 3
Molecules % NO at the half life	0 11	0 10	0 09	0 07	0 07	0 08	0 09

Nitrous oxide from cylinder (97 % N₂O)   0 0065 mols % NO

Discussion

The results obtained with the low pressure apparatus, which are shown in fig 4, are clearly in agreement with the observations of Hinshelwood and Burk and Musgrave and Hinshelwood (*loc cit*), since straight-lines can be drawn for $1/t_1$ against the pressure as far as 2000 mm Hg   From the work of Musgrave and Hinshelwood we know that these lines can be expected to bend sharply towards the origin at some pressure in the neighbourhood of 60 mm. Hg,

Table VIII.—Temperature 888° K

1	2	3	4	5	6	7	8
Pressure kg./cm.²	Reacting molecules = 2·5 × colliding molecules	$e - \kappa r$	Ratio Col. 2/Col. 3	$f(E)$ $n = 4$	Ratio Col. 2/Col. 5	$f(E)$ $n = 6$	Ratio Col. 2/Col. 7
0 64	1 89 × 10⁻¹⁴	0 3 × 10⁻¹⁴	30 7	1 44 × 10⁻¹⁴	1 31	11 8 × 10⁻¹⁴	0 164
2 44	0 856 × 10⁻¹⁴	0 01 × 10⁻¹⁴	17 1	79 × 10⁻¹⁴	1 08	8 55 × 10⁻¹⁴	0 130
3 40	0 87 × 10⁻¹⁴	3 17 × 10⁻¹⁴	20 8	66 × 10⁻¹⁴	1 32	5 60 × 10⁻¹⁴	0 138
3 97	0 78 × 10⁻¹⁴	3 89 × 10⁻¹⁴	20 0	34 × 10⁻¹⁴	1 25	5 15 × 10⁻¹⁴	0 152
4 65	0 738 × 10⁻¹⁴	3 39 × 10⁻¹⁴	21 7	50 × 10⁻¹⁴	1 36	4 50 × 10⁻¹⁴	0 164
5 64	0 63 × 10⁻¹⁴	3 16 × 10⁻¹⁴	19 9	47 1 × 10⁻¹⁴	1 25	4 24 × 10⁻¹⁴	0 148
6 70	0 52 × 10⁻¹⁴	2 96 × 10⁻¹⁴	19 6	40 1 × 10⁻¹⁴	1 19	3 97 × 10⁻¹⁴	0 132
8 20	0 478 × 10⁻¹⁴	2 34 × 10⁻¹⁴	19 0	37 b × 10⁻¹⁴	1 11	3 40 × 10⁻¹⁴	0 140
10 63	0 39 × 10⁻¹⁴	2 04 × 10⁻¹⁴	18 9	32 9 × 10⁻¹⁴	1 04	3 19 × 10⁻¹⁴	0 122
12 50	0 385 × 10⁻¹⁴	2 08 × 10⁻¹⁴	18 9	32 9 × 10⁻¹⁴	1 17	2 80 × 10⁻¹⁴	0 130
12 84	0 366 × 10⁻¹⁴	2 04 × 10⁻¹⁴	24 4	32 9 × 10⁻¹⁴	1 11	2 80 × 10⁻¹⁴	0 130
19 20	0 404 × 10⁻¹⁴	1 66 × 10⁻¹⁴	17 8	26 4 × 10⁻¹⁴	1 50	2 02 × 10⁻¹⁴	0 176
24 61	0 295 × 10⁻¹⁴	1 45 × 10⁻¹⁴	18 0	22 0 × 10⁻¹⁴	1 09	2 08 × 10⁻¹⁴	0 130
26 67	0 240 × 10⁻¹⁴	1 35 × 10⁻¹⁴	18 5	29 0 × 10⁻¹⁴	1 11	1 90 × 10⁻¹⁴	0 128
30 40	0 223 × 10⁻¹⁴	1 23 × 10⁻¹⁴	17 5	19 7 × 10⁻¹⁴	1 08	1 74 × 10⁻¹⁴	0 124
32 38	0 207 × 10⁻¹⁴	1 18 × 10⁻¹⁴	17 7	17 5 × 10⁻¹⁴	1 09	1 67 × 10⁻¹⁴	0 124
35 45	0 190 × 10⁻¹⁴	1 07 × 10⁻¹⁴	17 b	16 4 × 10⁻¹⁴	1 07	1 42 × 10⁻¹⁴	0 124
39 26	0 176 × 10⁻¹⁴	1 00 × 10⁻¹⁴					
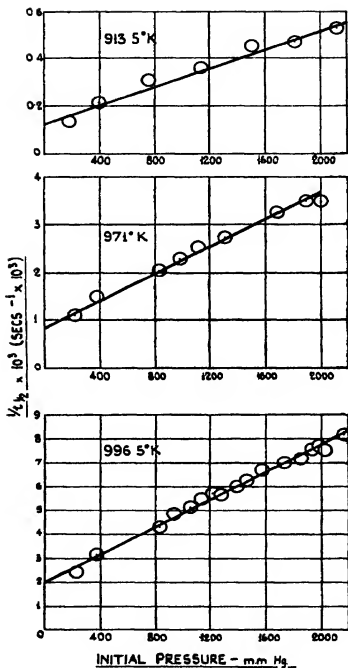
FIG 4

At 2000 mm. Hg, a pressure at which Volmer found an approach to true unimolecular velocity constants, there are no indications whatever of the line $1/t_{\frac{1}{2}}$ against p tending to become horizontal

The curve for the complete pressure range at 888° K is shown in fig 5, the straight line extending to at least 3 kg/cm² in fig 4 is found to bend over fairly sharply at about 4 kg/cm² to another straight line of smaller slope which persists to about 26 kg/cm² before curving away Above 30 kg/cm² the half-life is almost independent of pressure
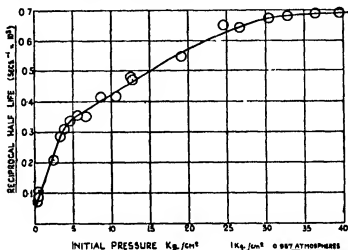
Fig 5

The measurements given in Tables IV and V were made to see whether any shifting of the bend at 4 kg/cm² with change of temperature could be discovered The curves of fig 6 show that within the range of temperature employed, change of temperature produces no definite change of the pressure at which the bend occurs

The results of Table VII, which show the amount of nitric oxide formed during reaction, give an assurance that at high pressures catalysis by this by-product is no more serious than it is at low pressures Musgrave and Hinshelwood found that at an initial pressure of 200 mm Hg of nitrous oxide, about 3¼% of nitric oxide was formed during reaction, at 500 mm Hg this had fallen to less than 2% Table VII shows that the percentage of nitric oxide formed continues to decrease with rising pressure

The results of measurements made to determine the activation energy are given in Table VI For each series straight lines are obtained by plotting

$1/K°$ against $\log 1/t_{\frac{1}{2}}$ The values of $\log 1/t_{\frac{1}{2}}$ calculated back from these straight lines are tabulated in column 4 The inferior accuracy of the two series at the lowest pressures, 75 and 100 mm Hg, is due to the difficulty of measuring accurately with an ordinary manometer, a pressure increase of only 18 to 25 mm Hg An attempt was made to carry out each series at constant initial concentration of N_2O rather than at constant initial pressure, by taking into account the variation of pressure with temperature at constant concentration, and adjusting the initial pressures accordingly The activation energies, calculated on the assumption that the slopes of the lines $1/K°$ against

Fig 6
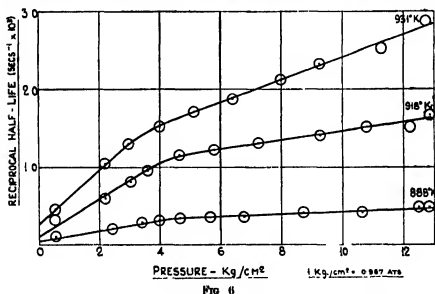
log₍ₑ₎ $1/t_{\frac{1}{2}}$ at constant initial concentration are equal to E/R, are given in column 5, and are plotted against the pressure in fig 7 In this graph the results of Musgrave and Hinshelwood for zero pressure, Hinshelwood and Burk for pressures between 100 and 400 mm, and M A Hunter for atmospheric pressure are included Between 0 and 4 kg /cm ² there is a great increase of activation energy with increasing pressure Above this pressure there is little further change to 40 kg /cm.² These results are at variance with those of Volmer and Nagasako,* who give an activation energy of 53,000 cal /gm mol for all pressures up to 10 kg /cm.² There is little doubt, however, that fig 7 shows the true behaviour, since it is supported both by the satisfactory results of Table VI and by the results of other workers. It is likely that we

* 'Z phys. Chem ,' B, vol 9, p 141 (1930)

are concerned with at least two, and possibly more, simultaneous reactions, each with a different activation energy   It remains to be decided whether or not the hypothesis that a unimolecular reaction proceeds alongside a bimolecular one is sufficient   Fig 5 shows that it is not   The straight line for $1/t_{\frac{1}{2}} - p$ does not continue indefinitely, but bends to another practically straight line of smaller slope, which in turn is succeeded by one which is almost horizontal

Recent work on the thermal decomposition of acetaldehyde by Hinshelwood and Fletcher* has produced results which correspond closely to those for
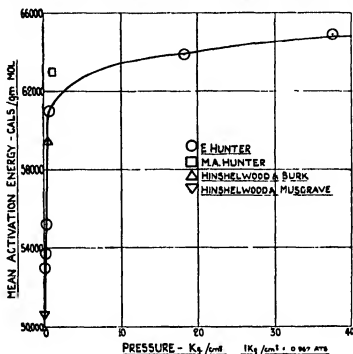
Fig 7

nitrous oxide, except for their much smaller pressure scale   The same type of segmented curve was obtained, with sharp bends at 3, 45, and 250 mm Hg In order to account for the behaviour of acetaldehyde the theory was put forward that the molecule can be activated in a definite number of different ways, according to the manner in which the energy is divided within the molecule between the different modes of vibration or rotation   In quasi-unimolecular reactions the time lapse between the instant of activation of the molecule by collision and the instant of its decomposition probably arises

* 'Proc Roy Soc,' A, vol 141, p 41 (1933)

from the necessity for a re-arrangement of the energy within the molecule before a state favouring decomposition is brought about It is conceivable that the time taken for this re-arrangement will depend on how the energy has been distributed between the modes of vibration according to the particular way in which the molecule has been activated If a definite number of different ways of activation are possible they will lead to the same definite number of independent quasi-unimolecular reactions.

In their paper, Hinshelwood and Fletcher made a rough analysis of a curve of the type of fig 5 and succeeded in showing that such a curve represents the combined effect of three separate quasi-unimolecular reactions

For each reaction an equation of the type

$$K_1 p^2 - K_2 pa - K_3 a = 0,$$

holds, where $K_1 p^2$ is the rate of activation by collision, $K_2 pa$ the rate of de-activation of active molecules by collision with normal molecules, and $K_3 a$ the rate of decomposition of activated molecules, or rate of reaction If there are three types of activated state the observed velocity is

$$- dp/dt = \frac{K_1 p^2}{1 + K_2 p/K_3} + \frac{K'_1 p^2}{1 + K'_2 p/K'_3} + \frac{K''_1 p^2}{1 + K''_2 p/K''_3}$$

If the three types of activated molecule have fairly widely different probabilities of reaction, $K_3 > K'_3 > K''_3$, and it can be shown that the curve for $1/t_1$ against the initial pressure starts from the origin as

$$1/t_1 = (K_1 + K'_1 + K''_1) p_0$$

This is the line OA of fig 8 It is succeeded by a practically straight line of slope approximately $(K_1 + K'_1)$ which makes an intercept of about $K''_1 K''_3/K''_2 \log 2$, on the axis of $1/t_1$ This line, AB in fig 8, represents the reaction velocities at pressures between 50 and about 3000 mm Hg, and its intercept is that which appears in figs 4 and 5 In this region one of the three reactions has reached its limiting velocity constant At a higher pressure the second reaction reaches its limiting velocity constant, and the line of slope $(K_1 + K'_1)$ is followed by a line of slope K_1, directed to a still larger intercept on the axis of $1/t_1$ This third line is BC in fig 8 which eventually becomes practically horizontal as the rising pressure causes the third reaction to approach its limiting velocity constant

The methods of this analysis give for the nitrous oxide decomposition the three quasi-unimolecular curves OEF, OGH, and OJK of fig 8 Although it

is clear that three separate curves can account for the shape of the experimental curve OABCD, fig 8 does not show more than the approximate magnitudes and shapes of the three curves, since the limiting velocity constants LF, LH, and LK are not sufficiently widely separated to fulfil the condition K_3 K'_3 K''_3, which is necessary before the above analysis can be expected to hold almost quantitatively

It is now possible to explain the activation energy curve of fig 7 Each of the three reactions has its own activation energy At low pressures (< 50 mm

INITIAL PRESSURE Kg /cm²   1 Kg /cm² 0 0e v v
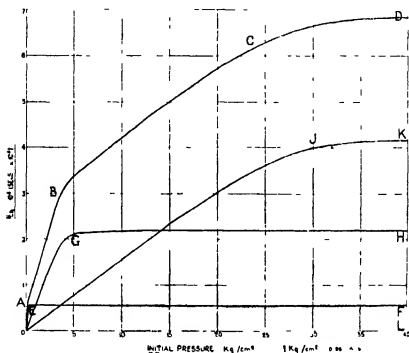
Fig 8

Hg) the low pressure reaction OEF of fig 8 contributes a greater fraction to the decomposition than either the medium pressure reaction OGH, or the high pressure reaction OJK, but as the pressure rises these latter two reactions participate to a greater and greater extent   The curve for the average activation energy consequently shows a rapid change in E with increasing pressure At about 5 kg /cm², however, both the low pressure and the medium pressure reactions are giving their maximum possible reaction velocities, and their combined contributions are quite a large fraction of the total.   The increase in

velocity on increasing the pressure above about 5 kg /cm.² is due solely to the growth of the high pressure reaction OJK of fig 8 and the measured mean activation energy no longer shows such a rapid change with increasing pressure Above a pressure of about 40 kg /cm² the limiting velocity constants of all three reactions are reached and the observed activation energy becomes independent of pressure, since the relative contributions of the three reactions do not vary with pressure

The absolute values of all three activation energies cannot be deduced from fig 7 since each may itself vary continuously with pressure It is apparent that the low pressure reaction is associated with an activation energy of about 50,500 cal /gm mol The activation energy of the high pressure reaction must be above 65,000 cals /gm mol, and the value for the medium pressure reaction is probably between 50,500 and 62,000 cal /gm mol Since the first reaction with activation energy 50,500 /gm mol gives a maximum velocity less than that for the second reaction with activation energy approximately 60,000 cals /gm mol, and this second reaction in its turn gives a maximum velocity less than that of the third reaction with an activation energy greater than 65,000 cal /gm mol, the probability of the decomposition of the activated molecule of the first reaction is smaller than that of the second, which again is smaller than that of the third reaction with the highest of the three activation energies

In Table VIII the results of some calculations based on the data of Tables III and VI are given Since the reaction is a compound one it was not justifiable to assume that the number of molecules reacting per cubic centimetre per second at any given pressure could be calculated directly from the particular value of the unimolecular velocity "constant" $ln\ 2/t_{\frac{1}{2}}$, or the bimolecular constant, $1/at_{\frac{1}{2}}$ at that pressure However, the tangent dp/dt at the time origin of each reaction curve can be used to calculate the number of molecules reacting, since the pressure increase is brought about by the formation of three molecules in place of two of nitrous oxide It was found that the number calculated in this way always agreed to within 10% of the number calculated from the different values of $ln\ 2/t_{\frac{1}{2}}$ (the unimolecular ' constant ") over the pressure range The numbers calculated in the latter way were used in Table VIII since the values of $t_{\frac{1}{2}}$ were known more accurately than the values of the tangents at the very start of the reactions, which were not easy to determine accurately

In column 2 of Table VIII is shown the ratio, reacting molecules/(2 5 × calc. no of colliding molecules) The number of collisions was calculated

on the assumption that the diameter of the nitrous oxide molecule is 3 32 × 10^{-8} cm. The factor 2 5 is used to compensate for the increased number of collisions due to the higher than average velocity of the high translational energy molecules which are likely to be concerned in activating collisions and for the possibility that a particular orientation of the molecules at the moment of impact is necessary

The values calculated for the expression $e^{-E/RT}$ from the data of Table VI are given in column 3 of Table VIII, and it will be seen that activation energy associated with only two square terms can only account for one-twentieth of the observed reaction, as is shown in column 4

The fraction of the molecules possessing energy greater than E, distributed between a number of degrees of freedom is given as a sufficient approximation by the expression

$$e^{-\left(\frac{E+(\frac{1}{2}n-1)RT}{RT}\right)} \frac{[E/RT + (\frac{1}{2}n+1)]^{\frac{1}{2}n-1}}{\lfloor\frac{1}{2}n-1}$$

where n represents the number of "square terms" between which the energy is distributed This expression worked out for nitrous oxide, gives for $n = 4$ and $n = 6$, the values which appear in columns 5 and 7, respectively of Table VIII The ratios in columns 6 and 8 show that the rate of activation can be equated to the rate of reaction if $n = 4$ and is greater than the rate of reaction if $n = 6$ This implies a distribution of energy between two, or at most three degrees of freedom, so that activation energy can be distributed between translational energy and one or perhaps two modes of vibrational energy within the molecule It is now fairly generally accepted that the atoms of the nitrous oxide molecule lie in a straight line in the order NNO, two or even three degrees of freedom is therefore not an unreasonable number

Since the observed reaction can be regarded as the resultant of three quasi-unimolecular reactions, the thermal decomposition of nitrous oxide is principally concerned with the isolated molecule, which presumably breaks up according to the scheme $N_2O \longrightarrow N_2 + O$ This free oxygen atom must react rapidly, either with a second free atom, $O + O \longrightarrow O_2$, or with a fresh nitrous oxide molecule $O + N_2O \longrightarrow N_2 + O_2$, and the measured pressure increase will be that corresponding to the stoichiometric equation $2N_2O \longrightarrow 2N_2 + O_2$.

2 E 2

Summary

Apparatus for the study of gas reactions by the static method at pressures up to 100 atms and at temperatures up to 900° C is described

Results of measurements of the velocity of thermal decomposition of nitrous oxide at pressures up to 40 atms are given   In conjunction with the work of Musgrave and Hinshelwood[*] they show clearly that the observed reaction is the resultant of three separate quasi-unimolecular reactions which become independent of pressure at approximately 0 08, 5, and 30 atms , respectively

The average activation energy of the reaction has been measured at different pressures and is found to rise rapidly from the value 50,500 cal /gm mol at zero pressure until a pressure of about 6 atms is reached   As the pressure rises above 6 atms it becomes less and less dependent upon pressure, and is practically independent of pressure above 30 atms

The behaviour of the reaction suggests that there are three separate modes of activation, each with a different mean activation energy and a different probability of decomposition of the activated molecule

* ' Proc Roy Soc ,' A, vol 135, p 23 (1932)

A Relativistic Basis of the Quantum Theory

By H T Flint, Reader in Physics, University of London, King's College

(Communicated by O W Richardson, F R S —Received December 2, 1933)

Introduction

In a previous communication* it was pointed out that the problem of the quantum equations could be regarded as having developed into a search for a modification of the Riemannian covariant differentiation

This view of the problem appears from many of the more recent publications, some of which are quoted below †

Various underlying geometrical or analytical theories have been employed to determine the modification of the Christoffel bracket expression, which we write here $\Gamma_{\mu\nu}{}^\sigma$, but in general the effect is to introduce a new quantity $T_{\mu\nu}{}^\sigma$ which must be added to $\Gamma_{\mu\nu}{}^\sigma$. The construction of $T_{\mu\nu}{}^\sigma$ depends upon the theory adopted, and it is sometimes symmetrical in μ, ν and sometimes not

Frequently the attempts have been successful to the extent of uniting gravitational and electromagnetic theory but the quantum equations, though fitting in well with the particular geometrical background, stand aside somewhat and are not absorbed completely into the scheme As an example of this Fisher and Flint (loc cit infra) found that Dirac's first order equations could be expressed in the form of a vanishing divergence and from the equations so obtained the second order wave equation containing the 'spin' terms was deduced without the introduction of further hypothesis But this method merely placed the equations into the scheme and it was only by a somewhat indirect process that they could be shown to have a geometrical significance ‡

Nevertheless, the actual form of the first order equations in this notation raises the hope of a possible union of gravitational, electromagnetic and quantum theories The present paper is a result of this discovery The underlying idea of this earlier attack on the problem was simple The track of a charged particle in a gravitational and electromagnetic field was regarded as a null geodesic Associated with this track was a set of equations was adopted,

based on the analogy that exists between the track of a photon and Maxwell's equations The equations so obtained turned out to be in the form of the quantum equations

In the light of the present study of the problem we shall have to regard this as an approximate theory, but it may be that in this close analogy to the wave theory of light we have the basis of the wave theory of matter We may see in examining the extent to which the analogy may be extended just how far we can go with the wave theory of matter

The other view of the quantum problem, which we suggested* was that it has become a search for quantities more fundamental in character than the $g_{\mu\nu}$ in the expression, $ds^2 = q_{\mu\nu}\, dx^\mu\, dx^\nu$, for the line element

The first to express this definitely appears to have been Tetrode † Fock (loc cit) worked out a detailed theory, using a relation of Tetrode's shortly afterwards

More recently Schroedinger (loc cit) has developed a theory of invariance with a generalized set of quantum equations, with which we shall have occasion to compare the results of this paper

The basis of this line of attack is the introduction of matrices α_m, which are more general than those originally introduced by Dirac and which satisfy the equations

$$\alpha_n\alpha_m + \alpha_n\alpha_m = q_{ma}\mathrm{I},\tag{1}$$

where I is the unit matrix

This method has much in common in its form with Einstein's theory of parallelism,‡ which he showed lent itself readily to the expression of the quantum equations as a vanishing divergence § It was therefore thought that the geometrical representation might succeed best in the framework of that theory and a study of the question was published ‖ A close analogy was discovered with Schroedinger's method but nothing emerged from the theory which would help to decide upon the particular type of space-time geometry appropriate to natural phenomena The mathematical form of the theory appears to permit of some variation in this particular

We must just mention here the work of Veblen and Hoffmann and the very general theory of Schouten and van Dantzig The latter have given a very

* ' Proc Roy Soc ,' A, vol. 141, p. 370 (1933)

† ' Z Physik,' vol 50, p 336 (1928)

‡ Einstein, ' SitzBer Preuss. Akad. Wiss.,' No. 17, p 217 (1928)

§ Flint, ' Proc Roy Soc ,' A, vol. 121, p 676 (1928)

‖ Ibid., vol. 141, p 363 (1933)

general formulation of the field theory, and it appears to include most of the important notations already proposed

The Basis of the Present Theory

The method we adopt here is based on a modification of the Riemannian covariant derivative

Instead of taking this to be

$$\frac{\partial A_\mu}{\partial x^\nu} - \Gamma_{\mu\nu}{}^\alpha A_\alpha, \tag{2}$$

we shall suppose it to be

$$\frac{\partial A_\mu}{\partial x^\nu} - \Delta_{\mu\nu}{}^\alpha A_\alpha, \tag{3}$$

and we shall write

$$\Delta_{\mu\nu}{}^\alpha = \Gamma_{\mu\nu}{}^\alpha + T_{\mu\nu}{}^\alpha \tag{4}$$

$T_{\mu\nu}{}^\alpha$ will not be supposed symmetrical in μ, ν as $\Gamma_{\mu\nu}{}^\alpha$ is, but we shall divide it into an antisymmetrical part $\Lambda_{\mu\nu}{}^\alpha$ and a symmetrical $\Theta_{\mu\nu}{}^\alpha$, writing

$$T_{\mu\nu}{}^\alpha = \Lambda_{\mu\nu}{}^\alpha - \Theta_{\mu\nu}{}^\alpha \tag{5}$$

It will be seen that we are using the same notation as Einstein employed This is for the reason mentioned above that his theory of parallelism suggests the mathematical form appropriate to our purpose.   We do not adopt the system of parallelism introduced by him   We shall, at any rate, have no occasion to refer to it   The idea is to leave open questions of this sort in order to free the notation of the limitations which geometry imposes on the form of $T_{\mu\nu}{}^\alpha$ It will be noticed that we have left ourselves unrestricted with regard to symmetry

It must also be made clear that we propose to make use of a system of five co-ordinates, x_μ, ($\mu = 1, 2, 3, 4, 5$) Every particle in our theory has five degrees of freedom   This is a point which has not met with general acceptance on the ground that the space-time of Physics is four-dimensional and no definite meaning can be given to the fifth co-ordinate

Our use of the fifth co-ordinate here is solely to enable us to make an appeal to mathematical form   If we are correct in the sense that our results correspond accurately with those of experiment, we can never presume to say more than that the physical world can be described as if it were five dimensional The success of the four-dimensional theory of the universe allows us to say no more than this with regard to the four-dimensional world   One may only exclaim in the excitement of discovery that space and time have henceforth vanished to shadows.

But as we have stated above, it is not our intention to insist upon the geometrical aspect of the theory

The more serious objections to the theory in the form of Kaluza and Klein are that the general covariance is destroyed by the "cylindrical" condition that the $q_{\mu\nu}$ do not contain x^5 and that q_{55} is taken as constant

For this reason many writers have sought to maintain a four-dimensional continuum, introducing five variables as auxiliary quantities, related to the four co ordinates, e g, Pauli's method of homogeneous co-ordinates makes the space-time co ordinates homogeneous functions of zero degree in the homogeneous variables

In the theory of Einstein and Mayer* vectors are introduced which are related to four-dimensional vectors, but the co ordinate system is four dimensional This theory is a unitary theory of gravitation and electricity

Such theories necessarily include many definitions and assumptions about the quantities introduced and extensions to the inclusion of the quantum theory involve some complications

We shall try to meet these objections by developing a more general theory than has been attempted hitherto It will be seen that the results obtained follow very naturally from the application of the methods of the theory of relativity

We shall then regard the special use of the cylindrical condition and the assumption about the way x^5 occurs in the functions as an approximation required by our need to eliminate x^5, in interpreting our results in the light of our present knowledge of physical phenomena We have to adopt a somewhat similar process in writing $x^4 = ut$, when we use the four co-ordinates x^1, x^2, x^3, x^4, in the theory of relativity We cannot, of course, claim that x^5 is in such a good case in this respect as x^4 This is our apology, if apology be needed, for the practical use of x^5 in this restricted way

Curvature

Following the suggestion that the geometrical notation gives, we shall describe the quantity $P_{\mu\nu\sigma}{}^{\bullet}$ as the curvature tensor In the notation of (3) the expression for this quantity is

$$P_{\mu\nu\sigma}{}^{\bullet} = \Delta_{\mu\sigma}{}_{,\nu}{}^{\bullet} - \Delta_{\mu\nu}{}_{,\sigma}{}^{\bullet} + \Delta_{\rho\nu}{}^{\bullet}\Delta_{\mu\sigma}{}^{\rho} - \Delta_{\rho\sigma}{}^{\bullet}\Delta_{\mu\nu}{}^{\rho} \qquad (6)$$

The use of the comma before a suffix denotes ordinary differentiation with

respect to the corresponding variable, e g, $\Delta_{\mu\sigma}{}^{\epsilon}{}_{,\nu} = \dfrac{\partial \Delta_{\mu\sigma}{}^{\epsilon}}{\partial x^{\nu}}$ We shall denote

covariant differentiation by the symbol ,ν It must be understood that the Greek affixes can have the values 1–5

If the substitution of (4) be made it follows that

$$P_{\mu,\epsilon}{}^{\epsilon} = R_{\mu\nu,\epsilon}{}^{\epsilon} - T_{\mu\nu}{}_{,\epsilon}{}^{\epsilon} + T_{\mu\sigma}{}^{\epsilon}{}_{,\nu}{}^{\epsilon} - T_{\mu\sigma}{}^{\epsilon}T_{\mu\epsilon}{}^{\rho} + T_{\rho\epsilon}{}^{\epsilon}T_{\mu\sigma}{}^{\rho} \tag{7}$$

This may be compared with the corresponding expression in the theory of relativity* where the quantity $T_{\mu\nu}{}^{\epsilon}$ is symmetrical in μ, ν The contracted curvature tensor obtained by writing ε = σ is

$$P_{\mu\nu} = R_{\mu\nu} \quad T_{\mu\nu}{}_{,\sigma}{}^{\sigma} + T_{\mu\sigma}{}^{\sigma}{}_{,\nu} - T_{\rho\sigma}{}^{\sigma}T_{\mu\nu}{}^{\rho} + T_{\rho\sigma}{}^{\sigma}T_{\mu\nu}{}^{\rho} \tag{8}$$

The Value of $T_{\mu\nu}{}^{\epsilon}$ and the Second Order Equation

In imposing a restriction upon this quantity we shall be guided again by the geometrical methods

One suggestion that arises is to write

$$T_{\mu\nu}{}^{\epsilon} - \gamma_{\mu\nu}\Pi^{\epsilon} - \gamma_{\mu}{}^{\epsilon}\Pi_{\nu} - \gamma_{\nu}{}^{\epsilon}\Pi_{\mu} \tag{9}$$

where the quantities $\gamma_{\mu\nu}$, $\gamma_{\mu}{}^{\epsilon}$, $\gamma_{\nu}{}^{\epsilon}$ have their usual meanings We write for the five-dimensional line element

$$d\sigma^2 - \int_{\mu\nu} dx^{\mu} dx^{\nu}, \tag{10}$$

so that the $\gamma_{\mu\nu}$ are analogous to the $g_{\mu\nu}$ of Riemannian geometry

This suggestion comes directly from the theory of Eddington and Weyl * It is the suggestion made formerly† which proved very fruitful in the expression for Dirac's equations as a vanishing divergence But we find it too restricted for our present purpose It may be noted that in this form $T_{\mu\nu}{}^{\epsilon}$ is symmetrical in μ, ν

We return rather to a form used in Einstein's theory‡

$$T_{\mu\nu}{}^{\epsilon} = \Lambda_{\mu\nu}{}^{\epsilon} - \gamma^{\epsilon\tau}\gamma_{\mu\rho}\Lambda_{\tau\nu}{}^{\rho} - \gamma^{\epsilon\tau}\gamma_{\nu\rho}\Lambda_{\tau\mu}{}^{\rho} \tag{11}$$

$\Lambda_{\mu\nu}{}^{\epsilon}$ is antisymmetric in μ, ν and it will be seen that the remaining terms on the right, taken together, are symmetric in μ, ν Thus the value of $\Theta_{\mu\nu}{}^{\epsilon}$ is the sum of these terms

* Eddington, "Mathematical Theory of Relativity," 2nd ed , p 218

† Fisher and Flint, loc. cit (1930)

‡ See also Flint, 'Proc Roy Soc ,' A, vol 141, p 371 (1933)

We have thus assumed that $T_{\mu\nu}{}^\epsilon$ depends upon a single quantity with components $\Lambda_{\mu\nu}{}^\epsilon$ except, of course, for the $\gamma_{\mu\nu}$.

We can without very much calculation substitute for $T_{\mu\nu}{}^\epsilon$ in the contracted curvature (8) The work is rendered much lighter if we remember that the covariant derivatives of the $\gamma_{\mu\nu}$ vanish

We find that it is important for us to consider the quantity $\gamma^{\mu\nu}P_{\mu\nu}$ so that we can omit the separate calculation of $P_{\mu\nu}$

We find that

$$\gamma^{\mu\nu}P_{\mu\nu} = \gamma^{\mu\nu}R_{\mu\nu} - 4\gamma^{\mu\nu}\Lambda_{\sigma\mu}{}^\sigma{}_{,\nu} + 4\gamma^{\sigma\nu}\Lambda_{\rho\sigma}{}^\epsilon\Lambda_{\nu\epsilon}{}^\rho + \gamma^{\rho\tau}\left(\gamma^{\sigma\eta}\gamma_{\alpha\epsilon} + 2\delta_\epsilon{}^\eta\delta_\alpha{}^\theta\right)\Lambda_{\tau\epsilon}{}^\alpha\Lambda_{\beta\rho}{}^\epsilon \quad (12)$$

Let us write $\Lambda_{\sigma\mu}{}^\sigma = \dfrac{a}{\psi}\dfrac{\partial\psi}{\partial x^\mu}$

Then

$$\gamma^{\mu\nu}\Lambda_{\sigma\mu}{}^\sigma{}_{,\nu} = a\gamma^{\mu\nu}\left\{\frac{\partial}{\partial x^\nu}\left(\frac{1}{\psi}\frac{\partial\psi}{\partial x^\mu}\right) - \Gamma_{\mu\nu}{}^r\left(\frac{1}{\psi}\frac{\partial\psi}{\partial x^r}\right)\right\}$$

$$= \frac{a}{\sqrt{\gamma}}\frac{\partial}{\partial x^\nu}\left\{\sqrt{\gamma}\gamma^{\mu\nu}\frac{1}{\psi}\frac{\partial\psi}{\partial x^\mu}\right\}$$

$$= \frac{a}{\psi}\frac{1}{\sqrt{\gamma}}\frac{\partial}{\partial x^\nu}\left\{\sqrt{\gamma}\gamma^{\mu\nu}\frac{\partial\psi}{\partial x^\mu}\right\} - \frac{a}{\psi^2}\gamma^{\mu\nu}\frac{\partial\psi}{\partial x^\nu}\frac{\partial\psi}{\partial x^\mu}$$

$$= \frac{a}{\psi}\frac{1}{\sqrt{\gamma}}\frac{\partial}{\partial x^\nu}\left\{\sqrt{\gamma}\gamma^{\mu\nu}\frac{\partial\psi}{\partial x^\mu}\right\} - \frac{\gamma^{\mu\nu}}{a}\Lambda_{\sigma\mu}{}^\sigma\Lambda_{\nu\epsilon}{}^\epsilon$$

If a be made equal to -1, we eliminate the third term on the right of (12), which may now be written

$$\frac{1}{\psi}\bigtriangleup\psi + \tfrac{1}{4}\gamma^{\rho\tau}\left(\gamma^{\sigma\eta}\gamma_{\alpha\epsilon} + 2\delta_\epsilon{}^\eta\delta_\alpha{}^\theta\right)\Lambda_{\tau\epsilon}{}^\alpha\Lambda_{\beta\rho}{}^\epsilon + \tfrac{1}{4}\gamma^{\mu\nu}R_{\mu\nu} = \tfrac{1}{4}\gamma^{\mu\nu}P_{\mu\nu}, \quad (13)$$

$\gamma^{\mu\nu}R_{\mu\nu}$ is the Gaussian curvature, i e, if we regard space as five-dimensional Riemannian space, we can speak of it as the curvature of that space We shall denote it by R and it corresponds to the G of relativity theory We shall denote $\gamma^{\mu\nu}P_{\mu\nu}$ by P

The symbol $\bigtriangleup\psi$ is familiar in the theory of Klein It corresponds to the Laplacian operator and in Klein's theory

$$\bigtriangleup\psi = 0 \quad (14)$$

is Schroedinger's equation for an electron without spin in a gravitational and electromagnetic field

We make the suggestion that the complete second order wave equation of the quantum theory in its relativistic form is (13)

The reason for this suggestion will be made clear by considering the approximate form obtained by the usual method of eliminating x^5

Reduction of the General Equation

In order to compare (13) with the equations proposed hitherto we shall adopt the Klein-Kaluza values of the $\gamma_{\mu\nu}$

If m, n, represent values 1–4, the values are

$$\left.\begin{array}{l} \gamma_{mn} = g_{mn} + \gamma_{55}\alpha^2\phi_m\phi_n, \qquad \gamma_{m5} = \gamma_{5m} = \gamma_{55}\alpha\phi_m, \\[2mm] \gamma^{mn} = g^{mn}, \qquad \gamma^{m5} = \gamma^{5m} = -\alpha\phi^m, \qquad \gamma^{55} = \alpha^2\phi_m\phi^m + \dfrac{1}{\gamma_{55}}, \\[2mm] \gamma_{55}\alpha^2 = -\dfrac{16\pi K}{c^2}, \end{array}\right\} \quad (15)$$

ϕ_m is a component of the electromagnetic potential and K is the Newtonian constant of gravitation

With this set of values the track of a charged particle is a geodesic in five-dimensional space and by writing $\alpha = e/mc$, it becomes a null geodesic [*] But however suggestive this may be it appears to be numerically incorrect in further applications of the theory

We shall further make use of de Broglie's suggestion that x^5 occurs in such a way in those quantities that depend upon it that differentiation with respect to this variable is equivalent to multiplication to multiplication $2\pi ie/h\kappa$, α being the constant in (15) and e the value of the fundamental electric charge

If $\alpha = e/mc$, this is equivalent to multiplication by $2\pi imc/h$, which is often taken to replace $\partial/\partial x^5$, but this makes the theory too restricted and de Broglie has considerably helped the theory by not introducing the mass in this operation

With these limitations and taking the value of $\sqrt{-\gamma}$ as unity, as in the theory of relativity, we obtain

$$\bigcirc\psi = \square^2\psi - \frac{4\pi i}{h}\frac{e}{c}\phi^m\frac{\partial\psi}{\partial x^m} - \frac{4\pi^2}{h^2}\left(\frac{e^2}{c^2}\phi_m\phi^m + \frac{e^2}{\alpha^2\gamma_{55}}\right) \qquad (16)$$

We notice that additional terms occur in (13), one of these must represent the

[*] Fisher, 'Proc Roy Soc,' A, vol 123, p 489 (1929)

spin term and another the mass of the particle considered   The third term $\gamma^{\mu\nu}R_{\mu\nu}$ is the curvature, and its value is known*

$$\gamma^{\mu\nu}R_{\mu\nu} = G - \frac{8\pi K}{c^2}H \qquad (17)$$

$$H = F^{il}F_{il} \qquad (18)$$

$$F_{il} = \frac{\partial\phi_i}{\partial x^k} - \frac{\partial\phi_k}{\partial x^i}, \qquad (19)$$

G is the four-dimensional curvature

The occurrence of the curvature in the wave equation has been previously noticed by *Schroedinger* (*loc cit*) and a comparison of (13) with his equation (74) reveals a striking resemblance

An interesting point in connection with our equation is that we have not yet introduced the mass   This mass term has caused a difficulty in the derivation of a general equation, for it has always been necessary to introduce the mass of the electron or proton arbitrarily

There seems no doubt here how it must be introduced   In the notation of *Klein* the mass of a particle takes a secondary position and is replaced by a quantity $1/\iota$,

$$I^2 = m^2c^2 + \frac{e^2}{\alpha^2\gamma_{55}} \qquad (20)$$

In the case when the geodesic is a null geodesic and $\gamma_{55} = -1$, I is zero Thus we have the further analogy between mass point and photon   I for the one is zero, the rest mass is zero for the other   But we cannot accept this as a general result   We must admit a non-vanishing value for I   We shall suppose that

$$\tfrac{1}{4}\gamma^{\mu\nu}P_{\mu\nu} = -\frac{4\pi^2 I^2}{h^2} = -\frac{4\pi^2}{h^2}\left(m^2c^2 + \frac{e^2}{\alpha^2\gamma_{55}}\right) \qquad (21)$$

Thus the quantity, which we might call the generalized curvature, is determined by the mass and charge of the particle situated at the point where the curvature is measured

This geometrical analogy gives a satisfactory way of introducing the mass into our equation

The negative sign appears to be rather arbitrarily chosen but the deciding factor is that we know from *Schroedinger's* equation that $4\pi^2m^2c^2/h^2$ occurs with a positive sign when taken over to the side of $\bigcirc\psi$ It will be seen at

* Rosenfeld, ' Bull. Acad. Roy Belgique,' vol. 13, p 304 (1927).

the same time that $e^2/\alpha^2\gamma_{88}$ cancels from the equation taking with it the gravitational constant Gravitation is represented in this part of the equation by the curvature G We have shown previously that the " spin " terms occur in the form of a term

$$- \frac{2\pi i e}{h} (\mathrm{H}_1 \mathrm{A}^{23} + \mathrm{H}_2 \mathrm{A}^{31} + \mathrm{H}_3 \mathrm{A}^{12} - i\mathrm{E}_1 \mathrm{A}^{14} - i\mathrm{E}_2 \mathrm{A}^{24} - i\mathrm{E}_3 \mathrm{A}^{34}),$$

and in Schroedinger's equation (74) of his paper (*loc cit*) they are represented by $- \frac{1}{2} f_{\mu\nu} s^{kl}$

Our additional term is of this type and we shall write it in the form

$$- \frac{2\pi i e}{h} \mathrm{F}_{\mu\nu} \mathrm{A}^{\mu\nu}$$

to bring it into the same notation

Thus the reduced equation becomes

$$\frac{1}{\psi} \,\square^2 \psi - \frac{4\pi i}{h} \,\frac{e}{c} \,\phi^m \frac{1}{\psi} \frac{\partial\psi}{\partial x^m} - \frac{2\pi i e}{h} \mathrm{F}_{\mu\nu} \mathrm{A}^{\mu\nu} + \frac{1}{4} \left(\mathrm{G} - \frac{4\pi \mathrm{K}}{c^2} \mathrm{H}\right)$$
$$+ \frac{4\pi^2}{h^2} \left(m^2 c^2 + \frac{e^2}{c^2} \,\phi_m \phi^m\right) = 0 \quad (22)$$

We can write this in a rather more general form by giving to the $\square \psi$ of (16) the value it has in (13) We then obtain

$$\frac{\gamma^{\mu\nu}}{\psi} \left(\frac{\partial^2\psi}{\partial x^\mu \partial x^\nu} - \Gamma^s_{\mu\nu} \frac{\partial\psi}{\partial x^s}\right) - \frac{2\pi i e}{h} \mathrm{F}_{\mu\nu} \mathrm{A}^{\mu\nu} + \frac{1}{4} \left(\mathrm{G} - \frac{4\pi \mathrm{K}}{c^2} \mathrm{H}\right)$$
$$+ \frac{4\pi^2}{h^2} \left(m^2 c^2 - \frac{e^2 c^2}{16\pi \mathrm{K}}\right) = 0 \quad (23)$$

This form should be compared with an equation of the electron without spin given by de Broglie [*]

The term in the curvature is of very great theoretical interest but much too small, compared with the term in m, to effect an appreciable result

The importance of the derivation of (13) or (23) is that it arises quite naturally from relativistic methods and is nothing else than the equation of curvature

The Relation to Matrix Theory

So far no matrices have been used in the theory The equation (23) contains a scalar quantity ψ introduced through $\Lambda_{\mu\nu}{}^s$ and is of the same form as the earlier Schroedinger equations

* ' J Phys Rad.,' vol 8, p. 65 (1927)

Matrices are introduced in attempting to replace the $\gamma_{\mu\nu}$ by more fundamental quantities

The way this is done is indicated in equation (1)

As we have previously pointed out there is a strong resemblance between these quantities and Einsteins' $h_{\mu s}$ of the theory of parallelism We therefore subject the α_μ to the following condition

$$\frac{\partial \alpha_\mu}{\partial \lambda^\lambda} - \Gamma_{\mu\lambda}{}^\beta \alpha_\beta - T_{\mu\lambda}{}^\beta \alpha_\beta = 0 \qquad (24)$$

This may be compared with equation (14) of an earlier paper *

Bargmann† has pointed out that this leads directly to Schroedinger's method, if it is postulated that $T_{\mu\lambda}{}^\beta \alpha_\beta$ is of such a form that

$$T_{\mu\lambda}{}^\beta \alpha_\beta = \Gamma_\lambda \alpha_\mu - \alpha_\mu \Gamma_\lambda \qquad (25)$$

Equation (24) is similar to the Riemannian relation

$$\gamma_{\mu\nu\lambda} = 0 \qquad (26)$$

Γ_λ is a matrix of importance in Schroedinger's theory

It is of interest to examine (26) in the light of (24)

If we write (24) in the form $\alpha_{\mu\lambda} = 0$, we can shorten the process, remembering that

$$\alpha_{\mu\lambda} = \alpha_{\mu\lambda} - T_{\mu\lambda}{}^\beta \alpha_\beta = 0 \qquad (27)$$

Now

$$2\gamma_{\mu\nu} = \alpha_\mu \alpha_\nu + \alpha_\nu \alpha_\mu,$$

omitting the unit matrix for convenience Thus

$$2\gamma_{\mu\nu\lambda} = \alpha_\mu \alpha_{\nu\lambda} + \alpha_{\mu\lambda} \alpha_\nu + \alpha_\nu \alpha_{\mu\lambda} + \alpha_\nu \alpha_\mu$$

On substituting from (27) the right-hand side becomes

$$T_{\nu\lambda}{}^\beta (\alpha_\mu \alpha_\beta + \alpha_\beta \alpha_\mu) + T_{\mu\lambda}{}^\beta (\alpha_\beta \alpha_\nu + \alpha_\nu \alpha_\beta) = 2\gamma_{\mu\beta} T_{\nu\lambda}{}^\beta + 2\gamma_{\nu\beta} T_{\mu\lambda}{}^\beta$$

This vanishes and (26) is preserved if

$$\gamma_{\mu\beta} T_{\nu\lambda}{}^\beta + \gamma_{\nu\beta} T_{\mu\lambda}{}^\beta = 0 \qquad (28)$$

With the form (11) for $T_{\mu\lambda}{}^\nu$, this relation holds or the important equation (26) is preserved

The remarks made on the relation between the notation of the earlier paper and Schroedinger's apply to the notation employed here Certain differences

* 'Proc Roy Soc,' A, vol 141, p 363 (1933)

† 'SitaBer. Preuss. Akad. Wiss,' No 24, p. 346 (1932)

between this method and that of Schroedinger's are brought to light in the discussion We can now see the connection between our theory and that of matrices Bargmann's suggestion (equation (25)) leads from one to the other

The relation may be satisfied by writing

$$\Gamma_\lambda = \tfrac{1}{4}\alpha^\sigma\alpha^\sigma \mathrm{T}_{\sigma\lambda\rho},$$ (29)

where

$$\mathrm{T}_{\sigma\lambda\rho} = \gamma_{\rho\beta}\mathrm{T}_{\sigma\lambda}{}^\beta$$ (30)

The result follows at once from the matrix relation

$$\alpha_\mu\alpha^\nu + \alpha^\nu\alpha_\mu = 2\delta_\nu{}^\nu\mathrm{I}$$ (31)

and from (28), which is equivalent to

$$\mathrm{T}_{\nu\lambda\mu} + \mathrm{T}_{\mu\lambda\nu} = 0$$ (32)

The further points of contact of the matrix method and that of this paper will be appreciated by a study of Schroedinger's work, any further development here could only be a repetition of it

The value of Γ_λ should be obtained in terms of the $\Lambda_{\sigma\rho}{}^\beta$, since these quantities are made the most fundamental of the theory The necessary calculation follows at once from (11) and (29) If we make use of the matrix $s^{\mu\nu}$ given by

$$\alpha^\mu\alpha^\nu + \alpha^\nu\alpha^\mu = 2s^{\mu\nu}$$ (33)

we find

$$\Gamma_\lambda = \tfrac{1}{2}\Lambda_{\lambda\sigma}{}^\beta\delta_\beta{}^\sigma - \tfrac{1}{4}\gamma_{\lambda\beta}\Lambda_{\sigma\rho}\Lambda_{\sigma\rho}s^{\rho\sigma},$$ (34)

$\delta_\beta{}^\sigma$ is written for $\delta_\beta{}^\sigma$I (31)

Schroedinger regards "spur Γ_λ" as $4\phi_\lambda$, where ϕ_λ is the electromagnetic potential

In our work we have taken

$$\text{"Spur } \Gamma_\lambda\text{"} \propto \Lambda_{\lambda\sigma}{}^\sigma$$

$$\propto \frac{1}{\psi}\frac{\partial\psi}{\partial x^\lambda}$$ (35)

This quantity thus occupies a position similar to the electromagnetic potential in the four-dimensional theory We have previously suggested that the corresponding quantity in the five-dimensional theory is Wilson's vector

$$\pi_\lambda = p_\lambda + \frac{e}{c}\phi_\lambda$$

If this can be extended to the present case we can write

$$\frac{1}{\psi} \frac{\partial \psi}{\partial x^\lambda} \propto \pi_\lambda \qquad (36)$$

The Invariance of the Quantum Equations

From the result of the formulation and study of the problem given here, it would seem that the second order equation of the quantum theory in the form (13) is invariant in the system proposed here and the suggestion is that this is the type of invariance which is applicable to the quantum equations.

With regard to the first order equations, it is as if we would pass backward from the wave equation for electromagnetic waves to Maxwell's equations Their invariant form can be determined by the introduction of matrices and adapting them to fit the notation introduced here

If we are correct in our suggestion that the second order equation is nothing but the curvature equation then the test will be that having satisfied the notation the first order equations lead to (13)

It would appear that Schroedinger's system satisfies both these requirements, but we suggest that it should be five-dimensional

Summary

The paper gives a relativistic treatment of the second order equation of the quantum theory This equation turns out to be the curvature equation in the system proposed, corresponding to the equation of the theory of relativity, $G_{\mu\nu} = 4\lambda$ The basis of the work is a modification of the Riemannian' covariant operator and it is shown that the geometric background of the theory permits of some latitude For this reason an appeal is made to geometrical methods to obtain an indication of the form of the equations but no special theory of parallelism is introduced directly

The relation to the matrix theory, especially in the form recently developed by Schroedinger is discussed and the two theories are found to be in harmony

The equation proposed is invariant and throws light on the kind of invariance appropriate to the quantum theory It is, moreover, an advance on previous equations in that it contains terms appropriate to the gravitational and electromagnetic fields, which come in only with difficulty in other methods

─────────

possible to decide confidently between the two possibilities on experimental grounds

The arguments used in this paper are based entirely on the need of securing a steady state of electrolysis when a steady current flows through the solution There must be no time variable concentrations in any part of the solution or on the electrodes The effective separations found are achieved in such steady states It is thought that perhaps the full implications of the steady state requirements have not always been realized by workers in this field, and there fore that the attempt, here presented at a full and careful exposition of them may not be without some general interest

In NaOH (or other alkaline) solutions the current is usually regarded as being carried by the movement of the ions Na^+ and $(OH)^-$ both more or less hydrated We can think of $(OH)^-$ as moving to the anode and Na^+, or owing to the hydration $(NaOH_2)^+$ if we prefer it, as moving to the cathode where it surrenders H^+ and becomes again $(Na^+ \ OH^-)$ This process is formally equivalent to the surrender of an H^+ by an OH_2 water molecule, an $(OH)^-$ being left behind in the solution free to travel to the anode That this process of surrender may require the presence of Na^+ before it can occur does not affect its essential form At the anode $(OH)^-$ ions become discharged on arrival and oxygen gas O_2 is finally evolved by some such chain of surface reactions as $2(OH)^- + OH_2 + O$, $2O \rightarrow O_2$ (gas) But as these processes do not evolve hydrogen they are of little interest to us here and we shall not have much occasion to refer to them again In the next section we shall have occasion to examine more closely the steady state requirements as to the movement of ions, when it will appear, of course, that in the steady electrolysis of water the Na^+ ions on the average do not move and the whole current is carried by the $(OH)^-$ ions

We shall in general in this paper discuss directly only alkaline solutions, since it is for such solutions that most is known But all our arguments apply with obvious slight changes to electrolysis in acids in which the positive $(OH_2)^+$ ions alone move and convey the current

§ 2 *General Description of the various Processes assumed to occur* —The arguments which we shall apply will often be general enough not to need any *detailed* specification of the mechanism by which a particular process is occur ing It is none the less necessary for clarity to specify the broad outlines of the processes occuring at and near the cathode, to which almost any special mechanism must conform It is therefore convenient to start by distinguishing three phases (1) the interior of the solution generally , (2) its boundary layer

in contact with the cathode , and (3) the surface of the cathode itself When, if ever, a valid distinction is to be drawn between (1) and (2) is a matter for investigation (§ 5) When a steady current flows we must consider the exchanges of the two hydrogens between these three phases and the evolved gas No accumulations can form anywhere except in the evolved gas which is ultimately formed at the expense only of the general body of hydrogen in the water of the interior of the solution

From the boundary layer of the solution hydrogen is fed on to the surface of the cathode This is an essential part of the current carrying process It will be necessary to consider whether or not the only exchanges of hydrogen between the cathode and the boundary layer are the current carrying depositions of hydrogen atoms, or whether important balanced exchanges take place in addition Finally since the hydrogen is certainly supplied to the cathode surface phase as atoms by the above process and evolved into the gas phase as molecules, it is necessary to consider a final process in the evolution of hydrogen gas in which atoms of hydrogen combine to form molecules on the cathode surface

§ 3 *Passage of Hydrogen from the Boundary Layer to the Cathode* —As we have said in the introductory section the essential action on the cathode which enables the current to flow is the break up of a water molecule OH_3 which surrenders a proton H^+ to the cathode and leaves an extra $(OH)^-$ ion behind in the water free to move to the anode It is a matter of comparative indifference whether or not the action involves intimately the presence of Na^+ so as to be more accurately described as

$$(NaOH_3)^+ \rightarrow (Na^+ (OH)^-) + H^1 \text{ (on cathode)}$$

This process has been visualized by Gurney rather as a process of discharge of the ion $(NaOH_3)^+$ by an electron jump from the cathode followed by a process of ejection of the unstable extra H atom from $NaOH_3$ which then becomes $Na^+ (OH)^-$ while the H atom combines with the metal cathode (The word " combine " is here used loosely) Whatever the correct version may be, it is agreed universally that the process is atomic and that H not H_2 is supplied to the cathode

If $n_1{}^s$, $n_2{}^s$ are the concentrations of H^1 and H^2 in the cathode boundary layer, then as the process is atomic and a first order reaction we may assume that H^1 atoms are deposited at a rate $\kappa_1 n_1{}^s$ and H^2 atoms at a rate $\kappa_2 n_2{}^s$, where κ_1, κ_2 are independent of $n_1{}^s$, $n_2{}^s$ It is *not* necessarily true that κ_1 equals κ_2 The κ's might depend on the amount of hydrogen already present on the

surface, on the temperature, and on the voltage drop from the cathode boundary layer to the cathode (the over-potential) So far as we know at present the concentrations of the hydrogens which are in a state to be transferred to the electrode, because, for example, they are attached to positive ions will be the same as their concentrations on the complete boundary layer

If the κ's depend on the hydrogen already present on the cathode, let n_1' and n_2' be the concentrations of the two sorts of hydrogen in the cathode surface Then the only dependence of the κ's on n_1' and n_2' which is at all likely is that the κ's are of the form

$$\kappa_1\{1 - \gamma(n_1' + n_2')\}, \quad \kappa_2\{1 - \gamma(n_1' + n_2')\}$$

so that their ratio would be unaffected This dependence would occur if the hydrogen to be deposited required a vacant metal atom to combine with It would be indifferent to prior occupation by H¹ or by H²

If the current carrying process is the only means by which hydrogen is conveyed from the solution or rather its boundary layer to the cathode then the whole exchange will be at the rates $\kappa_1 n_1^b$, $\kappa_2 n_2^b$ and all in the one direction , $\kappa_1 n_1^b + \kappa_2 n_2^b$ will be fixed by the current density It is, however, uncertain whether this does constitute the major part of the hydrogen exchange There is some evidence that even when no current is flowing there may be some considerable balanced exchange of hydrogen between the electrode and the water, particularly the ions of the boundary layer We shall then have an equilibrium state controlled by the equations,

$$\kappa_1 n_1^b = \mu_1 n_1', \quad \kappa_2 n_2^b = \mu_2 n_2',$$

where $\mu_1 n_1'$, $\mu_2 n_2'$ are the rates of transfer from the electrode back to the solution, and μ_1, μ_2 are independent of the n's In this case all the rates may be large compared with the rates demanded by any ordinary current density and then these equilibrium conditions will not be seriously disturbed by the passage of the current

The two conditions detailed above are, of course, the two possible limiting cases and every intermediate case is possible We shall, however, for simplicity only discuss these two limits which are sufficient for illustration

§ 4 *The Evolution of Hydrogen Gas at the Cathode* —The process of formation of H_2 gas appears to be one which takes place actually on the surface or in the immediate surface layer of the metal—in a metallic phase, that is, which is rich in adsorbed or absorbed H atoms This process must clearly be assumed to be a second order reaction The relevant concentrations of the H¹ and H²

atoms will be $n_1{}^s$ and $n_2{}^s$ as already defined [Conceivably the relevant concentrations might differ from these values, but if so they could only differ by factors which can be ignored because they could be absorbed in the λ's shortly to be defined] Molecules H^1H^1 H^1H^2 and H^2H^2 may therefore be assumed to be formed respectively at rates

$$\lambda_{11} (n_1{}^s)^2 \qquad \lambda_{12} n_1{}^s n_2{}^s \qquad \lambda_{22} (n_2{}^s)^2$$

where the λ's are independent of the n's

At this stage again there appear a priori to be two possible limiting cases though now they do not lead to distinct forms There may be an equilibrium concentration of hydrogen molecules in and on the metal surface which is practically zero so that effectively all the molecules formed immediately escape as gas In this case the rate of removal of H^1 atoms from the water will be

$$2\lambda_{11} (n_1{}')^2 + \lambda_{12} n_1{}' n_2{}', \qquad (2)$$

and the rate of removal of H^2 atoms

$$2\lambda_{22} (n_2{}')^2 + \lambda_{12} n_1{}' n_2{}' \qquad (3)$$

The λ's need not be equal

On the other hand, there may be a significant equilibrium concentration of molecules in the metal maintained by rates of formation and destruction sufficiently rapid for the evolution of gas required by the current transport not to disturb it In that case we must obviously expect that the rates of evolution of H_2 molecules of each type will be proportional to their equilibrium concentrations in the metal surface $n_{11}{}''$, $n_{12}{}''$ and $n_{22}{}''$ respectively

The rate of removal of H^1 atoms from the water will then be

$$2\nu_{11} n_{11}{}'' + \nu_{12} n_{12}{}',$$

and the rate of removal of H^2 atoms

$$2\nu_{22} n_{22}{}'' + \nu_{12} n_{12}{}''$$

Since, however, we must expect equilibrium relationships between the various n''s similar to those of a perfect gas, and of the forms

$$n_{11}{}'' = f_{11} (n_1{}')^2, \quad n_{12}{}' = f_{12} n_1{}' n_2{}', \quad n_{22}{}'' = f_{22} (n_2{}')^2,$$

where the f's are independent of the n's, these formulae of this limiting case reduce to (2) and (3) Presumably, therefore, it is not necessary to distinguish here between these limits, or any of the possible intermediate cases

§ 5 *Transport of Hydrogen to and fro between the Cathode Boundary Layer and the Interior of the Solution* — In any steady state the Na⁺ ions may not accumulate and therefore cannot be moving, so that the whole current is carried by the movement of the (OH) ions to the anode This movement "conveys" hydrogen to the cathode by allowing an (OH) ion to be replaced by an OH_2 molecule Besides, this transport the process of diffusion (molecular and turbulent) conveys hydrogen (in the water molecules and ions) to and fro between the boundary and the interior

It all diffusion could be neglected, since there are no accumulations anywhere in the boundary region the two hydrogens would be evolved (no matter what the mechanism) at rates in the ratio of the currents carried by the two types of hydrogens—that is, in the ratio

$$E_1 \quad E_2 = p D_1 \quad D_2, \qquad (4)$$

where p is the ratio of the mobilities of the two hydrogens The yield of each must equal the supply The mobility of H¹ means here the rate of effective movement due to the replacement of the grouping $(OH H^1)$ $(OH)^-$ by (OH) (OHH^1), where the unindexed H may be either H¹ or H², with a similar meaning for the mobility of H² The factor p is probably* about 1 5, but we shall not stay to discuss it more closely, since it can be shown that diffusion will always mask the current transport and keep the hydrogen concentrations in the boundary layer effectively in the ratio D_1 D_2, which is that of the water as a whole We now proceed to consider this effect of diffusion

Let n_1 and n_2 be the total concentration of the two hydrogens at any point in the water—hydrogen nuclei to be precise Then since the number of water ions can be locally variable it is not necessary that $n_1 + n_2 = \text{const}$ They are independently variable Under the influence of a given field let the number of H¹ and H² nuclei which cross unit area in unit time be $\alpha_1 n_1$ and $\alpha_2 n_2$ respectively The α's are proportional to the mean velocities of drift of the two nuclei and independent of the n's, but they are not *mobilities* since n_1 and n_2 are total molecular not ionic concentrations When any concentration gradient is set up, along the x axis for example, the numbers of H¹ and H² nuclei which diffuse back per cm² per second owing to the self diffusion of the water molecules, are respectively

$$-d_1 \frac{\partial n_1}{\partial x}, \quad -d_2 \frac{\partial n_2}{\partial x}$$

---

* See Lewis and Doody, 'J Amer Chem Soc,' vol 55 p 3504 (1933) for measurements on the replacement of $(OH_2)^+ OH_2$ by $(OH_2)(OH_2)^+$ For a theory which allows for these mobilities to be different for H¹ and H² see Bernal and Fowler ('J Chem Phys,' vol 1, p 515 (1933))

The d's are probably nearly equal, and in order of magnitude equal to the coefficient of self-diffusion of water   We may suppose that the whole flow takes place along the x axis   Then since no accumulations are occurring

$$\alpha_1 n_1 - d_1 \frac{\partial n_1}{\partial x} = \mathrm{E}_1, \quad \alpha_2 n_2 - d \frac{\partial n_2}{\partial x} = \mathrm{E}_2 \tag{5}$$

The equations hold for values of x from the cathode ($x = 0$) so far into the solution that the water between such value of x and the cathode is an appreciable fraction of the whole solution   Since the field gradients are not constant owing to space charge the α's strictly depend on x, but this can be ignored here   We return to it in § 8

Equations (5) can be solved at once and give

$$n_1 = \frac{\mathrm{E}_1}{\alpha_1} + \mathrm{C}_1 e^{\alpha_1 x/d_1}, \quad n_2 = \frac{\mathrm{E}_2}{\alpha_2} + \mathrm{C}_2 e^{\alpha_2 x/d_2} \tag{6}$$

The constants C_1 and C_2 must be adjusted to give the correct boundary values to n_1 and n_2 at $x = 0$ required to transfer the observed quantities E_1 and E_2 of evolved gas   These boundary values do depend, therefore, on the cathode mechanism   It is clear at once that if α_1/d_1 is so large that while formulæ (6) still apply $\alpha_1 x/d_1$ becomes effectively $-\infty$, then since at the same time $n_1/n_2 \to \mathrm{D}_1/\mathrm{D}_2$, we have $\mathrm{E}_1/\mathrm{E}_2 = (\alpha_1/\alpha_2)\,\mathrm{D}_1/\mathrm{D}_2 = p\mathrm{D}_1/\mathrm{D}_2$ as already stated   If, however, α_1/d_1 is so small that $\alpha_1 x/d_1 \approx 0$ throughout the region of validity of (6) then there is perfect mixing by diffusion in spite of the current and $n_1/n_2 = n_1{}^b/n_2{}^b$ everywhere, so that

$$n_1{}^b/n_2{}^b = \mathrm{D}_1/\mathrm{D}_2. \tag{7}$$

Everything then depends on the numerical order of $\alpha l/d$ where l is the scale of the cell, say, the distance between the electrodes   The numerical value of α can, of course, be derived from the mobility, but it is more simply derived by observing that $\alpha_1 n_1$ is approximately equal to E_1 A current of 1 ampere/cm^2 requires a net flow of 6×10^{18} protons per cm^2 per second   Since n_1 is of the order 7×10^{22} protons per cm^2 a $\frac{1}{2}$ 10^{-4}, and n_2 is of the same order   The numerical value of d_1 or d_2 is not yet known by direct observation of the molecular diffusion of heavy water into ordinary water, but its order can probably be safely derived from the known values for the diffusion coefficient for the diffusion of other small molecules into water   The values of all such coefficients of diffusion are of the order 10^{-5} cm.^{2}/sec   Thus

$$\alpha l/d \approx 10^{-2}.$$

For smaller current densities the coefficient is proportionately smaller Thus, except for obviously large scale apparatus molecular diffusion is capable of keeping the boundary concentrations normal for current densities up to 10 amp /cm.², which are greater than any hitherto used

Theoretically relation (7) might fail for very great current densities, but these are so great that they would induce other and more efficient means of mixing by turbulence due to the formation of bubbles on the cathode It is therefore doubtful if (7) ever fails

§ 6 *The Equations of Steady (Alkaline) Electrolysis* —Having thus cleared the ground we can write down the general equations of electrolysis to which the process will conform no matter what its detailed mechanism When the process is steady any differential coefficients such as dn/dt must vanish The concentrations of the two hydrogens in the boundary layer are D_1 D_2 for the reasons given in § 5 These equations are

$$\frac{dn_1{}^e}{dt} = \kappa_1 D_1 - \mu_1 n_1{}^e - E_1 = 0 \tag{8}$$

$$\frac{dn_2{}^e}{dt} = \kappa_2 D_2 - \mu_2 n_2{}^e - E_2 = 0, \tag{9}$$

$$E_1 = 2\lambda_{11} (n_1{}^e)^2 + \lambda_{12} n_1{}^e n_2{}^e, \tag{10}$$

$$E_2 = 2\lambda_{22} (n_2{}^e)^2 + \lambda_{12} n_1{}^e n_2{}^e. \tag{11}$$

There are some important special cases

Case (1) --*The to and fro exchange of hydrogen between the solution and the electrode small compared with* E_1, E_2 Under these conditions $\mu_1 n_1{}^e$ and $\mu_2 n_2{}^e$ can be neglected in (8) and (9), and we find simply *no matter what values the* λ's *have*

$$\frac{E_1}{E_2} = \frac{\kappa_1}{\kappa_2} \frac{D_1}{D_2} \tag{12}$$

This specifies an evolution of gas of the observed form if under the best working conditions $\kappa_1/\kappa_2 \lessgtr 6$ This case provides, of course, the explanation proposed by Polanyi for the observed separations The κ s could have such a ratio if the controlling mechanism of the deposition of hydrogen on the cathode is the passage of the hydrogen nuclei through a small potential barrier by the tunnel effect when the rate of penetration of H¹ for a given concentration can easily exceed that of H² by a factor of the order of 10 Gurney's theory of the hydrogen over-potential would then be inapplicable to the phenomenon *

[* *Note added February 20th* —The κ's could still have such a ratio on Gurney's theory *See* Bell and Wolfenden, 'Nature,' vol 133, p 25 (1934)]

It is, however, not certain that the conditions of case (i) are fulfilled It is known from the observations of Polanyi* himself, stimulated by observations of Oliphant,† that a very considerable exchange of hydrogen can take place between water and hydrogen gas in contact with a suitable catalysing surface in Polanyi's case platinum black This exchange, as is pointed out, appears to be precisely that with which we are concerned here, but its rate can hardly be estimated from what is yet known The action might be of one or both of two kinds (a) a simultaneous interchange of two hydrogen nuclei, one in a water molecule and one adsorbed on the surface by a process of the type OHH' + H"Me ⇌ OHH' + H'Me, (b) a continual formation and discharge of water ions in the neighbourhood of the catalytic surface leading to balanced reactions of the types (i) $(OH_2)^i$ + Me⁻ ⇌ OH_2 + HMe and (ii) $(OH)^-$ + HMe⁺ ⇌ OH_2 + Me It is, therefore, important to discuss equations (8)–(11) in other conditions than those of case (i)

Case (ii) —*The to and fro exchange of hydrogen between the solution and the electrode large compared with* E_1 *and* E_2. Under these conditions E_1 and E_2 can be neglected in (8) and (9) We, therefore, obtain from them

$$n_1^s = f_1 D_1, \quad n_2^s = f_2 D_2$$

The coefficients f_1 and f_2 may well be functions of the over-potential, that is, the voltage drop at the cathode surface required to carry a given current density It may, therefore, be well to write them sometimes as f_1 (V), f_2 (V) or as f_1 (I), f_2 (I) to recall this probable dependence Equations (10) and (11) then give

$$\frac{E_1}{E_2} = \frac{2\lambda_{11}f_1^2D_1 + \lambda_{12}f_1f_2D_1D_2}{2\lambda_{22}f_2^2D_2 + \lambda_{12}f_1f_2D_1D_2} \tag{13}$$

This equation cannot be of the observed form unless it reduces to $E_1/E_2 = \alpha D_1/D_2$ It *can*, however, so reduce if

$$\frac{2\lambda_{11}}{\lambda_{12}} - \frac{\lambda_{12}}{2\lambda_{22}} = q, \tag{14}$$

when

$$\frac{E_1}{E_2} = q \frac{f_1}{f_2} \frac{D_1}{D_2} \tag{15}$$

This equation will, of course, represent the results of the best experiments with nickel electrodes and currents of the order 1 amp /cm.² if then $qf_1/f_2 = 6$

---

* Horiuti and Polanyi, ' Nature,' vol 132, p 819 (1933)

† ' Nature,' vol 132, p 675 (1933)

Both q and the f's should depend on the temperature, but q should not depend on the voltage and therefore not on the current density

At first sight it is hardly to be expected that there is any reason why (14) should be satisfied—even approximately It requires the relationship $\lambda_{11}\lambda_{22}/\lambda_{12}{}^2 = \frac{1}{4}$ to hold between the λ's, but there is after all some *a priori* reason to expect such a connection

Let us, for example, take that view of the mechanism of gas evolution which regards the λ's as collision recombination rates for the formation of H_2 molecules on the metal surface Let us then consider the H atoms on the surface as an ideal quasi-gaseous mixture of atoms H^1 and H^2 of concentrations $n_1{}^{\bullet}$ and $n_2{}^{\bullet}$ The total numbers of effective collisions have been defined as $\lambda_{11}(n_1{}')^2$, $\lambda_{12}n_1{}'n_2{}'$ and $\lambda_{22}(n_2{}')^2$ If these were the total number of collisions of freely moving gas atoms then

$$\lambda_{11} \propto \tfrac{1}{2}\bar{C}_{11}, \quad \lambda_{12} \propto \bar{C}_{12} \quad \lambda_{22} \propto \tfrac{1}{2}\bar{C}_{22},$$

where the C's are the mean relative velocities of the two sorts of atom. If there is an excitation energy required for the success of the recombination then the number of favourable collisions might be proportional respectively to

$$\tfrac{1}{2}\bar{C}_{11}\,e^{-\chi_{11}/kT}, \quad \bar{C}_{12}\,e^{-\chi_{12}/kT}, \quad \tfrac{1}{2}\bar{C}_{22}\,e^{-\chi_{22}/kT}$$

But

$$\bar{C}_{11} \quad \bar{C}_{12} \quad \bar{C}_{22} = \sqrt{\left\{\frac{1}{m_1} + \frac{1}{m_1}\right\}} \quad \sqrt{\left\{\frac{1}{m_1} + \frac{1}{m_2}\right\}} \quad \sqrt{\left\{\frac{1}{m_2} + \frac{1}{m_2}\right\}}$$

Hence

$$\frac{\lambda_{11}\lambda_{22}}{\lambda_{12}{}^2} = \frac{1}{4}\frac{2(m_1 m_2)^{\frac{1}{2}}}{m_1 + m_2}\,e^{-(\chi_{11} + \chi_{22} - \chi_{12})/kT} \tag{16}$$

Now it can well happen that $\chi_{11} + \chi_{22} - 2\chi_{12} \cong 0$ For though the activation energy required by H^2H^2 may well be substantially greater than that required by H^1H^1, in that case the energy required for H^1H^2 is likely to be very nearly the mean value of the other two The mass factor is $2\sqrt{2/3} = 0.94$ even for masses so different as those of H^1 and H^2 Thus $\lambda_{11}\lambda_{22}/\lambda_{12}{}^2$ does not on this view seem likely to deviate much from $\frac{1}{4}$ and may well be almost exactly equal to it, even if $2\lambda_{11}/\lambda_{12} = q$ is distinctly different from unity A similar close equality between $\lambda_{11}\lambda_{22}/\lambda_{12}{}^2$ and $\frac{1}{4}$ can be shown to be expected if we take the other view of the mechanism in which the λ's represent velocities of escape of already formed molecules, and account is taken of the equilibrium constants of the dissociating quasi-gas on the metal surface

In this case we see that it is easily possible that the whole differential factor in the rates of evolution of H^1 and H^2 may come from preferential molecule

formation on the electrode surface—the factor f_1/f_2 being then close to unity, but with separation still possible owing to the factor q

It is not maintained here that case (ii) represents a true view of the electrode mechanism—only that it is at present a possible one which is not ruled out by any experiments yet reported It is important to note that if it were a true view then Gurney's explanation of the hydrogen over-potential might still stand

There is, however, one piece of evidence in this field which may possibly if correctly interpreted, lead to a discrimination against Gurney's version, or rather against any theory which allows $\kappa_1 \gtreqqless \kappa_2$ and casts the onus for separation on the surface recombination—that is, the apparently reduced efficiency of the separation at lower current densities or at lower over-potentials It seems possible that this means that at the higher current densities we have case (i) fully developed, but at lower current densities the to and fro exchanges are no longer negligible by comparison so that we tend to move towards the conditions of case (ii) It does not seem possible to refer this observed variation directly to variations of κ_1/κ_2 with over potential, for in that case the higher the over-potential the more nearer equal one must expect the κ's to become and the efficiency should be least at high current densities where it appears to be greatest Since this explanation may be important we consider a third special case which might apply to it

Case (iii)—Neither the μn's nor the E's negligible in (8) and (9) but $\lambda_{11} \lambda_{22}/\lambda_{12}^2 = \frac{1}{4}$ These are the simplest type of conditions intermediate between those of cases (i) and (ii) We find

$$\frac{E_1}{E_2} = \frac{2\lambda_{11}}{\lambda_{12}} \frac{\mu_2}{\mu_1} \frac{\kappa_1 D_1 - E_1}{\kappa_2 D_2 - E_2} \tag{17}$$

It may with the help of this equation be possible to trace a transition between the two limits in which

$$\frac{E_1}{E_2} = \frac{2\lambda_{11}}{\lambda_{12}} \frac{f_1}{f_2} \frac{D_1}{D_2} \qquad \frac{\kappa_1 D_1}{\kappa_2 D_2}$$

for low and high current densities respectively It must be remembered that the κ's at least are functions of the over-voltage and therefore of the current or $E_1 + E_2$.

§ 7 *Conclusions*—We may summarize this discussion as follows —

(1) If the transport of hydrogen by the current could overwhelm the transport by the natural processes of diffusion the rates of evolution of H^1 and H^2 would be in the ratio of the mobilities of the two hydrogen ions no matter

what the electrode mechanism. This condition, however, is never fulfilled in practice and diffusion is always ample to keep the two hydrogens in normal concentration ratios on the cathode boundary

(2) If the reversible exchange of hydrogen atoms between the cathode surface and the boundary layer of the liquid can be neglected compared with the hydrogen deposited by the current, i e , at sufficiently high current densities the ratio of the rates of evolution will be of the form $\kappa_1 D_1/\kappa_2 D_2$. This form is in agreement with observation

(3) If the reversible exchange of hydrogen atoms between the cathode surface and the boundary layer of the liquid is fast compared with the hydrogen deposited by the current—i e , at sufficiently low current densities—then equilibrium concentrations of the hydrogens on the cathode will be in the ratio $f_1 D_1/f_2 D_2$, where f_1/f_2 will in general depend on the over potential. The ratio of the rates of evolution of the hydrogen atoms will be $q f_1 D_1/f_2 D_2$ if a certain natural condition is satisfied so that the separation may be effected by $q (f_1/f_2 \gtrless 1)$ which is a factor arising from the relative efficiency of H¹H¹ and H²H² collisions in forming molecules, or it may be effected by $f_1/f_2 (q \gtrless 1)$ and so be a result of different over-voltages for the two hydrogens

(4) It is not possible yet to conclude that the over-potential factors κ_1/κ_2 or f_1/f_2 are necessarily the separating agency. Thus we cannot immediately rule out Gurney's theory of the hydrogen electrode. There is, however, this factor in favour of throwing the onus for the best separation factor (about 6) on to κ_1/κ_2—that the separation appears to fall off at lower current densities. If we refer the high current high efficiency to κ_1/κ_2 we can refer the lowering at lower currents to a change over towards $q f_1/f_2$

§ 8 *The Equations of Steady Electrolysis in an Alkaline Solution* —In this section we are no longer concerned with separation of the two hydrogens, but strictly speaking consider only the way in which the current is conveyed through an alkaline electrolyte when the electrolysis of pure water (either light or heavy) is proceeding steadily. It appears that, familiar as this problem is, something more can be said about the theory of it, by bringing in the ideas of space charge used so successfully in the theory of electron currents in high vacua

Suppose that the current is flowing everywhere parallel to the x-axis between plane parallel electrodes. In the solution there are Na^+ ions (or other positives) which on the whole cannot move and therefore have the sole function of creating a space charge $e n_+$, where n_+ is their concentration per unit volume

Let V be the electrostatic potential in the solution and let the cathode surface

be $x = 0$ and $V(0) = 0$ Then since the state of the positive ions is an equilibrium state in a field of potential $V(x)$.

$$n_+ = n_1{}^o e^{-\epsilon V/kT} \tag{18}$$

The $(OH)^-$ ions have a concentration n^-, produce a space charge $-\epsilon n^-$ and carry the current by their movement   If α is their effective mobility under unit field strength then $\alpha\epsilon\partial V/\partial x$ is their average velocity and the current density at any point in the fluid is $-\alpha\epsilon^2 n^- \partial V/\partial x$ in the direction of V increasing We may call this current I (since the conventional current flows in the direction of V decreasing) so that

$$I = \alpha\epsilon^2 n^- \frac{\partial V}{\partial x} \tag{19}$$

The potential V satisfies Poisson's equation,

$$\frac{d^2V}{dx^2} = -\frac{4\pi\epsilon}{K}(n^+ + n^-), \tag{20}$$

where K is the dielectric constant of water assumed independent of x This is the only place in these equations where K occurs   Then combining (18), (19) and (20) we obtain an equation which can be integrated once giving

$$\left(\frac{dV}{dx}\right)^2 - \left(\frac{dV}{dx}\right)_0^2 = -\frac{8\pi kT}{K} n_+{}^o \{1 - e^{-\epsilon V/kT}\} + \frac{8\pi}{K}\frac{I}{\alpha\epsilon} x \tag{21}$$

We have here assumed that V and $\partial V/\partial x$ are continuous functions of x and that in particular $V(0) = 0$, the potential of the cathode The value of $(\partial V/\partial x)_0$, on this version of the theory, must represent the over-potential, which here appears not as a discontinuity but as a steep initial potential gradient   On any theory of the cathode mechanism there will be a relationship of the form

$$\left(\frac{dV}{dx}\right)_0 = f(I), \tag{22}$$

or possibly more significantly of the form

$$\left(\frac{dV}{dx}\right)_0 = f(n_0{}^-, I) \tag{23}$$

This is one of the boundary conditions of the problem

A second integration in finite terms is not possible   But if we put

$$\epsilon V/kT = \phi$$

equation (21) becomes

$$\left(\frac{d\phi}{dx}\right)^2 - \left(\frac{d\phi}{dx}\right)_0^2 = -\frac{8\pi\epsilon^2 n_+^0}{K k T}\{1 - e^{-\phi}\} + \frac{8\pi I\epsilon}{\alpha K k^2 T^2}\,x \qquad (24)$$

If now we put

$$x = \mu\xi \qquad \mu = \left(\frac{K k T}{8\pi\epsilon^2 n_+^0}\right)^{\frac{1}{2}},$$

then

$$\left(\frac{d\phi}{d\xi}\right)^2 - \left(\frac{d\phi}{d\xi}\right)_0^2 = -(1 - e^{-\phi}) + \lambda\xi, \qquad (25)$$

where

$$\lambda \qquad \frac{K^{\frac{1}{2}} I}{(8\pi k T)^{\frac{1}{2}}\,\alpha\epsilon^2\,(n_0{}^+)^{3/2}} \qquad (26)$$

Equation (25) depends on the two parameters $(\partial\phi/\partial\xi)_0$ and λ and it is a not impossibly laborious task to compute its solutions numerically   We could thus determine

$$\phi = \phi\left(\xi,\ \lambda,\ \left(\frac{\partial\phi}{\partial\xi}\right)_0\right), \qquad (27)$$

and the final boundary condition which has to be applied is to make V take the correct value on the other electrode   Thus (27) really means

$$V\,(l) = V_0 = \Phi\,(l,\ I,\ n_0{}^+,\ \partial V/\partial x_0) \qquad (28)$$

Again from equation (27) since ϕ is known $n_0{}^+$ can be determined in terms of the total concentration of electrolyte in the whole cell, which is fixed   Thus (23) and (28) together give the current voltage relationship of the cell and (27) the distribution of potential, from which the other distributions follow   We have apparently not satisfied a second boundary condition analogous to (23) at the anode, namely,

$$\left(\frac{dV}{dx}\right)_l = g\,(n_0{}^-,\ I),$$

but the state of the anode is not fixed since the number of available $(OH)^-$ ions is not fixed, and therefore the anode can and must adjust itself until it can accept a current of the proper density from the boundary layer of the solution in its determined state   It is only by a crude approximation that these molar equations can be used right down to the boundary layer itself   But there is this essential difference between the requirements of the two electrodes when one of the ions is present in fixed amount and the other is indefinite

Further study of the equations of this section will be undertaken

Summary

This paper discusses in a general way the theory of the separation of hydrogen and diplogen by the electrolysis of water   It is an amplified account of remarks made at the recent discussion on heavy hydrogen and included in the published report   In discussing the theory of this separation, it is necessary to remember that the process is a steady one and that no accumulations of any substance are going on anywhere except in the evolved gas where hydrogen and diplogen accumulate at the expense of the general water supply   The requirements of a steady state are systematically applied to the various possible mechanisms of the hydrogen electrode which have been suggested   It is shown that the self diffusion of water is important and suffices to keep the H/D ratio near the cathode normal in spite of the different mobilities of the hydrogen and diplogen ions   It is next shown that if there were no to and fro exchange of hydrogen between the solution and the cathode, then the separation would depend on differential rates of transition for protons and diplons according to the suggestions put forward by Polanyi, but that this exchange certainly exists so that Polanyi's explanation, though still possible, is no longer unique   The conditions for this more general state of affairs are then discussed, and it is shown that so far as existing evidence goes, the separation may be due either to different over-potentials as proposed by Polanyi, or to different combination rates for molecule formation on the surface, or partly to one and partly to the other   The paper concludes with a formulation of the general space charge equations which must govern a steady electrolytic current in the alkaline electrolysis of water

Experiments on Heavy Hydrogen *—Part I

By Adalbert Farkas and Ladislas Farkas Colloid Science Laboratory, Cambridge

Method of Analysis

With the exception of those investigations in which spectroscopic† or mass spectrographic‡ methods were applicable, earlier workers on the heavy hydrogen isotope (deuterium or diplogen denoted by H^2 or by D) have determined the ratio H to D from measurements of the specific gravity§ of the water obtained from the heavy hydrogen One per cent of diplogen causes an increase of about one part in 1000 in the specific gravity The density measurement may be made with great accuracy, but at least 3–4 mg of water are required for every determination ‖

A convenient and reliable determination can be made with a very much smaller quantity of material, both accurately and rapidly, utilizing the thermal conductivity of the gas to indicate its composition in the following manner ¶

In fig 1 the specific heats of normal H_2, D_2, and by D) HD are plotted against the absolute temperature The rotational specific heats were calculated according to the general formula**

$$C_{rot} = -R\,\frac{d}{dT}\frac{d\,lnQ}{d\,1/T}, \qquad Q = \Sigma p_j\, e^{-\frac{j(j+1)h^2}{8\pi^2JkT}},$$

---

* ' Nature,' vol 132, p 894 (1933)

† Urey, Brickwedde, and Murphy, 'Phys Rev ,' vol 40 p 1 (1932)

‡ Bleakney, ' Phys Rev ,' vol. 41, p 32 (1932), Bleakney and Gould, ibid., vol 44, p 365 (1933)

§ Lewis and Macdonald, ' J Chem Phys ,' vol. 1, p. 341 (1933), Washburn, Smith, and Frandsen, ' Bur Stand J Res.,' vol 11, p. 453 (1933) More recently a refractive index method was worked out by Lewis and D B Luten, junr (' J Amer Chem Soc ,' vol 55, p 5061 (1933)) and by Crist, Murphy, and Urev (' J Amer Chem Soc ,' vol 55, p. 5060 (1933))

‖ Gilfillan and Polanyi, ' Z phys Chem.,' A, vol 166, p 255 (1933)

¶ Cf A Farkas, ' Z phys. Chem ,' B, vol 22, p 344 (1933) Evidently the normal thermal conductivity method as developed by Schleiermacher and applied by Bonhoeffer and Harteck to their experiments on ortho and para hydrogen (' Z phys Chem ' B, vol 4, p. 113 (1929)) may be used, but over a thousand times the quantity of gas would be required for each measurement, than in the micro-method.

** See, for example, Giauque, ' J Amer Chem Soc ,' vol. 52, pp. 4808, 4816 (1930)

where p_j is the quantum weight of the rotational state with the quantum number
j and J is the moment of inertia   For H_2 and D_2 the corresponding expressions
of Dennison* were used which treat hydrogen as a mixture of the ortho- and
para-modifications   ($H_2 = \frac{3}{4}$ ortho $H_2 + \frac{1}{4}$ para H_2, $D_2 = 2/3$ ortho $D_2 +$
$1/3$ para-D_2) (see Part II)   For the moments of inertia J of D_2 and HD the
values given by Urey and Rittenberg† were employed
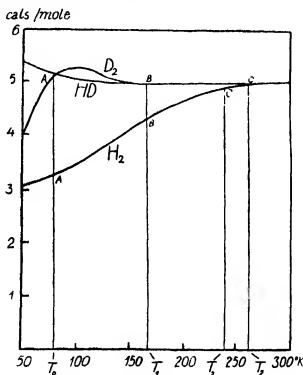
Fig 1

The heat lost by an electrically heated wire stretched in a narrow tube
containing the gas under a low pressure owing to the thermal conductivity of
the gas is proportional to the expression $\int_{T_0}^{T_1} C dT$, or on fig 1 to the area $T_0 T_1 BA$,
where T_0 is the temperature of the surrounding walls of the vessel and T_1 the
temperature to which the wire has been heated by a definite current t_1 If
now the current is increased to t_2 so that the heat given up by the wire to the
gas is, say, twice as great as previously the temperature of the wire rises to T_2

* 'Proc Roy Soc,' A, vol 115, p 483 (1927)
† 'J Chem. Phys.,' vol. 1, p. 137 (1933).

If the hydrogen in the tube be now replaced by diplogen and the pressure of the gas so regulated that the wire returns to the original temperature T_1 for the current s_1, this pressure is clearly given by

$$P_{D_2} = P_{H_2} \frac{T_0 T_1 AB}{T_0 T_1 A'B'},$$

but when the current s_2 is again switched on to the wire the temperature attained is now no longer T_2 but T'_2, where

$$\frac{T_0 T_1 BA}{T_0 T_2 CA} \simeq \frac{T_0 T_1 B'A'}{T_0 T_2 C'A'}*$$

From the temperature difference $T'_2 - T_2$ the D content of the gas may be determined from a calibration curve. In our experimental arrangement (0.01 mm diameter platinum wire, 5 cm long in gas at a pressure of ca 0.04 mm) $T'_2 - T_2$ for the pair of gases hydrogen and diplogen is about 20° and corresponds to a difference in resistance of about 6 ohms. From fig 1 it is seen that the temperature variation of the specific heat of HD is so similar to that of D_2 that they will give nearly the same results by this method (see below). The method differs from that of Schleiermacher in that the absolute thermal conductivity of the gas does not have to be considered, but rather the variation of this quantity with the temperature. It may be observed that the temperature variation of the accommodation coefficient should also be taken into account, but since the effect is quite small, the simplified treatment employed above is found to be legitimate.

Calibration

The method was tested and the wire calibrated with water containing known amounts, from 3% to nearly 100% of diplogen. These samples were prepared by Dr P. Harteck in the Cavendish Laboratory, and we are most grateful to him for his kindness in supplying them. The water was decomposed on a tungsten wire at 1000° C (see W, fig 2). It was necessary to ensure complete decomposition of the sample so that there might not be any difference between the D content of the gas and the water from which it was obtained. Tungsten possesses several advantages as a reducing agent, for complete outgassing at 2000° C eliminates the possibility of any contamination of the recovered gas and the tungstic oxide formed is volatile and distils off so that a fresh metal surface is always being presented to the vapour; while with care it is possible

---

* For the exact formula, see A. Farkas, 'Z. phys. Chem.,' B, vol. 22, p. 344 (1933).

to obtain 30 c c of gas at N T P from a wire 0 2 mm. in thickness and 20 cm long before it burns through   The hydrogen produced was then removed with the aid of a Toplur pump (T) and collected in a storage vessel (D_2) from which it could be admitted to the measuring cell

The cell (C) possessed a volume of about 10 c c , the gas was admitted through the mercury pump P_1, fig 2, and the pressure in the cell was adjusted
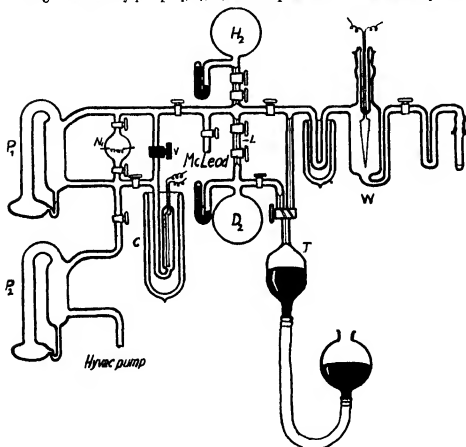
Fig 2

to the right range with the aid of a carefully ground needle valve (V)   A volume of about 0 002 c c of gas at N T P is required for a single measurement,*

* It is seen from fig 2 that the sample of gas did not fill only the cell but the dead space of the pump as well.   Naturally it would be possible to reduce this volume and to carry out the measurements at a still lower pressure than 0 04 mm Hg using a thinner wire if it were found desirable to reduce still further the amount of gas required for a single measurement.

which may, with practice, be made in about 2 minutes This small amount of
gas was measured by means of a capillary (L) having a volume of 0 1–0 2 c c

The actual readings of the resistances of the wire in the conductivity cell
corresponding to the temperatures T_2 and T'_2, fig 1, were found to be —

> For normal hydrogen- -104, 55 ohms
>
> For heavy hydrogen—-110, 44 ohms

Thereafter these figures will be referred to as the resistance values of the
respective hydrogen-diplogen sample In fig 3 the calibration curve obtained
in this way is shown
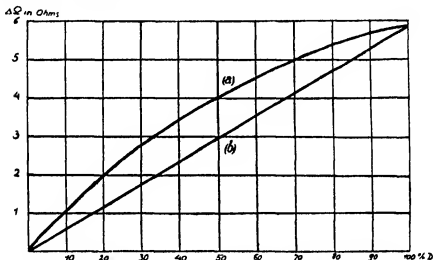
Fig 3.—Calibration curve. (a) $H_2 + D_2 + HD$ in equilibrium , (b) $H_2 + D_2$.

The straight line shows the relationship obtained between the resistance of
the wire and the D content for mixtures containing only D_2 and H_2 and none
of the mixed HD molecules, such mixtures having been prepared from normal
H_2 and pure D_2 The curved line shows the resistance obtained when H_2,
D_2, and HD are all present in thermodynamical equilibrium (see below), these
mixtures having been prepared either by passing the gas over a catalyst or
by the complete decomposition of a sample of water of known D content
The difference between the curves is due to the fact to which attention has
already been called, namely that the HD and D_2 are so similar in their thermal
conductivity variation with temperature that they give nearly the same effect
in the measuring vessel , and thus the total HD + D_2 content increases faster
with small D contents than with higher ones

The Equilibrium $H_2 + D_2 \rightleftharpoons 2HD$

Since the formation of the equilibrium mixture from a pure H_2 and D_2 mixture results in a marked increase in the resistance value of the hydrogen under examination, the technique described above permits the percentages of all three molecules in the mixture to be determined in any given experiment The formation of the equilibrium mixture containing HD molecules from a 50% H_2 and D_2 mixture results in an increase of the resistance value by about 1 ohm   To determine the quantities of all three gases, it is only necessary after the first measurement of the resistance value, to cause the equilibrium mixture to be formed, return the gas to the cell, and re determine its resistance value , the difference between these quantities will then give the amount of HD formed

The theoretical equilibrium between the three molecules H_2, D_2, and HD has been discussed by Urey and Rittenberg *   The equilibrium constant

$$K \quad \frac{[HD]^2}{[H_2][D_2]} \text{ in the range } 200° \text{ K to } 800° \text{ K is given by the expression}$$

$$- \ln K = \frac{\Delta E_0}{RT} - \tfrac{3}{2} \ln \frac{M^2_{HD}}{M_{H_2} \, M_{D_2}} - \ln \frac{J^2_{HD}}{J_{H_2} \, J_{D_2}} , - \ln^a$$

where J denotes the respective moments of inertia, M the masses and ΔE_0 the heat of the reaction ΔE_0 is about 180 cals , and is the difference in the zero point energy (ε) of the molecules taking part in the reaction, i e ,

$$\Delta E \quad 2\varepsilon_{HD} - (\varepsilon_{H_2} + \varepsilon_{D_2}),$$

since ΔE_0 is so very small, K is practically independent of the temperature

Experimental examination of the theoretical equilibrium constant in the following manner was carried out †   The increase in the resistance value of a 50% H_2–50% D_2 mixture when equilibrium has been attained has been assumed to be proportional to the theoretical value , and the single resistance value so obtained is then used to calibrate the wire in terms of the amounts of HD formed in all the other mixtures   The maximum increase in the resistance value results from the formation of HD from a 50% H_2, 50% D_2 mixture, and in our measuring cell is 1 07 ohms, so that approximately 1%HD will give

---

an increase of 0 02 ohms Fig 4 shows that with this procedure the amounts of HD obtained when equilbrium from various mixtures of H_2 and D_2 is obtained he with remarkable accuracy on the theoretical curve In this particular experiment it was desired to test the applicability of the method of measurement, rather than to determine the absolute value* of the equilibrium constant, but attention may be called to the fact that these experiments show that there is no appreciable alteration in the equilibrium constant with temperature, for when an equilibrium mixture prepared at 20° C (by the decomposition

The $H_2 + D_2 \rightleftharpoons 2HD$ equilibrium

$$K = \frac{[HD]^2}{[H_2][D_2]}$$

Fig 4
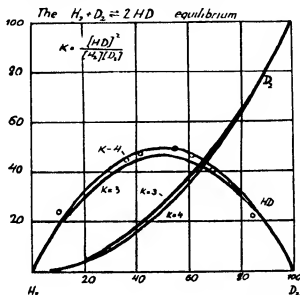
of heavy water by sodium) is heated to 600° C on a nickel wire there is no appreciable alteration in the resistance value is observed

It is found that the formation of the equilibrium mixture at 600° C on a nickel wire occurs in a few seconds Thus to determine the amount of HD in a sample, its resistance value having been determined, it was pumped from the measuring cell into a vessel containing a hot nickel wire, Ni, fig 2, left in contact with the wire for a few seconds, pumped back to the measuring cell and its resistance value again determined With this procedure, it is important that the nickel wire should not retain or evolve any hydrogen, so that the

---

* In some experiments to be published in detail later (*cf* 'Nature,' *loc. cit*) on the rate at which this equilibrium is attained the absolute value of K need not be known, for only the relative change is under consideration

amount of the gas used in the two measurements is the same   The wire must
be maintained scrupulously clean, and have been perfectly outgassed, for
every trace of foreign gas present in such minute amounts of material would
cause a large error in the measurement

More detailed measurements of the formation of HD from H_2 and D_2 on
nickel and other metals will be carried out shortly, but it is already possible to
propose a mechanism for this process   The hydrogen molecules are adsorbed
and dissociated into atoms on the surface of the metal, and naturally on de-
sorption combine in the adsorption layer to give H_2, D_2 and HD molecules
whose relative amounts are determined by the value of this equilibrium constant
at the temperature of the catalyst   This mechanism is identical with the so-
called high temperature mechanism of the catalytic conversion of para hydro-
gen [*]

We have also attempted to bring about the reaction

$$H_2 + D_2 \rightleftarrows 2HD$$
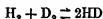
at low temperatures, by adsorbing the gases on charcoal but with negative
results   0 01 c c of a 50% H_2 and 50% D_2 mixture were adsorbed for 15
hours on 20 mg charcoal at 77 3° K , and on desorption no formation of HD
could be detected, though in theory at this temperature the equilibrium con-
centration is about 40%   This negative result shows rather beautifully that
adsorption or desorption on charcoal causes no rupture of the molecules for
if such did actually occur an exchange of D and H atoms would take place in
the surface layer resulting in the formation of HD   The work of Bonhoeffer,
Farkas and Rummel on the mechanism of the heterogeneous conversion of
para- to ortho-hydrogen would also lead us to anticipate such a result, for the
latter reaction is unimolecular in the adsorbed phase and involves no exchange
mechanism [†]

Since it is apparent that the equilibrium at low temperatures is not attainable
by means of a catalyst, it will be necessary, if measurements in this region are
to be made, to obtain the diplogen-hydrogen-mixture *in statu nascendi* either
photochemically or by a suitably chosen chemical reaction   On recombination
the equilibrium mixture of H_2, D_2 and HD will be obtained   Such measure-

---

[*] *Cf* Bonhoeffer, Farkas, and Rummel, ' Z phys Chem ,' B, vol 21, p 225 (1933)

[†] The establishment of the ortho- and para-hydrogen equilibrium on charcoal results
from the inhomogeneous magnetic field set up by unsaturated para magnetic carbon atoms
in the surface allowing a reversal of the nuclear spin to take place   On the above-mentioned
charcoal the ortho-para-hydrogen equilibrium was established within a few minutes at
78° K.

ments would, as Urey and Rittenberg (*loc cit*) have already pointed out, have particular interest since they should give direct information on the nuclear spin and the statistics of the molecules under consideration

Separation by Diffusion

Certain irregularities which we had observed in measurements of the concentrations of various mixtures led us to examine the possible separation of the isotopes occurring as a result of their different molecular velocities Such separation might be expected to occur when the mixed gases stream at low pressures through such narrow openings as partially closed taps or valves, and was, in fact, particularly marked where the measuring cell had initially been filled with too great a charge of hydrogen and its pressure later adjusted to the correct value by pumping off the excess gas through a very fine regulating valve A concentration of the heavy isotope takes place in the cell while the diplogen content of the gas pumped off is naturally less The magnitude of the effect may be calculated from Rayleigh's formula for fractional distillation which is valid for the range of pressure where the mean free path of gases effusing from a narrow opening is much greater than the diameter of the nozzle

$$\frac{\left(\frac{H_0}{H}\right)}{\left(\frac{D_0}{D}\right)} = \left(\frac{p_1}{p_0}\right)^{s-1},$$

(H_0), (D_0), (H) and (D) denoting the initial and the final concentration of the hydrogen, s being the ratio of the molecular velocities, i e, in this case $\sqrt{2}$, p_0 the initial pressure and p the final pressure equal to 0 04 mm Hg, i e, the same pressure which was maintained in the conductivity cell in all measurements

Table I shows that the theory accounts well for the results obtained

Table I

p_0/p	% D observed	% D calculated
1	47 5	—
1 5	50 7	50 7
2	53 0	53 0
3 25	56 0	57 8

2 I 2

The small discrepancy in the last experiment is probably due to the fact that
the pressure at which the experiment was carried out (about 0 13 mm Hg)
was too high for the nozzle of the valve, and the conditions of ideal effusion
were no longer maintained

A similar effect is also to be expected when H_2, D_2 and HD are all present
in their equilibrium concentrations, but now the theoretical treatment of the
problem is more involved, and the estimation of the concentrations is tech-
nically more difficult since the equilibrium is somewhat modified through the
separation that takes place The effect is, however, revealed in the alteration
in the resistance of the wire on pumping off the gas, and naturally such an
effect is not to be anticipated when pure hydrogen or a high percentage diplogen
concentrate are in the cell No such alteration is actually observed under
these conditions, and thus may be used as a convenient test for the purity of
the diplogen In all the later measurements careful control of the dimensions
of the apparatus in all parts where the flow of gas was at all restricted,
and the admission of only just the right amount of gas to the cell ensured
that all such variations in the measurements of the concentrations were
eliminated

No preferential adsorption of the diplogen occurs on exposure of the two
hydrogen isotopes to charcoal In an experiment in which 96% of a 30%

hydrogen-diplogen mixture was adsorbed on charcoal
at 78° K, the gas remaining above the charcoal had the
same H/D ratio as the original mixture Enrichment
of the D in the mixture residue occurs only if the gas
above the charcoal is pumped off, and is due to the
different diffusion velocities of the three molecular
species present

The Diffusion of the Isotopes through Palladium

The diffusion of the two hydrogen isotopes from
mixtures containing 40% to 50% of D through pal-
ladium at different temperatures has been studied

The gas at a pressure of about 5 mm was allowed to
diffuse through a thin hot palladium tube at constant
temperature, fig 5, as measured by a thermo-element,
into a vacuum from which it could be pumped off into

Fig 5 —Th = thermo-
element.

the measuring vessel and its composition determined From time to time measure-
ments were also made of the concentration of the gas remaining behind It was

found that the gas which had diffused through the palladium always had a lower D content than the original mixture, but that the difference in the D contents of the original gas and that of the gas diffused through the palladium decreased as the temperature of the palladium tube was increased Further the H/D ratio of the diffused gas did not depend on whether the initial mixture was composed only of H_2 and D_2 or of mixtures of H_2, D_2, and HD of the same H/D ratio * This would naturally be expected, since it is sure that inside the metal all these molecules are fully dissociated Accordingly, the gas diffusing through, and also after a time the initial sample, contains the equilibrium mixture of the three molecules In fig 6 the ratio

$$\alpha = \frac{\left(\dfrac{H}{D}\right) \text{ diffused}}{\left(\dfrac{H}{D}\right) \text{ original}}$$

is shown as a function of the temperature
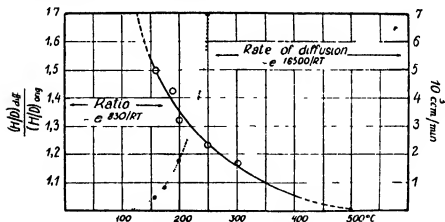
Fic 6 —Pressure 5 mm Hg

The figure shows that at higher temperatures the curve becomes asymptotic approaching unity as a limit, indicating that then the H and D are diffusing through the palladium with equal velocities The ratio gives directly the relative velocities of the two forms

---

* For diffusion through a thin quartz tube, this would not necessarily be true, since in this experiment molecules might diffuse through without previous dissociation.

The dependence of the diffusion (v) of H and D through palladium with temperature can be expressed by the relation

$$v = v_H + v_D = C \ e^{-A/RT},$$

where A is the so-called activation energy of diffusion.

The dotted curve in fig 6 shows these amounts plotted against the temperature, for which A has the value 16,500 cals The amounts of H and D which diffuse through palladium may, also to a first approximation, be expressed by the two equations

$$v_H = v \ (H)_{diff} = C_H \ (H)_{orig} \ e^{-A_H \ RT},$$

$$v_D = v \ (D)_{diff} - C_D \ (D)_{orig} \ e^{-A_D \ RT}$$

From these two expressions the magnitude

$$\alpha = e^{(A_D - A_H)/RT}$$

is obtained and is plotted in fig 6 (provided that the constants C_H and C_D, in both expressions are equal, see below) From the values shown in the figures $A_D - A_H = 830$ cals , which value is then the excess of the activation energy for the diffusion of D over that of H and is, in fact, about 5% of the whole (The value A = 16,500 cals is the average of A_H and A_D)

As a result of the difference in the velocities of diffusion of H and D the hydrogen in the original vessel from which diffusion is taking place gets gradually richer in the heavy isotope It is easily seen that the amount of concentration is again given by the Rayleigh formula

Fig 6 shows that at temperatures higher than 300° C α is very nearly equal to unity, and thus at these temperatures no marked separation is to be antici pated It is for this reason that attempts to use the diffusion of hydrogen through palladium as a means of concentrating the isotope have failed At lower temperatures, when the separation factor is relatively great, the amount of gas passing through is unfortunately so small that any separation by simple methods such as passing hydrogen at atmospheric pressure through a tube of ordinary dimension is quite impracticable

The difference between the two diffusion velocities may be considered to arise in the following ways

Fig 7 shows the energy levels of the two isotopes during the sorption process The difference in energy of the H_2 and D_2 gases arises from the difference of their zero-point energies The level for HD lies fairly exactly midway between that for H_2 and D_2 In the sorbed state the gases are dissociated

into atoms and corresponding to the different sorption complexes Pd-H and Pd-D, have still different zero-point energies

In the stationary state the velocity of diffusion must be determined by the velocity of sorption, as the same amount of gas must always be taken up as is being desorbed   Thus it is clear that the velocities of sorption of the two hydrogen isotopes must actually be different because of the different activation energies, which have been shown to differ by about 830 cals , i e , about the same as the difference in the zero point energy of $\frac{1}{2}H_2$ and $\frac{1}{2}D_2$, i e , 890 cals None the less there must certainly be a difference of the same order of magnitude in the heats of adsorption of the two molecules, resulting in a greater solubility or sorption of the heavier than the lighter isotope
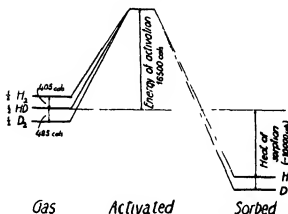
Fig 7

This consideration is merely schematic with a very simplified model , for it is assumed that the rate of diffusion is not determined by the migration of the hydrogen through the lattice (this is true for an infinitely thin palladium layer) or that, at least, the rates of migration are equal for both hydrogen isotopes

In this connection also, it can be reasonably suggested that the electrolytic separation owes its efficacy to a similar effect , and it is remarkable that if the factor $\alpha = e^{-(A_D - A_H)/T f}$ is extrapolated to room temperature a separation factor of five results, in agreement with the results first obtained by Lewis and Macdonald *   It should be observed that the difference in the energies of activation will be nearly independent of the metal surface, for the zero point energies of the various metal-hydrogen complexes will vary only slightly from

* 'J Chem Phys , vol 1, p 345 (1933)

metal to metal, thus the separation factor on different metals by electrolysis will be nearly independent of the metal surface, a conclusion in agreement with the experiments of Bell and Wolfenden * †

We are very much indebted to Professor E K Rideal, F R S, both for discussions and for his interest in our work, to Dr O H Wansbrough-Jones for translation of our manuscript and to the Central British Fund for German Jewry for a financial grant

Summary

(1) A method based on the different specific heats of the hydrogen isotopes is described permitting a determination of the concentration of the heavy hydrogen isotope in a mixture with an accuracy of 0 2% in a sample of 0 002 c c N T P of gas

(2) It is shown that in a mixture of hydrogen and diplogen the equilibrium

$$H_2 + D_2 \rightleftarrows HD$$

is readily established at the surface of a hot nickel wire   The equilibrium constant is, in agreement with theory, about 4 and nearly independent of temperature

(3) This establishment of the equilibrium is used to estimate the ratios of the molecules H_2, D_2, and HD in a given sample of hydrogen

(4) By pumping hydrogen-diplogen mixtures at low pressures through a fine nozzle a slight separation occurs due to the different molecular velocities of the hydrogen isotopes

(5) If a hydrogen-diplogen mixture diffuses through a palladium tube the H D ratio of the diffusing gas is the greater the lower the temperature of the tube   Above 300° C the H D ratio of the diffusing gas is equal to that of the original gas   This may be explained by assuming that the energy of activation for the diffusion of diplogen is greater than that for hydrogen on account of the difference in their zero point energies

---

* 'Nature,' vol 133, p 26 (1934)

† Topley ond Eyring, 'Nature,' vol 133, p 292 (1934), 'J Amer Chem ' vol 55, p 5058 (1933)

Experiments on Heavy Hydrogen   II —*The Ortho-para Conversion*

By A FARKAS, L FARKAS, and P HARTECK (Rockefeller Foundation Fellow), Laboratory of Colloid Science, Cambridge University

(Communicated by Eric K Rideal, F R S —Received March 2, 1934)

Ortho- and para-modifications should exist in all diatomic molecules of identical atoms with nuclear spin, since the law of prohibition of the ortho-para intercombination is generally applicable * The rotational states consist alternately of ortho- and para-levels   the ortho-levels being those which possess on the average the higher quantum weight and represent the states with the symmetrical nuclear-spin eigenfunctions, whereas the para-levels correspond to the antisymmetrical nuclear-spin function

The rotational quantum numbers possessed by the ortho- and para-levels depend on the statistics valid for the nuclei and on the symmetry of the electronic eigenfunctions   For even electronic eigenfunction (for hydrogen and diplogen the ground states of which are $^1\Sigma_g$) if the Fermi Dirac statistics are valid the ortho-modifications are in the rotational states with odd quantum numbers and the para states in the even ones, whilst the Bose Einstein statistics lead one to expect the reverse to be true

The existence of the two sets in the molecule becomes apparent on studying the specific heats,[†] the spectrum,[‡] and the equilibrium of the two modifications [§] With ordinary hydrogen these three effects were observed in that order , for diplogen it has already been shown that alternating intensities occur in the emission spectrum[||] and in this paper we shall substantiate the differences in the rotational specific heat and examine the ortho-para equilibrium

The ratio of the concentration of the ortho- and para-modification in equilibrium with each other may be derived in the following way[¶]   let t be the

---

* *Cf e g* L. Farkas, ' Ergbn exact Naturw ,' vol 12, p 163 (1933)

† Dennison, ' Proc Roy Soc ,' A, vol 115, p 483 (1927) , Eucken, ' SitzBer Preuss Akad. Wiss Berlin,' No 141, p 141 (1912)

‡ Heisenberg, ' Z Physik ,' vol 38, p 41 (1926) , vol 41, p 239 (1927) , Hund, ' Z. Physik,' vol 42, p 93 (1927)

§ Bonhoeffer and Harteck, ' Z phys Chem ,' B, vol 4, p 113 (1929) , Eucken and Hiller, ' Z phys Chem ,' B, vol 4, p 142 (1929)

|| Lewis and Ashley, ' Phys Rev ,' vol 43, p 837 (1933)

¶ Weizel, " Bandenspectren," ' Wien-Harms Handbuch der Exp. Physik,' (1933)

nuclear spin of the atom then the resulting spin T of the molecule may have
$2t + 1$ different values

$$T = 2t, \quad \underline{2t - 1}, \quad 2t - 2, \quad \underline{2t - 3}, \qquad , 0$$

the values underlined corresponding to the antisymmetrical spin function,
i e , to the para states   As each resulting nuclear spin T is $2T + 1$ fold
degenerated, the normal or high temperature ortho-para ratio is given by the
ratio of the total multiplicity (g) of the ortho states to that of the para states,
viz ,

$$\frac{g_{\text{ortho}}}{g_{\text{para}}} = \frac{\sum\limits_{n = \text{even}} 2 \, (2t - n) + 1}{\sum\limits_{n = \text{odd}} 2 \, (2t - n) + 1} = \frac{(t + 1) \, (2t + 1)}{t \, (2t + 1)} = \frac{t + 1}{t}$$

The distribution of the molecules in different rotational levels and thus the
dependence on temperature of the ortho-para equilibrium is governed by the
Boltzmann law

$$N_J = N_0 g \, (2j + 1) \, e^{-E_J/kT},$$

N_J denoting the fraction of the molecule of the total number (N_0) in the rota-
tional level j with the energy

$$E_J = \frac{j \, (j + 1) \, h^2}{8\pi^2 J}$$

(J — moment of inertia), g is the nuclear statistical weight, being $(t + 1)$
$(2t + 1)$ for the ortho states, and $t \, (2t + 1)$ for the para states
    The fraction of the molecules in the para and ortho states is given by

$$b_{\text{para}} = \frac{\sum\limits_{\text{para}} g_{\text{para}} (2j + 1) \, e^{-E_J/kT}}{\sum\limits_{\text{ortho}} g_{\text{ortho}} (2j + 1) \, e^{-E_J/kT} + \sum\limits_{\text{para}} g_{\text{para}} (2j + 1) \, e^{-E_J/kT}} = \frac{Q_{\text{para}}}{Q_{\text{ortho}} + Q_{\text{para}}}$$

$$b_{\text{ortho}} = \frac{Q_{\text{ortho}}}{Q_{\text{ortho}} + Q_{\text{para}}}$$

The index ortho or para under Σ denotes that the summation must be extended
over the ortho or para states
    Experiments were carried out in order to demonstrate the ortho-para con-
version in diplogen and to determine from the equilibrium ratio the spin and
statistics of the diplogen nucleus
    The experiments were planned on the assumption that diplogen would
behave in a manner analogous to hydrogen , that is to say, that the attainment
of the equilibrium ratio which, on account of the impossibility of the ortho-
para intercombination taking place in pure hydrogen, is extremely slow, could

be accelerated by suitable catalysts and that the gas removed from the catalyst, being stable under ordinary conditions, retains the ortho-para concentration which is in equilibrium at the temperature of the catalyst

As catalysts for the rapid production of the ortho para diplogen equilibrium mixture an active charcoal, which effected a very rapid ortho para conversion in hydrogen even at the temperature of liquid hydrogen, was employed   The sample of diplogen was of about 90% purity   It is evident that these experiments could be performed more readily with pure diplogen for the 90% diplogen contains the following five constituents   ortho hydrogen, para-hydrogen, HD molecules, ortho-diplogen, and para-diplogen   It was, however, found possible to determine the concentration of each constituent and thus overcome this difficulty

For the determination of the different forms of hydrogen and diplogen the micro method of A Farkas,* which gives measurements of high precision with amounts of gas as small as 0 002 c c at N T P, was employed   This method was applicable since a difference in the rotational specific heats of ortho- and para diplogen was to be expected similar to that found in ortho- and para-hydrogen (*cf* fig 2)   The actual measurements were carried out in two thermal conductivity cells having wires of different length and thickness extended down the axis of each cell

The calibration readings† were as follows —

Table I

	Cell I	Cell II
	ohms	ohms
Normal hydrogen	105 23	128 39
Para hydrogen	106 45	131 44
Normal diplogen (90% D)	111 23	1 16 73

For hydrogen it was shown that for these cells the excess concentration of para-hydrogen relative to normal hydrogen was proportional to the corresponding differences in the values found for the resistance, according to the formula

$$(p - 25) = \text{prop} (R_p - R_{25})$$

where p denotes the para-hydrogen concentration in percentage of the sample, R_p its resistance value and R_{25} the resistance value of normal or 25% para-hydrogen

* ' Z phys Chem ,' B, vol 22, p 344 (1933)
† A Farkas and L Farkas, ' Nature,' vol 132, p 894 (1933)

To determine the exact equilibrium between ortho- and para-diplogen three series of experiments were carried out at the temperatures 20 4° K ,[*] 53° K and 78° K   The first run was carried out at 20 4° K   The catalyst consisting of about 0 2 gram of active charcoal, enclosed in a thin glass tube of a few cubic centimetres capacity, absorbed at 20 4° K about 50 c c of diplogen, but the pressure over the charcoal was not higher than a few tenths of a millimetre of mercury   The first samples of gas were extracted from the charcoal tube after the diplogen had been in contact with the catalyst for some minutes, and its resistance value was found to be (cell I) 111 58 ohms compared with 111 23 ohms for the original gas

A change in the resistance value may be due to four different causes —

(1) Through separation of the hydrogen isotopes on pumping off the samples owing to the higher diffusibility of the lighter hydrogen, Part 1

(2) Through the possible readjustment of the $H_2 + D_2 \rightleftharpoons 2HD$ equilibrium

(3) Through the ortho-para conversion of the ordinary hydrogen present in the original sample or formed by reaction (2)

(4) Through the ortho para diplogen conversion

From the calibration experiments, it is evident that a separation of the hydrogen isotope in pumping off the samples cannot cause a rise in the resistance value but must lower it owing to the lower diplogen content of the gas pumped off

Previous experiments, made on charcoal indicated that the readjustment of the $H_2 + D_2 \rightleftharpoons 2HD$ equilibrium did not occur at the temperature of liquid nitrogen and, therefore, it is very improbable that the change in the resistance value is due to such an effect at the temperature of liquid hydrogen, but if (2) does not occur there is very little probability that the effect found is due to the ortho-para conversion of ordinary hydrogen since the original gas (90% D) could not contain more than 1% H_2, and such a small amount (even if somewhat concentrated by the pumping) would not cause the observed change in the resistance value when converted to parahydrogen

This single measurement, therefore, makes it very probable that we are dealing with a true para-ortho diplogen conversion   This was confirmed by the following experiment

* The liquid hydrogen was kept in a liquid air cooled Dewar container of 350 c c   By daily renewal of the liquid air the liquid hydrogen could be preserved for 4 days.

The gas pumped off from the charcoal cooled by liquid hydrogen was re-adsorbed on charcoal at 78° K and then completely re-evaporated, this sample showed a resistance value of 110 75 ohms, i e , 0 83 ohms lower than the sample taken from the charcoal at 20 4° K In this case it is evident that the processes (1) and (2) could not occur, the actual fall in the resistance value was, therefore, due to the adjustment of the ortho-diplogen para-diplogen equilibrium from 20 4° K to 78° K

We cannot attribute this change in the resistance value to the hydrogen content of the sample, for so great a change could only be caused by the ortho-para conversion of pure hydrogen Finally, this sample of gas was brought into contact with a hot nickel wire and the resistance value obtained after this operation was 110 25 ohms This further fall was to be anticipated since the excess of HD contained in the sample pumped off the charcoal cooled by liquid hydrogen was transformed according to the equation

$$2HD \rightleftarrows H_2 + D_2$$

From this final resistance value we calculate the D content to be about 67%* and from the difference 110 75–110 25 after taking into account a small change due to the readjustment of the ortho-para-equilibrium of diplogen (see below) we find that about 12% HD has disappeared, i e , when the original gas had a composition of

$$90\% \ D = 81\% \ D_2 + 18\% \ HD + 1\% \ H_2,$$

the gas pumped off from the charcoal cooled by liquid hydrogen contained

$$67\% \ D = 39\% \ D_2 + 56\% \ HD + 5\% \ H_2$$

the equilibrium mixture being

$$45\% \ D_2 + 44\% \ HD + 11\% \ H_2$$

This procedure was repeated several times and always led to practically the same result and conclusion Since, even by continuous pumping, we failed to get off the charcoal cooled in liquid hydrogen a gas containing more than 70% D (the whole amount pumped off in 10 hours was not more than 1/10 of that originally adsorbed) the liquid hydrogen container was suddenly removed and the greatest part of the adsorbed gas was recovered In the earlier experiments of Bonhoeffer and Harteck† with para-hydrogen, it was found

---

* This separation compared with 90% D of the original gas is due to a slightly preferential adsorption which does not occur at higher temperatures

† 'Z phys. Chem.,' B, vol 4, p 113 (1929)

A Farkas, L Farkas and P Harteck

that when para-hydrogen is suddenly liberated in this manner the ortho-para hydrogen equilibrium is not readjusted to the actual temperature of the charcoal as the desorption takes place with a greater velocity than the re-conversion

A sample of this gas gave a resistance value of 112 61 ohms which was reduced by contact with a hot nickel wire to 111 25 ohms, i e, practically to the value of the original sample   The corresponding readings in cell II were 138 93 ohms and 136 73 ohms respectively

As no separation whatever could occur the whole change was entirely due to the ortho para diplogen conversion

To determine the temperature dependence of the ortho-para diplogen equilibrium further series of measurements were made at 53° K and 78° K In Table II the changes are recorded in the resistance value for the samples relative to the normal diplogen and their ratios

Table II

Temperature, k	Cell I *		Cell II	
	Change	Ratio	Change	Ratio
20 4	1 40	9 2	2 20	8 8
53	0 51	3 4	0 85	3 4
78	0 15	1	0 25	1

* More weight is to be assigned to the values from cell I than to those from cell II, since they include a greater number of measurements

Since previous experiments with hydrogen had shown that the changes in the resistance value were proportional to the changes in the para-hydrogen content of the gas, an attempt was made to estimate from these readings the actual concentration of the ortho and para component in the following way

Fig 1 shows the dependence of the concentration of ortho-diplogen on the temperature adopting the Dirac-Fermi or Bose-Einstein statistics and for nuclear spins of $\frac{1}{2}$ and 1 (higher values of t are most improbable)   Table III contains the ratios of the excess concentration of ortho- and para-diplogen at 20·4° K, 53° K, and 78° K

If we compare the relative changes in the concentration with the ratio of the changes in the resistance value we can certainly exclude the Dirac-Fermi statistics   If the Bose-Einstein statistics are applicable to diplogen then the lowest rotational level with the quantum number 0, and thus all rotational states with even quantum numbers, are ortho states, and have the higher

statistical weight This result is in agreement with the statement of Lewis and Ashley who found that in the emission spectrum of the diplogen molecule the lines in the Q-branches of the Fulcher-bands corresponding to the transitions between rotational levels with even quantum numbers are more intense Our ratios agree better with the spin $t = 1$ which is the value to be expected from the analogy with other elements, $i\,e$, those with even atomic weight having integer nuclear spins *
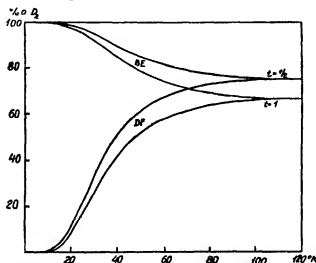
Fig 1 —B E calculated according to the Bose Einstein statistics , D F according to the Dirac Fermi statistics

Table III

Temperature, °K.	Dirac Fermi statistics		Bose Einstein statistics	
	$t = \frac{1}{2}$	$t = 1$	$t = \frac{1}{2}$	$t = 1$
20 4	31 2	14 7	8 4	9 5
54	3 8	3 2	1 1	3 2
78	1	1	1	1

For the nuclear spin 1 the lowest rotational state with the quantum number 0 has the following constitution The spins of the nuclei are either parallel

* It may be added that the measurements cannot exclude definitely a nuclear spin of $\frac{1}{2}$ as the relative changes in the concentrations (in this substance) are very similar to those for $t = 1$ The same difficulty appears in the spectroscopic measurement of the alternating intensity A conclusive determination of the nuclear spin can only be made by the absolute measurement of the specific heats as was carried out by Eucken for hydrogen

or antiparallel having the resultant spin $T = 2$ or 0, respectively   The state
with $T = 2$ is $2T + 1 = 5$-fold whereas the state $T = 0$ is single   The latter
has the lowest energy when this 6-fold degenerated state is split up at extremely
low temperatures for example in the crystal   Transition between these two
sets would also involve a change in the multiplicity of the nuclear spins similar
to the para-ortho hydrogen transition, we should therefore expect a pro-
hibition for this transition

If we compare the dependence on temperature of the ortho-diplogen con-
centration with hydrogen we note a remarkable difference owing to the different
statistics   while in hydrogen the ortho-hydrogen, i e, the component present
in excess at high temperatures, disappears on lowering the temperature, in
diplogen the ortho modification is the only stable form at low temperatures
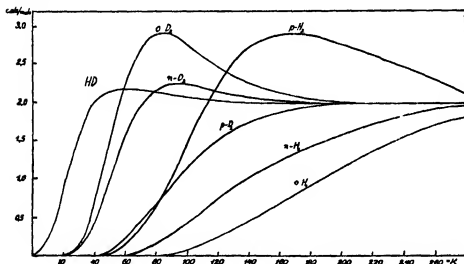
Fig 2

In fig 2 the rotational specific heats curves are shown for normal diplogen
(n-D_2), ortho-diplogen (o-D_2), para-diplogen (p-D_2), normal hydrogen (n-H_2),
para-hydrogen (p-H_2), ortho-hydrogen (o-H_2) and for the mixed molecule
gas HD   As normal diplogen and normal hydrogen are designated those
mixtures of ortho- and para-molecules which correspond to the distribution
at high temperatures, i e,

$$n\text{-}D_2 = \tfrac{2}{3}\, o\text{-}D_2 + \tfrac{1}{3}\, p\text{-}D_2,$$

$$n\text{-}H_2 = \tfrac{3}{4}\, o\text{-}H_2 + \tfrac{1}{4}\, p\text{-}H_2.$$

The specific heat curves were calculated on the basis of the Dennison formulæ (*loc cit*)

$$C_{rot}^{p-D_2} = R\sigma^2 \frac{d^2 \ln Q_{para}}{d\sigma^2},$$

$$C_{rot}^{o-D_2} = R\sigma^2 \frac{d^2 \ln Q_{ortho}}{d\sigma^2},$$

$$C_{rot}^{p-D_2} = \tfrac{2}{3} C_{rot}^{o-D_2} + \tfrac{1}{3} C_{rot}^{p-D_2} \quad \text{with } \sigma = \frac{\sigma_{H_2}}{2} = \frac{85}{2T},$$

on account of the double moment of inertia of D_2 compared with H_2 For HD the method of computation was based upon the analysis of Gregory [*]

A comparison has been made between the reaction velocity of the ortho-para conversion of diplogen in two characteristic examples with the corresponding reaction of hydrogen, firstly the heterogeneous ortho-diplogen formation at 20 4° K. and secondly the re-conversion of ortho-diplogen at room temperatures catalysed by gaseous oxygen.
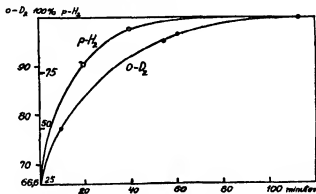
FIG. 3.

Since, as we have seen, the formation of ortho-diplogen is very rapid on charcoal another catalyst was employed consisting of a glass tube which, owing to some impurities, catalysed the para-ortho-diplogen conversion with a conveniently measurable speed. On this catalyst the diplogen conversion proceeded slightly more slowly than the hydrogen conversion as shown in fig 3, namely, with a half life time[†] of about 19 and 11 minutes respectively

[*] 'Z Physik,' vol 78, p 791 (1932)

[†] As was shown for hydrogen this type of reaction proceeds according to the formula $p_t - p_\infty = (p_0 - p_\infty) e^{-kt}$, p_0, p_t, and p_∞ denoting the para hydrogen concentration at a time $t = 0$, t and $t = \infty$ Then the reaction rate is given by the half life $\tau = \ln 2/k$

The mechanism of the catalytic ortho-para conversion of diplogen is most probably the same as for hydrogen,[*][†][‡], we have again two independent mechanisms one of them acting at low temperatures and the other at high temperatures, one is connected with the normal or van der Waals' adsorption and the second with the chemi- or atomic adsorption. The low temperature mechanism (e g, catalysis by charcoal) involves only one molecule and the twisting of the nuclear spin from the para position to the ortho position is effected by the magnetic forces of the catalyst. The probability of this twisting is nearly independent of the temperature and the reaction rate is governed by the amount adsorbed. The high temperature mechanism (e g, catalysis by metals) consists in atomic adsorption of diplogen (or hydrogen) when the adsorbed molecules are split into atoms and the ortho- and para-molecules re-evaporate in a ratio corresponding to the equilibrium at the actual temperature of the catalyst.

The homogeneous reconversion of ortho-diplogen in the presence of oxygen was next investigated, for it provides us with valuable information on the value of the nuclear magnetic moment of the diplon. As has been recently shown by L. Farkas and Sachsse[‡] paramagnetic molecules or ions convert para-hydrogen to normal hydrogen according to the reaction

$$p\text{-}H_2 + X \rightleftarrows o\text{-}H_2 + X$$
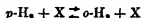
The rate of the reaction is given by

$$p_t - p_\infty = (p_0 - p_\infty) e^{-(k_{p \to o} + k_{o \to p})[X]t},$$

where $k_{p \to o}$ and $k_{o \to p}$ are the reaction velocity constants of the respective reactions and [X] is the concentration of the paramagnetic substance. At temperatures above 200° K $k_{p \to o}/k_{o \to p}$ is 3, because the ratio $p\text{-}H_2/o\text{-}H_2$ is maintained at a ratio of 1/3. Since the conversion is effected by the perturbation of the inhomogeneous magnetic field of the paramagnetic molecule upon the nuclear magnetic moment it was to be expected that a similar re-conversion would take place with ortho-diplogen as had been observed with para-hydrogen. For the ortho-diplogen conversion above 100° K we have

$$\frac{k_{o \to p}}{k_{p \to o}} = \frac{1}{2}$$

since the composition of normal diplogen is 2/3 o-D_2 + 1/3 p-D_2.

* Bonhoeffer and A Farkas, 'Trans. Faraday Soc,' vol. 28, pp. 242, 561 (1932)

† Bonhoeffer, A Farkas, and Rummel, 'Z phys. Chem.,' B, vol. 21, p. 225 (1933)

‡ 'SitzBer Preuss. Akad. Wiss. Berlin,' p 268 (1933), 'Z phys. Chem ,' B, vol. 23, pp. 1, 19 (1933).

The experimental arrangement for investigating the ortho-diplogen re-conversion was very simple. Ortho-diplogen, prepared at 20 4° K on charcoal, was mixed with oxygen and samples of this mixture were taken from time to time for measurement of the ortho-diplogen concentration. The samples passed through a trap, cooled with liquid hydrogen in order to freeze out the oxygen, before reaching the measuring cell. The mixture of ortho-diplogen and oxygen was kept in a gas burette over mercury and its pressure could be adjusted very conveniently by altering the level of the mercury in the burette.

As mean value for the half life time at 10 mm oxygen pressure (293° K) a value of 2200 minutes was obtained corresponding to a velocity constant of

$$\frac{\ln 2}{2200} \cdot \frac{22 \cdot 4 \cdot 760}{10} \cdot \frac{293}{273} = 0 \cdot 57 \text{ litre/mole minute}$$

The velocity constant is thus 16 times smaller than the velocity constant of the corresponding hydrogen reaction, namely, 9 16 litre/mole minute

This great difference in the velocity constant can be interpreted on the basis of the theoretical investigations of Wigner * According to this author the theoretical collision efficiency of the ortho-para transition from the rotational state $j = 0$ to the rotational state $j = 1$ is given by

$$Z_{01} = \frac{8\pi^3 J_{H_2} \mu_p^2 \mu_X^2}{9h^2 kTa^6} \, e^{-E_1/kT},$$

where J_{H_2} is the moment of inertia of H_2, μ_p the magnetic moment of the proton $(2 \cdot 5 \cdot 0 \cdot 5 \cdot 10^{-23}$ C G S units),† μ_X the magnetic moment of the colliding paramagnetic molecule and a the closest distance of approach on collision The factor $e^{-E_1/kT}$ is due to the fact that this transition is endothermic From the value Z_{01} the collision efficiency can be derived for the whole para-ortho reaction $(Z_{p \to o})$ which includes all the para-ortho transitions $j = 0 \to 1$, $2 \to 1$, $2 \to 1$, etc, and which is connected with the observed velocity constant by the relation

$$Z_{p \to o} = \frac{3}{4} \frac{(k_{p \to o} + k_{1 \to p})}{\text{number of collisions per minute}},$$

and is given by

$$Z_{p \to o} = \frac{8\pi^3 J_{H_2} \mu_p^2 \mu_X^2}{9h^2 kTa^6} \left(\frac{e^{-E_1/kT} + 2e^{-E_0/kT} + 3e^{-F_0/kT} + }{1 + 5e^{-E_0/kT} + 9e^{-E_0/kT} + } \right)$$

---

* 'Z phys. Chem,' B, vol 23, p 28 (1933)

† Estermann, Frisch, and Stern, 'Nature,' vol. 132, p 169 (1933), Estermann and Stern, 'Z Physik,' vol. 85, p 17 (1933), Frisch and Stern, 'Z Physik,' vol 85, p 4 (1933)

If we employ a similar expression for $Z_{o \to p}$ in the case of ortho-diplogen and adopt the same value of a in both cases we obtain for the ratio

$$\frac{Z_{p \to o}^{p H_2}}{Z_{o \to p}^{o D_2}} = \frac{\frac{1}{4} \; 9 \cdot 16 \; \sqrt{\frac{2 \; 32}{34}}}{\frac{1}{6} \; 0 \; 57 \; \sqrt{\frac{32 \; 4}{36}}} = \frac{\mu_P^2}{\mu_D^2} \frac{J_{H_2}}{J_{D_2}} \frac{\alpha}{\alpha'} = \frac{\mu_P^2}{\mu_D^2} \; \frac{1}{1} \frac{0 \; 4}{0 \; 7},$$

where α and α' denote expressions in the brackets in the theoretical formulæ for $Z_{p \to o}^{p H_2}$ and $Z_{o \to p}^{o D_2}$. We thus obtain for the ratio μ^2_P/μ^2_D a value of about 30 so that the magnetic moment of the diplon is about 5 5 times smaller than that of the proton being about 0 2 10^{-23} C G S units

In this calculation we have assumed that the value of a for the collision is the same for both reaction $p\text{-}H_2 + O_2$ and $o\text{-}D_2 + O_2$ and that the validity of the theoretical formulæ is retained It is hoped to confirm this ratio of μ_P/μ_D by comparing the relative efficiencies of other paramagnetic reactions in the two cases, and to estimate the probable difference in a due to the different zero point vibrations of H_2 and D_2. In fact one would expect the closest distance of approach a to be somewhat smaller for D_2 than for H_2, leading to an even smaller value for the magnetic moment of the diplon Stern and Estermann[*] came to the same qualitative result in their direct determination of the magnetic moment of the diplon by molecular ray methods Thus it is clear that the diplon has definitely a finite magnetic moment and an abnormal low ratio of $\dfrac{\text{magnetic moment}}{\text{mechanical moment}}$, whereas the proton has an abnormally high one, both at present inexplicable

Summary

It is shown that the ortho-para conversion of diplogen can be catalysed by charcoal and the actual conversion measured by thermal conductivity methods From the dependence of the ortho-para diplogen equilibrium on temperature

* 'Z Physik,' vol. 86, p 132 (1933)

it is found that for the diplogen nucleus the Bose Einstein statistics are valid, the lowest rotational state being an ortho level, furthermore, that the most probable value of the nuclear spin of diplogen is 1 The heterogeneous ortho-para conversion at 20 4° K proceeds under the experimental conditions at nearly the same rate both for hydrogen and for diplogen The re-conversion of ortho-diplogen to normal diplogen by the paramagnetic molecular oxygen is 16 times smaller than the corresponding reaction for hydrogen, indicating that the magnetic moment of the diplon is about 1/5 of the magnetic moment of the proton

———————————

The Thermal Conductivity of Air

By T. H. Laby, F.R.S.

When Miss Nelson and the writer prepared in 1929 an article for the 'International Critical Tables' on the thermal conductivity of gases, we found that the value for air had been measured by 19 observers and that the mean departure from the mean was 7%. Further the values obtained by the hot wire method by Weber, Gregory and Archer, and Schneider were higher than the value (5·40 × 10⁻⁵ cal cm⁻¹ sec⁻¹ deg⁻¹)* which Hercus and the writer had found by a parallel plate method and by 13 of the 14 determinations (including hot wire ones) made previous to 1918. In view of these facts it was desirable to repeat the parallel plate method and to obtain evidence as to whether or not there was a systematic difference between the two methods mentioned.

The hot wire method, as used by the experimenters named, has the practical advantages that the temperature of the wire can be kept constant and be accurately measured, and it is convenient and simple. As carried out in the experiments referred to in which fine wires were used it has the disadvantages that the elimination of the convection effects is not attained with certainty, the temperature gradient in the gas is large (which introduces both theoretical and practical difficulties) and there is a temperature discontinuity at the surface of the wire which has to be determined. Hercus and Sutherland have nearly completed in this laboratory a measurement of the thermal conductivity of air with a parallel plate apparatus. This method has the inherent advantages that there are no convection currents in the horizontal lamina of gas used, that the temperature gradient may be made small, and the temperature discontinuity at the surface of the plate is of no significance. In the experiments now in progress radiation is eliminated by using the metal plates at two different separations and considerable improvements have been made as compared with the experiment of Hercus and the writer by the use of a better technique, in the steadiness of the temperatures and in their measurement.

Kannuluik noticed while the experiment just described was in progress that a development of Kundsen's hot wire method which he had used for measuring the thermal conductivity of the metal of the wire could be used for measuring

---

* This and the other values given in this paper for the thermal conductivity of air are for air at 0° C

gas conductivities He and Martin in a paper already published and in the one which follows this describe this hot wire method as it is used for measuring gas conductivities The apparatus is of the simplest construction and the method has an exact theory *As a thick wire* is used in this apparatus it is free from two of the disadvantages mentioned above, for the temperature gradient can be made small, and the temperature discontinuity is almost or actually negligible By the use of narrow metal tubes convection effects have been eliminated before molecular conduction begins

Kannuluik and Martin obtain a value for the conductivity of air of $5\ 76 \times 10^{-5}$ cal cm $^{-1}$ deg $^{-1}$ sec $^{-1}$ which is higher than that obtained in the older determinations Hercus and Sutherland's experiments with the parallel plate method give a value $5\ 72 \times 10^{-5}$ which agrees to better than 1% with the value of Kannuluik and Martin

Thus these two investigations confirm the value* found by Weber, namely, $5\ 74 \times 10^{-5}$, and show that the parallel plate and certain hot wire methods agree The accuracy and convenience with which thermal conductivities of gases can be measured appear to have been considerably improved by the method described in the following paper

We are indebted to Dr J K Roberts for reading the proofs

---

* Gregory and Archer's value, $5\ 83 \times 10^{-5}$, is not very different

The Thermal Conductivity of some Gases at 0° C

By W G KANNULUIK, B Sc , and L H MARTIN, Ph D , University of Melbourne

(Communicated by T H Laby, F R S —Received September 25, 1933)

Introduction.

During recent years an increased interest has been displayed in the phenomena of gas conduction, particularly in their application to the observation of molecular changes and chemical dissociations While relative measurements usually suffice for these purposes, there have also been carefully planned researches on the absolute thermal conductivities of gases, the results of which are of value in the development of the kinetic theory

A comprehensive account of the methods which have been employed in the past for the measurement of the thermal conductivity of gases is given in a recent paper by Trautz and Zündel,[*] who include also a table of the available data to 1931 for air, hydrogen, and carbon dioxide The lack of agreement between the values obtained by different workers shown in this table can be explained by the smallness of the quantity measured, and by the difficulty of eliminating the heat transfers by convection and by radiation, one or both of which are always present

The principal methods which have been used in absolute determinations are (1) the parallel plate method, successfully adapted by Hercus and Laby,[†] and (2) the hot wire method, and its variants, of which the most satisfactory forms are found in the experiments of Weber[‡] and of Gregory and Archer,[§] and Gregory and Marshall ||

The most important work in recent years has been carried out with some form of hot wire method, and the conductivities obtained, notably for air, have been consistently higher than the values obtained with the parallel plate method

The parallel plate method has many advantages of a fundamental character, and as the hot wire methods have not always been above criticism in matters

---

[*] 'Z tech Phys.,' vol 12, p 273 (1931)

[†] 'Proc Roy Soc ,' A, vol 95, p 190 (1919)

[‡] 'Ann. Physik,' vol 54, p 325 (1917) , vol 82, p 479 (1927)

[§] 'Proc Roy Soc ,' A, vol 110, p 91 (1926)

[||] 'Proc Roy Soc ,' A, vol 114, p 354 (1927) , vol 118, p 594 (1928)

of detail it was believed that a new series of measurements would be of value if a hot wire method could be developed which met these criticisms satisfactorily The present paper describes the measurement of the conductivities of a number of gases using a new form of hot wire method in which an exact theory is completely realized with a single simple apparatus

All hot wire methods are faced with the initial difficulties of eliminating convection, and of making adequate correction for the temperature discontinuity at the wire surface The problem of separating convection and conduction has been studied by Weber and it is now possible to design a hot wire apparatus in which convection is absent Briefly, the tube must be vertical, and not too wide One of the most serious criticisms which can be levelled at recent work is associated with errors introduced by the temperature discontinuity at the wire In some cases the correction has been neglected, and in others, on account of the small diameter of the wire and the low gas pressures used, the correction has been much larger than is desirable The temperature discontinuity at the wire surface is related to the accommodation coefficient of the wire for the gas molecules, and it is thus possible to use values of the accommodation coefficients found by other workers in making the necessary correction, but this procedure is not desirable as the coefficient depends on the state of the metal surface It is preferable to measure the accommodation coefficient with the actual apparatus used for the conductivity experiments, or better, to employ a graphical method, described later, which gives the gas conductivity directly without having to evaluate the accommodation coefficient

In order to compare the results of different workers, final values of k are usually reduced to 0° C In the past this reduction has sometimes involved a considerable extrapolation based on a series of measurements carried out in a relatively short range of temperatures

In the present experiments the mean temperature of the gas is never greater than 3 3° C and is usually nearer 2° C so that no appreciable error is introduced in reducing the conductivities to 0° C For this purpose we preferred to employ the temperature coefficients given in the ' International Critical Tables '* by Laby and Nelson as these are based on experiments made over a wide range of temperature

The method and tube design are such as to reduce the above sources of error to a minimum For the majority of gases, there is no convection over a pressure range of some 50 cm of Hg The wires used are all so thick that,

with the possible exception of hydrogen, within this pressure range the correction for the temperature discontinuity can be neglected

Method and Theory

Before describing the method used in these measurements it will be useful to recall the general principles of the hot wire method

A metal wire, which is heated by an electric current, is mounted axially in a glass tube immersed in a constant temperature bath   The wire serves in the dual capacity of a resistance thermometer, and a heater which is at a uniform temperature along a central portion, which will be relatively greater the longer the wire and the smaller its diameter   The lateral heat transfer through the gas is therefore radial only for a limited central portion of the tube   This difficulty has been met in the past by two distinct methods of procedure   In the first, due to Schleiermacher,* a long thin wire is used and the resistance of a central portion which is at a uniform temperature is measured by introducing two very fine potential leads through the side walls of the tube   In a second method which was devised by Goldschmidt† two tubes are employed, one long and the other short , the differential measurements then refer to a central portion of the longer tube where radial flow conditions hold

Whichever of these two variants is adopted inconveniently long apparatus are required containing relatively fine wires the mean diameters of which in most experiments have only been determined by weighing methods   As the temperature gradient at the surface of a fine wire is very great it is necessary that it should be exactly circular in cross-section, and of constant diameter, requirements which are best verified by contact methods

These limitations have been removed in our experiments which are based on the general theory of the distribution of temperature along the wire and in the gas, and makes possible the use of a thick wire mounted in a single short metal tube

A brief description of the general principles of the present method is as follows   With the ends of the wire and the wall of the tube at 0° C the conductivity of the gas can be calculated from the rate of input of electrical energy, the thermal conductivity of the wire, and its mean temperature   Part of the heat generated is conducted laterally through the gas, while the remainder is dissipated at the ends of the wire   The theory takes into account both of these processes

* ' Wied Ann ,' vol 34, p. 623 (1888)

† ' Phys Z ,' vol 12, p 418 (1911)

With the short thick wires used in this experiment and with gases like air, which are relatively poor conductors, approximately 50%, of the total heat generated is dissipated at the ends of the wire It follows that the accuracy of the gas conductivity determinations depends ultimately on the accuracy with which the thermal conductivity of the wire can be measured This quantity is measured with the apparatus unchanged in any way, the wire *in situ*, and in the same physical condition as it was when used to measure gas conductivities The accuracy of this measurement is better than 1 in 300 (see Table II)

Theory—A wire of thermal conductivity λ is mounted axially in a tube which is maintained at 0° C The annular space between wire and tube is filled with a gas of conductivity k It follows then that

$$\pi b^2 \lambda \frac{\partial^2 \theta}{\partial z^2} + 2\pi b k \frac{\partial \theta}{\partial r}\Big|_{r=b} + I^2 \rho_0 (1 + \alpha\theta)/J = 0, \qquad (1)$$

where $\rho_0 (1 + \alpha\theta)$ is the resistance per unit length of the wire at the temperature $\theta°$ C and b is the radius of the wire

The first two terms multiplied by dz represent the net rate of inflow of heat into the element dz along the wire and over its surface, while the last term multiplied by dz is the rate of generation of heat in dz

If the heat flow from the wire through the gas to the wall of the tube is strictly radial, equation (1) becomes

$$\pi b^2 \lambda \frac{d^2\theta}{dz^2} + 2\pi b h \theta + I^2 \rho_0 (1 + \alpha\theta)/J = 0, \qquad (2)$$

where

$$h = k/b \log_e a/b, \qquad (3)$$

and a is the internal radius of the tube

The solution[*] of equation (2) is as follows

$$\left(\frac{1}{\beta l}\right)^2 \left(1 - \frac{\tanh \beta l}{\beta l}\right) = \frac{2\pi b^2 \lambda J (\bar{R} - R_0)}{R_0^2 I^2 \alpha l}$$

where

$$\beta^2 = \frac{2h}{b\lambda} - \frac{I^2 R_0 \alpha}{2\pi b^2 J \lambda l} \qquad (4)$$

and $2l$ is the length of the wire inside the tube

The substitution in this solution of the necessary measured quantities provides an evaluation of h, which when used with equation (3) yields the gas conductivity k

[*] Kannuluik, 'Proc Roy Soc,' A, vol 131, p 320 (1931), and Weber, 'Ann. Physik, vol 54, p 165 (1917)

An exact solution of equation (1) takes into consideration the fact that the flow through the gas is not radial, but follows lines of heat flow which show some curvature, particularly at the ends of the tube The effect of this curvature on the space factor $b \log_e a/b$ proves to be very small

The exact solution of equation (1) has already been given in detail in a previous paper,* and here the final equation only is shown

$$\pi \,(\bar{R} - R_0)/2R_0 \alpha = C_1 N_{01} - 1/3 \; C_3 N_{03} + 1/5 \; C_5 N_{05} - \quad , \qquad (5)$$

where

$$N_{0n} = I_0\,(nm)/I_0\,(np) - K_0\,(nm)/K_0\,(np),$$

n being odd, and $m \equiv \dfrac{\pi b}{2l}$, $p \equiv \dfrac{\pi a}{2l}$, and

$$C_n = \pm \; 4I^2 \rho_0/n\pi J - \left(\left[\pi b^2 \lambda \left(\frac{n\pi}{2l} \right)^2 - I^2 \rho_0 \alpha/J \right] N_{0n} - 2\pi b k \left(\frac{n\pi}{2l} \right) N_{1n} \right),$$

positive for $n = 1, 5, 9, \quad ,$

negative for $n = 3, 7, 11, \quad ,$

with

$$2\pi b N_{1n} = 2\pi b \; I_1\,(nm)/I_0\,(np) \; N_{0n} + 4l/nl_0\,(nm) \; K_0\,(np),$$

n being odd

The expansions of the Bessel functions I_0, I_1, and K_0 are given in Whittaker and Watson, " Modern Analysis," chap 17

The series on the right-hand side of (5) converges rapidly and the calculation of the first three terms allows k to be obtained by successive approximations

Equations (4) and (5) have each been used in the calculation of k for a number of different representative experiments with each tube In this way the correction is determined, which must be applied to the values of k deduced from the simpler equation (4) The correction is less than 1%

Before equation (4) can be used, λ for the wire must be determined The same apparatus is used to determine both λ and k The tube is evacuated to a pressure of the order 10^{-4} mm. Hg, when the lateral loss by molecular conduction is small enough to be neglected

It has been shown† that λ is given by

$$\lambda = \tfrac{1}{6} \; \frac{\bar{R} R_0 I^2 \alpha l}{\pi b^2 J \,(\bar{R} - R_0)} \left(1 + \tfrac{1}{15} \, \frac{R_0 I^2 \alpha l}{\pi b^2 J \lambda} \right) \left(1 - \tfrac{1}{3} \, \frac{h_r I^2}{b \lambda} \right), \qquad (6)$$

---

* Kannuluık and Martın, ' Proc Roy Soc.,' A, vol 141, p. 144 (1933) We are indebted to Professor T Cherry for this solution.

† Kannuluık, loc. cıt., and Weber, loc. cıt.

where h, cal cm $^{-2}$ sec $^{-1}$ deg $^{-1}$ is the small residual lateral loss of heat by radiation This radiation correction reaches a maximum value in our experiments of 0 5%

Description of Apparatus —We have departed from the usual practice in hot wire work of mounting the wire in a glass tube, preferring with Eucken* to use metal tubes which have the following advantages —

(1) The ends of the wire are maintained exactly at the temperature of the bath, the wire being soldered through thin copper caps, which close the tube

(2) It is unnecessary to correct for a temperature drop through the wall of the tube, and the gas at the wall is everywhere at the temperature of the bath

(3) Eucken† has pointed out that with glass tubes thermal equilibrium is attained very slowly The use of metal tubes considerably decreases the time taken for the steady state to be reached and it can therefore be detected with greater certainty

A thorough test of the possible sources of error in the method and apparatus has been made The space factor has been varied by using two copper tubes of different dimensions, each provided with a copper wire, while the wire material has been varied as well as the space factor, by constructing a third tube of stainless steel provided with a platinum wire In this way two wires are used, the conductivity of one being more than five times that of the other

The principles followed in the construction of the tubes may be inferred from the diagram, fig 1, and a detailed description of the third tube

This tube was of " Two score "‡ stainless steel of internal diameter 1 277 cm and length 10 61 cm The wall was 1 mm thick The tube is closed by thin copper caps approximately 1 mm thick, the lower one being insulated from the tube proper by a copper-glass joint A platinum wire 1 490 mm in

FIG 1

diameter is mounted axially in the tube by soldering it through holes in the end caps which were bored accurately central with respect to the tube by rotating this in a lathe Measurements of the coefficients of linear expansion of different varieties of steel showed that " Two score " had a coefficient of expansion, 0 000010, which is only slightly greater than that of platinum A platinum wire mounted in a stainless steel tube provides a permanent apparatus, and it was used for measuring the conductivity of a series of different gases.

All three tubes were thus compensated for the expansion which occurs in baths of different temperatures The dimensions of the copper tubes are shown in the following table –

Table I —Dimensions of Tubes

Apparatus	Length	Internal diameter	Outer diameter	Diameter of wire
	cm	cm	c m	cm
Cu (1)	15 93	0 950	1 526	0 06106
Cu (2)	10 21	1 592	2 207	0 06120
Pt	10 61	1 277	1 472	0 1490

The copper wires for Cu (1) and Cu (2) were drawn from a piece of Hilger's spectroscopically pure copper rod , the platinum wire was a very pure specimen of this metal by Heraeus The diameters of the wires were measured in terms of standard Johansson gauges using contact methods. Each wire used was circular in section

The metal tubes were constructed in the following manner A length of drawn tube, or solid rod through which a hole had been bored, had forced through it a steel ball-bearing the diameter of which was slightly greater than that of the hole

This produced a smooth central channel which was fairly circular in section but was not quite straight The tube was pressed as near straight as possible, and was then internally lapped with a series of mild steel laps of increasing diameter, the graded abrasive being held in a spiral groove cut in the lap The tube was now mounted with a press fit on a hardened steel mandril which had been carefully ground on centres to be straight (as tested against a Brown and Sharp surface plate) and accurately circular in section The outside was next ground to produce a wall of uniform thickness Great care was taken in this operation as the outer surface controls the centring of the wire The tube

was now relapped until it was found that a steel ball fell through it with a slow uniform speed, when the tube was held vertically with one end closed with adhesive tape

A central section of the tube produced in this manner was used in the construction of the apparatus, the diameter being measured by means of a series of " go " and " no go " plug gauges   The internal diameter of the tube was also contoured by dropping into it a ball bearing, the diameter of which was varied, by heating it to different known temperatures   The greatest variation in diameter found in any tube amounted to 0 002 cm

It may be mentioned here that a slight displacement δ of the wire from the axis of the tube does not lead to appreciable error in the space factor   The expression $b \log_e a/b$ of equation (3) must be replaced by

$$b \log_e \{a/b - a/b \cdot δ^2/(a^2 - b^2)\},$$

and substitution for particular cases shows that in our experiments the positioning was carried out with more than sufficient accuracy

The following sources of error have been the most serious in previous hot wire methods* —

(1) The transfer of heat through the ends of the wire
(2) The temperature discontinuity at the surface of the wire
(3) Heat losses by convection

In our experiments these sources of error are reduced to a minimum   The thermal conductivity λ of the wire is determined with the wire in position   As a result of the temperature discontinuity at the wire and wall surfaces the normal space factor $b \log_e a/b$ must be replaced by

$$b \{\log_e a/b + γ (1/a + 1/b)\},$$

where γ is related to the temperature discontinuity ΔT by the equation of Kundt and Warburg

$$ΔT = -γ \frac{dT}{dn}$$

The wires used by us are much thicker than those used by previous workers so that the term containing γ in the space factor is much decreased   Moreover with our apparatus it is unnecessary to work at low gas pressures   when γ becomes large, in order to eliminate convection   For example, for air, the gas conductivities are independent of the pressure from 60 to 10 cm Hg   It was considered that the independence of k of p over such a wide pressure

* Weber, ' Ann Physik,' vol 82, p 479 (1927).

range constituted sufficient evidence of the absence of convection in this range Accommodation coefficients determined at low pressures are in good agreement with existing data, but in obtaining mean values of k, we have preferred to consider only those values which lie within the pressure range where the effect of the temperature discontinuity has not yet become appreciable

Experimental Procedure

Apart from measuring the geometrical constants of the wire and tube, the experimental part of the work involves the determination of —

(1) The electrical constants, R_0 ohm the resistance of the wire at $0°$ C , and α the temperature coefficient of the wire at $0°$ C

(2) The thermal conductivity λ of the wire

(3) The small change in resistance $(R - R_0)$ ohm of the wire when heated by a suitable current 1 amp

As the success of the experiments depends on the accurate determination of a small change in resistance $(R - R_0)$ corresponding in the majority of cases to a mean rise of temperature of the wire of $4°$ to $6°$ only, it is necessary to make very precise determinations of R_0 For this purpose the pressure of air in the tube is reduced to less than 10^{-4} mm Hg so that the conditions for the application of equation (6) are satisfied For our tubes the term $\left(1 + \frac{1}{10} \cdot \frac{R_0 I^2 \alpha l}{\pi b^3 J \lambda}\right)$ in (6) is only slightly greater than unity and may be calculated with ample accuracy using approximate values of R_0 and λ It is evident from (6) that $1/R$ is a linear function of I^2 multiplied by the factor mentioned above, so that $1/R_0$ can be obtained by extrapolating $1/R$ to zero current This method yields very accurate values of R_0

To determine α the tube is filled with hydrogen, and a very small heating current I is passed through the wire, the resistance of which is determined at the ice point, the steam point and the transition point of sodium sulphate $32\ 383°$ C Assuming that the resistance of the wire is a quadratic function of the temperature, α can be determined from the relation

$$R_t = R_0 (1 + \alpha t + \beta t^2)$$

For the copper wires β is positive, for the platinum wire it is negative While the transition point of sodium sulphate is an excellent fixed point, only material of the highest purity may be used [*] Merck's C R was used

To determine λ the apparatus is evacuated with charcoal and liquid air, and corresponding values of $\bar{R}$ are obtained for a number of different values of I, when λ can be calculated from (6) The calculation of the radiation correction has been described in a previous paper * In these experiments it amounts to approximately 0 5%, being smaller for the tubes (1) and (2) than for (3)

A three dial type of the " thermo-kraft-frei " potentiometer by Wolff is used to measure $\bar{R}$ and R_0, and also the current I amps in terms of a standard 0 01 ohm resistance and a Weston Standard cell

After evaluating λ, the additional measurements required to determine k are a series of corresponding values of $\bar{R}$ and I when the tube is filled with a gas at a series of different pressures The pressures are measured with a U-tube mercury manometer The apparatus is immersed in a Dewar flask containing pure ice and water which is hand stirred vertically The approximate values of k are obtained from equation (4) and these are later reduced so that they agree with the values which would be obtained directly from h

The electrical and thermal constants of each of the three wires are given in Table II

Table II —Constants of Wires

Constants	Cu 1	Cu 2	Pt
R_0 (ohm)	0 00864717	0 00547941	0 00601815
α	0 004257	0 004244	0 003967
β	0 0,42	0 0,37	−0 0,63
λ cal cm $^{-1}$ sec $^{-1}$ deg $^{-1}$	0 949 ± 0 001	0 929 ± 0 001	0 1672 ± 0 0003

The thermal conductivity λ for Cu 2 is somewhat lower than for Cu 1 although each wire was drawn from the same rod of Hilger's spectroscopically pure copper This difference is due to different heat treatment, specimen (2) being rapidly cooled after being heated in an annealing furnace No attempt was made to remove this difference since it provided two copper wires of slightly different conductivity and so gave a check on the method The mean values of λ are obtained from at least six different corresponding values of $\bar{R}$ and I

Representative runs for air, neon, and hydrogen are shown in Tables III, IV, and V respectively In these tables, column five, under the heading of f, gives values of $(1/\beta l)^2 (1 - \tanh \beta l/\beta l)$ The values of k' given in the last

column need to be corrected to the true space factor, and for the temperature of the gas

It will be noticed that the effect of the temperature discontinuity for hydrogen appears at relatively high pressures For the present purpose it is convenient to divide the phenomenon of gas conduction as a function of the

Table III—Conductivity of dry air measured with tube 1   Mean temperature of gas 3 3° C

Pressure	I	$\bar{R} - R_o$	f	β^2	$L' \quad 10^4$
cm	amps	ohm			
75 3	3 7585$_6$	0 00024024	0 1560	0 04814	5 875
60 1	3 7547$_4$	24052	0 1563	0 04800	5 857
44 0	3 7538$_8$	24041	0 1564	0 04793	5 849
28 5	3 7536$_1$	24040	0 1563	0 04800	5 857
17 3	3 7535$_9$	24052	0 1564	0 04792	5 849
19 3	3 7570$_0$	24036	0 1564	0 04792	5 849
5 0	3 7516$_6$	24058	0 1566	0 04782	5 836
0 9	3 7504$_6$	24242	0 1579	0 04712	5 750

Mean L' in pressure range 60 to 10 cm   5 85$_6$ ± 0 007 × 10^{-4} at 3 3° C   Mean k' at 0° C , using a temperature coefficient 0 003, 5 793 × 10^{-4} On using correct space factor, k_o = 5 748 × 10^{-5} cal cm^{-1} sec^{-1} deg^{-1}

Table IV—Conductivity of pure neon measured with tube 3   Mean temperature of gas 1 7° C

Pressure	I	$\bar{R} \quad R_o$	f	β^2	$L' \times 10^5$
cm	amps	ohm			
67 0	4 3280$_6$	0 00008918	0 1503	0 1132	11 28
67 0	4 3280$_4$	8795	0 1503	0 1132	11 28
55 6	4 3261$_2$	8755	0 1502	0 1133	11 29
42 4	4 3262$_4$	8791	0 1502	0 1133	11 29
30 6	4 3264$_9$	8785	0 1501	0 1134	11 30
19 4	4 3263$_6$	8785	0 1501	0 1134	11 30
19 4	3 5475$_5$	5870	0 1492	0 1135	11 31*

* Mean temperature 1 1° C
Mean k' in pressure range 67 0 to 19 4 cm , 11 29$_5$ ± 0 01 × 10^{-5} at 1 7° C   Mean k' at 0° C using a temperature coefficient 0 003, 11 23 × 10^{-5} Using correct space factor k_o = 11 12 × 10^{-5} cal cm^{-1} sec^{-1} deg^{-1}

pressure into two regimes   At relatively high pressures the conductivity is independent of pressure, while at moderately low pressures there is a range determined by the geometry of the apparatus and the mean free path of the gas where the effect of the temperature discontinuity must be taken into account.

This is accomplished by replacing the normal temperature gradient θ/d by $\theta/(d + \Delta)$ where Δ is inversely proportional to the pressure If this correction be introduced into the space factor of the apparatus it can be shown[*] that p/k_0 is proportional to p down to pressures at which molecular conduction appears If p/k_0 and p are plotted using all the data in Table V, a straight line is obtained from which the conductivity is deduced from the cotangent of the angle made with the pressure axis The value so obtained, $k' = 41\ 85 \times 10^6$, is in excellent agreement with the value given above This procedure does not involve a knowledge of the accommodation coefficient itself

Table V —Conductivity of pure hydrogen measured with tube *l* Mean temperature of gas 0 9° C

Pressure	I	R̄ - R_s	f	β²	k × 10⁶
cm	amps	ohm			
63 1	4 2215₄	0 00004280	0 08414	0 2957	41 82
52 6	4 2217₆	4290	8432	0 2951	41 74
38 8	4 2221₆	4284	8402	0 2963	41 90
31 2	4 2318₆	4298	8408	0 2961	41 87
21 8	4 2349₆	4325	8453	0 2940	41 57
10 5	4 2368₆	4362	8515	0 2911	41 16
5 3	4 2371₆	4402	8592	0 2875	40 65
2 6	4 2374₆	4729	9230	0 2617	37 01

Mean k' in pressure range 63 to 31 cm , 41 83 ± 0 05 × 10⁻⁶ at 0 9° C   Mean k' at 0° C , using a temperature coefficient 0 003 = 41 71 × 10⁻⁶ On using correct space factor, $k_0 = 41\ 3 \times 10^{-6}$ cal sec⁻⁴ cm⁻¹ deg⁻¹

It has already been mentioned that a difficulty arises in reducing k to 0° C on account of some uncertainty in the values of the temperature coefficients of k The correction is a small one in this work and it has been sufficient to use one significant figure in the values of the coefficients adopted.

Experimental Results

The methods employed in the preparation of pure gases are those recommended in Traver's " Study of Gases " and in the " Handbuch der Arbeits Methoden in der Anorganischen Chemie," vol 4

Air —The air was dried by passing it through phosphorus pentoxide The carbon dioxide was not removed, as Weber has shown that its presence does not appreciably affect the conductivity of air The results for air are shown in Table VI The values of k' in column 3 are the mean values obtained with each tube, the corresponding gas temperatures being shown in column 2 Column 5 gives the conductivity corrected for temperature, and column 6 the final value for each tube after a correction has been made for the curvature of

---

[*] Gregory and Archer, ' Phil. Mag.,' vol 15, p 301 (1933) , see also Kannuluk and Martin, ' Proc Roy Soc ,' A, vol 141, p 144 (1933)

the lınes of heat flow   Thıs descrıptıon also applıes to further tables gıvıng results for other gases

Table VI —Air

Apparatus	Mean temperature of gas	$k' \times 10^5$	Temperature coefficient	$k' \times 10^5$ at 0° C	$k_0 < 10^{+5}$
	° C				
Cu 1	1 3	$5\ 85_2 \pm 0\ 007$	0 003	5 79	5 75
Cu 2	1 7	$5\ 83_1 \pm 0\ 009$	0 003	5 81	5 76
Pt	1 7	$5\ 84_1 \pm 0\ 006$	0 003	5 82	5 76

Mean value of $k_0 = 5\ 76 \times 10^{-5}$ cal cm $^{-1}$ sec $^{-1}$ deg $^{-1}$

The agreement between the three tubes ıs satısfactory and ıs certaınly much better than we had hoped to obtaın when plannıng these experıments We belıeve that the absolute accuracy ıs somewhat less than ıs ındıcated by thıs table, and ıs probably better than 0 5%

Hydrogen —The apparatus was fırst pumped to an X-ray vacuum, and then fılled wıth pure hydrogen whıch was prepared by passıng commercıal hydrogen through a palladıum tube heated electrıcally to a brıght red   The whole apparatus was washed out several tımes wıth hydrogen so prepared

Table VII —Hydrogen

Apparatus	Mean temperature of gas	$k' \times 10^3$	Temperature coefficient	$k' \times 10^3$ at 0° C	$k_0 \times 10^3$
	° C				
Cu 1	1 3	$41\ 83 \pm 0\ 10$	0 003	41 66	41 3
Cu 2	0 9	$41\ 83 \pm 0\ 05$	0 003	41 71	41 3
Pt	1 7	$41\ 71 \pm 0\ 07$	0 003	41 52	41 2

Mean value of $k_0 = 41\ 3 \times 10^{-5}$ cal cm $^{-1}$ sec $^{-1}$ deg $^{-1}$

Carbon Dıoxıde —Two methods were used to produce pure carbon dıoxıde For tube 1, the gas was produced by heatıng pure magnesıum carbonate, the gas beıng passed through concentrated sulphurıc acıd, and then through phosphorus pentoxıde   For tube 2, pure gas was obtaıned by Lord Rayleıgh's method, ın whıch the gas ıs drawn off an ınverted cylınder after a consıderable volume has been blown off from the cylınder ın the erect posıtıon   The gas was drıed by passıng ıt through phosphorus pentoxıde   As for all gases, the apparatus was fırst pumped to an X-ray vacuum, and was then washed out several tımes wıth the gas, before beıng fılled

Table VIII —Carbon Dioxide

Tube	Mean temperature of gas	$k' \times 10^5$	Temperature coefficient	$k' \times 10^5$ at 0° C	$k_0 \times 10^5$
Cu 1	2 4	3 492 + 0 024	0 004	3 46	3 44
Pt	2 0	3 508 ± 0 008	0 004	3 48	3 43

Mean value of $k_0 = 3\ 43 \times 10^{-5}$ cal cm^{-1} sec^{-1} deg^{-1}

Oxygen —The gas was prepared by heating potassium permanganate and was then passed through concentrated sulphuric acid and over phosphorus pentoxide

Table IX —Oxygen

Tube	Mean temperature of gas	$k \times 10^5$	Temperature coefficient	$k \times 10^5$ at 0° C	$k_0 \times 10^5$
	°C				
Cu 1	2 7	5 929 + 0 006	0 003	5 88	5 84
Pt	1 7	5 913 ± 0 009	0 003	5 88	5 82

Mean value of $k_0 = 5\ 83 \times 10^{-5}$ cal cm^{-1} sec^{-1} deg^{-1}

In view of the excellent agreement in the results obtained with the different tubes for air, hydrogen, carbon dioxide, and oxygen, the conductivities of the remaining gases, carbon monoxide, nitrous oxide, and the inert gases, helium, neon, and argon, have been measured with the platinum wire tube only

Carbon Monoxide and Nitrous Oxide —Carbon monoxide was obtained by the interaction of pure concentrated sulphuric acid and pure sodium formate The carbon dioxide present was removed by passing the gas through caustic potash, and the gas was finally dried by passing it through phosphorus pentoxide

Nitrous oxide was generated by heating pure ammonium nitrate to a temperature not greater than 250° C , thus preventing the formation of nitric oxide The gas was passed over caustic potash and then through concentrated sulphuric acid and phosphorus pentoxide

Monatomic Gases —The helium and neon used in this work were obtained from the British Oxygen Company, and the argon from Philips Lamp Company (Holland) The certificates supplied with these gases gave the neon and argon as 100% pure and the helium 100% pure except for a trace of neon. The conductivities of helium were determined for the gas as received and after it

Table X —Carbon Monoxide and Nitrous Oxide

Gas	Mean temperature of gas	$k' \times 10^5$	Temperature coefficient	$k' \times 10^5$ at 0° C	$k_a \times 10^5$
	°C				
Carbon monoxide	1 7	5 447 +0 008	0 001	5 420	5 37
Nitrous oxide	2 0	3 677 ±0 006	0 004	3 645	3 61

had been passed through charcoal immersed in liquid air   It was found that the second value was approximately 2% greater than the first, and this is probably due to the adsorption by the charcoal of the trace of neon stated to be present   The same procedure was adopted with neon, but here no change was observed in the conductivity

It was also our intention to pass the argon over heated calcium to eliminate possible impurities, but on account of an accident to the apparatus this has been postponed to a further series of experiments on temperature coefficients   However, the conductivity of the argon as received has been measured, and comparison of the value obtained with the values of other observers seems to imply the absence of any appreciable impurity, as this would certainly lead to a higher value

Table XI —Inert Gases

Gas	Mean Temperature of gas	$k' \times 10^5$	Temperature coefficient	$k' \times 10^5$ at 0° C	$k_a \times 10^5$
Helium	2 0	34 83 ±0 02	0 003	34 62	34 30
Neon	1 7	11 29 +0 01	0 003	11 23	11 12
Argon	2 0	3 88 ±0 009	0 003	3 86	3 82

Discussion of Results

Table XII contains the thermal conductivities at 0° C obtained by the authors, together with those for the same gases obtained by Weber and by Gregory, Archer, and Marshall, all of whom have carried out extensive series of very careful measurements using some form of the hot wire method   Our values appear to be in fair agreement with those given by Weber, particularly with his more recent values for air, carbon dioxide, and neon. There is some divergence, however, between our values and those of Gregory, Archer, and Marshall, who obtain values which are, for some gases, 2% or 3% greater than ours.   Unfortunately serious errors may easily be introduced in reducing

Table XII —$k_0 \times 10^5$ cal sec $^{-1}$ deg $^{-1}$ cm $^{-1}$

| Gas | K and M | Weber | | G A and M |
		1917	1927	
Air	5 76	5 68	5 740	5 85
H₂	41 3	41 65	—	40 43
CO₂	3 43	3 393	3 431	3 60
O₂	5 83	5 768		5 89
CO	5 37	—		5 63
N₂O	3 61	3 530	—	3 74
He	34 3	34 38		—
Ne	11 12	10 89	11 04	—
Ar	7 82	7 850		—

conductivities to 0° C For example, with air, Gregory and Archer studied the conductivity over a temperature range 7 4° C to 12 1° C and in reducing the conductivity to 0° C were obliged to extrapolate some 7° The value of the temperature coefficient implied in this extrapolation was 0 00297 Weber has studied the variation of the conductivity of air over a range of temperatures extending from 3° C to 18 5° C and finds a temperature coefficient of 0 00365, which he points out if used to reduce the data of Gregory and Archer leads to a value for the conductivity at 0° C of $5\ 76 \times 10^{-5}$ This value agrees with that found by Weber and ourselves It may be added, however, that the value of the temperature coefficient used by Gregory and Archer is in excellent agreement with the value given by Laby and Nelson in the International Critical Tables

In the single experiment on hydrogen, Gregory and Archer give a smaller conductivity than either Weber or ourselves An examination of the results of Gregory and Archer lead us to suppose that they have not made a sufficient correction for the temperature "discontinuity," and that when the necessary correction is applied, their result is in excellent agreement with ours

The value found by Weber for this gas is nearly 1% greater than ours As Weber in his purification process passed the gas slowly over charcoal immersed in liquid air, this discrepancy may be accounted for by the presence in his hydrogen of a greater proportion of para-hydrogen than is typical of the ordinary gas

It has been shown* that ordinary hydrogen, which is a mixture of ortho- and para-hydrogen present in the ratio of 3 to 1, if allowed to remain in contact

---

* Bonhoeffer and Harteck, ' Z phys. Chem ,' B, vol 4, p. 113 (1929), Eucken and Hiller, ' Z. phys Chem ,' B, vol 4, p 163 (1929), Dennison, 'Proc Roy Soc ,' A, vol 115, p 483 (1927)

with charcoal at the temperature of liquid air suffers a transformation, the equilibrium mixture now being one in which the ratio of ortho- to para- is 1 2 1   This mixture is quite stable and persists for a considerable time after the gas has been raised again to room temperature   The specific heat of the ordinary 3 to 1 mixture is 2 44R, while that of the mixture characteristic of the liquid air temperature is 2 49R, and since the thermal conductivity is proportional to the specific heat, a 2% increase in conductivity might be expected as a result of the change at the low temperature

While it is probable that in Weber's purification process the gas was moving too quickly through the charcoal to be transformed to the equilibrium mixture, Senftleben[†] has shown that a very marked change (sufficiently great to be easily demonstrated to a large audience) takes place even in a minute or two, and it might therefore be reasonably expected that Weber's value will be higher than the real value for ordinary hydrogen

Maxwell's Relation $k_0 = \varepsilon \eta_0 c_v$ —Table XIII gives values of k_0, the viscosity η, and c_v, while the fifth column shows the constant ε for the different gases calculated from

$$\varepsilon = k_0 / \eta_0 c_v$$

The values obtained for ε for helium, argon, and neon agree well with the value 2 5 deduced theoretically for monatomic gases by Maxwell, Chapman, and Enskog[‡]

Table XIII

Gas	$L_0 \times 10^5$	$\eta_0 \times 10^5$	c_v	ε	$\frac{1}{4}(9\gamma - 5)$
He	34 3	18 76	0 746	2 45	2 44
Ne	11 12	29 81	(0 150)*	(2 50)	2 44
Ar	3 82	21 02	0 0745	2 44	2 44
H_2	41 3	8 60	2 43	2 00	1 90
Air	5 76	17 22	0 171	1 96	1 91
O_2	5 83	19 31	0 157	1 92	1 95
CO	5 37	16 65	0 178	1 81	1 91
CO_2	3 43	13 74	0 153	1 64	1 72
N_2O	3 61	13 66	0 155	1 71	1 73

c_v values   Partington and Shilling, ' Specific Heats of Gases, ' p 201 (1924), Landolt and Bornstein, ' Supp.,' vol 2, Table 264A, p 1227 (1931)
η_0 values   Landolt and Bornstein (*loc cit*)
* c_v calculated from $\frac{5}{2}R$

[†] ' Z, phys Chem.,' B, vol. 4, p 169 (1929)
[‡] Jeans, " The Dynamical Theory of Gases," chap 12

Eucken has suggested a formal combination of Chapman's expression $k_0 = 5/2 \eta_0 c_v$ and the well-known equation $c_v = 3/2 (1 + \beta) R/Jm$ for polyatomic gases The sixth column contains the values of $\frac{1}{4} (9\gamma - 5)$ which according to this method of introducing the rotational energy of polyatomic molecules should equal ϵ

Summary

The thermal conductivities of the gases, air, H_2, CO_2, O_2, CO, N_2O, He, Ne, and Ar, have been measured using a hot wire method The method is based on an exact theory for the flow of heat from an electrically heated short thick wire mounted axially in a metal tube maintained at a uniform temperature

The apparatus realizes completely the requirements of the theory, is simple in construction and rapid in working Measurements carried out on several gases with three separate pieces of apparatus show excellent agreement These differ not only in their dimensions, but also in the material of the axial wire

Possible sources of error in hot wire methods generally are discussed, and our results are compared with previous determinations for the above gases by other workers

The constant ϵ in the kinetic theory relation $k_0 = \epsilon \eta_0 c_v$ is evaluated for the above gases The values of ϵ obtained for He, Ne, and Ar are in good agreement with Chapman's theoretical value 2 5 for a monatomic gas

The Calculation of Wave Resistance

By T H Havelock, F R S

1 The wave resistance of a body moving in a frictionless liquid has been calculated by various methods In a few cases it has been found directly as the resultant of the fluid pressures on the surface of the body Another method, which has been more generally useful, involves the introduction of a certain type of fluid friction into the equations of motion The wave resistance is then found by calculating the rate of dissipation of energy and taking the limiting value when the frictional coefficient is made vanishingly small This method has certain important analytical advantages, nevertheless it is highly artificial A third method, dealing directly with a frictionless liquid, consists in examining the flow of energy in the wave motion , this has hitherto been used only for two-dimensional problems when the wave motion consists of simple waves with straight parallel crests, the usual theory of group velocity being directly applicable

In the following note this method is extended to three-dimensional fluid motion Although no new special results are obtained so far as expressions for wave resistance are concerned, it seemed of sufficient interest to obtain them by this direct method, namely, by considering the flow of energy and the rate of work across planes far in advance and far in the rear of the moving body

These quantities are examined first for a free wave pattern of simple type Then a general expression is given for wave resistance in terms of the velocity potential of the free wave pattern to which the disturbance approximates at a great distance in the rear, and this is applied to a general form of wave pattern and to some special cases Finally, a similar examination is made of a certain problem when the water is of finite depth

2 With the origin O in the free surface of deep water, and Oz vertically upwards, the surface condition is

$$\frac{\partial^2 \phi}{\partial t^2} - g \frac{\partial \zeta}{\partial t} = 0, \qquad z = 0, \tag{1}$$

where ϕ is the velocity potential and ζ the surface elevation For a wave

pattern advancing steadily with velocity c in the direction Ox, we may write (1) in the form

$$\frac{\partial^2 \phi}{\partial z^2} + \kappa_0 \frac{\partial \phi}{\partial z} = 0, \qquad z = 0, \tag{2}$$

with $\kappa_0 = g/c^2$

A simple plane wave advancing in a direction making an angle θ with Ox is given by

$$\left. \begin{array}{l} \zeta = a \sin \{\kappa_0 \sec^2 \theta \ (x \cos \theta + y \sin \theta - ct \cos \theta)\} \\[2mm] \phi = ac \cos \theta\, e^{\kappa_0 z \sec^2 \theta} \cos \{\kappa_0 \sec^2 \theta \ (x \cos \theta + y \sin \theta - ct \cos \theta)\} \end{array} \right\} \tag{3}$$

We may generalize this to obtain a free wave pattern made up of plane waves advancing in all directions, so that the pattern itself moves steadily with velocity c in the direction Ox, we have then

$$\zeta = \int_{-\frac{1}{2}\pi}^{\frac{1}{2}\pi} f(\theta) \sin \{\kappa_0 \sec^2 \theta \ (x \cos \theta + y \sin \theta - ct \cos \theta)\}\, d\theta \tag{4}$$

We shall suppose in the first place that the pattern is symmetrical with respect to Ox, so that we have

$$\left. \begin{array}{l} \zeta = 2 \int_0^{\frac{1}{2}\pi} f(\theta) \sin (\kappa_0 x' \sec \theta) \cos (\kappa_0 y \sin \theta \sec^2 \theta)\, d\theta \\[2mm] \phi = 2c \int_0^{\frac{1}{2}\pi} f(\theta)\, e^{\kappa_0 z \sec^2 \theta} \cos (\kappa_0 x' \sec \theta) \cos (\kappa_0 y \sin \theta \sec^2 \theta) \cos \theta\, d\theta \end{array} \right\}, \tag{5}$$

with $z' = x - ct$

Consider a fixed vertical plane $x = \text{constant}$ The rate of flow of total energy across this plane is given by

$$\tfrac{1}{2}\rho c \int_{-\infty}^{0} dz \int_{-\infty}^{\infty} \left\{ \left(\frac{\partial \phi}{\partial x}\right)^2 + \left(\frac{\partial \phi}{\partial y}\right)^2 + \left(\frac{\partial \phi}{\partial z}\right)^2 \right\} dy + \tfrac{1}{2} g \rho c \int_{-\infty}^{\infty} \zeta^2\, dy \tag{6}$$

The variable part of the fluid pressure being $\rho \partial \phi / \partial t$, or $- \rho c \partial \phi / \partial x$, the rate at which work is being done across the same plane is

$$\rho c \int_{-\infty}^{0} dz \int_{-\infty}^{\infty} \left(\frac{\partial \phi}{\partial x}\right)^2 dy \tag{7}$$

We shall assume that the wave pattern is such that these quantities are finite and determinate

To evaluate these expressions with the values (5) for ϕ and ζ we use the following theorem

If

$$F_1(y) = \int_0^\infty (A_1 \cos yu + B_1 \sin yu)\, du,$$
$$F_2(y) = \int_0^\infty (A_2 \cos yu + B_2 \sin yu)\, du,$$

(8)

A, B, being functions of u, then

$$\int_{-\infty}^\infty F_1(y)\, F_2(y)\, dy = \pi \int_0^\infty (A_1 A_2 + B_1 B_2)\, du,$$

(9)

assuming that the integrals are convergent

To take one of the integrals in (6) as an example we have

$$\frac{\partial \phi}{\partial x} = -2\kappa_0 c \int_0^{\frac12 \pi} f(\theta)\, e^{\kappa_0 z \sec^2 \theta} \sin (\kappa_0 x' \sec \theta) \cos (\kappa_0 y \sin \theta \sec^2 \theta)\, d\theta$$

(10)

To put this into the form (8), we write $u = \kappa_0 \sin \theta \sec^2 \theta$, then carry out the process (9) and finally replace the variable u in terms of θ, it is clear that we shall have to introduce into the integral in the final form a factor $d\theta/du$, that is, a factor $\cos^2 \theta/\kappa_0 (1 + \sin^2 \theta)$ Thus we have

$$\int_{-\infty}^0 dz \int_{-\infty}^\infty \left(\frac{\partial \phi}{\partial x}\right)^2 dy$$
$$= 4\pi\kappa_0 c^2 \int_{-\infty}^0 dz \int_0^{\frac12 \pi} \{f(\theta)\}^2\, e^{2\kappa_0 z \sec^2 \theta} \sin^2 (\kappa_0 x' \sec \theta)\, \frac{\cos^2 \theta\, d\theta}{1 + \sin^2 \theta}$$
$$= 2\pi c^2 \int_0^{\frac12 \pi} \{f(\theta)\}^2 \sin^2 (\kappa_0 x' \sec \theta)\, \frac{\cos^2 \theta\, d\theta}{1 + \sin^2 \theta}$$

(11)

From (6) we find in this way that the rate of flow of total energy across the vertical plane is

$$\pi \rho c^3 \int_0^{\frac12 \pi} \{f(\theta)\}^2 \{(3 - \sin^2 \theta) \sin^2 (\kappa_0 x' \sec \theta)$$
$$+ (1 + \sin^2 \theta) \cos^2 (\kappa_0 x' \sec \theta)\} \frac{\cos^2 \theta\, d\theta}{1 + \sin^2 \theta},$$

(12)

and that the rate at which work is being done across this plane is

$$2\pi \rho c^3 \int_0^{\frac12 \pi} \{f(\theta)\}^2 \sin^2 (\kappa_0 x' \sec \theta)\, \frac{\cos^2 \theta\, d\theta}{1 + \sin^2 \theta}$$

(13)

It is the difference of these two quantities that is significant for our purpose, it is, as would be expected, independent of the time and of the position of the

plane Subtracting (13) from (12), we find that the rate at which energy is being propagated less the rate of work reduces to the simple expression

$$\pi \rho c^3 \int_0^{\frac{1}{2}\pi} \{f(\theta)\}^2 \cos^3 \theta \, d\theta \tag{14}$$

It may be noted that if we take mean values of (12) and (13) we have as the mean rate of flow of energy

$$2\pi \rho c^2 \int_0^{\frac{1}{2}\pi} \{f(\theta)\}^2 \frac{\cos^3 \theta}{1 + \sin^2 \theta} \, d\theta, \tag{15}$$

and as the mean rate of work

$$\pi \rho c^3 \int_0^{\frac{1}{2}\pi} \{f(\theta)\}^2 \frac{\cos^5 \theta}{1 + \sin^2 \theta} \, d\theta \tag{16}$$

The connection indicated in (15) and (16) is a generalization of the well-known result for simple plane waves that the mean rate of work is half the mean rate of flow of energy

3 Consider now the forced wave pattern produced by a body moving through the liquid, or by a localized pressure disturbance The complete surface elevation may be separated into a local disturbance and a wave pattern In a frictionless liquid a possible solution is one in which the wave pattern extends to an infinite distance in advance of the body as well as in the rear The determinate practical solution is that for which the wave pattern vanishes at a great distance in advance, and we may suppose this obtained by superposing over the whole surface a suitable free wave pattern In that case, considering the flow of energy and rate of work across two fixed vertical planes, one far in advance and the other far in the rear, we see that (14) is equal to Rc, where R is the wave resistance Hence we have

$$R = \pi \rho c^2 \int_0^{\frac{1}{2}\pi} \{f(\theta)\}^2 \cos^3 \theta \, d\theta, \tag{17}$$

when the wave pattern at a great distance to the rear approximates to the form (4)

For example, the forced wave pattern produced by a submerged sphere, or more precisely by a horizontal doublet of moment M moving at depth f, approximates at a great distance behind the disturbance, to the free wave pattern

$$\zeta = \frac{4\kappa_0 M}{c} \int_{-\frac{1}{2}\pi}^{\frac{1}{2}\pi} \sec^4 \theta \, e^{-\kappa_0 f \sec^2 \theta} \sin \{\kappa_0 (x' \cos \theta + y \sin \theta) \sec^2 \theta\} \, d\theta \tag{18}$$

Hence, from (17), the wave resistance is

$$R = 16\pi\kappa_0 M^2 \int_0^{\frac{1}{2}\pi} \sec^5\theta \, e^{-2\kappa_0 f \sec^2\theta} \, d\theta, \tag{19}$$

which is the known result for this case

4 Before generalizing these results we may put (6) and (7) into an explicit form for the wave resistance

The kinetic energy of the liquid in a strip between two parallel vertical planes at a distance δx apart is

$$\tfrac{1}{2}\rho \, \delta x \int_{-\infty}^{\infty} dz \int_{-\infty}^{0} \left\{ \left(\frac{\partial\phi}{\partial x}\right)^2 + \left(\frac{\partial\phi}{\partial y}\right)^2 + \left(\frac{\partial\phi}{\partial z}\right)^2 \right\} dy \tag{23}$$

Transform (23) into the equivalent form of a surface integral over the boundaries of this portion of fluid, assuming the wave pattern to be such that the various integrals are convergent Thus we obtain the rate of flow of kinetic energy across a vertical plane as

$$\tfrac{1}{2}\rho c \int_{-\infty}^{\infty} \left(\phi \, \frac{\partial\phi}{\partial z} \right)_{z=0} dy + \tfrac{1}{2}\rho c \int_{-\infty}^{0} dz \int_{-\infty}^{\infty} \left\{ \phi \, \frac{\partial^2\phi}{\partial x^2} + \left(\frac{\partial\phi}{\partial x}\right)^2 \right\} dy \tag{24}$$

Further, we may transform the other terms in (6) and (7) by using the surface condition (2) together with $g\zeta = -c\partial\phi/\partial x$ at $z = 0$

Finally, equating the difference between (6) and (7) to Rc, we obtain for the wave resistance

$$R = \frac{\rho}{2\kappa_0} \int_{-\infty}^{\infty} \left\{ \left(\frac{\partial\phi}{\partial x}\right)^2 - \phi \, \frac{\partial^2\phi}{\partial x^2} \right\}_{z=0} dy - \tfrac{1}{2}\rho \int_{-\infty}^{0} dz \int_{-\infty}^{\infty} \left\{ \left(\frac{\partial\phi}{\partial x}\right)^2 - \phi \, \frac{\partial^2\phi}{\partial x^2} \right\} dy \tag{25}$$

In this expression ϕ is the velocity potential of the free wave pattern to which the disturbance approximates at a great distance in the rear Considering the disturbance produced by a body of any form, it appears that this free wave pattern must be expressible, in general, in the form

$$\zeta = \int_{-\frac{1}{2}\pi}^{\frac{1}{2}\pi} f(\theta) \sin\{\kappa_0 \sec^2\theta \,(x'\cos\theta + y\sin\theta)\} d\theta$$

$$+ \int_{-\frac{1}{2}\pi}^{\frac{1}{2}\pi} F(\theta) \cos\{\kappa_0 \sec^2\theta \,(x'\cos\theta + y\sin\theta)\} d\theta, \tag{26}$$

that is, in the form

$$\zeta = \int_0^{\frac{1}{2}\pi} (P_1 \sin A \cos B + P_2 \cos A \sin B + P_3 \cos A \cos B + P_4 \sin A \sin B) \, d\theta,$$

where $A = \kappa_0 x' \sec\theta$, $B = \kappa_0 y \sin\theta \sec^2\theta$ \hfill (27)

The corresponding velocity potential is

$$\phi = c \int_0^{\frac{1}{2}\pi} (P_1 \cos A \cos B - P_2 \sin A \sin B - P_3 \sin A \cos B$$
$$+ P_4 \cos A \sin B) \, e^{\kappa_0 \sec^2 \theta} \cos \theta \, d\theta \quad (28)$$

With this value of ϕ in (25), we use (8) and (9) to evaluate the integrations with respect to y as in § 2, and we obtain readily the general result

$$R = \frac{1}{2}\pi\rho c^2 \int_0^{\frac{1}{2}\pi} (P_1^2 + P_2^2 + P_3^2 + P_4^2) \cos^3 \theta \, d\theta \quad (29)$$

The actual calculation of the quantities P for a body of given form is, of course, another problem. Methods in use at present amount to replacing the body by some approximately equivalent system of sources and sinks; the functions P then appear, in general, in the form of integrals taken over the surface of the body. We need not consider these here as the expressions for R given above lead to the same results as those obtained previously by different methods.

5. It is of interest to examine a similar problem when the water is of finite depth h. It is clear from the derivation of (25) that we may use it in this case also, taking the lower limit of integration with respect to z to be $-h$ instead of $-\infty$.

For the simple symmetrical type of free wave pattern given by (4), the corresponding velocity potential is

$$\phi = 2c \int_0^{\frac{1}{2}\pi} f(\theta) \, \frac{\cosh \kappa (z + h)}{\sinh \kappa h} \cos (\kappa z' \cos \theta) \cos (\kappa y \sin \theta) \cos \theta \, d\theta, \quad (30)$$

the relation between κ and θ being

$$\kappa - \kappa_0 \sec^2 \theta \tanh \kappa h = 0 \quad (31)$$

We shall assume first $\kappa_0 h > 1$, that is $c^2 < gh$, so that (31) as an equation for κ has one real root for each value of θ in the range of integration. In evaluating (25) we carry out the integrations with respect to y by means of (8) and (9). For this we have to change from an integration in θ to one in a variable u given by

$$u = \kappa \sin \theta, \quad (32)$$

together with (31). The corresponding factor $d\theta/du$ has now the value

$$\frac{\cos^2 \theta (\coth \kappa h - \kappa h \operatorname{cosech}^2 \kappa h)}{\kappa_0 (1 + \sin^2 \theta - \kappa_0 h \operatorname{sech}^2 \kappa h)} \quad (33)$$

We have, for example,

$$\int_{-h}^{0} dz \int_{-\infty}^{\infty} \left(\frac{\partial \phi}{\partial x}\right)^2 dy$$

$$= 4\pi c^2 \int_{-h}^{0} dz \int_{0}^{\frac{1}{2}\pi} \{f(\theta)\}^2 \frac{\cosh^2 \kappa (z+h) (\coth \kappa h - \kappa h \operatorname{cosech}^2 \kappa h)}{\kappa_0 \sinh^2 \kappa h (1 + \sin^2 \theta - \kappa_0 h \operatorname{sech}^2 \kappa h)}$$

$$\times \sin^2 (\kappa x' \cos \theta) \kappa^2 \cos^2 \theta \, d\theta$$

$$= 2\pi c^2 \int_{0}^{\frac{1}{2}\pi} \{f(\theta)\}^2 \frac{\coth^2 \kappa h - \kappa^2 h^2 \operatorname{cosech}^2 \kappa h}{\kappa_0 (1 + \sin^2 \theta - \kappa_0 h \operatorname{sech}^2 \kappa h)} \sin^2 (\kappa x' \cos \theta) \kappa \cos^2 \theta \, d\theta \quad (34)$$

Evaluating the remaining terms in (25), we obtain after a little reduction the result

$$R = \pi \rho c^2 \int_{0}^{\frac{1}{2}\pi} \{f(\theta)\}^2 (\coth \kappa h - \kappa h \operatorname{cosech}^2 \kappa h) \cos^3 \theta \, d\theta, \quad (35)$$

with κ given in terms of θ by (31)

This may be compared with (17) for the similar wave pattern in deep water

For a horizontal doublet M at depth f in water of depth h, an expression for the complete surface elevation can be derived from results given previously [*] We have

$$\zeta = \frac{M}{\pi c} \int_{-\pi}^{\pi} d\theta \int_{0}^{\infty} \frac{\cosh \kappa (h-f) e^{i\kappa (x \cos \theta + y \sin \theta)}}{\cosh \kappa h (\kappa - \kappa_0 \sec^2 \theta \tanh \kappa h + i \mu \sec \theta)} \kappa^3 d\kappa, \quad (36)$$

where we take the limiting value of the real part for $\mu \to 0$

From this we may easily deduce the free wave pattern to which the disturbance approximates at a great distance in the rear It is given by

$$\zeta = \frac{4\kappa_0 M}{c} \int_{-\frac{1}{2}\pi}^{\frac{1}{2}\pi} \frac{\cosh \kappa (h-f) \tanh^2 \kappa h \sec^4 \theta}{\cosh \kappa h (1 - \kappa_0 h \sec^2 \theta \operatorname{sech}^2 \kappa h)} \sin \{\kappa (x' \cos \theta + y \sin \theta)\} \, d\theta \quad (37)$$

From (35) this gives

$$R = 16\pi \rho \kappa_0 M^2 \int_{0}^{\frac{1}{2}\pi} \frac{\kappa^2 \cos \theta \cosh^2 \kappa (h-f)}{\cosh^2 \kappa h (1 - \kappa_0 h \sec^2 \theta \operatorname{sech}^2 \kappa h)} \, d\theta \quad (38)$$

It will be found that this agrees with the result obtained by a different method in the paper just quoted, when the previous expression is corrected for an obvious slip, in formula (37) of that paper 32 should be replaced by 16 and $\tanh \kappa h (1 + \tanh \kappa h)$ by $(1 + \tanh \kappa h)^2$

---

[*] 'Proc Roy Soc,' A, vol 118, p 32 (1928)

When $\kappa_0 h < 1$, that is $c^2 > gh$, the equation (31) for κ has a real root only for a more limited range of values of θ, the lower limit being $\theta_0 = \cos^{-1}\sqrt{(\kappa_0 h)}$ instead of zero It is readily seen that the expression for R will be as in (38) with θ_0 as the lower limit of the integral

Summary

An examination is made of the transfer of energy in a free wave pattern, and expressions for wave resistance are deduced These are applied to certain cases both for deep water and for water of finite depth

---

Structures of the Metallic Carbonyl and Nitrosyl Compounds

By N V Sidgwick, F R S, and R W Bailey

Our knowledge of the compounds containing carbonyl and nitrosyl (NO) groups attached to metallic atoms has been greatly extended in recent years, largely through the work of Hieber and Manchot and their collaborators , but the structures which have been suggested, especially for the nitrosyl derivatives, are not in every way satisfactory In this paper an attempt is made to establish the structures of these compounds on a firmer basis

1 Carbonyl Compounds

The nature of the linkage formed between carbon monoxide and a metallic atom is now well established In its complexes the CO group occupies one co-ordination place as donor—it provides two electrons to form a single link — as is shown, for example, by the ferrous pentacyano-compounds of the general formula $M_3[Fe(CN)_5X]^*$ where X may be CO, H_2O, NH_3, pyridine, etc This formation of a single link is in agreement with the Langmuir formula for carbon monoxide,[†]

$$\text{I} \quad \text{C} \ \ \text{O} \quad \bar{\text{C}} \equiv \overset{+}{\text{O}} \qquad \text{II} \quad \text{M} \ \ \text{C} \ \ \text{O} \quad \bar{\text{M}} - \text{C} \equiv \overset{+}{\text{O}}[‡]$$

which has been shown[§] to be supported by the electrical dipole moment, the

---

* Gmelin-Kraut, " Handbuch d. anorg Chem ," ' Iron,' B, pp 740, 1046, 1066, etc

† ' J Amer Chem Soc ,' vol 41, p. 1543 (1919)

‡ In the structural formulae given above, the charges assigned to the atoms are those which they would have if the electrons were equally shared. For the purpose of this paper the symbol $\bar{\text{A}} - \overset{+}{\text{B}}$ for the co-ordinate link is more convenient than $\text{A} \leftarrow \text{B}$, which means the same thing.

§ See Hammick, New, Sidgwick and Sutton, ' J Chem Soc ,' p 1876 (1930) , Sidgwick, ' Chem. Rev ,' vol 9, p 77 (1931)

interatomic distance, the heat of formation, the force constant and the parachor The CO molecule is obviously capable of co-ordinating as donor with another atom, either through the carbon or the oxygen It is more probable that the link is formed through the carbon as in II, since (I) the 4-covalent condition is the normal state of the carbon atom, whereas it only rarely (e g , in " basic " beryllium acetate $Be_4O(O \cdot CO \cdot CH_3)_6$) occurs with oxygen, and (2) similar types of co-ordination compounds are formed by the isocyanides, for example with the cyanides of the metals Co, Ni, Cu, Ag, Cd, and with other salts, as in $[Pt(CH_3NC)_4]PtCl$ and $[Pt(CH_3NC)_6Cl_2]$ * Here the link must be formed through the carbon (which is in precisely the same state as in carbon monoxide), since the nitrogen has no unshared electrons The arguments that follow would not, however, be affected if we supposed the carbonyl group to be attached through the oxygen

This structure (II above), involving a triple link between the carbon and the oxygen, is strongly supported by the observation of Sutton and Bentley† that the electrical dipole moment of nickel carbonyl is zero Unless the M—C—O group were linear, the molecule must have a moment owing to the rotation of the groups, as occurs with methyl and ethyl orthocarbonic esters $C(O \cdot CO \cdot R)_4$ The fact that a CO group can replace an H_2O or NH_3 in a complex shows that the link to the metal is single, and this is only compatible with a linear grouping of the atoms M—C—O if the C—O link is triple The Raman spectrum of nickel carbonyl confirms the presence in it of a triple link of carbon to oxygen ‡

We may therefore accept the structure $\overset{-}{M}-C \equiv \overset{+}{O}$ as established Now five monometallic carbonyls (i e , containing only one metallic atom in the molecule) are known

	$Cr(CO)_6$§	$Fe(CO)_5$‖	$N(CO)_4$	$Mo(CO)_6$¶	$W(CO)_6$**
E A N	Cr 36	Fe 36	Ni 36	Mo 54	W 86

* Hofmann and Bugge, ' Ber deuts chem Ges,' vol. 40, p 1774 (1907), Tschugaev and Teearu, ibid , vol. 47, p 570 (1914)

† ' Nature,' vol. 130, p 314 (1932), Sutton, New and Bentley, ' J Chem Soc,' p 652, (1933)

‡ Anderson, ' Nature,' vol 130, p 1002 (1932)

§ Job and Cassal, ' Bull. Soc Chim ,' vol. 41, p. 1041 (1927)

‖ Mond and Langer, ' J Chem Soc ,' vol. 59, p 1091 (1891) , Gmelin Kraut, " Handbuch d anorg. Chem.," ' Iron,' B, p 486

¶ Mond, Hirtz and Cowlap, ' J Chem Soc ,' vol. 97, p 798 (1910) , Mond and Wallis, ibid., vol 121, p 34 (1922) The analyses varied between $Mo(CO)_5$ and $Mo(CO)_6$, but the analogy of the chromium and tungsten compounds fixes the composition.

** Job and Rouvillois, ' C R Acad. Sci. Paris,' vol 187, p. 564 (1928)

It is generally recognised that in all these the effective atomic number (E A N the total number of electrons, shared and unshared, in the molecule , in these compounds the atomic number increased by 2 for every CO) of the metallic atom is that of the next following inert gas, as is shown above * This fact, which explains why monometallic carbonyls are not formed by elements of odd atomic number, is very remarkable As a rule it is found that the stability of a molecule depends, not on the total number of electrons in the E A N , but separately on the number in the core and that in the valency group In these substances, however (which are all derivatives of the transitional elements of Periodic Groups VI, VII and VIII), the determining factor seems to be the total number, irrespective of how it is divided between the shared and the unshared electrons , thus the numbers are (the shared electrons are underlined) —

$$Cr(CO) \quad Cr = \quad 2, 8, 14, \underline{12} = 36$$
$$Fe(CO) \quad Fe = \quad 2, 8, 16, \underline{10} = 36$$
$$Ni(CO) \quad Ni = \quad 2, 8, 18, \underline{8} = 36$$
$$Mo(CO) \quad Mo = \quad 2, 8, 18, 14 \ \underline{12} = 54$$
$$W(CO) \quad W = \quad 2, 8, 18, 32, 14, \underline{12} = 86$$

It does not, however, seem to have been noticed that there is a further remarkable regularity in the composition of the carbonyls, which extends to those that contain more than one atom of metal in the molecule (the poly-metallic carbonyls) If we calculate the average E A N of the metallic atoms, by adding 2 to the atomic numbers for every CO, then the difference between the result and the atomic number of the next inert gas is always found to be one less than the number of metallic atoms in the molecule If we write the compound $M_x(CO)_y$, and if m is the atomic number of M, and G that of the next inert gas, then the equation

$$G - \frac{x \ m + 2y}{x} = x - 1 \qquad (1)$$

is always found to be true Where $x = 1$ (monometallic carbonyls) we have seen that this holds throughout The other known pure carbonyls (containing only metallic atoms and CO groups) are the following , the molecular

---

* This was given by Langmuir ('Science,' vol. 54, p 65 (1921)) as the cause of the stability of iron and nickel carbonyls, and also accounts for the diamagnetism of these compounds , Oxley, 'Proc Camb Phil Soc ,' vol 16, p 102 (1911)

weights of all are known, and they are all derivatives of iron or cobalt, so that G always equals 36

$$Fe_2(CO)_9*† \quad \frac{2 \times 26 + 2 \times 9}{2} = 35 \quad x = 2$$

$$Fe_3(CO)_{12}‡ \quad \frac{3 \times 26 + 2 \times 12}{3} = 34 \quad x = 3$$

$$Co_2(CO)_8† \quad \frac{2 \times 27 + 2 \times 8}{2} = 35 \quad x = 2$$

$$Co_4(CO)_{12}§ \quad \frac{4 \times 27 + 2 \times 12}{4} = 33 \quad x = 4$$

This equation, with the appropriate modifications for other groups in the molecule, can be shown to hold also for the great majority of metallic derivatives containing carbonyl groups, and, if we accept the view of the nitrosyl group proposed in the second part of this paper, for the majority of the nitrosyl derivatives as well We may fairly assume that in these polymetallic compounds the rule still applies that the E A.N is that of the next inert gas|| and that the necessary increase in the number of available electrons is secured by further co-ordination, which holds these atoms together It is very improbable that the metallic atoms are united directly, as this form of linkage is practically unknown except with mercury, but it is obvious that the CO group is capable of forming a second co-ordinate link through the oxygen as donor, as in $M \leftarrow C \equiv O \rightarrow M$ or $M \xleftarrow{-} \overset{+}{C} \equiv \overset{-}{O} \to M$ Since equation (1) holds for these compounds, it follows that when the number of M atoms in the molecule is 2, 3 and 4, the number of extra electrons needed in the molecule to make up the E A N of every M to that of the next inert gas is 2, 6 and 12, and hence the number of new co-ordinate links required is 1, 3, and 6 respectively This implies that every metallic atom in the molecule is joined to every other

---

* Mond and Langer, 'J Chem Soc' vol 59, p 1092 (1891), Dewar and Jones, 'Proc Roy Soc,' A, vol 76, p 573 (1905), Speyer and Wolf, 'Ber deuts chem Ges, vol 60, p 1424 (1927)

† Mond, Hirtz and Cowap, 'J Chem Soc,' vol 97, p 798 (1910)

‡ Dewar and Jones, 'Proc Roy Soc,' A, vol 79, p 75 (1907), Freundlich and Cuy, 'Ber deuts chem Ges,' vol 56, p 2265 (1923)

§ Hieber, Mühlbauer and Ehmann, 'Ber deuts chem Ges.,' vol 65, p 1090 (1932)

|| This is supported by the fact that $Fe_2(CO)_9$ and $Fe_3(CO)_{12}$ are diamagnetic, like $Fe(CO)_5$ and $Ni(CO)_4$, Freundlich, 'Ber deuts chem Ges,' vol 56, p 2264 (1923), Berkmann and Zocher, 'Z phys Chem,' vol 124, p 318 (1926)

through a link of this kind   For two such atoms this is secured by joining them through a single CO, for three, by placing them at the angular points of a triangle with a CO on each side, and for four by placing them at those of a tetrahedron, with a CO group on each edge

These curious relations may be regarded in two ways   either (a) they depend on the validity of equation (1), or (b) they are connected with the linear, triangular, and tetrahedral structures   For $x = 2$, 3, or 4, either hypothesis gives the same result, but for higher values of x they differ   If equation (1) is the determining factor, then since that involves a link between every metallic atom and every other, and since for physical reasons these links must obviously be of the same length, no value of x greater than 4 is possible, for we cannot have more than four points equidistant from one another in space   As a fact no carbonyls with more than four metallic atoms in the molecules are known, and this may be the reason , or it may only be an accident that they have not yet been discovered   If the real principle is the adoption of a series of simple geometrical forms (together with the attainment of the inert gas number), then we might expect the tetrahedron to be followed by an octahedron, and that by a cube   For an octahedron, with a CO on each edge, the formulæ which would give each M an inert gas number are $Fe_6(CO)_{12}$, $Co_6(CO)_{15}$, and $Ni_6(CO)_{18}$ These do not satisfy equation (1), which would require x to be 5, not 6   A cube, with 8 points and 12 sides, would give the same result as a tetrahedron (4 and 6) and so is not likely to occur

The structures assigned on this hypothesis to $Fe_2(CO)_9$, $Fe_3(CO)_{12}$, and $Co_4(CO)_{12}$, $Fe_4(CO)_{14}$, which we should expect to exist, have not been obtained are given in figs 1 to 3

The crystal structures of the first two of these structures have been examined by Brill *   We are much indebted to Mr H M Powell for the following note on Brill's results—

With $Fe_2(CO)_9$ Brill finds that the substance crystallizes in the hexagonal system, and concludes that the symmetry of the molecule is either C_3, C_{3v}, C_{3h}, D_3, or D_{3h}, but he does not determine the atomic positions   The structure he suggests is different from that given in fig 1, and has three layers of three CO's each, with the two iron atoms, which must both lie on a threefold symmetry axis, between them   But in a note (p 89) he says " It is possible to bring some of the CO's into onefold positions   This leads to crowding of the threefold axis, and is chemically

---

* $Fe_2(CO)_9$, ' Z Kristallog ,' vol 65, p 89 (1927), $Fe_3(CO)_{12}$, *ibid*, vol 77, p 36 (1931)

not very probable " The proposed formula I has the symmetry C_{3v}, or, if one group of three CO's is rotated relative to the other through an arbitrary angle, C_3 it could therefore be put into some of the possible space groups found by Brill   We have no independent evidence of the disposition in space of five covalencies (which cannot in any event be
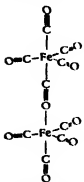
FIG 1—Fe₂(Co)₉.
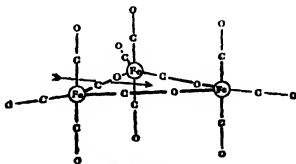
FIG 2—Fe₃(CO)₁₂.
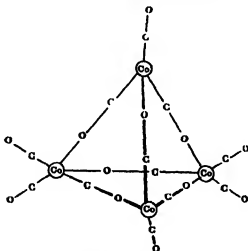
FIG 3.—Co₄(CO)₁₂.

symmetrically equivalent in three dimensions), but that given in fig 1 is at least as probable as any   Moreover, the dimensions required by the formula agree with Brill's observations   The long vertical axis is $O = C - Fe - C = O - Fe - C = O$, if we may assume the two valencies of the iron to be at 180° this must be linear, as the X-ray results show it to be , if we take the lengths of the links to be C = O

1 14   C — Fe 0 77 + 1 27 = 2 04   O — Fe 0 70 + 1 27 = 1 97,*
the distance between the centres of the terminal oxygen atoms should
be 11 5 A   The whole height of the cell according to Brill is 15 8 A ,
which means that the distance between the centres of two neighbouring
oxygens in different molecules is 4 3 A   This is about the usual value ,
in graphite two carbon atoms in different sheets (*i e ,* molecules) are
3 4 A apart, in benzene hexachloride two such chlorines are 3 74 A
apart †   Thus there is no undue crowding on the threefold axis, and
the structure, fig 1, proposed for $Fe_2(CO)_9$ in no way conflicts with the
X-ray evidence

With $Fe_3(CO)_{12}$ the X-ray evidence is less easy to interpret   The molecule
has symmetry C_3 Formula 11, fig 2, can be given symmetry very near
to C_2 if we distort the triangle slightly in the direction of the arrow
shown in the figure, which then represents the twofold axis   This is on
the assumption that a carbon and an oxygen atom are indistinguishable,
which is probable since on the proposed structure each has the same
number of electrons   The formula which Brill prefers requires at least
as much distortion to make it fit the observations

It might be objected to these formulae that they involve too great a strain
in the ring, the chain of atoms M — C ≡ O — Fe being in its unstrained con-
dition linear   But we may assume that the natural angle between the two
nearest valencies of a 5-covalent atom does not exceed 90°, as in fig 1   Hence
in the triangle, fig 2, the total strain is 3 (90° — 60°) = 90°, and this is
divided among 9 atoms, giving only 10° per atom, which is to be compared
with the strain of 50° per atom in cyclopropane, or 20° per atom in cyclo-
butane

In addition to the pure carbonyls, there are a large number of mixed deriva-
tives which contain CO groups, and of these the majority, though not all,
when their E A N 's are calculated in the usual way, give the values required
by equation (1) , they must therefore be supposed to have similar structures.
Thus we can have one or more of the CO groups replaced by an equal number
of other donor molecules such as ammonia or pyridine (*py*), or two CO groups
by a chelate molecule (*i e.,* one containing two donor atoms in positions suitable
for forming a ring) such as ethylene diamine (*en*) (I), the di-ethyl ether of
dithioglycol (*th*) (II), or *o*-phenanthroline (*phth*) (III)

---

* These distances are taken from Sidgwick, " The Covalent Link," pp. 85, 88 (1933)

† Hendricks and Bilicke, ' J Amer Chem Soc.,' vol. 48, p. 3007 (1926)

Examples are $Fe(CO)_2(py)\ddagger$, $Fe(CO)_2(py)_2\|\|$, $-(NH_2)_2\S$, $Fe(CO)_2(en)\|\|**$,
$-(phth)\dagger\dagger$, $Ni(CO)_2(phth)\ddagger\ddagger$, and among the polymetallic compounds
$Fe_2(CO)_5(en)_2*\dagger**$, $-(phth)\dagger\dagger$ and $Ni_2(CO)_4(py)_2\ddagger\ddagger$ In all these the E A N
remains 36, and the covalency of the simpler carbonyls (5 for iron, 4 for
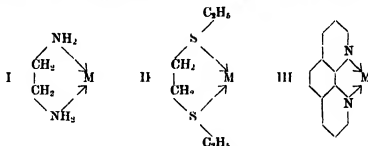
nickel)   In another series we find the E A N preserved, but the covalency
increased for iron from 5 to 6   The most remarkable of these is the volatile
hydrogen compound $H_2Fe(CO)_4$ §§   This is a volatile unstable yellow liquid
melting about $-68°$ C, which is formed by the action of alkalis on iron penta-
carbonyl

$$Fe(CO)_5 + 2[OH]^- = Fe(CO_4)H_2 + [CO_3]^{--}$$
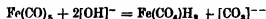
It is obvious from its volatility that it is covalent, and it gives a series of deriva-
tives in which the hydrogens are replaced by halogens, as in $Fe(CO)_4Cl_2$,
$-Br_2$, $-I_2,\|\|$ or by mercury, as in $Fe(CO)_4Hg$ $Fe(CO)_4(HgCl)_2$, $-(HgBr)_2$,
$-(HgI)_2,\|\|$ or they can be replaced by metals with the formation of salts,
and the reduction of the covalency to 5 or 4, as in $Fe(CO)_4H[Na]$,
$Fe(CO)_4H_2Ba]$, $Fe(CO)_4[Cd]$ ¶¶   Similar derivatives are known with
several metallic atoms in the molecule, and these still satisfy equation (1),
examples are $Fe_2(CO)_7Br_2\|\|$ and $Fe_3(CO)_9Br_6$ (molecular weight determined) ¶
We also find compounds containing both halogens and co-ordinated molecules,
such as $Fe(CO)_2Cl_2(phth)$, $-Br_2(phth)$, $Fe(CO)_2I_2(th)$, $-(py)_2$ ¶

---

* Hieber and Sonnekalb, 'Ber deuts chem Ges,' vol 61, p 558 (1928)

† Hieber and Bader, ibid , p 1717 (1928)

‡ Hieber and Sonnekalb, ibid , p 2421

§ Hieber, 'SitzBer heidelberg Akad. Wiss,' vol 3, p 4 (1929)

‖ Hieber and Becker, 'Ber deuts chem Ges,' vol 63, p 1405 (1930)

¶ Hieber, 'Z anorg Chem,' vol 201, p 329 (1931)

** Hieber and Leutert, 'Ber deuts chem Ges,' vol 64, p 2832 (1931)

†† Hieber and Mühlbauer, ibid , vol 65, p 1082 (1932)

‡‡ Hieber, Mühlbauer and Ehmann, ibid , p 1090

§§ Hieber and Leutert, 'Naturwiss,' vol 19, p 360 (1931)

‖‖ Gmelin Kraut, "Handbuch d. anorg. Chem ," 'Iron,' B, pp 499–502

¶¶ Feigl and Krumholz, 'Z anorg Chem,' vol 215, p 242 (1933)

Some examples of the working out of the E A.N and of the size of the valency group may be given —

$$Fe(CO)_3(en) \qquad 26 + 2 \times 3 + 4 \qquad = 36 \quad 2, 8, 16, \underline{10,}$$

$$H_2Fe(CO)_4 \qquad 26 + 2 \times 2 \times 4 \qquad = 36 \quad 2, 8, 14, \underline{12,}$$

$$Fe(CO)_4H[Na] \qquad 26 + 2 \times 4 + 1 + 1 \qquad = 36 \quad 2, 8, 16, \underline{10,}$$

$$Fe_2(CO)_5(en)_2 \qquad \frac{2 \times 26 + 2 \times 5 + 2 \times 4}{2} = 35 \qquad x = 2,$$

$$Fe_2(CO)_6Br_6 \qquad \frac{3 \times 26 + 2 \times 9 + 6}{3} = 34 \qquad x = 3$$

The rule is obeyed equally by other series of compounds in which CO replaces water or ammonia in recognized complexes, as in the pentacyano-compounds $M_3[Fe(CH)_5(CO)]$ already mentioned   It is clear that this rule expresses the condition of stability of metallic atoms of the transitional elements attached to carbonyl groups

II *Nitrosyl Compounds*

The nitrosyl compounds have one or more NO groups attached to a metallic atom   In their preparation and properties they show a close analogy to the carbonyls   They are commonly formed by the same metals , they are usually prepared by the direct action of nitric oxide, as the carbonyls are by that of carbon monoxide, and often these two gases can drive one another out of their respective compounds *   We may therefore expect to find that the nitrosyls and the carbonyls have analogous structures

The suggestion that the metallic nitrosyls are derivatives of hyponitrous acid

N—OH
$\|$ has been sufficiently refuted by Manchot †   They are formed from
N—OH

nitric oxide and not from hyponitrous acid, except under conditions where the latter forms nitric oxide, they readily liberate nitric oxide (as the carbonyls liberate carbon monoxide) with acids, whereas the hyponitrites with acids give nitrous oxide   Also this assumption would require us to double the formulae of many of them, such as the nitroprussides and generally those which have

---

* Manchot and Schmidt, 'Z anorg Chem ,' vol 216, p 99 (1933)

† Manchot and Davidson, 'Ber deuts chem Ges.,' vol 62, p 684 (1929)   See also Manchot and Schmidt, 'Z anorg Chem ,' vol 216, p 103 (1933)   It is not impossible that metallic complexes derived from hyponitrous acid may occur, but they are not found among the normal nitrosyls.

one NO to one metallic atom , there is no evidence in favour of this, and much against it

We may therefore conclude that each NO group is separately attached to the metal, and the first question is what is the nature of the attachment   It can be shown that this is a single co-ordinate link M ← by the fact that it is possible to replace a CO by an NO in a series of complexes of the co-ordination number 6   Examples of these are given in Table I

Table I

K₄[Mn(CN)₅(NO)]*	K₄[Fe(CN)₅(CO)]	K₃[Mn(CN)₆]
K₄[Fe(CN)₄(NO)]†	K₄[Fe(CN)₅(H₂O)]	K₄[Fe(CN)₆]
K₃[Ru₂(CN)₄(NO)]††		
K₂RuCl₄(NO)‡		K₄[Ru(CN)₆]
[Ru(NH₃)₄Cl(NO)] Br₂§		
K₄[OsCl₄(NO)]‖		K₃[OsCl₆]
		K₄[Os(CN)₆]

* Manchot and Schmidt, ' Ber deuts. chem Ges.,' vol 59, p 2360 (1926)
† Manchot and Düsing, ibid , vol. 63, p 1226 (1930)
‡ Joly, ' C. R. Acad Sci Paris,' vol 107, p. 994 (1888) , Howe, ' J Amer Chem Soc ,' vol
16, p. 388 (1894) , Manchot and Schmidt, ' Z anorg Chem ,' vol 216, p 99 (1933)
§ Rosenbohm, ' Z. phys. Chem ,' vol 93, p 693 (1919)
‖ Wintrebert, ' Ann Chim Phys , vol 28, p 15 (1903)

Of these compounds the nitroprussides M₂[Fe(CN)₅(NO)] are the most familiar, and in this anion, as we have seen, the NO can be replaced not only by CO, but also by H₂O, NH₃, and other molecules , the replacement is always accompanied by a fall in the electrovalency of the anion, which will be discussed later   The suggestion that the NO is doubly linked to the metal cannot be entertained   The co-ordination number 6 (group of 12 shared electrons) is universal in complexes of the pentacyano-type, and is, as Werner showed, the commonest of all complex forms , a co-ordination number 7 is almost unknown throughout chemistry, and has never been observed with these transitional metals   Moreover, for iron and manganese a co-ordination number greater than 6 is not only unknown, but is impossible according to the covalency rule *   We may therefore take it as proved that the metal is joined to the NO by a single co-ordinate link   That the attachment is through the nitrogen is shown by the fact that the nitroso-group in these compounds can be oxidized to a nitro-group

If we accept these conclusions, there are three structures possible for the M—N—O group

* Sidgwick, " Electronic Theory of Valency," p 152 (1927).

(1) It may contain a true nitroso-group M — N = O, as in the organic nitroso-compounds This view cannot be maintained, the nitrosyls are devoid of the characteristic tendency of the nitroso-compounds to polymerize with loss (or change) of colour, also this structure would involve the assumption of valencies for the metallic atoms for which there is no parallel elsewhere, such as the quadrivalency of iron in the nitroprussides. Moreover, Werner and Karrer* have obtained a complex salt which has the characteristics of such a true nitroso-derivative This is [Co(NH₃)₅(NO)]X₂, a series of salts were prepared They occur in a black monomolecular form which changes to a red dimeric form These belong to quite a different type from the nitrosyls, regarded as nitroso-compounds they correspond to [Co(NH₃)₅Cl]Cl₂, and the cobalt is trivalent, as it normally is in its 6-co-ordination compounds

(2) It might be supposed that they are formed by simple co-ordination, by the sharing of a lone pair of electrons of the nitrogen in the nitric oxide molecule with the metal, without any further change occurring Then the mysterious link—presumably of 5 electrons—which exists in nitric oxide must be maintained in the nitrosyls This link, however, is, so far as we know, except in nitric oxide and perhaps in a few of its organic derivatives, too unstable to exist, and it may be expected to pass over in the complex into some more normal form Moreover on this hypothesis that the N—O link is the same in the complex as in nitric oxide (which is the one most generally accepted for the nitroprussides), the replacement of CO by NO should involve no other change in the molecule, whereas in fact it is always accompanied by a change in the electrovalency, as from K₄Fe(CN)₆(CO)] to K₄Fe(CN)₆(NO)] (see Table I) This second hypothesis is quite unable to account for such changes

(3) The close similarity between nitric oxide and carbon monoxide, and between the nitrosyls and the carbonyls, suggests that the structures of the latter are similar, and that there is a triple link between the nitrogen and the oxygen giving M — N ≡ O, corresponding to M — C ≡ O But nitric oxide has one more electron than carbon monoxide (balanced of course by an extra positive charge on the nitrogen nucleus), this electron, if it does not remain as part of an "odd-electron" N—O link, must go somewhere We have evidence of this tendency of the NO link to lose an electron in the existence of positive [NO]⁺ ion, which has been established by Hantzsch and Berger † They have shown that nitrosyl perchlorate [NO]ClO₄ is anhydrous, and gives a conducting solution in nitromethane, and that the so-called "nitrosulphonic

---

* 'Helv Chem Acta,' vol 1, p 54 (1918).

† 'Z. anorg. Chem,' vol 190, p. 321 (1930)

acid " which is usually written NO_2SO_3H, is dissociated in concentrated
sulphuric acid, and is no doubt nitrosyl hydrogen sulphate $[NO]\,SO_4\,H$. Another
salt of this type is nitrosyl fluoborate $[NO]BF_4$, obtained* by treating con-
centrated aqueous fluoboric acid with oxides of nitrogen, which has been shown†
to have this composition and is no doubt free from water   It is thus evident that
a cation $[NO]^+$ can exist   This forms with $[CN]$ and CO a series of diatomic
molecules with identical electronic arrangements, as shown in Table II   The
positions of the electrical charges, on the simplifying assumption that the
electrons are shared equally, are given in the second line of symbols ; every
atom in these molecules has 2 unshared and 6 shared electrons, equivalent
to a total of 5, which gives the residual charges as $C - 1$, N zero, $O + 1$
If we suppose a combination of the neutral groups CN, CO, NO with a metallic
atom M, we get the structures given in the table for M—C—N, etc , the CN
group contributes one electron to the E A N of the metal (normal covalency),
the CO two (co-ordinate link), while the NO, in addition to the 2 for the co-
ordinate link, adds a third, by the total transference of an electron from
the NO to the M, and thus contributes three   These charges diminish the
electrovalency of the complex by 1 and 2 respectively, as is shown in the
formulæ of the pentacyano-compounds at the foot of the table

Table II

$[\,C \quad N\,]^-$	$C \quad O$	$[\,N \quad O\,]^+$
$\bar{C} \quad N$	$\bar{C} \quad \overset{+}{O}$	$N \quad \overset{+}{O}$
$M \quad C \quad N$	$M \quad C \quad O$	$M \quad N \quad O$
$M — C \equiv N$	$\bar{M} — \bar{C} - \overset{+}{O}$	$\overset{--}{M} - \overset{+}{N} - \overset{+}{O}$
$K_4[Fe(CN)_6]$	$K_3[Fe(CN)_5(CO)]$	$K_2[Fe(CN)_5(NO)]$

If we make this assumption that the NO group, though it is only attached
to the metal by a single link of two shared electrons, yet contributes a further
electron, and counts as 3 towards the E A N of M, the whole series of nitrosyl
compounds given in the left-hand column of Table I is brought into
line with the other complexes of these metals, in the other two columns ‡

---

* Wilke Dörfurt and Balz, *ibid.*, vol 159, p 197 (1927)

† 'Z anorg Chem ,' vol 190, p 321 (1930)

‡ Reiff, 'Z anorg Chem ,' vol 202, p 376 (1931) suggests that this contribution of
three electrons made by the NO to the E A N of the metallic atom explains the existence
and the diamagnetism of $Co(CO)_3(NO)$ (see below), but he does not seriously discuss the
nature of the linkage

Thus the nitroprussides are $M_2[Fe(CN)_5(NO)]$ while the corresponding carbonyl compounds are $M_3[Fe(CN)_5(CO)]$, if we allow for the extra electron going to the iron in the former, this makes the nitroprussides, like their carbonyl analogues, ferrous and not ferric compounds Now among all the known compounds of the type $M_n[Fe(CN)_5X]$, where X may be CN, NO_2, AsO_2, SO_3, H_2O, NH_3, or CO,* it is always found that the ferrous are more stable than the ferric, the latter when they occur have ferrous analogues, but the reverse is not true, in particular, there is no ferric analogue of $M_3[Fe(CN)_5(CO)]$ It is therefore definitely in favour of this view that it represents the nitroprussides as ferrous compounds, the anomaly of a stable ferric pentacyano-compound with no ferrous equivalent is thereby removed In the same way the manganese in the compound in Table I has the same valency as in the colourless cyanide $K_3[Mn(CN)_6]$, and the ruthenium compound as in the only stable cyanide of ruthenium $K_4[Ru(CN)_6]$ Further, the E A N of the elements in Table I is Mn, Fe 36 Os 86, that is, the nitrosyl like the carbonyl derivatives follow the inert gas rule

Another way of retaining the E A N when a CO is replaced by an NO is to replace at the same time the central atom by an atom with an atomic number less by 1 This is illustrated by the remarkable series of volatile compounds analogous to nickel carbonyl

	$Ni(CO)_4$	$Co(CO)_3(NO)$ †	$Fe(CO)_2(NO)_2$‡
	°C	°C	°C
B Pt	43	78 6	110
M Pt	−23	−1 1	+18

Hieber and Anderson who prepared the iron compound from iron ennea-carbonyl $Fe_3(CO)_9$, draw attention to this parallelism, and recognize (as Reiff also does with respect to the cobalt compound) that the NO group contributes an extra electron, they point out that we might expect to get $Mn(CO)(NO)_3$ and $Cr(NO)_4$, although the marked instability of the iron derivative make this rather improbable They suppose, however, that the NO is attached by a double link (four shared electrons) to the metal, which would make the cobalt 5- and the iron 6-covalent This is not only an unnecessary complication, but

---

* See Gmelin Kraut, "Handbuch d anorg Chem, 'Iron,' B, pp 732–742

† Mond and Wallis, 'J Chem Soc,' vol 121, p 34 (1922), Reiff, 'Z anorg Chem,' vol 202, p 375 (1931), Hieber and Anderson, *ibid.,* vol 211, p 132 (1933)

‡ Hieber and Anderson, *loc cit.,* and *ibid*, vol 208, p 238 (1932), the boiling point of the cobalt compound is given by mistake as 48 6°

as we have seen it cannot be applied to the manganese and iron nitrosyl compounds in Table I, because it would give them a covalency of 7, which is above their maximum   The marked rise in the boiling point as we go from the nickel to the iron compound is sufficiently accounted for by the considerable dipole moment which the $\overset{+}{M} - \overset{+}{N} \equiv \overset{+}{O}$ group must give to the molecule

This method of formulation further explains the characteristic colour reaction of the nitroprussides with the sulphides   They do not react with hydrogen sulphide, but on addition of alkali or of an alkaline sulphide to the solution the deep purple colour of $M_4[Fe(CN)_5(NOS)]$ at once appears, showing that the reaction is with the sulphide ion *   In the same way hydroxyl ions convert the nitroprussides into nitro-compounds $M_4[Fe(CN)_5(NO_2)]$ †   It is evident that the strongly positive $\overset{+}{N} \equiv \overset{+}{O}$ group attracts the negative OH^- or S^- (or HS^-) ions, with the production of a nitro or thionitro-group

$$M - \overset{+}{N} \equiv \overset{+}{O} \quad \longrightarrow \quad M - N\overset{\textstyle O}{\underset{\textstyle O}{\diagup}} \quad \text{or} \quad M - N\overset{\textstyle S}{\underset{\textstyle O}{\diagup}}$$
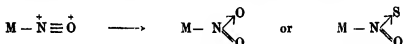
This reaction involves the withdrawal of two electrons from the central atom, and hence, in order to maintain the E A N, an increase of the electrovalency by two, the products having four atoms of M instead of two in the molecule

It is particularly to be observed that in all the nitrosyl compounds hitherto mentioned this method of formulation involves the inert gas rule being maintained   This rule is so nearly universal among the carbonyls that it is a strong support of our hypothesis that it involves its extension to the nitrosyls as well   For a molecule $M_x(CO)_y(NO)_z$ we get the equation

$$G - \frac{xm + 2y + 3z}{x} = x - 1, \qquad (2)$$

which expresses the composition of the carbonyl-nitrosyls of iron and cobalt given above   Many mixed nitrosyl derivatives comply with this equation, such as $Fe(NO)_2(phth)$ and $Co(CO)(NO)(phth)$ ‡   It is important to note that equation (2) holds for nitrosyls containing more than one metallic atom

---

* Virgili, 'Z analyt Chem ,' vol 45, p 409 (1906)

† Cambi and Szegö, 'Rend Acc Lincei,' vol 5, p 737 (1927), 'Gazz Chim Ital,' vol 58, p 71 (1928)   This is usually formulated as a nitrito-compound $M - O - N = O$, but according to Werner, "Neuere Anschauungen," pp 131, 339 (1913), the stable form when M is a transitional element is the true-nitro-form $M - NO_2$

‡ Hieber and Anderson, 'Z anorg Chem ,' vol 211, p 132 (1933)

ın the molecule   One example ıs $Fe_2(NO)_6(py)_2$, * here, sınce each pyrıdıne molecule, lıke a CO, adds two electrons, we have

$$g - \frac{2 \times 26 + 3 \times 4 + 2 \times 3}{2} = 36 - 35 = 1$$

$$(x = 2)$$

Others are the curıous " red and black salts of Roussın," whıch have long been known †   Theır formulæ are $M_2[Fe_2(NO)_4S_2]$ (red, unstable) and $M[Fe_4(NO)_7S_3]$ [black, stable]   The black salts are obtaıned by the actıon of nıtrıc oxıde or nıtrıtes on ıron salts ın the presence of sulphıdes , alkalıes convert them ınto the red serıes, whıch are unstable and readıly revert to the black The molecular weıghts of the black salts have been confırmed by conductıvıty measurements ‡   Those of the red serıes are known through theır esters, whıch Hofmann and Wıede§ prepared by the actıon of nıtrıc oxıde on a mıxture of ferrous sulphate and ethyl mercaptan , they found theır molecular weıght ın solutıon to correspond to the formula $(C_2H_5)_2Fe_2(NO)_4S_2$ On the probable assumptıon that the sulphur ıs doubly lınked to the metal (ın the ıon as $Fe = S$,

contrıbutıng two electrons, ın the ester as $\overrightarrow{Fe} = \overset{+}{S} - C_2H_5$, contrıbutıng three, and so compensatıng for the dısappearance of the ıonıc charge) these compounds satısfy equatıon (2)

$$M_2[Fe_2(NO)_4S_2] \qquad \frac{2 \times 26 + 3 \times 4 + 2 \times 2 + 2}{2} = 35 \qquad x = 2$$

$$Fe_2(NO)_4(S \quad C_2H_5)_2 \qquad \frac{2 \times 26 + 3 \times 4 + 2 \times 3}{2} = 35 \qquad x = 2$$

$$M[Fe_4(NO)_7S_3] \qquad \frac{4 \times 26 + 3 \times 7 + 3 \times 2 + 1}{2} = 33 \qquad x = 4$$

Thıs ımplıes for the black salts a tetrahedral structure, lıke that gıven for $Co_4(CO)_{12}$ ın fıg 3

Among the nıtrosyl compounds descrıbed ın the lıterature there are a number whıch do not comply wıth thıs rule   Some could be brought ınto lıne wıth ıt by assumıng a suffıcıent degree of polymerızatıon, and the substances ın

---

* Hıeber and Anderson, Z anorg Chem,' vol 211, p 132 (1933)

† Gmelın Kraut, *loc cıt*, 'Iron,' B, pp 471-487 , Manchot and Lınckh, 'Ber deuts chem Ges,' vol 59, p 407 (1926), Manchot and Gall, *ıbıd* , vol 60, p 2318 (1927) , Manchot and Lehmann, 'Lıebıgs Ann ,' vol 470, p 255 (1929)

‡ Marchlewskı and Sachs, 'Z anorg. Chem ,' vol 2, p 181 (1892) , Belluccı and Carne valı, 'Rend. Acc Lınceı,' vol 16, p 654 (1907)

§ 'Z anorg Chem ,' vol 9, p 301 (1895)

question are obviously polymerized, but we do not know to what extent
Some give support to our general theory of the structure of the nitrosyl group,
though not to the particular rule   Such are the carbonyl and nitrosyl deriva-
tives of copper   The molecular weights and hence the complete structures of
these compounds are unknown, but it is clear that the stable forms contain one
carbonyl* or one nitrosyl† group to one copper atom. Now the carbonyl
compounds are all derived from cuprous copper, as Cu(CO)Br, and the nitrosyls
from cupric copper, as Cu(NO)Cl₂ and Cu(NO)SO₄   It is evident that the
extra electron contributed by the NO balances the defect in the copper   Other
substances, such as Manchot's iron tetranitrosyl (Fe(NO)₄)ₙ,‡ must obviously
have some totally different structure   But it is submitted that the method
of formulation which we have proposed accounts for the composition and
behaviour of the great majority of nitrosyl compounds, and brings their
structures into conformity with those of the very similar carbonyls

Summary

1 *Carbonyl Compounds* —These contain the group $\overset{-}{M} - C \equiv \overset{+}{O}$ For all
carbonyls $M_x(CO)_y$, $G = \dfrac{x \, m + 2y}{x} = x - 1$ (m = atomic number of M, G of
next inert gas) $x = 1$, 2, 3, or 4   When $x = 1$, M has effective atomic
number (E A N) of inert gas   Assuming this to be true when $x > 1$, M atoms
must be held together thus $\overset{-}{M} - \overset{+}{C} \equiv \overset{-}{O} - \overset{+}{M}$, if the molecule contains 2M
they must have one such link , if 3, they must be at the angles of a triangle
with a CO in each side , if 4, at the points of a tetrahedron with a CO on each
edge   The crystal structures of $Fe_2(CO)_9$ and $Fe_3(CO)_{12}$ are compatible with
this   Nearly all carbonyl derivatives follow these rules, with necessary
modifications for the other groups present

II *Nitrosyl Compounds* —In $M - N - O$ the nitrogen is attached by two
shared electrons to M   But when NO replaces CO in a complex the negative
electrovalency falls by 1 $M_3[Fe(CN)_5(CO)]$, $M_2[Fe(CN)_5(NO)]$ This is
explained if the structure is M N   O   or $\overset{-}{M} - N \equiv \overset{+}{O}$, corresponding to

M C   O   or $\overset{-}{M} - C \equiv \overset{+}{O}$, and the NO contributes there electrons to the
E A N of M, as CO contributes two

* Wagner, 'Z anorg Chem ,' vol 196, p 364 (1931)
† Manchot, 'Liebigs Ann ,' vol 375, p 308 (1910) , 'Ber deuts chem Ges.,' vol 47,
p 1601 (1914), Manchot and Linckh, *ibid.*, vol. 59, p 407 (1926)
‡ Manchot and Enk, 'Liebigs Ann ,' vol. 470, p. 275 (1929)

On this hypothesis the structures of the great majority of nitrosyl derivatives are shown to follow precisely the same rules as the carbonyls The changes in electrovalency of the anions, and the similarity of the volatile compounds $Ni(CO)_4$, $Co(CO)_3(NO)$, $Fe(CO)_2(NO)_2$ are explained, and the nitrosyls with several metallic atoms in the molecules are shown to obey an equation corresponding to that given above

---

An Annual Perturbation in the Range of Tide

By R H Corkan, M Sc , Liverpool Observatory and Tidal Institute

(Communicated by A T Doodson, F R S —Received November 17, 1933)

1 Introduction

In the following paper the existence is established of an annual perturbation in the range of tide The perturbation became evident during an intensive examination, by a method* described in the paper, of the residual semi-diurnal tide at Liverpool Direct analysis† of hourly heights for an annual perturbation in the principal constituent of semi-diurnal tide showed the perturbation to be consistent from year to year, and to exist generally in British Waters, and throughout the world at large Analysis of high and low waters further confirmed the results A study of the general distribution of the perturbation provided a number of interesting results, as also did a study of its relation with local meteorological conditions

The paper concludes with a short discussion on possible causes of an annual perturbation in the range of tide

2 Observed and Synthesized Tides

It is a noteworthy feature of Doodson's method of analysis in that it provides for each species of tide (diurnal, semi-diurnal, etc) two numerical quantities for each solar day Thus the hourly heights are treated in the

---

* The method, which is new, is described in detail in Appendix I It is dependent upon Doodson's method of tidal analysis, and was first indicated in his paper on the " Analysis of Tidal Observations," ' Phil Trans.' A, vol 227, p 223 (1928).

† See Appendix II

first place as though the tide were solar and the semi-diurnal part of it expressible in the form

$$R \cos (30° \, t - \varepsilon) = P \cos 30° \, t + Q \sin 30° \, t,$$

where

$t =$ the time in solar hours from a fixed hour of the day,

$\varepsilon/30 =$ the time of high water in solar hours,

$$P = R \cos \varepsilon \quad \text{and} \quad Q = R \sin \varepsilon$$

The numerical processes of analysis give each day two quantities, related to P and Q, which are almost entirely free from perturbations by diurnal and other species of tide The values change from day to day, and computed quantities are precisely defined at a certain fixed hour of the day Essentially therefore, P and Q determine what we may regard as the average tide for the day The observational values not only show the regular variations to be expected from the normal tidal constituents but they also show erratic day to day changes, obvious on account of their magnitude It is clear, therefore, that the method is of very great value, even if the analysis for the tidal constituents is not affected, in providing observational data for meteorological perturbations of the semi-diurnal tides (and similarly of all other species of tide and of sea level) If, however, the analysis is completed so that the harmonic constituents are determined, then it is possible to synthesize these constituents (say for the semi-diurnal species only) to give synthesized values of P and Q which we can call P_s and Q_s. Alternatively the whole of the data can be expressed in the form R, ε, R_s, and ε_s.

It was the examination of the quantities

$$\lambda = R/R_s \quad \text{and} \quad \eta = \varepsilon - \varepsilon_s,$$

which led originally to the present investigation

The synthesized semi-diurnal tide will include all the principal tidal constituents, and thus λ and η will reveal—

(i) Harmonic constituents neglected in the synthesis ,

(ii) Harmonic constituents of unknown origin ,

(iii) Erratic variations, probably due to meteorological changes.

Further details of the method are given in Appendix I

3 Perturbations of the Semi-diurnal Tide

The method already described was applied to the semi-diurnal tide at Liverpool for the year 1918 Values of R and ε had already been tabulated

at the time of the analysis, whilst R_a and ε_a were obtained from quantities generated on the predicting machine from the 1918 Harmonic Constants

Daily values of the quantities λ and η are given in Table I

A cursory examination of the results shows that in general the perturbations occur more or less casually, though on several occasions they remain noticeably consistent over a period of several days The maximum perturbation is about 15 minutes in times and 1 5 feet in range It seems reasonable to suppose that eventually the casual variations will be explained in terms of the meteorological conditions Up to the present, however, correlation methods which have been applied have shown little success This would further indicate, ' that in the ultimate solution of the meteorological tide, dynamical methods must largely replace the statical methods of the past "

Table I also contains monthly averages of the quantities η and λ which we shall call η_m and λ_m

Monthly time errors of the synthesized tide are indicated by η_m It will be seen that in April the average time error amounted to 3 minutes, whilst in the remaining months of the year it was 2 minutes or under There is no obvious periodicity in the values, but it is noticeable that in April and again in August, when the time errors were greatest, the range was nearest normal
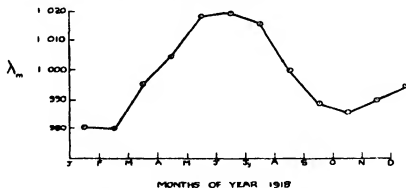
FIG 1 —Annual perturbation in the range of semi-diurnal tide at Liverpool, 1918

Monthly range errors are indicated by λ_m These show a prominent perturbation which is illustrated in fig 1 It is clear that the actual tide is less than the synthesized tide during the winter months and greater than the synthesized tide during the summer months, the discrepancy in range being of the order of 2% With an average semi-range of 10 feet this indicates an average discrepancy of nearly 3 inches in semi-range of tide during the summer months

Table I.—Daily Perturbations η and λ

Day	January		February		March		April		May		June		July		August		September		October		November		December	
	η	λ	η	λ	η	λ	η	λ	η	λ	η	λ	η	λ	η	λ	η	λ	η	λ	η	λ	η	λ

Monthly Perturbations η_m and λ_m

η_{Jan}	λ_{Jan}	η_{Feb}	λ_{Feb}	η_{Mar}	λ_{Mar}	η_{Apr}	λ_{Apr}	η_{May}	λ_{May}	η_{Jun}	λ_{Jun}	η_{Jul}	λ_{Jul}	η_{Aug}	λ_{Aug}	η_{Sep}	λ_{Sep}	η_{Oct}	λ_{Oct}	η_{Nov}	λ_{Nov}	η_{Dec}	λ_{Dec}
0 7	0 983	0 0	0 980	-0 7	0 996	0 907	1 5	1 008	0 0	1 010	0 7	1 020	0 7	1 016	1 1	0 999	-0 1	0 988	-0 7	0 968	0 7	0 990	0 7

The existence of a perturbation of this magnitude, whether casual or continued, is of considerable practical importance quite apart from any theoretical interest it may possess, and it is with a more complete investigation of the annual portion of this perturbation that the present paper is concerned   If the phenomenon were due to a single harmonic semi-diurnal constituent of amplitude 0 2 feet we should expect it to disturb high and low water times by 2 minutes, but the observed disturbance of times is not as great as this   We shall show later that the disturbance can be expressed by means of two harmonic constituents

4 *Annual Perturbation of the Principal Constituent of Semi-diurnal Tide*

Tidal analysis in the past has been restricted to a search for constituents indicated by the tide generating potential and by the shallow water theory In the Report of the British Association for 1923 Proudman has shown that additional frictional constituents are possible

None of the above suggests an annual variation in the range of tide

For the purpose of continuing the investigation, a direct method of analysis for such an annual perturbation was considered desirable, and in Appendix II Doodson's tables for the analysis of tidal observations have been extended to include two new constituents which have been called MA_2 and Ma_2, and which perturb M_2, the principal lunar constituent, once in the year   These constituents, which are conjugates with respect to M_2, have been chosen so that MA_2 loses and Ma_2 gains on M_2 very approximately 1 degree per day

For comparison purposes a method is also given whereby the constants obtained for MA_2 and Ma_2 may be combined so as to give an expression for the annual perturbation in semi-range of M_2 in the form

$$R \cos (\alpha + 1^\circ d),$$

where

R = the amplitude of the perturbation (semi-range),

α = the phase lag of the perturbation on January 1,

d = the number of days elapsed from January 1

5 *Analytical Results at Liverpool*

Five years' observations of the Liverpool tides, 1918, 1920, 1922, 1924 and 1930, have been analysed for the new constituents, and the results are given in Table II

We may summarize our observations on this table as follows —

(i) There can be little doubt of the continued existence at Liverpool of an annual perturbation of M_2.

(ii) The perturbation shows a definite consistency of phase from year to year. In all five years the range of phase lies within 55°, whilst if we exclude the year 1924 the range is within 30°. (A phase difference of 30° corresponds to a time difference of 1 month.)

Table II —Analytical Results at Liverpool

Year	MA₁		Ma₂		R cos (α + 1° d)		% H(MA₁)/H(M₂)	% H(Ma₂)/H(M₂)	% R/H(M₂)
	H	g	H	g	R	a			
1918	0 125	217	0 102	20	0 198	196	1 22	1 01	1 98
1920	0 118	230	0 069	289	0 087	220	1 17	0 69	0 87
1922	0 127	228	0 033	305	0 115	105	1 26	0 3J	1 65
1924	0 045	275	0 057	342	0 098	248	0 45	0 57	0 98
1930	0 193	324	0 173	93	0 166	222	1 90	1 71	1 66
Vector average	0 086	256	0 040	24	0 126	213	0 86	0 40	1 25

(iii) In 1918 the perturbation was unusually large, amounting to nearly 2% of M_2. In 1920 it was less than half this value. Over the five years examined the average perturbation was 1 25% of M_2.

A rather interesting fact is that the year to year magnitude would appear to follow the year to year magnitude of M_2.

(iv) If we confine our attention to the constituents, MA_1 would appear to be the more important of the two, with an amplitude averaging double that of Ma_2. There is also an apparent tendency for the phase lag of MA_1 to increase steadily with a period of roughly 40 years. This tendency was first noticed in the years 1918 to 1924 and is further confirmed by the year 1930. If further observations show this steady increase to be maintained, it will mean that the true period of the phenomenon is not exactly 1 year but slightly less.

It is convenient here to compare the results obtained from the monthly averages of λ with those from the direct analysis of hourly heights. In order to do this the twelve mean values of λ were analysed, and the results expressed in the form R cos (α + 1° d). The actual expression obtained from the analysis was

$$0\ 212 \cos (197 + 1°\ d),$$

as compared with

$$0 \ 198 \cos (196 + 1° \ d),$$

from the 1918 analysis of hourly heights

These results show conclusively that the annual perturbation in range originally found in the semi-diurnal tide may be considered to be adequately represented by these two new constituents

6 *Perturbations in the High and Low Water Range of Tide*

In the preceding sections an examination was made first of the semi-diurnal tide as a whole, and then of the principal constituent of the semi-diurnal tide   We shall now extend this examination to the tide as observed at the times of high and low water

The simplest method of proceeding would be to analyse the monthly averages of the differences between observed and predicted tides   A more satisfactory method is to make use of existing analyses for shallow water constituents

[The method of analysis for shallow water constituents, though devised by Doodson several years ago has not yet been published   The quantities analysed are the daily differences between observed and predicted times and heights of high and low waters   A search for annual (Sa) variations in these quantities is included in the method   Simple differences between the Sa term for high water, and that for low water, give the perturbation in the range of tide   The semi-range of the perturbation may then be easily expressed in the form R cos $(α + 1° \ d)$]

One year's observations, 1924, have been analysed for Liverpool by the above method, and the expression obtained for the annual perturbation was

$$0 \ 110 \cos (228 + 1° \ d),$$

as compared with $0 \ 098 \cos (248 + 1° \ d),$

from the analysis of 1924 hourly heights

The main difference, that of 20° in phase, is not considerable, and could easily arise from the independent methods of analysis, one of hourly heights, and the other of high and low waters   It is possible, however, through variable shallow water effects, to have an annual perturbation in the high and low waters, independent of one in the semi-diurnal tide   This may also partially account for the difference

7 *Annual Perturbation in British Waters*

(I) *From Hourly Heights*—Proceeding to the region of the British Isles generally, Table III gives the values of the constants MA_2 and Ma_2, and the

deduced perturbation R cos $(\alpha + 1° d)$ at all places in these regions for which analyses of hourly heights already existed at the Tidal Institute Additional quantities are given in which amplitudes are expressed as a percentage of the amplitude of M_2 These quantities are also given in the tables for Liverpool, and are later used for comparison purposes They will be referred to as "relative amplitudes"

Table III —British Waters, Annual Perturbation from Analysis of Hourly Heights.

Place	Year	MA₂		Ma₂		R cos $(\alpha + 1° d)$		% $\frac{H (MA_2)}{H (M_2)}$	% $\frac{H (Ma_2)}{H (M_2)}$	% $\frac{R}{H (M_2)}$
		H	g	H.	g	R	α			
Stornoway	1929	0 020	57	0 055	153	0 038	321	0 44	1 20	0 83
Aberdeen	1910	0 030	261	0 016	221	0 038	133	0 70	0 35	0 89
Immingham	1926	0 139	13	0 160	158	0 076	223	1 39	2 19	1 04
Harwich	1931	0 073	276	0 045	113	0 082	196	1 72	1 06	1 92
Southend	1926	0 181	330	0 077	182	0 141	201	2 75	1 17	2 15
Southampton	1924	0 063	198	0 021	106	0 093	147	1 42	0 47	2 08
Portland	1924	0 055	151	0 011	231	0 061	245	2 67	0 53	2 70
Avonmouth	1924	0 108	161	0 084	200	0 180	257	0 77	0 60	1 79

The tables indicate at once that the perturbation exists generally in British waters , and at a number of places is of even greater importance than at Liverpool An examination of the changes from place to place, in phase and amplitude of the constituents and perturbation, lead to the following interesting results

Commencing at Stornoway the phase lag of MA_2 steadily increases as one proceeds southwards down the North Sea, reaches a maximum at Immingham, and then diminishes slightly at Harwich and Southend In the lower approaches it increases as one proceeds into the Irish Sea and also up the English Channel This increase in phase lag as one advances from the Atlantic into the neighbouring seas is precisely what one would expect, were the constituent generated in the open sea, and propagated in a manner similar to that of an ordinary astronomical tide

The changes of phase of Ma_2 are not nearly so definite as those of its conjugate constituent Over the whole of the North Sea and English Channel the phase is, within a range of 100 degrees, more or less constant At Liverpool, in the Irish Sea, it differs by roughly 180 degrees from that in the above two regions.

Concerning the variations in relative amplitudes of the constituents, of the two, MA_2 is clearly the more important, though there are occasions, as at Stornoway and Immingham, where the reverse is true Over the southern

North Sea and English Channel, the relative amplitude of MA₂ is roughly 2% of M_2, and it is striking that this is more than double its value in the Irish Sea and on the Scottish coasts

The constituent Ms₂ is practically constant over the Irish Sea and English Channel, where its relative amplitude is approximately 0 5% of M_2 In the North Sea its relative amplitude is somewhat greater, and at Immingham rises to a prominent maximum of 2% of M_2

If we confine our attention to the resultant annual perturbation the indications are, with the possible exception of one station, Aberdeen, that the perturbation occurs steadily later in the year as one proceeds inward from the Atlantic

At the approaches, both North and South, the maximum perturbation occurs between the middle and end of February   At Southend and Harwich it occurs in June, whilst at Liverpool it occurs about half a month earlier

If we take an average of α over the whole region we get a value of 214° If we take an average of the corresponding phase for the change in sea level, we get a value of 76°   The difference between the two is roughly 140°   This might suggest a tendency for the perturbation in range to be opposite in phase to the perturbation in sea level   This would mean a maximum perturbation in range to be associated with a minimum sea level, and *vice versa*

As to the changes in the relative amplitude of the perturbation, in the Irish Sea and English Channel the perturbation would appear to decrease in amplitude as one proceeds inwards from the Atlantic   In the North Sea an opposite result is found   Between Stornoway and Immingham the perturbation is practically constant, whilst a very rapid increase occurs at Harwich, and this is further maintained at Southend

The importance of the perturbation relative to M_2 is at Immingham and Aberdeen 1% of M_2 and at all other places 2% of M_2

(II) *From High and Low Waters* -Table IV gives the expressions for the annual perturbation as derived from existing shallow water analyses   For the majority of places the results are in fair agreement with those from hourly heights   It is noticeable that where agreement is least, particularly in phase, shallow water constituents are abnormally large

It will be noticed that up to the moment no mention has been made of London Bridge   This was unnecessary because of the close agreement of the results with those of Southend

The stations are, however, worth comparing one with another, because of light they may throw on variations in the perturbation in a large tidal river

Comparisons between yearly amplitudes and phases at the two places show that abnormal values at the one are associated with corresponding abnormalities at the other, whilst the five year average indicates the perturbation at London Bridge to be slightly greater, and to occur a little later than at Southend   It

Table IV —British Waters, Annual Perturbation from Harmonic Shallow Water Analysis.

Place	Year	$R \cos (a + 1° d)$		$\% \frac{R}{H} (M_4)$
		R	a.	
Harwich	1931	0 085	181	2 00
Southend*	1925	0 085	230	1 30
	1926	0 054	224	0 83
	1927	0 101	181	1 54
	1928	0 095	225	1 45
	1931	0 151	188	2 30
	Vector average	0 091	205	1 39
London Bridge*	1925	0 077	201	0 96
	1926	0 074	218	0 93
	1927	0 148	178	1 86
	1928	0 078	215	0 98
	1931	0 141	192	1 77
	Vector average	0 097	199	1 22
Southampton	1924	0 070	252	1 58
Portland	1924	0 058	301	2 80
Avonmouth*	1924	0 150	284	1 07
	1925	0 108	257	0 78
	1926	0 172	249	1 23
	Vector average	0 137	263	0 99
Liverpool	1924	0 110	228	1 09

* The vector average refers only to Southend, London Bridge and Avonmouth

is difficult from the results to imagine the origin of the perturbation to be in the river , the indications are much more in favour of it being propagated inwards from the mouth.

8 Perturbation in General

Table V contains the results of analyses, at a small number of places, widely distributed over the surface of the globe.

St John, N B, is situated in the Bay of Fundy in a region where resonance effects may be expected. The results both in amplitude and phase are very similar to those at certain places in the British Isles, in particular to Harwich and Southend   Two years of analyses exist and it is clear, as in previous cases, that considerable variation in amplitude, and to a less degree in phase, can occur from year to year   It is interesting that the results further confirm what was previously found to exist at Liverpool, viz, that yearly changes in

Table V —Perturbation in General

Place	Year	MA_2		Ma_2		$R \cos (a + 1° d)$		$a_1 \frac{H(MA_2)}{H(M_2)}$	$a_1 \frac{H(Ma_2)}{H(M_2)}$	$\% \frac{R}{H(M_2)}$
		H	g	H	g	R	a.	°	°	
St. John, N B	1930	0 174	283	0 024	158	0 162	246	1 75	0 24	1 63
,,	1931	0 231	265	0 094	152	0 296	168	2 30	0 94	2 95
Ponta Delgada	1924	0 084	248	0 049	134	0 013	222	3 48	3 15	0 84
Johore Bahru	1929	0 071	178	0 020	113	0 081	152	2 55	0 72	2 90
Port Hedland	1927	0 047	317	0 047	58	0 050	229	0 82	0 82	0 87
Newchwang	1924	0 362	196	0 203	190	0 122	150	9 20	5 10	3 40

the amplitude of the perturbation are accompanied by yearly changes in the amplitude of M_2 Thus in

$$1930 \qquad H \text{ of } M_2 = 9\ 957 \text{ whilst } R = 0\ 162$$
$$1931 \qquad H \text{ of } M_2 = 10\ 083 \text{ whilst } R = 0\ 296$$

Ponta Delgada, in the Azores is suitably situated to be typical of tides in the middle of the Atlantic   It is very striking that the magnitude of the perturbation found here should be practically the same as at Stornoway and Aberdeen on the open Scottish coasts

Port Hedland, which is placed on the North-west coast of Australia, is in an open position comparable with Ponta Delgada, but on the opposite side of the globe   The magnitude of the perturbation at the two places is much the same

Johore Bahru, in the Singapore Strait, has a prominent perturbation larger than at any place in the British Isles   The conditions at this place are peculiar, for it is situated in a comparatively deep channel, but the flow of water through the channel is restricted by an artificial causeway   The winds along the direction of the channel have an annual variation.

Newchwang, on a tidal river in the Yellow Sea, is icebound for a portion of the year   As a result, considerable freshet effects are experienced at times, and this makes the results of particular importance   The existence of a large perturbation in the range of tide at Newchwang has been known for a number of years, and it has always been attributed to the very abnormal conditions What is of importance is that practically the whole of the perturbation exists in the semi-diurnal tide, and does not arise, except to a very minor extent, from variations in the shallow water constituents

9   *Annual Perturbation and Local Meteorological Conditions*

It was stated early in the paper, that little success had resulted from an attempt to correlate the day to day changes in the perturbation with the local meteorological conditions   It is now proposed to replace day to day values by mean values for the month   Also an assumption (similar to that adopted by Doodson when considering mean sea level variations[*]) will be made that the average perturbation in range of tide can be expressed as a linear function, of the departure from the mean of the local pressure, and of the local east and north pressure gradients   Thus if

> B = the departure from the mean of the average local pressure for the month,
>
> E = the departure from the mean of the average local easterly pressure gradient for the month,
>
> N = the departure from the mean of the average local northerly pressure gradient for the month

then the average range perturbation for the month $(\lambda_m) = \alpha B + \beta E + \gamma N$, where α, β, γ, are constants depending upon the correlation and also on the units used

Twelve mean monthly values of λ_m at Liverpool were obtained from the curve for the average perturbation, for the years 1918, 1920, 1922, 1924, 1930

Monthly averages for B, E, N, at Liverpool were obtained from " The Weather of the British Coasts M O 230 "   The figures are based upon the 7-hour observations at the Telegraphic Reporting Stations of the Meteorological Office in the ten years 1906 to 1915

With special reference to Liverpool

> B = the monthly average of the departure from the mean of the pressure at Liverpool,

E = the monthly average of the departure from the mean of the
    pressure between Spurn Head and Blacksod Point,

N = the monthly average of the departure from the mean of the
    pressure between Thurso and Plymouth

These quantities are given in Table VI The twelve equations obtained
from the above values were solved by the method of least squares for α, β, γ
The results gave

$$\lambda_m = 0 \ 7B - 8 \ 0E + 2 \ 8N$$

Fig 2 shows the annual perturbation, together with the perturbation as
deduced from the meteorological conditions by substitution in the above
formula

Table VI —Value of B, E, N, at Liverpool from 10 year Average

	Jan	Feb	Mar	Apr	May	June	July	Aug	Sept	Oct	Nov	Dec
B	1 6	−3 2	−2 5	1 8	1 8	2 3	2 0	0 8	5 3	−1 2	−2 2	−7 3
E	0 8	0 4	−1 0	0 1	0 3	−1 1	−1 5	−0 7	−0 2	2 4	−0 8	+1 4
N	−4 J	−4 3	−0 9	0 9	J 3	2 4	1 4	0 5	1 9	3 7	−1 5	−2 6

The annual variation is undoubtedly reproduced by the meteorological
conditions, though there are marked differences in many of the monthly
values   A tendency for the results from the meteorological conditions to lag
roughly one month behind the actual perturbation is hard to explain   It is
possibly due to the selection of local meteorological conditions instead of
those far out at sea

The contributions from B, E, N, to the perturbation in fig 2 as deduced
from the meteorological conditions, were in the ratio 21 86 70   From
this we would infer the effects from easterly pressure gradients to be slightly
greater than those from northerly pressure gradients, and roughly four times
greater than the effect from local barometric pressure

10 Previous Experience of an Annual Perturbation

The earliest reference to a seasonal change in semi-diurnal tide is to be found
in Darwin's paper on the "Harmonic Analysis of the Antarctic Tidal Observa-
tions of the 'Discovery'"   The observations discussed in his paper were
taken during the years 1902 and 1903 at a position on the south-eastern

extremity of Ross Island For analytical purposes the observations were
grouped into periods of one month The feature of these monthly analyses
which was of particular interest was that the M_2 tide showed a progressive
annual change both in amplitude and phase during each of the two seasons
analysed The change was such that the average range was least and the
average tide most retarded during the months of June, July and August
The magnitude of the change was even greater than at any of the places
discussed in the present paper, having a relative amplitude of 38% It is
particularly interesting that no other constituent showed this progressive
annual change Darwin also found that an inequality of 13 months would
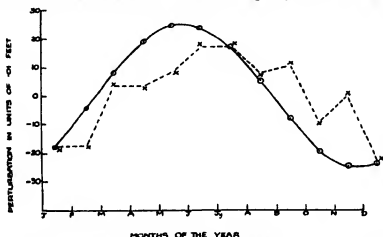
FIG 2 —Perturbation as deduced from meteorological conditions   Perturbation,
——— actual ; – – – as deduced from meteorological conditions

satisfy the conditions better than one of 12 months and from this he suggested
a possible connection with the 14 months period for the variation in latitude
    In recent years several references to an annual perturbation in the range of
tide have appeared in special publications of the U S Coast and Geodetic
Survey The references have been based upon monthly averages of the
observed high and low waters at individual places In Special Publication
No 162, " On the tides and currents in Chesapeake Bay and Tributaries," we
find the following remarks —" At Philadelphia on the Delaware River, the
average seasonal variation in range is about 1 foot, whereas at Boston near the
open coast it is only 0 2 feet It appears, therefore, that such a variation is
largely a river effect, and it is probably due to the varying quantities of
drainage water in the river " The existence of the perturbation at Newchwang
was discovered in 1925 following a series of monthly analyses made at the

Tidal Institute   The perturbation was so prominent and so regular that it has been included in the Newchwang predictions since 1927

Analyses for shallow water constituents were commenced in 1924 and the unequal annual changes in the high and low waters were obvious from that time   The small number of these analyses available prevented an examination of the perturbation at an earlier date

11 *Discussion*

Perhaps the most fundamental of all the causes likely to produce a perturbation in the range of tide, is a periodic change in the boundary conditions   This cause will not provide a universal explanation of the phenomenon, but it should be particularly applicable to the seas of the polar regions   Darwin found that in the Antarctic the least range and greatest retardation of tide occurred during the months June, July and August, when the Antarctic seas are frozen over to their greatest extent   When we consider that it is during these months that the greatest restrictions to the free flow of the currents will be present, the occurrence of a reduced range of tide during this period is exactly what we should expect

In a tidal river the perturbation may arise in several ways, provided there is an annual change in the average depth or in the non-tidal current in the river   A change in the average depth from the ordinary law for the propagation of a wave in a canal will affect the speed and consequently the phase at a particular place to a first order, whilst it will affect the range to a second order The phase and range of tide will also change with any variation of the non-tidal current in the river   This may be seen as follows :—

The equations of motion for the tides in a canal of rectangular section will be found in Lamb's "Hydrodynamics"   If we neglect second order terms other than those arising from the interaction of tidal and non-tidal current and consider the currents as made up of two parts, one a tidal portion u and the other a non-tidal portion U, the modified equations of motion become

$$\frac{\partial u}{\partial t} + g\,\frac{\partial \zeta}{\partial x} = -\,U\,\frac{\partial u}{\partial x}$$

$$\frac{\partial \zeta}{\partial t} + h\,\frac{\partial u}{\partial x} = -\,U\,\frac{\partial \zeta}{\partial x},$$

where x is the distance from the origin along the length of the canal , g is the acceleration due to gravity , t is the time , ζ is the elevation of the surface from the mean level.

Solving these differential equations in the usual manner and assuming a tidal oscillation of the form $\mathrm{Re}^{i\sigma t}$, where σ is the speed, the expression for ζ becomes

$$\zeta = A e^{i\sigma\left[\frac{x}{c-U}+t\right]} + B e^{i\sigma\left[\frac{x}{c+U}-t\right]},$$

where A and B are constants and $c^2 = gh$

The real part of this may be written in the form $\zeta = \mathrm{R}\cos(\sigma t - \varepsilon)$, where

$$\mathrm{R}^2 = \mathrm{A}^2 + \mathrm{B}^2 + 2\mathrm{AB}\cos\frac{\sigma x}{c^2 - \mathrm{U}^2}$$

$$\tan\varepsilon = -\frac{A\sin\dfrac{\sigma x}{c-U} - B\sin\dfrac{\sigma x}{c+U}}{A\cos\dfrac{\sigma x}{c-U} + B\cos\dfrac{\sigma x}{c+U}}$$

Clearly, then, provided A and B are neither equal to zero, any change in U will produce a corresponding change in R and ε

The range of tide in a river may also be affected by changes in certain of the shallow water constituents which themselves may vary from changes in the average depth and of the constant current

The observational data already discussed in this paper have shown that though in particular cases, as in the Delaware River, the changes can largely be explained as a river effect, this is not universally so, and the explanation is not applicable to the River Thames where the perturbations at Southend and London Bridge are found to be practically the same

The formula, deduced above for a tidal oscillation and a variable non-tidal current, is also applicable to an open ocean, provided we can prove the existence of a variable non-tidal current The existence of such a current in the Atlantic having an annual variation, is now a well-established fact in oceanographical research, and is confirmed by the sea level changes in the marginal seas and by observations of sea temperature, salinity, density, distribution and character of plankton, both in the Atlantic Ocean, and in the marginal seas, and also in the connecting channels Clearly, however, from the relations between c and U in the open ocean the changes in U must be much greater than can be reasonably expected if they are to produce the changes that are observed Again, the present paper has shown that in the open ocean the magnitude of the perturbation is of the same order as the change in the mean sea level This would practically rule out any explanation of the perturbation in terms of sea level changes in the open ocean We

must admit then, that no satisfactory explanation of the perturbation in the open ocean has yet been found

Conclusion.

We have seen established an annual perturbation in the range of tide, which at a number of places is of sufficient importance for inclusion in future tidal predictions   Under what conditions is the additional labour, which such an inclusion would involve, justified ?

Considering the yearly variations in the perturbation, the results have shown, that though the consistency in phase can generally be relied upon, the value of the amplitude may vary considerably from year to year   This would lead us to proceed with caution where the amplitude is concerned, and it would appear advisable for this reason alone, to have two, and possibly three, years' analyses available, previous to considering the inclusion of this perturbation in predictions   A reasonable limit for the amplitude of the perturbation, would be one greater than 1% of that of M_2, though for places of particular consistency the limit might easily be fixed at a lower value

As is necessary in a paper of this type, attention has been drawn to indications which later observations may, or may not, prove to be true   It is intended that these be taken, purely for what they are worth, on the information available, and that they be kept in mind as future data come to hand   More definite and satisfying conclusions should be possible by a revision, and expansion of the paper, in, say, ten years' time

Acknowledgments.

APPENDICES

In the following appendices constant reference will be made to Doodson's paper on the "Analysis of Tidal Observations," and it will be assumed that the reader is familiar with both the notation and theoretical basis of this paper

APPENDIX I

Let

ζ = the tidal elevation above a known datum

σ = the increment in phase of a constituent, in degrees per mean solar hour

ρ = the increment in phase in degrees per mean solar day with integral multiples of 360° omitted

t = the number of hours measured from the origin of time

T = the number of complete days measured from the origin in time

R = amplitude of the constituent

$R \cos (\sigma t - \varepsilon)$ = a typical tidal constituent with phase $-\varepsilon$ at the origin of time

H = the hour of the day measured from midnight

Taking a tidal constituent in the form

$$R \cos (\sigma t - \varepsilon),$$

the height of tide due to this constituent at hour H on the day T may be written in the form

$$R \cos (\sigma H + \rho T - \varepsilon)$$

If we take any combination of hourly heights such as $\zeta_H + \zeta_{H+2} + \zeta_{H+3}$ then it can be shown that the results may be expressed in the form

$$JR \cos (\sigma H + \rho T - \varepsilon + \eta),$$

where J and η are constants depending upon the combination used

Doodson has shown that it is possible to obtain daily expressions of the above form which are functions of one species only   For the semi-diurnal tide two such expressions are obtained

$$X = JR \cos (\rho T - \varepsilon + \eta')$$

$$Y = JR \cos (\rho T - \varepsilon + \eta'')$$

The quantities η' and η'' are chosen so that the initial hour of X is midnight preceding the day, whilst that of Y is 3 hours later

The computation of the initial phase of the amplitude require two further expressions

$$A = X + Y$$

$$B = X - Y,$$

of the form

$$A = aR \cos (\delta - \rho T) \quad \text{and} \quad B = bR \sin (\delta - \rho T),$$

so that

$$a = 2J \cos \tfrac{1}{2} (\eta' - \eta'') \quad \text{and} \quad b = -2J \sin \tfrac{1}{2} (\eta' - \eta''),$$

$$\delta = \varepsilon - \Delta \quad \text{and} \quad \Delta = \tfrac{1}{2} (\eta' + \eta'')$$

It will thus be seen that for any particular day the phase of both A and B—

(1) as obtained from observations through X and Y,

(2) as obtained by generation from the final constants, at intervals of 24 hours from the time origin (taken as zero hour of the central day),

is the phase of the tidal constituent (1) from observation, (2) from synthesis, Δ/σ hours after the preceding midnight

The value of Δ/σ for the average semi-diurnal tide is 15 5 hours   Thus if on any day we write the semi-diurnal tide in the form

$$R \cos (30° t - \varepsilon') = P \cos 30° t + Q \sin 30° t,$$

where $t =$ the time in solar hours measured from 15 5 hours after the preceding midnight , $-\varepsilon' =$ the phase of the semi-diurnal tide at this time

$$P = R \cos \varepsilon' \quad \text{and} \quad Q = R \sin \varepsilon',$$

then

$$\frac{b}{a} \tan \varepsilon' = \frac{\Sigma B \text{ (for the semi-diurnal constituents)}}{\Sigma A \text{ (for the semi-diurnal constituents)}},$$

and

$$\Sigma (a^2 + b^2) R^2 = \Sigma A^2 + \Sigma B^2$$

To a first approximation the magnitude of both a and b for the semi-diurnal tide may be taken as 34

The values of R and ε' from observation are easily found through ΣX and ΣY the quantities tabulated daily in the analysis   Values of R_s and ε_s, the synthesized quantities, are obtained from ΣA_s and ΣB_s, which are generated on the predicting machine   The quantities R and δ necessary in the synthesis are obtained from the completed analysis, whilst values of a and b are given in Doodson's paper

The Légé predicting machine which was used for the purpose provides for ten semi-diurnal constituents as follows —

$$2SM_2, \ 2N_2, \ \mu_2, \ N_2, \ \nu_2, \ M_2, \ L_2, \ T_2, \ S_2, \ K_2.$$

Since we are only interested in daily increments of the constituents it is possible

to generate additional minor constituents by making use of the following relationships

$$MNS_2 \text{ has the same } \rho \text{ as } MN_4$$
$$R_2 \text{ has the same } \rho \text{ as } K_1 \text{ (very approx.)}$$
$$MSN_2 \text{ has the same } \rho \text{ as } Mm$$
$$OP_2 \text{ has the same } \rho \text{ as } Mf \text{ but of opposite sign}$$
$$\lambda_2 \text{ has the same } \rho \text{ as } Mm \text{ but of opposite sign}$$

The constituents MSN_2 and λ_2 were generated as compound constituents.

Much care was taken in the reading of ΣA_s and ΣB_s. The scale used was 4 cm to 1000 units, readings being to the nearest 0 05 cm.

APPENDIX II.

Analysis Tables for an Annual Perturbation of M_2

Constituents which will produce an annual perturbation of M_2 may be considered as having either of the following arguments

$$[(\text{Argument of } M_2) - h]$$

or

$$[(\text{Argument of } M_2) + h],$$

where h is the mean longitude of the sun

In the present section Doodson's analysis tables have been extended to include the above two constituents which have been called MA_2 and Ma_2, respectively

The eight new functions which it is necessary to calculate for the determination of the new constituents are in the notation of Doodson's paper, for

$$R \cos \delta \quad - A_{221}, B_{222}, B_{201}, A_{204},$$

and for

$$R \sin \delta \quad - B_{221}, A_{222}, A_{201}, B_{204}$$

Table VII contains values of σ, ρ, Δ, a, b, D, M, for MA_2 and Ma_2. The quantities σ and ρ are the hourly and daily speeds of the constituents, whilst Δ is a constant used in determining the final constants a, b, D, M, are necessary for the calculation of the number of contributions from MA_2 and Ma_2 to the various functions

Table VIII sets out in tabular form the correction process for $[R \cos \delta]$ and $[R \sin \delta]$ whereby contributions from all constituents other than MA_2 and Ma_2 are eliminated. Except for a correction through the terms A_{181},

and B_{1ac} for an annual perturbation which arises from O_1, and also the use of a uniform divisor of 10,000, the tables are similar in form to those of Doodson. Table IX contains the factors for the calculation of R cos δ and R sin δ from [R cos δ] and [R sin δ].

Table VII.—Data relative to MA₂ and Ma₂

	MA₂	Ma₂
σ	28 943036	29 025173
p	−25 367146	−23 395851
Δ	88 5	89 9
a₂	35 276	35 146
b₂	33 377	−33 446
D₀	− 1 482	2 024
D₁	− 2 862	1 488
D₂	28 064	30 476
D₃	31 574	30 132
D₄	2 342	− 0 832
D₅	− 1 220	0 092
M₀	0 457	0 372
M₁	11 272	11 216
M₂	−14 020	15 124
M₃	− 0 464	0 274

Table VIII.
Correction Tables for the Calculation of [R cos δ]

Principal function	Correction terms—Multiples of										Divisor	Symbol
	A_{2a1}	A_{2a2}	A_{2a1}	B_{2a0}	A_{2a0}	A_{2a1}	A_{2a0}	A_{2a0}	A_{2a0}	A_{2a1}		
A_{2a1}	0 004	0 002	−0 023	0 039	−0 009	0 026	−0 073	0 003	−0 010	0 083	10,000	A
B_{2a0}	−0 005	0 001	0 081	−0 018	0 005	−0 140	0 007	—	0 012	−0 040	10,000	B
B_{2a1}	0 084	−0 023	−0 029	0 067	−0 008	0 041	−0 040	0 001	0 008	0 029	10,000	C
A_{2a0}	0 109	0 012	−0 160	0 016	−0 008	0 086	−0 039	—	0 012	0 094	10,000	D

Correction Tables for the Calculation of [R sin δ]

Principal function	Correction terms—Multiples of										Divisor	Symbol
	B_{2a1}	A_{2a2}	B_{2a1}	A_{2a0}	B_{2a0}	B_{2a1}	A_{2a0}	B_{2a0}	B_{2a0}	B_{2a0}		
B_{2a1}	0 004	—	−0 022	−0 039	−0 009	0 027	0 062	0 002	−0 009	0 040	10,000	A'
A_{2a0}	0 005	0 002	−0 086	−0 018	−0 006	0 164	0 007	−0 001	−0 010	0 130	10,000	B'
A_{2a1}	−0 085	−0 019	0 031	0 067	0 009	−0 048	−0 040	−0 002	−0 006	−0 095	10,000	C'
B_{2a0}	0 109	−0 004	−0 161	−0 015	−0 008	0 086	0 039	0 001	0 008	0 045	10,000	D'

Constituents expressed as a Perturbation in Range of M_2.

Let H_1, H_2, H_3, be the amplitudes and g_1, g_2, g_3, the phase lags of M_2, MA_2, Ma_2, respectively

Then the phases of the constituents relative to M_2 are, of MA_2

$$(g_1 - g_2 - h),$$

and of Ma_2

$$(g_1 - g_3 + h)$$

Table IX —Calculation of R cos δ and R sin δ from [R cos δ] and [R sin δ]

Constituent	R cos δ				R sin δ			
	Multiples of—				Multiples of—			
	A.	B	C	D	A′	B′	C′	D′
MA_2	0 41	−0 32			−0 43	−0 30		
MA_4	0 41	0 34			−0 42	0 32		
Ma_2			0 48	0 34			0 45	−0 35
Ma_4			0 42	−0 32			0 40	0 35

The perturbation in the semi-range of M_2 is given by

$$[H_2 \cos \{h - (g_1 - g_2)\} + H_3 \cos \{h + (g_1 - g_3)\}],$$

which may be expressed in the form

$$R \cos (h + \beta),$$

where

$$\tan \beta = \frac{H_3 \sin (g_1 - g_3) - H_2 \sin (g_1 - g_2)}{H_3 \cos (g_1 - g_3) + H_2 \cos (g_1 - g_2)},$$

and

$$R^2 = [H_2^2 + H_3^2 + 2H_2H_3 \{\cos (2g_1 - g_2 - g_3)\}]$$

If α is the phase of the constituent on January 1 when the value of h is 280°, and if d are the number of days elapsed from January 1, then since the daily increment in h is with sufficient accuracy equal to 1° per day, an alternative form for the annual perturbation is

$$R \cos \{(\alpha + 280 + \beta) + 1° d\}$$

This is the form used in the paper

Summary

The paper establishes the existence of an annual perturbation in the range of tide   The perturbation became evident during an intensive examination, by a method which should be of particular interest, in the residual semi-diurnal tide at Liverpool   Direct analysis of hourly heights for an annual perturbation in the principal constituent of semi-diurnal tide showed the perturbation to be consistent from year to year, and to exist generally in British waters and throughout the world at large   Analysis of high and low waters further confirmed the results   A study of the distribution of the perturbation provided a number of interesting results as also did a study of its relation with local meteorological conditions   The paper concludes with a short discussion on possible causes of an annual perturbation in the range of tide   Appendices describe the method by which the residual tide was obtained, and also contain tables for the direct analysis of hourly heights for an annual perturbation in the range of tide

---

The Production of Showers by Cosmic Radiation

By C. W. Gilbert, B A

Introduction

The production of secondary particles by the passage of cosmic radiation through matter is a well-known feature of the cosmic ray phenomenon.   Cloud chamber photographs of Blackett and Occhialini,[*] Anderson,[†] and Kuntze[‡] show that the secondaries often occur in groups, which have been named "showers"   The production of these showers was investigated by observing the simultaneous discharges of three Geiger-Müller counters so arranged that they only recorded showers of at least three particles   The main experiments were carried out at the Forschungs-station Jungfraujoch, in Switzerland, at a height of 3500 metres   Other experiments were made at Eigergletscher

---

[*] 'Proc Roy Soc ,' A, vol. 139, p 699 (1933)
[†] 'Phys. Rev ,' vol. 43, p 368 (1933) , vol. 44, p 406 (1933)
[‡] 'Z Physik,' vol. 80, p 559 (1933)

(2300 m) and Zürich (500 m.) to investigate the variation of frequency of the showers with altitude

Experimental Method

The experimental arrangement was similar to that used by Rossi* and by Fünfer † Three Geiger-Müller counters were used, arranged as shown in fig 1 The lead under investigation was placed above in such a position
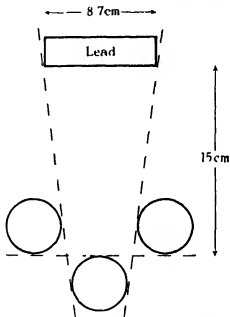
FIG 1 —Experimental arrangement of counters and lead.

that no particle coming from the lead could go through more than one counter The triple coincidences due to the presence of the lead must thus be due to showers of at least three particles The coincidences were recorded by a method described by Rossi ‡ The impulse from a fourth valve was fed to the grid of a thyratron by resistance capacity coupling, fig 2 This impulse was a *negative* kick, but the accompanying positive back-kick was sufficient to trip the thyratron This arrangement rendered the circuit very stable and free from external pickup

* 'Z. Physik,' vol. 82, p 151 (1933).

† *Ibid.*, vol. 83, p. 92 (1933).

‡ 'Nature,' vol 125, p. 636 (1930)

The counters used were 20 cm long × 4 2 cm diameter These gave about 120 counts per minute at sea level and between 200 and 300 per minute at 3500 m , at this rate the mechanical telephone counter used could not respond to all the counts The number of casual triple coincidences was only 2 or 3 per hour From the number of casual double coincidences the resolving power was found to be 10⁻³ seconds The rate of casual triple coincidences was very much smaller than the rate of counting of triple coincidences and so no correction was made for them
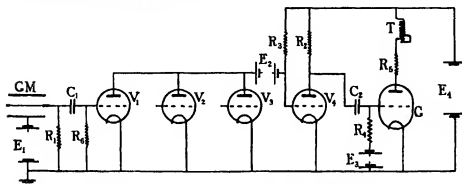
FIG 2 —GM, Geiger Müller counter, T, telephone counter and break, R_1, 4 × 10⁵ ω , R_2, 20,000 ω , $R_3R_4R_5$, 10⁷ ω , R_6, 800 ω , E_1, about 1500 v , E_2, about 10 v , E_3, about 10 v , E_4, about 100 v

Difficulty was encountered at the Forschungs-station Jungfraujoch, on account of the damp atmosphere , and the roof of the building was so thick that satisfactory measurements were only possible on the roof So the counters and recording set were placed in a tin box which stood on the roof, which was then protected by a wooden box from snow and sun Leads were taken from the tin box through a length of large bore rubber tube into the building for the L T supply, counter HT, telephone counter, etc The air in the tin box was dried with P_2O_5 and the box heated by two 40-watt lamps The voltage for the counters was supplied by a 1500-volt dry battery and it was found necessary to place this near a heater to keep it sufficiently dry at night By these means it was possible to work the counters on the roof, day and night under all weather conditions *

The coincidences were recorded on a telephone counter and also on an automatic recorder supplied by the Cambridge Instrument Company This recorded each coincidence on a slowly moving paper disc, and gave a useful

* The mean atmospheric temperature in July was about 1° C It frequently snowed and was often very misty

check on the performance of the apparatus, as well as the necessary data for investigating the distribution of counts in time

Experimental Results

Triple coincidences were observed at Jungfraujoch with the arrangement shown in fig 1, with varying thicknesses of lead over the counters As the thickness of lead was increased the number of coincidences was found to rise to a maximum at 2 2 cm and then to fall off rapidly (Table I and fig 3) The curve

Table I —Dependence of showers on the thickness of lead

Thickness of lead in cm	0 0	0 77	1 35	1 90	2 19	2 48	2 67	3 69	5 77	7 67	9 46
Number of periods of counting	7	7	6	8	4	3	4	6	5	4	3
Total time in hours and minutes	11 01	8 28	7 49	13 39	7 31	7 14	10 27	5 33	6 40	6 15	6 44
Total count	559	545	562	1069	614	560	791	383	393	336	386
Mean count per hour	50 9	64 5	72 0	78 4	81 9	77 9	75 6	69 1	58 0	53 8	57 3
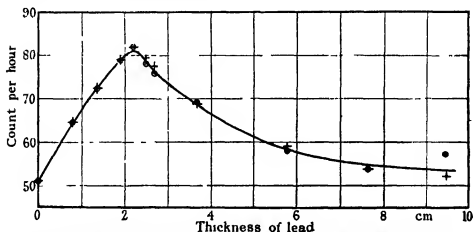
FIG 3—Showers observed with different thicknesses of lead above the counter at 3500 m O, observed points , +, calculated.

is very similar to curves obtained by Rossi and Fünfer at sea level The most notable difference is the different position of the maximum, which for Rossi's and Fünfer's curves was at 1 6 cm.

With no lead triple coincidences are obtained at a greater rate than the rate of casual coincidences, which are due to showers originating in the atmosphere

This background count will not be greatly affected by the presence of the lead After subtracting this background the fall away from the maximum is exponential with a coefficient of μ = 0 38 cm $^{-1}$ Rossi's and Fünfer's curves give rather lower values The curve will be discussed in more detail later

Fünfer observed that the lead side screens round his counters gave an increased count which was dependent on the count from the lead over the counters He found that the maximum effect was reached with a thickness of the side screens of 0 6 cm He obtained a similar effect with lead under the counters * To investigate this 2 0 cm of lead were placed over the counters and varying thicknesses placed underneath , an increase in the counting rate was obtained which reached a maximum at 0 6 cm , fig 4 Then 2 0 cm of
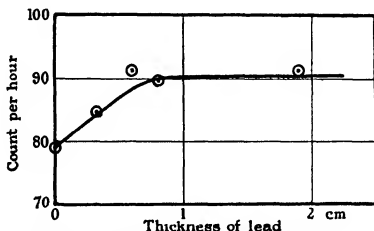
FIG 4 —Showers observed with different thicknesses of lead under the counter

lead were placed under the counters and the lead above varied The curve obtained, fig 5, was similar to the one without lead underneath The difference between the curves of figs 3 and 5 also shows a maximum, fig 6 Because of the statistical errors the position of this maximum cannot be fixed at all accurately, but it almost certainly lies not far from 2 cm The maximum increase is about 40% of the count due to the upper lead Fünfer had attributed this effect to reflection by the lower lead of the shower particles from the upper lead However, such an explanation would require that about 20% of the shower particles would be reflected back through nearly 180° Cloud chamber photographs show that there is no such large backward scattering Further, Blackett and Occhialini obtained conclusive evidence of high

* 'Z Physik,' p 83, vol 92 (1933)

energy particles thrown backwards from showers The explanation thus
appears to be that the increase is due to particles thrown in a backward
direction from showers occurring in the lower lead

Measurements were made at Jungfraujoch, Eigergletscher* and Zürich† to
determine how the increase with altitude of the frequency of the showers
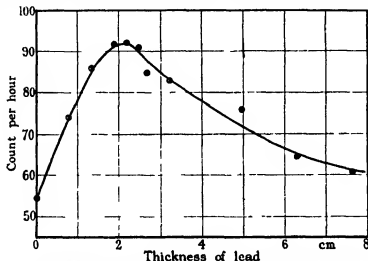
FIG 5—Showers observed with 2 0 cm of lead under the counters and different thick-
    nesses above.
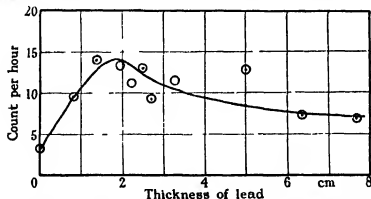
FIG 6 —Showers due to lead under the counter with different thicknesses of lead over the
    counter   Difference between curves of fig 3 and fig 5

compared with the increase of the general cosmic radiation. At these places measurements were made with the arrangement shown in fig 1 with 2 2 cm of lead over the counters, the frequency of showers being taken as the difference in counting rate with and without the lead Measurements were also made with the three counters one above the other in a vertical plane This gave a measure of the general cosmic ray intensity Since the maximum of the showers at Zurich is below 2 2 cm the frequency of showers for this station must be corrected This is done by estimating the number, using the curve of fig 3, that would have been recorded if the shower particles had had sufficient energy to reach the counters The results are shown in Table II

Table II —Comparison of frequency of showers and cosmic radiation intensity

	Jungfraujoch	Figergletscher	Zürich
Atmospheric pressure, in cm of Hg	50 7	57 6	72 3
Showers from 2 2 cm of lead, count per hour	31 0	24 3	11 6
Corrected	—	—	14 4
Counters in vertical plane, count per minute	5 45	4 40	2 50
Ionization intensity, ions per c c per sec	5 68	4 21	2 74
Showers	1 00	0 78	0 46
Cosmic radiation intensity—			
Counters	1 00	0 80	0 45
Ionization	1 00	0 73	0 48

The first line gives the showers observed from 2 2 cm of lead, the second line the rate of counting with the counters in a vertical plane The third line shows the cosmic ray intensity measured by Wollan with an ionization chamber * The next three lines are the same measurements reduced so that the value at Jungfraujoch is 1 00 The number of showers thus increases with altitude at about the same rate as the general cosmic ray intensity, as measured by both the total ionization and the number of particles producing coincidences in these three counters placed in a vertical plane

The Transition Curve for Lead

The curve showing the dependence of the number of showers recorded on the thickness of lead above is very similar to those obtained by Rossi and by Fünfer The chief difference is the change of the position of the peak. The

* Compton, 'Phys Rev,' vol 43, p 394 (1933)

position of the maximum observed at Jungfraujoch was 2 2 cm   Both Rossi and Fünfer located the maximum at 1 6 cm   Preliminary measurements made at Cambridge before going to Jungfraujoch had shown the peak to occur at about 1 6 cm , and later measurements made at Cambridge confirm this, fig 7

It appears certain that the curve must be interpreted* to be a transition effect on passing from air to lead   The shower particles to which the counters respond must be charged since they produce ionization in the counters, and so they have a range in lead †   When the thickness of lead is greater than the range of the shower particles the showers from the upper part of the lead can
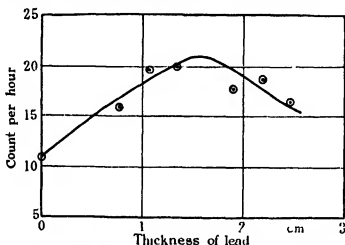
Fig 7 —Showers observed with different thicknesses of lead above the counters at sea level

no longer be recorded   Hence the curve will have a maximum at the thickness of lead equal to the range of the shower particles in lead   The curve must then fall off with the absorption coefficient of the radiation producing the showers   Since this absorption coefficient is very much larger than the absorption coefficient of the general radiation, 0 38 cm $^{-1}$ in lead as compared with 0 006 cm.$^{-1}$, the immediate cause of the showers cannot be the general cosmic

---

* Rossi, ' Nature,' vol 132, p 173 (1933) , see also Johnson's '' Analyses of Schindler's transition curves," ' Phys Rev ,' vol 41, p 545 (1932)

† A charged particle loses energy continually and so has a definite maximum range   But the particles of an uncharged radiation lose all or at least a considerable portion of their energy in a single event, so the radiation is absorbed exponentially   There is, therefore, a finite probability that some of the radiation will travel any given distance and have no maximum range

radiation. Since the absorption coefficient of the radiation producing the showers is so large and also the absorption exponential, the production of showers is probably the main cause of absorption. We shall call this radiation the shower-producing radiation. This radiation could not penetrate the whole of the atmosphere and so must be produced by some other radiation, which we shall call the primary radiation. After traversing sufficient depth of homogeneous matter an equilibrium will be reached between the amount of primary and shower producing radiation present. The curves obtained are thus transition curves due to the readjustment of this equilibrium in passing from one medium to another.

Suppose that the shower producing particles are produced by a primary radiation with absorption coefficient μ and so the intensity of the primary at any depth x in the atmosphere is $I = I_0 e^{-\mu x}$, treating the problem as one-dimensional, where x is measured downwards.

Let I_p be the intensity of the shower-producing radiation at depth x and let μ_p be the absorption coefficient, and α the coefficient of production of shower-producing radiation by the primary. α may be considerably less than μ since the production of shower-producing radiation may not be the only means of absorption of the primary.

Then

$$\frac{dI_p}{dx} = -\mu_p I_p + \alpha I$$

The solution is

$$I_p = Be^{-\mu_p x} + \frac{\alpha}{\mu_p - \mu} I_0 e^{-\mu x}$$

$$= Be^{-\mu_p x} + AI,$$

on writing

$$A = \frac{\alpha}{\mu_p - \mu}$$

If $\mu < \mu_p$ then after traversing a large thickness of matter the second term is the only significant one, and so the equilibrium intensity of the shower-producing radiation is given by

$$I_p = AI$$

A is a constant for any homogeneous medium but may vary from medium to medium.

Consider now the effect of putting varying thicknesses of a material over the counters, see fig 8

Let

S be the number of showers observed

a the mean range of the shower particles in the material

Z the thickness of material whose upper surface is at $x = 0$

Let the index (1) denote coefficients in the air and index (2) coefficients in the material
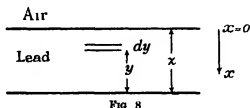
Fig 8

We have

$$I_p^{(2)} = Be^{-\mu_p^{(2)}x} + A^{(2)} I$$

But at $x = 0$

$$I_p^{(2)} = I_p^{(1)} - A^{(1)} I,$$

and so

$$B = (A^{(1)} - A^{(2)}) I$$

We thus have, where $\beta = z$ if $z < a$ and a if $z \geqslant a$,

$$S = C \int_0^\beta \mu_p^{(2)} I_p^{(2)} (z - y) \, dy,$$

$$= C \int_0^\beta \mu_p I_0 \{(A^{(1)} - A^{(2)}) e^{-(\mu_p + \mu)(z-y)} + A^{(2)} e^{-\mu(z-y)}\} \, dy,$$

$$= \begin{cases} C(A^{(1)} - A^{(2)}) I_0 \dfrac{\mu_p}{\mu_p + \mu} (1 - e^{-(\mu_p + \mu)z}) + CA^{(2)} I_0 \dfrac{\mu_p}{\mu} (1 - e^{-\mu z}) \text{ for } z \leqslant a, \\[3mm] C(A^{(1)} - A^{(2)}) I_0 \dfrac{\mu_p}{\mu_p + \mu} (e^{(\mu_p + \mu)a} - 1) e^{-(\mu_p + \mu)z} + CA^{(2)} I_0 \dfrac{\mu_p}{\mu} (e^{\mu a} - 1) e^{-\mu z} \\ \hfill \text{ for } z \geqslant a, \end{cases}$$

where C is a constant depending on the chance of observing a shower   To this number of showers must be added the background   Thus, in the experimental arrangement of fig 1, will be approximately constant   Denote this background by D   If $\mu < \mu_p$, then the second term has little effect on the shape of the curve until a considerable thickness has been reached   Thus for small thicknesses the shape of the curve is given by

$$S = \begin{cases} C'(1 - e^{-\mu_p z}) + D & \text{for } z \leqslant a \\[2mm] C'(e^{\mu_p z} - 1) e^{-\mu_p z} + D & \text{for } z \geqslant a \end{cases}$$

This formula agrees very well with the experimental results with the values

$$a = 2 \ 2 \ \text{cm}$$

$$\mu = 0 \ 38 \ \text{cm}^{-1}$$

$$C' = 53 \ 9 \ \text{counts per hour}$$

$$D = 51 \ 0 \ \text{counts per hour}$$

The points calculated using these values are shown by crosses in fig 3.

For large thicknesses of material the tail of the curve falls away less rapidly and finally has an absorption coefficient μ * The sharpness of the peak of the experimental curve suggests that the energy of the shower particles is fairly homogeneous † The curves of Rossi and Funfer have not such sharp peaks. This may be due to the fact that they used much wider sheets of lead and so many showers would be recorded that had come through the lead at an angle

The shape of this transition curve is similar to the transition curves (Übergangskurven) obtained by Schindler using an ionization chamber ‡ The fall of his curves immediately past the maximum gives an absorption coefficient which agrees well with the values obtained with counters The position of the maximum is also in rough agreement It thus appears certain that the transition effects observed by Steinke,§ Schindler (*loc cit*) and others with ionization chambers are essentially the same as those observed with counters, and therefore are mainly an effect due to the showers

The Shower Particles

The position of the peak of the curve varies from 1 6 cm at sea level to 2 2 cm. at 3500 m The corresponding energies of the shower particles as calculated from Heisenberg's‖ formula are 70 and 95 million electron volts, if the particles are positive and negative electrons. The measurements of Anderson¶ confirm Heisenberg's data at these high energies That the particles are positive and negative electrons seems certain from the expansion chamber photographs of Blackett and Occhialini (*loc cit*) and Anderson **

* Rossi, ' Nature,' *loc cit*

† Bhabha, 'Z Physik,' vol 86, p. 120 (1933)

‡ Schindler, ' Z Physik,' vol. 72, p 625 (1931)

§ ' Z. Physik,' vol 48, p 647 (1928)

‖ ' Ann. Physik,' vol 13, p. 430 (1932)

¶ ' Phys. Rev ,' vol. 43, p. 381 A (1933) , vol. 44, p. 406 (1933)

** ' Phys. Rev ,' vol. 44, p. 406 (1933).

Fünfer's (*loc cit*) results give the ranges of the shower particles of showers produced in lead, iron and aluminium as 1 6 cm , 2 5 cm and 7 0 cm in lead iron and aluminium respectively All these values correspond to an energy of approximately 70 million electron volts Thus it appears that the energy of the shower particles does not vary greatly with the atomic number of the material

Shower Producing Radiation

The absorption coefficient of the shower producing radiation as observed at Jungfraujoch is 0 38 cm $^{-1}$ in lead Since the absorption coefficient is exponential the absorption probably takes place through single, or at the most a few, events Thus the greater part of the absorption is probably due to the production of showers The relation

$$\mu = N\sigma,$$

where N is the number of nuclei per unit volume and σ the effective cross-section for production of a shower, gives the value of cross-section for this absorption coefficient as 11 4 × 10^{-24} sq cm (radius 1 90 × 10^{-12} cm.) This is a very large cross-section, being larger than the nucleus itself From the data of various workers the cross-section for production of a shower can be estimated for lead, iron and aluminium. The results are shown in Table III Thus

Table III —Effective cross section for production of a shower

	Lead	Iron	Aluminium.
Absorption coefficient of shower producing radiation in cm.$^{-1}$ of the material	0 30* 0 29† 0 38‡ 0 34§	0 064* 0 11† — —	0 017* — — —
Radius of cross-section × 10^{13} cm. Atomic number, Z	17 5 82	5 8 26	3 0 13
$\dfrac{\text{Area cross-section}}{Z^2} \times 10^{27}$	1 43	1 54	1 66

* Fünfer, *loc cit.*
† Rossi, ' Z Physik,' vol 82, p. 151 (1933)
‡ The author
§ Schindler, ' Z Physik,' vol. 72, p. 628 (1931)

the area of cross-section varies nearly as the *square* of the atomic number This is in striking contrast to the usual *mass* absorption rule holding for cosmic radiation in general Recent calculations of Oppenheimer and Plesset‖

‖ ' Phys. Rev ,' vol. 44, p 53 (1933)

show that for γ-rays of high energy the cross-section for production of a pair of positive and negative electrons is given by

$$\sigma \sim \frac{Z^2}{137} \frac{e^4}{m^2 c^4}$$

Furry and Carlson* show that for high energy electrons the cross section is of the same order For lead the cross-section derived by Oppenheimer and Plesset is $3 \ 9 \times 10^{-24}$ sq cm as compared with the observed value of $11 \ 4 \times 10^{-24}$ sq cm for the absorption coefficient of the shower-producing radiation †

The mechanism of production of the showers by the shower-producing radiation is probably that pairs of electrons are produced in the field of the nucleus. Oppenheimer and Plesset have only dealt with the production of a single pair, but it is possible that in the showers many pairs are produced simultaneously The showers thus appear to be creation of particles and not, as at first looked probable, the disintegration of the nucleus

The experiment with lead under the counters shows that there are showers with particles thrown backward with a range in lead of approximately 0 6 cm that is an energy of about 30 million electron volts Further, these showers depend in some way on the showers produced in the lead above, for as the thickness of the lead above is increased the number of showers from the lower lead increases, reaches a maximum lying between 1 and 3 cm. and then decreases

Thus the showers from the upper lead must contain some kind of radiation which is capable of producing showers in the lower lead. This is in agreement with the remark of Blackett and Occhialini (*loc cit*, p 717) that " when one shower occurs there is a surprisingly large chance that another will occur a short way below it This leads one to the view that a shower-producing radiation can be produced in the showers themselves, but as is shown later, this cannot be the main cause of the shower-producing radiation

About the nature of the shower-producing radiation little can be said Its chief means of absorption is probably the production of showers and since the mean free path for this is so small no information is given by its absorption as to whether it is charged or not. It may possibly consist of gamma radiation

* ' Phys. Rev ,' vol. 44, p 237 (1933)

† Heitler and Santer, ' Nature,' vol. 132, p 892 (1933), obtain a cross section for production of positive and negative electrons in lead of 33×10^{-24} sq cm for γ rays of energy 50 million electron volts

Primary Radiation

Since the shower-producing radiation has such a small mean free path, there must be some mechanism of reproducing the radiation   We have seen that it can be reproduced in the showers themselves, but this cannot be the only method for this alone cannot give the transition effects observed   These require that the shower producing radiation be in equilibrium with some other radiation and that the equilibrium value changes on passing from one material to another   It thus appears necessary that the shower-producing radiation is produced by a primary radiation which traverses the whole atmosphere

For large thicknesses of material the number of showers falls off with the absorption coefficient of the primary radiation   Further, the number of showers increases with altitude at the same rate as the general radiation   So the absorption of the primaries is probably the same as that of the general cosmic radiation   Now the absorption of the general radiation in large thicknesses of different material obeys approximately the mass absorption rule   Hence the primary radiation probably obeys the same rule   From the absorption measurements of cosmic radiation in large thicknesses of material we can get an upper limit for the cross-section of *production* of the shower-producing radiation by the primary radiation (Table IV)

Table IV —Effective cross-section of absorption of primary radiation

	Lead	Iron	Water
Absorption coefficient in cm.$^{-1}$ of the material	0 0064*	0 0070*	0 00021†
Area of cross section × 10^{23} cm	2 5	1 7	0 44

* Schindler, ' Z Physik,' vol 72, p. 628 (1931)
† Regener, ' Phys Z,' vol. 34, p. 306 (1933)

The majority of the particles present in the cosmic ray stream in the atmosphere may have originated in showers   the primaries would then probably be charged so as to give the observed latitude variation

Energy Relations

The fact that the energy of the showers increases upwards in the atmosphere suggests that the energy of the showers comes from the primary radiation and is not released from the nucleus as some trigger action.

The energy carried by the shower particles is probably of the order of 1 5 × 10^9 electron volts at sea level, assuming 20 particles in a shower   Since

the energy required for an electron to penetrate the atmosphere is 5×10^9 electron volts, the energy of the primary radiation is probably of the order of 10^{10} electron volts Particles of this order are required by the theory of Lemaitre and Vallarta* to explain the observed latitude effect On going from 3500 m to sea level an electron which had 10^{10} electron volts energy when it entered the atmosphere will suffer a 26% decrease in energy This compares favourably with the 25% decrease of the energy of the shower particles between these levels

Summary

Experiments made with triple coincidence counters show that the frequency of showers produced in lead by the passage of cosmic radiation is proportional to the general cosmic radiation The transition curves for air to lead were obtained at 3500 m and it was found that there the energy of the shower particles was greater than at sea level To explain the curves obtained, three types of radiation are needed, a primary radiation, a shower-producing radiation and the shower particles The nature and properties of these radiations are summarized in Table V

Table V

Radiation	Kind	Evidence	Absorption.
Primary	Probably charged	Latitude effect	Mass absorption $\sigma \propto \gamma$
Shower producing	Unknown		Exponential absorption $\sigma \sim \dfrac{Z^2}{137} \dfrac{e^4}{m^2 c^4}$
Shower particles	Positive and negative electrons	Wilson cloud chamber photographs	Mass absorption range $\sim 1/\rho$.

* ' Phys. Rev.,' vol 42, p. 914 (1932)

The Nuclear Spin of Tin

By S. Tolansky, Ph.D. (1851 Exhibition Senior Student), Imperial College of Science, London

Introduction

In a previous note to 'Nature,'[†] the author has briefly reported the main conclusions arrived at from an investigation of the fine structures of the lines of the spark spectrum of tin. It was stated there that the nuclear spin of the two main odd isotopes of tin was $\frac{1}{2}$, the magnetic moments being negative, and also identical in value for both. Almost immediately after this note appeared, an independent report was published by Schüler and Westmeyer,[‡] who reached identical conclusions about the spins. The present paper gives a detailed account of the author's observations on the Sn II spectrum. In addition to this, the value of the nuclear spin has been confirmed by measurements in the Sn I spectrum.

Aston has reported 11 isotopes in tin, the relative abundances of which are shown in Table I.

Table I

Isotope	112	114	115	116	117	118	119	120	121	122	124
% abundance	1·1	0·7	0·4*	14·2	9·8*	21·5	11·0*	27·0	2·9*	5·0	6·2

The odd isotopes, indicated by asterisks, comprise about 24% of the total. In accordance with what has usually been observed in atoms containing a mixture of odd and even isotopes, it is to be expected that the even isotopes will have zero nuclear spin, or at least very small nuclear magnetic moments. Each even isotope will contribute a single component to the pattern of a given line, and if there is no isotope displacement effect these will all superpose, producing a single strong component.

On the other hand, the odd isotopes will possess nuclear mechanical and magnetic moments, and the coupling of the nuclear magnetic moment with the external electron magnetic moment of the atom will cause the terms to split, such that the even isotope in each term is at the centre of gravity of the split

term As a result, the expected line patterns will consist of tiny multiplet groups, the summed intensity of which will be 24% of the total, and at the centre of gravity of each group will be a single strong line comprising 76% of the total intensity, and representing the contribution of the even isotopes If this central strong component is split up or even appreciably broadened, this is an indication that even isotope displacement is taking place

The present investigation is largely concerned with the Sn II lines emitted by a hollow cathode discharge in tin The term scheme of this spectrum has been given by Green and Loring[*] and further details have been reported by Lang[†]

The transitions which have been studied here are shown in the term scheme in fig 1 Other transitions lie in a region unsuited to the silvered Fabry-Pérot interferometer which was used as the resolving instrument In the normal state, the tin ion has a $5s^2$ $5p$ electron configuration, so that a group of doublet terms is built up by the $5p$ electron going into various orbits From the point of view of fine structure analysis, the closed $5s^2$ group can be neglected and the doublet terms treated as if they arise from a one electron system Such a procedure is entirely justified both on theoretical grounds and by previous experimental evidence However, Lang (*loc cit*) has shown that in addition to the doublet group discussed above, there exists a doublet and quartet system based upon $5s$ $5p^2$ The observed terms due to this configuration are shown to the right of fig 1 and it will be shown later that there is evidence that fine structure perturbations take place between the ^2D terms of the two configurations

Experimental

The Sn II spectrum was excited both in water cooled and hot hollow cathode discharges The tubes employed were slight modifications of the type used so successfully by Schüler for the production of intense lines free from broadening effects Helium was continuously circulated through the tubes at about a millimetre pressure and currents of 200–300 milliamperes employed The resulting tin spectrum was extremely bright The lines were examined for fine structure by means of a variable gap, silvered, Fabry-Pérot interferometer of large aperture, crossed with a two prism spectrograph Using Ilford hyper sensitive plates the pattern of the strongest line could be photographed in a few minutes, although it includes a relatively weak component whose intensity is only 5% of that of the complete pattern

The observed structures are shown in Table II As usual, the separations are given in cm $^{-1} \times 10^{-3}$, and the visual estimates of intensity indicated below each component in brackets.
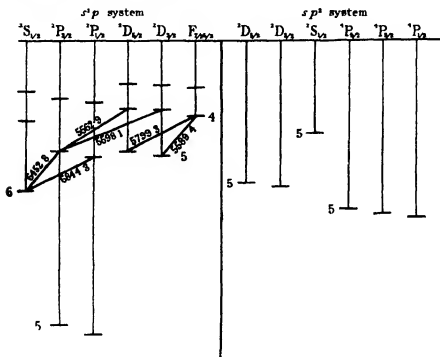
Fig 1

Table II

Wave length	Allocation	Structure					Total width.
							cm $^{-1} \times 10^{-3}$
6844 3	$6s\ ^2D_{1/2} - 6p\ ^2P_{1/2}$	$\dagger$	100	65	0	181	281
			(1)	(2)	(15)	(1)	
6452 8	$6s\ ^2D_{3/2} - 6p\ ^2P_{3/2}$	$+$	53	0	154	$-$	207
			(3)	(15)	(1)		
5799 3	$5d\ ^2D_{3/2} - 4f\ ^2F$	$+$	152	0	239	$-$	391
			(3)	(15)	(2)		
5598 1	$6p\ ^2P_{3/2} - 6d\ ^2D_{3/2}$	Single—sharp					—
5589 4	$5d\ ^2D_{3/2} - 4f\ ^2F$	Single – diffuse					~ 75
5562 9	$6p\ ^2P_{1/2} - 6d\ ^2D_{3/2}$	Single—sharp					▶—
5545 9*	?	$+$	115	54	0	81	250
			(2)	(3)	(6)	(1)	
4511 5*	?	$+$	69	0	186	—	255
			(1)	(2)	(2)		

* It is not quite certain that these two lines belong to the Sn II spectrum

Analysis of Structures.

The analysis of each line will now be separately dealt with, and it will be shown that all the structures are completely accounted for on a nuclear spin of $\frac{1}{2}$ for the two main odd isotopes, and a zero spin (or minute nuclear magnetic moment) for the even isotopes. The lines will be considered in the order best suited for analysis.

λ 6452 8 $(6s\ ^3S_{1/2} - 6p\ ^3P_{3/2})$.—The structure in this line consists of a strong central component contributing about 75% of the total intensity of the pattern, flanked on either side by two weak components whose intensity ratio is 3 : 1. It is at once apparent that the central strong component arises from the even isotopes and as the two odd isotopes 117 and 119 are present to the extent of 9 8% and 11 0% respectively, the two weak satellites are almost entirely produced by these, any contribution from 121 being difficult to observe since its components will only be of intensity 1% and therefore practically negligible. The 3 : 1 intensity ratio of the components shows that both isotopes contribute to each component. The ratio of the intervals between the satellites and the central strong component is exactly 1 : 3, so that the strong line is at the optical centre of gravity of the pattern. The lower term is a $6s\ ^3S_{1/2}$ term, and as it involves a penetrating s electron it will show fine structure. On the other hand, it is already well known that the $6p\ ^3P_{3/2}$ term should show a relatively very minute structure, for all $p\ ^3P_{3/2}$ terms yet investigated have conformed to this rule. It follows that the structure in the line is the structure of the lower term.

The number of fine structure levels in a term is $2J + 1$ when the spin, I, is greater than J, or $2I + 1$ when $J > I$. From this it is seen that a term with $J = \frac{1}{2}$ always splits up into two fine structure levels, no matter what the value of I. An intensity ratio of 3 : 1 is only produced by a spin of $\frac{1}{2}$, the next value, namely, 3/2 giving an intensity ratio of 5 : 3 which could not be confused with the previous value. However, it will be shown later that the $^3D_{5/2}$ term is also double, and as the J value is 5/2 here, this proves conclusively that the spin is $\frac{1}{2}$. In addition, it will be further shown that a spin of $\frac{1}{2}$ is unambiguously deduced from fine structures in the Sn I spectrum.

The analysis for the line under consideration is shown in fig 2. The upper term is single. The nuclear spin $\frac{1}{2}$ combines with the lower $J = \frac{1}{2}$ to give the fine structure quantum numbers $F = 0$ and 1. Both the odd isotopes must be treated as one, since otherwise four satellites instead of two would appear. The dotted lines show the even isotope transition, and in order to get this the

lower even isotope term has been placed at the centre of gravity of the lower term, i e, one-fourth of the distance from the level with $F = 1$ (the quantum weight of a fine structure level F is $2F + 1$)   As the stronger satellite is to the violet, the fine structure levels are inverted, the higher F term lying deeper This means that the nuclear moment is negative, so that $I = -\frac{1}{2}$ It will be observed that the calculated position of the even isotope line is 155 units
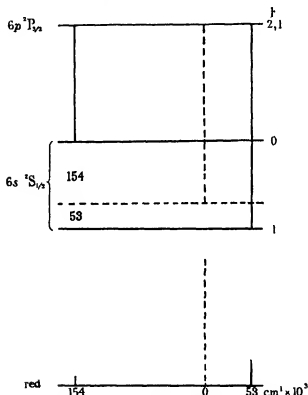
FIG 2 —Fine structure of λ 6452 8 (6s $^2S_{1/2}$—6p $^2P_{3/2}$)

from the weaker component and experimentally it is found to be 154 units away   This is considered to be exact agreement

λ 6844 3 (6s $^2S_{1/2}$—6p $^2P_{1/2}$) —The structure of the upper term can be directly obtained It was found experimentally that the intense even isotope line blurred the near by component of intensity 2, making accurate measurement of the position of this component very difficult   However, this does not invalidate the analysis, for it will be

seen from fig 3 that the structure of the upper term is determined by the separation of the remaining outer components The even isotope level is again placed at the optical centre of gravity in both terms The calculated structure is shown at A and the observed pattern at B The agreement is
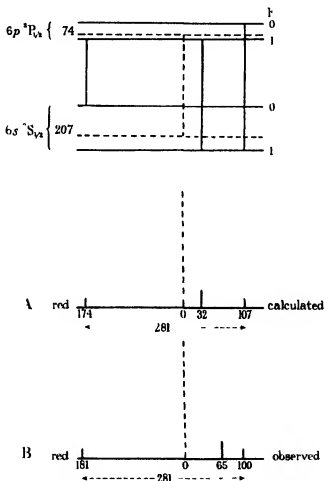
Fig 3 — Fine structure of λ 6844 ⅓ ($6s$ $^5S_{1/2}$—$6p$ $^2P_{1/2}$)

fairly satisfactory when account is taken both of the smallness of the separations and the difficulties caused by the over-exposed even isotope central component

The upper term has a structure 74 units in width, with an uncertainty of perhaps 10 units at the utmost As in the lower term the levels are inverted The transition $\Delta F = 0 \rightarrow 0$ is, of course, absent

λ 5598 1 ($6p$ $^2P_{3/2}$—$6d$ $^2D_{3/2}$) .—This line shows no trace of structure, thus confirming the previous conclusion that the $6p$ $^2P_{3/2}$ term is single It proves that the upper term, $6d$ $^2D_{3/2}$ also shows no structure

λ 5799 3 ($5d$ $^2D_{5/2}$—$4f$ ^2F) —There is a strong central component due to the even isotopes, but instead of being quite sharp, as in the previous lines, it is distinctly diffuse In addition, there are two weak satellites arising from the odd isotopes, the structure being relatively quite wide, for the components are 391 units apart The odd isotope structure is due entirely to the lower term, for it will be shown later that the $4f$ ^2F term is single This is also shown by —

(a) The fact that the even isotope is almost at the centre of gravity of the doublet

(b) The fact that the stronger component is nearer to the violet shows that the structure is in the lower term, since the spin is negative

The analysis of the line is shown in fig 4 Of particular importance is the fact that the lower term has only two fine structure components, for this at once proves that the spin is = $\frac{1}{2}$

The diffuse nature of the central component indicates a very small even isotope displacement

λ 5589 4 ($5d$ $^2D_{3/2}$—$4f$ ^2F) —This line is also single but is diffuse The absence of weak components shows that the structure in both upper and lower odd isotope terms is extremely minute This therefore confirms the previous conclusion that $4f$ ^2F shows no structure It is difficult to tell whether the small isotope displacement is in the lower or the upper term An approximate estimate of the width of the line is 75 units, which would indicate a displacement between the even isotopes of the order of 20 units This tentative value can only indicate the order of the effect

λ 5562 9 ($6p$ $^2P_{3/2}$—$6d$ $^2D_{5/2}$) —This line is very sharp and single, and as the lower term has already been proved to be single by two other lines, it follows that the upper $6d$ $^2D_{5/2}$ term is also single

Two other lines, namely, λλ 5545 9, 4511 5, show peculiar structures, but it is not known whether they belong to the spectrum of Sn II These are quite strong, however, and have not been identified with any probable impurity lines λ 4511 5 is particularly intense and is reported by Homsalech as a weak tin line occurring in the spark Although none of the remaining observers quoted in Kayser's 'Handbuch der Spektroskopie,' vol 6, have observed this line, it appears with great intensity in the discharge tube employed That

does not, however, show whether or not it is an impurity line   The structures in these two lines are quite different from those in all the other lines examined, for neither possesses a strong central even isotope component   If these lines do belong to tin, then they both show large even isotope displacement effects   In particular the intensities of the components of λ 5545 9 agree fairly well with the abundance ratios of the even isotopes, when it is remembered that the odd isotope components will be distributed amongst them   If this is correct,
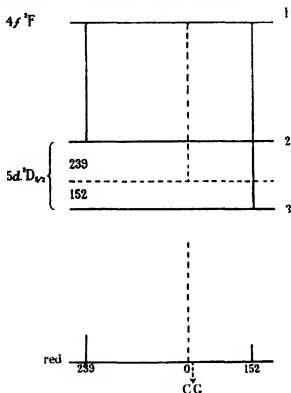
FIG 4 —Fine structure of λ 5799 3 $(5d\ ^3D_{3/2}–4f\ ^3F)$

it would imply an even isotope displacement of the order of 60 units   The peculiar structure in the other line could also arise from the superposition of a large isotope displacement effect on a small spin structure   It is, however, entirely unsafe to speculate about either of these lines since it is not known with certainty if they are tin lines or not

Discussion

It is seen that the fine structures are consistently explained by attributing a nuclear spin of $-\frac{1}{2}$ to the two main odd isotopes   Both of these isotopes

have the same magnetic as well as the same mechanical moments, so that their respective patterns superpose exactly There is no evidence of any measurable displacement effect between the two odd isotopes That the spin must be $\frac{1}{2}$ is proved by the structure of the $5d$ $^2D_{5/2}$ term, for if I had any other value than this more than two components would have resulted Furthermore the even isotope lines only fall at the centres of gravity of the patterns if the spin is taken to be $\frac{1}{2}$ As the higher valued F level lies deeper in all the terms, the spin is negative for both the isotopes, as for the neighbouring atom cadmium

It is possible to deduce the interval factors in a number of terms, and these are shown in Table III According to the interval rule, the interval between two fine structure levels F + 1 and F, is given by A (F + 1) where A is a constant for a term and is called the interval factor The values in the table refer only to the odd isotopes

Table III

Term	Width of structure	Interval factor
$6s$ $^2S_{1/2}$	207	207
$6p$ $^2P_{1/2}$	74	74
$6p$ $^2P_{3/2}$	small	small
$5d$ $^2D_{5/2}$	391	130
$5d$ $^2D_{3/2}$	small	small
$6d$ $^2D_{5/2}$	small	small
$6d$ $^2D_{3/2}$	small	small
$4f$ ^2F	small	small

In accordance with theoretical expectations, the $6s$ $^2S_{1/2}$ term has a relatively wide structure, since it possesses a penetrating s electron The structure in the $6p$ $^2P_{3/2}$ term is too small to measure and this fact is in complete agreement with what has been found in other spectra The interval factor for the $6p$ $^2P_{1/2}$ term is 74 As in other one-electron spectra this is quite appreciable and appears to be due to the fact that in heavy atoms a $p_{1/2}$ electron is relatively penetrating * Since the d and f electrons are non-penetrating, no observable fine structures are to be expected in terms involving them. It appears therefore that the interval factor 130 for $5d$ $^2D_{5/2}$ is anomalously great Associated with this is the question of the observed small even isotope displacement This occurs in two lines $5d$ $^2D_{5/2}$—$4f$ ^2F and $5d$ $^2D_{3/2}$—$4f$ ^2F, but appears to be slightly more marked in the latter line, although this is difficult to decide

* Brent, 'Phys Rev.,' vol. 38, p. 462 (1931)

The multiplet separation of the ^3F term is not resolved * It follows that the even isotope displacement occurs either in the two ^3D terms or in the ^3F term It will now be shown that the ^3D terms are probably responsible, although it is not unambiguously proved

It is very probable that the $5d$ ^3D terms are perturbed in the Sn II spectrum, for both Green and Loring (*loc cit*) and Lang (*loc cit*) have shown that in addition to the normal doublet system having s^2 p as its basic configuration, there exists a parallel s p^2 system of doublets and quartets It is seen from fig 1 that the 5 ^3D terms of these two systems lie fairly close to each other Russell and Shenstone† have shown that it is just such terms, namely those with the same n, L, J values, but arising from different electron configurations, that perturb very strongly, even if a large interval separates them The Pb II spectrum is very similar in structure, and the two sets of ^3D terms are almost identically situated in both spectra It is known that there is a strong perturbation between these terms in Pb II so that the same will be likely in Sn II These perturbed terms in Pb II show abnormally wide even isotope displacement ‡ It is therefore to be expected that even isotope displacement should occur in both the $5d$ $^3D_{5/2}$ and the $5d$ $^3D_{3/2}$ terms of Sn II, and as shown previously, the experimental evidence supports this

The abnormally large value of the $5d$ $^3D_{5/2}$ interval factor is also very probably a result of the same perturbation that produces the isotope displacement It was shown by Schüler and Jones§ that when fine structure perturbations occur between two terms there is an apparent repulsion between levels of the same F value The repulsions are proportional to F so that if all the levels of a term are perturbed (which is the case when the J values of the two perturbing terms are the same) the interval rule still holds in the perturbed structures The perturbation may either close or open up a structure, depending on the relative positions of the perturbing levels Jones‖ also pointed out that the strongly perturbed $^1P_1$ term in Hg I and the $6d$ ^3D terms of Pb II are associated with a very large even isotope displacement Taking all the evidence into consideration, it suggests that the explanation of the abnormal ^3D structures is probably to be sought in perturbations In this respect it may be noticed that the even isotope line in $5d$ $^3D_{5/2}$—$4f$ ^3F is not exactly at the calculated centre of gravity of the fine structure multiplet, but is dis-

---

* An analogous case exists in the very similar Pb II spectrum

† ' Phys Rev ,' vol 39, p 415 (1932)

‡ Schüler and Jones, ' Z Physik,' vol 75, p 563 (1932)

§ ' Z Physik,' vol 77, p 801 (1932)

‖ ' Proc Phys Soc ,' vol 45, p 501 (1933)

placed to the violet by 10 units, which, although small, is apparently real
Such a displacement would arise if a perturbation took place, as can easily be
shown

Nuclear Magnetic Moment

Recent theoretical developments due to Goudsmit[*] make it possible to
calculate the nuclear magnetic moment, for a one-electron spectrum, with a
high degree of certainty, if the necessary fine structures are known The
values of the nuclear magnetic moments are just as important as the values
of the mechanical moments, for although the latter are quantized, the former
are not, showing that although the nuclear particles have half integral
mechanical spins, these spins are associated with different magnetic moments
for different kinds of particles Goudsmit has shown that, if g (I) is the ratio
of the magnetic to the mechanical moment of a nucleus, the former being
expressed in Bohr magnetons, the following relationship holds for the structure
in an s $^2S_{1/2}$ term

$$g\,(\mathrm{I}) = \frac{3a}{8} \frac{n_0{}^3}{R a^2} \frac{1838}{Z_i Z_0{}^2 \; \kappa\,(\tfrac{1}{2},\,Z_i)}$$

The symbols have the following values for the present term under considera-
tion —

   a is the interval factor of the term and is equal to 0 207 cm.$^{-1}$

   $n_0 = 2$ 685 is the Rydberg denominator of the term which in this case
          is the 6s $^2S_{1/2}$ term

   $R = 109,737$ is the Rydberg constant

   Z_i is the effective nuclear charge in the inner portion of the penetrating
        orbit, and as the fine structure interaction comes from the region
        very close to the nucleus, $Z_i = Z$ where Z is the atomic number
        For tin this is 50

   Z_0 is the charge in the outer portion of the orbit and since the spectrum
        is that of Sn II, equals 2

   $\kappa\,(\tfrac{1}{2},\,Z_i)$ is a calculated relativity correction depending on the value of
        Z and J and is in this case 1 30

   a^2 is the spectroscopic doublet constant = 5 305 $\times$ 10^{-5}

On substituting these values into the above equation, the value obtained for
g (I) is -1 78 Alternatively, the magnetic moment is -0 89 Bohr
proton magnetons or 1/2060 that of the electron

* ' Phys Rev ,' vol. 43, p. 636 (1933)

Fine Structure in the Sn I Spectrum.

When the pressure of helium in the tube was reduced, the Sn I line 5631 9 ($2p$ $^1S_0$—$3s$ $^3P_1$) came up very strongly   The structure of this line is as follows :—

$$+ \quad 158 \qquad 0 \qquad 82 \quad -$$
$$(1) \qquad (10) \qquad (2)$$

As in the Sn II lines, the central strong sharp component is due to the even isotopes and the weaker components to the odd   The analysis of this line is
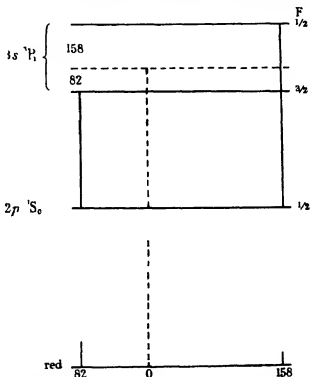
Fig 5 —Fine structure of the Sn I line λ 5631 9 ($2p$ $^1S_0$—$3s$ $^3P_1$)

of particular value, since the lower term has a $J = 0$ and therefore remains single, no matter what the value of the spin ($2J + 1 = 1$)   The two satellites therefore give the structure of the upper term, and as the J value of this term is 1, the doublet fine structure proves that the spin is $\frac{1}{2}$, for any other value would result in a triplet structure   The analysis of the line is shown in fig 5   The bigger F level lies deeper, again proving that the magnetic moment is negative   The even isotope line falls extremely close to the calculated optical

centre of gravity of the pattern   The F values being $\frac{1}{2}$ and 3/2, the quantum weights of the levels are in the ratio 1   2, so that the centre of gravity is 80 units from the stronger component   The measurements give it at 82, which is extremely good agreement

The interval factor for the 3s $^3P_1$ term of Sn I is 160   It may therefore be taken as definitely proved that the nuclear spin of tin is $-\frac{1}{2}$, for this value is obtained from independent analysis of Sn I and Sn II lines   This is true for the two stronger odd isotopes 117 and 119   It is usually considered that as the even isotopes show no structure, this is due to a zero spin, but it is well to point out the no structure is produced when the nuclear magnetic moment is small   even when associated with a mechanical moment   It can therefore only be concluded with certainty that the nuclear magnetic moments of 116, 118, 120, 122, 124 are very small, possibly zero   Unfortunately nothing can be said about the weak tin isotopes 115 and 121   These are isobaric with indium and antimony respectively and a comparison of isobaric spins would have been of value   Cadmium is the only other atom in which both the odd isotopes are known to possess negative spins   Table IV is of interest, showing how abruptly the spins change from small negative to large positive values, although the atomic weights form a regular series

Table IV

Atom	Cd	Cd	In	Sn	Sn	Sb	Sb
Isotope	111	113	115	117	119	121	123
Spin	$-1/2$	$-1/2$	9/2	$-1/2$	$-1/2$	5/2	7/2

I wish to take this opportunity of expressing my thanks to Professor A Fowler, F R S, for his continual assistance and encouragement during this work, and for the excellent facilities he has afforded me in his laboratory I also wish to thank Professor W E Curtis, of Newcastle, for the loan of a pair of interferometer plates

Summary

The fine structures of the visible lines of the Sn II spectrum have been analysed by means of a silvered Fabry-Pérot interferometer   The structures of eight terms have been observed, and it is shown that the nuclear spin of the two main odd isotopes 117 and 119 is $-\frac{1}{2}$ The nuclear magnetic moment for these isotopes has been calculated and g (I) found to be -1 78, giving a magnetic moment 1/2060 that of the electron.

Even isotope displacement is found in some lines, and it is shown that this is probably due to perturbations taking place between the ^3D terms arising from the s^2 d and the s p^2 electron configurations, as in the Pb II spectrum.

The fine structure of the $2p$ $^1S_0$—$3s$ $^3P_1$ line of the Sn I spectrum is reported and analysed, and from this a nuclear spin of $-\frac{1}{2}$ is also deduced, thereby confirming the value obtained from Sn II

Attention is drawn to the very abrupt changes which take place in the signs and values of the nuclear spins in the series of odd isotopes between 111 and 123

Hyperfine Structure in the Arc Spectrum of Xenon

By E GWYNNE JONES, Beit Scientific Research Fellow, Imperial College of Science, London

(Communicated by A Fowler, F R S—Received November 22, 1933)

The spectrum of neutral xenon (Xe–I) was first analysed by Meggers, de Bruin and Humphreys[*] in 1929 One of the objects of their investigation was to determine whether any of the lines of xenon would be suitable for consideration as wave-length standards to replace the λ 6438 of cadmium, which is considered[†] to be unsuitable in many respects The analysis showed that the strongest lines in the region $\lambda\lambda$ 4200 to 8800 are $s - p$ transitions and are therefore theoretically suitable as standards, in the event of their not possessing hyperfine structures, since they are not subject to Stark displacements in the electric field of the discharge [‡] It is thus important that the spectrum should be thoroughly examined, with apparatus of the highest resolving power, for hyperfine structure

Apparatus

Xenon, on account of its high atomic weight, emits very sharp lines in ordinary light-sources, so that no great precautions were necessary beyond care that lines involving metastable terms (in particular $1s_5$) should not be produced under conditions that would permit self-absorption to occur

The lines were excited, by means of a transformer supplying about 10,000 volts A.C., in a Pyrex discharge tube, of H-shape, so that both the " end-on "

* ' Bur Stand J Res,' vol 3, p 731 (1929)

† ' 7th Conf. Gen Poids et Mesures, p. 52 (1927)

‡ Harkness and Heard, ' Proc Roy Soc ,' A, vol. 139, p 416 (1933)

and " side on " positions could be used   The lower ends of the tube, which
contained the aluminium electrodes, were much lengthened in order to keep
the capillary free from sputtered material, as xenon causes very excessive
electrode sputtering   Currents ranging from 1/10 to 5 mA were employed—
only the weakest excitations being used for lines ending on metastable levels—
with exposure times varying from $\frac{1}{4}$ minute to $7\frac{1}{2}$ hours

Fabry-Pérot étalons, mounted in the " parallel beam " of a large-aperture
spectrograph, provided the necessary interferometric apparatus   The étalons
were of the fixed separation type, with various thicknesses from 5 to 25 mm ,
the plates being silvered by cathodic sputtering in argon to suitable densities
for the different spectral regions   The spectra were recorded on Ilford
Monarch, hypersensitive panchromatic or infra-red plates according to the
region examined   It was necessary to " sensitise " the infra-red plates with
ammonia for all but the strongest lines   About 85 photographs, obtained
with various étalon separations, were retained for measurement

Experimental Results

It was established that the majority of the lines investigated possess fairly
complex structures   A few, notably some of those involving the term $1s_4$,
have no appreciable structures but are slightly broadened ; the analysis of
other line structures shows that this is due to the small structure of the term
$1s_4$, which is only recognizable when in combination with another term possess-
ing a greater structure   In general, the line patterns consist of an intense
central component, together with a number of fainter lines whose total intensity
is roughly the same as that of the central component   In view of Aston's*
abundance ratios and of all other previously analysed hyperfine structures
of elements with " odd " and " even " isotopes, it is clear that this strong
central component represents the unresolved even isotopes (mass numbers
124, 126, 128, 130, 132, 134, and 136, totalling 52 2% of the whole) and that
the outer, less intense, components are due to the action of nuclear moments
in the odd isotopes (129 and 131, respectively 27 1% and 20 7%)

The problem is now to analyse these fainter components into a scheme that
will relate the observed structures to definite terms and to assign nuclear
moments to account for these structures   It has been found possible† to
allocate the line structures to the various terms, to assign the nuclear moment

$I = \frac{1}{2}$ to Xe_{129} and to assert that for Xe_{131}, $I > 3/2$ Owing to the fact that the less abundant odd isotope has the larger nuclear spin, it has not been possible to obtain the complete patterns since, for an atom with a nuclear moment greater than $\frac{1}{2}$, these contain numerous faint components which are difficult to recognize, particularly when the structures are comparatively narrow Nevertheless, the analysis can be carried out with certainty for Xe_{129} ($I = \frac{1}{2}$), and the term separations for one odd isotope suffice to give a complete survey of the hyperfine structures occurring in the spectrum For terms of given J value, the Xe_{131} separations will always bear a constant ratio to those of Xe_{129}, and thus do not add to the knowledge of the coupling between the nucleus and the valency electrons

In a very brief note (in which no details are given) Kopfermann* states that he has also analysed a number of xenon line structures and assigned the nuclear moments $I_{129} = \frac{1}{2}$ and $I_{131} > 3/2$ The two independent analyses thus lead to the same result

Convincing proof of the correctness of the above interpretation is obtained when the various xenon line structures are compared with those of corresponding mercury lines a striking similarity is at once evident--the xenon line structures are usually perfect mirror images, on a smaller scale, of the mercury structures It has been shown†‡ that, for mercury, the even isotopes have zero nuclear spins ($I = 0$), while for the more abundant odd isotope, Hg_{199}, $I = \frac{1}{2}$ and for the other, Hg_{201}, $I = 3/2$ Thus a complete analogy between the structures is to be expected

Notation

The term notation adopted by Humphreys and Meggers§ is retained in the present work, but the appropriate J-value is added as a superscript to the term symbols.

The Analysis of the Line Structures

The observed line structures and the analysis for Xe_{129} are shown in the figs 1 to 9, in which the positions of the components are given in units of 10^{-3} cm^{-1} The intensities of the various components, according to a rough visual estimate, are proportional to the heights of the lines and the theoretical

---

* ' Naturwiss ,' vol 39, p 704 (1933)

† Schüler and Keyston, ' Z Physik,' vol 72, p 423 (1931)

‡ Schüler and Jones, ' Z Physik,' vol 74, p 631 (1932) , vol 77, p 801 (1932)

§ ' Bur Stand J Res ,' vol 10, p 139 (1933)

intensities—calculated from the appropriate intensity rules* and Aston's
abundance ratios—are found in the term schemes The components assigned
to Xe_{129} are indicated by capital letters, and those assigned to Xe_{131} by small
letters

The structure of the line $\lambda 7967$ $(1s_5^0 - 3p_7^1)$ is of particular importance,
since the appearance of four components—apart from the central one—proves
that the two odd isotopes have different nuclear moments The term $1s_5^0$ is
characterized by $J = 0$ and thus, in the absence of isotopic displacements,
can have no hyperfine structure ; hence, the term $3p_7^1$ has at least four hyper-
fine sub-levels arising from the odd isotopes Isotopic displacements are
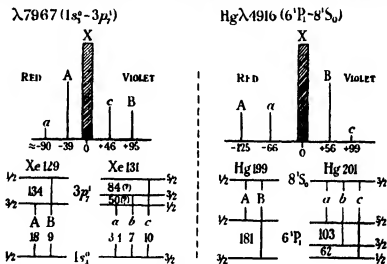
Fig 1

ruled out by the sharpness of the central component, X, in all lines Now,
$3p_7^1$ has $J = 1$ and thus cannot have more than a three-fold hyperfine structure
unless isotopes with more than one nuclear moment are involved In view of
the fact that Xe_{129} is the more abundant odd isotope, the strongest com-
ponents in the line patterns will belong to it , accordingly in $\lambda 7967$, " A "
and " B ", fig 1, are assigned to Xe_{129} Their relative intensities ($\simeq 2\ 1$)
and positions with respect to the " null-line " indicate that $I_{129} = \frac{1}{2}$, as other-
wise another component (approximately half the intensity of B) would be
required on the " violet " side and also the centre of gravity of this new pattern
would no longer coincide with " X " The components " a " and " b " are
assigned to Xe_{131}, but a third component, between a and X, is required in

* Güttinger and Pauli, ' Z. Physik,' vol. 67, p 743 (1931)

order that the centre of gravity of Xe_{131} should coincide with X The complete analysis is presented in fig 1, which also contains the structure and analysis of Hg $\lambda 4916$, likewise a $J = 0 \rightarrow 1$ transition, and therefore completely analogous to Xe $\lambda 7967$

The lines $\lambda 7887$ $(1s_2{}^1 - 2p_4{}^0)$ and $\lambda 7642$ $(1s_2{}^0 - 2p_5{}^1)$ have structures that may be similarly analysed, fig 2 These two lines are not so favourable as $\lambda 7967$ for the observation of faint components
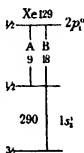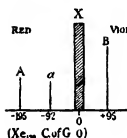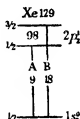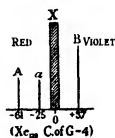
FIG 2

The structures of the lines $\lambda 8409$ $(1s_5{}^2 - 2p_7{}^1)$ and $\lambda 4792$ $(1s_5{}^2 - 3p_{10}{}^1)$ need special comment They are both exactly analogous to the mercury line $\lambda 5769$, this agreement is very satisfactory, in all these cases, both upper and lower terms possess structures and, as a result, the line patterns are rather complex, figs 3 and 4
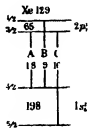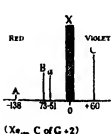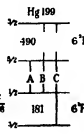
FIG 3

The structures of the terms $1s_5{}^2$ and $2p_8{}^1$ being now determined, it is possible to calculate the positions of the strongest satellites of Xe_{129} for $\lambda 4500$ $(1s_5{}^2 - 2p_8{}^1)$ The agreement with experiment is very close. The structure of the

term $1s_3^2$ permits the analysis of the lines λλ 4203, 4524, 8231, 8819, 4624, 4671, 4697, and 4792, from which the Xe_{129}-structures can be derived for the terms 4Y, $2p_8^2$, $2p_4^2$, $2p_6^2$, $3p_2^2$, $3p_8^2$, $3p_6^2$, and $3p_{10}^1$.
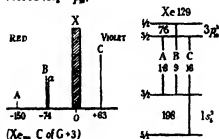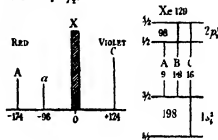
Fig 4

The lines λ 4734 ($1s_4^1 - 2p_2^2$) and λ 4524 ($1s_4^2 - 2p_2^2$) give the structures of $2p_2^2$ and the important term $1s_4^1$ The former term structure is again checked by the line λ 8346 ($1s_4^1 - 2p_3^2$), which also shows two of the strongest Xe_{131} components, a ($F = 5/2 \rightarrow 3/2$) and b ($F = 5/2 \rightarrow 5/2$), indicating that the total separation of the Xe_{131}-hyperfine structure is about 0 235 cm ^{1} for $1s_4^1$ The separation assigned to the term $2p_2^1$ is only approximate, as it is estimated from the fact that λ 4690 ($1s_5^2 - 2p_4^1$) possesses no marked structure —showing that the separations of the terms $1s_5^2$ and $2p_4^1$ are nearly equal This estimated structure is in qualitative agreement with the incompletely observed hyperfine structure of the line λ 4916 ($1s_4^1 - 2p_4^1$).
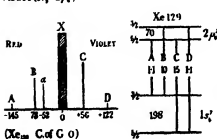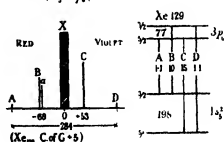
Fig 5

The total separations of the terms of Xe_{131} appear to be slightly less than those of Xe_{129}, and are always " inverted " with respect to those of the lighter isotope, proving that the nuclear magnetic moments are of opposite sign It

may also be shown, by the construction of tentative schemes for Xe_{131}, that no additional intense components are to be expected in observable positions for any of the lines   Thus the proposed analysis explains all the observed structures of the 20 principal Xe–I lines
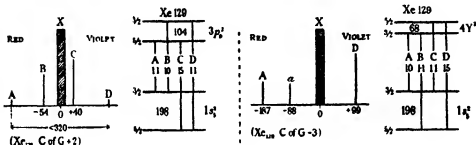
Fig 6

Discussion of Results

The hyperfine separations (for the isotope Xe_{129}) of the terms of the Xe–I spectrum, as derived from the preceding analysis of the line structures, are collected in Table I, which also shows the lines that were used in the determination of the particular term structure   It is noteworthy that, in all terms
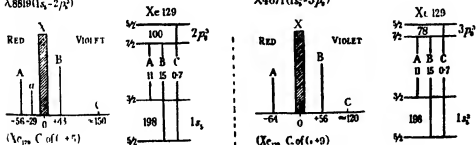
Fig 7.

except $2p_2$ and $4Y$, the hyperfine level of greater F-value is lower in the energy diagram (i e   the hyperfine levels of Xe_{129} are usually " inverted ")

No trace of an isotopic displacement was observed in any of the lines , the component (X) due to the even isotopes is always quite sharp

Table I — Hyperfine separations of the terms of Xe$_{129}$ (I = $\frac{1}{2}$)

Term	J value	Hyperfine separation	Landé interval factor	Lines involved
		cm^{-1}	cm^{-1}	λ
$1s_2{}^1$	1	$-0\ 290$	$-0\ 193$	7887, 8346
$1s_3{}^1$	0	$0\ 0$	$0\ 0$	7967, 7642
$1s_4{}^1$	1	$-0\ 057$	$-0\ 038$	4734
$1s_5{}^1$	2	$-0\ 198$	$-0\ 079$	8409, 4792, 4500, 8231, 4624 4203, 8819, 4671, 4524, 4697
$2p_1{}^0$	0	$0\ 0$	$0\ 0$	
$2p_2{}^1$	1	$+0\ 098$	$+0\ 065$	7887, 4582
$2p_3{}^1$	2	$-0\ 250$	$-0\ 100$	7642, 4500
$2p_4{}^1$	1	$\approx -0\ 220$	$-0\ 147$	(4916), (4690)
$2p_5{}^0$	0	$0\ 0$	$0\ 0$	8280
$2p_6{}^1$	2	$-0\ 070$	$-0\ 028$	8231
$2p_7{}^1$	1	$-0\ 065$	$-0\ 043$	8409
$2p_8{}^1$	3	$-0\ 100$	$-0\ 029$	8819
$3p_5{}^0$	0	$0\ 0$	$0\ 0$	4807
$3p_6{}^1$	2	$-0\ 076$	$-0\ 030$	4624
$3p_7{}^1$	1	$-0\ 134$	$-0\ 089$	7967
$3p_8{}^1$	3	$-0\ 078$	$-0\ 022$	4671
$3p_9{}^1$	2	$-0\ 104$	$-0\ 042$	4697
$3p_2{}^1$	1	$-0\ 076$	$-0\ 051$	4792
$4Y$	2	$+0\ 068$	$+0\ 027$	4203

The ^{1} — sign indicates that the hyperfine levels are inverted

λ4734 ($1s_4{}^1$ - $2p_2{}^1$)   λ4524 ($1s_5{}^1$-$2p_3{}^1$)
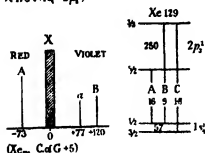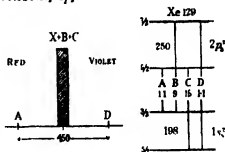
Fig 8

The mp_7- and mp_8-series show the existence of selective perturbations in the hyperfine structures of the members with $m = 3$, each perturbation is perceptible as an anomalous increase in the hyperfine separation of the term when compared with the lowest member The quantum defects of the terms are also anomalous and likewise indicate the presence of perturbations at $m = 3$ Exactly similar perturbations of hyperfine structures have been described* in the spectra Hg-I and Pb-II

* E. G Jones, 'Proc Phys. Soc,' vol 45, p. 501 (1933)

In conclusion, the writer wishes to express his thanks to Professor A Fowler, F R S , in whose laboratories the work was carried out, for his kindly interest and encouragement

Summary

(1) All the important lines in the region λλ 4200 to 8800 of the spectrum of neutral xenon have been investigated, with Fabry-Pérot étalons, for hyperfine structure   It was found that 16 lines were complex, so that it may be concluded that the lines of Xe-I are not suitable as wave-length standards

Fig 9
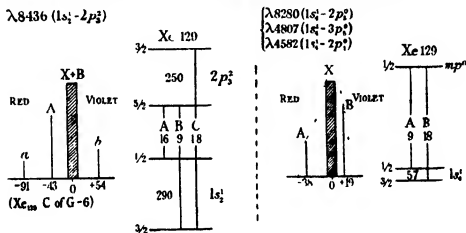
(2) The observed line structures have been analysed and the corresponding term structures determined   These structures are explicable if the nuclear moments I = 0 be assigned to the even isotopes, I = $\frac{1}{2}$ to Xe_{129} and I ⩾ 3/2 to Xe_{131} The nuclear magnetic moment of Xe_{131} has a sign opposite to that of Xe_{129}

(3) No isotopic displacements were found in any of the lines and the observed intensities of the components in the line patterns indicate that the even mass-numbers represent about 50% of the xenon isotopes

The Scattering of Electrons in Ionizing Collisions with Gas Atoms

By C. B. O. Mohr, Ph.D., Trinity College, Cambridge, and F. H. Nicoll,
M.Sc., Trinity College, Cambridge, 1851 Exhibitioner, University of
Saskatchewan

Introduction

When electrons lose energy by colliding with gas atoms, they may do so
either in definite amounts by exciting the atom to a discrete level, or by ionizing
the atom, in which case the electrons may lose any amount of their energy
over and above the minimum required for ionization. The first process has
now been studied in several aspects by a number of investigators, in particular,
the authors[*] have dealt with the angular distribution of the scattered electrons.

The study of ionizing collisions, however, has so far been confined largely
to the measurement of collision cross-sections,[†] while only slight attention
has been paid to the angular distribution and the energy distribution of the
scattered electrons.[‡] The most valuable information concerning the collision
process is to be derived from a detailed study of the angular distribution of the
scattered electrons, and such an investigation is described in the present
paper.

Little work has so far been done on the angular distribution of electrons
scattered in ionizing collisions. Tate and Palmer (loc. cit.) have carried out
a few measurements in mercury vapour, in which the collected electrons were
separated into groups having a large energy spread. In view of the results
of the present paper, however, it is clear that reasonably good velocity resolu-
tion of the collected electrons is necessary in order to observe the interesting
phenomena which occur. Hughes and McMillen (loc. cit.) have given some
scattering curves in argon and hydrogen for collected electrons which had only
a few volts energy. The results they have obtained will be discussed later.

The present paper describes experiments on the angular distribution of
electrons which have lost different amounts of energy over and above the

* 'Proc. Roy. Soc.,' A, vol. 142, pp. 320, 647 (1933).

† Bleakney, 'Phys. Rev.,' vol. 35, p. 139 (1930), Smith, 'Phys. Rev.,' vol. 36, p. 1293
(1930), Tate and Smith, 'Phys. Rev.,' vol. 39, p. 270 (1931).

‡ Tate and Palmer, 'Phys. Rev.,' vol. 40, p. 731 (1932), Hughes and McMillen, 'Phys.
Rev.,' vol. 39, p. 585 (1932), vol. 41, p. 39 (1932).

amount required for ionization, and the investigation includes measurements on electrons which leave the atom with certain definite velocities   Electrons with different incident energies have been used, and measurements have been carried out in hydrogen, helium, nitrogen, methane, neon, argon, and mercury vapour

Method

The apparatus used in the present work has already been described in detail in a previous paper *   The essential parts are a collision chamber containing the gas at a low pressure, and a highly evacuated chamber containing an electrostatic analyser   Scattered electrons entering the analyser are subjected to a velocity analysis, and the number of electrons with the desired energy is measured as a function of the angle of scattering by rotating the electron gun

The precautions taken in obtaining measurements have been discussed elsewhere† in connection with the discrete losses, *i e*, losses corresponding to excitation of the atom to a discrete level   With ionization losses there are no peaks in the velocity distribution of the collected electrons such as occur for the main discrete losses, and one must be certain that the measured effects are not partly due to 'background'   Consideration shows that background may arise from two causes   (a) stray scattering in the collision chamber, most probably from the slits and walls, (b) stray electrons in the analyser reaching the collector with energies different from that which the analyser is adjusted to focus   The following tests indicated that such background effects were quite unimportant in the present work—

   (i) When there was no gas in the collision chamber, the collected current was only a small fraction of that when gas was present

   (ii) The intensity of collected electrons with energies between those of the elastically and inelastically scattered electrons was always small compared with the intensity of the electrons which had made ionizing collisions

   (iii) For investigations on electrons which retained only a few volts energy after collision, it was convenient to accelerate the scattered electrons up to 30 volts energy before they entered the analyser   Under these circumstances the intensity of the collected current fell abruptly to a very small value when the analyser was adjusted to focus electrons with energies slightly less than 30 volts

Test (i) shows that background due to stray scattering in the collision chamber was small compared with the scattering by the gas, and tests (ii) and (iii) showed the absence of appreciable background due to stray electrons getting around the analyser and entering the collector Further evidence of the reliability of the results was obtained from the fact that the curves were closely reproducible at different gas pressures

Results

(a) *Argon and Mercury Vapour* – The ionization potential of argon is 15 7 volts, and angular distributions were measured for electrons which had lost this or a greater amount of energy in the scattering process In fig 1* curves are given† for incident electrons of 100, 60, 40, 30 and 20-volts energy The 100-volt curves are for electrons which have lost 15 7, 25, 40, 65, 75 and 95-volts energy in the collision similarly, curves for various losses greater than the ionization potential are given for the other incident velocities The ionization potential of mercury vapour is 10 4 volts, and in fig 2 curves are given for incident electrons of 60, 40, 30, 20 and 14-volts energy

These curves exhibit some features which are also present in the curves for the other gases studied These features are –

  (i) A close similarity between the curves for the ionization loss and the corresponding curves for the main discrete loss, though at small angles the former curves are less steep than the latter , this last effect is more marked at the lower incident voltages

  (ii) For incident electrons of any particular energy, the curves for electrons which have lost the larger amounts of energy are flatter than those which have lost smaller amounts in the collision Further, the change in steepness is particularly rapid within a range of a few volts near the voltage at which the scattered electrons have half the energy of the incident electrons , this effect, however, is not so marked in the curves for argon, and is even less so for mercury vapour

Turning now to the curves for argon and mercury vapour in particular, we observe further features of interest Diffraction effects, in the form of a maximum and a rise at large angles, are present in the curves even when the collected electrons have only a few volts energy Moreover, the curves for

---

* In this and subsequent figures, all the curves are drawn to arbitrary scales
† The zeros of the successive curves are given on the right-hand side

electrons which have only 5 volts energy after the collision are markedly similar for all incident electron energies   Such curves for argon are different from the corresponding ones for mercury vapour, in which the rise at small angles is more pronounced
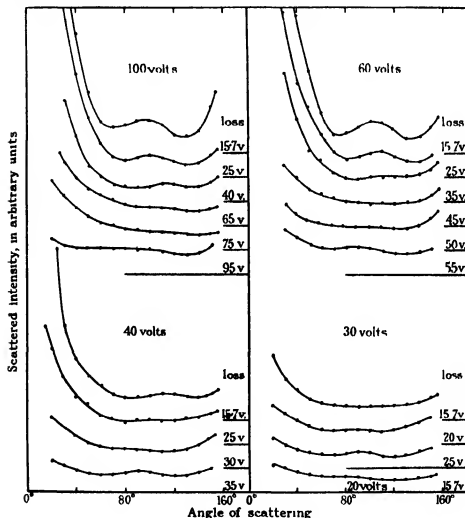
Fig 1 —Scattering in argon

In the curves for argon, as the energy lost by the electron increases, the maximum tends to move out to a slightly larger angle and then moves in to a smaller angle, while its prominence decreases and then increases again slightly Similar but less pronounced effects are present in the curves for mercury vapour

Hughes and McMillen (*loc cut*) have given curves for the scattering of electrons in argon and hydrogen for collected electrons with energies of 1, 3, 5 5 and 8-volts energy Most of these curves show very sharp maxima at large angles, the curves being otherwise fairly flat Our attempts to verify
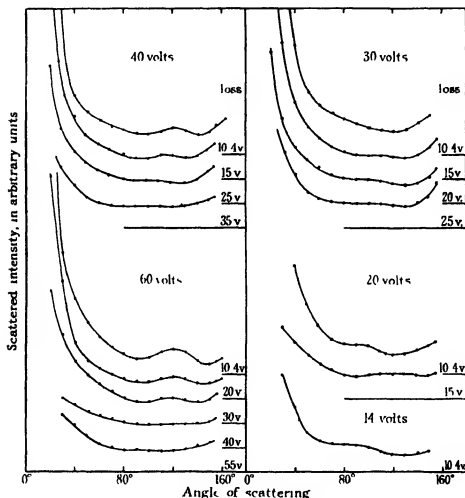
Fig 2 —Scattering in mercury vapour

the presence of such maxima were unsuccessful , however, too much importance should not be attached to this result, since in some experiments when studying collected electrons of very low energy, there was a background due to slow electrons ejected from the walls of the scattering chamber Background effects were, of course, quite small for all the curves given in this paper

(b) *Helium*.—In fig 3 scattering curves are given for electrons with incident energies of 200, 100, 60 and 40 volts, and for various losses greater than the ionization potential of 24 5 volts At large angles all the curves are quite flat, and in general they show the characteristics (i) and (ii) already mentioned above In addition to these characteristics some of the curves show a kink, a feature which is seen later to be of some significance
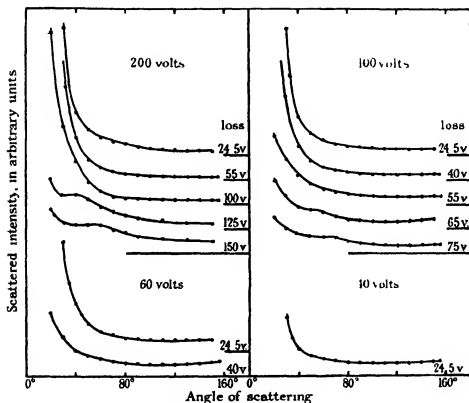
Fig 3 —Scattering in helium

(c) *Hydrogen*.—In fig 4 curves are given for the scattering of 300, 200, 100, 60, 40, 30 and 20-volt electrons in hydrogen, the ionization potential of which is 15 9 volts At the higher voltages, many of the curves are seen to exhibit a striking and unusual feature in the occurrence of a prominent maximum, which moves regularly as the energy loss changes As the amount of energy lost by the electron decreases, the maximum moves into smaller angles, until it is finally lost in the increased steepness of the curves This type of maximum is not present in the inelastic curves for the main discrete loss, and it will be

Fig 4 —Scattering in hydrogen
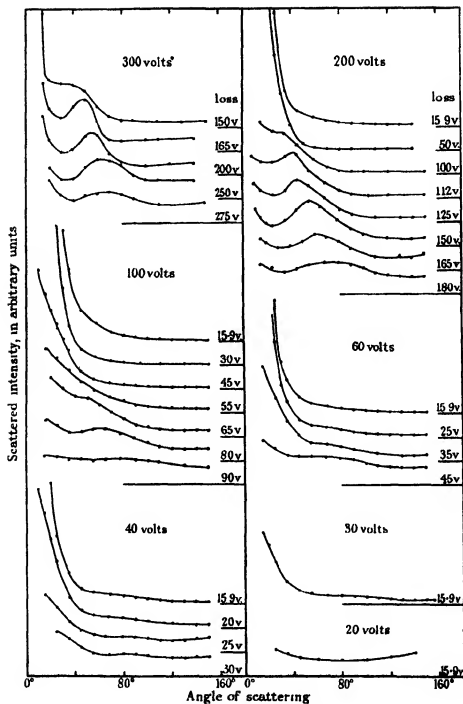
clear that it is of quite a different nature to that observed at large angles in the curves for argon and mercury vapour   At the lower incident voltages the effect is still present although much less pronounced, the maximum being reduced to a slight undulation

(d) *Nitrogen, Methane and Neon* – Since the very interesting feature observed in hydrogen was also noticeable to a slight extent in helium, it was clearly of interest to investigate other light gases at higher voltages where the effect would be more pronounced   Measurements were therefore obtained for the scattering of 300, 200 and 100-volt electrons in nitrogen, and for 200-volt
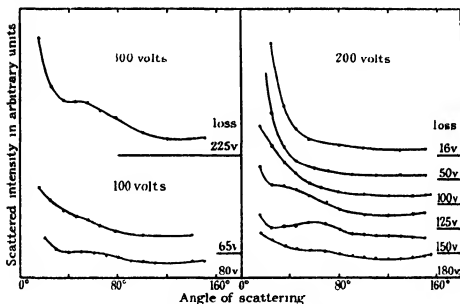
Fig 5 —Scattering in nitrogen

electrons in methane and neon   the resulting curves are shown in figs 5 and 6

The effect observed in hydrogen and helium is also present to a slight degree in these curves, although for neon, the heaviest of the three gases, it has almost disappeared   The main point of interest is that the position of the maximum in corresponding curves for the same incident voltage is independent of the nature of the gas

Discussion

The chief interest attached to the scattering of electrons by the heavier atoms lies in the occurrence of diffraction maxima and minima at large angles

The presence of these diffraction effects is due to the distortion of the incident and outgoing electron waves by the field of the atom. In a previous paper* the authors have given a qualitative explanation of inelastic scattering in different gases for electrons which have lost a discrete amount of energy. It was shown that when the wave lengths of the incident and outgoing electrons are nearly the same, the curves for inelastic scattering will exhibit a diffraction effect † For the same reasons it is to be expected that curves for the ionization loss will be similar to the corresponding curves for the discrete loss, provided that the energy of the incident electrons is large compared with the ionization potential However, when the incident electrons lose an amount of energy
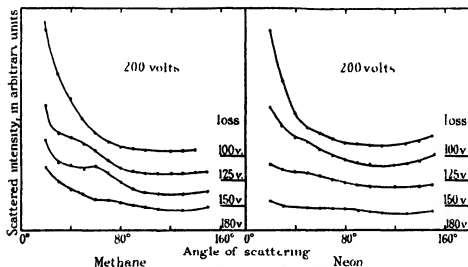
Fig 6 —Scattering in methane and neon

considerably more than is required to ionize the atom, the wave-lengths of the incident and outgoing electrons are appreciably different, and so the diffraction effect in the curves becomes less prominent These features are observed in the curves for argon and mercury vapour Now, when electrons leave the atom with only a very few volts energy, they are moving slowly in the comparatively strong field of the ionized atom, an influence which is independent of, and more important than the energy of the incident electrons Thus, we expect the angular distributions of electrons leaving the atom with 5-volts

---

* ' Proc Roy Soc ,' A, vol. 138, p 469 (1932)

† [Note added in proof, January 9, 1934 —Detailed calculations (to appear shortly) have since been carried out by Massey and Mohr and their results establish this explanation]

energy (see figs 1 and 2) to be similar for all energies of the incident electron

Let us now turn to the results obtained for the scattering by light elements In some of the angular distributions a maximum appears which is particularly marked for hydrogen This maximum becomes less prominent as the energy of the incident electrons decreases, whereas this is not so for the usual diffraction maxima which occur at large angles Further, the position of the maximum depends only on the energies of the incident and outgoing electrons, and not on the nature of the gas The effect therefore involves, not the atom, but the atomic electrons, and so considerations of energy and momentum should explain the phenomenon

Let us therefore consider the collision of an incident and an atomic electron neglecting the effect of the atomic field Let V be the energy of the incident electron in volts, v, v' the energies of the two electrons after the collision, θ, θ' the angle which the directions of the two outgoing electrons make with the incident electron, and V_0 the ionization potential of the atom The energy and momentum relations then give

$$V^{\frac{1}{2}} = v^{\frac{1}{2}} \cos \theta + v'^{\frac{1}{2}} \cos \theta',$$

$$0 = v^{\frac{1}{2}} \sin \theta - v'^{\frac{1}{2}} \sin \theta',$$

$$V = v + v' + V_0$$

It follows that

$$\cos \theta = \frac{v + \frac{1}{2} V_0}{V^{\frac{1}{2}} v^{\frac{1}{2}}} \tag{1}$$

From this relation we obtain the angle at which electrons with energy v leave the atom after the collision We should therefore expect a maximum at an angle θ in the angular distribution of collected electrons of energy v This maximum will, of course, be superimposed on the angular distribution owing to the scattering by the atomic field In Table I are compared the observed and calculated angles at which the maximum appears in the various curves for hydrogen, and it is seen that there is remarkably good agreement This agreement will also hold for other gases, since the calculated position of the maximum depends only slightly on the ionization potential of the atom

Let us now consider the application of quantum theory to the calculation of the actual form of the curves Using Born's formula, Massey and Mohr[*] and Wetzel[†] have carried out calculations for the ionization of the simplest

---

[*] 'Proc Roy Soc,' A, vol 140, p 613 (1933)

[†] 'Phys Rev,' vol 44, p 25 (1933)

elements, hydrogen and helium, by electron impact Wetzel uses the somewhat
doubtful approximation of taking plane waves to represent the electron ejected
from the atom, while the more exact continuous wave functions were used by
Massey and Mohr Only a few curves were given in their paper owing to the
tedious nature of the calculations, and Wetzel does not give curves for hydrogen
or for the larger energy losses in helium Additional curves were therefore

Table I —Calculated and Observed Positions of the Maxima in the Angular
Distributions for Hydrogen

V (volts)	v (volts)	θ calculated (degrees)	θ observed (degrees)
300	150	42	40
	135	45	48
	100	51	54
	60	63	64
	25	68	68
200	88	43	42
	75	47	44
	50	54	55
	35	59	58
	20	64	72
100	35	4 ?	48
	20	51	60

calculated, using Massey and Mohr's formulæ, so as to enable direct comparison
with the experimental curves In fig 7 theoretical and experimental curves
are given for the scattering at small angles in hydrogen and helium, and it is
seen that they agree fairly well except in one case In fig 8 a number of
theoretical curves are given for the scattering of 200-volt electrons in hydrogen
and helium Now the experimental measurements include both electrons
scattered by the atom and those ejected from the atom in the collision process,
as the two types are experimentally indistinguishable It would therefore
be necessary to calculate the angular distributions for both types and combine
them in the appropriate manner for comparison with the experimental curves
It is seen, however, in fig 8 that the two types of electrons have very similar
angular distributions, as might be expected, and so it is usually sufficient to
calculate merely the angular distribution of the scattered electrons

Comparing the theoretical curves in fig 8 with the corresponding
experimental curves for hydrogen and helium in figs 3 and 4 respectively,
we see that there is qualitative agreement in the form of the curves,
and that the position of the maximum, when it occurs is also given

correctly The theory, however, does not give sufficient scattering at large angles. This also occurs when Born's formula is used to calculate the inelastic scattering for the discrete loss, and it has been shown[*] that this is due to neglect of the distortion of the incident and outgoing electron waves by the atomic field Inclusion of this effect for ionizing collisions would, as for the discrete loss, increase the calculated scattering at large angles The theoretical curves
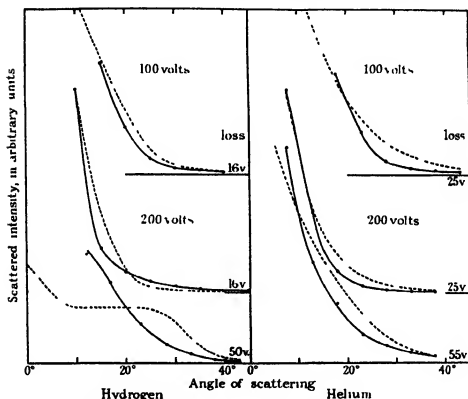
Fig 7 □ — Experimental curves , - - - theoretical curves

show a less pronounced and broader maximum for helium than for hydrogen, and inspection of the formula which was used shows that for electrons of the same incident velocity, the maximum becomes much less pronounced for atoms of greater atomic number , the formula also shows that the maximum becomes more prominent at higher velocities The experimental curves exhibit all these features, as we have already seen

* Massey and Mohr, 'Proc Roy Soc ,' A, vol 139, p. 187 (1933)

One of us (C B O M.) is indebted to the Department of Scientific and Industrial Research for a Senior Research Grant during the latter portion of this work   In conclusion, the authors wish to thank Lord Rutherford and Dr J Chadwick for their interest and encouragement
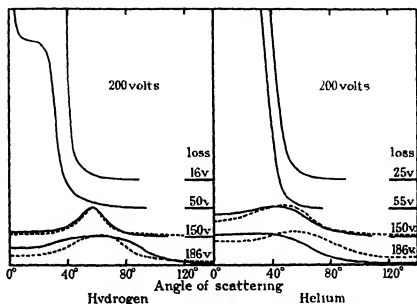
FIG 8 —Theoretical curves , ——— scattered electrons , - - - ejected electrons

Summary

An apparatus, described in a previous paper, has been used for investigations on the angular distribution of the scattering of electrons in gases for ionizing collisions   Measurements were carried out for electrons which had lost various definite amounts of their incident energy over and above that required for ionization   Results have been obtained for hydrogen, helium, nitrogen methane, neon, argon, and mercury vapour, and curves are given for several incident energies below 300 volts

The curves obtained exhibit several features which are discussed in detail An interesting effect is observed in the light gases, particularly in hydrogen, namely, the occurrence of a single pronounced maximum in the angular distribution at certain angles between 30° and 80°   This effect, which is more pronounced at higher velocities, is explained by simple momentum and energy considerations, and curves are obtained with the use of quantum theory which are in fair agreement with the experimental curves

An Extension of Southwell's Method of Analysing Experimental Observations in Problems of Elastic Stability

By H. R. Fisher, B.A.

1. Introduction

In a recent paper* Southwell deals with a well-known type of elastic instability which he exemplifies by considering an axially loaded strut. When a system having such instability is subjected to some type of load P there corresponds to each one of certain kinematically possible modes of distortion a certain critical load, P_1, at which this mode becomes unstable. If before loading the system has already a small distortion answering to the mode considered, then the application of P increases the amplitude of this mode, and hence the representative deflection, in the ratio $P_1/(P_1 - P)$. Alternatively it may be said that owing to the application of P there occurs an *additional deflection* δ equal to $P_1/(P_1 - P)$ times the initial deflection δ_0, that is

$$\frac{P_1 - P}{P} \delta = \delta_0,$$

or

$$P_1 v - \delta = \delta_0, \tag{1}$$

if v be written for δ/P.

In most practical cases only the mode which is associated with lowest P_1 (that is, the "fundamental mode") will be important, but it will often be difficult to measure δ or δ_0 without including components arising from other modes of deflection, and then (1), regarded as an equation in δ the measured additional deflection, will be only an approximation, which, however, becomes increasingly close as the approach of P towards P_1 causes the fundamental mode to predominate.

In the paper cited, Southwell pointed out that, in accordance with (1) above, the points obtained by plotting δ (the observed deflection) against v (the deflection divided by the load) may be expected to lie upon a straight line whose slope defines the critical load P_1 (see fig. 1). In the problem of the axially loaded strut P is the axial load, δ_0 and δ are the initial and additional small transverse deflections at the mid-length, and P_1 is the well-known Euler

* 'Proc. Roy. Soc.,' A, vol. 135, p. 601 (1932).

buckling load $\pi^2 EI/(2l)^2$, where EI is the flexural rigidity and $2l$ the length of the strut *

Southwell's method of plotting has proved useful in the analysis of experiments on the instability of strips or panels of thin metal sheet subjected to shear † Here P is the shearing stress, and if (as usually happens) there is initially any slight deviation from planeness whose fundamental component is δ_0, δ is the additional depth of the waves or corrugations which are exhibited as the load is increased
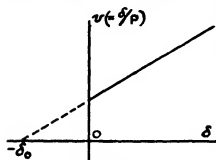
Fig 1—Ideal e δ relation

1 1 The following notes develop the idea, suggested by Southwell's example, that the straight-line plotting indicated by (1) might be applicable to the analysis of the mechanical tests which are regularly made on aeroplane spars of new design   The theoretical results may be of interest inasmuch as they illustrate a few elaborations of the method which are apparently of general application

In the tests referred to, a specimen, chosen of such length as to represent an appropriate portion of the whole spar, is subjected to gradually increasing loads approximating in type to those which the spar sustains in service   In a
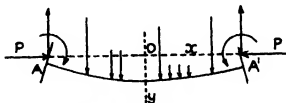
Fig 2—Methods of loading a spar

biplane, or braced monoplane, the loads on a spar (which extends horizontally in the wing from root to tip) consist of compressive axial loads due to the horizontal components of the forces in the external diagonal bracing, combined with transverse loads due to the vertical aerodynamic forces transmitted through the fabric and ribs   The types of loading which would accordingly be employed in testing are those indicated in fig 2, AA' being the centre line of

---

* In Southwell's paper (loc. cit.) the length of the strut is denoted by l.

† Gough and Cox, ' Proc Roy Soc,' A, vol 137, p. 145 (1932).

the spar   Actual conditions would usually be symmetrical about the mid-length, but asymmetry will be permitted in what follows, since it introduces little complication   If, in fact, only the mid-length deflection is considered, the anti-symmetrical components of the loads and end eccentricities have no effect

In spar tests of the standard type the main transverse loads are kept proportional to the end load P while P is varied, although constant transverse loads (such, for example, as the weight of the spar) may co-exist   In the present paper both kinds of loading will be taken into account, and it will be shown that in a sufficiently wide range of circumstances an equation of type (1) does theoretically hold with close approximation   The practical advantages of this result are manifest   By fitting a straight line by eye to points plotted on a δ, v diagram, a sufficiently accurate value of the flexural rigidity of a spar can be obtained from a large number of experimental readings in a few minutes, and every observation is given weight in arriving at this experimental estimate   Also anomalous behaviour of a tested spar—due, for example, to the limit of proportional elasticity having been exceeded—is immediately recognizable in a departure from straightness of the δ, v line   Since δ and v can quite practicably be plotted concurrently with the progress of the test, it is thus possible to obtain early warning of the approach of failure when, as usually, this occurs by yielding or wrinkling of the material at loads well below the critical load P_1

1 2   The problem to be considered in this paper can accordingly be enunciated as follows   "By what simple methods is it possible to describe or analyse the behaviour of a uniform beam, initially slightly bowed, which is subjected to the combination of loads shown in fig 2 ?"   These loads, with the requisite notation, are detailed below

(i) Compressive loads P (which are varied during the test) are applied at fixed points in the end cross-sections of the beam   The beam is assumed to be not perfectly straight, and the end thrusts P are assumed to be applied with some small eccentricity   thus if the line of action of P be taken as Ox, with O at mid-length and Oy perpendicular as shown, the equation of the unstrained centre line is taken as given by $y = \eta(x)$, where η is a function at present unspecified   The end eccentricities are $\eta(\pm l)$ where $2l$ is the length of the beam

(ii) Forces proportional to P are applied parallel to Oy at various points along the beam, and couples proportional to P are applied in the plane Ozy at the ends   These loads, with the requisite reactions at the ends, are defined

by saying that they produce, in the absence of other loads, a bending moment P times N (z) at a distance z from O

(iii) Constant forces parallel to Oy are applied at various points along the beam, and constant couples in the plane Ozy are applied at the ends   These loads, with the requisite reactions at the ends, are defined by saying that they produce, in the absence of other loads, a bending moment M (z) at a distance x from O, and a consequent deflection relative to the ends of amount m (x), where

$$- \text{EI} \frac{d^2 m}{dx^2} = \text{M},$$ (1A)

EI being the flexural rigidity

The problem here presented can, of course, be solved exactly on the basis of the ordinary theory of flexure, the suggested interest of the treatment to be given in this paper centres in the illustration which it affords of principles and methods believed to have applications in other cases of elastic instability It will be shown that equation (1), regarded as a first approximation, will apply in a wide range of systems, the order of its approximation will be examined, and a second approximation of high accuracy will be suggested

2 Theory

Exact Form of the v — δ Relation   The Function F (θ, z)

2 1 In the notation of § 1 2, and if δ (x) is the additional deflection due to P and its associated loads—that is, the deflection which ensues on the application of (i) and (ii) after (iii) has already been applied—the bending moment at a distance x from O, fig 2, is

$$Py + M (x) + P \quad N (x),$$

where

$$y = \eta (x) + m (x) + \delta (x),$$

and this bending moment is to be equated to EI times the excess of the curvature over that implied by η (x)   So we have

$$- \text{EI} \frac{d^2}{dx^2} \{\delta (x) + m (x)\} = \text{P} \{\eta (x) + m (x) + \delta (x)\} + \text{M} (x) + \text{P} \quad \text{N} (x)$$

Remembering equation (1A) and putting P/EI = μ², we may write this equation in the form

$$\left[\frac{d^2}{dx^2} + \mu^2 \right] \delta (x) = - \mu^2 \{\eta (x) + \text{N} (x) + m (x)\},$$
$$= - \mu^2 \text{H} (x), \quad \text{say}$$ (2)

The deflection $\delta(x)$ is determined by (2) and by the condition $\delta = 0$ at $x = \pm l$. We observe that there is an exact correspondence between η, N, and m, in that only their sum, H, affects δ. Thus initial bowing, end-eccentricity, and transverse loads and end-couples, whether proportional to P or constant, all combine to form one total equivalent eccentricity *

It is convenient to use instead of x a co-ordinate θ varying linearly from 0 to π along the beam. On introducing the substitutions

$$\theta = (l + x)\frac{\pi}{2l}, \qquad D \equiv \frac{d}{d\theta} = \frac{2l}{\pi}\frac{d}{dx},$$

we may write (2) in the form

$$[D^2 + z]\delta = -zH(\theta), \qquad (3)$$

where

$$z = \mu^2 \frac{(2l)^2}{\pi^2} = P\frac{(2l)^2}{\pi^2 EI} \qquad (4)$$

Now let $H(\theta)$ be expanded in the range $(0 < \theta < \pi)$ in the Fourier series

$$H(\theta) = H_1 \sin\theta + H_2 \sin 2\theta + \quad + H_n \sin n\theta + \quad (5)$$

On assuming a similar series for δ, substituting in (3) and equating the coefficients of corresponding terms, we deduce that

$$\delta = \frac{z}{1-z}H_1 \sin\theta + \frac{z}{4-z}H_2 \sin 2\theta + \quad + \frac{z}{n^2-z}H_n \sin n\theta + \quad , \quad (6)$$

provided that certain operations on the infinite series are justified. The justification is clear if H is continuous and zero at the end-points, as was assumed in Southwell's paper. The latter condition is not necessary, however, as will be shown later

Equation (6) illustrates the opening remarks of this paper. In the expression for δ, $H_1 \sin\theta$, the fundamental component of H, is multiplied by $z/(1-z)$, that is, from (4), by $P/(P_1 - P)$ if (as in the case of the simple strut) we write P_1 for $\pi^2 EI/4l^2$, the Euler buckling load. Thus z measures the end-load in units of P_1. If we neglect all terms in the series (6) except the first, and

---

* We could have foreseen the equivalence of N and η as regards constant additions, since the same net loading is obtained by decreasing the end-eccentricities and increasing by the same amount the contribution of the end-couples to N. Nor is it to be supposed that the idea of a general correspondence is new; it is implicit in the various approximate formulæ, well known to engineers, which have been given by Perry, Berry, Webb and others for applications to problems of beams loaded axially and transversely

multiply by $(1 - z)/z$, we obtain equation (1), except that δ_θ is replaced by $H_1 \sin \theta$

The complete equation (6) may be written in the form

$$\frac{1-z}{z} \delta = P_1 v - \delta = H(\theta) \frac{H_1 \sin \theta + \quad + \frac{1-z}{n^2 - z} H_n \sin n\theta +}{H_1 \sin \theta + \quad + H_n \sin n\theta +}$$

$$= H(\theta) F_H(\theta, z), \text{ say}, \qquad (7)$$

where $v = \delta/P$ as before   The form of the non-dimensional ' error-function "
F_H as thus defined does not depend upon the magnitude of H, but only on its
distribution along the beam's length

In order that the graph of v against δ should be a straight line with slope
$1/P_1$, it would be necessary that $F_H(\theta, z)$ should be independent of z As a rule
this is not exactly true , but since the coefficient of $H_n \sin n\theta$ in the numerator
varies from only $1/n^2$ to 0 when z varies from 0 to 1, the variation of F_H will be
extremely small if, as usually happens, $H_1 \neq 0$ and the following few coefficients
H_n are comparatively small   If H is symmetrical or δ is measured at the mid-
length only, the second (and all even) terms in the numerator are absent, and
the variation is further reduced *

Validity of the Series for δ

2 11 Let H be continuous, and have limited total fluctuation,† in $0 \leqslant \theta \leqslant \pi$
Then $H = \Sigma [H_n \sin n\theta]$ in $0 < \theta < \pi$, and

$$H_n \equiv O(1/n) \ddagger \qquad (9)$$

Let

$$\delta = \Sigma \left[\frac{z}{n^2 - z} H_n \sin n\theta \right] \qquad (6) \, bis$$

The convergence of this series is uniform with respect to θ in $0 \leqslant \theta \leqslant \pi$.
Hence it is continuous, and so equal to 0 at the end-points $\theta = 0, \pi$ Term
by term differentiation yields

$$\frac{d\delta}{d\theta} = \Sigma \left[\frac{nz}{n^2 - z} H_n \cos n\theta \right],$$

since (9) makes this series uniformly convergent in $0 \leqslant \theta \leqslant \pi$ $d\delta/d\theta$ is

---

* Cf Southwell (loc cit), § 8.
† Whittaker and Watson, "Modern Analysis," §§ 3 64.
‡ Whittaker and Watson, "Modern Analysis," §§ 9 21

continuous in $0 \leqslant \theta \leqslant \pi$ for the same reason   A second differentiation shows that

$$\frac{d^2\delta}{d\theta^2} = \Sigma \left[\frac{-n^2z}{n^2-z} \, \mathrm{H}_n \sin n\theta \right],$$

whenever this series is uniformly convergent   *i e*,

$$\frac{d^2\delta}{d\theta^2} = -z \left(\Sigma \left[\mathrm{H}_n \sin n\theta \right] + \Sigma \left[\frac{z}{n^2-z} \, \mathrm{H}_n \sin n\theta \right] \right)$$

$$= -z \, (\mathrm{H} + \delta),$$

whenever the series for H and δ are uniformly convergent

The series for δ is uniformly convergent in $0 \leqslant \theta \leqslant \pi$, and the series in H is uniformly convergent in any interval (α, β) where $0 \prec \alpha \prec \beta \prec \pi$ *   Hence

$$\frac{d^2\delta}{d\theta^2} + z\delta = -z\mathrm{H} \qquad (3) \ bis$$

at all points of $(0, \pi)$, except possibly the end-points , and the doubt as to end-points may be removed, since by the continuity of $d\delta/d\theta$ and $\delta + \mathrm{H}$

$$\left(\frac{d^2\delta}{d\theta^2} \right)_0 = \lim_{\theta \to 0} \frac{1}{\theta} \lim_{\alpha \to 0} \int_\alpha^\theta \frac{d^2\delta}{d\theta^2} \, d\theta \qquad (0 \prec \alpha \prec \theta)$$

$$= \lim_{\theta \to 0} \frac{1}{\theta} \lim_{\alpha \to 0} \int_\alpha^\theta -z \, (\mathrm{H} + \delta) \, d\theta$$

$$= -z \, (\mathrm{H} + \delta)_{0^*}$$

A similar argument holds at the end-point π

We have proved that if H is continuous the series (6) is zero at $\theta = 0$, π, and satisfies the equation (3) at all points of $(0, \pi)$ The proof is easily extended to the case when H has a finite number of points of discontinuity such as would correspond to loading by couples proportional to P and applied at intermediate points of the beam

Evaluation of the Function $\mathrm{F}_{\mathrm{II}} (\theta, z)$

2 2 The variation of F_{H} as z passes from 0 to 1 is a measure of the deviation from linearity of the exact theoretical δ, v curve   Equation (7) indicates that such variations are likely to be small, and it could be used in any particular case to give numerical values , when, however, the loading can be simply expressed analytically, the simplest method is to solve equation (2), or its equivalent (3), in finite terms.

* Whittaker and Watson, " Modern Analysis," § 9 24

We have from (3)

$$\delta = \frac{-z}{D^2 + z} H(\theta),$$

where D means $d/d\theta$ as before   Also

$$\frac{1-z}{z}\delta = H(\theta) \quad F_H(\theta, z) \qquad (7) \ bis$$

Therefore

$$F_H = \frac{1}{H} \frac{1-z}{z} \frac{-z}{D+z} H,$$

$$= \frac{1}{H} \frac{-1+z}{D^2+z} H, \qquad (10)$$

where the operator is to be interpreted so that δ is 0 at $\theta = 0, \pi$

The following notation will be adopted for the forms which F_H takes in particular conditions of loading   The suffix to F will designate the source of "equivalent eccentricity"   If the suffix designating a load stands alone the load is supposed to remain constant while P varies, and if the suffix is followed by /P the load is supposed to be kept proportional to P   This will be made clear by the following examples, which relate to the simple symmetrical cases, some of common occurrence, used later in this paper as illustrations —

F_h corresponds with equal end-eccentricities h

F_w ,,   constant uniformly distributed transverse load w,

$F_{w\,1}$,,   transverse load w, as above, but proportional to P,

F_R ,,   two constant concentrated transverse loads R, applied at two given points symmetrical about the mid length cf fig 3 (a),

$F_{R/P}$,,   transverse loads R as above, but proportional to P (this is the loading usually adopted in spar-tests) ,

F_Q ,,   equal constant terminal couples Q ,

$F_{Q\,P}$,,   terminal couples Q, as above, but proportional to P. (In accordance with the footnote to §2 1, $F_{Q/P} = F_h$)

2 21 Numerical calculation is facilitated by taking advantage of a simple relation between some of the F-functions, which we now proceed to derive Let W represent any form of loading by transverse forces or couples, and let

M be the resulting bending moment and (as before) m the deflection resulting from M in the absence of other load Concentrating now on any one pair of values of the loads P and W, we may calculate the total resulting deflection (δ', say), either on the assumption that P and W have been gradually applied simultaneously in constant proportion, or on the assumption that W was applied first, up to its full value, and then kept constant while P was applied On the former assumption H has in equation (2) the form N (z), which is now M/P—that is, M/zP₁, and δ' is the same as δ Hence we have from (7)

$$\frac{1-z}{z}\, \delta' = HF_H = \frac{M}{zP_1}\, F_{W/P}\,(z),$$

so that

$$\delta' = \frac{1}{1-z}\, \frac{M}{P_1}\, F_{W/P}\,(z) \tag{11}$$

Equation (11) holds for all values of M and z greater than 0 Letting z tend to zero with M unchanged, we deduce by continuity

$$m = \lim_{z \to 0} \delta' = \frac{M}{P_1}\, F_{W/P}\,(0) \tag{12}$$

If now we take the latter assumption that W was applied first and then kept constant, δ is $\delta' - m$, and H (x) is m (x) in equation (2) hence, by (7),

$$\frac{1-z}{z}\, (\delta' - m) = HF_H = m F_W\,(z),$$

and

$$\delta' = \frac{1}{1-z}\, m \left[1 + z\,\{F_W\,(z) - 1\}\right] \tag{13}$$

Comparing (13) with (11) and (12), we obtain the relation

$$F_{W/P}\,(z) = F_{W/P}\,(0)\,[1 + z\,\{F_W\,(z) - 1\}], \tag{14}$$

or, on re-arrangement and insertion of the argument θ as a reminder that the result is true for deflection measured at any point of the beam,

$$F_W\,(z,\,\theta) = 1 + \frac{1}{z}\left\{\frac{F_{W/P}\,(z,\,\theta)}{F_{W/P}\,(0,\,\theta)} - 1\right\} \tag{15}$$

The identity (15) may also be obtained by algebraic manipulation of the symbolic definition (10)

It will be remembered that the form of an error function depends only on the distribution with respect to z (or θ) of the contribution made to H by the

relevant source of equivalent eccentricity In the above work F_W corresponds with a contribution to H which is distributed like the *deflection* due to W alone, this deflection is typified by $m(x)$ in equation (2) $F_{W/P}$ corresponds with a contribution to H which distributed like the *bending moment* due to W alone, this bending moment is typified by $N(x)$ in equation (2)

It follows that the identity (15) holds between the functions corresponding with *any* two sources of equivalent eccentricity, if the contribution to H of the first source is distributed with respect to x *like the deflection which would result from bending moments distributed like the contribution of the second* Since the relation of deflection to bending moment is (for beams of uniform section) similar to the relation of bending moment to load distribution, the words in *italics* may be replaced by "*like the bending moment which would result from transverse loading distributed like the contribution of the second*" Provided that W does not include terminal couples, we deduce that (15) also holds when F_W is replaced by $F_{W/P}$ and $F_{W/P}$ is replaced by the F-function which corresponds with an initial deflection having the form of the curve of load distribution W   Accordingly, if the last F-function is known, all that is required to find F_W is two successive applications of (15)

The foregoing method is illustrated by a tabular example, Table I, in which W is taken to be a uniformly distributed load w The connection with loading by terminal couples is also shown   Each of the diagrams in the third column shows the distribution along the beam's length of the contribution to H appropriate to the row in which it stands   The diagram in one row shows the form of deflection (or of bending moment) due to the form of bending moment (or of loading) shown in the diagram immediately below   Consequently an error function in one compartment is obtained by (15) from the error function in the compartment immediately below   We have $F_h \equiv F_{Q/P}$, as already noticed, because the initial form of the centre line when the loading is by eccentric end load is similar to the distribution of bending moment which results from terminal couples, and $F_{w/P} \equiv F_Q$, because the distribution of bending moment due to uniform transverse load is similar to the deflection due to terminal couples

2 22 The relation (15) fails when $z = 0$, and at this point a limiting process is necessary   Denoting by $F_{n+1}(z)$ the function derived from $F_n(z)$ in the way that F_W is derived from $F_{W/P}$, we may rewrite (15), divided by $(1 - z)$, as
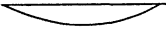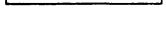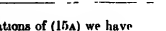
$$\frac{F_{n+1}(z)}{1 - z} = \frac{1}{zF_n(0)} \left\{ \frac{F_n(z)}{1 - z} - F_n(0) \right\} \tag{15A}$$

Now assume that $F_n(z)/(1-z)$ can be expanded in powers of z, that is, let

$$\frac{F_n(z)}{1-z} = c_0 + c_1 z + c_2 z^2 + c_3 z^3 +$$

The c's are, of course, functions of θ.

Table I

Source of equivalent eccentricity	Error function	Contribution to H	
Uniform load w, $w \div$ constant	F_w		Deflection due to w
Uniform load w $w/P =$ constant	$F_{w/P}$ and F_Q		Bending moment due to w
End couples Q, $Q =$ constant			Deflection due to Q
End-eccentricities	F_h and $F_{Q/P}$		Graph of uniform load ing w
End couples Q, $Q/P =$ constant			Initial position of centre line when end load is eccentric
			Bending moment due to Q

Then by repeated applications of (15A) we have

$$\frac{F_{n+1}(z)}{1-z} = \frac{1}{c_0}(c_1 + c_2 z + c_3 z^2 +)$$

$$\frac{F_{n+2}(z)}{1-z} = \frac{1}{c_1}(c_2 + c_3 z + c_4 z^2 +),$$

and so on, so that $F_{n+1}(0) = c_1/c_0$, $F_{n+2}(0) = c_2/c_1$, etc. Thus we see that the values at $z = 0$ of the functions derived from F_n are the ratios of consecutive pairs of coefficients in the expansion of $F_n/(1-z)$ in powers of z.

2·23 Returning to our particular example, we can easily show, when H is made a constant in (3), that the form of $F_H(\theta, z)$ as given by (7) or (10)—that is, of F_h (§ 2·2)—is given by

$$F_h(\xi, z) = (\cos \frac{\sqrt{z}\,\xi\,\pi}{2} \sec \frac{\sqrt{z}\,\pi}{2} - 1) \frac{1-z}{z}, \qquad (16)$$

where ξ, which equals x/l or $(\theta - \frac{1}{2}\pi)/(\frac{1}{2}\pi)$, defines the point on the beam at which δ is measured

By taking the limit $z \to 1$, we have

$$F_h(\xi, 1) = \frac{4}{\pi} \cos \xi \frac{\pi}{2}$$

Also, on division of F_h by $1 - z$ and expansion in positive powers of z, the first coefficient and the ratios of following coefficients yield the values

$$F_h(\xi, 0) = \frac{\pi^2}{8}(1 - \xi^2)$$

$$F_{w,r}(\xi, 0) = \frac{\pi^2}{9 \cdot 6}(1 - \tfrac{1}{6}\xi^2)$$

$$F_w(\xi, 0) = \frac{\pi^2}{10} \frac{d^2}{(61 - 14\tfrac{5}{6}\xi^2 + \xi^4)}{1 - \tfrac{1}{6}\xi^2},$$

and with the aid of these and equations (16) and (15) Table II is easily constructed   The percentage variation shown in the last column is

Table II

	z	0	0 2	0 4	0 5	0 6	0 8	1 0	% variation
$\xi \cdot - 0$	F_h	1 23370	1 24081	1 24829	1 23217	1 25616	1 26447	1 27324	+3 205
	$F_{w/r}$	1 02808	1 02880	1 02955	1 02994	1 03034	1 03118	1 03205	+0 386
	F_w	1 00341	1 00349	1 00358	1 00362	1 00367	1 00376	1 00386	+0 046
$\xi = \tfrac{1}{2}$	F_h	1 09662	1 09778	1 09897	1 09957	1 10017	1 10140	1 10266	+0 550
	F_{w} r	1 00524	1 00529	1 00534	1 00537	1 00539	1 00545	1 00550	+0 026
	F_w	1 00025	1 00025	1 00026	1 00026	1 00026	1 00026	1 00026	+0 001
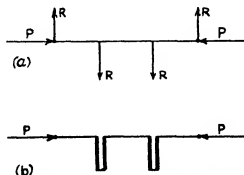
Fig 3.—(a) Usual test loading. (b) Beam whose limiting form is the loading-curve of (a)

$100 \{F(1)/F(0) - 1\}$ Values are shown for $\xi = 1/3$ because at this point $\sin 3\theta = 0$, so that (if, as here, even harmonics in H are absent) only the fifth and higher odd harmonics in H affect the constancy of the F-function

2 24   As a further illustration of the method, some F-functions for the R-loading (§ 2 2 and fig 3, a) are tabulated below, al is the distance from the ends of the points of application of R   These functions may be obtained by (15) from the limit (F_A, say) of the function corresponding with the beam shown in fig 3, b, when the areas of the rectangular excursions remain constant as their breadth tends to zero   The vertical connecting parts, together with the right angle joints at their ends, are of course supposed rigid †   On taking the limit, we have

$$F_A \propto (1 - z) \frac{2}{\sqrt{z}\,\alpha\pi} \sin \frac{\sqrt{z}\,\alpha\pi}{2} \cos \frac{\sqrt{z}\,\xi\,\pi}{2} \sec \frac{\sqrt{z}\,\pi}{2},$$

when $\xi < 1 - \alpha$,
and hence, by expansion of $F_A/(1 - z)$

$$F_{R\,P}(0) = \frac{\pi^2}{8}(1 \quad \xi^2 - \tfrac{1}{3}\alpha^2),$$

$$F_R(0) = \frac{5\pi^2}{48} \frac{(1 - \xi^2)(1 - \tfrac{1}{5}\xi^2 - \tfrac{2}{5}\alpha^2) + \tfrac{1}{15}\alpha^4}{1 - \xi^2 - \tfrac{1}{3}\alpha^2}$$

Table III

	z	0	1	% variation
$a = \tfrac{1}{2}$ $\}$ $\xi = 0$ $\}$	$F_{R/P}$ F_R	1 05093 1 00186	1 05296 1 00193	+0 193 +0 007
$a = \tfrac{2}{3}$ $\}$ $\xi = \tfrac{1}{3}$ $\}$	$F_{R/P}$ F_R	0 91385 0 99793	0 91189 0 99785	−0 215 −0 007
$a = 1$ $\}$ $\xi = 0$ $\}$	$F_{R\,P}$ F_R	0 82247 0 98499	0 81037 0 98553	−1 447 0 145
$a = 1$ $\}$ $\xi = \tfrac{1}{3}$ $\}$	$F_{R/P}^*$ F_R^*	1 05093 1 00186	1 05296 1 00193	+0 193 +0 007

* Since here $\xi > 1 - a$, the functions have different analytical forms from those given above It is easily verified that when $F \equiv F_{R/P}$ or F_R, $F(a, \xi, z) = F(1 - \xi, 1 \quad a, z)$ This is the extension of a well known reciprocal theorem to the case when P is present

Range of Application of the Linear $r - \delta$ Relation

2 3   From numerical results, of which the above are typical, it appears that in all ordinary cases in which either the loading is symmetrical, or in which δ

† It would perhaps be logically simpler to adopt a more cumbersome procedure, and obtain an algebraic expression for $F_{R/P}$ from first principles by solving equation (3) with the appropriate (discontinuous) form for H   The result is, of course,

$$F_{R/P} = 1 + \frac{1}{z}\left\{\frac{F_A(z)}{F_A(0)} - 1\right\},$$

where F_A is as given above

is measured so as to be unaffected by anti-symmetrical deflection, the variation in the F-functions is small , except possibly for F_h, it is less than could ordinarily be detected experimentally   Neglecting the variation, and noticing that the contributions to δ of the various components of H are additive, we may summarize the results so far obtained as showing that an equation analogous to (1), viz ,

$$P_1 x - \delta = C \text{ (a constant)}, \qquad (17)$$

will hold very approximately in relation to a wide range of loadings.   The constant C represents an "equivalent eccentricity" composed of—

(i) the initial (unstressed) bowing at the point where the deflection is measured, multiplied by a factor which is nearly 1 if the bowing is nearly in the form sin θ,

(ii) the mean eccentricity of end-load, multiplied by a factor which is 1 25 (a mean value of F_h in Table II) for mid-length deflection,[*]

(iii) the deflection produced without end-load by any transverse loads or end couples which remain constant during test, multiplied by a factor nearly equal to 1,

(iv) equivalent deflections corresponding with any transverse loads or end couples which are kept proportional to P during test , these deflections are independent of the flexural rigidity, being given by

$$\frac{\begin{pmatrix} \text{Bending moment due to such transverse} \\ \text{load or end couples at the point where} \\ \text{the deflection is measured} \end{pmatrix}}{\text{(End load)}} \times \begin{cases} \text{a factor depending upon} \\ \text{the distribution of the} \\ \text{loads, and usually lying} \\ \text{between 0 8 and 1 25.} \end{cases}$$

Equation (12) shows that these are the deflections produced without end load by transverse loads or end couples proportional to the Euler critical end load, P_1

In tests made by standard methods on aeroplane spars, the transverse loading is by intention entirely proportional to P , hence, apart from quantities of the nature of small corrections which can be estimated, C arises from (iv) above and depends on known quantities only   The experimental δ, v points, therefore, may be expected to lie on a line which is not merely straight but also passes through a known point $(-C, 0)$ This fact adds to the already noticed

---

[*] This is in effect a well-known result, given by Perry ('The Engineer,' vol 62, pp. 464 and 513 (1886)), where a value 5/6 (clearly a misprint for 6/5) is suggested as equivalent to our F_h

advantages of the possibility of linear plotting, for example, an equivalent flexural rigidity corresponding to only one experimental point may be obtained from the slope of the line joining this point to the theoretical point ($-C$, 0).

Equation (12) deserves attention, since, $F_{W/P}$ being usually nearly unity, it shows that M/P_r is a fair approximation to the deflection due to the bending moment M. Equation (12) might also be derived as the limit of (10) as $z \rightarrow 0$.

A Second Approximation to the $v - \delta$ Relation

2 4. Before passing to experimental examples it may be of interest to examine further the nature of the approximation made in deriving equation (17)

2 41. We have, in effect, neglected all terms but the first in the numerator of the expression for F_{II} which is given by (7). If one more term is taken into account, say, the rth, then

$$F_{II}(z) = F_{II}(1) - \frac{1-z}{1 - z/r^2} \{F_{If}(1) - F_{II}(0)\}$$

In the case of mid-length deflection the modifying term will ordinarily arise from the third harmonic, so that $r^2 = 9$. More generally, the approximate formula

$$F_n(z) = F_n(1) - \frac{1-z}{1-kz} \{F_n(1) - F_n(0)\}, \tag{18}$$

may be adopted, the constant k being adjustable. In (18) $F_n(z)$ is supposed to be one of a series of functions connected as before by (15)

Equation (18) gives F_n truly at $z = 0$, $z = 1$, and a value, $k(z_1)$ say, may be assigned to k in order to ensure exact agreement at any chosen third point $z = z_1$. As $z_1 \rightarrow 0$ or 1, $k(z_1)$ tends to the value of k necessary to ensure agreement of the derivative F'_n at $z = 0$ or 1 respectively. On taking limits and using (15),

$$k(0) = \frac{F_{n+1}(1) - F_{n+1}(0)}{F_{n+1}(1) - 1}, \qquad k(1) = 1 - \frac{F_n(1) - F_n(0)}{F'_n(1)}.$$

The most appropriate value of k will ordinarily lie between $k(0)$ and $k(1)$

The function F_n, with its comparatively large variation, affords a convenient numerical example. Values of $k(z_1)$ are given in Table IV for the case $\xi = 0$

Table IV.

z	0	0 2	0 4	0 5	0 6	0 8	1 0	% variation
$k(z_1)$	0 12373	0 12353	0 12334	0 12324	0 12313	0 12293	0 12273	-0 807

Thus $k(z_1)$ is practically independent of z_1 If a mean value, $0\ 123234$, be given to k, the formula (18) yields values of F_k agreeing to at least six significant figures with the true values shown in Table II

2 42 If (18) be assumed true, the δ, v relation (17) is replaced by

$$P_1 v - \delta = C_1 - \frac{1-z}{1-kz}(C_1 - C_0),$$

where C_0 and C_1 are the values of the right-hand side at $z = 0$ and 1 respectively Remembering the definitions $v = \delta/P$, $z = P/P_1$, we write $z = \delta/P_1 v$ in the above, and thus obtain

$$P_1 v - \delta = C_1 - \frac{P_1 v - \delta}{P_1 v - k\delta}(C_1 - C_0),$$

which becomes, on reduction,

$$(P_1 v - \delta - C_1)(P_1 v - k\delta + C_1 - C_0) = -C_1(C_1 - C_0) \qquad (19)$$

In the δ, v diagram this represents a hyperbola passing through the origin A typical form is sketched in fig 4
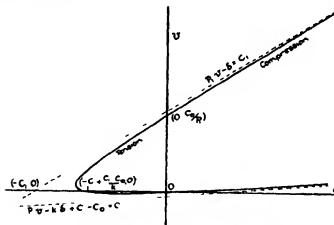
Fig 4.—Hyperbolic approximation

End Tension.

2 5 Hitherto P and z, and consequently δ, have been assumed positive, attention being thus confined to the right-hand halves of figs. 1 and 4 The analysis is equally applicable, however, when P and z are negative, the end forces being then tensional The solutions in finite terms now involve hyperbolic instead of circular functions thus $\sec \sqrt{s}\pi/2$ in (16) is replaced by the

analytically identical form sech $\sqrt{-z\pi/2}$) but the solution in series, as given by (7), is unchanged   The convergence of the numerator of the fraction in (7) being uniform in z for $1 \gg z \gg -\infty$,[*] $F_h \to 1$ as $z \to -\infty$ Hence, when $F_H(\theta, 0) \approx 1$, the linear and hyperbolic approximations to the δ, v relation may be expected to remain good for end tension   Actually the hyperbolic approximation (18), with the given value of k inserted, gives F_h with an error of less than 1% for end tensions less than $15P_1$, and less than 5% for all end tensions   Fig 5 reproduces the left-hand part of fig 4, and shows for this case (eccentric end load) both the true curve and the approximate hyperbola (19)   The true value of $dv/d\delta \to \infty$ as $\delta \to -1$
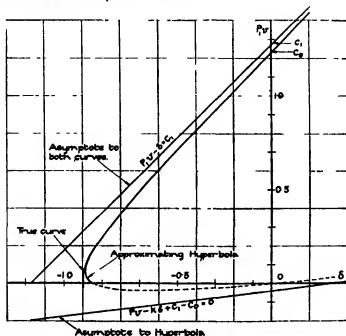
Fɪɢ 5 —Hyperbolic approximation and ideal relation for end tension with unit end eccentricity

Effects of Zero Errors

2 6 All of the preceding work depends on the assumption that δ is the *additional* deflection—that is, the deflection which ensues when P and any loads proportional to P are applied   In actual tests, especially of "built up" spars, δ may be subject to considerable zero error, of amount difficult to deter-

---

[*] By Abel's test. *Cf* Bromwich, "Introduction to the Theory of Infinite Series," § 44 (2), or Whittaker and Watson, "Modern Analysis," § 3 35

mine directly, on account of minor settlements, etc , in the early stages of the loading process It would not be fair to regard the effects of these as showing that the specimen differed materially in its behaviour from an ideal beam.

2 61 Let δ be the true additional deflection in a test of an ideal beam, and let $v = \delta/P$ Let δ' be the crude deflection (that is, the quantity measured instead of δ), and let $v' = \delta'/P$ Also let $\delta = \delta' + \varepsilon$, ε being the constant correction which should be added to the measurements to give the true additional deflection.
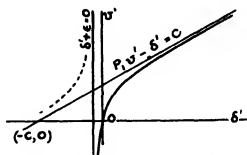
FIG 6 —Effect of zero error in δ' (ε positive)
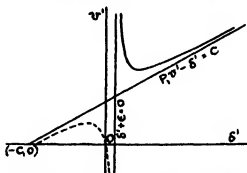
FIG 7 —Effect of zero error in δ' (ε negative).

Variation of the F-functions being neglected, we have

$$P_1 v - \delta = C,$$

that is

$$(\delta' + \varepsilon)\left(P_1 \frac{v'}{\delta'} - 1\right) = C,$$

or

$$(P_1 v' - \delta' - C)(\delta' + \varepsilon) = -C\varepsilon \qquad (20)$$

Hence the curve relating δ' and v' is a hyperbola passing through the origin, of which the asymptotes are $P_1 v' - \delta' = C$ and $\delta' + \varepsilon = 0$ Figs 6 and 7 show the forms of this hyperbola for ε positive and negative respectively

2 62 In tests of actual material ε will not be measured directly If we assume that over a sufficient range the behaviour is like that of some ideal beam, ε is easily found from three points on the corresponding range of the δ', v' curve Arithmetical methods may be used, but the geometrical method which follows has been found very satisfactory in practice

2 621 Given O and three other points on the hyperbola (20), we wish to find the position of the vertical asymptote Calling the three points 1, 2, 3, fig 8, we apply Pascal's hexagram theorem to O, 1, 2, 3, and the coincident points at infinity at which this asymptote meets the hyperbola, and obtain the
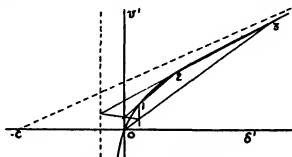
FIG 8 —Geometrical construction for zero error

following construction *the line joining the intersection of 2 1 and the ordinate through O with the intersection of 3 O and the ordinate through 1 meets 2 3 at a point on the asymptote*

The other asymptote gives the required δ, v relation, and may be obtained geometrically from the fact that any chord of a hyperbola makes equal intercepts between the curve and the asymptotes.

The corresponding arithmetical formula, and various "least-square" methods of solution, may be deduced without difficulty

EXPERIMENTAL ILLUSTRATIONS

Some practical examples of the method are exhibited in figs 9 and 10

The tests of fig 9 were undertaken with the special object of testing the theory To avoid frictional errors at the end-pins the transverse loading was made self-balancing, both up and down forces being applied by means of a single dead weight connected to a system of levers, at each stage of transverse load the mid-length deflection was measured as the end-load was increased from zero up to a safe maximum A test with eccentric end load only is included.
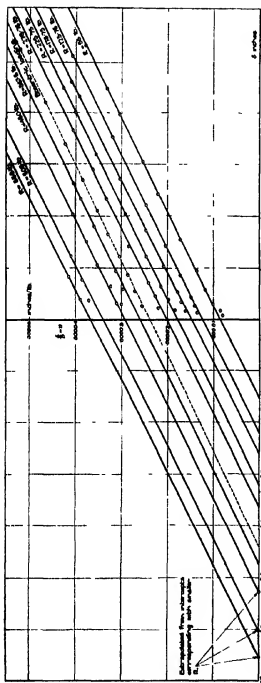
Fig 9 —Solid rectangular steel bar $\frac{3}{8}$ and $\frac{1}{2}$ for (1) variable end load P with various constant values of transverse load R, as in fig. 3 (a) (full lines) (2) variable end load P applied eccentrically (broken line)

			weight attached
(1) for R = 555 lb	C = 0 6530	} extrapolated	
R = 505 lb	C = 0 6025		
R = 430 lb.	C = 0 5270		
R = 367 5 lb	C = 0 4788		
R = 273 75 lb	C = 0 3651		
R = 223·75 lb	C = 0 3206		
R = 178 75 lb	C = 0 263		
R = 123 75 lb	C = 0 2232		
R = 55 0 lb	C = 0 1545		

$P_8 = 17,700$	1
$P_7 = 17,605$	2
$P_6 = 18,000$	3
$P_5 = 18,170$	4
$P_4 = 17,960$	5
$P_3 = 18,020$	6
$P_2 = 17,700$	7
$P_1 = 18,000$	8
$P_1 = 18,120$	

Weighted $\overline{P_1} = 18,000$

$\overline{P_1} = 18,480$

(2) for eccentric loading $C = 0 442$

Fig 10 shows an airworthiness acceptance test of an aeroplane spar built up of steel strip, transverse and end loads being here proportional Southwell's method of plotting reveals features of the test, such as the point at which the breakdown of elasticity begins, which it would be almost impossible to recognize by other methods It is interesting to observe the similarity of these results to those obtained by Gough and Cox[*] from tests on strip buckling under shear.
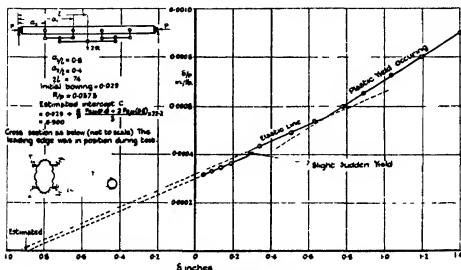
FIG 10 —Aeroplane spar

Acknowledgments.

The author is indebted to the Aeronautical Research Committee and to the Director of Scientific Research at the Air Ministry for permitting publication of this paper, and to the Secretary and Staff of the Committee for assistance in the preparation of the diagrams , to Mr W D Douglas, head of the Mechanical Testing Department of the Royal Aircraft Establishment, for having first drawn his attention to the problem, and to Mr D Seed of that Department, for arithmetical assistance Finally he has specially to thank Professor Southwell for ready encouragement and advice

Summary

The conventional theory of a beam subjected to combined transverse loads and axial end load is put into a form demonstrating an exact correspondence of transverse loads, either constant or proportional to end load, with initial (unstressed) deformation of the beam A method of linear plotting suggested

* *Loc cit* , fig 2

by Southwell for the analysis of experiments in elastic stability thus becomes available for the analysis of experiments in which "transverse" loads are operative and tend directly to increase the mode of deformation which becomes unstable An examination in particular cases of the approximation implied by the linear plotting is facilitated by simple relations (derived from the above mentioned correspondence) between the functions expressing the error

A very accurate second approximation is given, in which Southwell's straight line is replaced by a hyperbola.

Zero errors in the measurement of the deflection would destroy the collinearity of plotted observations, but methods are described for estimating and eliminating their effects

---

The Structure of Symm (1–3–5) Triphenylbenzene   Part I

By Boris Orelkin and Kathleen Lonsdale

Note —Boris Orelkin died on December 25, 1931 The X-ray investigation of symm. (1-3-5) triphenylbenzene was begun by him at the Davy Faraday Research Laboratory, where he worked as Research Fellow of the International Board of Education, but it was not completed at the time The following paper contains his results and further preliminary data leading to an approximate structure A full account of the detailed structure and of the magnetic properties will be published later

Chemical and Crystallographic Data

The chemical structure of the symmetrical triphenylbenzene is determined by its preparation It is obtained (*cf* the formation of mesitylene from acetone) by the action of dry HCl gas on acetophenone, HCl removing water according to the reaction

C_6H_5-C
$CH\ H_2$
O
$O\ C-C_6H_5$
HCH_2
H_2CH
C
O
C_6H_5
→ →
C_6H_5 C_6H_5
C_6H_5
$+ 3H_2O$
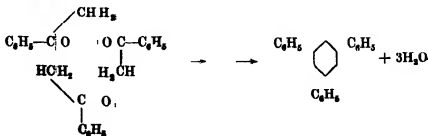
In the course of the reaction there are different intermediate products corresponding to the gradual condensation of acetophenone

The melting point of the crystals prepared in this way (by B O) was 169° to 170° C   A sample supplied later by Messrs Eastman Kodaks, and once recrystallized, melted at 173° C

Very fine crystals of any weight from about 0 1 gm downwards can be obtained by crystallization from ether or ether + alcohol   These have exceptionally sharp bright faces, and the smaller ones sparkle like brilliants in a bright light   The larger crystals have a pronounced yellow tinge

Symm triphenylbenzene has been investigated crystallographically by Knop, using crystals prepared by Arzruni   Their results are quoted by Groth† who gives diagrams of typical habits   The description and list of observed forms indicate that the crystals belong to the orthorhombic holohedral class, but, as will be shown later, they are, in fact, only hemihedral   The "imperfect cleavage" mentioned by Groth has not been observed on any of the crystals used in this investigation, a conchoidal fracture only being obtained   The habit and the supposed existence of this cleavage suggested to Fedorow that these crystals might be considered as "orthorhombic hexagonaloidal," and he gave them the habit symbol

$$
\begin{array}{c}
6 \\
37°\ 44' , \\
0°\ 25'
\end{array}
$$

where 6 denotes the "hexagonaloidal" character, 37° 44' the angle (1110 1000) [(10$\bar{1}$1) (0001) in the usual notation] and 0° 25' is the deviation from the hexagonal angle in the vertical zone [(010) (110)—60°]

The habit is usually such that all the forms corresponding to the pseudo-hexagonal bipyramid and prism of the same order are represented, the ortho-rhombic nature of the crystals being indicated by the presence of other forms only occasionally developed   On the other hand, the development of the different planes in the pseudohexagonal forms is by no means even   In the crystallographic description the pseudohexagonal axis has been adopted as the c axis and the axial ratio is given as

$$
a^* \ b^* \ c^* = 0\ 5662\ 1\ 0\ 7666,
$$

the observed forms being {110} {010} {011} and less frequently {$\bar{1}$12} {012} {100} {310}

† 'Chem Kristallog ,' vol 5, p 341 (1919).

Actually the so-called a^* axis of these crystals has now been found to be a polar axis, and, moreover, the c^* axis must be halved   Taking the polar axis as our new c axis (according to the usual crystallographic convention) the correct axial ratio becomes

$$a \quad b \quad c = \frac{c^*}{2} \quad b^* \quad a^* = 0 \ 3833 \quad 1 \quad 0 \ 5662$$

The planes (expressed in the correct notation, hereafter adopted throughout the paper) which have been observed during the course of the investigation now described are {011} {010} {120} and less frequently {001} {111} and {013}   {110} and {100} have also been observed, but at one end only   The {011} {120} planes are always much better developed than the {010} {111} planes, the last named being only occasionally developed   Usually the larger crystals are tabular on one pair of {011} faces.
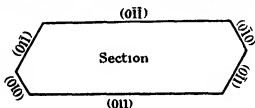
(0$\bar{1}$1)

(0$\bar{1}$0)   (010)

Section

(010)   (0$\bar{1}$0)

(011)

Fig 1

The specific gravity, measured by Schroder,† is 1 205₅ (the exact temperature not stated)

On the basis of 4 molecules of $C_6H_5(C_3H_5)_2$, molecular weight 306 14, in a unit cell of dimensions 7 55 × 19 76 × 11·22 A³, the specific gravity is 1·205   These dimensions, obtained from rotation photographs taken at a plate distance of 10 cm , give an axial ratio

$$a \quad b \quad c = 0 \ 382 \quad 1 \quad 0 \ 568$$

Space-group Determination

Rotation and oscillation photographs about the three crystallographic axes, ionization spectrometer measurements and Weissenberg photographs of the three axial zones all agree in showing that the reflections from the following planes are absent —

(0kl) if $(k + l)$ is odd ,

($h0l$) if h is odd

† ' Ber deuts chem Ges ,' vol 14, p 2516 (1881)

The absence of these reflections is characteristic of the space-groups —

Q_h^{16} (*Pnam*) in the holohedral class, and

C_{2v}^9 (*Pna*) in the hemihedral class

In order to decide between these alternatives, the crystals were tested for the pyroelectric and piezo-electric effects† in the following way   A crystal measuring about 3 mm across was placed in a Pyrex test-tube and gripped between two insulated copper wires so that the latter made as good contact as possible with opposite (001) faces. The wires passed out through the cork of the test-tube, one being connected to earth, the other to the leaf of a sensitive Wilson tilted electroscope ‡   When the surrounding test-tube was cooled by means of liquid air, the temperature of the crystal fell quickly and a small charge was developed at each end of the [001] axis   The leaf of the electroscope moved 10–12 divisions in repeated experiments   If both wires are earthed while the crystal is being cooled down, and then the same wire is connected to the electroscope, an opposite charge is indicated as the temperature rises Reversal of the wires, of course, reverses the whole effect Using a crystal of rock salt as a control, under similar conditions, a maximum

Electroscope

Fig 2

deflection of 1 division was observed   Crystals of resorcinol and tartaric acid gave deflections of over 100 divisions, that is, greater than the whole length of the eyepiece scale   Since symm. triphenylbenzene shows this small, but positive, result for the piezo-electric (or pyro-electric) test, the space-group must be one in which there is *no centre of symmetry*

---
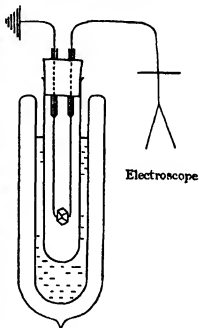
† The strains set up by a change of temperature give a piezo-electric effect which is not distinguishable from a true pyro-electric effect   For references see 'Phil Mag.,' vol 6, p 437 (1928)

‡ Sir William Bragg used an experiment similar to this in the course of a Royal Institution lecture, in order to demonstrate the polarity of resorcinol crystals

The space-group therefore is Pna, in which there is a glide-plane of translation $(b + c)/2$ parallel to (100), a glide-plane of translation $a/2$ parallel to (010) and a two-fold screw axis parallel to [001]

The co-ordinates of equivalent points are

$$(x\ y\ z)\ (\bar{x}\ \ \bar{y}\ \tfrac{1}{2} + z)\ (\tfrac{1}{2} - x\ \tfrac{1}{2} + y\tfrac{1}{2} + z)\ (\tfrac{1}{2} + x\ \tfrac{1}{2} - y\ z)$$

the structure factor for any plane (hkl) being given by

$$|F(hkl)| = \Sigma f_e (A^2 + B^2)^{\frac{1}{2}}$$

(neglecting hydrogen atoms) where

f_e = scattering power of carbon atom for plane (hkl)

$$A = \Sigma \cos 2\pi\ (hx + ky + lz)$$
$$= 4 \cos 2\pi \left(hx - \frac{h + k + l}{4}\right) \cos 2\pi \left(ky + \frac{h + k}{4}\right) \cos 2\pi \left(lz + \frac{l}{4}\right),$$

$$B = \Sigma \sin 2\pi\ (hx + ky + lz)$$
$$= 4 \cos 2\pi \left(hx - \frac{h + k + l}{4}\right) \cos 2\pi \left(ky + \frac{h + k}{4}\right) \sin 2\pi \left(lz + \frac{l}{4}\right)$$
$$= 0 \text{ if } l = 0$$

The electron density at any point XYZ is given by

$$\rho(XYZ) = \frac{1}{V_c} \sum_{-\infty}^{\infty} \sum_{-\infty}^{\infty} \sum_{-\infty}^{\infty} |F(hkl)| \cos\left[2\pi \left(\frac{hX}{a} + \frac{kY}{b} + \frac{lZ}{c}\right) - \alpha(hkl)\right],\dagger$$

where the phase $\alpha(hkl) = \tan^{-1} \frac{\Sigma B}{\Sigma A}$ (since there is only one kind of scattering

material in the cell if hydrogens are neglected), and

$$F(000) = \text{total number of electrons in the unit cell}$$
$$= 96 \times 6 + 72 = 648$$

If $l = 0$, $\alpha(hkl) = 0$ (A positive) or π (A negative), that is to say, the projection of the structure on the plane (001) is centrosymmetrical For this zone, (hk0), the electron density is

$$\rho(XY) = \frac{1}{ab} \sum_{-\infty}^{\infty} \sum_{-\infty}^{\infty} F(hk0) \cos 2\pi \left(\frac{hX}{a} + \frac{kY}{b}\right)$$

F (hk0) being positive or negative according to the sign of ΣA.

Since there are four molecules in the unit cell, each molecule is asymmetric This was to have been expected since no symmetry has ever been found with certainty for the benzene nucleus other than a centre of symmetry[†] and, in one instance, a threefold axis [‡] The formula of symm. triphenylbenzene precludes the possibility of a centre of symmetry, while the space-group forbids a threefold axis

On the other hand the chemical formula strongly suggests a pseudo-trigonal axis in the molecule, in which case this would probably coincide, or make only a small angle with the pseudo-hexagonal crystal axis *a* This arrangement can be tested by means of the optical and magnetic properties and by X-ray intensities

Optical and Magnetic Properties

The crystals show very strong negative birifringence, typical of the "layer lattice" structure type §

The following data are given by Groth (*loc cit*) but are now referred to the correct axes

The plane of the optic axes is (010), *a* being the acute bisectrix   The refractive indices have the following values —

	α	β	γ
Li	1 5202	—	—
Na	1 5241	1 8670	1 8725
Tl	1 5291	1 8848	1 8897

2V	9° 50'	Na	2E	17° 48'	Li
(calc)	10° 17'	Tl	(obs)	18° 25'	Na
				19° 27'	Tl

These values may be compared with the following —

	α	β	γ
Naphthalene	1 442	1 775	1 932
Anthracene	1 43	1 79	2 04
Phenanthrene	1 335	1 538	1 625
Diphenyl	1 554	1 586	1 647
Hexamethylbenzene	1 503	1 747	1 801

[†] For references see 'Trans Faraday Soc ,' vol 25, p 352 (1929)

[‡] Knaggs, 'Proc Roy Soc ,' A, vol 131, p 312 (1931)

[§] Wooster, 'Z Kristallog ,' vol 80, p 495 (1931)

In each of these structures the vibration direction of the fast ray (corresponding to the minimum refractive index) is perpendicular or most nearly perpendicular to the plane of the molecule, that of the slow ray (maximum refractive index) being parallel or nearly parallel to its longest dimension With symm. triphenylbenzene it is clear that the plane of the molecule must be nearly perpendicular to the acute bisectrix a (that is, to the pseudo-hexagonal axis), while the arrangement of atoms in the (100) plane is such as to form an approximately uniaxial structure, β and γ being very nearly equal The increased birefringence of triphenylbenzene relative to hexamethylbenzene points to an increased *area* of the molecule in its own plane

Large optical birefringence in hydrocarbons is accompanied by strong diamagnetic anisotropy,† the (numerically) maximum diamagnetic susceptibility corresponding to the vibration direction of the fast ray Experiment shows that for these crystals the susceptibility in the [100] direction is, in fact, very much larger than that along either of the other two axes, the susceptibility being a minimum (numerically) in the [001] direction A more detailed account of the magnetic measurements will be published later

X-ray Measurements

A study of the measured intensities confirms the above molecular arrangement, in that the reflection from the (200) plane is very strong indeed, while the higher order reflections fall off steadily in intensity The falling off is, however, more rapid than is consistent with an absolutely plane arrangement in the (200) planes Moreover, if the atoms all lay in the (200) planes then x would always be 0 or $\frac{1}{4}$, giving

$$\begin{cases} A = 4 \cos 2\pi \dfrac{h+k+l}{4} \cos 2\pi \left(ky + \dfrac{h+k}{4}\right) \cos 2\pi \left(lz + \dfrac{l}{4}\right) \\ B = 4 \cos 2\pi \dfrac{h+k+l}{4} \cos 2\pi \left(ky + \dfrac{h+k}{4}\right) \sin 2\pi \left(l_z + \dfrac{l}{4}\right) \end{cases}$$

if $x = 0$, or

$$\begin{cases} A = 4 \cos 2\pi \dfrac{k+l}{4} \cos 2\pi \left(ky + \dfrac{h+k}{4}\right) \cos 2\pi \left(lz + \dfrac{l}{4}\right) \\ B = 4 \cos 2\pi \dfrac{k+l}{4} \cos 2\pi \left(ky + \dfrac{h+k}{4}\right) \sin 2\pi \left(lz + \dfrac{l}{4}\right) \end{cases}$$

if $x = \frac{1}{4}$

† Bhagavantam, 'Indian J Phys,' vol 4, p 1 (1929)

In either case there would disappear certain sets of reflections (for example, from planes (hkl) having $h + k + l$ odd, in the first case) which have, in fact, been observed

Signs of pseudo-trigonal symmetry exist in the observed structure factors of the $(0kl)$ planes, fig 3 For example, the planes $(01\bar{5})$, $(07\bar{5})$, (082), which

F

(031) — (010)

$(03\bar{1})$ — $(01\bar{1})$

(001) — (011)

Fig 3
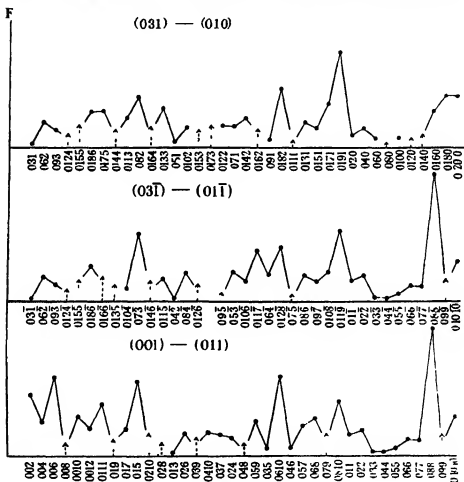
have nearly the same spacing and lie at 60° to each other, all have a large structure factor Similar groups of three planes are $(0, 6, 10)$, $(0, 12, \bar{8})$, $(0, 18, 2)$, and $(0, 8, 10)$, $(0, 11, \bar{9})$, $(0, 19, 1)$ On the other hand, the (002) structure factor is large, while that of its "pseudo-hexagonal" repetition, (031), is particularly small On passing to the general planes (hkl), having no zero index, the pseudo-

hexagonal symmetry has almost entirely disappeared, so that a Laue photograph taken perpendicular to the [100] axis shows no trace of it The slight tilt of the molecules to the (100) plane probably accounts partly for this effect, but it is also undoubtedly due to the introduction of the variable parameters consequent on reflection across the (100) and (010) planes It is clear that even if the molecules were very nearly trigonal, and lay very nearly parallel to the (100) planes, suitable translations of the four molecules relative to each other would eliminate all pseudo-hexagonal symmetry from the structure as revealed by X-rays, though retaining it in the external form The "centres" of the four molecules will lie at the points

$$(p \; q \; 0) \; (\bar{p} \; \bar{q} \; \tfrac{1}{2}) \; (\tfrac{1}{2} - p \; \tfrac{1}{2} + q \; \tfrac{1}{2}) \; (\tfrac{1}{2} + p \; \tfrac{1}{2} - q \; 0),$$

so that the (00l) planes are the only ones the structure factors of which are independent of p and q Good agreement for all observed planes (00l),† up
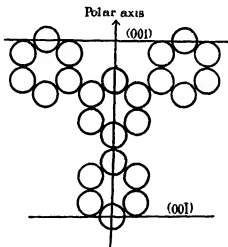
FIG 4.

to $l = 12$, is obtained by placing a plane pseudo-trigonal molecule of 1–3–5 triphenylbenzene with one of its "arms" very nearly parallel to [001], and in no other position. The polar axis of the crystal thus has a very real physical significance, owing to the fact that at one end of the crystal there are, in effect, twice as many carbon atoms in the surface as at the other end. Any redistribution of electron density due to temperature or other cause of strain will have twice as much effect at one (001) face as at the other (00$\bar{1}$) face

† Mr B W Robinson very kindly made absolute measurements of the (002), (004), and (006) reflections

A detailed study of other hydrocarbons, notably of anthracene and naphthalene,[†] has shown that while the distance between the centres of carbon atoms in the same molecule is 1·54 A or less, the corresponding distance between carbon atoms in different molecules is never less than 3·4 A (as in graphite) and is usually about 3·7 A for closest approach of neighbouring molecules.[‡] Thus the van der Waals' forces between the molecules in the crystal may be represented by the enclosure of each carbon atom in a sphere of diameter 3·7 A, within which no corresponding sphere from another molecule may be allowed to penetrate. This is a most useful rule, which can often be used to determine the most probable molecule arrangements in the crystal cell.

Taking the centre of the middle benzene nucleus as a representative point in the molecule, corresponding points in the four molecules are situated as follows —

Molecule 1 . $(p, q, 0)$

Molecule 2 (reflection of molecule 1 in $(100)_{\frac{1}{4}}$ translated
$\frac{1}{4}b + \frac{1}{4}c$) $(\frac{1}{2} - p \frac{1}{2} + q \frac{1}{4})$

Molecule 3 (reflection of molecule 1 in $(010)_{\frac{1}{4}}$ translated
$\frac{1}{4}a$) . $(\frac{1}{4} + p \frac{1}{2} - q \ 0)$

Molecule 4 (reflection of molecule 2 in $(010)_{\frac{1}{4}}$ translated $\frac{1}{4}a$) $(\bar{p}, \bar{q}, \frac{1}{2})$.

Consider the planes $(p, 0, 0)$ and $(1 + p, 0, 0)$, passing through eight molecules of type 1, which we know to be tilted a little out of the (100) plane, fig. 5.

The molecule which occupies the space between four molecules of type 1 must lie very near to the centre of gravity of the four, in order that the van der Waals' "spheres of force" shall not interpenetrate. This molecule can be either of type 2, or of type 4 (type 3 being in the plane $(1 + p, 0, 0)$). If it is of type 2, then p and $\frac{1}{2} - p$ must be nearly equal (their difference being not bigger than about $\frac{1}{10}$), while if it is of type 4, then q must be very nearly equal to $\frac{1}{4}$ (say $\frac{1}{4} \pm \frac{1}{10}$). The latter arrangement would give a complete structure as shown in fig. 6. This would not explain the big difference in the intensities of (002) and (031). It would, in fact, involve a much greater degree of pseudo-trigonal symmetry than is actually found, and so is out of the question.

Placing a molecule of type 2 in this position, it is clear that the very small intensity of (031) is best explained by making $q = 0$, $\frac{1}{2}$ or $-\frac{1}{2}$ (nearly), so that if molecules 1 and 2 lie in the (031) planes, molecules 3 and 4 just interleave

those planes, but all four molecules lie in successive (002) planes These
values of the parameters give arrangements as shown in fig 7

Fig 6 (a) shows that if $q = 0$ the reflections from (011), (051), (015) planes
should be very much weakened by comparison with those from (020), (042),

a

Space for two molecules
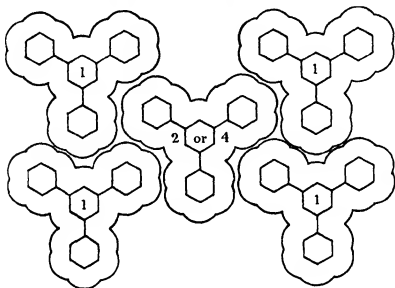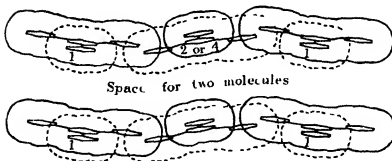
b

Fig 5

(082) which are inclined at 60° to them This is not so, as fig 3 shows, and
therefore we are left with $p = \frac{1}{4} \pm$ ($< \frac{1}{16}$) and $q = \frac{1}{4}$ or $-\frac{1}{4}$, the differences
in the corresponding structures being too small to be settled by any but the
most detailed structure factor comparisons.

Fig 6

a

b

c
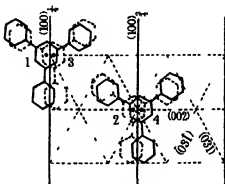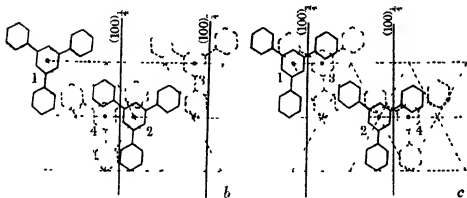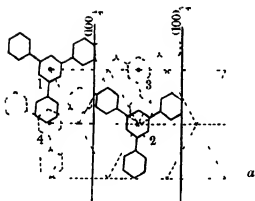
Fig 7

Discussion of further structural details, such as the exact molecular direction cosines, the distance between carbon atoms in a single nucleus and in different nuclei of the same molecule, will be left for the second part of this paper

Summary

1-3-5 triphenylbenzene crystallizes in the orthorhombic hemihedral class, space-group Pna (C_{2v}^{9})   The unit cell contains four molecules and is of dimensions $a = 7\ 55$ A., $b = 19\ 76$ A , $c = 11\ 22$ A   The crystal habit is pseudo-hexagonal, with a as the pseudo-principal axis   The optical and magnetic properties of the crystal and the X-ray measurements upon it show that the structure approximates to the "layer lattice" type   Pseudo-trigonal molecules are inclined at a relatively small angle to the (100) planes, with one "biphenyl" arm nearly parallel to the [001] axis, so that there are, in effect, twice as many carbon atoms in the crystal surface at one end of the polar axis as at the other end   The co-ordinates of representative points of the molecules are given to a first approximation

The Effect of Solvent on Reaction Velocity   V — The Interaction of N-Chloroacetanilide and Hydrobromic Acid in Dilute Aqueous Solution.

By ISLWYN JONES and F G SOPER.

(Communicated by J L Simonsen, F R S — Received December 13, 1933)

The interaction of N-chloroacetanilide and hydrobromic acid to form p-bromoacetanilide and hydrochloric acid has, unlike the corresponding reaction with hydrochloric acid,[†] received comparatively little attention from a kinetic standpoint   It possesses, however, the advantage over the hydrochloric acid reaction, that its speed is much greater   It thus allows of the examination of mixtures containing only 0 001 M hydrobromic acid and of salt effects in the region of dilute concentration where the Debye-Hückel theory applies

The mechanism of the interaction is analogous to that of the chloroamine-hydrochloric acid reaction, where the first stage

$$C_6H_5NClAc + HCl \rightleftharpoons Cl_2 + C_6H_5NHAc \overset{\text{II}}{\rightarrow} ClC_6H_4NHAc + HCl$$
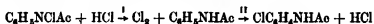
determines[‡] the rate of transformation of the chloroamine in aqueous solution Two corrections are necessary in this reaction if the true rate of interaction of chloroamine and acid is to be determined   The first correction is for the hydrolysis of the chloroamine under the influence of the acid, a rate mainly dependent on the H ion concentration   Since the rate of the transformation depends on the product of the H⁺ and Cl⁻ ion concentrations, the correction for hydrolysis cannot be regarded as forming a constant fraction of the observed speed, particularly when the ratio of these ion concentrations is widely varied The second correction is for the simultaneous formation of the chloroamines of the chloroanilides present   These chloroamines, which are formed pro-

---

* Acree and Johnson, 'Amer Chem J,' vol. 37, p 410 (1907), Orton and Jones, 'Rep. British Ass.,' p. 85 (1910) , Richardson and Soper, 'J Chem Soc ,' p 1873 (1929)

† Orton and Jones (loc. cit.), Rivett, 'Z phys Chem ,' vol 82, p 201 , vol 85, p. 113 (1913) , Harned and Seltz, 'J Amer Chem Soc ,' vol 44, p 1476 (1922) , Åkerlof, 'Medd. Nobel Inst.,' vol 6, No 2 (1925) , Soper, 'J Phys Chem ,' vol 31, p 1192 (1927) , Soper and Pryde, 'J Chem Soc ,' p 2761 (1927) , Fontein, 'Rec trav chim ,' vol 47, p 635 (1928) , Barnes and Porter, 'J Amer Chem Soc ,' vol 52, p. 2973 (1930) , Belton, 'J Chem. Soc ,' p. 116 (1930) , Dawson and Millet, 'J Chem Soc ,' p. 1920 (1932)

‡ Comparison of the observed rate of transformation with the value calculated for stage I from the equilibrium constant and the reverse velocity coefficient shows good agreement (Soper, loc. cit)

gressively, appear in the chloramine titre and cause the measured reaction rate to be slower by 4–10% than the actual rate of production of chlorine This complication can be avoided by the presence of easily chlorinated substances, such as anisole, p-cresol,* or acetanilide, which remove the chlorine as formed †

In the analogous hydrobromic acid reaction, the first stage

$$C_6H_5NClAc + HBr \xrightarrow{I} C_6H_5NHAc + ClBr \xrightarrow{II} BrC_6H_4NHAc + HCl$$
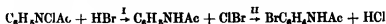
determines the rate in water The correction for hydrolysis of the chloroamine is negligible in comparison with the measured rate of interaction, which is approximately 20,000 times faster than that of the hydrochloric acid reaction The complication due to simultaneous formation of bromoamines by interaction of p-bromoacetanilide and ClBr also appears to be of much less magnitude and is completely eliminated by working in the presence of slight excess of acetanilide

Before considering the salt effects observed in the present investigation at low ionic strengths, it is necessary to refer briefly to the conclusions reached from a study of the chloroamine-hydrochloric acid reaction These conclusions, particularly those relating to the reactivity of the acid, depend largely on the fundamental reaction velocity equation adopted Rivett (loc cit)

---

* Balton (loc cit) regards the two corrections as eliminating each other and reports that he was unable to obtain consistent results using p-cresol We have not experienced this difficulty when the p-cresol is quite colourless

† Barnes and Porter (loc cit) have criticized this explanation of the reaction mechanism, particularly in regard to the effect of the addition of readily chlorinated substances on the rate of reaction The experiments of Barnes and Porter were carried out in glacial acetic acid In this medium the second stage determines the reaction rate (Orton and Jones, loc. cit), the change of solvent having slowed up the interaction of chlorine and acetanilide and increased that of the chloroamine and hydrochloric acid The state of affairs may be represented

$$HCl + NClAc \longleftrightarrow Cl_2 + NHAc \longrightarrow ClC_6H_4NHAc + HCl$$

where $[Cl_2] / [NHAc] / [HCl] / [NClAc] = K$ The reaction rate, v, is given by

$$v = k_1[Cl_2] [NHAc] = k_1K [HCl] [NClAc] = k_1 [NClAc]$$

following a unimolecular law

Addition of acetanilide increases both the concentration products [HCl] [NClAc] and [Cl$_2$] [NHAc] equally and increases the rate of disappearance of chlorine The cause of the increase of the observed speed is different from that of the increased speed in water on addition of acetanilide The presence of the more readily chlorinated β-acetonaphthalide in the glacial acetic acid medium, examined by Barnes and Porter, will obviously cause a more rapid disappearance of chlorine than the presence of a similar amount of acetanilide

assigned separate reactivities to the un-ionized hydrogen chloride and to the H' and Cl' ions, using the classical equation in which velocity is strictly dependent on concentration. Harned and Seltz (*loc cit*) concluded that the speed was proportional to the chloramine concentration and to the thermodynamic activity of the H' and Cl' ions. Soper and Pryde correcting for the two simultaneous reactions, previously referred to, found the speed proportional to the thermodynamic activity of both the chloramine and hydrochloric acid molecules. Richardson and Soper suggested that this unusual concordance with the activity rate theory, might be associated with the constant surface tension and cohesion of the hydrochloric acid solutions examined. It was found, in the analogous reaction with hydrobromic acid that the activity rate theory held approximately for sucrose solutions, where there was little change in the cohesion of the solvent medium, but that divergencies were observed in opposite directions in aqueous alcohol and in salt solutions.

The agreement of results with the activity rate theory where the cohesion of the solvent medium remains constant is suggestive and may be due to the fact that under these conditions, the thermodynamic activities of the chloramine and hydrochloric acid are proportional to the number of unsolvated or un-ionized molecules, respectively, able to pass a *constant* energy barrier at the interface at which the activity is determined, and thus measure the number of such molecules in unit free space. If the cohesion of the medium is not constant the energy barrier at the interface varies and the number of molecules escaping in unit time is not simply related to their concentration. The activity rate equation would appear to reduce to a true concentration reaction velocity equation when the medium is of constant cohesion and, further, this constancy results in uniformity of ease of formation or of resolution of the intermediate critical complex and results in the agreement observed.

Recently two papers have been published on the chloramine-hydrochloric acid reaction by Belton and by Dawson and Millet, in which the results are regarded as supporting a theory of strict dependence of reaction speed on molecular concentration, over a range of considerable changes in the salt content of the reaction medium. According to Dawson and Millet, the reaction rate, being determined by the concentration of un-ionized hydrochloric acid, is proportional to the product of the concentrations of the H' and Cl' ions and their activity coefficients. The kinetic results are well accounted for if the activity coefficients are assigned values given by the equation,

$$\log f = -0.28 \sqrt{\mu} + b\mu,$$

where b varies with the nature of the salt These kinetically deduced values of the activity coefficients, however, differ considerably from those given by equilibrium measurements, and the discrepancy may be due partly to the non-correction of the observed speeds for simultaneous reactions and possibly also to a specific medium effect on the reaction process caused by the changes in the salt content of the solution
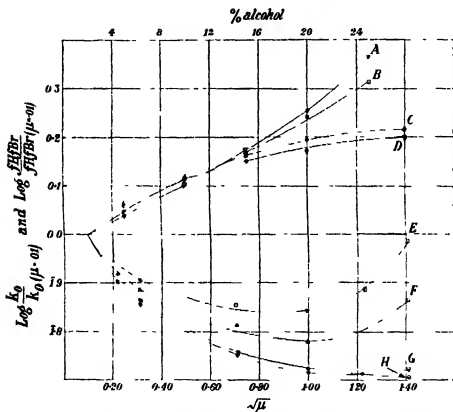
FIG 1 —A, k_0 in EtOH , B, k_0 in MeOH , C, $f_H f_{Br'}$ in EtOH , D, $f_H f_{Br}$ in MeOH , E, $f_H f_{Br}$ in NaNO₃ , F, $f_H f_{Br}$ in KNO₃ ; G, k_0 in KNO₃ , H, k_0 in NaNO₃.

Actual comparison of the velocity coefficients, k_0, of the hydrobromic acid reaction (where $v = k_0 c \cdot_{\text{H}} c_{\text{H}} c_{\text{Br'}}$) with the measured thermodynamic activity coefficients of the H˙ and Br′ ions in various aqueous media, was made by Richardson and Soper These results are shown graphically in fig 1, the relative change in the velocity coefficient caused by the various additions to the aqueous solution being compared with the relative change in the activity coefficients of the ions of the acid These curves bring out the fact that in

sodium and potassium nitrate solutions the velocity coefficient, k_0, is depressed below the product of the activity coefficients whilst in alcoholic solution the reverse is true, k_0 increasing more rapidly than the activity coefficient product The specific rate of reaction of un-ionised hydrobromic acid with chloroamine is thus depressed in salt solution and increased in alcoholic solutions. These divergencies were regarded as specific solvent effects connected with the relative polar nature of the reagents and products and the cohesion of the solvent, which was regarded as assisting the intermediate critical complex to break up into those substances for which it has the greater affinity

Comparison* of the effect of ionic strength on the following types of ionic reactions

$$A' + B'' = C''' + D \qquad (1)$$

$$A' + B'' = C'' + D' \qquad (2)$$

showed that increase of ionic strength, even in the range 0 001–0 03 μ increased the speed of reaction (1) above that of (2), as though the medium effect observed with neutral molecules were superimposed on the Bronsted primary salt effect As high-valent ions were involved in the above comparison, with possible attendant anomalies, the investigation in dilute solution of the hydrobromic acid-chloroamine reaction, in which no ions have a higher charge than unity, was thought likely to be of interest

Details of the method of following this reaction speed have previously been recorded. Sharp titration of the iodine liberated on addition of the mixture containing N-chloroacetanilide to aqueous potassium iodide was achieved, using N/500 thiosulphate and freshly prepared starch, by carrying out the operation in a current of nitrogen The salts of the alkali metals and alkaline earths used as neutral salts in the investigation were B D H , A.R chemicals and were dried to constant weight at 110° The p_H of each solution was tested using brom-thymol blue and was shown to lie within the range 6 6 to 6 9 The nitric and perchloric acids were distilled from their constant boiling mixtures, diluted to the approximate strength required and estimated iodometrically Conductivity water was used in all experiments The velocity follows the equations for a bimolecular reaction, since in any one experiment, the H' ion concentration is constant, i.e., $v = k_2 c_{.NCl} c_H c_{Br'} = k_2' c_{.NCl} c_{Br'}$, where $k_2 = k_2' c_H$ The unusually good consistency of the bimolecular constants obtained may be illustrated by two typical experiments, recorded in Table I

The collected results are given in Table II and for each series the slope of the log $k - \sqrt{\mu}$ curve has been calculated by the method of least squares An estimate of the precision of the slope has been obtained by considering the

Table I

Initial concentrations [.NCl] = [HBr] = 0 001 M , [PhNHAc] = 0 01 M , Ba(NO₃)₂ = 0 00500, $\mu = 0$ 01601 thiosulphate = 1 044 N/500								
Time (mins)	0	75	163	240	319	395	472	580
25 c c titre (c c thio)	21 28	17 51	14 55	12 64	11 12	9 84	9 00	7 96
k_2	—	3 14	3 16	3 16	3 16	3 15	3 13	3 16

Initial concentrations [NCl] = [HBr] = 0 001 M [PhNHAc] = 0 01 M , [HClO₄] = 0 01601 M., $\mu = 0$ 01601 , thiosulphate = 1 044 N/500							
Time (mins)	0	5 00	10 00	15 00	20 00	25 91	33 00
25 c c titre	20 02	16 48	13 99	12 04	10 70	9 35	8 17
$k_2 \times 10^{-2}$	—	3 19	3 21	3 22	3 18	3 21	3 20
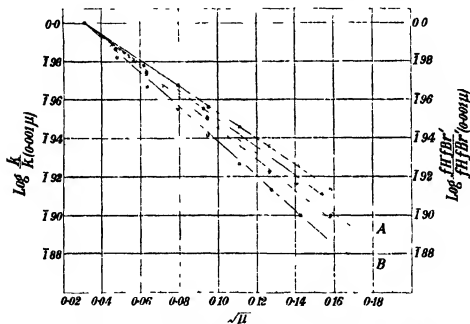
Fıg 2—O, HClO₄ , □, NaNO₃ , ●, Ba(NO₃)₂ , Δ, HNO₃ , A, f_H f_{Br} = f_H f_{Cl} B, f_H f_{Cl} ın KCl.

separate slopes of lines joinıng each poınt of the series to the calculated initial poınt of the series ($\mu = 0$ 001) The mean deviation of these slopes from the recorded value has been determined and the average error range of the slope of the series stated. In connection with each fresh salt series, a control

experiment on the reaction rate of chloroamine and hydrobromic acid, each at 0 001 M initial concentration, was carried out in the same thermostat and simultaneously with the fresh series of salt mixtures. The slopes of the curves, which appear to be linear up to $\mu = 0\ 01$, vary between $-0\ 89$ and $-0\ 64$ with an average precision of $\pm\ 0\ 01$. The results of four series are shown in fig 2

Table II

Salt added = KNO_3 Initial concentration $[NCl] = [HBr] = 0\ 001$ M

Temperature = $25\ 00 \pm 0\ 02°$ C

Conc of KNO_3	$\sqrt{\mu}$	k_s range $\times 10^3$	Mean k_s $\times 10^{-3}$	No of values of k_s	Log k_s
0 0000	0 03162	3 69–3 77	3 71	10	3 5694
0 00125	0 04793	3 54–3 60	3 56	10	3 5516
0 00299	0 06324	3 44–3 60	3 46	10	3 5389
0 005248	0 07905	3 37–3 40	3 38	12	3 5289
0 007999	0 09486	3 26–3 32	3 28	12	3 5152
0 011280	0 11070	3 13–3 18	3 15	12	3 4980
0 01501	0 12650	3 02–3 06	3 05	11	3 4843
0 01925	0 14230	2 92–2 99	2 95	12	3 4698
0 02400	0 15810	2 86–2 92	2 88	12	3 4594
0 03499	0 18972	2 60–2 74	2 715	12	3 4346
0 04800	0 22114	2 57 2 63	2 60	12	3 4150
0 06300	0 25296	2 50–2 54	2 52	12	3 4014
0 07996	0 28458	2 36–2 43	2 40	12	3 3793
0 09000	0 31620	2 33–2 38	2 35	12	3 3711
0 1200	0 34782	2 26–2 30	2 28	12	3 3579
0 1430	0 37944	2 21–2 27	2 24	12	3 3502

Slope of the log $k - \sqrt{\mu}$ curve $= -0\ 871 + 0\ 012$

Addition of Magnesium Nitrate

Conc of $MgSO_4$	$\sqrt{\mu}$	k range $\times 10^3$	Mean k_s $\times 10^{-3}$	No of values of k_s	Log k_s
0 0000	0 03162	3 69–3 77	3 71	10	3 5694
0 0007475	0 06324	3 38–3 44	3 40	12	3 5318
0 00200	0 09486	3 10–3 14	3 115	12	3 4949
0 003752	0 12650	2 70–2 77	2 725	12	3 4354
0 0060000	0 15810	2 49–2 57	2 525	12	3 4023
0 008745	0 18972	2 26–2 32	2 285	12	3 3589
0 01200	0 22134	2 12–2 18	2 145	12	3 3324
0 01575	0 25296	1 87–1 92	1 89	12	3 2765
0 019999	0 28458	1 74–1 80	1 765	12	3 2467
0 02475	0 31620	1 59–1 65	1 626	12	3 2186
0 03000	0 34782	1 48–1 52	1 509	12	3 1786
0 03575	0 37944	1 39–1 44	1 417	12	3 1513

Slope of the log $k - \sqrt{\mu}$ curve $= -1\ 26$

Table II—(continued)

Addition of Sodium Nitrate

Conc of NaNO$_3$	$\sqrt{\mu}$	k_0 range × 10^{-3}	Mean k_0 × 10^{-3}	No of values of k_0	Log k_0
0 0000	0 03162	3 69–3 77	3 71	10	3 5694
0 00125	0 04743	3 53–3 58	3 575	10	3 5583
0 00299	0 06324	3 37–3 44	3 420	10	3 5354
0 005248	0 07005	3 36–3 39	3 38	10	3 5248
0 007999	0 09486	3 23–3 26	3 24	10	3 5105
0 011260	0 11070	3 10–3 15	3 13	10	3 4955
0 01501	0 12650	2 98–3 05	3 035	12	3 4821
0 01125	0 14230	2 91–2 97	2 9475	12	3 4694
0 02400	0 15810	2 86–2 90	2 88	12	3 4594

Slope of the log k − $\sqrt{\mu}$ curve = − 0 876 ± 0 0082

Addition of Lithium Nitrate

Conc of LiNO$_3$	$\sqrt{\mu}$	k_0 range × 10^{-3}	Mean k_0 × 10^{-3}	No of values of k_0	Log k_0
0 0000	0 03162	3 68–3 75	3 71	10	3 5694
0 002493	0 05910	3 46–3 54	3 52	7	3 5465
0 006866	0 08870	3 31–3 38	3 34	7	3 5237
0 01300	0 1183	3 11–3 18	3 14	7	3 4969
0 02085	0 1473	2 93–2 99	2 95	7	3 4698

Slope of the log k − $\sqrt{\mu}$ curve = − 0 854 ± 0 008

Addition of Barium Nitrate   Temperature = 25 05 ± 0 02° C

Conc of Ba(NO$_2$)$_2$	$\sqrt{\mu}$	k_0 range × 10^{-3}	Mean k_0 × 10^{-3}	No of values of k_0	Log k_0
0 0000	0 03162	3 71–3 80	3 77	7	3 5763
0 000999	0 06324	3 52–3 58	3 55	7	3 5502
0 00266	0 09486	3 34–3 38	3 37	7	3 5276
0 00500	0 12650	3 13–3 16	3 15	7	3 4963
0 00800	0 15810	2 99–3 04	3 01	7	3 4786

Slope of the log k − $\sqrt{\mu}$ curve = − 0 7827 ± 0 01

Addition of Strontium Nitrate   Temperature = 25 05 ± 0 02° C

Conc of Sr(NO$_2$)$_2$	$\sqrt{\mu}$	k_0 range × 10^{-3}	Mean k_0 × 10^{-3}	No of values of k_0	Log k_0
0 0000	0 03162	3 71–3 80	3 77	7	3 5763
0 000999	0 06324	3 53–3 59	3 54	7	3 5490
0 00266	0 09486	3 30–3 36	3 335	7	3 5230
0 00500	0 12650	3 09–3 15	3 13	7	3 4955
0 00800	0 15810	2 96–3 03	3 00	7	3 4711

Slope of the log k − $\sqrt{\mu}$ curve = − 0 7980 ± 0 01

Table II—(continued)

Addition of Perchloric Acid Temperature = 25 00 ± 0 02° C

Conc of HClO₄	√μ	k_s range × 10⁻³	Mean k_s × 10⁻³	No of values of k_s	Log k_s
0 0000	0 03162	3 67–3 73	3 71	10	3 5694
0 00125	0 04743	3 50–3 57	3 55	7	3 5502
0 00299	0 06324	3 46–3 52	3 49	7	3 5428
0 005248	0 07905	3 39–3 47	3 44	7	3 5366
0 00799	0 09486	3 32–3 38	3 36	7	3 5263
0 011260	0 11070	3 26–3 29	3 27	7	3 5143
0 01501	0 12650	3 18–3 21	3 20	7	3 5051
0 01925	0 14230	3 08–3 16	3 13	7	3 4955
0 02400	0 15810	3 00–3 07	3 04	7	3 4829

Slope of the log k — √μ curve — 0 6406 ± 0 008

Addition of Nitric Acid

Conc of HNO₃	√μ	k_s range × 10⁻³	Mean k_s × 10⁻³	No of values of k_s	Log k_s
0 0000	0 03162	3 67–3 73	3 71	7	3 5694
0 002829	0 06190	3 47–3 54	3 52	7	3 5468
0 00799	0 09251	3 30–3 36	3 34	7	3 5237
0 01430	0 12330	3 11–3 17	3 15	7	3 4983
0 02268	0 15390	3 00–3 04	3 02	7	3 4800

Slope of the log k — √μ curve — — 0 741 ± 0 008

Addition of Sodium Chloride

Conc of NaCl.	√μ	k_s range × 10⁻³	Mean k_s × 10⁻³	No of values of k_s.	Log k_s
0 0000	0 03162	3 67–3 75	3 73	7	3 5717
0 00299	0 06324	3 48–3 55	3 515	7	3 5459
0 00799	0 09486	3 22–3 30	3 27	7	3 5145
0 01501	0 12650	3 06–3 12	3 10	7	3 4914
0 02400	0 15810	2 84–2 89	2 87	7	3 4599

Slope of the log k — √μ curve — — 0 8932 ± 0 015

Temperature = 34 80 ± 0 02° C

0 000	0 03162	8 19–8 28	8 23	14	3 9154

No values for the activity coefficient of HBr in the presence of neutral salt at low ionic strength are recorded, but Livingston[*] found that the activity coefficients of HCl and HBr are indistinguishable at concentrations below 0 1 M   According to the Bronsted theory of reaction velocity, the speed of the reaction will be given by $v = Cc_H \ c_{Br'} \ c_{\, \text{\tiny NCl}} f_H \ f_{Br} \ f_{\text{\tiny NCl}}/f_x$, and in dilute solution by $v = Cc_H \ c_{Br} \ c_{\, \text{\tiny NCl}} f_H \ f_{Br}$ Comparison with the expression for the concentration velocity coefficient, k_0, shows that log k_0 should be given by

$$\log k_0 = \log C + \log f_H \ f_{Br},$$

and the curve of log $k_0 - \sqrt{\mu}$ should be exactly similar to one of log $f_H \ f_{Br} - \sqrt{\mu}$ The values for the activity coefficient product are shown as a broken line curve in fig 2, falling in the centre of the pencil of velocity curves Data for the activity coefficients of hydrochloric acid[†] in the presence of neutral salts show that at constant ionic strength the salt effects are of similar magnitude to those observed kinetically, the divergences which exist in the solutions of higher salt concentration tending to disappear in dilute solution   For purposes of comparison, the activity coefficient of hydrochloric acid in the presence of potassium chloride is indicated in fig 2   A minor discrepancy exists in the order of the salt effects in the two cases   For the activity coefficients of hydrochloric acid at an ionic strength of unity, the order of $f_H \ f_{Cl}$ is

$$HCl > LiCl > NaCl > KCl > SrCl_2 > BaCl_2,$$
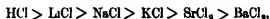
whilst for k_0 the order is

$$HClO_4 > HNO_3 > Ba(NO_3)_2 > Sr(NO_3)_2 > LiNO_3 > NaNO_3, KNO_3 > NaCl,$$

the relative positions of the alkali metal and alkaline earth salts being reversed   The great effect of magnesium sulphate on the reaction speed is largely due to removal of H-ion by the reaction $SO_4'' + H' = HSO_4'$

The considerable variation in the slopes observed clearly demonstrates the specific nature of the salt effects and renders the comparison of the log $k - \sqrt{\mu}$ curves of ionic reactions of different types of uncertain value   In the present investigation with uni-valent ions, there is no evidence for a medium effect superimposed on the Bronsted primary salt effect in dilute solution   At higher salt concentrations the medium effect may possibly be expressed in the residual term $f_{\text{\tiny NCl}}/f_x$ of the Bronsted equation, or, as previously suggested, may be due to an environmental influence assisting or preventing the break-up of the critical complex into the products

---

* 'J Amer Chem Soc,' vol 48, p. 45 (1926)

† Harned and Åkerlöf, 'Phys. Z.,' vol 27, p. 411 (1926)

In Table III the slopes of the log $k - \sqrt{\mu}$ curves are collected and compared with the relative cohesions of the various salt and acid solutions

<div style="text-align:center">Table III</div>

Salt	Reciprocal of relative compressibility of 0 5 M solution	Surface tension of solution at $\mu = 1\ 5$ $\Delta\gamma$	Slope of log $k - \sqrt{\mu}$ curve
NaCl	1 178	2 45	$-0\ 893 \pm 0\ 015$
NaNO$_3$	1 139	1 76	$-0\ 876 + 0\ 008$
KNO$_3$	1 110	1 55	$-0\ 871 \pm 0\ 012$
LiNO$_3$	1 120	1 82	$-0\ 854 \pm 0\ 008$
Sr(NO$_3$)$_2$	—	1 27	$-0\ 798 \pm 0\ 010$
Ba(NO$_3$)$_2$	—	1 00	$-0\ 783 \pm 0\ 010$
HNO$_3$	1 020	$-1\ 10$	$-0\ 741 + 0\ 008$
HBr	1 029	$-0\ 69$	—
HClO$_4$	—	—	$-0\ 641 + 0\ 008$

The surface tensions and the reciprocals of the relative compressibilities of the salt solutions indicate that the cohesions are in the order   NaCl > alkali nitrates > alkaline earth nitrates > acids   This order is in agreement with the retarding effects of these solutions at constant ionic strength and in approximate agreement with the inverse order of the activity coefficients of hydrochloric acid in these solutions   At constant ionic strength, activity coefficients are regarded as affected by the average ion diameters and by the influence of the salts on the dielectric constant of the medium, but in view of the anomalous behaviour of the activity coefficients of the alkali hydroxides,* where $f_K > f_{Na} > f_{Li}$, it is possible that other factors may sometimes dominate If, for example, the equilibrium between co-valent hydrogen chloride and its ions varies in different solutions, this variation would be reflected in its activity coefficient   The effect of solvent on equilibrium is such that a change of solvent displaces the equilibrium, $A \rightleftharpoons P$, to form the substance, the solubility of which is the more increased by the change   By analogy with the behaviour of other co-valent gases,† increase of the internal pressure of an aqueous solution, which may be caused by the addition of salt, will decrease the solubility of co-valent hydrogen chloride and displace the equilibrium, $HCl = H^+ + Cl^-$, in the direction of the ions   In salt solutions at constant ionic strength,

---

* Harned, 'J Amer Chem Soc,' vol. 47, pp 684, 689 (1925), Harned and Swindells, *ibid.,* vol 48, p 126 (1926)

† Euler, 'Z phys. Chem ,' vol. 31, p. 368 (1898), Hildebrand, "Solubility," N Y (1924)

increase of internal pressure would decrease the fugacity and the activity coefficient of the acid, as is observed   This effect would be additional to those from other causes   For the alkali hydroxides, an equilibrium of doublets with the free ions probably exists, and it is tentatively suggested that the anomalous order of activity coefficients for these substances, may be due to the opposite effect of internal pressure on the equilibrium of the ions, increase of internal pressure increasing the number of doublets and increasing the activity coefficient

The critical increment of the reaction has been calculated from measurements at 25° and 35°, permitting the expression of k_0, referred to unit activity coefficient of the acid, by the equation

$$k_0 = 10^{14\ 39}\,e^{\ 14,580/RT}$$

The corresponding expression for the reaction of hydrochloric acid with the chloroamine, using the data of Harned and Seltz at 25° and 35° is

$$k_0 = 10^{16\ 00}\,e^{\ 21\ 370/RT},$$

the difference in the reactivity of the two acids being almost entirely due to the change in the critical increment from 14,580 to 21,370 cals   The products and reagents of contrasted nature in these reactions are hydrobromic acid and bromine chloride in the one reaction and hydrochloric acid and chlorine in the other   In both the contrast is similar, as also occurs in the chlorination of phenols, ethers and anilides,* where chlorine and hydrochloric acid appear on opposite sides of the equation in all the reactions   This similar contrast in the nature of the products and reagents appears to confer constancy on the solvent effect in the series of reactions   In chlorinations, the changes in the reaction speeds are due, within experimental error, to changes in the energy of activation, as though the probability factor P, representing the influence of solvent on the ease of formation or of disruption of the critical complex into the products, is constant for the series   This factor, not unexpectedly, appears to be constant in the interactions of N-chloracetanilide with hydrobromic and hydrochloric acids.

* For references, *vide* Roberts and Soper, ' Proc Roy Soc ,' A, vol. 140, p 71 (1933)

Summary

(1) The effect of neutral salt on the rate of interaction of hydrobromic acid and N-chloroacetanilide has been studied over the range of ionic strength, 0 001–0 025 μ, and the slopes of the log $k - \sqrt{\mu}$ curves, evaluated by the method of least squares, found to vary from $- 0\ 64$ to $- 0\ 89$ with the nature of the added electrolyte

(2) The order of salt effects is approximately that of the activity coefficient of the acid and also that of the internal pressures of the solutions

(3) The difference (20,000-fold) in the speeds of interaction of the chloroamine with hydrochloric and hydrobromic acids is due almost entirely to the change in the energy of activation of the two reactions This fact is regarded as supporting the interpretation of solvent effects previously advanced

---

Optical Rotatory Power I.—A Theoretical Calculation for a Molecule containing only Isotropic Refractive Centres

By S F Boys, A.R.C S , B Sc , Beit Scientific Research Fellow, Imperial College of Science and Technology, London

Introduction.

Ever since the time of van't Hoff and Le Bel the number of investigations dependent on optical activity, or attempting to elucidate optical activity, has been very great, and it is remarkable that, even at the present time, there is no theoretical formula which gives the relation between the magnitude of the rotation and the chemical structure of the molecule concerned The present communication supplies this want with regard to the molecule of the simplest asymmetric type the molecule with four different groups attached to one central atom

Various special hypotheses have been postulated to explain optical activity, but a few investigators have shown quite definitely that there is no necessity for any of these hypotheses Born[*] and Oseen[†] have shown independently

---

[*] 'Phys Z,' vol. 16, p 251 (1915), 'Ann Physik,' vol 55, p 177 (1918).

[†] 'Ann. Physik,' vol. 48, p 1 (1915).

that, if the molecule has a dissymmetric structure, the ordinary refractive properties of the atoms will account for an optical rotation Gray* and de Mallemann† have attempted calculations of formulæ for optical rotatory power on this basis However, it has not been possible to condense the numerous algebraic terms which occur in these calculations into a compact form

De Mallemann approached the nearest to the desired formula when he applied his calculation to a molecule of four atoms where one atom may be regarded as the origin of a set of rectangular axes and the other three atoms must lie on these axes De Mallemann‡ showed that, if CHClBrI has a structure of this shape, the predicted rotation would be of the order of ordinary optical rotatory powers However, there do not seem to be any compounds which are known to have the postulated structure, and the formula has no practical use

By the following analysis it is possible to find a formula for the optical rotatory power of the general molecule of refractive structure , and this rotation has been expressed in a precise form by means of determinants The expression is in a manageable form and simplifies by purely algebraic processes when it is applied to a particular type of molecule It first became apparent to me that the ordinary properties of a dissymmetric molecule account for its optical activity, when I realized a complete analogy in a simple mechanical system It is probably this analogy which has provided the clue for the solution of the complicated mathematical expressions which occur in the evaluation of the rotation caused by these refractive properties

It is possible to construct a medium which shows a rotatory power for an ordinary transverse elastic wave This is formed when we have an elastic solid with heavy masses embedded in it , as an example we may consider a gelatine gel with ball bearings as heavy particles These balls are arranged in sets of four , all these sets are exactly alike, but the balls in each separate set may be different and may be at the corners of an irregular tetrahedron These tetrahedral sets are distributed entirely at random, so that the gel as a whole is isotropic There are two kinds of model, related to each other as an object to its mirror image , and hence a gel containing only one " enantiomorph " corresponds to an optically active liquid Each ball vibrates under the influence of a passing wave and has an effect on neighbouring balls, e g , if a certain ball A vibrates up and down, then a smaller ball B a little farther

* ' Phys Rev ,' vol. 7, p 472 (1916)
† ' Rev gén. sci ,' vol. 38, p. 453 (1927).
‡ ' C R. Acad Sci Paris,' vol 181, p 298 (1925)

along the path of the wave, a little to one side, and a little above A, is dragged to and fro in a horizontal direction by the motion of A   The secondary wavelets caused by all these vibrators have to be added to the original wave and, if the total effect of these is not exactly in the same direction as the original wave, the plane of polarization is altered   For a medium containing a symmetrical model the resultant of these secondary wavelets would be in the same direction as the inducing wave, but with an unsymmetrical model this condition does not hold and the medium is " mechanically active "

This model bears the same relation to the natural optically active molecule as the Sellmeier vibrators in the early theory of optical dispersion do to the
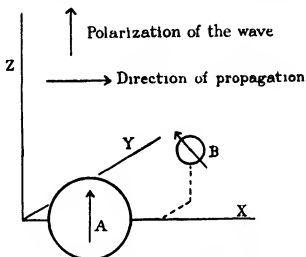
Fig 1 —Direction of oscillation of B, a small ball embedded near a large ball A in an elastic medium

modern electron structure   Replace the ball bearings by atoms containing electrons free to move under the influence of an electric field , replace the elasticity of the gel by the equations of electricity, and the model becomes an asymmetric molecule under the influence of a light wave   Under the action of the electric field of a light wave each atom becomes an oscillating electric doublet   Inside the molecule the electric field of the wave is altered by the fields of the doublets themselves, and, making allowance for this, the exact polarizations of the molecule can be calculated.   When the polarizations in a medium can be expressed in terms of the electrical fields, it is possible to find the velocity of a light wave in this medium by use of Maxwell's equations   Fresnel has shown that an active medium can be regarded as a medium in

which the velocities of circularly polarized waves of opposite sense are different, and the rotation can be calculated from this difference   Hence, having found the expression for the total polarization we can derive the formula for the rotation

The method of evaluating the electric interactions of induced doublets in adjacent atoms has been employed successfully in other phenomena   W L Bragg,* using the atom spacing found by X-rays, has calculated the various refractive indices of calcite and aragonite, and thus explained the strong double refraction of this type of crystal   Ramanathan† has deduced the anisotropy of various simple polyatomic molecules from the interaction of the atomic doublets, and has shown that the results agree with those obtained by the scattering of light

To evaluate the electric interactions of the doublets it is necessary to know the size of these and the exact spacing of the atoms or groups in which they are induced   The size of an atomic doublet is obtained directly from the tables on atomic refractivity, but, while the spacing can be obtained directly for crystals, the shape of the active molecule has to be deduced from other data

It is established now that the valency bonds in a molecule are easily flexible, and, in this calculation, it is assumed that the spacing in the molecule is very dependent on the close-packing of the atoms according to their size , the shape of the asymmetric molecule is taken as that determined by the close-packing of four spheres corresponding to the four different groups of the molecule

The first stage of the calculation is carried out in this paper   A general expression is obtained for the rotatory power of any arrangement of polarizable centres in a molecule   Throughout the whole treatment Heaviside's rational units will be employed   In order to avoid repetition the theory of refraction according to Lorentz will be assumed

The Interactions of Induced Doublets in a Molecule and the Rotation of the Plane of Polarization

The mechanical analogy suggests that the optical rotatory power may be due to the ordinary refractive properties of the atoms in the molecules , the interaction of the induced doublets can be calculated by the laws of electricity and the resultant electromagnetic properties of the whole molecule may be the

* 'Proc Roy Soc ,' A, vol 105, p 370 (1924)
† 'Proc. Roy Soc ,' A, vol 107, p. 684 (1924)

origin of a rotatory power It is necessary to calculate the electromagnetic properties of a fixed arrangement of polarizable particles in the molecule while neglecting all other chemical properties which do not interfere with the calculation. I have found it most convenient to define a hypothetical model and calculate exactly the relation between its dimensions and rotatory power, before examining how far its properties correspond to those of a chemical molecule The generality of this treatment is so great that it shows that a model of conducting spheres joined together with insulating rods might twist the plane of polarization of a Hertzian wave, and that the amount of the twist could be calculated by the final formula

We shall consider a medium with the following properties —

(1) The medium as a whole is perfectly isotropic, since it contains a large number of models distributed entirely at random

(2) In accordance with the Lorentz treatment of refractivity, the field acting on any model is taken as $E + aP$ where E is the electrostatic field of the electromagnetic wave, P the corresponding polarization and a is taken as $\frac{1}{3}$ This is tantamount to assuming that, owing to the random distribution, the medium external to the molecule is isotropic

(3) The model consists of a rigid arrangement of particles which become polarized in an electric field The particles are thus analogous to the refractive atoms in the ordinary molecule

(4) The linear dimensions of the model are small compared with the wavelength of the electromagnetic wave

(5) The polarization of each particle is proportional to, and in the same direction as the applied field when this field has a definite frequency

(6) The particles are sufficiently symmetrical for the electric field of the induced doublet to be evaluated as if the doublet was concentrated at the centre of the particle

(7) The changes in the doublets produced by the fields of local doublets are small compared with the magnitude of the doublet induced directly by the electric field of the electromagnetic wave

When a single plane polarised wave acts on a model, an oscillating electric doublet is induced in each particle and, as one component of this may be out of phase with the inducing wave, we need two vectors to represent this The electric field at a particle consists of the field of the light wave and the oscillating fields of the other doublets in the same model To find the exact induced dipole in any one of a set of n particles it is necessary to solve $6n$ equations in the components of these vectors. Later it is shown that the simplest active

molecule contains more than four atoms and so even for this molecule, there are twenty four equations for solution   A direct solution of these must be abandoned, but there is a method of evaluation which expresses the induced dipole as the sum of a series, every term of which is of the same kind and can be dealt with very simply, as shown in the following analysis

The oscillating fields due to adjacent vibrators are small compared with the field due to the main light wave, and the magnitudes and directions of the vibrations can be obtained by successive approximations   The main field acting on a particle is that of the light wave, and the result is an induced dipole in phase with this   This initial dipole has an appreciable field at the positions of the adjacent atoms   On the initial dipole there are superimposed smaller dipoles due to the fields of initial dipoles of the adjacent atoms   This can be regarded as a second approximation and, passing to a third approximation we must consider the effects of these superimposed dipoles on the other vibrators, and so *ad infinitum*   The essential point is that the resultant dipole of any atom is obtained by the addition, vectorial with regard both to phase and direction, of a number of dipoles, each of which has been relayed by a definite path and has a definite source   Each of these is proportional to the dipole from which it originated and some constant depending on the course of the relays   Thus we can represent the vibration of A as made up of terms [A], [BA], [CA], [DA], [CBA], [ABA], [DCBA], etc , with these terms becoming less as their order increases

· If we resolve the initial dipole at A in three directions, every relay effect is included in the following type   H an induced dipole along the vector α at A causes by means of the relay path [A   B] a proportional induced dipole at B in the direction β Letting AB be represented by γ, we have the whole system of interactions made up from terms of the type $\alpha - \gamma - \beta$ The effect of such a system on the difference in velocity of two oppositely circularly polarized waves can be found, and then this effect summed for all the systems in the molecule until these are of negligible size   It is most convenient to find the effect of this general relay system on the rotatory power before finding the exact value of any of the relay systems in the model

When the model is situated in a variable electric field E with a value E_{A1} at A at a time t, the polarization along α will be proportional to $(\alpha \ E_{A1})$ and the relayed polarization to B can be written $h\beta(\alpha \ E_{A1})$ where h is the constant of the relay system   Let δ be the time lag during transmission   For the construction of the general electromagnetic equations of the medium it is necessary to express the polarization in terms of the electric field at the same point and

the same time   Since the model is small the relation between the field E_{A1} and the field E acting at B after δ seconds is

$$E_{A1} = E - \frac{\partial E}{\partial x} \gamma_x - \frac{\partial E}{\partial y} \gamma_y - \frac{\partial E}{\partial z} \gamma_z$$
$$- \delta E + \delta \frac{\partial E}{\partial x} \gamma_x + \delta \frac{\partial E}{\partial y} \gamma_y + \delta \frac{\partial E}{\partial z} \gamma_z \qquad (1)$$
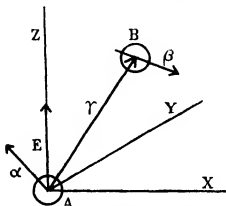
Fig 2 —The relayed polarization

Substituting in the expression for relayed polarization we have the relation between the applied field and the polarization at the same point

The expression may be split into two similar parts dependent on E and $- \delta E$ respectively   Since it will only be found necessary to consider relay terms of a low order, and the wave-length of the wave will thus be long compared with the relay path, the term $- \delta E$ must be very small compared with E The terms dependent on $- \delta E$ will be neglected from this stage because if the analysis were completed it would be found that these have no appreciable influence on the rotatory power

It is necessary to integrate the expression

$$h\beta \, [(\alpha \cdot E) - \left(\alpha \cdot \frac{\partial E}{\partial x} \right) \gamma_x - \left(\alpha \cdot \frac{\partial E}{\partial y} \right) \gamma_y - \left(\alpha \cdot \frac{\partial E}{\partial z} \right) \gamma_z] \qquad (2)$$

where the vectors α, etc , can have any direction so long as the relative configuration of these vectors remains the same   For the integration it is desirable to express the orientation in terms of independent variables, and this is performed by considering the position of the molecule as derived from the initial position $\alpha_1 - \gamma_1 - \beta_1$ by the Eulerian rotations, θ about the Y axis, ϕ about the X axis, and ψ about the new position of γ The rectangular axes X, Y,

and Z, with the corresponding unit vectors **i**, **j**, and **k** are taken in the usual positive sense so that $\mathbf{i} \wedge \mathbf{j} = \mathbf{k}$ The position of any vector after performing the above rotations is obtained by operating with the tensor T whose coefficients are given in the table   The coefficients of the first row multiply the dyads **ii**, **ij**, and **ik**

cos θ	sin ψ sin θ	− cos ψ sin θ
sin φ sin θ	cos ψ cos φ − sin ψ sin φ cos θ	sin ψ cos φ + cos ψ sin φ cos θ
cos φ sin θ	− cos ψ sin φ − sin ψ cos φ cos θ	− sin ψ sin φ + cos ψ cos φ cos θ

$$(3)$$

If $T\alpha_1$, etc , are substituted in expression (2) we have the value of the polarization expressed in invariable vectors and functions of variable angles , and , since the number of molecules within the limits θ to θ + dθ, etc , is

$$(N/8\pi^2)\ \sin\theta\, d\theta\, d\phi\, d\psi,$$

we can find the total value of the expression (2) for N molecules

For simplicity we shall carry out the integration of the various parts of (2) separately, and, taking the first term, we shall evaluate

$$(N/8\pi^2)\int_0^{2\pi} d\psi \int_0^{2\pi} d\phi \int_0^{\pi} AT\boldsymbol{\beta}_1\,(T\alpha_1 \quad E)\ \sin\theta\, d\theta \qquad (4)$$

In the expansions of $T\alpha_1$ and $T\beta_1$ there are terms corresponding to the whole of the array of the tensor   Fortunately most of the coefficients become zero on integrating between the required limits, and we shall only construct the necessary vector terms after evaluating the coefficients   With regard to the integration $\int_0^{2\pi} d\psi$ the expression is of the type

$$(A_1 + B_1 \sin\psi + C_1 \cos\psi)\,(A_2 + B_2 \sin\psi + C_2 \cos\psi),$$

and, after integration between the limits 0 and 2π, the only terms which remain are due to $A_1 A_2$, $B_1 B_2 \sin^2\psi$, and $C_1 C_2 \cos^2\psi$ Only the corresponding terms remain in the integration $\int_0^{2\pi} d\phi$ In the third integration $\int_0^{\pi} \sin\theta\, d\theta$ there is the extra factor sin θ and the terms which do not vanish are $A_1 A_2 \sin\theta$, $(A_1 B_2 + A_2 B_1) \sin^2\theta$, $B_1 B_2 \sin^3\theta$, and $C_1 C_2 \sin\theta\ \cos^2\theta$ By inspection of the product formed by squaring the array, it is seen that the only coefficients satisfying the above conditions are the squares of the original coefficients,

$i \, e$, a_{11}^2, a_{12}^2, etc Direct evaluation of these gives a total polarization of $(N/3) \hbar E (\alpha \quad \beta)$ The actual value of this is unnecessary in the calculation of optical rotation, but it is important that this portion of the polarization is in the same direction as **E** This last result might have been considered obvious from considerations of symmetry

Returning to the second term in the expression (2) we find that it is necessary to evaluate

$$- (N/8\pi^2) \int_0^{2\pi} d\psi \int_0^{2\pi} d\phi \int_0^{\pi} k T \beta_1 \left(T\alpha_1 \frac{\partial E}{\partial x} \right) \gamma_x \sin\theta \, d\theta \qquad (5)$$

By the system of rotations adopted γ_x is equal to $\gamma \cos\theta$ With regard to the scalar coefficients in the expansion, this expression is the same as above, but with the extra factor $\cos\theta$ Proceeding as previously to find the characteristics of the terms which do not disappear on integration, we find that the conditions for ψ and ϕ are as above, but only one term in θ does not vanish $i \, e$, $\cos^2\theta \sin\theta$ These conditions limit the coefficients to $a_{22}a_{23}$, $a_{23}a_{22}$, $a_{22}a_{33}$, and $a_{33}a_{32}$ The portions of these coefficients which do not vanish on integration are

$$a_{22}a_{32} = -\cos^2\psi \sin^2\phi \cos\theta - \sin^2\psi \cos^2\phi \cos\theta$$

$$a_{23}a_{33} = \cos^2\psi \cos^2\phi \cos\theta + \sin^2\psi \sin^2\phi \cos\theta,$$

giving

$$(N/8\pi^2) \int_0^{2\pi} \int_0^{2\pi} \int_0^{\pi} a_{22}a_{32} \cos\theta \sin\theta \, d\theta \, d\phi \, d\psi = -N/6$$

$$(N/8\pi^2) \int_0^{2\pi} \int_0^{2\pi} \int_0^{\pi} a_{23}a_{33} \cos\theta \sin\theta \, d\theta \, d\phi \, d\psi = N/6$$

The value of integral (5) is obtained by constructing the corresponding vectorial terms

$$-\frac{N\hbar}{6} \left[-\mathbf{j}(\mathbf{k} \quad \boldsymbol{\beta}_1)(\mathbf{j} \quad \boldsymbol{\alpha}_1) \left(\mathbf{k} \, \frac{\partial E}{\partial x} \right) \gamma + \mathbf{j}(\mathbf{j} \quad \boldsymbol{\beta}_1)(\mathbf{k} \quad \boldsymbol{\alpha}_1) \left(\mathbf{k} \, \frac{\partial E}{\partial x} \right) \gamma \right.$$

$$\left. - \mathbf{k}(\mathbf{j} \quad \boldsymbol{\beta}_1)(\mathbf{k} \quad \boldsymbol{\alpha}_1) \left(\mathbf{j} \, \frac{\partial E}{\partial x} \right) \gamma + \mathbf{k}(\mathbf{k} \quad \boldsymbol{\beta}_1)(\mathbf{j} \quad \boldsymbol{\alpha}_1) \left(\mathbf{j} \, \frac{\partial E}{\partial x} \right) \gamma \right]$$

$$= + \frac{N\hbar}{6} \left[\mathbf{k} \left(\mathbf{j} \, \frac{\partial E}{\partial x} \right) - \mathbf{j} \left(\mathbf{k} \, \frac{\partial E}{\partial x} \right) \right] [(\mathbf{j} \quad \boldsymbol{\beta}_1)(\mathbf{k} \quad \boldsymbol{\alpha}_1) - (\mathbf{j} \quad \boldsymbol{\alpha}_1)(\mathbf{k} \quad \boldsymbol{\beta}_1)] \gamma \quad (6)$$

The last factor becomes

$$\gamma (\mathbf{k}_\wedge \mathbf{j} \quad \boldsymbol{\alpha}_1 \wedge \boldsymbol{\beta}_1) = -\gamma (\mathbf{i} \quad \boldsymbol{\alpha}_1 \wedge \boldsymbol{\beta}_1) = [\alpha_1 \gamma_1 \beta_1] = [\alpha \gamma \beta]$$

If the integrals corresponding to the other terms of expression (2) are calculated the only change is in the first bracket of the above expression, and these

factors together constitute curl **E**   Thus the total polarization due to N molecules containing the system of interactions α — γ — β is

$$NE (\alpha \quad \beta) (h/3) + N \text{ curl } E [\alpha\gamma\beta] (h/6) \qquad (7)$$

To obtain the total polarization of the medium this must be summed for all systems in all the molecules present, though it must be noted that many systems, while giving a value for the first term, will give a zero value for the triple scalar product in the second term

Drude[*] was aware that, when a term proportional to curl **E** occurs in the expression for the average polarization of a molecule under the influence of an electromagnetic wave the medium containing this type of molecule will rotate the plane of polarization of the wave   He suggested that the electrons might be forced to vibrate in spiral paths, and after showing that this introduced a term of the type curl **E**, he calculated the resulting rotatory power However, there is not any other evidence of such a spiral path, and since the ordinary interactions of the doublets induced in the polarizable centres give a term of this type there is no necessity for the hypothesis of spiral movements

For complete specification of the electrical properties, we require, in addition to the above relation, a knowledge of any magnetic induction due to the fields of the wave   In the ordinary refractivity treatment it is assumed that for the frequency of light waves the magnetic susceptibility is zero, and the molecule has no magnetic polarization   However, in this case there is a suggestion of a circular current in some of the polarizations of the molecule , this is especially apparent in the spiral motions which were introduced by Drude as a mathematical artifice, but which correspond mathematically to the present treatment   The possibility of a magnetic polarization has been frequently ignored in early examinations of this type, but recently it has been generally accepted   Gans[†] criticizing the analysis carried out by Born, has indicated the necessity for this, and the derivation of the value has been put in very clear form by Försterling [‡] I had hoped to derive this magnetic moment directly from the spatial distribution of the oscillating polarizations in the molecule, but, though this method gives the same value, it is doubtful whether the method is absolutely rigorous   Hence, all justification for the use of this movement is based on the treatment as given by Försterling   When

* "Theory of Optics," p 401 (1902)
† ' Ann Physik.,' vol 79, p 547 (1926)
‡ " Lehrbuch der Optik," Leipzig (1928), p 188

the energy of the wave is considered, it is shown that a term f curl E in the electric polarization can only exist at the same time as a varying magnetic moment of value (f/c) E

Taking N as the Avogadro number and q as the concentration in gram-molecules per cubic centimetre we can write the electrostatic polarization P and the magnetic polarization M per cubic centimetre for any electromagnetic disturbance

$$P = Nq \{ E\Sigma\lambda (\alpha \quad \beta)/3 + \text{curl } E \Sigma h \lfloor\alpha\gamma\beta\rfloor/6 \} \atop M = Nq \{ E\Sigma\lambda \lfloor\alpha\gamma\beta\rfloor/6c\} \} \tag{8}$$

The medium is perfectly isotropic and the only double refraction which can occur is a difference in the velocities of the two circularly polarized waves We shall first find the refractive index of the medium for the circularly polarized wave

$$E_1 = kE_0 \cos \left(2\pi nt - \frac{2\pi x}{\lambda_1} \right) - jE_0 \sin \left(2\pi nt - \frac{2\pi x}{\lambda_1} \right) \tag{9}$$

We have the polarizations expressed as dependent on the applied field, but according to the Lorentz treatment the applied field is equal to $E_1 + aP$, where E_1 is the field of the wave We can evaluate P exactly for this particular wave, since curl $E_1 = 2\pi E_1/\lambda_1$ and since P is in phase with this we have curl $E = 2\pi (E_1 + aP)/\lambda_1$ Substituting in equation (8) we obtain

$$E = E_1/\{1 - aNq \Sigma(h (\alpha \quad \beta)/3 + 2\pi h \lfloor\alpha\gamma\beta\rfloor/6\lambda_1)\} \tag{10}$$

To simplify write

$$\varepsilon = Nq\Sigma h (\alpha \quad \beta)/3 \atop \rho = Nq\Sigma h \lfloor\alpha\gamma\beta\rfloor/6 \atop \phi - 1 = aNq \Sigma(h (\alpha \quad \beta)/3 + 2\pi h \lfloor\alpha\gamma\beta\rfloor/6\lambda_1) \} \tag{11}$$

Substituting for curl E_1 by the second law of Maxwell curl $E_1 = -B/c$, equations (8) become

$$P = (\varepsilon E_1 - \rho B/c)/\phi \atop M = \rho E_1/c\phi \} \tag{12}$$

Writing Maxwell's equations in the modified form for an isotropic medium we have the following equations to complete the solution, where D is the electrostatic displacement, B the magnetic induction and s is unit vector in the direction of propagation

$$D = E_1 + P \qquad B = H + M \atop B = \mu s_\wedge E_1 \qquad D = -\mu s_\wedge H \} \tag{13}$$

μ is the refractive index and we can relate this to the electrical properties of the medium.

$$\mu s_\wedge [\mu s_\wedge E_1] = \mu s_\wedge B \left.\begin{array}{l} \\ = \mu s_\wedge H + \mu s_\wedge M \\ - D + (\rho/c\phi)\, \mu s_\wedge E_1 \\ - E_1(1 + \varepsilon/\phi) + 2\,(\rho/c\phi)\,\mu s_\wedge E_1 \end{array}\right\}, \qquad (14)$$

but

$$\mu s_\wedge [\mu s_\wedge E_1] = \mu^2 s(s \quad E_1) - \mu^2 E_1 = - \mu^2 E_1$$

Hence

$$E_1(\mu^2 - 1 - \varepsilon/\phi) = - 2\,(\rho/c\phi)\,\mu s_\wedge E_1 \qquad (15)$$

Applying the relations solely to the circularly polarized wave represented in equation (9), whose field is E_1 and whose particular refractive index is μ_1 we have,

$$s \wedge E_1 = - 2\pi n E_1$$

$$(\mu_1^2 - 1 - \varepsilon/\phi) = 4\pi\mu_1\rho/\phi\lambda,$$

λ is the wave length of the light *in vacuo*

$$(\mu_1^2 - 1) = (\varepsilon + 4\pi\mu_1\rho/\lambda)/[1 - a\,(\varepsilon + 2\pi\mu_1\rho/\lambda)] \left.\begin{array}{l} \\ \dfrac{\mu_1^2 - 1}{a\,(\mu_1^2 - 1) + 1} \quad \varepsilon + \dfrac{2\pi\mu_1\rho}{\lambda} + \dfrac{2\pi\mu_1\rho}{\lambda} \dfrac{1}{a\,(\mu_1^2 - 1) + 1} \end{array}\right\} \qquad (16)$$

This gives μ_1 the refractive index of the light corresponding to equation (9) but if the opposite kind of circularly polarized light is considered we obtain

$$\frac{\mu_2^2 - 1}{a\,(\mu_2^2 - 1) + 1} = \varepsilon - \frac{2\pi\mu_2\rho}{\lambda} - \frac{2\pi\mu_2\rho}{\lambda} \frac{1}{a\,(\mu_2^2 - 1) + 1}$$

From these two equations we can obtain the value of $(\mu_1^2 - \mu_2^2)$ by subtraction

$$\frac{\mu_1^2 - \mu_2^2}{[a\,(\mu_1^2 - 1) + 1][a\,(\mu_2^2 - 1) + 1]}$$

$$\frac{2\pi\rho}{\lambda} \left(\mu_1 + \mu_2 + \frac{(\mu_1 + \mu_2)\,[a\,(\mu_1\mu_2 - 1) + 1]}{[a\,(\mu_1^2 - 1) + 1][a\,(\mu_2^2 - 1) + 1]} \right)$$

The only term involving a difference of μ_1 and μ_2 is $\mu_1^2 - \mu_2^2$ and, since the

difference in these refractive indices is very small, a mean value will be taken throughout the rest of the expression

$$\mu_1 - \mu_2 = \frac{2\pi N g \Sigma h [\alpha\gamma\beta]}{6\lambda} [1 + a (\mu^2 - 1)][2 + a (\mu^2 - 1)] \quad (17)$$

The circularly polarized waves to which μ_1 and μ_2 apply respectively are given by the equations

$$\left.\begin{array}{l} \mathbf{E}_1 = \mathbf{k}E_0 \cos\left(2\pi nt - \dfrac{2\pi x}{\lambda_1}\right) - \mathbf{j}E_0 \sin\left(2\pi nt - \dfrac{2\pi x}{\lambda_1}\right) \\[3mm] \mathbf{E}_2 = \mathbf{k}E_0 \cos\left(2\pi nt - \dfrac{2\pi x}{\lambda_2}\right) + \mathbf{j}E_0 \sin\left(2\pi nt - \dfrac{2\pi x}{\lambda_2}\right) \end{array}\right\} \quad (18)$$

Combining these two equations we obtain a plane polarized wave whose plane of polarization will rotate if λ_1 and λ_2 are unequal

$$\mathbf{E}_1 + \mathbf{E}_2 = 2\left\{\mathbf{k}E_0 \cos \pi x\left(\frac{1}{\lambda_1} - \frac{1}{\lambda_2}\right) + \mathbf{j}E_0 \sin \pi x\left(\frac{1}{\lambda_1} - \frac{1}{\lambda_2}\right)\right\}$$
$$\times \left[\cos\left(2\pi nt - \pi x\left(\frac{1}{\lambda_1} + \frac{1}{\lambda_2}\right)\right)\right] \quad (19)$$

Thus the vector determining the plane of polarization rotates on passing along the X axis When $x = 0$ the wave is polarized along the Z axis, but as x becomes larger the plane of polarization turns towards the Y axis, i e, in a counter-clockwise direction when looking along the X axis, but in a clockwise direction when looking back along the X axis to receive the light From the point of view of the observer the plane of polarization rotates $(1/\lambda_1 - 1/\lambda_2)$ radians in a dextro or clockwise direction, and by equation (17)

$$\theta = \pi l \left(\frac{1}{\lambda_1} - \frac{1}{\lambda_2}\right) = \frac{\pi l}{\lambda} (\mu_1 - \mu_2)$$
$$= \frac{[a (\mu^2 - 1) + 1][a (\mu^2 - 1) + 2] \pi^2 N g l \Sigma h [\alpha\gamma\beta]}{3\lambda^2} \quad (20)$$

This is the rotation due to one compound of which there are Ng molecules per cubic centimetre when the light passes through l cm of the medium of refractive index μ

This method of solution for the different refractive indices tends to be very formal, and it is advisable to consider the actual mechanism by which the difference arises Considering the first wave (9) referred to above, we can resolve this into two plane waves travelling along the X axis When the electrostatic field of the first is a maximum up the Z axis at the origin, the other

plane wave is a maximum at $x = \lambda/4$ but acting along the Y axis. When part of the polarization of the molecule is dependent on curl E, not only does the Z wave cause a polarization up the Z axis, but it also causes a polarization a quarter of a period ahead and acting along the Y axis If this extra polarization is positive, the polarizations in phase with each component of the circularly polarized wave are increased In the circularly polarized wave of opposite sense the advance portion may be regarded as acting along $-Y$ Thus, while in one case the waves mutually reinforce each other by virtue of the curl E term, in the other they tend to annul each other This causes a difference in effective dielectric constant and, neglecting magnetic effects, this gives an optical rotation When the magnetic moment is taken into account the rotation is approximately doubled instead of the factor $[a(\mu^2 - 1) + 1]^2$, which would be obtained if there were no magnetic effects, we have obtained the factor $[a(\mu^2 - 1) + 1][a(\mu^2 - 1) + 2]$

The factor $[a(\mu^2 - 1) + 1][a(\mu^2 - 1) + 2]$ has been retained until the present stage to illustrate the generality of the treatment and, though in future this will be written $(\mu^2 + 2)(\mu^2 + 5)/9$ in accordance with the Lorentz theory, it would be quite possible to replace it by the appropriate factor in accordance with another theory of refractivity, such as that of Gladstone and Dale

It may be noted that, even in entire absence of any chemical interaction, the rotation depends on the medium by means of the factor $(\mu^2 + 2)(\mu^2 + 5)$ In a mixture of two optically active substances the rotation will not obey a simple mixture law even if in every other respect the mixture is purely a physical one The ordinary method of calculating the specific rotatory power, taking this as a property of the substance, tacitly assumes a simple mixture law and, though in the following analysis the value of the specific rotatory power is expressed, it must be recalled that this is only a constant for the compound under the special conditions of measurement The specific rotation of a compound of which Mg gm per cubic centimetre give a rotation of θ radians in a column of length l cm is

$$[\alpha] = \frac{1800 \; \theta}{\pi g M l},$$

where M is the molecular weight

The specific rotatory power of a compound in a medium of refractive index μ is obtained from (20)

$$[\alpha] = \frac{(\mu^2 + 2)(\mu^2 + 5) \, 1800 \pi N}{27 M \lambda^3} \, \Sigma \, h[\alpha \gamma \beta], \tag{21}$$

where the summation Σ is carried out for every system $\alpha - \gamma - \beta$ within the molecule

We have assumed that the exact magnitude of the doublets can be expressed in a converging series, and since these terms rapidly become more complex it will be very convenient if we can approximate at any stage by neglecting all higher terms This is a definite approximation, but there is reasonable evidence in favour of this in the general optical properties of compounds the fact that molecular refractivities can be calculated so accurately from atomic refractivities suggests that interactions between the doublets are small compared with direct polarizations, and the smallness of double refraction in crystals, compared with the mean refraction, indicates the relayed effects to be small compared with the primary polarizations It will be shown presently that the optical activity is dependent on polarizations thrice relayed, and since the usual magnitude of optical rotations corresponds to a difference in the refractive indices of opposite circularly polarized waves of about 10^{-6} it is apparent that the process of relaying decreases the magnitude of the polarizations considerably Hence, when it is proved that a three relay system is responsible for an optical rotation, all higher relay terms will be neglected

It is necessary to know the exact size of the electric doublet induced in any vibrator by a known electric field In applying the formula to molecules these data can be obtained from the tables tabulated either by Bruhl or by Eisenlohr Lorentz proved that, for a gram-molecule of a compound of refractive index μ and density d the total polarization per unit applied field is $3M (\mu^2 - 1)/(\mu^2 + 2) d$, and it has been shown experimentally that each element makes a definite contribution, so that atomic polarizations can be found The function tabulated, i e, $A (\mu^2 - 1)/(\mu^2 + 2) d$, where A is the atomic weight, represents one-third of the absolute atomic polarizability and is called the atomic refractivity The moment induced in any chemical group is thus $ER (3/N)$ where R is the sum of the atomic refractivities of the constituents of the group The polarizability of the particle will be taken in this form for convenience in the application to chemical molecules

In each particle of the model there is an oscillating dipole, and, since the wave-length of the electromagnetic wave is long compared with the distances at which the field acts on the other particles of the model, and since the dipole is considered as concentrated in a very small volume, the field is expressed by $[1/4 \pi r^3] [3r (r D) - D r^2]$ This is the simple electrostatic field at the

end of the vector r from a point dipole D   At A the initial dipole is $\mathbf{E}\,(3\mathbf{R}_A/N)$, and the field of this at B will cause a secondary dipole of value

$$\frac{9\mathbf{R}_A\mathbf{R}_B}{4\pi N^2 AB^5}\,[3AB\,(AB\quad E) - EAB^2]$$

The first term of this represents a relayed effect which is proportional to the component of the field acting along AB at A and transmits a polarization along AB to B giving a polarization which also acts along AB   Thus using the general notation for a relayed effect we have $\alpha = \gamma = \beta = AB$, but since the effect on the optical activity is given by $[\alpha\gamma\beta]$ it is apparent that the interactions responsible for a rotation must be much more complex than this

The polarization [ABC] relayed to C is

$$\frac{27\mathbf{R}_A\mathbf{R}_B\mathbf{R}_C}{(4\pi)^2 N^3 AB^5 BC^5}\,[9BC\,(BC\quad AB)(AB\quad E) - 3AB\,(AB\quad E)\,BC - 3BC\,(BC\quad E)\,AB^2 + EBC^2\quad AB^2]$$

The polarization [ABCD] relayed to D is

$$\frac{81\mathbf{R}_A\mathbf{R}_B\mathbf{R}_C\mathbf{R}}{(4\pi)^3 N^4 AB^5 BC^5 CD^5}\,[27CD\,(CD\quad BC)(BC\quad AB)(AB\quad E)$$
$$- 9BC\,(BC\quad AB)(AB\quad E)\,CD^2$$
$$- 9CD\,(CD\quad AB)(AB\quad E)\,BC^2 + 3AB\,(AB\quad E)\,CD^2 BC^2$$
$$- 9CD\,(CD\quad BC)(BC\quad E)\,AB^2 + 3BC\,(BC\quad E)\,CD^2 AB^2$$
$$+ 3CD\,(CD\quad E)\,BC^2 AB^2 - ECD^2\quad BC^2\quad AB^2] \qquad (22)$$

As might have been predicted from considerations of symmetry the relay effect involving the interactions of the four particles A, B, C, and D is the simplest effect to give a contribution to the rotatory power   Examining (22) we find that the 1st, 2nd, 3rd, and 5th terms give a definite value for $[\alpha\gamma\beta]$, e.g , in the 1st term $AB = \alpha$, $CD = \beta$, $AD = \gamma$,   and

$$h = \frac{81\mathbf{R}_A\mathbf{R}\;\mathbf{R}\;\mathbf{R}_D}{(4\pi)^3 N^4\,AB^5\;BC^5\;CD^5}\,(CD\quad BC)(BC\quad AB)$$

A polarization $h\beta\,(\alpha\quad E)$ relayed along γ makes a contribution to the rotatory which is given by (21)   The total rotatory power due to the relay path [ABCD] is

$$\frac{1800\pi\,(\mu^2 + 2)\,(\mu^2 + 5)}{27\lambda^2\,MN^2}\frac{81\mathbf{R}_A\mathbf{R}_B\mathbf{R}_C\mathbf{R}_D}{(4\pi)^3\,N^4\,AB^5\;BC^5\;CD^5}\,[27\,[AB\;AD\;CD]\,(CD\quad BC)\,(BC\quad AB)$$
$$- 9\,[AB\;AD\;BC]\,(BC\quad AB)\,CD^2 - 9\,[AB\;AD\;CD]\,(CD\quad AB)\,BC^2$$
$$- 9\,[BC\;AD\;CD]\,(CD\quad BC)\,AB^2] \qquad (23)$$

All the triple scalar products are equal to $\pm 6V$ where V is the volume of the tetrahedron ABCD and if we take $[AB\ AD\ CD] = +6V$ then

$$[AB\ AD\ BC] = [BC\ AD\ CD] = -6V$$

The scalar products can easily be expressed in terms of the edges of the tetrahedron, e g,

$$(CD\quad BC) = -CD\quad BC \cos BCD = -(BC^2 + CD^2 - BD^2)/2$$

We can express the contribution of $[ABCD]$ to the rotatory power completely in scalar quantities by these substitutions

$$\frac{1800\pi\,(\mu^2+2)\,(\mu^2+5)\,81R_AR_BR_CR_D}{27\lambda^2MN^2\,(4\pi)^3\,AB^5\quad BC^5\quad CD^5}$$

$$\times \frac{27V}{2}\,[3\,(CD^2+BC^2-BD^2)\,(AB^2+BC^2-AC^2)$$

$$-\,2BC^2\,(AD^2+BC^2-AC^2-BD^2)-2CD^2\,(AB^2+BC^2-AC^2)$$

$$-\,2AB^2\,(BC^2+CD^2-BD^2)]\quad(24)$$

We shall only consider relayed effects of this type $i\,e$, $[ABCD]$, as the paths $[ABCA]$, etc, have no rotatory power and the higher terms such as $[ABCDE]$ are assumed to be small compared with the terms of three relays Hence for the total rotatory power of the model it is only necessary to consider all the combinations of four particles in the model and take all the relay paths within each set by considering all the permutations of these four

We shall examine the rotatory power due to the interaction within the four particles A, B, C, and D The rotatory contribution of any other path can be derived from the expression for $[ABCD]$ by the obvious interchange of the letters, but the substitution must also be carried out in the triple scalar product represented by 6V the value of this is perfectly constant, but the sign is changed The triple scalar product for any path is found to have a value $(-1)^n\,6V$ where n is the number of inversions in the order of ABCD in the relay path

The numerical value of V actually depends upon which "enantiomorph" is being considered and V will be considered as positive, thus making the whole analysis apply to a tetrahedral arrangement of the configuration shown in fig 3 It can be noted that the configuration is defined by stating that when looking at the other particles from A these appear in a clockwise order in the order BCD

The rule of signs for V is very suggestive of a simple method of expressing the sum of all these terms, since exactly the same rule of signs occurs in the expansion of a determinant. It appears as if there are twenty-four permutations to be considered, but owing to the symmetry of the expression, pairs of paths such as [ABCD] and [DCBA] give the same expression and there are only twelve different terms. Taking $\Sigma \pm$ to mean the sum of all the terms
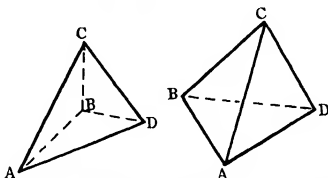
Fig 3—Tetrahedra of the configuration which gives [AB AD CD] a positive value

with the signs chosen correctly we will omit the constants and consider only the following factor of the expression (24),

$$\Sigma \pm \frac{1}{AB^5 BC^5 CD^5} [BC^4 - 2AD^2 \; BC^2 + BC^2 (AB^2 + CD^2 - AC^2 - BD^2)$$

$$+ 2AC^2 \; BD^2 - 2AB^2 CD^2 + (AB^2 \; CD^2 + AC^2 \; BD^2 - AC^2 \; CD^2 - AB^2 \; BD^2)]$$

$$= R^{-5} \Sigma \pm CA^5 \; AD^5 \; DB^5 \; (BC^4 - 2AD^2 \; BC^2 \qquad\qquad), \qquad (25)$$

where

$$R^5 = AB^5 \; CD^5 \; AC^5 \; BD^5 \; AD^5 \; BC^5$$

Writing out the terms for some of the paths for $\Sigma \pm CA^5 \; AD^5 \; DB^5 \; BC^4$, the first term in the above expression,

$$[A\;B\;C\;D] + [D\;C\;B\;A] = 2CA^5 \; DB^5 \; AD^5 \; BC^4$$

$$[A\;C\;B\;D] + [D\;B\;C\;A] = -\,2BA^5 \; DC^5 \; AD^5 \; BC^4$$

$$[B\;A\;D\;C] + [C\;D\;A\;B] = 2CA^5 \; DB^5 \; BC^5 \; AD^4$$

$$[B\;D\;A\;C] + [C\;A\;D\;B] = -\,2BA^5 \; DC^5 \; BC^5 \; AD^4$$

By addition we get $2(AD^5 \; BC^4 + BC^5 \; AD^4)(AC^5. BD^5 - AB^5. CD^5)$

which is a minor of the following determinant, which is found to express all the terms of $\Sigma \pm CA^5 \; AD^5 \; DB^5 \; BC^4$

$$
\begin{vmatrix}
2 & 2 & 2 \\
(AB^5 \; CD^4 + AB^4 \; CD^5) & (AD^5 \; BC^4 + AD^4 \; BC^5) & (AC^5 \; BD^4 + AC^4 \; BD^5) \\
AB^5 \; CD^5 & AD^5 \; BC^5 & AC^5 \; BD^5
\end{vmatrix}
$$

In future only the first columns of the determinants will be given as the succeeding columns can easily be constructed from these. Each of the other terms can be put into a corresponding determinant and the specific rotation due to the four particles A, B, C, and D is given by

$$[\alpha] = \frac{72900 \, (\mu^2 + 2) \, (\mu^2 + 5) \, R_A R_B R_C R_D \, I}{32 \, \pi^2 \, \lambda^2 \, MN^3}, \tag{26}$$

where

$$
\begin{aligned}
I = \frac{V}{R^3} \Bigg\{ &
\begin{vmatrix} 1 \\ AB^5 \; CD^4 + AB^4 \; CD^5 \\ AB^5 \; CD^5 \end{vmatrix}
- 2 \begin{vmatrix} 1 \\ AB^7 \; CD^2 + AB^2 \; CD^7 \\ AB^5 \; CD^5 \end{vmatrix} \\[2ex]
& + \begin{vmatrix} AB^2 + CD^2 \\ AB^5 \; CD^2 + AB^2 \; CD^5 \\ AB^5 \; CD^5 \end{vmatrix}
- \begin{vmatrix} 1 \\ AB^5 \; CD^3 + AB^3 \; CD^5 \\ AB^5 \; CD^5(AB^2 + CD^2) \end{vmatrix} \\[2ex]
& + 2 \begin{vmatrix} 1 \\ AB^5 + CD^5 \\ AB^7 \; CD^7 \end{vmatrix}
- 2 \begin{vmatrix} AB^2 \; CD^2 \\ AB^5 + CD^5 \\ AB^5 \; CD^5 \end{vmatrix} \\[2ex]
& + \begin{vmatrix} 1 \\ AB^5(AD^2 \; BC^2 + AC^2 \; BD^2 - AC^2 \; CB^2 - AD^2 \; DB^2) \\ + CD^5(AD^2 \; BC^2 + AC^2 \; BD^2 - AC^2 \; AD^2 - CB^2 \; BD^2) \\ AB^5 \; CD^5 \end{vmatrix} \Bigg\}
\end{aligned}
\tag{27}
$$

The interactions of the four particles A, B, C, and D cause a rotatory power of $[\alpha]$ and, if there are more than four particles in the model, the total rotatory power is obtained by summing all the contributions from all the combinations of four particles in a single model.

If there is a plane of symmetry in the tetrahedron ABCD, or for more than four particles if the model is symmetrical as a whole, it is apparent that the

rotatory power is zero   Regarding a molecule as an atomic model we see that the same conditions seem to apply to natural rotatory power, active molecules are always dissymmetric from a chemical point of view, and it is obvious that the difference in the sizes of the various atoms will make the spatial arrangement dissymmetric

In a liquid we have an almost random distribution of molecules, each of which consists of a definite structure of atoms   The ordinary refractivity data show the various parts of the molecule to be polarized by the electric field of a light wave, and, if we use, as an illuminant, light of a wave-length considerably longer than X rays, whose wave-length is comparable with atomic dimensions, we have a molecular system fulfilling the properties of the hypothetical model used above   The conditions 5 7 were approximations made for the sake of simplicity in the mathematical treatment, but these will hold fairly accurately for a molecular system   Formula (26) gives the rotatory power of a chemical compound in terms of the atomic refractivities and the internal dimensions of the molecule

A definite approximation has been made when the particles are considered as isotropic, and it is of special interest to examine this more closely since Kuhn* attributes the rotatory power to the anisotropy of radicals in the molecule   In the present calculation it is not at all essential for the particles to be isotropic in order that the molecule be optically active, but our knowledge of anisotropy is very vague, and so this is a very convenient approximation If we are to connect optical rotatory power with known data, we shall have to neglect this variation in refractivity with direction   In many simple molecules which are optically active there is no evidence of anisotropy, and since the anisotropy is not necessary for the existence of optical activity it can be classed as a secondary effect   Hence it is probable that even in more complex compounds the rotatory power will be given fairly accurately by considering only the average refractive properties

By formula (26), the rotatory power of any molecule could be calculated In a straightforward application of the formula to a given compound, each atom could be taken as a refractive centre   The distances AB, etc, would be the distances between the centres of pairs of atoms   Formula (26) gives the contribution of a combination of four atoms to the total rotatory power, and all the contributions (i e, from every possible combination of four atoms) would have to be summed   Unfortunately the complexity of the formula makes such a procedure impossible, even if the calculation were practicable,

* 'Trans. Faraday Soc.,' vol 22, p. 457 (1930)

there is no direct way of measuring all the interatomic distances   The formula is only fit for a practical use if it can be applied to a particular type of atomic structure so that (a) it becomes much simpler in form, and (b) the distances AB can be easily expressed in terms of some atomic property which is already known

The paper following this contains the account of the application of the formula to the simplest type of optically active molecule

At the present stage we have established that the magnitude of the optical rotation as well as its sense is completely determined by the arrangement of refractive centres in the molecule   The optical rotatory power is expressed in a precise formula which must be applied to the various structural types of optically active compounds in order to obtain for them a practical theoretical formula

---

Optical Rotatory Power   II.—The Calculation of the Rotatory Power of a Molecule containing Four Refractive Radicals at the Corners of an Irregular Tetrahedron

By S F Boys, A R C S, B Sc, Beit Scientific Research Fellow, Imperial College of Science and Technology, London

It has been shown in the previous paper that, where there are four refractive centres arranged dissymmetrically in a molecule, there is a definite rotatory power depending on the dimensions of the molecule   In the simple active molecule of four different radicals we seem to have been provided directly with four different refractive centres   It is, however, necessary to examine if a chemical radical fulfils all the properties which were assigned to the hypothetical particle in the general calculation ; but, if this is true, we can substitute dimensions of such a molecule in the general formula to derive a simpler formula for the rotation

If the radical is to have the same properties as the polarizable particle, it will have a definite refractivity for a fixed wave-length and its electric field in the polarized state must approximate to that of a dipole of equal value situated at its centre   A chemical radical has a definite refractivity for a given frequency, but it is only if the radical is small and fairly compact that its

field in the polarized state may be taken as that of a dipole concentrated at a single point Consequently this paper will be limited to the calculation for molecules containing radicals of only a few atoms in length The refractive properties will be regarded as concentrated at the geometric centre of these small radicals

When different radicals are attached to a common atom, the Thorpe-Ingold theory postulates that the positions of the radicals are largely controlled by their respective volumes This conception of atomic close-packing within the molecule has been found necessary to explain the physico-chemical properties of many compounds , and more recently it has been directly confirmed by the X-ray diffraction and electron diffraction experiments of Debye and Wierl[*] respectively and their collaborators , these investigators have measured the dimensions of the molecules CCl_4, $CHCl_3$, and CH_2Cl_2 in the vapour state, and have shown the configuration to be determined by the sizes of the Cl and H atoms It appears that radicals linked to the same central atom are drawn into contact and that the valencies have little or no directing effect This is very convenient for the calculation of the shape of the tetrahedron of centres when four different radicals are present since the radicals are small we can regard each as having a sphere of repulsion and the distance between any two centres will be the sum of the radii, $i e$, $AB = (a + b)$, etc

We shall proceed to calculate the rotatory power of four refractive centres of value R_A, R_B, R_C, and R_D situated at the apices of a tetrahedron whose edges have the lengths $(a + b)$, $(b + c)$, etc This rotatory power is equal to that of an asymmetric molecule containing four different radicals which are fairly short in length and have the values a, b, c, and d for their radii of repulsion

The substitution $AB = (a + b)$, etc , in the determinants expresses the rotatory power completely in terms of the properties of the individual radicals It is apparent that the expression must contain the differences $(a - b)$, etc., as factors, and probably the remaining factor will be a symmetrical function of almost constant value It is convenient to resolve the determinants into alternants of the following type —

$$\begin{vmatrix} x \\ y \\ z \end{vmatrix} = \begin{vmatrix} L_1{}^x & L_2{}^x & L_3{}^x \\ L_1{}^y & L_2{}^y & L_3{}^y \\ L_1{}^z & L_2{}^z & L_3{}^z \end{vmatrix} \qquad \begin{aligned} \text{where } & L_1 = AB \quad CD \\ & L_2 = BC \quad AD \\ & L_3 = AC \quad BD. \end{aligned}$$

The advantage of this process is that every alternant can be resolved into the

product of a symmetrical function and the simplest alternant, and this last factor is equal to the difference product

$$\begin{vmatrix} 0 \\ 1 \\ 2 \end{vmatrix} = (L_1 - L_2)(L_2 - L_3)(L_3 - L_1)$$
$$= -(a - b)(a - c)(a - d)$$
$$\times (b - c)(b - d)$$
$$\times (c - d) = -W \qquad (28)$$

The tetrahedron which is being considered is of a special class, since

$$AB + CD = BC + AD = AC + BD = a + b + c + d = K,$$

and this relation enables the determinants of (27) to be resolved into alternants in a fairly straightforward manner. The general method is to separate the determinant so that symmetrical functions can be removed from a whole row leaving each element in terms of L_1, L_2, and L_3. The resolution of the first and second determinants is carried out as follows :—

$$\text{(I)} \quad \begin{vmatrix} 1 \\ AB^5 \quad CD^4 + AB^4 \quad CD^5 \\ AB^5 \quad CD^5 \end{vmatrix} = \begin{vmatrix} 1 \\ L_1^4(AB + CD) \\ L_1^5 \end{vmatrix} = K \begin{vmatrix} 0 \\ 4 \\ 5 \end{vmatrix}$$

$$\text{(II)} \quad -2 \begin{vmatrix} 1 \\ L_1^2(AB^3 + CD^3) \\ L_1^5 \end{vmatrix} = -2 \begin{vmatrix} 1 \\ L_1^2(K^3 - 5K^2L_1 + 5KL_1) \\ L_1^5 \end{vmatrix}$$

$$= -2K^3 \begin{vmatrix} 0 \\ 2 \\ 5 \end{vmatrix} + 10K^2 \begin{vmatrix} 0 \\ 3 \\ 5 \end{vmatrix} - 10K \begin{vmatrix} 0 \\ 4 \\ 5 \end{vmatrix} \qquad (29)$$

The resolution of the other determinants follows a similar course, though the last determinant is rather more complicated. It is necessary to use the following symmetrical functions :—

$$\left.\begin{array}{ll} p = \Sigma\, a, & K = AB + CD \\ q = \Sigma\, ab, & P = \Sigma\, L_1 \\ r = \Sigma\, abc, & Q = \Sigma\, L_1 L_2 \\ s = abcd, & R = L_1 L_2 L_3 \end{array}\right\} \qquad (30)$$

These are related and we have

$$K = p, \qquad\qquad\qquad P = 2q$$
$$Q = q^2 + pr - 4s, \qquad R = pqr - r^2 - ps \qquad \left.\right\} \quad (31)$$

After complete resolution I is given by

$$I = 2KVR^{-5} \left\{ \quad -12 \begin{vmatrix} 0 \\ 4 \\ 5 \end{vmatrix} + (10K^2 + 5P) \begin{vmatrix} 0 \\ 3 \\ 5 \end{vmatrix} \right.$$

$$+ (2K^2P - 16Q + 2P^2 + 8s) \begin{vmatrix} 0 \\ 2 \\ 5 \end{vmatrix}$$

$$+ (10K^2Q - 6K^2P^2 + 5PQ - 5R - 24K^4s) \begin{vmatrix} 0 \\ 1 \\ 5 \end{vmatrix}$$

$$\left. + 3R \begin{vmatrix} 0 \\ 2 \\ 4 \end{vmatrix} + (3PR - 12K^2R) \begin{vmatrix} 0 \\ 1 \\ 4 \end{vmatrix} \right\} \qquad (32)$$

All alternants can be resolved into a product of the lowest alternant and a symmetrical function of the same variables   Thus by the ordinary methods of manipulation of determinants we have the following identities —

$$\begin{vmatrix} 0 \\ 1 \\ 4 \end{vmatrix} = (P^2 - Q)(-W), \qquad\qquad \begin{vmatrix} 0 \\ 2 \\ 4 \end{vmatrix} = (PQ - R)(-W),$$

$$\begin{vmatrix} 0 \\ 1 \\ 5 \end{vmatrix} = (P^3 - 2PQ + R)(-W), \qquad \begin{vmatrix} 0 \\ 2 \\ 5 \end{vmatrix} = (P^2Q - Q^2 - PR)(-W),$$

$$\begin{vmatrix} 0 \\ 3 \\ 5 \end{vmatrix} = (PQ^2 - QR - P^2R)(-W), \qquad \begin{vmatrix} 0 \\ 4 \\ 5 \end{vmatrix} = (Q^3 - 2PQR + R^2)(-W)$$

$$(33)$$

Substituting these in (21)

$$I = 2KWVR^{-5} (6K^3P^5 - 24K^3P^3Q + 24K^3P^3s + 30K^3P^2R$$
$$+ 12K^3PQ^2 - 48KPQs - 12K^2QR + 24K^2sR$$
$$- 7P^4Q + 2JP^2Q^3 - 8P^2Qs - 50PQR + 8PsR - 4Q^3$$
$$+ 8Q^2s + 20R^2) \qquad (34)$$

At the present stage it would be quite possible to evaluate the specific rotatory powers of actual compounds, but the evaluation of the symmetrical function S, contained in the brackets, for each compound would be very laborious The value of S is not very sensitive to the differences of a, b, etc , and an approximation can be made by replacing $a, b, c,$ and d by the mean value $(a + b + c + d)/4$, i e , K/4 In the case of amyl alcohol this involves an error of 10% We can make a more accurate approximation by a substitution of the following symmetrical functions for those in (34) retaining K

$$\Sigma \, (3a - b - c - d)^2/(a + b + c + d)^2 = \Sigma \, (4a - K)^2/K^2 = \Delta_2$$
$$\Sigma \, (4a - K)^3/K^3 = \Delta_3$$
$$\Sigma \, (4a - K)^4/K^4 = \Delta_4 \qquad (35)$$

The result is a series such as

$$S = AK^{12}(1 + A_2\Delta_2 + A_3\Delta_3 + A_4\Delta_4 + A_{22}\Delta_2{}^2 + A_{23}\Delta_2\Delta_3 \quad),$$

where the first term AK^{12} is the first approximation, obtained when K/4 is substituted for $a, b, c,$ and d, and the higher terms are purely difference terms giving a more accurate value of S The value of Δ_4 and $\Delta_2\Delta_3$ terms are very small and accordingly all higher terms will be neglected

The substitution of Δ_2, etc , in (34) is carried out by the identities

$$\left.\begin{array}{l} 16q/K^2 = 6 - \tfrac{1}{2}\Delta_2 \\ 64r/K^3 = 4 - \Delta_2 + \tfrac{1}{2}\Delta_3 \\ 256s/K^4 = 1 - \Delta_2 + \tfrac{1}{2}\Delta_3 - \tfrac{1}{4}\Delta_4 + \tfrac{1}{2}\Delta_2{}^2 \end{array}\right\} \qquad (36)$$

and

$$\left.\begin{array}{l} P/K^4 = \tfrac{3}{4}(1 - \tfrac{1}{12}\Delta_2) \\ Q/K^4 = \tfrac{7}{16}(1 - \tfrac{1}{8}\Delta_2 + \tfrac{1}{48}\Delta_4 - \tfrac{1}{192}\Delta_2{}^2) \\ R/K^6 = \tfrac{1}{14}(1 - \tfrac{1}{4}\Delta_2 + \tfrac{1}{16}\Delta_4 + \tfrac{1}{14}\Delta_2{}^2 - \tfrac{7}{48}\Delta_2{}^3) \end{array}\right\} \qquad (37)$$

These values have been substituted in each term of S and by addition of these expressions, while all terms higher than $\Delta_2\Delta_3$ are neglected, we obtain

$$S = K^{12}16^{-3}(207\ 5 - 92\ 25\ \Delta_2 + 17\ 5\ \Delta_3 - 51\ 9\ \Delta_4 + 42\ 5\ \Delta_2{}^2$$
$$- 4\ 2\ \Delta_2\Delta_3) \qquad (38)$$

This method of expression, which is valuable when the values of a, b, c, and d are very close together, can be extended further to V and R^{-5}, both of which are symmetrical functions These can be obtained in similar series and combined with S so that only one function need be evaluated We have by the binomial theorem

$$R^{-5} = K^{-50} 2^{+30} (1 + 1\ 25\ \Delta_2 - 0\ 3125\ \Delta_4 + 1\ 015\ \Delta_2{}^2 \quad) \quad (39)$$

The volume of a tetrahedron of edges $(a + b)$, etc , is derived from the expression for the volume when the three angles at an apex are λ, μ, and ν and the lengths of the edges meeting at this apex are x, y, and z.

$$V = \tfrac{1}{6}xyz \sqrt{(1 - \cos^2 \lambda - \cos^2 \mu - \cos^2 \nu + 2 \cos \lambda \cos \mu \cos \nu)}$$
$$= \tfrac{1}{3}\sqrt{(2\Sigma a^2 b^2 cd - \Sigma a^4 b^2 c^2)} = \tfrac{1}{3}\sqrt{(4qs - r^2)}$$
$$= K^3 (\sqrt{2/96}) (1 - 0\ 375\ \Delta_2 + 0\ 333\ \Delta_2 - 0\ 375\ \Delta_4 + 0\ 117\ \Delta_2{}^2$$
$$+ 0\ 125\ \Delta_2\Delta_3) \quad (40)$$

Substituting values of S, V, and R^{-5} in (34)

$$I = \frac{W}{K^{14}} \frac{2\ 207\ 5\ \sqrt{2}\ 2^{30}}{16^3\ 96}$$
$$\times (1 + 0\ 430\ \Delta_2 + 0\ 418\ \Delta_3 - 0\ 938\ \Delta_4 + 0\ 480\ \Delta_2{}^2 + 0\ 447\Delta_2\Delta_3)$$
$$\quad (41)$$

We could easily obtain the final rotation by use of this value, but by means of a small approximation the value of the series can be tabulated We will substitute by the identity $\Delta_2\Delta_3 = \tfrac{2}{3}\Delta_6$ and make the approximation $\Delta_2{}^2 = 4\Delta_4$ This is true when $\Delta a^2 = \Delta b^2 = \Delta c^2 = \Delta d^2$, but is just an approximation in the ordinary case

Defining $\Delta a = (4a - K)/K$ we can split the series in (41) into separate series in powers of Δa, etc

$$f(\Delta a) = 0\ 430\ \Delta a^2 + 0\ 418\ \Delta a^3 + 0\ 982\ \Delta a^4 + 0\ 537\ \Delta a^5 \quad (42)$$

The value of $f(\Delta a)$ has been tabulated and is obtained from the value of $4a/K$ by the use of Table I The values of $f(\Delta b)$, etc , are obtained similarly from the corresponding values of $4b/K$, etc The value of the series is obtained by adding these quantities to unity

$$I = C_1 W K^{-14} (1 + f(\Delta a) + f(\Delta b) + f(\Delta c) + f(\Delta d)) = C_1 W K^{-14} (1 + F)$$

In an extreme case (e g , $4a/K = 1\ 6$) the quantities Δa, etc , might be in such a relation that errors up to 10% would be introduced, but for actual

compounds the error involved in using the table instead of the exact equation (41) will be much less

We are now in a position to put down the formula for the specific rotatory power of the classical optically active compound by putting I in equation (26)

$$[\alpha] = \frac{C(\mu^2+2)(\mu^2+5)R_A R_B R_C R_D(1+F)(a-b)(a-c)(a-d)(b-c)(b-d)(c-d)}{\lambda^2 M(a+b+c+d)^{14}},$$

(43)

μ is the refractive index of the medium in which the rotation is measured

Table I

$4a/K$	$f(\Delta a)$	$4a/K$	$f(\Delta a)$	$4a/K$	$f(\Delta a)$
0 40	0 150	0 60	0 062	1 44	0 165
0 42	0 139	0 70	0 034	1 46	0 187
0 44	0 129	0 80	0 015	1 48	0 211
0 46	0 119	0 90	0 003	1 50	0 238
0 48	0 109	1 00	0 000	1 52	0 267
0 50	0 100	1 10	0 005	1 54	0 300
0 52	0 091	1 20	0 022	1 56	0 335
0 54	0 084	1 30	0 059	1 58	0 373
0 56	0 075	1 40	0 126	1 60	0 414
0 58	0 069	1 42	0 145		

R_A, etc , are the total refractivities of each attached group, as given in the tables of Bruhl or Eisenlohr

a, b, c, and d are the effective radii of the groups in Angstrom units

$f(\Delta a)$, etc , have not much effect on the numerical result and, after finding $4a/(a+b+c+d)$ are obtained from Table I

λ is the wave-length of light used.

M is the molecular weight of the compound

C is a constant

$$C = \frac{72900 \ 207 \ 5 \ \sqrt{2} \ 2^{36} \ 2 \ 10^{64}}{32 \ \pi^3 \ 10^3 \ 96 N^3} = 16 \ 62 \ ,$$

taking the value $N = 6 \ 06 \times 10^{23}$ and introducing 10^{64} in order that the lengths of the tetrahedron might be expressed in Angstrom units

For light of D lines $C/\lambda^2 = 4 \ 786 \times 10^9$, and for this wave-length this is conveniently used as a constant

$[\alpha]$ is the specific rotation for a molecule of such configuration that, when the group A is placed nearest to the observer, the groups B, C, D appear in clockwise order This gives the interesting result that the actual spatial distribution is known and it is no longer necessary to refer the spatial distribution of

most compounds to some reference compound According to this analysis, we can say with absolute certainty that a dextro-compound has the configuration such that, when the largest group is nearest to the hypothetical observer, the other groups in order of diminishing size appear in a clockwise rotation It may be noted that this result depends on taking the positive sign for the square root in the evaluation of V by equation (31), this is essential as V was defined as $\frac{1}{6}$ [AB AD CD] which is positive for a tetrahedron of the configuration described above [α] was also taken as a rotation in the clockwise direction of the plane of polarization as seen by the observer at the receiving end of the polarimeter, thus is the accepted convention for terming compounds dextro, apart from such compounds as the sugars where the prefixes are used to denote the relation of the configuration to that of some reference compound The difference product has been put in the form $(a - b) (a - c) (a - d) (b - c) (b - d) (c - d)$ so that this is found to be positive when $a > b > c > d$

The final formula has now been derived and this gives the rotatory power of a compound containing four different radicals in terms of their properties, but only when the radicals are small If we have data giving the absolute magnitudes of R_A, a, etc , we can calculate the rotatory power of some compounds of this type, such as C_2H_5 CHOH CH_3 The evaluation of R_A and a must be examined to see how these depend on the atoms in the radical

The refractivity of a radical is obtained directly by the addition of the atomic refractivities of its constituents, but the effect of the central atom must also be considered The valency electrons of this atom will act almost as part of the attached radicals and move with these to take up a dissymmetric distribution If the central atom is small, as in carbon, since most of its refractivity is due to these electrons we can regard it as completely shared by the larger radicals, and we shall correct the refractivities of the radicals by adding one-quarter of that of the central atom.

The quantities a, etc , were termed the radii of repulsion of the radicals, but rather than representing any exact physical quantity they must be regarded more as parameters used to express the shape of the molecule The radical is usually more complex than a single atom In a single atom we might have regarded the radical as having a radius which could not be penetrated equal to that of the orbit of the outer electrons In several atoms joined together our knowledge of the repulsion effects is very vague and the simplest assumption is that the total volume guarded from penetration is equal to the sum of the atomic volumes. The atomic radii are obtained by finding the distance

between atomic nuclei in diatomic molecules, and taking the total distance as the sum of the radii of the two atoms concerned. It will be noted that the radius here has very much the same meaning as that in which we have employed it in the above treatment. The measurements of the molecular dimensions are mainly from rotation spectra, and have been confirmed by X-ray and electron diffraction of vapours. The atoms are considered as spheres to obtain their volumes and then the radical assumed spherical to deduce the radius from the total volume. The radical radius is thus the cube root of the sum of the cubes of the atomic radii. As with the refractivity we shall correct for the effect of the central atom by adding one-quarter of its volume, this should give the approximate effect since the volume of the central atom will prevent the radicals approaching when they are small, but will have little effect when the radicals are large.

We can represent the method of calculating R and a by

$$R_A = \Sigma_A R + R\ (c)/4 \quad \text{and} \quad a = (\Sigma_A^{\text{t}}\ r^3 + r\ (c)^3/4),$$

where R (c) and r (c) are refractivity and radius of the central atom.

In the following calculation the refractivities for the D lines according to Eisenlohr are taken from Landolt-Bornstein ' Tabellen,' 1923 edition. The atomic radii H 0 37 A, C 0 77 A, 0 70 A, and N 0 72 A, are taken from ' Ann Reps Chem Soc ,' vol 28, p 402 (1931), Table II, data from various sources, chiefly rotational spectra. In accordance with the suggestion in the Report, the radii for O and N have been corrected on the assumption that double and triple bonds cause 14% and 23% shortenings in length since the radii are taken from the molecules O_2 and N_2. The properties of the radicals C_2H_5, CH_3, OH, and H have been found and substituted in formula (43) to obtain the rotatory power of sec butyl alcohol, and the other calculations performed in a similar manner. The values of the refractive indices have been taken from Landolt-Bornstein ' Tabellen '

The experimental data are from sources commonly quoted for these compounds.

The concordance between the experimental and calculated values is better than the accuracy of the original data and the method of calculation warrants. This close agreement must be fortuitous, and the points of main importance are that the rotations forecasted are of the correct order and that the ratios of the values in the four compounds considered are very much the same in both the theoretical and experimental series. The four compounds chosen are the simplest active compounds, but they give a valuable proof that formula

(43) will apply for the calculation of the rotation of compounds in which we can regard the radicals as approximately spherical This is the first time that the absolute magnitudes of the rotatory powers of actual compounds have been calculated from data entirely independent of optical activity measurements

<div align="center">Table II —Specific Rotatory Powers $[\alpha]_D$</div>

	Calculated	Experimental	Observer
	°	°	
Amylamine	3 6	5 86	Marckwald, ' Ber deuts chem Ges,' vol 37, p 1045 (1904)
Amyl alcohol	4 0	5 90	Marckwald and McKenzie, ibid , vol. 34, p 490 (1901)
Sec butylamine	7 4	7 44	Thomé, ibid , vol. 36, p 586 (1903)
Sec butyl alcohol	9 3	13 9	Pickard and Kenyon, ' J Chem Soc , vol 99, p 45 (1911)

While we have employed formula (43) to forecast the absolute rotations from atomic data it is not in this direction that it will be most useful The method of obtaining the radical radii from atomic radii, uncertain quantities in themselves, precludes the application to more complex compounds , but having established formula (43) it is possible for us to use it to obtain relative rotations It seems to me that in the parachor we have a reliable method of obtaining an estimation of radical radius , the more so because this will already include any special repulsion effects To use the cube root of the parachor for quantitative predictions it would be necessary to obtain an empirical constant for the formula, but the idea may be useful for the qualitative study of the variations of rotation by substitution

In a large radical it appears that only the portion adjacent to the asymmetric centre will enter into the rotatory power interactions, and the only effect of those portions of the radical far removed from the asymmetric centre will be to repel the adjacent radicals slightly , thus substitution at the far end of a chain will only alter the rotatory power to the extent that it alters the configuration around the centre Substitution of a group with a large parachor should increase the effective radius of the group which it enters, and, if the relative sizes of the groups are known previously, it should be possible to forecast the direction of the change in rotation The effect will be much greater if the substitution is near the asymmetric centre

An examination of the parachors, especially of those portions near the asymmetric centre, should provide a means of estimating the absolute con-

figuration of any enantiomorph from the sense of its rotatory power   This can only be done with certainty when interactions of the solvent with the molecule or association are known to be absent, but, when a reliable estimation can be made, this should be of vital importance in the study of Walden Inversion reactions

In formula (43) we have the connecting link between rotation and chemical structure   Although the formula is only applicable in a quantitative manner to the extent that the molecule approximates to four spherical groups, it demonstrates clearly what variations in rotation are to be expected for known changes in the atomic structure

Rotatory Power, Rotatory Dispersion, and Molecular Structure

It is definitely established that, if a compound containing four groups attached to a central atom exhibits optical activity, all these groups must be different chemically   Since the very existence of a rotation depends on the differences of these groups, it appears that the magnitude of this rotation must depend on the difference of some specific property A of the groups, and that there must be a factor of the type $(A - B) (A - C) (A - D) (B - C)$ $(B - D) (C - D)$ in any theoretical expression for the optical rotation   This logical deduction was made independently by Crum Brown[*] and Guye,[†] but these investigators had no definite idea of the mechanisms involved in the actual twisting of the plane of polarization   Crum Brown also showed that, if one group could be changed in small increments so that the magnitude of this property in it approached the magnitude of this property in another group, the rotation would decrease to zero and then change sign as the first group surpassed the fixed group

It has been established in this paper that the rotatory power is given by a formula of the predicted kind, in which the effective radius is the property occurring in the continued difference product   If one group can be changed while the compound retains the same configuration, the sign of the rotation should change when the effective radius is increased above that of the next largest group   This has been shown experimentally if we can assume the effective radius of an aliphatic chain to increase with its length, Kuhn[‡] has observed that in the series of compounds $R_1 R_2 CHOH$, if these are prepared in a manner such that the configuration is definite, then the sign of the rotation

---

[*] 'Proc. Roy Soc , Edin.,' vol 17, p 181 (1890).
[†] 'C. R. Acad. Sci., Paris,' vol 110, p. 714 (1890)
[‡] 'Trans. Faraday Soc ,' vol 22, p. 457 (1930)

is constant if $R_1 > R_2$ Again in active amyl derivatives we find that —OH and —NH$_2$ are the only radicals which have less atomic volumes than the —CH$_2$ group, all other radicals cause the —CH$_x$X group to be larger than the adjacent —CH$_2$CH$_2$ group Thus amyl alcohol and amylamine should have the opposite sense of rotation to all other compounds prepared by substituting for —OH in amyl alcohol, and this is entirely fulfilled experimentally

It is interesting to note that we can ascertain the absolute configuration of the ordinary amyl alcohol, which is lævorotatory This is given in fig 1, when the CH$_2$OH group is placed nearest to the observer the other groups taken in clockwise order are C$_2$H$_5$, CH$_3$, and H
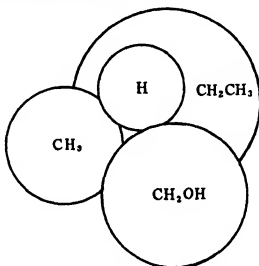
Fɪɢ 1 —Absolute configuration of lævorotatory amyl alcohol. For simplicity the radicals have been represented as spheres.

An examination of formula (43) shows that it divides quite naturally into three factors which seem almost independent, and the variations of the rotatory power under different conditions are easily classified by considering the changes in these three factors ($\mu^2 + 2$) ($\mu^2 + 5$) dependent solely on the medium ; R$_A$R$_B$R$_C$R$_D$/λ^2 dependent on the refractivities and the wavelength ; and

$$(1 + \mathrm{F})\, (a - b)\, (a - c)\, (a - d)\, (b - c)\, (b - d)\, (c - d)/(a + b + c + d)^{16}$$

totally dependent on the spatial arrangement

The first factor ($\mu^2 + 2$) ($\mu^2 + 5$) is more a property of the medium than of the active compound. In accurate work this factor should be corrected

for in order to obtain comparative results when working in different solvents and with different wave-lengths, but as a general rule the variations in the rotatory power brought about by this factor are very small

The second factor determines the variation in rotation with changing wave-lengths of light   In this examination the first factor will be neglected, or can be regarded as corrected for by suitable measurements on the refractive index of the medium at different wave-lengths   For many compounds there are regions in which R_A, etc, are almost indifferent to changes in wave-length, in these regions the rotatory dispersion is given by Biot's inverse square law   For other regions, since the refractivities R_A, etc, can be determined from ordinary refractive data, it is possible to predict exactly the rotatory dispersion   However, it is interesting to find the general form of the rotatory dispersion curve, which can be obtained since the general equation for refractive dispersion is known   For the sake of simplicity, the term corresponding to a dissipation of energy by absorption will be omitted and hence the resulting rotatory dispersion equation will only apply for wave-lengths outside absorption bands   The extra terms can be introduced if desired

According to the Drude treatment of refractivity as modified by Lorentz the refractivity of any group is obtained by summing for the motion of all its electrons,

$$3R = \frac{3\,(m^2-1)}{m^2+2} = \frac{3\,(K-1)}{K+2} + \frac{1}{4\pi^2 c} \Sigma \frac{\nu_s\, e_s\, \lambda_s^2}{m_s\,(\lambda^2 - \lambda_s^2)}$$

The first term represents the refractivity for infinitely long waves and the second the sum of the effects of absorption bands situated at λ_s, etc   For regions not very near an absorption band only the first term is large, and, as it is not very probable that two absorption bands in different groups will be at the same wave-length, we may evaluate $R_A R_B R_C R_D / \lambda^2$ neglecting portions which contain products of absorption terms

$$\frac{R_A R_B R_C R_D}{\lambda^2} = \frac{1}{\lambda^2}\Bigg[R_A'R_B'R_C'R_D' + R_C'R_B'R_C'\,\frac{K_D}{\lambda^2 - \lambda_D^2} + R_B'R_C'R_D'\,\frac{K_A}{\lambda^2 - \lambda_A^2} \Bigg]$$

and

$$[\alpha] = \frac{1}{\lambda^2}\Bigg[K_0 + \frac{K_1}{\lambda^2 - \lambda_1^2} + \frac{K_2}{\lambda^2 - \lambda_2^2} \Bigg] \qquad (44)$$

Only one absorption band has been written for each group, but it is obvious that, if there are more than one, all these must be included   The last equation is the most general form of the rotatory dispersion equation, where λ_1, λ_2, etc, are the wave-lengths at which there are absorption bands in the separate groups adjacent to the asymmetric centre

The form of equation which is generally used for expressing experimental results is that deduced by Drude on his hypothesis of spiral movements of electrons, and this equation has been well established by Lowry and his co-workers Though the Drude form does not appear the same as the above equation, these can be directly transformed into each other. Taking the two terms which Lowry finds sufficient to represent the behaviour of most compounds we have

$$[\alpha] = \frac{K_1}{\lambda^2 - \lambda_1^2} + \frac{K_2}{\lambda^2 - \lambda_2^2}$$

$$= \frac{1}{\lambda^2}\left[(K_1 + K_2) + \frac{\lambda_1^2 K_1}{\lambda^2 - \lambda_1^2} + \frac{\lambda_2^2 K_2}{\lambda^2 - \lambda_2}\right]$$

Since $\lambda_1^2 K_1$ and $\lambda_2^2 K_2$ are constants, this last equation has the same form as (44) The formula for the rotatory dispersion obtained on the assumption that the rotatory power of the molecule is due to the electric interactions of the induced electric doublets is just the same as that used in experiment and derived from other hypotheses , but it has the advantage that the significance of the constants are known exactly and their values can be derived independently from other sources

The Drude formula for the rotatory dispersion resolves the rotatory power into the sum of several terms, each of which appears to be the contribution of a separate group of electrons giving one or more definite absorption bands Occasionally a single term gives a very large contribution and it would appear that the electrons have a very dissymmetric structure For camphor the rotatory power in the ultra-violet region is dependent largely on a term $K/(\lambda^2 - \lambda_s^2)$ where λ_s is the absorption wave-length of the ketone CO group , but it seems impossible for a symmetrical group such as the ketone group to have a dissymmetric structure In order to meet this difficulty Lowry and Walker[*] formulated the interesting hypothesis that some influence could emanate from the asymmetric centre and induce asymmetry in adjacent groups such as the CO group However, in this analysis we do not regard the rotatory power as due to asymmetry concentrated in various centres, and this phenomenon should be completely explained according to the factor $R_A R_B R_C R_D / \lambda^2$

Considering the region just outside the absorption band we see that R_{CO}, the refractivity of the ketone group, will vary very rapidly with λ. This variation will be so great that, in comparison, we can regard $(R_A R_B R_C)$ as

* ' Nature,' vol. 113, p 565 (1924).

practically constant The ketone group is considered as the fourth refractive centre D and the remaining factor R_{CO}/λ^2 is expressed by $K/(\lambda^2 - \lambda^2_{CO})$ according to the ordinary theory of refractive dispersion λ_{CO} is the absorption wave-length of the ketone group and so the variation of the whole rotatory power is given by a single Drude term dependent on this wave-length This is just the experimental result and there is no necessity for any further assumptions

In the last factor

$$(1 + F)(a - b)(a - c)(a - d)(b - c)(b - d)(c - d)/(a + b + c + d)^{14}$$

we have an expression which is characteristic of a formula for optical activity The exact predictions and applications of this have already been discussed, but it is noteworthy that since this factor has a very differential nature most of the variation of activity from compound to compound is given by this factor The variations of R_A, etc , in different compounds are small and we may regard the spatial configuration as altogether the most important property in the determination of the rotatory power

The quantities a, b, c, and d were only given a meaning according to the Thorpe-Ingold theory of valency deflexion Since the numerical calculations for the simple compounds sec-butyl alcohol, etc , agree with the experimental data, this constitutes another point of evidence in favour of the Thorpe-Ingold theory

Hitherto we have ignored the occurrence of permanent dipoles in certain molecules A permanent dipole will not interfere with the electric inter-actions causing the rotatory power, but it may have a definite effect on the configuration A polar group may tend either to attract or repel the adjacent groups according to their nature We can see the influence of a polar group most clearly if we consider it at such a distance that its volume does not affect the configuration A dipole at the end of a long chain may still have an appreciable deforming influence on the portions around the asymmetric centre , the effect may be transmitted either as an electric field acting through space or as a polarization along the atoms linking with the centre We should expect the rotatory power to vary with the size of the dipole Rule[*] and his collaborators have studied several series of compounds with the dipoles at a distance from the centre, and it is probable that the alteration of configuration around the asymmetric centre explains the systematic variation in rotatory power which has been found.

---

[*] Rule and Smith, 'J. Chem. Soc.,' vol. 127, p. 2188 (1925).

In the experimental study of the dependence of the optical activity on chemical constitution, one of the great difficulties has been the sensitivity of the rotation of many compounds to changes in solvent and temperature   The present analysis seems to provide a logical basis by which one can understand and correlate these variations with other properties of the compounds and of the solvents   The optically active compounds will fall roughly into three classes according to their atomic structure   and these will give more or less distinct behaviours on variation of the physical conditions

When we consider a molecule with little or no polar groups and no groups which have a tendency to co-ordinate with any other group, even if this is dissolved in a strongly polar solvent, it cannot be appreciably deformed by the internal electric fields   The refractivities will be affected much less, and the only variation will be due to the factor $(\mu^2 + 2)(\mu^2 + 5)$ Thus, for changes from one solvent to another and for changes of concentration while in one solvent, the specific rotation should vary as $(\mu^2 + 2)(\mu^2 + 5)$ where μ is the refractive index of the solution under exactly the same conditions as in the measurement of the rotation

In a molecule containing a dipole we should expect this, by virtue of its local electric field, to exert a deforming influence in the molecule   The electric field will be partially transmitted through the space external to the molecule and its magnitude will be very dependent on the presence or absence of other polar molecules which will determine a mean dielectric constant of the external space   Thus in changing from solvent to solvent probably the variation of the specific rotation with $(\mu^2 + 2)(\mu^2 + 5)$ will be entirely masked by variations dependent on the dielectric constant   Thus for inert polar molecules the variation of the specific rotation should give exactly the same serial order as arranging the solvents in order of their dielectric constants   In this and the preceding cases the change of medium will not alter the chemical nature of any of the groups, and we should not expect any change in the form of the rotatory dispersion curves

In the molecule which contains a group which can co-ordinate with other molecules, whether of the same or a different kind, the system is very complicated   In solution, or even in the pure state when the compound associates, the system will be an equilibrium consisting, as regards optical activity, of entirely different molecules   The group that co-ordinates will have its effective radius very much increased by junction with another whole molecule and the magnitude and sign of the rotation may be altogether altered.   The direction of this change may be predicted if we know from chemical evidence

which group it is that co-ordinates However, in the loose linking with another molecule the chemical structure of the group may be so altered that the refractivity and refractive dispersion are changed Whereas all other types of compound retain the same rotatory dispersion curve even if the magnitude of the rotation is changed by concentration or solvent, this type of molecule which co-ordinates with another molecule may have both the rotation and rotatory dispersion entirely altered

There is no direct effect of the temperature apparent in the general case and the variations due to temperature are due to variations in the properties of the medium, e g , refractive index, dielectric constant, and equilibrium in association From the theoretical viewpoint the temperature and solvent action can be classified according to nature of the compound (1) The compound is inert and the rotation depends on the refractive index of the medium while the rotatory dispersion is constant (2) The compound is polar, but inert, and the rotation depends chiefly on the dielectric constant while the rotatory dispersion is constant (3) The compound is active chemically, tending to co-ordinate, and both rotation and rotatory dispersion vary with temperature and concentration

With regard to the relation of chemical constitution to rotatory power, rotatory dispersion, and solvent and temperature effects, the theoretical predictions seem to provide a clear understanding of the actions which lie behind these phenomena

In conclusion, it may be emphasized that, since the direct calculation of the polarizations in the various refractive centres of the active molecule predicts rotations of the observed magnitudes, there is no necessity for any special molecular structure to be assumed as an explanation of optical activity Indeed, since the actions which are the origin of the rotatory power are so well established by the electronic theory of dispersion, it appeared that this analysis could not be called an hypothesis, but could only be correctly named a calculation of optical activity

Summary

(1) The optical rotatory power of an asymmetric atom attached to four small radicals has been calculated and is expressed in a practical formula The rotation is dependent on the refractivities and the sizes of the radicals

(2) The formula has been confirmed by the calculation of the rotatory powers of amyl alcohol, amylamine, sec-butyl alcohol, and sec-butylamine

(3) The conclusions drawn from this calculation with regard to optical activity and chemical substitution and optical activity and physical conditions agree with the characteristic behaviour of optically active compounds

(4) An exact formula connecting the rotatory dispersion of the compound with the refractive dispersion of the radicals has been obtained

---

Transmutation Effects Observed with Heavy Hydrogen

By M. L. E. OLIPHANT, Ph D (Messel Research Fellow of the Royal Society),
P. HARTECK, Ph D, and Lord RUTHERFORD, O M, F R S

[PLATE 16]

In our paper " Transmutation of Elements by Protons,"[*] we showed that the transformation of some of the light elements by protons could be conveniently studied by the use of comparatively low voltages—of the order of 100,000 volts—by generating an intense narrow beam of protons which fell on the target of small area of about 1 sq cm   In the light of experience of the past year, the installation has been modified in several particulars and entirely reconstructed   By the addition of another 100,000-volt transformer in tandem and the use of appropriate condensers the D C voltage available has been raised from 200,000 to 400,000 volts   The main change, however, consists in the use of a horizontal instead of a vertical discharge tube   In place of glass, a corrugated porcelain wall bushing capable of withstanding high voltages has been used to insulate the positive electrode, while the earthed metal casing forming the negative electrode projects through a brick wall.   The arrangement of the internal electrodes is, in general, similar to that used in the

earlier apparatus The oil cooling circulation has been improved as the electrodes cannot now be cooled by radiation alone As before a magnetic field is applied to sort out the various types of ions generated in the discharge tube The use of the horizontal tube has many advantages, not only for assembling the controls at convenient points but also in the ease of handling the counting apparatus and absorbing screens

The new installation has worked smoothly and satisfactorily and we have been able to increase the number of disintegration particles available for study by a factor of 10 to 50 The thick brick wall acts as a complete screen for the X-radiation generated in the system

In our last paper* we gave an account of the transformations produced in lithium by the ions of heavy hydrogen The heavy water used for this purpose was generously presented to us by Professor G N Lewis For our present experiments we have depended on a supply of concentrated heavy water prepared in the Cavendish Laboratory by Dr P Harteck † For preliminary requirements a weak concentration of diplogen‡ of about 12% was generally used Stronger concentrations up to 30% mixture with helium§ were necessary in order to study the emission of neutrons and protons The action of diplons on diplons was studied by observation of the effects produced when diplons were used to bombard targets covered with a thin layer of a preparation containing heavy hydrogen These were ammonium chloride, ammonium sulphate, and orthophosphoric acid in which the normal hydrogen had been largely replaced by diplogen The method of preparation was very simple A small quantity of the normal ammonium salt or the phosphoric pentoxide was added to an excess of heavy water An equilibrium was at once established between the concentration of hydrogen and of diplogen in the compound and in the water,‖ and if a drop of the solution was placed upon a warm iron target and allowed to evaporate a stable but non uniform layer of a salt containing diplogen was left behind The ND_4Cl was also deposited upon the target in the form of a very thin and a uniform layer by means of sublimation, but this very property renders the target unstable and liable to disappear rapidly

* ' Proc Roy Soc ,' A, vol 141, p. 722 (1933)

† ' Proc Phys Soc Lond.,' vol. 46, p 277 (1934)

‡ In a discussion on Heavy Hydrogen before the Royal Society on December 14, 1933 (see ' Nature,' p 955 (1933)), the names diplogen (D) for the *new isotope* of hydrogen and diplon for its nucleus seemed to find favour Also ' Proc Roy Soc ,' A, vol 144, p 1 (1934)

§ *Cf* Oliphant, Kinsey, and Rutherford, ' Proc Roy Soc ,' A, vol 141, p 722 (1933)

‖ Lewis, ' Proc Amer Chem Soc ,' vol 55, p 3502 (1933)

under bombardment   The phosphoric acid remained as a liquid film over the surface of the target   Exceedingly small quantities of the substances are required

The Action of Diplons on Diplons

The Emission of Charged Particles—The most interesting and important reaction which we have observed is that of heavy hydrogen on heavy hydrogen itself   Experiment has shown* that diplogen is not appreciably affected by bombardment with α-particles from polonium, and we have been unable to detect any specific action of protons on diplogen for energies up to 300,000 e-volts   We were therefore surprised to find that on bombarding heavy hydrogen with diplons an enormous effect was produced   Fig 4, Plate 1b, shows a reproduction of portion of an oscillograph record obtained in our first experiment   We assumed at first that this was an effect due to radiation passing through the counting chamber as previous experiments had shown that X-rays could produce just the result observed, but subsequent observation at much lower bombarding potentials showed that we were dealing in reality with a very large emission of protons   Examples of an oscillograph record obtained under these conditions are given in figs 5 and 6, Plate 16   The original observations were made on ND_4Cl, but in order to establish that the effects observed came from the action of D on D and not from the nitrogen or chlorine, we bombarded targets of $(ND_4)_2SO_4$ and of D_3PO_4 The absorption curves obtained for the three substances are given in fig 1   The shape of these curves is due to the fact that protons gave too small a deflection in the oscillograph to be easily counted except over the last five centimetres of their path

It is evident from fig 1 that there are present in each case two very prominent groups of particles of ranges 14 3 and 1 6 cm. respectively   Careful counting of the records established that the numbers of these particles were identical within the errors of measurement   The maximum size of the deflections produced on the oscillograph record by the particles in each group indicated that they both consisted of singly charged particles   On these data it is natural to assume that these particles are emitted in pairs opposite one another, and that the difference in range arises from a difference in mass, and hence of the velocity and energy   The simplest reaction which we can assume is

$$_1D^2 + {}_1D^2 \rightarrow {}_2He^4 \rightarrow {}_1H^1 + {}_1H^3 \dagger \tag{1}$$

* Rutherford and Kempton, ' Proc. Roy Soc ,' A, vol 143, p. 724 (1934)

† It has been decided to put the symbol for the nuclear charge to the left and below the symbol for the element

While from the point of view of both experiment and theory, we have no information of the details of the nuclear changes involved and can only study the final result, yet it is often useful and may even be more correct to assume that the first step in the process is the capture of the bombarding particle to form a new and heavier nucleus   If this proves unstable, it then breaks up, possibly in a variety of ways   The recent discovery by M and Mme Curie-Johot,* and by Cockcroft and Walton,† that a type of radioactive nucleus is
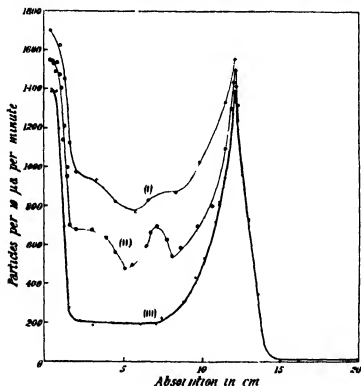
Fig 1 —(i) ND_4Cl , (ii) $(ND_4)_2SO_4$, (iii) D_3PO_4

formed by the capture of an α-particle, diplon, or proton lends support to this point of view   The time of transformation may vary over very wide limits and may sometimes be so short that the process cannot be experimentally followed   In the case which we are considering we are inclined to interpret the observations in the following way   The initial process is the union of two diplons to form a new nucleus of charge 2 and mass 4, *i e* , a helium nucleus

* 'C. R. Acad Sci Paris,' vol 196, p. 254 (1934).

† 'Nature,' vol 133, p 328 (1934).

If we neglect the energy of the bombarding particle and assume the mass of D to be that given by Bainbridge,* the mass of this helium atom must be 4 0272, and it therefore possesses an excess energy over the normal helium atom, of mass 4 0022, of about 23 million volts   This atom is unstable and may lose its energy in a variety of ways, some of which are considered later   We are considering here the breaking up of the helium nucleus into a proton and a hydrogen isotope of mass 3   The transformation follows so rapidly after the capture that no evidence of the existence of the excited helium nucleus has so far been obtained

The mass and energy relations on the right-hand side of equation (1) can be obtained in the following way   The $_1H^1$ particle possesses an energy of $3 \ 0 \times 10^6$ e-volts, corresponding to protons of the observed range of 14 3 cm   Then, from momentum considerations, the energy of the $_1H^3$ particle which is emitted in the opposite direction will be $1 \ 0 \times 10^6$ e-volts, i e, the total energy of the two particles will be $4 \ 0 \times 10^6$ e-volts, corresponding to a mass-change of 0 0043 units   Hence the mass of the $_1H^3$ atom will be

$$4 \ 0272 - (1 \ 0078 + 0 \ 0043),$$

i e, 3 0151   The ionization produced by the $_1H^3$ particle will be at every point of its path identical with that produced by a proton possessing the same velocity   However, owing to its greater momentum the $_1H^3$ particle will travel three times as far as the proton for a given reduction of velocity   Consequently it will have three times the range of a proton of the same initial speed   The initial velocity of the $_1H^3$, corresponding to an energy of 10^6 e-volts, is 8×10^8 cm /sec   The range of a proton with this velocity is 5 8 mm according to data given to us by Feather   Hence the range of the $_1H^3$ particle should be $3 \times 5 \ 8 = 1 \ 74$ cm   Considering the nature of the data available and the difficulties of determining the range of the short 1 6 cm group, we feel that this agreement is very satisfactory

Additional evidence of the truth of our assumption is afforded by observation of the way in which the ionization, as measured from the magnitude of the oscillograph deflections, varies near the end of the range of the particles   In fig 2 we have plotted the number of deflections above a given size against the absorption in the path of the particles, using a chamber 3 mm deep   It is seen that the14 cm group shows a very sharp peak which occurs about 2 cm short of the end of the range   The 1 6 cm group, on the other hand, rises rapidly to what appears to be a much broader maximum   This is just what

would be expected from a particle of greater mass, the velocity of which varies less rapidly with the length of path in the material than the proton

Still further confirmation of the truth of this mode of transformation would be provided if it could be shown that the $_1H^1$ and $_1H^3$ particles recoil in opposite directions This point has been carefully examined by Dee using the Wilson expansion chamber method, and in a recent letter to ' Nature '* he concludes that there is no doubt of its correctness

It seems clear that the production of this isotope of hydrogen of mass 3 in these reactions is established beyond doubt The mass of the $_1H^3$ atom is consistent with its possessing a stability of the same order as $_1H^2$ The possible existence of this isotope has been discussed by several writers and although a
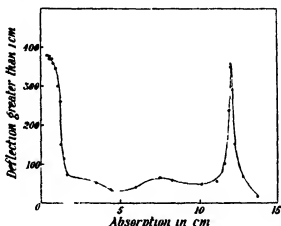
Fig 2 —$(ND_4)_2SO_4$

careful search has been made no evidence of its presence has been found It seems probable, however, that it could be formed by the process we have considered in sufficient quantity to be detected ultimately by spectroscopic or positive-ray methods.

Voltage Variation and Absolute Yield —The variation with energy of the bombarding diplons, of the emission of 14 3 cm protons, has been measured over a limited range of voltage The yield is so great that the number of particles entering the chamber soon became inconveniently large, and also we found that at high bombarding energies the heavy hydrogen compound is rapidly removed from the target Fig 3 gives the curve obtained with $(ND_4)_2SO_4$ It is evident that particles are detected at energies as low as 20,000 volts

* ' Nature,' vol. 133, p. 564, April 14th (1934)

and that the number increases rapidly with increase of accelerating potential * The nearly linear rise beyond 100,000 volts is probably due to the fact that, for potentials greater than this, the chance of disintegration in a collision is nearly constant, and the number of transformations therefore increases proportionally with the penetration of the bombarding particle into the target material
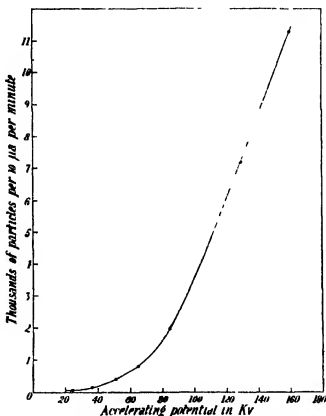
Fig 3 —$(ND_4)_2SO_4$, 12 cm absorber

From the solid angle subtended by the window, and the known composition of the target, we estimate that at 100,000 volts the absolute yield of disintegrations for collisions between D and D is of the order of magnitude of 1 in 10^6 This is a far greater yield than that obtained for any other disintegration process, even at much higher potentials Simple calculation shows that even a monomolecular layer of diplogen under the conditions of our

* It should be emphasized that the energy available in a collision between two particles of equal mass is only half the energy of the bombarding particle, since half the kinetic energy is retained by the composite nucleus formed by capture.

experiment would give a large effect Consequently every substance we have bombarded with diplons begins, after a short time, to show effects which are clearly due to traces of diplogen absorbed by or driven into the target We have also observed that when a compound containing hydrogen, such as ammonium sulphate or lithium hydroxide, is bombarded with a strong beam of diplons, the hydrogen in the compound is gradually replaced in part by diplogen After some time such compounds begin to behave as diplogen targets of appreciable concentration, and great care must be exercised to separate these effects from any others which are under investigation This deposition of diplogen from the beam itself, while easily distinguished by the appearance of protons of characteristic range, is much more difficult to allow for when observations are made on the neutron emission of elements For example, it is difficult to disentangle the emission of neutrons characteristic of lithium and beryllium from the spurious effect due to contamination by diplogen

The Emission of Neutrons —We have pointed out that the appearance of the oscillograph records obtained in our initial experiments on the effects produced on bombarding diplogen with diplogen were suggestive of the presence of a strong radiation The unstable form of He of mass 4 00272, formed by the union of two diplons, might be able to revert to the normal form of He of mass 4 0022 by losing the additional mass as energy of a gamma ray or rays of 23×10^6 e-volts energy Accordingly we searched for such a radiation with a Geiger-Müller counter It was at once evident that there was present a very intense radiation capable of producing an undiminished effect on the counter through 20 cm of lead As a check on this a search was made for recoil nuclei with the linear counter, and it was found that neutrons are emitted in numbers comparable with the number of 14 cm protons It is known that the Geiger counter is affected by neutrons both by the recoil nuclei produced in the counter itself, and also through the action of secondary radiations[*] produced when neutrons pass through matter Under these conditions it is impossible for us to decide, on the basis of our experiments, whether a gamma ray of high energy is present In order to establish the existence of such a radiation it will be necessary to search for high speed photo-electrons, either with the expansion chamber or with a system of coincidence counters

We have endeavoured to determine the properties of the neutrons by various methods The absorption in lead has been measured with the linear counter

---

[*] *Cf.* Lea, 'Nature,' vol 133, p 24 (1934) Experiments on these points have been made with the assistance of Mr Westcott, who provided the counters, and details will be published elsewhere

by observation of the number of recoil kicks produced with or without an absorbing screen of 5·5 cm of lead between the chamber and the target. The average of three measurements showed that the number of kicks was reduced by 44%, corresponding to a radius of cross-section for a collision between a neutron and a lead nucleus of 8 4 × 10⁻¹³ cm. This is to be compared with the value found by Chadwick for the neutrons from beryllium bombarded by polonium α-particles, *i.e.*, 7 × 10⁻¹³ cm * Chadwick states that the cross-section does not appear to change rapidly with the energy of the neutron except when the energy is very low, so that the result tells us nothing except that the neutrons appear to behave in very much the same way as the neutrons from beryllium, which we know to possess a large range of energies.

It is possible to obtain an approximate value for the maximum energy of the neutrons by observation of the maximum size of the kicks produced by recoil nuclei in the linear counting chamber From the mean size of the kicks produced by α-particles, and our knowledge of the energy loss of such particles in traversing the chamber, we can estimate the ionization produced by, and hence the energy of the recoil nuclei Thus we find that the maximum size of kick produced in the chamber by the recoil nuclei in air is about 6 mm., if we neglect the very large deflections of 2 cm. and over, which almost certainly result from disintegrations Assuming that the energy loss of the recoil particle per ion produced along its path is the same as for an α-particle, we find an energy for this nucleus of about 0 5 × 10⁶ e-volts Application of momentum considerations to a head-on collision between a nitrogen nucleus and a neutron leads to the conclusion that the energy of the colliding neutron must be about 2 × 10⁶ e-volts We have also made experiments on the energy of recoil nuclei produced in helium resulting in a slightly higher value of 2 2 × 10⁶ e-volts This gas is especially suited for neutron recoil observations as it does not suffer disintegration by neutrons.

In order to account for the production of neutrons of the observed energy and number we have been led to assume the transformation

$$_1D^2 + _1D^2 \rightarrow _2He^4 \rightarrow _2He^3 + _0n^1, \tag{2}$$
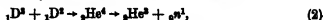
in which the unstable $_2He^4$ nucleus first formed breaks up into a helium isotope of mass 3 and a neutron The assumption of the formation of $_2He^3$ as a product of such a transformation is not without a precedent, as we have already con-

Fig. 4   First observation of 14 cm protons from D + D

Fig. 5 —14 cm protons from D + D (12 cm absorber)

Fig. 6 —₁H³ particles from D + D (11 cm absorber)

cluded that it is produced, together with a normal α-particle, as a result of the bombardment of $_3Li^6$ with protons.* We assumed

$$_3Li^6 + _1H^1 \rightarrow _4Be^7 \rightarrow _2He^3 + _2He^4, \tag{3}$$
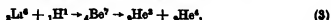
and found that the observed ranges of 11·5 and 6·8 mm were in good accord with the application of momentum considerations to this reaction Dee† has obtained very definite evidence that the two short-range particles are emitted in opposite directions, and we have confirmed that it is the $_3Li^6$ isotope which is concerned in this transformation ‡ It seems quite clear, therefore, that $_2He^3$ can exist under these conditions, and from the observed ranges of the particles we are able to calculate its mass in the following way The longer range of 11·5 mm is reasonably well known and it will correspond with the $_2He^3$ particle For the same velocity an α-particle would go 4/3 times as far because of its greater energy Hence the velocity of the $_2He^3$ is the same as the velocity of an α-particle the range of which is 1·53 cm., corresponding with an energy of 2·5 × 10⁶ e-volts The energy of the $_2He^3$ will be three-quarters of the energy of this α-particle, i e., 1·88 × 10⁶ e-volts The total energy produced in the transformation is thus 3·30 × 10⁶ e-volts, or the corresponding change in mass is 0·0035 units Hence the mass of the $_2He^3$ is

$$(6·0145 + 1·0078) - (4·0022 + 0·0035) = 3·0166,$$

using Bainbridge's (*loc cit.*) value for the mass of Li^6 On the other hand, we can use the mass 6·0157 calculated from the disintegration of $_3Li^6$ into two α-particles of 13·2 cm range under bombardment by diplons,§ the data for this transformation being extremely good From this transformation we obtain for $_2He^3$ a mass of 3·0178 units.

Substitution in reaction (3) of the masses calculated in the above manner leads to the appearance of excess masses of

$$(2·0136 + 2·0136) - (3·0166 + 1·0067) = 0·0039,$$

and

$$(2·0136 + 2·0136) - (3·0178 + 1·0067) = 0·0027,$$

respectively, corresponding to energies of 3·6 × 10⁶ and 2·5 × 10⁶ e-volts. The neutron would receive three-quarters of this energy, i e., 2·7 × 10⁶, or 1·9 × 10⁶ e-volts. Either of these two values are in good accord with the

* 'Proc. Roy. Soc.,' A, vol. 141, p. 259 (1933).
† 'Nature,' vol. 133, p. 564 (1934).
  'Nature,' vol. 133, p 377 (1934).
§ Oliphant, Kinsey, and Rutherford, 'Proc. Roy Soc ,' A, vol. 141, p. 722 (1933).

approximate value of 2×10^6 e-volts found from our experiments, but Dee[*] has now obtained expansion chamber photographs of the recoil nuclei, analysis of which suggests that the lower of the two figures is more nearly correct, and that the neutrons emitted at right angles to the bombarding beam of diplons are homogeneous in velocity, as required by our reaction

The recoiling $_2He^3$ nucleus possesses an energy of about $0\ 7 \times 10^6$ e-volts, i e, a range of 5-6 mm as a maximum.[†] The thinnest mica window we have been able to use has a stopping power of 3 mm of air, and the residual range of 2-3 mm is not sufficient for the particle to enter our counting chamber and produce a deflection of appreciable size We have searched very carefully for such a doubly charged particle, both with a special type of counting chamber of small depth, and by looking for scintillations produced on a screen of zinc sulphide placed inside the apparatus itself and covered with aluminium of 2 mm stopping power to prevent light and scattered diplons from reaching it In both cases the presence of a very intense radiation which is strongly absorbed in a fraction of a centimetre of air, gave rise to so much disturbance as to render counting impossible Thus, while we have not yet detected the $_2He^3$ particles which we believe to be present, we have not yet obtained any evidence that they do not exist

No evidence of the existence of an $_2He^3$ isotope has been obtained by ordinary methods, although the possibility of its existence has been suggested at various times It is not unlikely that while the new isotope may prove to be unstable over long periods it may yet have a sufficiently long life to be detected by counting methods and in the expansion chamber We have not detected any after-effects lasting for a few seconds or more, suggesting the expulsion of a positive electron or other charged particle If the $_2He^3$ nucleus is unstable, there are a number of possibilities as to the mode of transformation

It is evident that the experiments we have described suggest very strongly that the neutrons resulting from the bombardment of diplogen with diplogen are homogeneous in velocity, and since large yields are obtainable at comparatively low bombarding potentials they should serve as an almost ideal group for experimental work on the properties of neutrons.

In addition to a study of these transformations, we have made a number of observations on the neutrons, protons, and also α-particles emitted from

---

[*] Not yet published.

[†] The energy and range of the particle depends to some extent on the direction of emission relative to the bombarding particle, and will be greater in the forward direction

lithium, beryllium, carbon, and other elements under diplon bombardment We hope to give an account of these experiments in a subsequent paper

Summary

An account is given of the effects observed when diplons are used to bombard targets of compounds containing heavy hydrogen. It is found that a group of protons of 14 3 cm range is emitted in very large numbers   A shorter 1 6 cm. range group of singly charged particles is also observed, and it is shown that the two groups contain equal numbers of particles   A discussion of the reaction which gives rise to them is given, and reasons are advanced for supposing that the short-range group consists of nuclei of a new isotope of hydrogen of mass 3·0151   The number of particles emitted has been investigated as a function of the energy of the bombarding diplons, and the absolute yield for a pure diplon beam hitting a pure diplogen target is estimated to be about 1 in 10^6 at 100,000 volts

Neutrons have been observed in large numbers as a result of the same bombardment   It is shown that the energy of the neutrons is about 2×10^6 e-volts, and it is suggested that they arise from an alternative mode of breaking up of the unstable form of helium nucleus formed initially by the union of two diplons   This other mode results in the expulsion of a neutron and a helium isotope of mass 3 in directions opposite to one another   If we calculate the mass of $_2He^3$ from energy and momentum considerations of the ranges of the short-range groups emitted from $_3Li^6$ when bombarded by protons, the energy of the neutron can be deduced and agrees well with experiment.

Experiments with High Velocity Positive Ions   III —The Disintegration of Lithium, Boron, and Carbon by Heavy Hydrogen Ions

By J D COCKCROFT, Ph.D, and E T S WALTON, Ph D

(Communicated by Lord Rutherford, O M , F R S —Received April 4, 1934)

1 *Introduction*

An important enlargement of the field of nuclear research has been effected by the experiments of Lawrence, Lewis, and Livingstone,[*] who first used the ions of the heavy isotope of hydrogen to produce nuclear disintegrations These pioneer experiments showed that these ions, which will in future be termed "diplons,"[†] produced disintegrations of considerably greater complexity than those produced by protons of the same energies   Thus, Lawrence, Lewis, and Livingstone reported that from most of the substances bombarded, one or more groups of protons were emitted, whilst a group having a range of about 18 cm appeared to be emitted from every element investigated   This surprising result led these workers to the hypothesis that the "diplon" is unstable in a strong nuclear field and that it breaks up into a proton and a neutron with a liberation of energy of the order of 5 million volts, the neutron mass being taken to be 1 0006[‡] to explain the observed proton energies

In addition to the emission of long-range protons, Lawrence, Lewis, and Livingstone (*loc cit*) reported the emission of α-particles from lithium, beryllium, boron, nitrogen, magnesium, and aluminium   The experiments of Rutherford, Oliphant, and Kinsey[§] and the Wilson chamber photographs of Dee and Walton[||] showed that the 13 2 cm α-particles from lithium originated from the disintegration of Li^6 into two α-particles, and suggested that Li^7 disintegrated into two α-particles and a neutron   No detailed studies have been made of the disintegration of the other elements

The experiments described below have been made with a view to obtaining more evidence on the nature of the disintegrations in which protons are emitted , we have also studied the emission of α-particles from boron under diplon bombardment.

[*] ' Phys. Rev ,' vol 44, p 55 (1933)
[†] ' Proc Roy Soc ,' A, vol. 144, p 1 (1934)
[‡] ' Phys. Rev ,' vol. 44, p 778 (1933)
[§] ' Proc Roy Soc ,' A, vol. 141, p 722 (1933)
[||] ' Proc. Roy Soc ,' A, vol. 141, p 733 (1933)

2 *Apparatus*

In these experiments, we have used the high voltage D C generator described in our previous paper,* which gives a maximum steady potential of 700 kv. The tube for the acceleration of ions there described has been modified to give larger intensities of ions and more reliable operation   Porcelain cylinders of 12-inch diameter and 3 feet 6 inches length have been substituted for the glass cylinders used previously , a discharge tube of the type described by Rutherford and Oliphant† has been transferred from the apparatus of Dee and Walton to the new apparatus and the evacuation of the tube is now carried out by a Metropolitan-Vickers 04 Apiezon Oil Diffusion Pump which has a speed of 1200 litres/sec. for hydrogen. This great increase in pumping speed has increased considerably the reliability of operation of the tube , the new discharge tube enables total currents of 200 microamperes to be obtained, whilst, in spite of using double stage acceleration, the geometry of the electrodes is now such as to focus about 20 per cent of the ions into a beam having a diameter of only 1 cm in the experimental chamber, thereby increasing considerably the fraction of disintegration particles which can be made to enter the recording apparatus

3 *The Detection of High Speed Protons*

In most experiments we have used the scintillation method for fixing approximately the ranges of the particles emitted, carrying out a detailed study with the ionization chamber, linear amplifier, and oscillograph previously described   In interpreting records of proton emission, difficulty arises when the background disturbance of the oscillograph record due to electrical and acoustical " pickup " is comparable with the oscillograph deflection due to the protons   The greatest care has been taken to reduce as far as possible the magnitude of this pick up, but in practice there is often a disturbance due to the discharge tube or to soft radiation which gives a background oscillation on the oscillograph   Consequently it is often necessary to count only deflections above some arbitrary size corresponding to protons approaching the end of their range   The absorption curves obtained are thus of a differential type, maxima being obtained near the end of the range of a group of protons

In the present experiments we have not applied magnetic analysis to separate out the protons and diplons in our beams. Since we usually have a mixture of hydrogen and diplogen in our discharge tube, the beam of ions contains

* ‘ Proc Roy Soc ,’ A, vol 136, p. 619 (1932).
† ‘ Proc Roy Soc ,’ A, vol 141, p. 259 (1933).

protons of full and half energy and diplons of full and two-thirds energy
Thus spread of the energy causes the peaks in the absorption curves to be less
sharply defined, but does not prevent an accurate deduction of the range from
being made

In most of these experiments, an ionization chamber having a depth of 1 cm.
has been used , in general a correction of 0 5 cm has been made to the ranges
obtained from the absorption curves to allow for this depth

4 The Disintegration of Lithium

A target of pure Kahlbaum lithium, which on exposure becomes covered
with a layer of lithium hydroxide, was bombarded with a mixed beam of ions
obtained from hydrogen containing approximately 10 per cent of diplogen   A
target of 5 cm. diameter was used, the beam covering a diameter of about
1 cm. , the distance from centre of target to recorder was 5 cm., and the solid
angle subtended by the counter aperture at the recorder was about 1/30   With
this arrangement, the emission of particles having a range of about 30 cm. was
observed, and the absorption curve of fig 1 was obtained for an accelerating
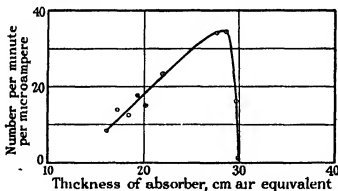
Fig 1 —Protons from lithium

potential of 500 kv   The maximum number of particles counted was about
700 per minute   The observations show that a group of protons having a
range of 30 5 cm. ± 1 cm for an accelerating potential of 500 kv is emitted
from lithium   Observations were not carried out at absorptions less than
14 cm. owing to the presence of the strong α-particle group of 13 2 cm. range
The range observed is consistent with the observation of Lawrence, Lewis, and
Livingstone that protons of range up to 40 cm were emitted from lithium
fluoride when bombarded with their more energetic particles

5 *The Mechanism of the Disintegration.*

If we make the assumption that the following nuclear reaction occurs

$$_3Li^6 + _1D^2 = _3Li^7 + _1H^1$$
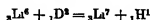
the kinetic energy change in the transmutation may be calculated from the mass change

$$(6 \cdot 0145 + 2 \ 0136) - (7 \ 0146 + 1 \cdot 0078)$$
$$= 0 \ 0057 \pm 0 \ 0007 = 5 \ 3 \pm 0 \ 6 \ \text{million volts}$$

Allowing for the kinetic energy of the diplons and the energy taken by the recoiling nucleus, the disintegration protons may be expected to have an energy of 5 0 ± 0 5 million volts If we adopt Duncanson's figures* for the range velocity function of the protons, protons of this energy would have a range 35 ± 5 cm. The observed ranges would thus be consistent with the hypothesis as to the nature of the disintegration. If, on the other hand, we take the masses of Li^6 and Li^7 to be fixed by disintegration data, the expected energy in the protons is 5 1 ± 0 2 million volts, which, from Duncanson's data would give a range of 35 ± 2 cm. The agreement while fair is not as good as might be expected , the discrepancy may be due to the uncertainties in the range velocity relation for protons, to the emission of radiation in the transmutation, or it may be possible that the unstable nucleus Be^8 may loose part of the energy imparted by the diplon before breaking up

Strong support for the proposed reaction is given by the experiments of Oliphant, Shire, and Crowther† on the transmutation of the separated isotopes of lithium, which showed that the 30 cm. protons result from the bombardment of Li^6 by H^2

6 *The Number of Disintegrations*

The absolute number of disintegrations cannot be obtained with any precision from our present experiments owing to the uncertainty in the composition of the beam For the same reason, no accurate determination of the variation of the number of disintegrations with voltage has been made. The results for the mixed beam are, however, given in fig 2 It is seen that there is no sharply defined lower limit to the voltage at which disintegrations can be observed, the curve being similar to that obtained for the 13 2 cm. α-particles emitted in the disintegration

$$_3Li^6 + _1D^2 \rightarrow 2_2He^4$$

* 'Proc Camb Phil Soc,' vol 30, p. 102 (1934)

† 'Nature,' vol. 133, p 377, March 10 (1934).

We find that the number of 13 2 cm. α-particles emitted is roughly twice the number of disintegration protons for diplon energies of 500 kv., so that the relative probability of the two types of disintegration is not very different.

7. *The Disintegration of Carbon.*

The absorption curves obtained for a target of Acheson graphite with the same experimental arrangement as for lithium are given in fig 3, the maximum number of disintegration particles being of the same order as that found for-
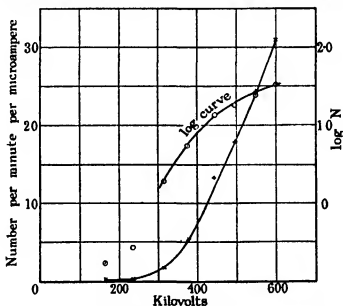
Fig 2 —Protons from lithium , 27 8 cm absorber

lithium   The curves suggest the presence of a group of particles having a range of 14 0 ± 1 cm for an accelerating potential of 500 kv   An analysis of the oscillograph deflections suggests that this group are protons, and it also indicates the presence of a weak proton group having a range of about 8 cm.

Taking the energy of the 14 cm. protons as 2 9 million volts, the kinetic energy change in the reaction is 2 6 ± 0 16 million volts

The range of the proton group obtained is about 1 cm. longer than would be expected from the observations of Lawrence, namely, that, using 1 2 million volt diplons, the proton range is 18 cm.

Since these experiments were completed, Lauritsen and Crane* have reported the emission of a γ-ray having an energy of about 3 million volts when carbon

* 'Phys. Rev.,' vol. 45, p. 345 (1934).

is bombarded with diplons. If we assume that the 14 cm. proton and the γ-ray are emitted at the same time from the reaction

$$_6C^{12} + _1D^2 = _6C^{13} + _1H^1 + h\nu,$$
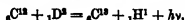
we obtain the following value for the mass of C^{13}.

$$12\ 0036 + 2\ 0136 - 1\ 0078 - 0\cdot0027 - 0\ 0032 = 13\ 0035 \pm 0\ 0006$$

The band spectrum mass for C^{13} is 13 0039 ± 0 0013 The mass obtained from the disintegration of B^{10} by α-particles is 13 0047 ± 0 0005 (Chadwick, Constable, and Pollard) *

If the reaction assumed is correct, it might be expected that some transmutations would occur in which no γ-ray was emitted, the full energy appearing in the form of kinetic energy, so that protons of about 40 cm range should be
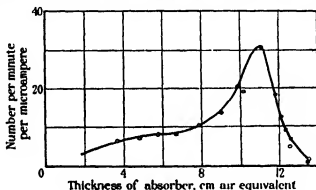
FIG 3 —Protons from carbon Diplon energy 500 kv

observed. It appears certain, however, that if they exist the number of such protons must be less than 1 in 500 of the number of 14 cm. protons

On the other hand, the emission of the γ-ray observed by Lauritsen and Crane may be connected with the transformation of C^{12} to N^{13} under proton bombardment with the subsequent emission of a positive electron.† If this is so, then the mass of C^{13} calculated from both reactions would be about 13 006

Evidence to be referred to later suggests that the 8 cm proton group may be due to a layer of adsorbed oxygen

Fig 4 gives the observed variation in the number of disintegrations with voltage These results were obtained from a beam of mixed ions, and an absolute determination of numbers has not yet been made.

---

* ' Proc Roy Soc ,' A, vol. 130, p. 463 (1933)

† Cockcroft, Gilbert, and Walton, 'Nature,' vol. 133, p 328 (1934).

8 *The Disintegration of Boron*

A study of the particles emitted from a target of boron under diplon bombardment has shown that very swift α-particles are emitted together with[*] at least three groups of protons   The absorption curve is given in fig 5

By combining deductions from the shape of the absorption curve, fig 5, with an analysis of the distribution of the size of oscillograph deflections we find that both α-particle and proton groups are present   A complete interpretation
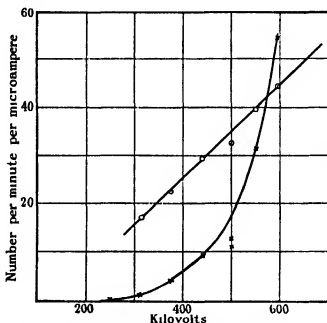
FIG 4 —Diplons on carbon target , absorber 8 9 cm of air

of these curves up to 16 cm is difficult owing to the probable superposition of one or more proton groups on a continuous distribution of α-particles.   The existence of the following groups of particles seems, however, to be certain —

(1) α-particles of all ranges up to a maximum of 15 0 ± 1 cm.

(2) A proton group of range 31 ± 2 cm.

(3) A proton group of range 58 ± 2 cm.

(4) A proton group of range 92 ± 2 cm.

The rise in the absorption curve from 6 to 10 cm. suggests the presence of another proton group, but until Wilson chamber photographs are available it is not possible to be certain of the interpretation.

The following tentative explanations are advanced for groups (1) to (4)

(1) The continuous distribution of α-particles corresponds to the disintegration of B^{10} into three α-particles

$$_5B^{10} + _1D^2 \rightarrow 3_2He^4$$
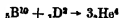
The absorption curve for this disintegration would be expected to be of a similar nature to that observed for the disintegration of B^{11} by protons * If
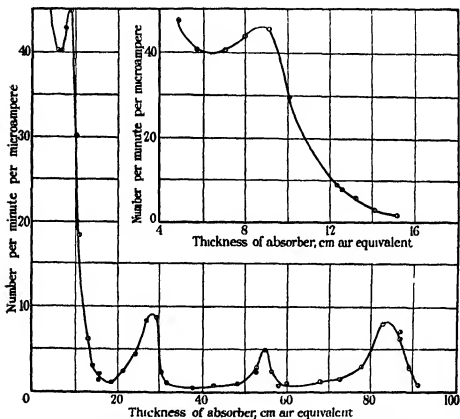
Fig 5 —α-particles and protons from boron   Diplon energy 500 kv

the hump in the curve at 9 cm. is due to a superposed homogeneous group of protons, then the residual curve would have a shape similar to the B^{11} curve

If the end-point of the α-particle curve corresponds to a disintegration in which one α-particle is ejected in a direction opposite to the other two, then

* Rutherford and Oliphant, 'Proc. Roy Soc ,' A, vol. 141, p 259 (1933)

thus α-particle possesses two-thirds of the total kinetic energy. The total kinetic energy in the disintegration particles would thus be

$$(12\ 3 \pm 0\ 30) \times 3/2 \text{ million volts} = 18\ 45 \pm 0\cdot45 \text{ million volts.}$$

If the mass of B^{10} be taken as $10\ 0135 \pm 0\ 0005$ the expected kinetic energy is $19\ 4 \pm 0\cdot6$ million volts. The agreement is satisfactory, but it is very desirable to have further evidence about this disintegration from Wilson chamber photographs. It should be noted that some of the α-particles from this reaction are swifter than any which have previously been discovered. The fastest α-particles from radioactive bodies have a range of $11\cdot5$ cm. whilst the α-particles discovered by Lawrence in the reaction $Li^6 + D$ had a range of 14 cm.

(2), (3), and (4) assuming Duncanson's range velocity relation for protons, these groups correspond to protons of energy $4\ 7$, $6\ 7$, and $8\ 8$ million volts, and could be explained by the following reaction.

$$_5B^{10} + _1D^2 = _5B^{11} + _1H^1 + h\nu.$$

If the proton of range 92 cm. is emitted when all the energy of the reaction goes into kinetic energy, we may calculate the difference of mass of B^{10} and B^{11} as follows

$$B^{11} - B^{10} = 2\ 0136 - 1\ 0078 + 0\ 0005 \text{ (K.E of } D^2)$$
$$- 0\ 0102 \text{ (K E after disintegration)}$$
$$= 0\ 9961 \pm 0\ 0004$$

The difference of mass from Aston's determination is $11\ 0110 - 10\ 0135 = 0\ 9975 \pm 0\ 0007$ Thus the agreement is not very good If, on the other hand, we were to assume that the masses of B^{10} and B^{11} could be obtained from the end-point of the continuous α-particle distributions in the transmutations by diplons and protons respectively, we should obtain very close agreement with these experiments.

The two groups of lower energy may correspond to disintegrations in which energy of 2 and 4 million volts respectively is emitted in the form of γ-radiation.

The total number of particles in groups (2), (3), and (4) is approximately one-third of the maximum number of α-particles observed This suggests that the disintegration leading to three α-particles has about the same probability as the disintegration leading to B^{11}.

9 *The Emission of Particles on the Bombardment of Heavy Elements by Diplons*

A detailed study has been made of the particles emitted from copper, copper oxide, iron, iron oxide, tungsten, and silver In order to facilitate comparison of these elements the target illustrated by fig 6 was constructed so that four targets could be interchanged by rotation of a ground joint With this arrangement the solid angle subtended by the window at the target was increased to 0 25 , a still further increase in the number of particles observed was obtained by using a helium-diplogen mixture containing 30% of diplogen A series of eight experiments was carried out, using diplon energies of 500 kv

(i) and (ii) The emission of particles from carbon, copper oxide, copper, and iron was compared in one series of experiments and of tungsten, silver, iron oxide, and iron in another, the absorption curves of figs 7, *a*, and 7, *b*, being obtained. Observations could not be carried out on silver at less absorber than 6 cm owing to the emission of soft radiation in considerable intensity

From these curves and from an analysis of the size of the oscillograph deflections we conclude—

Stream of ions

FIG 6

(*a*) that a group of protons of range about 14 cm is emitted from all these targets, the numbers from carbon being about ten times the numbers from other targets ;

(*b*) that a group of protons of range 8 cm is emitted from all the targets ;

(*c*) that a group of singly charged particles of range about 4 cm is common to all targets except carbon ,

(*d*) that α-particles are emitted from all the targets, the numbers falling rapidly for absorbers greater than 2 cm., a few particles being observed up to 5 cm

(*e*) that whilst the 8 cm group is stronger from Fe_3O_3 than from Fe, the relative strength of the 14 cm groups are reversed

(iii) A strip of the tungsten used in experiment (ii) was washed in succession in caustic soda, distilled water, ether, caustic soda, and distilled water and
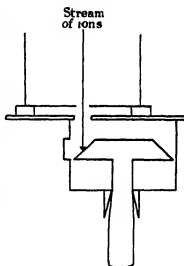
then bombarded. The absorption curve of fig 8, *b*, was then obtained, showing
that whereas the short range group of particles and the number of particles
at 8 cm. absorber had roughly the same relative magnitude as in experiment
(ii) the 14 cm peak was reduced in numbers to about one-third of the 8 cm.
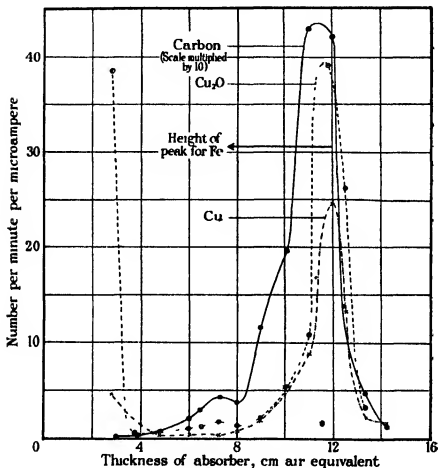
Fig. 7, *a*.

group In addition the residual group appears now to have a rather longer
range than that of the original group

(iv) At the suggestion of Dr Oliphant the target was heated in position to
about 2000° C by passing a heavy current through it, and the emission of
particles observed under these conditions and immediately after heating.
The results showed a considerable diminution in the number of particles in
the 8 cm. groups and short-range groups, whilst the numbers in the 14 cm.

group were reduced by a further factor of 2, the curve obtained after heating being shown on fig 8, *c*

(v) The target was left for 18 hours in the apparatus and then bombarded whilst cold The number of particles observed was if anything smaller than immediately after heating the target, showing that no new layers of impurities had been adsorbed during this period
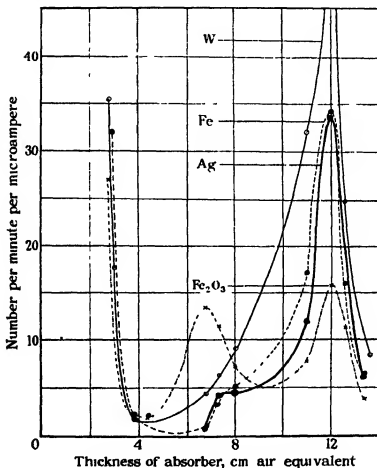
Fig 7, *b* —Diplon energy 500 kv

(vi) Carbon dioxide was admitted to the apparatus to a pressure of 1 cm, the target flashed at about 1600° C and again bombarded No change in the number of particles was observed from experiment (v), showing that no surface layer had been adsorbed in sufficient amount to give rise to an appreciable effect.

(vii) After being cleaned by heating, the target was taken out and oxidised by passing an electric current through it, replaced and again bombarded. The absorption curve obtained is shown in fig. 8, *d*. The short-range group and
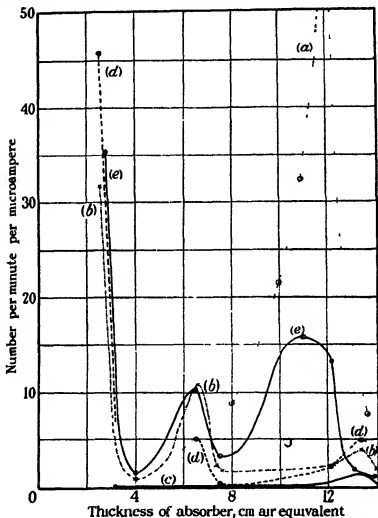
Fig. 8.—Diplon energy 500 kv.   (*a*) Original tungsten, (*b*) chemically cleaned tungsten, (*c*) after heating, (*d*) after oxidising, (*e*) after reheating.

8 cm. group have again appeared strongly together with a few particles at absorptions of 14 cm. about equal in numbers to those obtained in (iii).

(viii) The target was cleaned by heating in vacuum, was removed and oxidised and then handled in order to reproduce the treatment which a metal

might reasonably receive before mounting in an apparatus   The target was then replaced and bombarded and the curves of fig 8, *e*, were obtained   We see that all three peaks now appear strongly , the long-range peak is again stronger than the 8 cm peak and is now restored to its former position

These experiments may be summarized as follows : —

(i) The 8 cm proton group, the 4 cm proton group, and the short-range α-particle groups disappear when the target is heated strongly and reappear when the target is oxidized   The evidence suggests therefore that these groups are due to oxygen

Other experiments carried out by Rutherford and Oliphant* have lead to similar conclusions and they propose the following explanation for the reaction leading to the 8 cm protons

$$_8O^{16} + {_1}D^2 = {_8}O^{17} + {_1}H^1$$
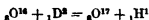
the observed range being in good accord with the accepted masses for O^{16} and O^{17} The explanation of the 4 cm proton group must await further experiments , the energy difference between the two groups is 0 75 million volts

(ii) The long-range proton group from the heavy elements appears to be complex, the greater part of the effect being removed by chemical cleaning of the surfaces, a small residual effect remaining due to protons having a slightly longer range   The coincidence of the range of the majority of the protons with the long-range group from carbon suggests therefore that a thin film of grease or other carbon impurity is responsible for the greater part of the effects

An alternative explanation seemed, however, to be offered by the experiments of Rutherford, Harteck, and Oliphant,† which showed that on bombarding by diplons, ammonium sulphate, in which the ordinary hydrogen had been largely replaced by diplogen, very great numbers of particles were emitted, half of the particles having a range of 1 7 cm and half a range of about 14 cm   It seemed, therefore, possible that the whole of our results might be explained by diplogen being absorbed on carbon from the bombarding stream, the adsorbed layer being then disintegrated by the diplon stream

In order to test this hypothesis, we have carefully compared the ranges of the proton groups emitted from $(ND_4)_2SO_4$ and carbon under identical conditions   If all the results are due to adsorbed diplogen, we ought to get the

same 14 cm. range from the two substances, and we ought to observe large numbers of singly charged particles having a range of about 2 cm. from carbon.

The results of these experiments are given by figs. 9 and 10 In fig 9 the absorption curves for the two substances are given, showing that the range of the protons from $(ND_4)_2SO_4$ is greater by about 1 cm. than the range of the protons from carbon   A still more conclusive proof of the difference between the two reactions is given by fig 10 in which we plot the distribution in size of the oscillograph deflections for the two substances for small absorptions Remembering that a large deflection corresponds to a proton near the end of
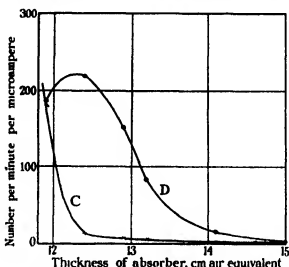
Fig 9 —Comparison of ranges of long range protons from $(ND_4)_2SO_4$ and C   D accelerating voltage of diplons 150 kv , proton range 14 ± 0 5 cm   C accelerating voltage of diplons 370 kv , proton range 12 5 ± 0 5 cm

its range, we see at once that there are very few short-range particles from carbon compared with the number from $(ND_4)_2SO_4$ Experiments with greater thickness of absorber showed that the number of 14 cm. protons are of the same order of magnitude for the two targets

We conclude that—

(1) most of the 14 cm. protons emitted from carbon are due to the transmutation of C^{12} into C^{13},

(2) there is probably a small additional group of protons of range 15 cm. at 500 kv due to the adsorption of diplogen and the subsequent disintegration of the adsorbed layer,

(3) the greater part of the effects observed with the heavy elements is due to thin films of grease or other form of carbon impurity adsorbed on the surface,

(4) a smaller number of 15 cm protons are emitted from the heavy elements due to the adsorption of diplogen from the bombarding stream

10 Conclusions

We may summarize the experimental results by stating (i) that the emission of long-range protons is in all substances investigated (D, Li, B, C, O) bound up
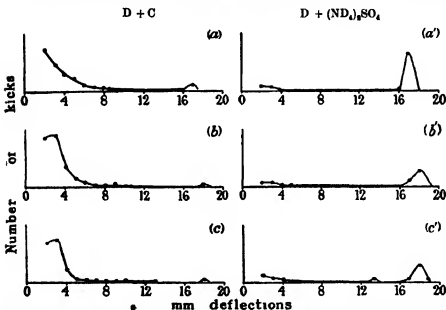
Fig 10 —Distribution in use of oscillograph deflections for C + D and $(ND_4)_2SO_4$ + D

(a) and (a') 0 63 cm absorber
(b) and (b') 1 23 cm absorber
(c) and (c') 2 cm absorber

with the transformation of an element into the next heavier isotope of that element, the neutron being captured and the proton ejected, (ii) that when transmutations leading to the emission of an α-particle are possible (Li, B) the probability of this transmutation is of the same order as that of the first type, (iii) that the emission of protons from the heavier elements (Cu, Fe, Ag, W) is in our experiments due to films of impurities of oxygen, carbon, and adsorbed diplogen.

Summary

The disintegration of lithium, boron, and carbon, when bombarded by fast ions of heavy hydrogen, has been examined   For lithium, a group of protons of 30 5 cm range has been observed , this can be interpreted as resulting from the transformation of Li^6 to Li^7 Boron gives proton groups of ranges 92 cm , 58 cm., and 31 cm together with a continuous distribution of α-particles with ranges up to a maximum of 15 cm   Carbon gives a group of protons with a range of 14 cm   These would correspond with the 18 cm. group observed by Lawrence from all targets if allowance is made for the higher energies of his bombarding particles.

A 14 cm group of protons has been observed from a number of heavy elements   Experiments have been carried out which indicate that these are probably due to carbon present on the surface in a thin film of grease   A smaller number of protons having a slightly longer range are also emitted, these are probably produced from the disintegration of diplogen adsorbed on the surface   Layers of oxygen on the surface may also give rise to spurious effects.

The emission of a fast group of protons always appears to be connected with the change of one isotope of an element into its next heavier isotope.

INDEX TO VOL CXLIV. (A)